# UNIVERSITY OF SOUTHAMPTON

FACULTY OF NATURAL AND ENVIRONMENTAL SCIENCES

Ocean and Earth Sciences

**Processes Influencing Phytoplankton Growth and Primary Production in a Shallow Temperate Estuary Christchurch Harbour, United Kingdom**

by

**Jiraporn Charoenvattanaporn**

Thesis for the degree of Doctor of Philosophy

September 2016

**UNIVERSITY OF SOUTHAMPTON**

# ABSTRACT

FACULTY OF NATURAL AND ENVIRONMENTAL SCIENCES

Ocean and Earth Sciences

Thesis for the degree of Doctor of Philosophy

## PROCESSES INFLUENCING PHYTOPLANKTON GROWTH AND PRIMARY PRODUCTION IN A SHALLOW TEMPERATE ESTUARY CHRISTCHURCH HARBOUR, UNITED KINGDOM

Jiraporn Charoenvattanaporn

The aim of this research project was to identify the factors controlling the phytoplankton community and primary production in the shallow temperate estuary of Christchurch Harbour and the two river systems flowing into the estuary. Christchurch Harbour is a small shallow micro-tidal enclosed estuary situated on the south coast of England. It is fed by the rivers Stour and Hampshire Avon, and exchanges with coastal waters through a narrow channel at Mudeford. An intensive programme of monitoring both the water quality and phytoplankton communities was undertaken at weekly intervals from April 2013 to April 2014 at the lowest river gauging stations on the Hampshire Avon at Knapp Mill and the Stour at Throop plus a further station at Iford Bridge just above the tidal limit of the estuary. In addition a similar set of measurements were made on the same dates at the entrance to the estuary at Mudeford Quay at low tide. During Spring/Summer 2014 eight estuarine surveys were conducted at fortnightly intervals with measurements of water quality, phytoplankton abundance, and production made at six stations along a transect throughout the estuary.

The riverine phytoplankton community in terms of carbon biomass and accessory pigments displayed a distinctive pattern of seasonal succession. A diatom group maximum was observed in spring and chlorophyte peak in summer. The nano-sized diatom (2.0 – 20.0 µm), *Stephanodiscus* sp., dominated the phytoplankton assemblage, reaching $4.4 \times 10^4$ cells $mL^{-1}$ and a chlorophyll concentration of 98.8 µg $L^{-1}$ on the Stour river during spring when river discharge had reduced following the winter flow peak. The summer chlorophyte bloom was composed of *Chlamydomonas* spp., reaching $7.9 \times 10^4$ cells $mL^{-1}$ and followed the diatom spring bloom. Multivariate analysis revealed that water temperature, river discharge, silicate, and phosphate concentration were major factors controlling phytoplankton carbon biomass at all the river study sites.

At Mudeford Quay, inorganic nutrient concentrations (nitrate, phosphate, and silicate) were generally low during periods of reduced river discharge, but increased during the winter high river flow periods. A chlorophyll *a* maximum was observed during the late spring and decreased during the autumn and winter similar to conditions on the rivers at Throop and Knapp Mill. Phytoplankton carbon biomass and accessory pigment concentration displayed a similar pattern. Diatoms dominated the phytoplankton biomass and community throughout most of the sampling period and were inversely correlated to silicate concentrations. The dinoflagellate *Kryptoperidinium foliaceum* was observed in high abundance during summer months at high salinity values and the freshwater diatom *Stephanodiscus* spp. dominated during the spring.

During the estuarine transect surveys conducted over high tide, high chlorophyll ‘bloom’ events (chlorophyll up to 98 µg $L^{-1}$) were detected in the middle of the estuary in waters of salinity values over 30. Reduced river discharge in summer months led to an increase in

higher salinity water in the mid estuary with these associated peaks in phytoplankton abundance. Different populations of estuarine phytoplankton were observed over the course of the summer with dinoflagellate blooms dominated by *K. foliaceum*, occurring in the mid-estuary followed by *Cryptomonas* spp. blooms. Multivariate analysis revealed that irradiance attenuation coefficient (*k*), salinity, oxygen saturation, temperature, nitrate, and silicate were the major factors controlling phytoplankton carbon biomass during the transect surveys. The results of the present study have provided an improved understanding of the factors controlling the production and distribution of estuarine phytoplankton communities in the shallow temperate, Christchurch Harbour estuary.

## Table of Contents

## List of Tables

**List of Figures**

## DECLARATION OF AUTHORSHIP

I, Jiraporn Charoenvattanaporn declare that this thesis and the work presented in it are my own and has been generated by me as the result of my own original research.

**Processes influencing phytoplankton growth and primary production in a shallow temperate estuary Christchurch Harbour, United Kingdom**

I confirm that:

1. This work was done wholly or mainly while in candidature for a research degree at this University;
2. Where any part of this thesis has previously been submitted for a degree or any other qualification at this University or any other institution, this has been clearly stated;
3. Where I have consulted the published work of others, this is always clearly attributed;
4. Where I have quoted from the work of others, the source is always given. With the exception of such quotations, this thesis is entirely my own work;
5. I have acknowledged all main sources of help;
6. Where the thesis is based on work done by myself jointly with others, I have made clear exactly what was done by others and what I have contributed myself;
7. None of this work has been published before submission.

Signed: .....

Date: .....

**Acknowledgements**

This doctoral study would not have been possible without the help of a number of people and organisations. First and foremost, I would like to acknowledge my main supervisor, Professor Duncan A. Purdie for his excellent supervision and guidance on my PhD research. Also, I would like to thank my second supervisor, Professor Peter J. Statham for his worthy guidance my research and Dr. Henry Ruhl for constructive comments and opinions in every PhD panel meeting. I would like to extend my gratitude to Dr. Anouska Panton for her considerable contribution and lots of supports throughout my PhD study, and Dr. Suree Satapoomin and Dr. Wanwiwa Tumnoi for their guiding and inspiring me to study in the United Kingdom. I would like to thank Royal Thai Government for a PhD scholarship. My grateful thanks are given to the Natural Environment Research Council (NERC) for a partial funding support to my PhD project.

I also gratefully thank the Macronutrients project colleagues, Dr. Anouska Panton, Dr. Fay Couceiro, Dr. Charlie Thompson, Jack Billinge, and Amani Alshatti for their help on field and laboratory works. I am also grateful to Barry Childs for his help during the transect sampling and Dr. Charlie Thompson for her help in the calculation of water residence time. I specially thank to Glaucia M. Fragoso, Christopher Bird, and Daniel Possee as wonderful officemates. Grateful thanks also expressed to Dr. John Gittins, Matt O'Shaughnessy, Nicola Pratt, and Dr. Amonsak Sawusdee who always guided and supported my work, and Akirat Abdulkade for her help in all sampling maps.

I would also like to thank colleagues at Phuket Marine Biological Center, Thailand. Finally, my special thanks go to my beloved family, my father and my mother, my husband Adisorn Charoenvattanaporn, my son Ruj Charoenvattanaporn, and younger brothers. Without their endless love, encouragement, and support, none of this success would have been possible.

| | |
|---|---|
| 19'But | 19'Butanoyloxyfucoxanthin |
| 19'Hex | 19'Hexanoyloxyfucoxanthin |
| Allo | Alloxanthin |
| Chl *a* | Chlorophyll *a* |
| Chl *b* | Chlorophyll *b* |
| Chl *c2* | Chlorophyll *c2* |
| Chl *c3* | Chlorophyll *c3* |
| Dia | Diadinoxanthin |
| DV Chl *a* | Divinyl chlorophyll *a* |
| Fuco | Fucoxanthin |
| Lut | Lutein |
| Per | Peridinin |
| Pra | Prasinoxanthin |
| Vio | Violaxanthin |
| Zea | Zeaxanthin |
| β car | β carotene |
| ANOSIM | Analysis of similarity |
| a.u. | Arbitrary unit (Fluorescence intensity) |
| CCA | Caconical correspondence analysis |
| DCCA | Detrending canonical correspondence analysis |
| $E_0$ | Surface incident irradiance |
| $E_d$ | Downwelling incident irradiance |
| $F_0$ | Initial fluorescence |
| $F_m$ | Maximal fluorescence |
| $F_v$ | Variable fluorescence ($F_m - F_0$) |
| FLO | Orange fluorescence |
| FLR | Red fluorescence |
| FLY | Yellow fluorescence |
| FWS | Forward scatter |
| HPLC | High performance liquid chromatography |
| $k$ | irradiance attenuation coefficient |
| MNC | Macronutrient cycles programme |
| nMDS | Non-matric multidimentional scaling |

| | |
|---|---|
| NTU | Nephelometric turbidity unit |
| PAR | Photosynthetic active radiation (400 – 700 nm) |
| PS II | Photosystem II |
| RDA | Redundancy analysis |
| SEM | Scanning electron microscopy |
| SFCM | Scanning flow cytometer |
| SIMPER | Similarity percentage analysis |
| SPM | Suspended particulate matter |
| SWS | Sideward angle scatter |

# Chapter 1: Introduction

## 1.1 Estuaries

An estuary is commonly defined as *" a semi-enclosed coastal body of water which has free connection to the open sea, extending into the rivers as far as the limit of tidal influence and within which seawater is measurably diluted with freshwater derived from land drainage"* (Dyer, 1997). Rivers concentrate discharges from the catchment area that are transported into the estuaries and coastal waters (Underwood and Kromkamp, 1999). Estuaries are valuable environments in terms of their ecology and economy and are highly complex aquatic systems. The morphology of an estuary can be divided into three sectors; a) a marine or lower estuary, in free connection with open sea; b) a middle estuary subject to strong salt and freshwater mixing; and c) an upper fluvial estuary, characterized by freshwater but subject to daily tidal action (McLusky and Elliott, 2004; Kaiser *et al.*, 2011). The limits between these sectors are variable, and subject to constant changes in the river discharge (Levinton, 2011). Freshwater discharge influences the salinity and nutrient variation along the estuary (Underwood and Kromkamp, 1999; Paerl and Justić, 2011). Spatial and temporal salinity variation has been considered to be the most important factor that influences the distribution and growth of estuarine organisms especially plankton (Kaiser *et al.*, 2011). In addition, freshwater discharge is the main source of nutrients to an estuary (Gillanders and Kingsford, 2002) and macronutrients (nitrogen, phosphorus, and silicon) are important factors influencing phytoplankton growth and production in estuaries (Mann, 2000). Hence, estuaries are considered some of the world's most productive ecosystems and a trophic gradient exists that decreases as salinity increases from estuarine to oceanic systems (Kaiser *et al.*, 2011; Levinton, 2011).

Estuarine ecology is influenced by the quality and quantity of riverine discharge. Most freshwater phytoplankton tend to dominate in the upper estuary and are gradually replaced by coastal or marine species in the lower estuary. Increased river flow raises organic and inorganic gradients into the estuary and turbidity that may affect the photosynthetic processes. On the other hand, low river discharge may increase residence time and reduce the rate of which material moves out of the estuary. In addition, estuaries are considerably influenced by local weather events such as flooding, droughts, and winds. Therefore, it can be argued that production of phytoplankton in estuarine ecosystems is influenced by several physical factors and biogeochemical processes.

## 1.2 Phytoplankton

Phytoplankton are aquatic microscopic plant-like organisms that are able to convert the energy of sunlight to chemical energy, assimilating carbon dioxide and inorganic nutrients (autotrophs). These organisms exist as single cells or simple multicellular forms and they have a large range of cell size (1 – 400 µm) and growth rates (Harris, 1986). Phytoplankton also play an important role in biogeochemical cycles as they are an integral part of the global carbon cycle (Falkowski *et al.*, 1998; Gregg *et al.*, 2003).

Phytoplankton are important components of estuarine ecosystem but rapid changes in their physical environment can influence the species composition (Underwood and Kromkamp, 1999). Estuaries occur adjacent to coastal waters where freshwater inputs from land and oceanic sources are mixed by hydrodynamic processes. The resulting distributions have important effects in regulating the populations and succession of phytoplankton dynamics in estuaries with the phytoplankton community structure mixing between freshwater and coastal species along the estuary.

### 1.2.1 Riverine phytoplankton

Phytoplankton in streams and rivers are important components of primary producers associated with the water column (Belcher and Swale, 1979; Reynolds, 1984; Wehr and Descy, 1998; Dudgeon, 2007; Bellinger and Sigee, 2010) and are used as important indicator of river water quality (Villegas and de Giner, 1973). Phytoplankton growth can cause problems in rivers with high nutrient enrichment and can result in oxygen depletion following blooms (Hilton *et al.*, 2006). Nevertheless, they can also provide an ecosystem service by improving water quality in rivers through nutrient uptake of industrial and agricultural contaminants (Wehr and Descy, 1998). Freshwater phytoplankton dynamics have been studied extensively in lakes and reservoirs, but comparatively little research has concentrated on factors that control phytoplankton biomass in streams and rivers (Reynolds, 2000; Hardenbicker *et al.*, 2014). There is little general literature concerning the factors that influence phytoplanktion dynamics in river ecosystems (Wehr and Thorp, 1997; Wu *et al.*, 2011), but as phytoplankton respond rapidly to local weather conditions and changes in river flow, they are sensitive to climate change (Reynolds, 1998).

Generally, when rivers flow through lowland areas they contain microalgae in suspension. In temperate regions, the addition of substances including macronutrients from agricultural land and sewage effluent from urban areas leads to increased algal growth in rivers leading

to phytoplankton blooms. Nutrients are usually in high concentration in rivers affected by urbanization and agriculture and accordingly rarely limit phytoplankton growth in these systems (Reynolds, 2006). Some biological factors like grazing can control phytoplankton populations in rivers (Schöl *et al.*, 1999) but moreover, they are considered as biological indicators or biomarkers by their presence under particular conditions of water quality (Bellinger and Sigee, 2010).

Several studies have reported that riverine phytoplankton abundance in temperate regions normally reach significant numbers only during the spring and summer months (Belcher and Swale, 1979; Phlips *et al.*, 2000; Hardenbicker *et al.*, 2014). The diatoms are predominant particular in the spring and the characteristic phytoplankton species belonging mainly to the centric diatom genera *Stephanodiscus* and *Cyclotella* occur in UK river ecosystems (Belcher and Swale, 1979). In North America, Wehr and Thorp (1997) reported on the planktonic organisms of the Ohio River between 1991 and 1992, observing the diatom *Melosira* spp. was abundant in summer and *Cyclotella* spp. in spring.

Various possible factors regulating the phytoplankton dynamics in rivers maybe chemical (e.g. nutrient concentrations), hydrological (water residence time, discharge), physical (light, temperature), and biological (grazing) (Belcher and Swale, 1979; Reynolds, 1984; Wehr and Thorp, 1997; Hardenbicker *et al.*, 2014). All these different parameters are known to alter phytoplankton populations in rivers, however, studies on the effect of conditions on phytoplankton growth in rivers are still rare (Wu *et al.*, 2011; Hardenbicker *et al.*, 2014).

### 1.2.2 Estuarine phytoplankton

Phytoplankton are described as important primary producers in estuarine planktonic food webs (Cloern, 2001; Harding Jr *et al.*, 2002; Paerl and Justić, 2011). Phytoplankton populations are present within the drainage channels and extensive biofilms of microalgae e.g. diatoms and euglenoids plus cyanobacteria can be found on the surface of mudflats (Underwood and Kromkamp, 1999). In estuarine and coastal ecosystems, phytoplankton can be divided into seven main groups including; diatoms, chlorophytes, cyanophytes, cryptophytes, chrysophytes, prymnesiophytes, and dinoflagellates.

### 1.2.3 Distribution of the main taxonomic phytoplankton groups

Diatoms are considered among the most abundant and productive phytoplankton in rivers, estuaries and oceanic waters, and support a central role in planktonic and benthic food webs (Tomas, 1997; Round *et al.*, 2007; Bellinger and Sigee, 2010). The diatoms tend to prefer waters with moderate to productive nutrient concentrations and favour blooming during springtime when relatively high nutrient levels are available and when water residence time is reduced in estuaries (Paerl and Justić, 2011). The distribution of some diatom species can be used as indicators of nutrient status in estuaries (Underwood *et al.*, 1998; Paerl *et al.*, 2003), and they support a key role in planktonic and benthic food webs (Tomas, 1997; Reynolds, 2006). In addition, diatoms can dominate summer blooms in some temperate estuaries (Carstensen *et al.*, 2007; Nixon *et al.*, 2009). Fucoxanthin is often used as a diagnostic photopigment of diatoms when present in both estuarine and marine ecosystems (Jeffrey and Vesk, 1997; Paerl *et al.*, 2003).

Chlorophytes or green algae are commonly found in freshwater, coastal, and ocean waters and are generally present in the low salinity or upper parts of estuaries (Tomas, 1997). They vary in size and shape and occur as coccoid cells (e.g. *Chlorella*), disk-shaped cells (e.g. *Cosmarium*), stacked cells (e.g. *Scenedesmus*), and include flagellated genera (e.g. *Chlamydomonas*) (Paerl and Justić, 2011) with chlorophyll *a* and *b* their main pigments (Jeffrey and Vesk, 1997). Chlorophytes have rapid growth rates and planktonic forms can grow in fast-flowing water with short residence time and in low salinity waters, where nutrients are enriched (Jeffrey and Vesk, 1997; Paerl and Justić, 2011). Chlorophytes are normally non-toxic although they can form blooms that may contribute to hypoxic conditions particularly in estuarine bottom waters after sedimention (GEOHAB, 2006).

Cyanobacteria or cyanophytes are prokaryotic phytoplankton most commonly found in filamentous forms and widely occurring in freshwater and seawater environments (Jeffrey and Vesk, 1997; Bellinger and Sigee, 2010). They are often abundant under eutrophic nutrient-enriched conditions in freshwaters and estuaries (Paerl *et al.*, 2003). Cyanophytes include several toxic species and some species can fix atmospheric nitrogen into ammonium. They contain zeaxanthin a diagnostic photopigment (Jeffrey and Humphrey, 1975).

Cryptophytes or cryptomonads are a well-defined group of photosynthetic nanoplanktonic flagellates and are similar in size to the chlorophytes (Jeffrey and Humphrey, 1975; Paerl and Justić, 2011). They are found both in freshwater and marine environments and are

common in temperate waters (Bellinger and Sigee, 2010). They prefer fresh to brackish nutrient enriched waters and as a result, some species are used as bioindicators of eutrophic status (Bellinger and Sigee, 2010). Alloxanthin is present as a main accessory pigment that indicates the presence of cryptophytes (Jeffrey and Vesk, 1997).

Most chrysophytes are found in freshwater environment as unicellular, colonial, and free swimming forms (flagellar). Their photosynthetic pigments include chlorophyll *a*, *c2*, *c3*, fucoxanthin, 19'Butanoyloxyfucoxanthin, and diadinoxanthin; excluding violaxanthin mainly present in some freshwater species (Jeffrey and Vesk, 1997). They are often used as indicators of oligotrophic conditions in terms of water monitoring and sediment analysis in lakes (Bellinger and Sigee, 2010).

Prymnesiophytes or haptophytes are photosynthetic cells possessing chlorophyll *a* and accessory pigments including diadinoxanthin and fucoxanthin (Jeffrey and Vesk, 1997; Bellinger and Sigee, 2010). Haptophytes of the genus *Chrysochromulina* form blooms that can cause serious aquaculture problems (Paerl and Justić, 2011).

Dinoflagellates are often dominant in surface marine water, with only about 220 species found in freshwater ecosystems (Bellinger and Sigee, 2010). They are important primary producers in estuarine ecosystems and can sustain the grazing component of food webs and higher trophic levels (Paerl *et al.*, 2003; Paerl and Justić, 2011). Dinoflagellates contain chlorophyll *a* and usually peridinin photopigments and they can form temporary cysts under unfavourable situation (Jeffrey and Vesk, 1997). They can form blooms and some form toxins that can contaminate the food chain in estuaries and may accumulate in shell fish. The growth rates of dinoflagellates are generally slower than diatoms, chlorophytes, and cryptomonads (Paerl and Justić, 2011).

### 1.2.4 Temperate estuarine phytoplankton

In temperate areas, estuarine zones are valuable ecological and economic environments that support fisheries, aquaculture, tourism, and recreation activities (Underwood and Kromkamp, 1999; De Jonge *et al.*, 2002). In some estuaries direct impacts of human activities have significantly contributed to decreasing water quality including increased nutrient concentrations from sewage and agricultural run off. Increasing nutrient loadings in estuaries can enhance primary production leading ultimately to eutrophication (Nedwell and Raffaelli, 1999; De Jonge *et al.*, 2002). The over enrichment of water by dissolved nutrients such as nitrogen and phosphorus can increase phytoplankton growth and

microbial production in the water column (Levinton, 2011). Through time, these changes will most probably be reflected at other trophic levels (Wetz *et al.*, 2011) and some estuaries have undergone significant eutrophication due to organic enrichment (Marques *et al.*, 2007; Wetz *et al.*, 2011; Maier *et al.*, 2012). Estuarine ecosystems are very dynamic systems where water circulation, river flow, and sewage input can induce changes in the distribution and structure of planktonic populations (Marques *et al.*, 2007). Because of the unusually dynamic conditions experienced in estuaries, the phytoplankton distribution is often spatially and temporally heterogeneous (e.g. the Taw estuary in north Devon) when compared to other aquatic ecosystems (Maier *et al.*, 2012). Several studies have investigated the environmental controls upon phytoplankton growth and primary production in temperate estuarine systems in recent years (Moore *et al.*, 2006; Wetz *et al.*, 2011; Maier *et al.*, 2012). The estuarine phytoplankton are an important component in eutrophic estuaries and have a key role in primary production in an estuary. McLusky and Elliott (2004) showed that high levels of primary production occur due mainly to the high nutrient levels in estuaries in comparison to the near shore waters or the open sea.

### 1.2.5 General characteristics of temperate estuarine phytoplankton in shallow estuaries

Estuarine ecosystems are very dynamic systems where water circulation river inputs and tides cause high variability in the distribution and structure of planktonic populations (Marques *et al.*, 2007). Phytoplankton are described as the major primary producers in estuaries and have a dynamic influence on the estuarine planktonic food web. McLusky and Elliott (2004) suggest that there may be two factors, shallowness and turbidity that limit the production rate of phytoplankton in shallow natural estuaries. Recent evidence suggests that larger phytoplankton may dominate in shallow coastal systems typified by high nutrient concentrations (Wetz *et al.*, 2011). Several studies investigating pico-phytoplankton (0.2 – 2 µm), however, have found that this size fraction are the dominant primary producers in some temperate estuaries (Sin *et al.*, 2000; Gaulke *et al.*, 2010). Thus, the role of small phytoplankton, such as pico-phytoplankton and nano-phytoplankton in estuarine food webs and biogeochemical cycles is still largely unresolved and understanding of environmental controls upon estuarine small phytoplankton in particular is limited (Wetz *et al.*, 2011). Several studies have investigated environmental control of phytoplankton growth and primary production in temperate estuarine systems in recent years (Moore *et al.*, 2006; Wetz *et al.*, 2011; Maier *et al.*, 2012). These studies have

identified many different factors controlling phytoplankton growth and productivity in the temperate shallow and river-dominated estuary.

### 1.2.6 Species succession and occurrence of blooms in estuaries

Carstensen *et al.* (2015) demonstrated that the occurrence of phytoplankton blooms are the driving phenomenon of the functioning of estuarine and coastal waters. The phytoplankton bloom may be defined as a population explosion of a particular species which is confined to a definite part of the water column and can develop in the course of a few days and be sustained for several weeks. Phytoplankton bloom events are often visible and the water colour shows the characteristics of the phytoplankton species (Allen *et al.*, 2008; Allen and Wolfe, 2013). An obvious spring bloom is commonly present in temperate estuarine and coastal systems and diatom dominated blooms in spring time are a general feature (Carstensen *et al.*, 2015). The occurrence of blooms in other seasons particularly summer and autumn has recently achieved consideration as a consequence of their increasing recurrence (Nixon *et al.*, 2009). Summer phytoplankton blooms have increased in magnitude and frequency in some estuarine and coastal areas (Carstensen *et al.*, 2007; Nixon *et al.*, 2009). Blooms occur at different times in different estuaries, depending on the environmental condition and nutrients available (Lucas *et al.*, 1999; Pinckney *et al.*, 1999). For instance, summer blooms in the shallow coastal waters of the northern Europe (the Kattegat strait) were consideration to be related to strong nutrients inputs from river discharge and resuspension from the bottom (Carstensen and Conley, 2004). In contrast, the occurrence of summer blooms seems to result from the germination of resting stages of different phytoplankton species particularly diatom and dinoflagellate species in Hakata Bay, Japan (Shikata *et al.*, 2008) and in the Gullmar Fjord, Sweden (McQuoid, 2005). These blooms response to environment variables, for example, increase in light intensity, water temperature, and nitrogen availability (McQuoid, 2005; Shikata *et al.*, 2008). In addition, the blooms may change the water colour, due to high chlorophyll concentration. Dinoflagellate blooms can result occurs in green or red colouration to the waters depending on the dominant species (GEOHAB, 2006). Dinoflagellate blooms often occur after massive rain events the coastal zone (Jeffrey and Vesk, 1997).

## 1.3 Important environmental factors influencing phytoplankton growth in temperate estuaries

Estuaries have complex ecosystems that can be affected by changes in hydrology, local weather, and human activities. The key environmental factors controlling the diversity and abundance of phytoplankton in estuaries are nutrients, light, water residence time, freshwater discharge, salinity, temperature, and grazing.

### 1.3.1 Nutrients

About half of the world's human populution live adjacent to estuaries leading to increasing levels of nutrients and sediment associated with coastal developments (Paerl *et al.*, 2005). McLusky and Elliott (2004) showed that the abundance of nutrients in estuaries may limit the production of estuarine phytoplankton. Generally phytoplankton require the following nutrients for growth; carbon, nitrogen, phosphorus, silicon, metal, and trace elements (Paerl and Justić, 2011). Kaiser *et al.* (2011) found that nitrogen (nitrite, nitrate, and ammonia) and phosphorus most frequently limit phytoplankton growth in the sea and silicon is also important for diatoms and silica-scaled *Prymnesiophytes.* In general, nitrate is the major source of nitrogen utilized by phytoplankton. In estuarine ecosystems, nitrogen is usually the limiting nutrient in the lower estuary near the sea, while phosphorus can be the limiting nutrient in the upper low salinity region of the estuary (Mann, 2000). Nitrogen and phosphate are most significant nutrients because they are in shortly supply relative to demand (Gaulke *et al.*, 2010). Nutrient concentration is higher in the upper estuary due to nutrients from the freshwater riverine discharge. Nedwell and Raffaelli (1999) point out that nutrient fluxes through estuaries to coastal waters are controlled by freshwater input from land, plant production, and tidal flow. Supporting this statement, Statham (2012) demonstrated nutrient behaviour in estuarine systems (see Figure 1-1) could be understood through knowledge of the underlying hydrodynamics and biogeochemical processes within these estuaries. As a result, the increasing nutrient levels in temperate estuaries can change the structure of phytoplankton community and primary productivity in the estuarine ecosystems.

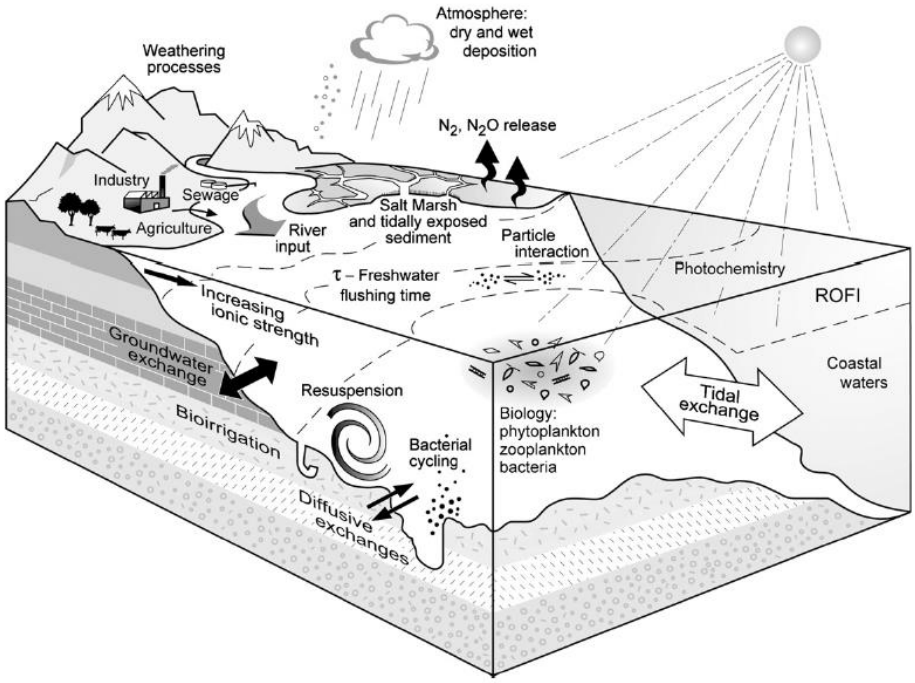


Figure 1-1: Processes and exchanges influencing the macronutrients Si, P and N in estuarine systems, ROFI = Region of Freshwater Influence (From Statham, 2012).

### 1.3.2 Light

Light is essentially important in controlling phytoplankton productivity and nutrient uptake in turbid coastal ecosystems (Lancelot and Muylaert, 2011; Paerl and Justić, 2011). In aquatic environments, particularly lakes and estuaries, the amount of light incident on the surface is rapidly decreased with depth by an exponential function. Light intensity is controlled largely by variations in the concentration of suspended material in the estuary and a threshold daily light input is needed before phytoplankton growth can commence in temperate regions (Paerl and Justić, 2011). The presence of suspended sediment does not directly affect the phytoplankton community, but indirectly affects the light intensity in the water column and thus microalgal growth rates. Some authors have found pico-phytoplankton productivity and biomass in North Carolina's Neuse River Estuary, USA were maximal in summer due to high suspended sediments (Gaulke *et al.*, 2010) and a clear seasonal pattern to the production of the pico-phytoplankton appears to be closely linked to turbidity variations. Turbidity in estuaries may be caused by suspended sediments, coloured dissolved organic matter content, and chlorophyll and other phytoplankton pigments (Paerl and Justić, 2011). Ferreira *et al.* (2011) demonstrated that estuarine turbidity not only dominates phytoplankton growth but also regulates the

community composition, with diatoms better adapted to the turbid conditions in many estuaries. As a result, light availability plays an important role in influencing the activity, biomass, distribution, and composition of phytoplankton in temperate estuaries due to turbidity limiting the penetration of light into the water column.

### 1.3.3 Water residence time/tide

A considerable amount of literature has been published on the effect of tidal movement and water residence time on phytoplankton growth in estuaries (Iriarte and Purdie, 1994; Trigueros and Orive, 2001; Monsen *et al.*, 2002; Maier *et al.*, 2012). Residence time is mainly dependent on river flow, although tidal movement and volume of the estuary are also factors (Dyer, 1997) and it is strong determinants of where the maximum importance of phytoplankton biomass can develop and grow in response to nutrient inputs within the estuaries (Paerl and Justić, 2011). Surveys such as that conducted by Trigueros and Orive (2001) have showed that the development of phytoplankton blooms in the Urdaibai Estuary, Spain is influenced by the water residence time. In temperate estuaries, the residence time is primarily influenced by river discharge and varies strongly over different seasons affecting development of phytoplankton populations (Lancelot and Muylaert, 2011). The estuarine residence time can be formulated using several methods, however, the basic fraction of freshwater method takes into consideration the effect of river flow and salinity variation on its estimation (Dyer, 1997). Many studies have argued that the spring and neap tidal cycle can influence net phytoplankton growth as demonstrated in the Taw Estuary, England (Maier *et al.*, 2012) and San Francisco Bay Estuary (Kimmerer *et al.*, 2012). During the neap cycle, longer water residence times and reduced suspended sediment level lead to increased phytoplankton growth rates, whereas increased mixing during spring tides can correlate with increased diatom growth, for example in the Southampton Water estuary, due to reduced sinking rates of algal cells (Iriarte and Purdie, 1994). Moreover, Howarth *et al.* (2000) demonstrated that dissolved inorganic nutrients are high in concentration throughout the year within the Lower Hudson estuary, USA, but that phytoplankton blooms did not occur in-spite of an availability of nutrients. It is argued that this finding was due to the flushing rate in the estuary, by which phytoplankton community is transported out to the coastal water before their division rates enable the development of phytoplankton blooms.

### 1.3.4 Freshwater discharge/river flow

There are generally negative impacts on the estuarine phytoplankton community from freshwater discharges due to osmotic shock, flushing out of phytoplankton populations and increasing turbidity (McLusky and Elliott, 2004). The residence time in many estuaries is primarily influenced by river discharges (Lancelot and Muylaert, 2011). Freshwater input also directly alters the salinity and nutrient concentration in estuaries. In temperate regions, river discharge increases during winter and is generally reduced in summer. In estuarine systems, the beginning of the phytoplankton bloom in spring often occurs simultaneously with a reduction in river discharge (Lancelot and Muylaert, 2011) and therefore, the influence of freshwater discharge controls the spatial distribution of estuarine organisms (Levinton, 2011). In the Taw Estuary (SW England) and the Asan Bay (Korea), river flow rate was a physical control on diatom growth and primary production dynamics (Sin *et al.*, 2000; Maier *et al.*, 2012). Kimmerer *et al.* (2012) found that the effect of freshwater flow into the San Francisco Bay Estuary (USA) also had a strong influence on primary production in the estuary. In Chesapeake Bay it was found that chlorophyll *a* concentration showed a significantly positive correlation with river flow in spring and summer (Adolf *et al.*, 2006). In summary freshwater inputs and river flow have a significant influence on phytoplankton communities in estuarine systems with a particular impact on small shallow estuaries.

### 1.3.5 Salinity

Estuarine ecosystems include a combination of freshwater and marine organisms. Although the distribution of organisms within each estuary is not solely controlled by salinity, this environmental factor is considered to be the most important in affecting the survival, growth and distribution of estuarine organisms (Kaiser *et al.*, 2011). Freshwater phytoplankton species experience large salinity changes during downstream transport in the estuary (Lancelot and Muylaert, 2011).Temporal variations of salinity in estuaries are influenced by seasonal changes due to freshwater discharge. Kimmerer *et al.* (2012) measured phytoplankton biomass and productivity in the San Francisco Estuary which has variable salinity but found no persistent patterns and only infrequent phytoplankton blooms. Therefore, organisms in the mid-estuary are affected by gradients in salinity moving between freshwater and marine waters as shown in the Remane diagram as shown in Figure 1-2 (Attrill and Rundle, 2002).

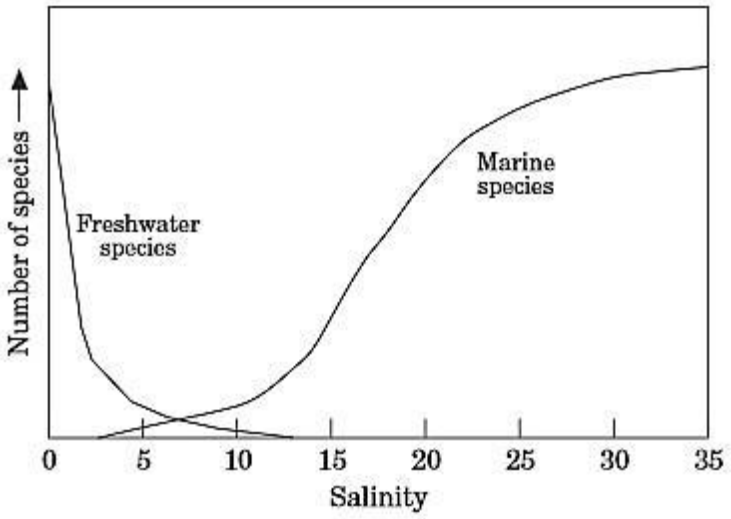


Figure 1-2: The Remane diagram with number of species plotted versus estuarine salinity gradient redrawn by Attrill and Rundle (2002).

### 1.3.6 Temperature

Phytoplankton growth rate is generally a function of water temperature assuming other factors such as light and nutrients are non-limiting. In temperate estuaries, the temperature normally limits plant growth in winter periods. Several previous studies have shown that during mid-summer, phytoplankton blooms appeared in estuaries (Eppley, 1972; Lancelot and Muylaert, 2011; Paerl and Justić, 2011). In summer, river flows are minimal and water temperature and surface light levels are high, therefore, phytoplankton growth rates are maximized during this productive period providing sufficient nutrients are available.

### 1.3.7 Top-down control

Top-down control of phytoplankton in estuary includes grazing by pelagic organisms (e.g. meso-zooplankton and micro-zooplankton) and benthic feeders (Lancelot and Muylaert, 2011). Zooplankton grazing control directly influences phytoplankton biomass when grazing rates are high in estuarine habitats (Griffin and Rippingale, 2001). Lionard *et al.* (2005) have reported that in the Schelde Estuary (Belgium/The Netherlands), microzooplankton had a significant controlling influence on the standing crops of phytoplankton in this shallow temperate estuary. Moreover, grazing by zooplankton in spring and summer was negatively associated with phytoplankton standing stock in the Pearl River Estuary, China (Tan *et al.*, 2004). Although phytoplankton is important as a food source for mesozooplankton in estuaries, including turbid estuaries (Kimmerer *et al.*,

1998), the top-down control of mesozooplankton on phytoplankton in estuaries is generally low compared to other aquatic systems (White and Roman, 1992). In some estuaries, benthic filter-feeders may be important grazers of phytoplankton (Lucas *et al.*, 1998), e.g. biomass of benthic bivalves is negatively correlated with chlorophyll *a* concentrations in Danish estuaries (Conley *et al.*, 2000). In addition, biological interactions, such as viral and bacterial infections can affect phytoplankton production and growth for example as seen in the San Francisco Bay (Cloern, 1996). However, McLusky and Elliott (2004) suggested that total primary production will not change due to grazing directly, but that nutrient concentrations and phytoplankton species composition will change under this influence. Phytoplankton can also be lost from the water column in estuaries by sedimentation or removed by flushing of cells during increased freshwater inputs from rivers or during large spring tidal exchanges.

## 1.4 Previous studies of phytoplankton in shallow temperate estuaries

Several previous studies of small and medium sized shallow temperate estuaries, including the Uradaibai Estuary (north Spain), the upper tidal Scheldt Estuary (Belgium), and Canal de Mira and North Carolina's Neuse River Estuary (USA) have described the dependence of phytoplankton growth on river flow and thus residence times (Trigueros and Orive, 2001; Lionard *et al.*, 2008; Gaulke *et al.*, 2010). In the Taw estuary (southwest England), researchers showed that phytoplankton biomass increased during low river flow and neap tides (Maier *et al.*, 2012). Similar patterns were observed in the Southampton Water Estuary (Crawford *et al.*, 1997) and the Guadiana Estuary, southwest Iberia (Domingues *et al.*, 2010). It is argued that during neap tides, water residence times are longer, leading to enhanced primary production. In contrast, diatom production was enhanced during spring tides in the Solent (England) and Ria de Aveiro Estuary (western Portugal) probably due to a reduction in phytoplankton sinking rates (Iriarte and Purdie, 1994; Resende *et al.*, 2005).

Many researchers studying different temperate estuaries have appeared to reach widely different conclusions regarding the controls upon phytoplankton growth and primary production. There are a large number of potential interactions between the key variables, such as temperature, light, residence time, nutrients, salinity, freshwater discharge, and zooplankton grazing, influencing the rate of phytoplankton growth in these dynamic systems. Therefore, phytoplankton growth and primary production would be predicted to show a rise along the increasing nutrient concentrations in estuaries, either because of a parallel increase along salinity gradient, or because of a decrease in sedimentary particles.

Some shallow temperate estuaries have been well researched over many decades, in part because algal bloom events are thought to be a symptom of eutrophication driven by human activities in the watershed. Most of this research has focused on phytoplankton community and water quality issues. Many questions still remain about what factors control phytoplankton biomass in temperate estuaries particularly in shallow systems. There is little evidence on what is influencing phytoplankton growth and primary production in shallow temperate microtidal estuaries like Christchurch Harbour. Understanding of the processes influencing the interactions between chemical and physical factors on phytoplankton growth and primary production in shallow temperate estuaries due to recent environmental change, such as influence of storm events for example, is still needed.

## 1.5 Christchurch Harbour and Hampshire Rivers

The Christchurch Harbour estuary is a small, shallow natural harbour in the southern part of the United Kingdom situated between Poole Bay and the Solent. This estuary has approximately an area of 2.39 $km^2$ and receives direct discharges of macronutrients from principally two rivers, the Hampshire Avon River and the Stour River, with a total catchment area of 2779 $km^2$ (Nedwell *et al.*, 2002). The two rivers combine south of Christchurch Priory and then discharge freshwater into the western end of the harbour. The combined waters of both rivers in the northwest Christchurch Harbour flow through a channel into the harbour and then towards the mouth (Murray, 1966). The harbour has extensive intertidal mudflats and saltmarshes (Murray, 1966) and is generally shallow with a depth of less than 2 m (Chart Datum) except in river and tidal channels (Gao and Collins, 1994). It is a micro-tidal and semi-diurnal estuary with a unique high tide system due to the tidal harmonics of the English Channel (Haskoning, 2009). The mean spring and neap tidal range at the mouth of Christchurch Harbour are only 1.4 m and 0.8 m, respectively (Gao and Collins, 1994). The residence time of the harbour is estimated to be 2.7 days during the spring (Thompson, personal con.).

There is little available chemical and biological data on the eutrophic status of the estuary and also little information on the dominant phytoplankton species present or of the presence of any toxic species in the estuary. Chlorophyll *a* concentrations have been measured by the Environment Agency and have been reported to reach over 50 $\mu g\ L^{-1}$, however, data on phytoplankton blooms occurring in this estuary is rare. Thus, monitoring of the changes of phytoplankton species and phytoplankton production rates as well as

measurements of macronutrient concentrations over the biologically productive seasons are needed for this economically important estuary.

## 1.6 Research questions

Our understanding of the interaction between the chemical environment and phytoplankton populations in shallow temperate estuarine environments is still limited. Christchurch Harbour provides such an estuarine environment, which has not been well studied in the past. The Macronutrient Cycles programme (MNC) on Christchurch Harbour provided an excellent environment to study phytoplankton population changes and associated chemical conditions (see Section 1.5). What drives annual variations in phytoplankton productivity (up to 50 µg $L^{-1}$, Environment Agency unpublished data) needs to be better understood, and the intensive fieldwork of the MNC provides a very good data resource for this phytoplankton study.

The following specific questions are addressed in the thesis:

- Do nutrient concentrations control estuarine phytoplankton growth in the Christchurch Harbour estuary?
- Does phytoplankton abundance present a clear annual pattern related to seasonal variations in both the lower Hampshire Avon and Stour rivers and the estuary?
- What are the dominant phytoplankton species present in the estuary?
- Do toxic phytoplankton occur in this estuary?
- How does the spatial distribution of phytoplankton change in the estuary?
- What are the most important factors controlling the phytoplankton growth in the estuary?

## 1.7 Aim of the thesis

This thesis has the overall aim of 'Identifying the factors controlling the phytoplankton community and primary production in the shallow temperate estuary Christchurch Harbour and the two river systems flowing into the estuary'.

The main objectives of the research are as follows:

- To monitor the annual changes in riverine phytoplankton in the lower Hampshire Avon and Stour Rivers in terms of species composition and cell size. This study

takes into account the whole phytoplankton community, in terms of its carbon biomass, accessory pigments and also in relation to the chlorophyll, size fractionated chlorophyll, and photosynthetic efficiency of phytoplankton.

- To determine the response of the estuarine phytoplankton community to changes in the macronutrient inputs to the Christchurch Harbour estuary.
- To relate variations in the lower rivers and estuarine phytoplankton community structure to environmental factors especially nutrients and river flow rate.
- To apply the CytoSense flow cytometer as a tool for measuring *in vivo* riverine and estuarine phytoplankton abundance and compare estimates of cell abundance from both the CytoSense and microscopic techniques.
- To evaluate the changes in phytoplankton uptake rates of nitrate and ammonium using stable isotope incubations conducted over the productive period at fortnightly intervals along a transect of the estuary.

## 1.8 Plan of the thesis

- Chapter 1 includes a review of temperate estuaries and their phytoplankton community, as well as the factors influencing estuarine phytoplankton growth. In addition a description of the study area and the main aim and objectives of this study are described.
- Chapter 2 includes a description of methods and details of sampling strategy conducted during an annual sampling period of both rivers and the estuary. The statistical analysis applied to calculate and determine the correlation of phytoplankton and environmental factors controlling phytoplankton growth is described.
- Chapter 3 includes a description of the phytoplankton community and pigments sampled on a weekly basis between April 2013 and April 2014 at the lowest river gauging stations on the Stour and Hampshire Avon Rivers. A range of environmental parameters were also measured to determine factors that influence phytoplankton populations in the rivers.
- Chapter 4 includes a description of the phytoplankton community and pigments plus a range of environmental parameters sampled on weekly basis between April 2013 and April 2014 at the entrance to the Christchurch Harbour estuary at Mudeford Quay at low tide.

- Chapter 5 presents the distribution of phytoplankton species, nutrient uptake and carbon production rates determined during eight two weekly transects along the Christchurch Harbour estuary from May to September in 2014.
- Chapter 6 includes a summary of the main results and conclusions of the research plus suggestions for further study.

# Chapter 2: Methods

## 2.1 Station locations and sampling

### 2.1.1 Spot sampling April 2013 – 2014

Four study sites were selected based on the local Environment Agency monitoring stations and the geo-hydromorphogical characteristics for each river section as shown in Figure 2-1 and Figure 2-2. Dates on which spot samples were collected at low tide from those sampling sites between 16th April 2013 and 10th April 2014 are shown in Appendix A.

#### 2.1.1.1 Christchurch Harbour Estuary at Mudeford Quay

The sampling position at the estuary entrance was at Mudeford Quay (50º 43' 4133 N, 1º 44' 5378 W) situated on the narrow channel known as the "Run" shown in Figure 2-1 A. To the west of the Run, where the estuary exchanges with coastal water of Christchurch Bay, there are two important sandbanks (Murray, 1966). Samples were collected at low tide at Mudeford Quay at weekly intervals from 16th April 2013 to 10th April 2014.

#### 2.1.1.2 Stour River at Throop and Iford Bridge

The Stour River enters Christchurch Harbour from the North West (see Figure 2-1). The river has a catchment area of 1073 $km^2$ based on tertiary deposits that includes clay (Murray, 1966; Nedwell *et al.*, 2002). Water samples were collected at Throop (Figure 2-1 D) which is also the lowest gauging station of the Environmental Agency (50º 45' 8290 N, 1º 50' 5158 W) on the Stour at weekly intervals from 16th April 2013 until 10th April 2014. Samples were additionally collected at Iford Bridge (50º 44' 4708 N, 1º 48' 3914 W) on the Stour which is downstream of Throop and just above the tidal limit of that branch of the estuary as shown in Figure 2-1 C. This position was chosen as it is directly downstream of the main sewage input from Holdenhurst Sewage Works. Samples were collected from Iford Bridge at weekly intervals from 6th June 2013 until 10th April 2014.

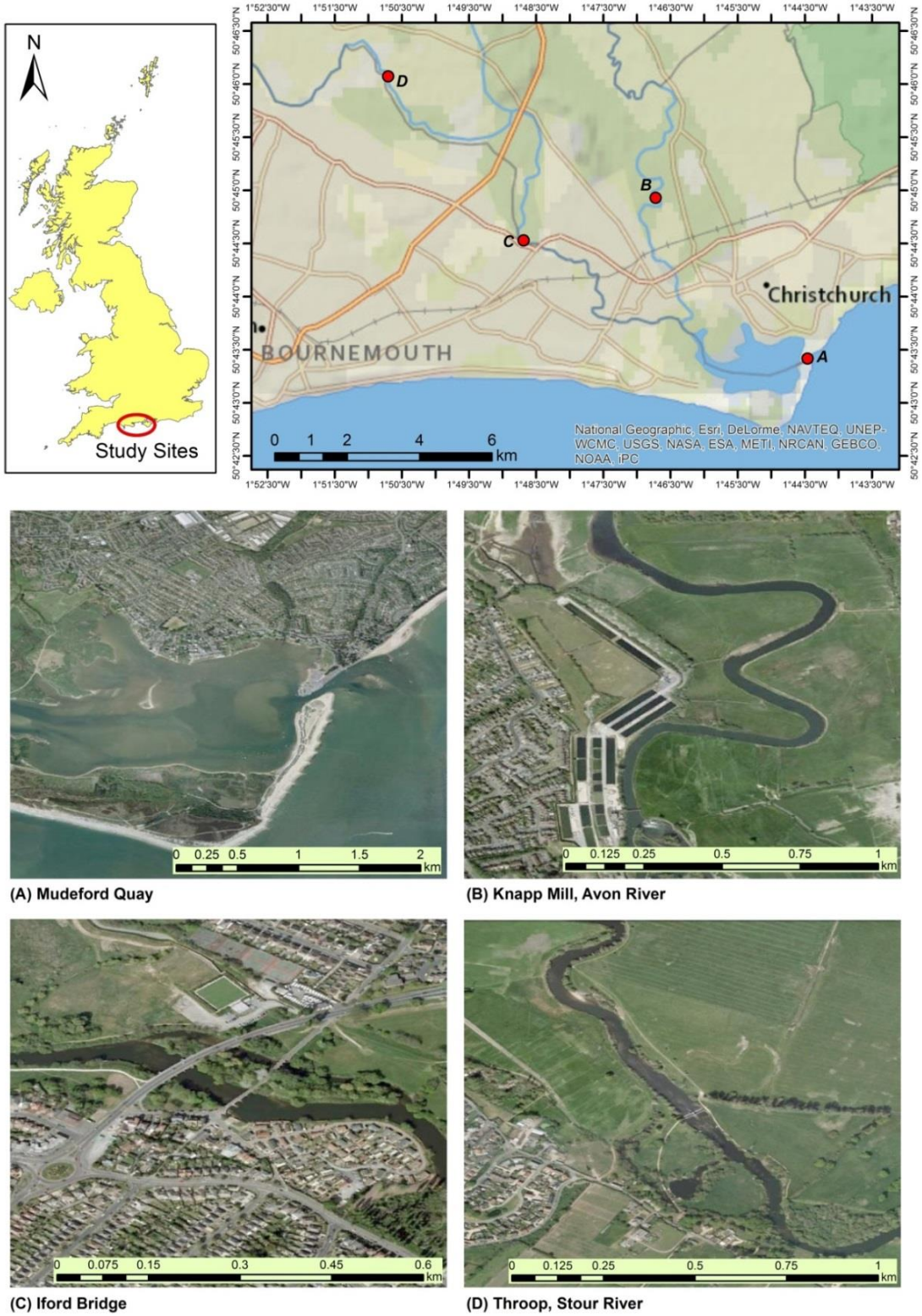


Figure 2-1: Map of Christchurch Harbour (A) and the lower reaches of the Hampshire Avon (B) and Stour rivers (C and D) showing four sampling sites.

### 2.1.1.3 Hampshire Avon River at Knapp Mill

The Hampshire Avon River enters the estuary from the north. The catchment area of the river is 1706 $km^2$ mainly on Chalk and derived from Chalk springs (Murray, 1966; Nedwell *et al.*, 2002; Heywood and Walling, 2003; Jarvie *et al.*, 2005b). In 2005, Jarvie *et al.* (2005a) reported the land use of the catchment area of Knapp Mill as 38.9% grazing land, 3.4% arable, 12% lowland pasture, 7.5% settlement and 1% urban. Water samples were collected at weekly intervals from 16th April 2013 until 10th April 2014 from immediately adjacent to the Environment Agency water gauging station at Knapp Mill (50º 44' 8852 N, 1º 46' 8119 W) which is within the Bournemouth Water SembCorp industrial site as shown in Figure 2-1 B.


Figure 2-2: Images of the four sites where water samples were collected during the Christchurch Harbour Macronutrients Project April 2013 – 2014.

### 2.1.2 Christchurch Harbour Estuary transect sampling in 2014

Water samples were collected during eight fortnightly transects of Christchurch Harbour at high tide from 27th May 2014 to 4th September 2014 using a small local boat (owned by Mr.Barry Childs). Six study sites were selected based on sampling positions previously used by the Environment Agency as show in Figure 2-3 and Figure 2-4 including; The Run

at Mudeford, Ferry Pontoon, Blackberry Point, Grimbury Marsh, Christchurch Quay, and Tuckton Bridge (see detail in Table 2-1).

Table 2-1: Study sites sampled during the Christchurch Harbour estuary transects in 2014. The distance in kilometres is from the estuary mouth.

| Study site | Position | Distance (km) |
|---|---|---|
| Run at Mudeford (RM) | 50º 43' 3995 N1º 44' 5548 W | 0.0 |
| Ferry Pontoon (FP) | 50º 43' 1961 N1º 44' 6223 W | 0.4 |
| Blackberry Point (BP) | 50º 43' 3465 N1º 45' 5715 W | 1.6 |
| Grimbury Marsh (GM) | 50º 43' 6581 N1º 46' 1374 W | 2.5 |
| Christchurch Quay (CQ) | 50º 43' 7940 N1º 46' 8870 W | 3.5 |
| Tuckton Bridge (TB) | 50º 43' 7794 N1º 47' 2560 W | 4.0 |

## 2.2 Water column measurements

During the weekly spot water sampling visits to each of the four sites, vertical profiles of water column properties were measured using initially a YSI 6600 (25th April to 14th August 2013) then later a EXO2 multi-parameter sonde (20th August 2013 to 10th April 2014) for temperature (ºC), conductivity (mS $cm^{-1}$), salinity (at Mudeford Quay), pH, turbidity (NTU), chlorophyll *a* (µg $L^{-1}$), oxygen saturation (%), dissolved oxygen (mg $L^{-1}$), and depth (m). The probes were rinsed with freshwater after each measurement and the data from the probe imported into Excel.

During the estuary transect sampling in 2014 the YSI 6600 was deployed to provide vertical profiles of environmental parameters at 0.5 m depth intervals at each station along the Christchurch Harbour estuary as shown in Figure 2-3. Water column profiles of photosynthetically available radiation (PAR unit, µmols $m^{-2}$ $s^{-1}$) were recorded at each site using a Li-COR LI-1400 data logger with both surface and depth light sensors. The data were recorded simultaneously from both the surface sensors ($E_0$) and the submerged depth sensor at 0.2, 0.5, 1.0, 1.5 up to 2.0 metres below the water surface ($E_d$) dependant on the maximum depth at each station. Values of the vertical diffuse attenuation coefficient, *k* ($m^{-1}$), were determined from the regression of loge ($E_d/E_0$) against depth.

Surface water samples for later laboratory analyses were collected from each of the four sites during the spot sampling using a clean white bucket then poured into twice rinsed clean 5-litre plastic bottles. During the estuary transect sampling a 5 litre Niskin water

sampler was used with the aim of collecting a single water sample from each of the six sites at the depth where chlorophyll concentration (detected by the YSI 6600 fluorometer) was maximum. The sample bottles were placed in a dark cool box with ice packs and taken back to the laboratory for further processing.

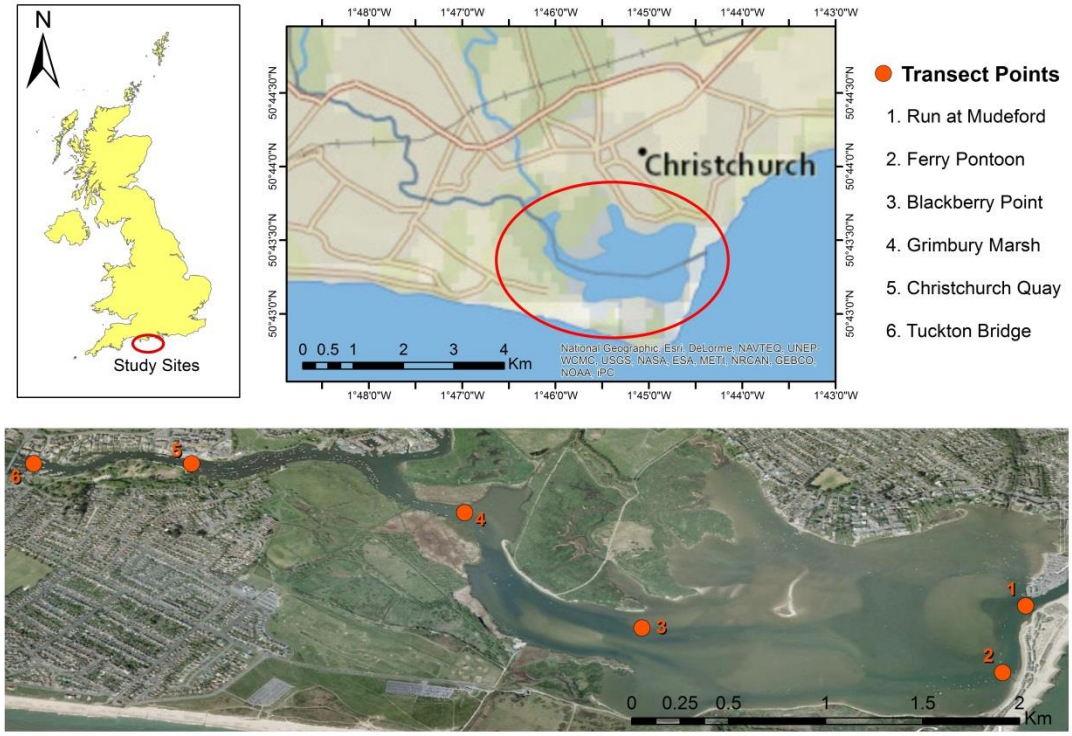


Figure 2-3: Map of Christchurch Harbour showing the six sampling sites along the estuary transects.

## 2.3 Suspended particulate matter (SPM)

The SPM data in this thesis was provided by Dr.Charlie Thompson (University of Southampton, National Oceanography Centre) under the NERC Christchurch Harbour Macronutrients Cycles Project. The SPM concentration in the water samples collected from each site was determined by filtering 50 – 550 mL of water through pre-weighed and dried 25 mm Fisherbrand$^{TM}$ GF/F filters (pore size 0.7 µm) in triplicate. The filtered samples were dried overnight at 80 ºC and then re-weighed. The concentration of SPM was calculated using the following equation:

SPM concentration (g $L^{-1}$) = ($W_2$ – $W_1$) / V

Where $W_1$ = Pre-weight of GF/F filter after drying (in grams)

$W_2$ = Post-weight of sample plus filter after drying (in grams)

V = Volume of water filtered in litres


Figure 2-4: Images of the six sites of the Christchurch Estuary transect sampling during 2014.

## 2.4 Pigment measurements

### 2.4.1 Chlorophyll *a* by fluorescence

Chlorophyll *a* concentration in the collected water samples was determined by measurement of fluorescence, according to the method of Parsons *et al.* (1984). 50 mL of

water was filtered in triplicate through 25 mm Fisherbrand$^{TM}$ GF/F filters using a syringe attached to an inline filter holder. The filters were folded in half and placed in a sealable plastic bag, labelled and stored in a -80 ºC freezer until further processing.

To measure chlorophyll *a* concentration, each filter was placed in a 15 mL plastic centrifuge tube and 7 mL of 90% (v/v) acetone added and shaken gently to extract the pigments. Preparation of chlorophyll extracts was conducted under subdued light. All samples were immediately sonicated for 30 seconds using a Vibracell sonicator to disrupt phytoplankton cells. The samples were then centrifuged in a Mistral 2000 centrifuge at 1500 rpm for 10 minutes at room temperature to remove filter debris and then the fluorescence of each extracted sample measured in a Turner Designs Model 10-AU Series fluorometer fitted with a F4T41/2B2 lamp, a 436 nm excitation filter and a 680 nm emission filter.

90% acetone was used as a blank and a standard solution of chlorophyll *a* (Sigma) in 90% acetone was used to calibrate the fluorometer before each set of measurements. The concentration of chlorophyll *a* (µg $L^{-1}$) was calculated using the following equation:

Chlorophyll *a* concentration (µg $L^{-1}$) = $C \times (v/V)$

Where C = concentration of chlorophyll in extract (in µg $L^{-1}$)

v = volume of acetone extract in mL

V = volume of seawater filtered in litres

The Turner fluorometer was regularly calibrated using dilutions of a standard chlorophyll *a* solution (Sigma Chemical Co.) in 90% acetone. The concentration of the chlorophyll standard was determined by spectrophotometry using the equation given by Jeffrey and Humphrey (1975). 90% acetone was placed into clean 1 cm path length glass cuvettes and placed in the sample holder of a Cecil spectrophotometer. The absorbance was then measured at each of 750, 664, 647, and 630 nm wavelengths to check the two cuvettes were matched. A standard solution of chlorophyll was then added to the second cuvette and wavelength adjusted to 750 nm. The absorbance measurement of the chlorophyll standard was determined at wavelengths of 664, 647, and 630 nm zeroing the instrument on the 90% acetone cuvette each time.

The absorbance value at each wavelength was used to calculate the concentration of chlorophyll in the standard following the equation:

Chlorophyll *a* concentration (mg $L^{-1}$ or µg $mL^{-1}$) = $(11.85 \times Ab_{664}) - (1.54 \times Ab_{647}) - (0.08 \times Ab_{630})$

Where $Ab_{664}$ = absorbance value at 664 nm

$Ab_{647}$ = absorbance value at 647 nm

$Ab_{630}$ = absorbance value at 630 nm

### 2.4.2 Size fractionated chlorophyll *a* by fluorescence

Size fractionated chlorophyll *a* concentration was measured by fluorescence using the method of Parsons *et al.* (1984) as described above. Chlorophyll *a* was size fractionated by initially passing 250 mL of water through 47 mm diameter nylon mesh filters with pore size of 20 µm filtered under gravity in triplicate. The filtrate was then passed through a sequence of 47 mm polycarbonate filters with pore size of 2.0 and 0.2 µm under gentle vacuum in triplicate. Chlorophyll *a* on the 20 µm net filters represents chlorophyll *a* concentration in micro-phytoplankton size fraction (> 20 µm), while chlorophyll *a* in nano-phytoplankton size fraction was determined in 2.0 – 20.0 µm size and pico-phytoplankton size fraction in < 2.0 µm size, respectively (Sieburth *et al.*, 1978). The filters were placed in a sealable plastic bag, labelled and stored in a -80 ºC freezer prior to extraction as described in Section 2.4.1.

### 2.4.3 High Performance Liquid Chromatography (HPLC) of phytoplankton pigments

Between 500 and 2000 mL of water was filtered through a 47 mm GF/F (Whatman) glass fibre filter on the day of sampling, giving triplicate samples from each station (except the Iford Bridge site), for later phytoplankton pigment analysis. The filters were stored at -80 ºC to prevent degradation prior to laboratory analysis. The pigments were subsequently extracted from each filter by placing them into 9 mL of HPLC grade 90% acetone in a 15 mL cooled centrifuge tube. The extracts were placed in a -80 ºC freezer for 10 – 20 minutes and then sonicated for 30 seconds using a Vibracell probe in order to break up the cells. Following the extraction the tube was centrifuged using a MSE Mistral at 4000 rpm for 10 minutes to remove cellular and filter debris. The tube was placed in a cool box with ice packs to prevent it warming during processing. The extracts were syringe filtered through a 0.2 µm 10 mm diameter nylon filter and then 1 mL of the extract was transferred

into a small brown glass vial, closed with a cap and placed in the sample tray for high performance liquid chromatography analysis in the HPLC auto-sampler. An aliquot of 500 µL of extract was mixed with 500 µL of 1M ammonium acetate and then 100 µL of the mixture was injected onto the HPLC column.

HPLC was used to analyse the pigments of collected samples as described by Gibb *et al.* (2001) and Barlow *et al.* (1997). A Perkin Elmer column was used to analyse all samples from this study. The system used was a Thermo Finigan HPLC with P2000 dual solvent pump, vacuum degasser, AS3000 auto-sampler, UV 6000LP detector, FL3000 fluorescence detector, and SN4000 system controller. The mobile phase consisted of a binary system using solvent A: 30% 1M ammonium acetate buffer and 70% methanol, solvent B: 100% methanol, solvent C: 1M ammonium acetate and methanol flush bottle. All reagents used were HPLC grade.

The pigments were identified by comparison to known system retention times for authentic pigment standards: chlorophyll *a*, chlorophyll *b* and β carotene were obtained from Sigma Chemical Company. The others pigments including chlorophyll *c3*, chlorophyll *c2*, peridinin, 19'Butanoyloxyfucoxanthin, fucoxanthin, 19'Hexanoyloxyfucoxanthin, violaxanthin, prasinoxanthin, diadinoxanthin, alloxanthin, zeaxanthin, lutein, chlorophyll *b*, divinyl chlorophyll *a*, chlorophyll *a*, and β carotene were previously obtained from DHI, Denmark. The Chromquest software on a Dell 1100 computer was used for data collection and integration. All data was compared with those of pure standards obtained from DHI, Denmark. Table 2-1 lists the major pigments present in phytoplankton groups and according to Jeffrey and Vesk (1997) and Paerl *et al.* (2003) and can be used as a guide to taxonomic identification of phytoplankton.

The concentration of each accessory pigment (Pc, µg $L^{-1}$), calculated using the following equation (Barlow *et al.*, 1993), allows for the chemo-taxonomical classification of phytoplankton communities:

$$Pc = \frac{Pa \times Ve \times 1000}{Pr \times Vi \times Vf \times 0.5}$$

Where Pa = the peak area at wavelength 440 nm

Ve = the volume of extracted 90% acetone in mL

Pr = the response factor of each pigment

Vi = the volume injected in the column (100 µL)

Vf = the volume of filtered sample in litres

0.5 = the buffer dilution factor

Table 2-2: Pigments found in selected taxonomic phytoplankton groups according to Jeffrey and Vesk (1997) and Paerl *et al.* (2003).

| **Pigments** | **Abbreviations** | **Designation** |
|---|---|---|
| Chlorophyll *c3* | Chl *c3* | Prymnesiophytes, Chrysophytes, Dinoflagellates, Diatoms |
| Chlorophyll *c2* | Chl *c2* | Most diatoms, Dinoflagellates, Prymnesiophytes, Cryptophytes |
| Peridinin | Per | Dinoflagellates |
| 19'Butanoyloxyfucoxanthin | 19'But | Some prymnesiophytes, Dinoflagellates |
| Fucoxanthin | Fuco | Diatoms, Prymnesiophytes, Chrysophytes, Several dinoflagellates |
| 19'Hexanoyloxyfucoxanthin | 19'Hex | Prymnesiophytes, Several dinoflagellates |
| Violaxanthin | Vio | Chlorophytes, Prasinophytes |
| Prasinoxanthin | Pra | Some prasinophytes |
| Diadinoxanthin | Dia | Diatoms, Dinoflagellates, Prymnesiophytes, Chrysophytes |
| Alloxanthin | Allo | Cryptophytes |
| Zeaxanthin | Zea | Cyanophytes, Prochlorophytes, Chlorophytes |
| Lutein | Lut | Chlorophytes, Prasinophytes |
| Chlorophyll *b* | Chl *b* | Chlorophytes, Prasinophytes, Euglenophytes |
| Divinyl chlorophyll *a* | DV Chl *a* | Prochlorophytes |
| Chlorophyll *a* | Chl *a* | All microalgae (except prochlorophytes) |
| β carotene | β car | All groups |

## 2.5 Phytoplankton microscope counts

Duplicate 100 mL screw topped water samples for phytoplankton identification and enumeration were placed in brown glass bottles and 1 mL of acidic Lugol's solution added. The samples were kept in a dark cupboard at room temperature for later analysis of cell counts and species identification.

Each Lugol's preserved sample was gently mixed and then a 10 mL subsample transferred to a 10 mL sedimentation chamber using a 10 mL automatic pipette. The chambers were

covered with a glass plate and left to settle for at least 24 hours before placing on a Leitz Fluovert inverted microscope to allow cells to be counted and identified according to the Utermöhl method (UNESCO, 2010). Tomas (1997); Belcher and Swale (1979); Round *et al.* (2007), and Kraberg *et al.* (2010) were used for identification of riverine and estuarine phytoplankton.

The whole base of the sedimentation chamber was initially viewed by transects under magnification of ×100. Cells were also counted on two cross diameters of the chambers under ×400 magnification (2 × 24 mm diameter × 0.43 mm wide field of view).

(diameter of chamber × width of field of view) × number of transects = Transect area

(1)

$$\text{Chamber area} = \pi\left(\frac{Diameter}{2}\right)^2$$

(2)

$$\frac{Chamber\ area}{Transected\ area} = \text{A}$$

(3)

Cells counted × A = cells in 10 mL

(4)

The calculations below were used to extrapolate the number of cells counted to the number of cells per mL. The equation uses the diameter of the chamber (24 mm), width of field of view (0.43 mm), number of transects (2), and volume of sample (10 mL)

$$\frac{(24 \times 0.43)\times 2}{\pi(\frac{24}{2})^2}$$

(5)

$$\frac{cells\ counted \times 23.45}{10} = cells\ per\ mL$$

(6)

## 2.6 Scanning electron microscope

20 – 50 mL of Lugol's sample was gently filtered onto a 25 mm diameter 0.8 µm pore size polycarbonate filter using a syringe filter unit to avoid damaging the phytoplankton cells. The filters were dried at 50 ºC overnight on a clean petri slide. Each filter was mounted on

an aluminium microscope stub with carbon tape and sputter coated with gold palladium before SEM examination.

## 2.7 Phytoplankton biomass estimation

The cell volume of each phytoplankton species was estimated using shape assimilation equivalent to known geometric forms and direct measurement of the main cellular dimensions of about 15 – 20 randomly selected individuals. Total cell volume was calculated by the addition of the bio-volume of each species present. Phytoplankton abundances were converted into cell volumes according to the different equivalent geometric shapes as describe by Hillebrand *et al.* (1999) and Sun and Liu (2003). Carbon biomass rather than cell number is considered a more appropriate estimate of phytoplankton composition as cell volume varies between species by several orders of magnitude. The carbon content of each species was calculated according to the carbon-to-volume relationships given by Menden-Deuer and Lessard (2000) using the following equations:

$$\text{pg C cell}^{-1} = 0.288 \times \text{volume}^{0.811} \quad (1)$$

$$\text{pg C cell}^{-1} = 0.216 \times \text{volume}^{0.939} \quad (2)$$

Where equation (1) is used for diatoms and equation (2) is for taxonomically diverse protists including dinoflagellates. The calculation of cell biomass is complicated because of cell shrinkage during preservation and due to intra-species variability in cell size (Montagnes *et al.*, 1994). Therefore, the carbon biomass estimates for individual phytoplankton species can only be considered as semi-quantitative. Within this study, the carbon volume of phytoplankton cells were also multiplied by 1.33 according to Montagnes *et al.* (1994) to allow for shrinkage of cells preserved in Lugol's solution.

## 2.8 Fluorescence Induction and Relaxation (FIRe)

The FIRe fluorometer system is a bench-top instrument manufactured by Satlantic Inc. The FIRe technique has been used to measure the photosynthetic characteristics of phytoplankton in many studies in freshwater and seawater (Suggett *et al.*, 2001; Kaiblinger and Dokulil, 2006). The initial fluorescence ($F_0$), the maximum fluorescence ($F_m$), and the maximum quantum efficiency of photosystem II (PSII) photochemistry were derived according to the biophysical equations of Kolber *et al.* (1998). The quantum efficiency of

PSII or the change in fluorescence was calculated from variable fluorescence ($F_v = F_m - F_0$, unit-less) normalised to $F_m$, indicating the proportion of functional PSII reaction centres (Geider *et al.*, 1993). The cross section of photosystem II (σPSII, $Å^2$ $quanta^{-1}$), is a measure of the size of the light-harvesting antenna system associated with the photochemical reaction centre PSII. Functional absorption cross-sections of σPSII are obtained from the rate at which fluorescence increases from $F_0$ to $F_m$. A Satlantic FIRe (Fluorescence Induction and Relaxation) system or Fire Fast Repetition Rate Fluorometry (Fire FRRF) was used to detect $F_v/F_m$ (variable fluorescence divided by the maximum fluorescence, a measure of photochemical efficiency of photosystem II, photochemical efficiency or normalised active fluorescence). $F_v/F_m$ is a measure of the efficiency of the conversion of light energy into photosynthesis (Kolber *et al.*, 1988).

Where: $F_v$ = variable fluorescence

$F_m$ = maximum fluorescence

Size fractionated water samples prepared for chlorophyll analysis as described above (see Section 2.4.2) were used for FIRe measurements. An unfiltered water sample plus filtrates (2 – 20 µm and 0.2 – 2 µm) for FIRe measurements were stored in a dark box prior to analysis. All samples were measured within 4 – 5 hours of collection. Milli-Q water was used as a blank and was analysed with the FIRe prior to each set of measurements according to Cullen and Davis (2003). Typically $F_v$ and $F_v/F_m$ values for Mili-Q blanks were <1.0 and <0.05 respectively. Each sample was placed in a clean glass cuvette attached to the FIRe light sensor to quantify the relative fraction of total chlorophyll associated with a certain size-group. The light projector provided 16 different light levels to the FIRe chamber. Data from the FIRe instrument were recorded and downloaded to a computer then analysed using MATLAB R2011a software. The photosynthetic parameters calculated from the FIRe profiles were based on the biophysical model of Kolber *et al.* (1988).

## 2.9 CytoSense flow cytometry

50 mL of discrete unfiltered water samples from the spot and estuary transect sampling was preserved with 1% final concentration of a 20% paraformaldehyde solution in a clean chemical reagent bottle. The fixed sample was stored in a laboratory fridge at -5 ºC for 20 minutes and then moved to a freezer at -80 ºC to prevent degradation prior to laboratory analysis. The frozen samples were subsequently defrosted in a dark cool box. The fixed

phytoplankton cells were analysed with a CytoSense Benchtop pulse-shape recording scanning flow cytometer (SFCM, Cytobouy b.v., The Netherlands), with a laser excitation wavelength of 488 nm, 20 mW. A range of sample volumes (50 – 100 µL) was initially analysed with the CytoSense to assess the optimal sample volume which was then set to 50 µL to process all collected samples. Individual cells were identified according to their different optical features: sideward angle scatter (SWS), forward scatter (FWS), red (FLR), orange (FLO), and yellow (FLY) fluorescence. Each cell flows through the laser beam (5 µm width) at a rate at 2 m $s^{-1}$. The CytoSense can analyse a wide size range of phytoplankton cells from 1 – 800 µm. Fluorescence beads of 3 µm (Cyto-Cal™) and 10 µm (Polybead®) in diameter were used before fully analysing the phytoplankton samples. Data recording was triggered on the red fluorescence signal at 15 mV for 5 – 10 minutes. A small magnetic stirrer was used to keep the fixed sample sufficiently mixed during analysis. CytoSense data was later analysed with the CytoClus© software.

Clusters of points on the cytograms were selected by taking into account the amplitude and the shape of the different optical signals. In addition to 5 average signal heights for forward scatter (FWS), sideward scatter (SWS), and for three fluorescence signals: red (FLR), orange (FLO), and yellow (FLY), some simple mathematical parameters were assigned to each signal shape: inertia fill factor, asymmetry, number of peaks, length, apparent size (Dubelaar *et al.*, 2004).

## 2.10 Nutrient uptake by stable isotope incubations

### 2.10.1 Incubation experiments and isotope analysis

Following each estuary transect survey during the summer months in 2014, a series of incubations were conducted in the laboratory to determine uptake rates of nutrients (nitrate and ammonium) and inorganic carbon by the natural estuarine phytoplankton populations. Water was divided into 2 sets of separate 500 mL polycarbonate bottles per station. To one 500 mL bottle 0.1 mL of a stock solution of 0.1µmol $L^{-1}$ of $^{15}$N-nitrate tracer ($K^{15}N$ 99 atom % $^{15}$N) was added and 0.1 mL of a 0.1 mmol $L^{-1}$ of $^{13}$C-carbon tracer ($NaH^{13}CO_3$ 98 atom % $^{13}$C) was added. To the other 500 mL bottle 0.1 mL of a stock solution 0.1 µmol $L^{-1}$ of $^{15}$N-ammonium tracer ($^{15}NH_4Cl$ 99 atom % $^{15}$N) was added. The incubated bottles were gently mixed after the tracer additions then incubated in a Mercian cooled incubator at incubation light level about 35 µmols $m^{-2}$ $s^{-1}$ for 4 hours generally starting between 13:00 – 14:15 hours (BST) at simulated *in situ* water temperature (15 to 20 ºC). All

incubations were terminated after 4 hours by filtration onto 25 mm pre-combusted (500 ºC, 4 hours) GF/F Whatman filters. 100 mL of incubated water was then filtered in duplicated at low vacuum (< 150 mm Hg). Filters were rinsed with pre-filterer estuarine water from the respective station to remove the excess tracer, and then stored frozen and in duplicate in clean labelled petri slides.

The filters were dried within the petri slides at 50 ºC for 24 hours. Each filter was cut in half and then packed into tin capsules (pressed, standard weight 8 × 5 mm). Isotopic composition and particulate nitrogen (PN) concentrations were determined using an Elemental Analyser Isotope Ratio Mass Spectrometry (EA-IRMS) at a commercial laboratory (Iso-Analytical Limited, Cheshire, UK).

### 2.10.2 Calculation of nitrogen and carbon uptake rates

The absolute nutrient uptake rates (ρ in μmol $L^{-1}$ $h^{-1}$) were calculated according to the equation in Dugdale and Wilkerson (1986), where the PON concentration is measured at the end of the incubation period. Uptake rates were not corrected for the effects of isotopic dilution as these are expected to be minimal during the 4 hour incubation used in this study (Harrison and Harris, 1986).

***Nitrogen uptake rate (nitrate and ammonium)***

$$\text{Nitrogen uptake rate } (\rho \text{ in } \mu\text{mol } L^{-1} h^{-1}) = [\text{PON}] \times \left(\frac{\text{PN}at\%}{\text{DIN}at\% \times t}\right):$$

Where: PON = the concentration of particulate organic nitrogen.

PN*at%* = the concentration of N label (atom % $^{15}N$) in each sample determined by mass spectrometry minus the natural isotopic abundance of $^{15}N$ (0.3663%)

DIN*at%* = the concentration of N label (atom % $^{15}N$) in the dissolved phase after 4 hours incubation.

t = incubation period (4 hours)

The calculation can be demonstrated with the following example. During a 4 hour incubation experiment a given volume of estuarine water sample was enriched to a concentration of 0.1 μmol $L^{-1}$ with $^{15}N$ enriched (99%) $K^{15}N$. The measured $NO_3^-$ concentration of the sample was 156.72 μmol $L^{-1}$. The concentration of PON collected by

filtration at the end of the incubation was 1.26 µmol $L^{-1}$ and was 0.3706% enriched with $^{15}N$ as determined by mass spectrometry. The calculation proceeded as follows,

$$\rho = 1.26 \times \left( \frac{0.3706 - 0.3663}{\left( \frac{(156.72 \times 0.3663) + (0.1 \times 99)}{156.72 + 0.1} - 0.3663 \right) \times 4} \right) = 0.02$$

The nitrate uptake rate in this example is 0.02 µmol-N $L^{-1}$ $h^{-1}$.

The ammonium uptake rate was calculated using a similar equation as the nitrate uptake rate.

***Carbon uptake rate***

The carbon uptake rate was calculated using the same equation used to calculate the nitrogen uptake rate. In this study the particulate organic carbon concentration [POC] of the sample collected by the filtration at the end of incubation replaced the [PON] in the equation above and the $^{13}C$ atom % enrichment, as determined by mass spectrometry, replaced PN*at%*. The $^{13}C$ atom % enrichment of the dissolved fraction in turn replaced the DIN*at%*. The natural abundance (atom percent) of $^{13}C$ used for this calculation was 1.092% (Bury *et al.*, 1995). The [DIC] was not directly measured in water collected from each site in the estuary but is usually conservative with salinity and shows a small range of [DIC] in most river domiated estuaries (Liu *et al.*, 2014). The concentration of total dissolved inorganic carbon [DIC] was estimated to be 2000 µmol $L^{-1}$ in calculating carbon fixation rates from all incubations (Stoll *et al.*, 2001; Ji *et al.*, 2009).

## 2.11 Nutrients

Nitrate, phosphate, and silicate concentration data presented in this report was provided by a team from the University of Portsmouth in the NERC Christchurch Harbour Macronutrients Cycles Project. Freshly collected water samples were filtered through 0.7 µm glass fibre filters into clean plastic vials and then 20 mL samples preserved with 5 µL per mL of sample of a 4 g $L^{-1}$ mercuric chloride solution ($HgCl_2$). Kirkwood (1992) recommended the addition of mercuric chloride to preserve an effective concentration of nitrate, phosphate, and silicate in water samples. All preserved samples were stored in a dark cupboard prior to analysis. All inorganic nutrients were determined using a QuAAtro segmented flow analysis system (Seal Analytical, UK) at the University of Portsmouth laboratory. Detection limits of nutrients were analysed as three times the standard deviation of measurements of 5 Milli-Q ultrapure water samples. Detection limits of

nitrate, phosphate, and silicate were 0.06, 0.01, and 0.05 µmol $L^{-1}$, respectively (Couceiro *et al.*, 2013).

## 2.12 Statistical method

Data analysis was undertaken using Excel 2010, Sigma Plot 12.5, PRIMER-E 7 (Plymouth Routines In Multivariate Ecological Research) and CANOCO 4.5 software (CANOCO, Microcomputer Power, Ithaca, NY). Excel was used to organise, display and complete simple data analyses tasks. Sigma Plot was applied to create graphs, including scatter, area, and line plots of environmental variables and stack plots of phytoplankton data. Parametric linear regressions were also performed using Sigma Plot statistical software. PRIMER-E was used for cluster analysis and non-metric multidimensional scaling (nMDS) to resolve the complexity of the phytoplankton community in terms of abundance, carbon biomass and pigment concentration, including environment variables. CANOCO software was used in this study to analyse the effect of environmental parameters on the phytoplankton species biomass and pigments.

***PRIMER software***

The principle of the multivariate techniques by the PRIMER-E programme used in this study included hierarchical clustering and a non-matric multidimensional scaling (nMDS). These were employed to attempt to reduce the complexity of the high dimensional phytoplankton community and environmental parameters by taking a low dimensional view of the structure it exhibits (Clarke and Warwick, 1994; Clarke *et al.*, 2014). The PRIMER-E version 7 was used to perform these analyses following the recommendations of Clarke *et al.* (2014).

*Phytoplankton carbon biomass and accessory pigments data*

The cluster analysis and the nMDS start from a triangular matrix of similarity coefficients computed between every pair of samples. The coefficient of similarity is a measure of how similar two samples are. The Bray-Curtis coefficient was used for the phytoplankton data (carbon biomass and accessory pigment), as it is a satisfactory coefficient for biological datasets on community structure (Clarke and Warwick, 1994; Clarke *et al.*, 2014). The Bray-Curtis coefficient reflects differences between two samples due both to differing community composition and differing total abundance.

Data transformation in community analysis is used to weight the contributions of common and rare species or concentrations in the non-parametric multivariate representations. It is acknowledged that the selection of which transformation to use can have a significant effect on the final ordination or clustering demonstration. The Christchurch Harbour estuary data were therefore the fourth-root transformed to down weight the importance of very abundant species/concentration so that the less dominant species/concentrations contributed something to the definition of similarity. The retention of some information on the prevalence of a species/concentration ensures that the common species/concentrations are generally given greater weight than the rare ones.

The cluster analysis is used to find natural grouping of samples such that samples within a group are more similar to each other than samples in different groups. It is appropriate for delineating groups with distinct community structure with different characteristic patterns of abundance found consistently in different groups (Clarke and Warwick, 1994; Clarke *et al.*, 2014). The outcome of a cluster analysis is represented by a dendrogram with the x axis defining the full set of samples and the y axis representing a similarity level at which two samples or groups are considered to have fused. For two different sample groups identified as the result of a cluster analysis, the species that primarily accounted for the observed assemblage difference were identified by a decomposition of the Bray-Curtis similarity into contributions from each species. The overall percentage contribution each species makes to the average dissimilarity between two groups is established and then the species are listed in decreasing order of their importance in discriminating the two sets of samples.

The nMDS aims to construct a configuration of the samples in a specified number of dimensions which attempt to satisfy all the conditions imposed by the rank similarity matrix (James and McCulloch, 1990; Clarke *et al.*, 2014). The nMDS plots can be arbitrary scaled, located, rotated or inverted as only relative similarity between samples can be interpreted. The nMDS diagram chooses a configuration of points which minimises this degree of stress. The combination of clustering and ordination analysis can be an effective way of checking the suitability and common consistency of both representations (Clarke *et al.*, 2014). The strength of the ordination is in displaying a gradation of community composition across a set of samples.

For each type of analysis, the similarity percentage analysis (SIMPER) was performed to calculate the percentage similarity of each sample group and the dissimilarity between each

pair of groups. Moreover, this analysis was used to identify the contributions from each taxon to the average overall similarity within group at similarity of 90% cumulative contribution. An analysis of similarities (one-way ANOSIM) was also applied to determine whether groups were statistically significantly different from each other in terms of their taxonomic composition.

A bubble plot was constructed in the nMDS plots to identify the associations between the peak of chlorophyll *a* events and some physical parameters. For this output, an average of chlorophyll *a* concentrations above 15 µg $L^{-1}$ for each group was applied to define a peak chlorophyll event at all study sites as undesirable Maier *et al.* (2009). A shade plot is an alternative to line plots undertaken with PRIMER-E. This plot displays in the form of the data matrix itself, with rows being species/concentrations and columns the samples and the entries rectangles whose grey shading deepens with high abundant species biomass/concentration. A white rectangle indicates absence of that species or biomass in that sample and full black represents the maximum abundance in the matrix (Clarke *et al.*, 2014).

*Environmental variables*

The environmental variables including, river flow, water temperature, oxygen saturation, suspended particulate matter, nitrate, phosphate, silicate concentration, irradiance attenuation coefficient (*k*), and turbidity were used as variables in the multivariate analysis. Irradiance attenuation coefficient (*k*) and turbidity data were not available for the multivariate analysis during the spot sampling in 2013 to 2014.

There are important differences between environmental variables and species or biomass data. Abiotic data are often on mixed measurement scales and the Bray-Curtis coefficient that assumes a common measurement scale is not relevant. Different transformations may be needed for different variables but in general it is preferable to use a common form of transformation for a variable of particular type (Clarke and Warwick, 1994).

Normalisation manages most effective when the environmental data are near as possible to normality. In general, the transformation is desirable to use a common form for a variable of a particular style and different transformation forms may be needed for different variables (Clarke *et al.*, 2014). Environmental variables of the Christchurch Harbour estuary data were log (x + 1) transformed.

Cluster and non-metric MDS analyses were performed using log transformed data and normalised Euclidean distances. The result of a cluster analysis is indicated by the dendrogram with the x axis defining the samples and the y axis indicating a Euclidean distance at which two samples or groups considered to have integrated. The nMDS plots can be an arbitrary distance between samples and choose a configuration of points which minimises the degree of stress as phytoplankton analysis.

For each type of analysis, the SIMPER analysis was used to calculate the average squared distance of each sample group and between each pair of groups. This analysis was indicated to identify the contributions from each environmental factor to the average overall similarity within group at similarity of 90% cumulative contribution using Euclidean distance.

***CANOCO software***

To assess interactions between environmental parameters and phytoplankton carbon biomass, a redundancy analysis (RDA) was carried out using the CANOCO 4.5 software package (Ter Braak and Šmilauer, 2002). This analysis determines the environmental variables (explanatory variables) that best explain the distribution of the main selected taxonomic groups, by selecting the linear combination of environmental variables that yields the smallest total residual sum of squares in the taxonomic data (Peterson *et al.*, 2007). Detrending canonical correspondence analysis (DCCA) was used *a priori* to determine whether the data ordination method was linear and suitable for RDA analysis or unimodal that is suitable for Caconical correspondence analysis (CCA). A relatively small gradient length (< 2.5 of standard deviation units according to DCCA analysis output) revealed that the ordination was linear-based and that the RDA analysis was suitable for the data (Lepš and Šmilauer, 2003). *A posteriori* analysis or forward-selection was used to identify a subset of environmental variables that significantly explained taxonomic distribution and community structure when analysed as single factor ($\lambda_1$, marginal effects) or included in the model where other forward-selected variables were analysed together ($\lambda_a$, conditional effects). Phytoplankton carbon biomass data were transformed by log (x+1) and Monte Carlo permutation test (n = 999), reduced model was applied to test the statistical significance ($P < 0.05$) of each of the forward-selected variables considered in the RDA.

# Chapter 3: Contrasting the annual pattern of two riverine phytoplankton communities in Hampshire Rivers

## 3.1 Abstract

Seasonal dynamics in the riverine phytoplankton community were investigated at the lowest gauging stations of the Stour and Hampshire Avon Rivers and at one additional site at Iford Bridge on the Stour River which is located between Throop and Christchurch Harbour (Southern UK) with regard to some major physical and chemical variables during an annual cycle. The riverine phytoplankton community in terms of carbon biomass and accessory pigments displayed a distinctive pattern of seasonal succession. The diatom group maxima were observed in spring and chlorophytes maxima in summer. The nano-sized diatom (2.0 – 20.0 µm), *Stephanodiscus* sp., dominated the assemblages, reaching 4.4 × $10^4$ cells $mL^{-1}$ and a chlorophyll *a* concentration of 98.8 µg $L^{-1}$ on the Stour River during the 2013 spring bloom. This diatom bloom was observed during a period of decreasing river discharge of between 8.4 and 8.8 $m^3$ $s^{-1}$ on the Stour and was also the blooming species during the same period on the Avon but was lower in cell numbers in comparison. A summer chlorophyte bloom on the Stour, composed of *Chlamydomonas* spp., reached 7.9 × $10^4$ cells $mL^{-1}$ and followed the diatom spring bloom. The nano-phytoplankton component was dominant in biomass and production during the spring-summer period in both rivers. Principal component analysis suggested that the structure of the phytoplankton communities in both rivers was determined by a variety of parameters including hydrology (river flow, suspended particulate matter, temperature, and oxygen saturation), and nutrients (nitrate, phosphate, and silicate concentrations). Multivariate analysis revealed that water temperature, river discharge, silicate, and phosphate concentration were major factors controlling phytoplankton carbon biomass at the three study sites. The results of the present study provide improved understanding into the composition and dynamics of phytoplankton communities on the Stour and Hampshire Avon Rivers immediately before the water passes into the shallow temperate, Christchurch Harbour estuary.

## 3.2 Introduction

The Stour and Hampshire Avon Rivers are principally a main sources of freshwater and nutrients to the Christchurch Harbour estuary. Both rivers have been variably affected by agriculture, urbanisation, and input from sewage treatment works (Jarvie *et al.*, 2005a). The rivers differ in their channel forms and in the extent to which hydrology is altered by both natural and artificial structures. During this study intensive surveys were investigated at the lowest gauging stations of both rivers and one additional position on the Stour at Iford Bridge to characterise seasonal changes in phytoplankton populations. The aims of this study were to describe the changes in species composition, biomass, and pigments of phytoplankton in the lower River Stour and Avon, and to investigate the relationship between phytoplankton populations and environmental variables.

## 3.3 Results

### 3.3.1 Environmental data

The hydrographic environment at Throop gauging station and Iford Bridge site on the Stour and Knapp Mill gauging station within the Bournemouth Water SembCorp site on the Avon River are described in this chapter (see the sampling dates in Appendix A). Average physical factors (suspended particulate matter, river flow, water temperature, and oxygen saturation) and nutrient concentrations (nitrate, phosphate, and silicate) were measured at these three study sites regularly by weekly between mid-April 2013 and mid-April 2014 as summarised in Table 3-1.

#### 3.3.1.1 River flow

Freshwater discharge from the Stour River at Throop and the Avon River at Knapp Mill between mid-April 2013 and mid-April 2014 (week 1 to 51) are shown in Figure 3-1. Both river flow records were provided by the Environment Agency. The average annual river flow at Throop was 20 $m^3 s^{-1}$ meanwhile at Knapp Mill it was 28 $m^3 s^{-1}$. The combined average annual flow of both rivers was 24 $m^3 s^{-1}$. The minimum values were recorded between July and mid-October 2013 (mean = 3 $m^3 s^{-1}$ at Throop, 7 $m^3 s^{-1}$ at Knapp Mill) and the maximum flows were observed in the winter between mid-December 2013 and mid-March 2014 (mean = 60 $m^3 s^{-1}$ at Throop, 75 $m^3 s^{-1}$ at Knapp Mill). An increase in flow also occurred between these minimum and maximum flows in November 2013

recorded in both rivers (mean = 20 $m^3$ $s^{-1}$). The river discharge observed in the Stour and Hampshire Avon Rivers shows a similar pattern with a decrease to a minimum (< 3 $m^3$ $s^{-1}$ at Throop and < 7 $m^3$ $s^{-1}$ at Knapp Mill) in August and October 2013 (week 18 to 26), respectively followed by a sudden winter peak up to 112 and 94 $m^3$ $s^{-1}$ (January 2014, week 38). This large increase in river flow caused widespread flooding along the lower reaches of both rivers as shown in Figure 3-2.

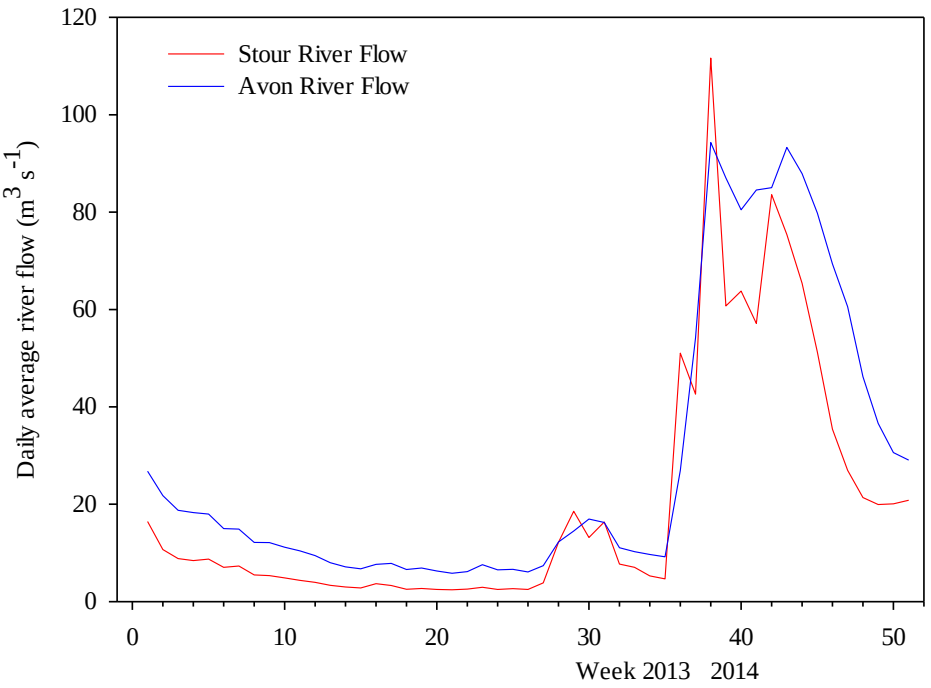


Figure 3-1: Daily average river flow ($m^3$ $s^{-1}$) from the Stour and the Hampshire Avon River for April 2013 to April 2014, obtained from the Environment Agency.

### 3.3.1.2 Suspended particulate matter

The annual pattern of suspended particulate matter (SPM) was influenced by the changes in river flow on both the rivers as shown in Figure 3-3. SPM concentration at Throop was normally below 0.003 g $L^{-1}$ and progressively increased up to 0.135 g $L^{-1}$ during the massive flooding event in winter (Figure 3-3 B). On the Hampshire Avon, SPM values at Knapp Mill were typically lower than at Throop and ranged from 0.001 – 0.038 g $L^{-1}$ (Figure 3-3 C). However, a maximum SPM concentration at Knapp Mill also occurred at the beginning of the high flow event in late December 2013 (week 36).


Figure 3-2: Images of the four sites where water samples were collected during the winter flood.

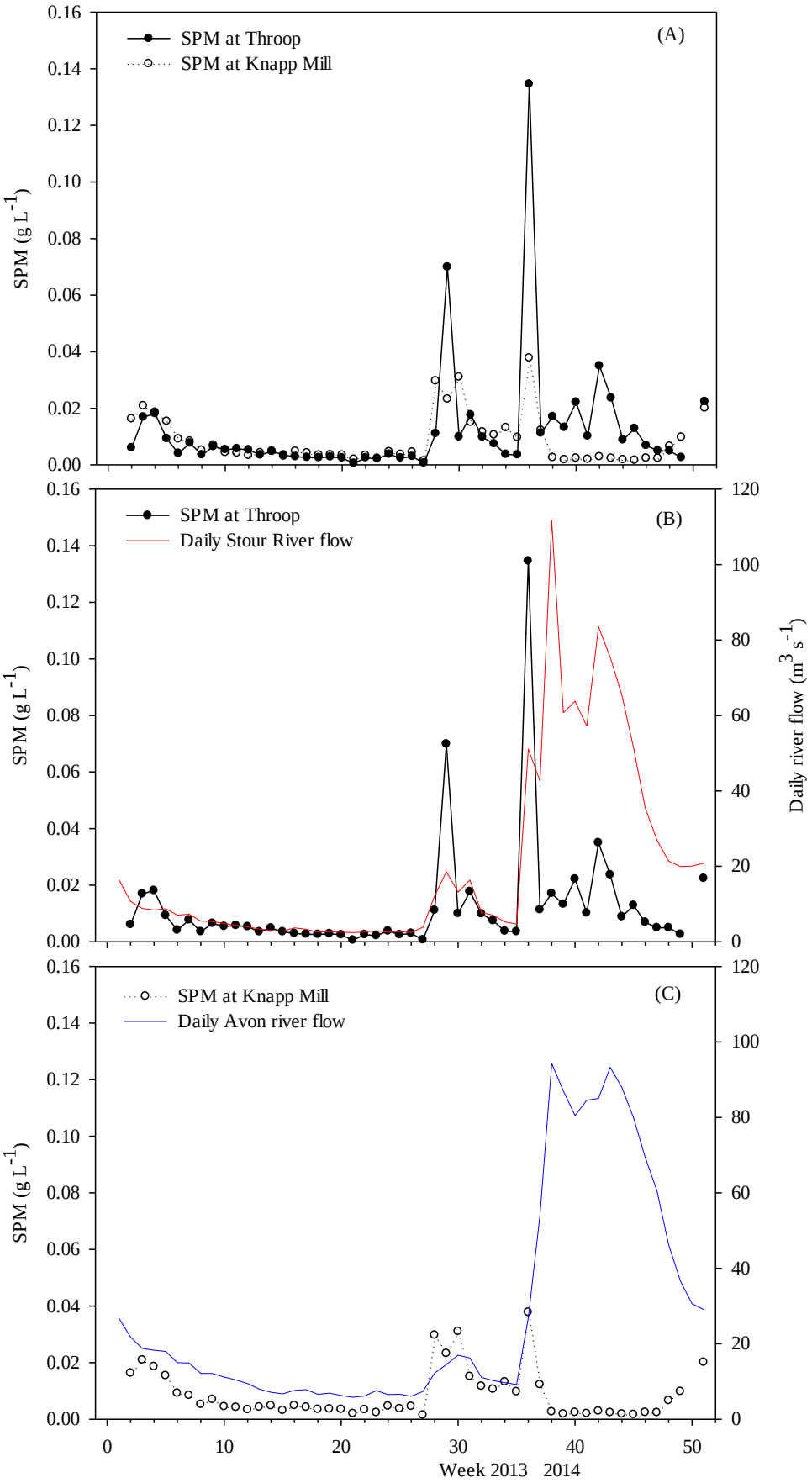


Figure 3-3: Suspended particulate matter (SPM) concentrations at Throop on the Stour River (A and B) and Knapp Mill on the Hampshire Avon River (A and C).

### 3.3.1.3 Chemical parameters: Inorganic nutrients

The concentration of the major inorganic nutrients, phosphate, nitrate, and silicate at the three river stations in general followed a pattern of relatively high concentrations in summer and autumn 2013 (week 8 to 28) and lower concentrations during winter and spring 2014 (week 30 to 51) as shown in Figure 3-4, Figure 3-5, and Table 3-1.

The mean concentration of nitrate, phosphate, and silicate on the Stour at Throop throughout the sampling period were 470 ± 75 (n=49), 10 ± 7 (n=49), and 109 ± 41 (n=49) µmol $L^{-1}$, respectively all being well above detection levels throughout the sampling period. Nitrate concentrations ranged from 315 µmol $L^{-1}$ (February 2014, week 42) to 611 µmol $L^{-1}$ (May 2013, week 6), phosphate concentrations ranged from 2 µmol $L^{-1}$ at the end of April 2013 (week 2) to 25 µmol $L^{-1}$ at the end of September 2013 (week 24), and silicate from 6 µmol $L^{-1}$ (May 2013, week 3) to 216 µmol $L^{-1}$ (October 2013, week 28) as shown in Figure 3-4. The highest nitrate, phosphate, and silicate concentrations were found in autumn months when riverine flow rate was less than 20 $m^3$ $s^{-1}$ at this station.

The Iford Bridge sampling site is downstream of Throop on the Stour and just above the tidal limit of that branch of the estuary. Phosphate and nitrate were generally detected at higher concentration than at Throop (Figure 3-4 A and B) but the concentration of silicate was very similar (Figure 3-4 C). Phosphate concentrations ranged from 3 µmol $L^{-1}$ in mid-February 2014 (week 44) to 49 µmol $L^{-1}$ in mid-October 2013 (week 27), nitrate from 332 µmol $L^{-1}$ (January 2014, week 38) to 824 µmol $L^{-1}$ (October 2013, week 27), and silicate from 48 µmol $L^{-1}$ (June 2013, week 8) to 191 µmol $L^{-1}$ (October 2013, week 28). The mean concentration of phosphate, nitrate, and silicate at Iford Bridge during the sampling period were 17 ± 12 (n=44), 543 ± 111 (n=44), and 113 ± 32 (n=44) µmol $L^{-1}$, respectively. The highest nitrate and silicate concentrations were found in autumn months when riverine flow rate measured at Throop was less than 20 $m^3$ $s^{-1}$.

The distribution of inorganic nutrients in the Hampshire Avon at Knapp Mill in general followed a pattern of relatively high concentrations in summer and autumn months and reduced concentrations during high winter river flow rates as shown in Figure 3-5. The mean concentration of phosphate, nitrate, and silicate concentrations at Knapp Mill during the sampling period were 2 ± 1 (n=50), 382 ± 56 (n=50), and 136 ± 68 (n=50) µmol $L^{-1}$, respectively. All three inorganic nutrients were above detection level at Knapp Mill throughout the sampling period. Phosphate concentrations ranged from ~0.1 µmol $L^{-1}$ at the end of April 2013 (week 2) to 4 µmol $L^{-1}$ in early January 2014 (week 38), nitrate from

272 µmol $L^{-1}$ (December 2013, week 36) to 493 µmol $L^{-1}$ (March 2014, week 48), and silicate from 4 µmol $L^{-1}$ (February 2014, week 45) to 240 µmol $L^{-1}$ (October 2013, week 29). The maximum phosphate and silicate concentrations were found in both the Avon and the Stour in autumn when river flow rates were less than 20 $m^3 s^{-1}$. The mean phosphate concentration in the Hampshire Avon at Knapp Mill was about sevenfold lower compared to the concentration in the Stour River at Throop.

Table 3-1: Mean environmental variables measured during the five study periods between spring 2013 and spring 2014 at Throop (Thr), Iford Bridge (IB), and Knapp Mill (KM).

| | Spring 2013 | | | Summer 2013 | | | Autumn 2013 | | | Winter 2013 | | | Spring 2014 | | |
|---|---|---|---|---|---|---|---|---|---|---|---|---|---|---|---|
| Variables | Thr | IB | KM | Thr | IB | KM | Thr | IB | KM | Thr | IB | KM | Thr | IB | KM |
| *Physical factors* | | | | | | | | | | | | | | | |
| SPM (g $L^{-1}$) | 0.010 | - | 0.015 | 0.004 | - | 0.004 | 0.011 | - | 0.011 | 0.025 | - | 0.008 | 0.008 | - | 0.008 |
| River flow ($m^3 s^{-1}$) | 9.6 | - | 19.1 | 3.7 | - | 8.6 | 7.3 | - | 9.8 | 56.1 | - | 99.0 | 24.1 | - | 45.4 |
| Temperature (°C) | 13.3 | - | 13.0 | 18.7 | 18.5 | 18.9 | 12.6 | 12.8 | 12.2 | 7.6 | 7.7 | 7.3 | 9.8 | 9.9 | 9.9 |
| Oxygen saturation | 119.1 | - | 103.8 | 94.2 | 84.3 | 111.6 | 89.5 | 86.2 | 93.9 | 89.6 | 89.9 | 99.2 | 98.3 | 97.2 | 103.5 |
| *Nutrients*(µmol $L^{-1}$) | | | | | | | | | | | | | | | |
| Nitrate | 562 | - | 430 | 482 | 593 | 364 | 493 | 543 | 358 | 419 | 455 | 368 | 394 | 607 | 458 |
| Phosphate | 6 | - | 1 | 14 | 26 | 2 | 16 | 23 | 2 | 4 | 7 | 2 | 3 | 7 | 1 |
| Silicate | 47 | - | 99 | 95 | 93 | 125 | 152 | 144 | 194 | 110 | 108 | 118 | 109 | 97 | 105 |

The nitrate to phosphate ratios (N:P) generally ranged between 20 and 485 at Throop (Figure 3-6 A). Meanwhile, on the same river at Iford Bridge the N:P ratios range was 15 – 136. These ratios are significantly greater than the Redfield ratio of 16 for typical marine waters. Silicate to phosphate ratios (Si:P) were generally between 2 and 40 at Throop, and 2 and 25 at Iford Bridge. The nitrate to silicate ratios (N:Si) were between 2 and 98 at Throop, and 2 and 14 at Iford Bridge. Both N:P and Si:P ratios at Throop increased to 380 and 40, respectively during the winter flood, when the lowest phosphate and nitrate concentrations were observed. By contrast, the N:Si ratios did not vary significantly at this time (Figure 3-6 B).

The N:P ratio at Knapp Mill generally ranged between 82 and 2,980 (Figure 3-7), significantly greater than both the Redfield ratio of 16 for typical marine waters and the N:P ratio on the Stour River. The Si:P ratios were generally between 12 and ~495. The N:Si ratios were between 1 and 86. Both N:P and Si:P ratio on the Hampshire Avon were greater than the ratios on the Stour River during the winter flood, when the lowest

phosphate and silicate concentrations were observed. Meanwhile, the highest N:Si ratio occurred at this time (Figure 3-7).

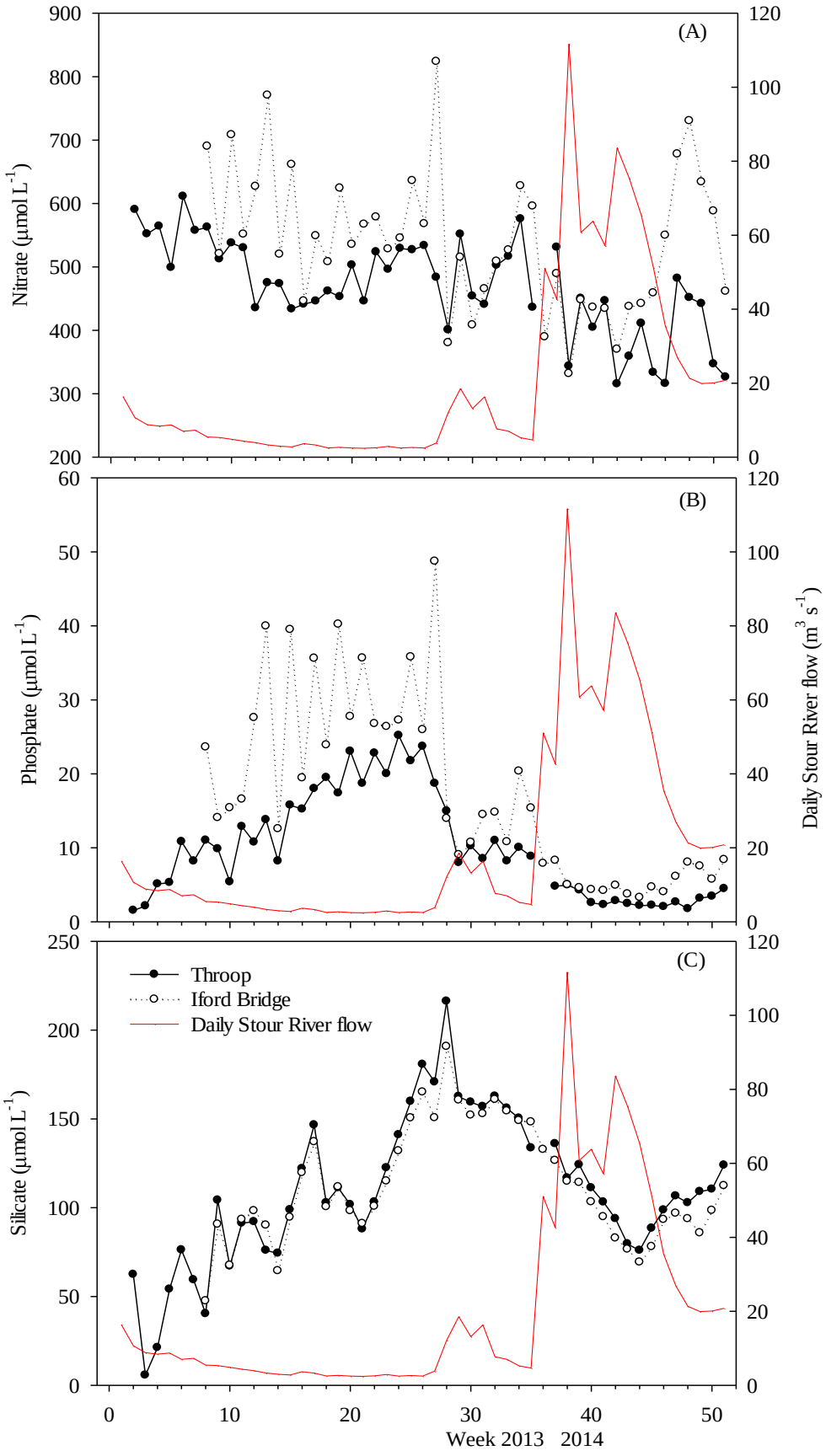


Figure 3-4: Surface nutrient concentrations (µmol $L^{-1}$) at Throop and Iford Bridge on the Stour River (A) nitrate, (B) phosphate, and (C) silicate. Symbols in lower panel apply to all panels.

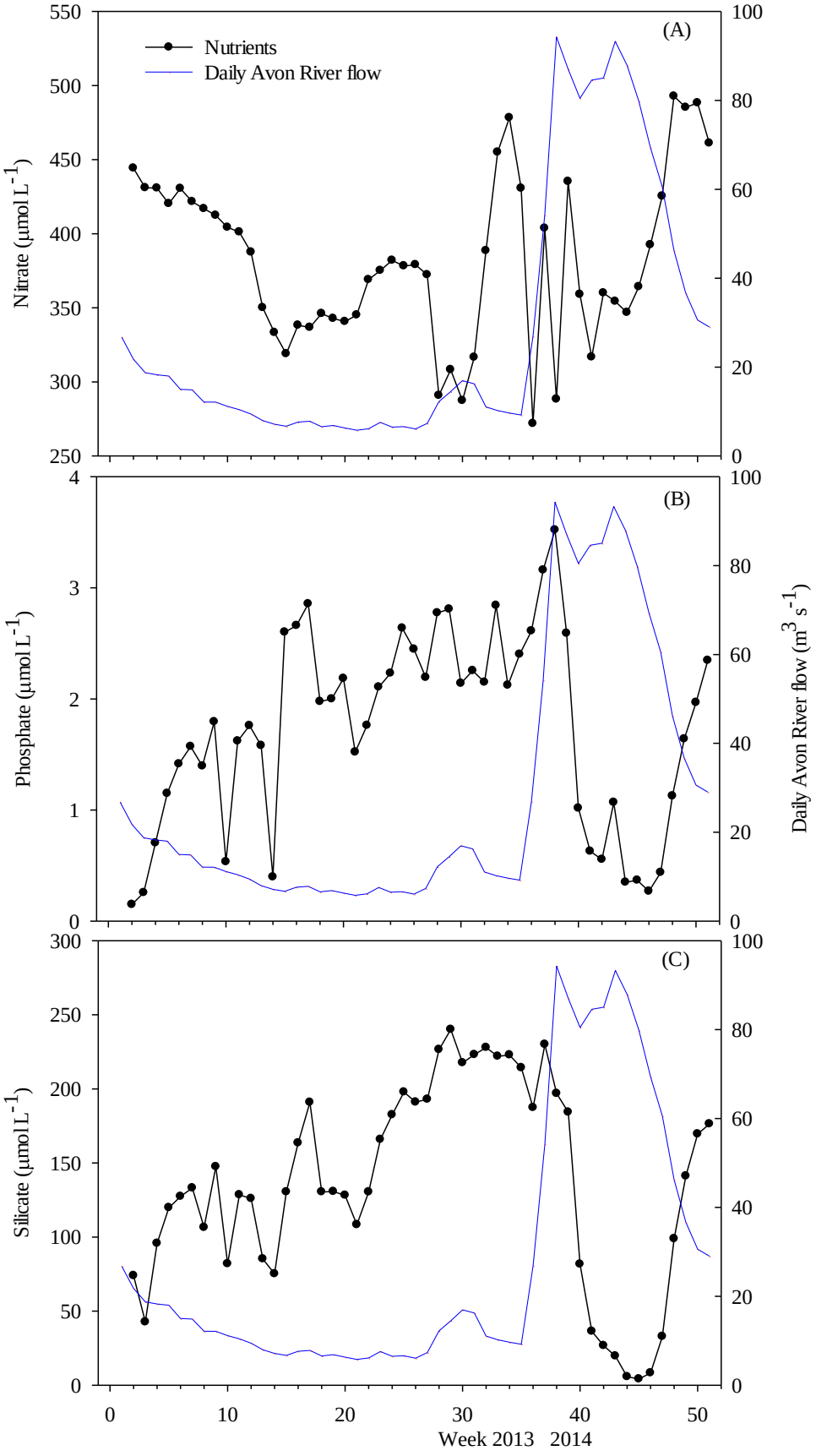


Figure 3-5: Surface nutrient concentrations (µmol $L^{-1}$) at Knapp Mill on the Hampshire Avon River (A) nitrate, (B) phosphate, and (C) silicate. Symbols in upper panel apply to all panels.

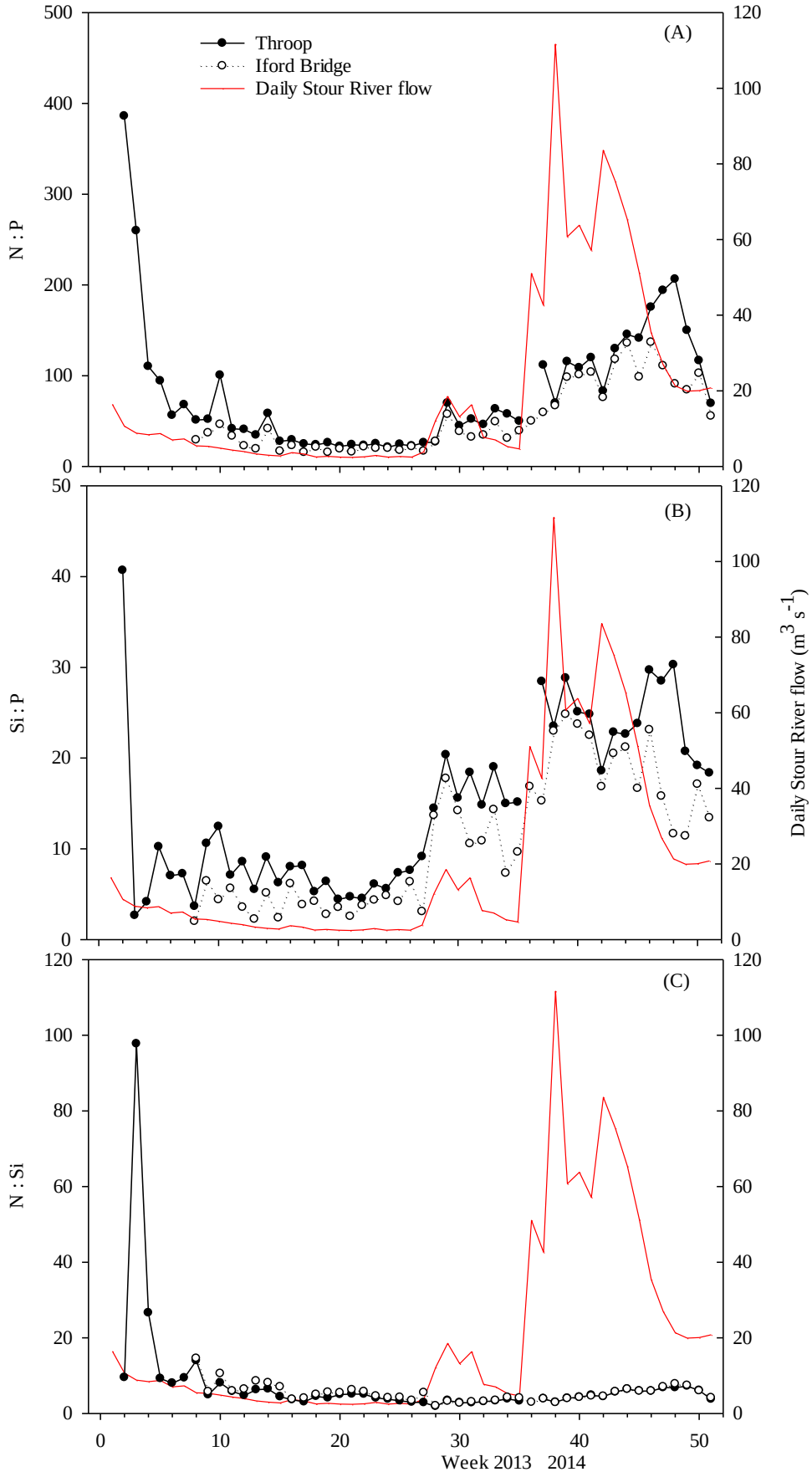


Figure 3-6: Si:P, N:P, and N:Si ratio at Throop and Iford Bridge on the Stour River. Symbols in upper panel apply to all panels.

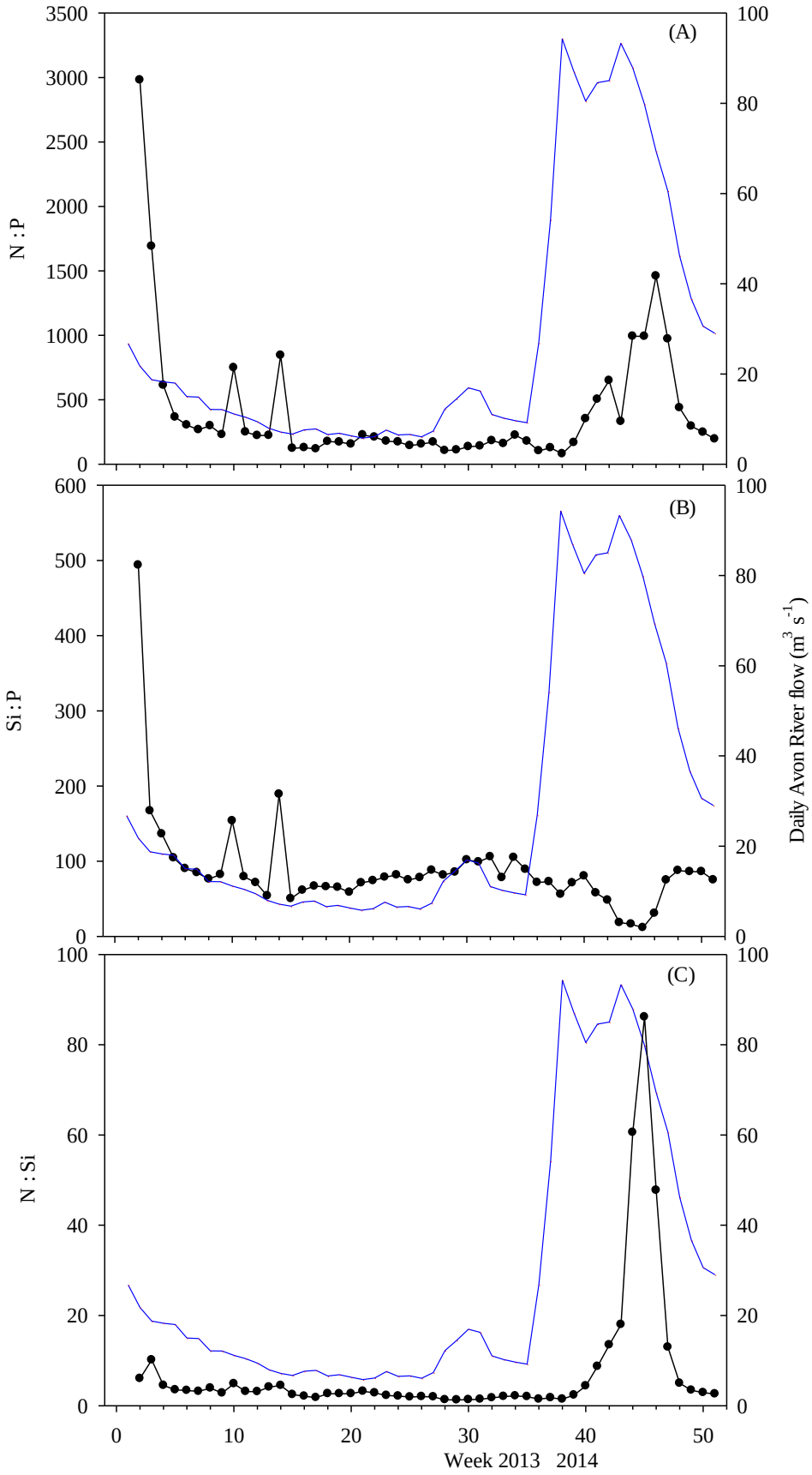


Figure 3-7: Si:P, N:P, and N:Si ratio at Knapp Mill on the Hampshire Avon River.

### 3.3.2 Phytoplankton pigments

#### 3.3.2.1 Total chlorophyll *a* and chlorophyll *a* size fractions

Changes in total surface chlorophyll *a* concentrations and chlorophyll *a* size fractions are shown in Figure 3-8. Total chlorophyll *a* values ranged from 0.7 µg $L^{-1}$ in December 2013 (week 34 and 35) to 98.8 µg $L^{-1}$ in May 2013 (week 4) at Throop, with larger peaks of ~65 to ~99 µg $L^{-1}$ in May 2013 (week 3, 4, 5) during the spring bloom event, followed by three small peaks of ~19 to ~29 µg $L^{-1}$ during May – July 2013 (week 7, 9, 12), and two final small peaks at the end of March (week 49) and in April 2013 (week 51) as shown in Figure 3-8 A. Meanwhile, total chlorophyll *a* concentrations at Iford Bridge showed the same pattern as the total chlorophyll concentration at Throop. The changes of total surface chlorophyll *a* values at Iford Bridge are presented in Figure 3-8 B. Total chlorophyll *a* concentrations ranged from 0.6 µg $L^{-1}$ in December 2013 (week 34) to 43.7 µg $L^{-1}$ in mid June 2013 (week 9), followed by a small peak of ~22 µg $L^{-1}$ at the end of June 2013 (week 12), and a final peak at the end of March 2014 (week 49).

The seasonal distribution of total chlorophyll *a* concentration at Knapp Mill is shown in Figure 3-8 C. Total chlorophyll *a* concentrations ranged from 0.9 µg $L^{-1}$ in January 2014 (week 39) to 35.5 µg $L^{-1}$ in May 2013 (week 3), with a large peak of 35.5 µg $L^{-1}$ at the early of May 2013 (week 3), followed by three small peaks throughout the weekly sampling in June 2013, February, and April 2014 (week 10, 42, 50). The highest chlorophyll *a* concentration at Knapp Mill was measured a week after the bloom event occurred at Throop. Chlorophyll *a* events (peaks) are numbered in series for each study site in Figure 3-8, Throop (T1 – 8), Iford Bridge (I1 – 3), and Knapp Mill (K1 – 4).

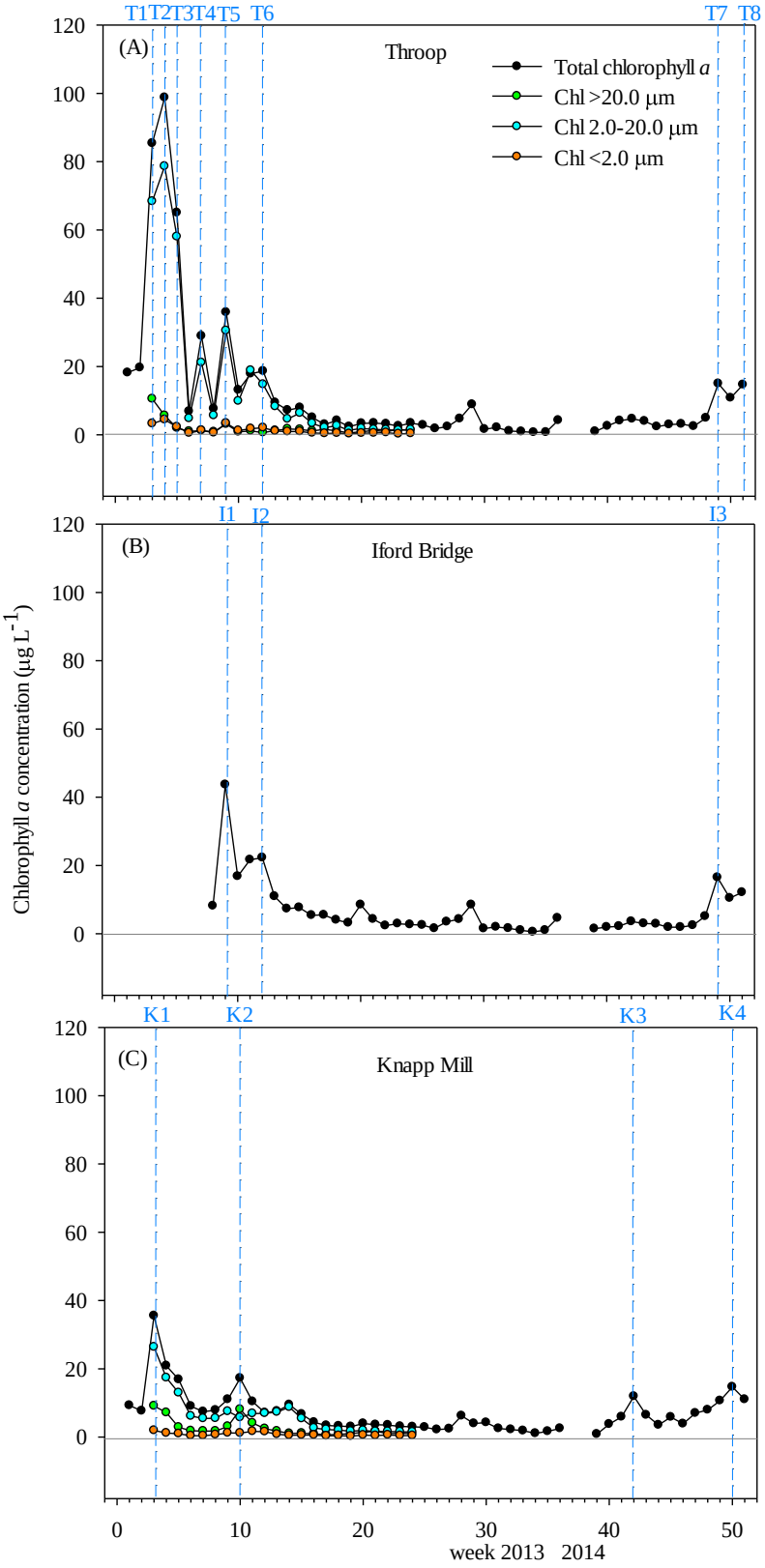


Figure 3-8: Seasonal distribution of total chlorophyll *a* at Throop (A), Iford Bridge (B), and Knapp Mill (C) and size fractionated chlorophyll *a* (< 0.2, 0.2 – 2.0, and > 20 µm) at Throop (A) and Knapp Mill (C) from week 3 to 24 only. The numbers and dash lines shown above the chlorophyll *a* curve identify each of the peak chlorophyll events. Symbols in upper panel apply to all panels.

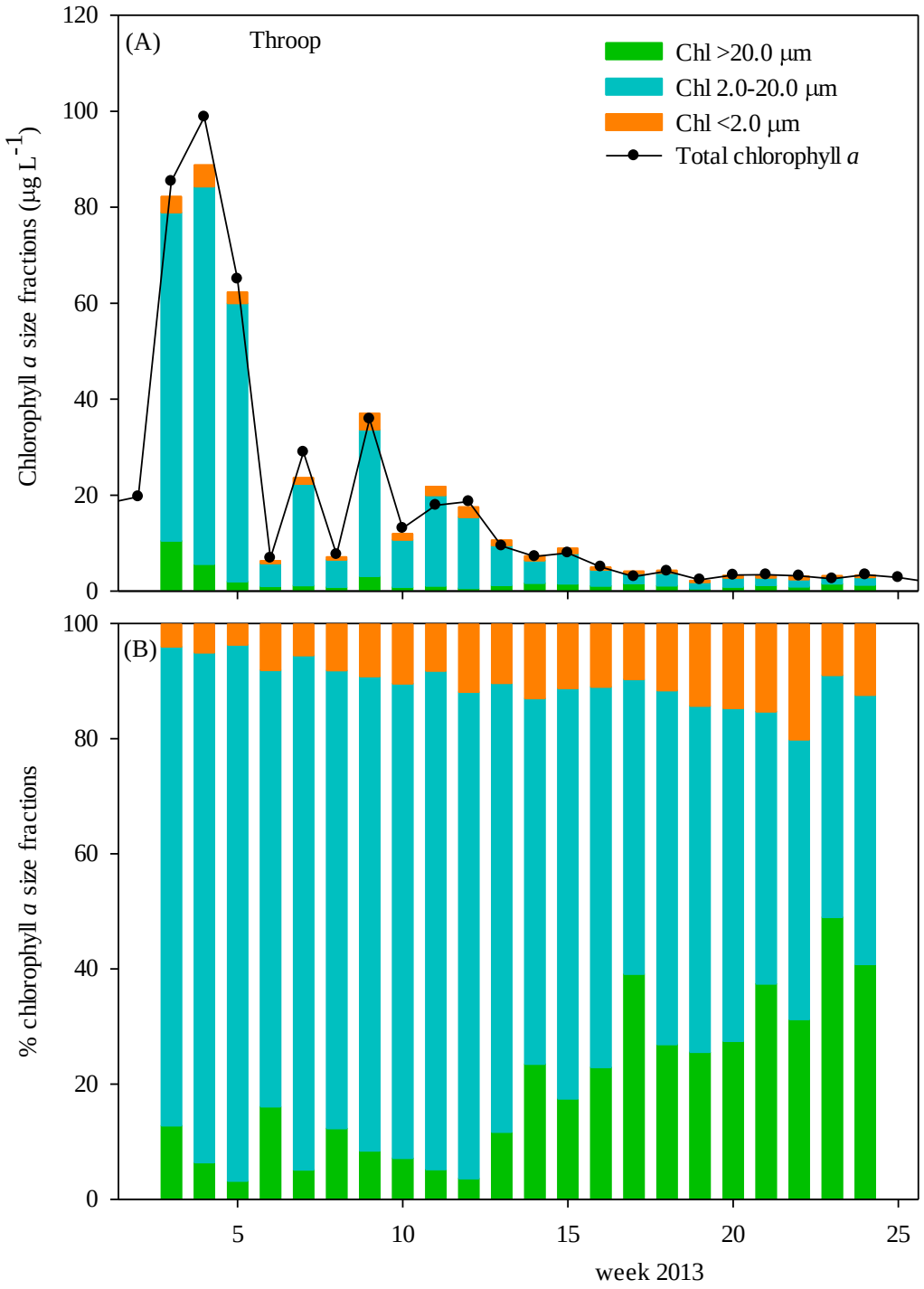


Figure 3-9: Distributions of chlorophyll *a* size fractions at Throop during the high productive period (A) and distributions of chlorophyll *a* size fractions expressed as percentages (B).

The distribution of the chlorophyll *a* size fractions at Throop on the Stour River is illustrated in absolute units and as percentages in Figure 3-9. The mean percentages for each size fraction were: > 20 µm, 20% (maximum 49% in week 23); 2 – 20 µm 70% (maximum 93% in week 5); < 2 µm 10% (maximum 20% in week 22).

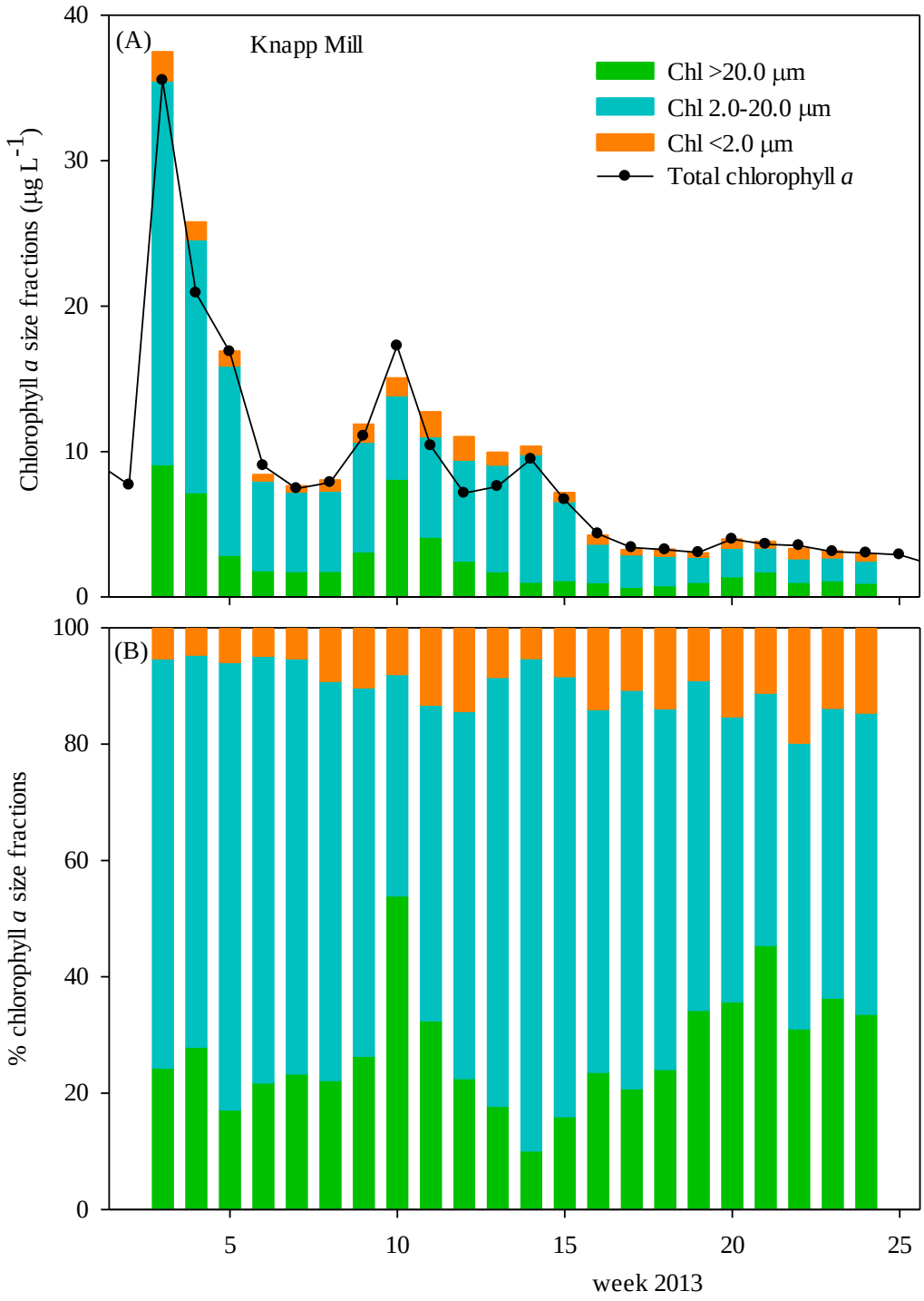


Figure 3-10: Distributions of chlorophyll *a* size fractions at Knapp Mill during the high productive period (A) and distributions of chlorophyll *a* size fractions expressed as percentages (B).

The distribution of the chlorophyll *a* size fractions at Knapp Mill on the Avon River is shown in absolute units and as percentages in Figure 3-10. The mean percentages for each size fraction were: > 20 µm, 27% (maximum 54% in week 10); 2 – 20 µm 63% (maximum 85% in week 14); < 2 µm 10% (maximum 20% in week 22).

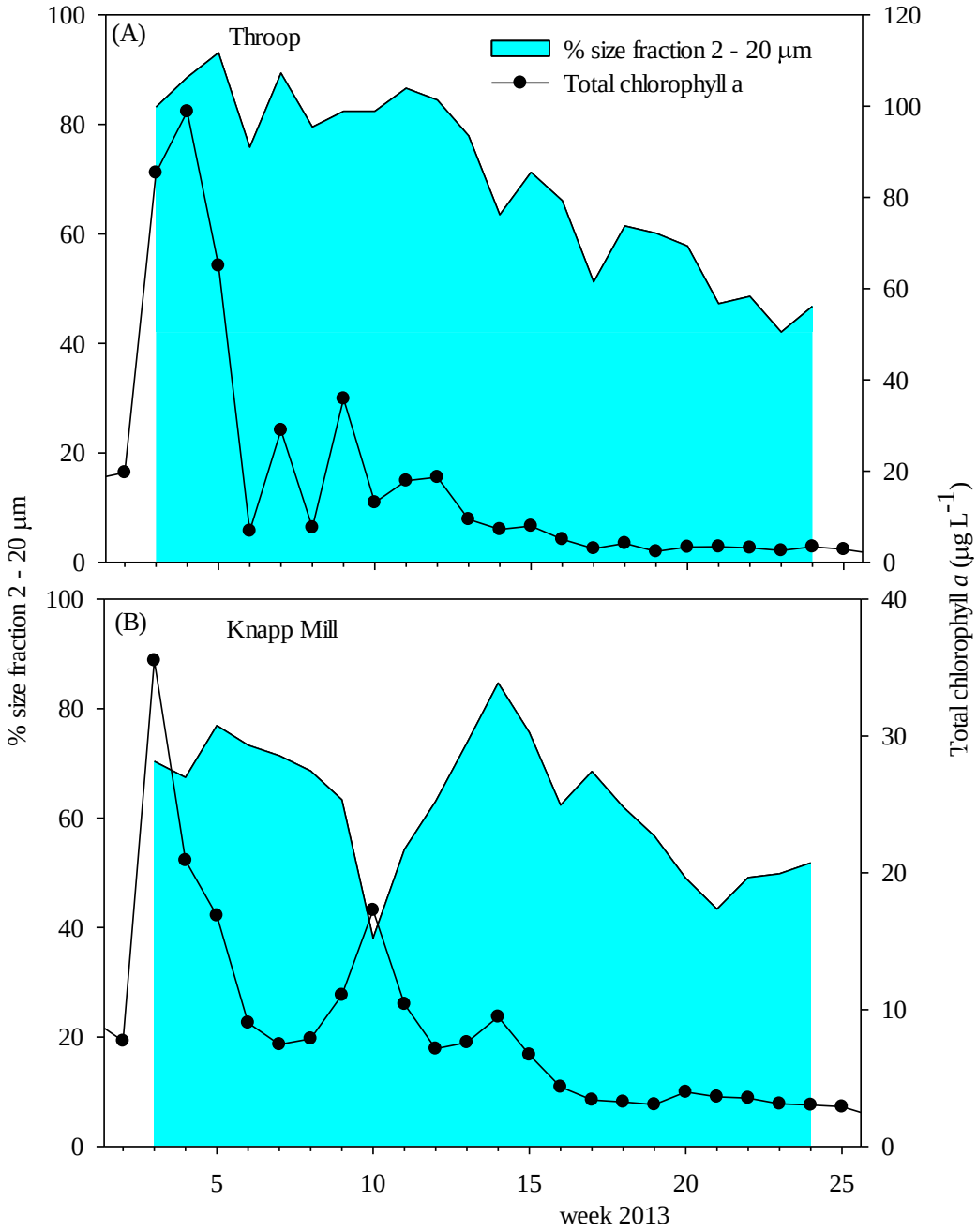


Figure 3-11: Total chlorophyll *a* and percentages of 2 – 20 µm chlorophyll *a* fraction at Throop (A) and Knapp Mill (B).

Figure 3-9 and Figure 3-10 indicate that the 2 – 20 µm size fraction was the dominant group at both sites. The mean percentage of the 2 – 20 µm fraction were found to be 70% (range 42 – 93%), and 62% (range 38 – 84%) in the Stour and the Hampshire Avon Rivers, respectively (Figure 3-11). The correlation between total chlorophyll *a* and the 2 – 20 µm gave $R^2 = 0.99$ (n = 22) at Throop and $R^2 = 0.91$ (n = 22) at Knapp Mill.

There was good agreement between the sum of the total chlorophyll *a* and three size fractions at both Throop and Knapp Mill, with slopes of 0.93 and 1.07, and an $R^2$ value of

0.99 and 0.97, respectively. This result gave confidence that the size fractionation procedure from the two sampling sites was not associated with significant loss of phytoplankton cells (Figure 3-12).

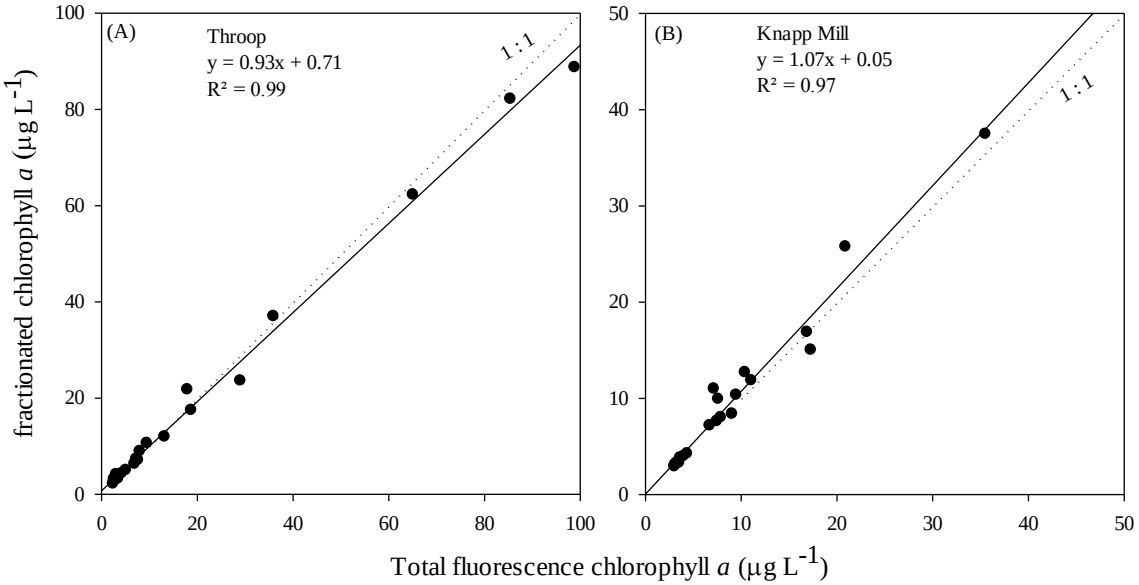


Figure 3-12: Correlation between total chlorophyll *a* and sum of the size fractions at (A) Throop and (B) Knapp Mill. The dash lines represent the 1:1 agreement line.

The relationship between phytoplankton biomass (chlorophyll *a*) and nutrient concentrations at all riverine stations are shown in Figure 3-13 for Throop and Iford Bridge and Figure 3-14 for Knapp Mill. Silicate and phosphate concentrations reduced during high chlorophyll concentrations in both rivers but not a clear pattern at Iford Bridge (Figure 3-13 B, C, E, F and Figure 3-14 B, C). It is probably water samples at this site have been collected later the spring bloom as occurred at Throop and Knapp Mill in May 2013 while nitrate concentrations did not show a correlation with the chlorophyll *a* concentrations from all study sites (Figure 3-13 A and Figure 3-14 A).

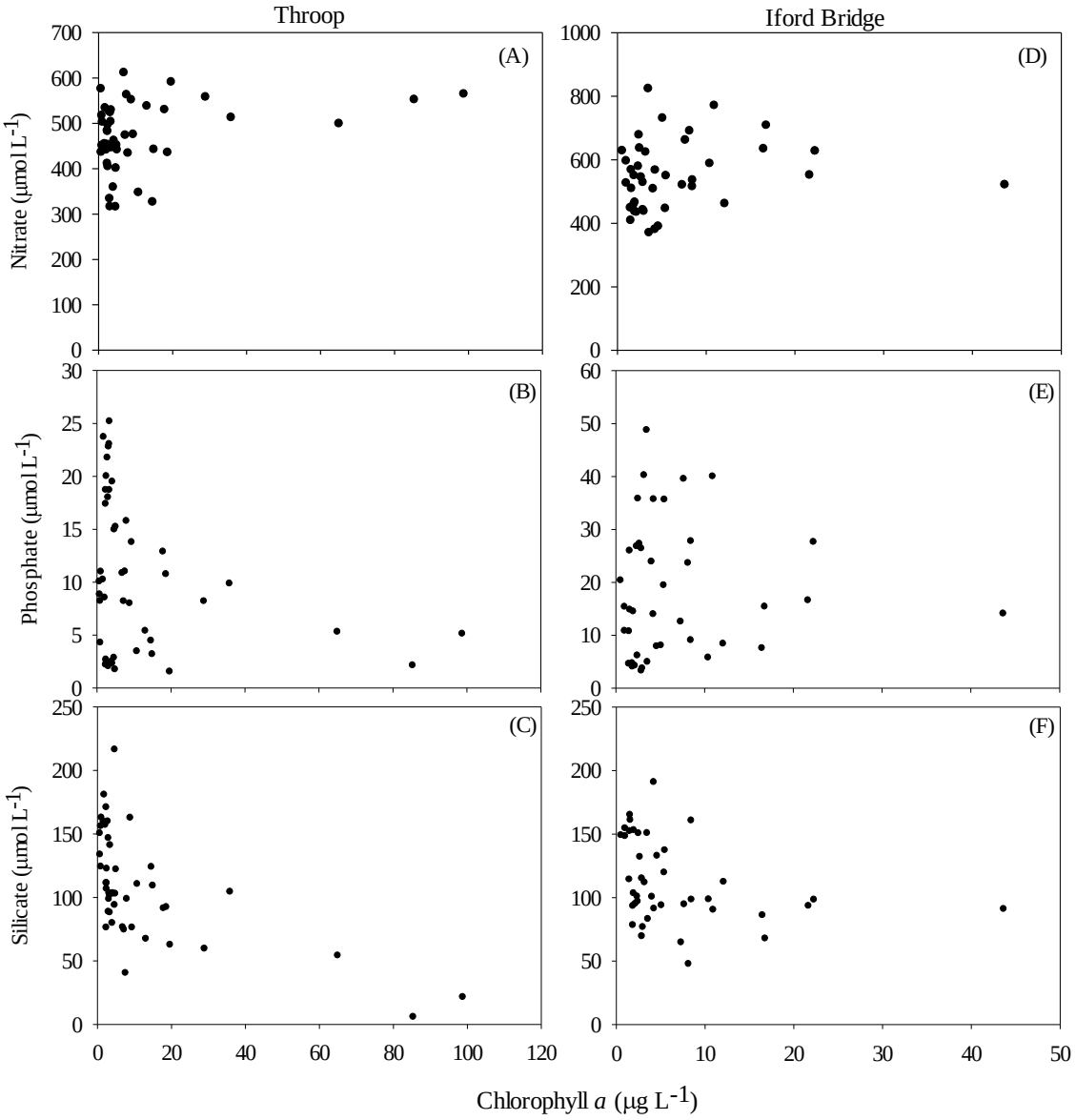


Figure 3-13: Relationship between inorganic nutrients and chlorophyll *a* concentration at Throop and Iford Bridge on the Stour, (A and D) nitrate, (B and E) phosphate, (C and F) silicate.

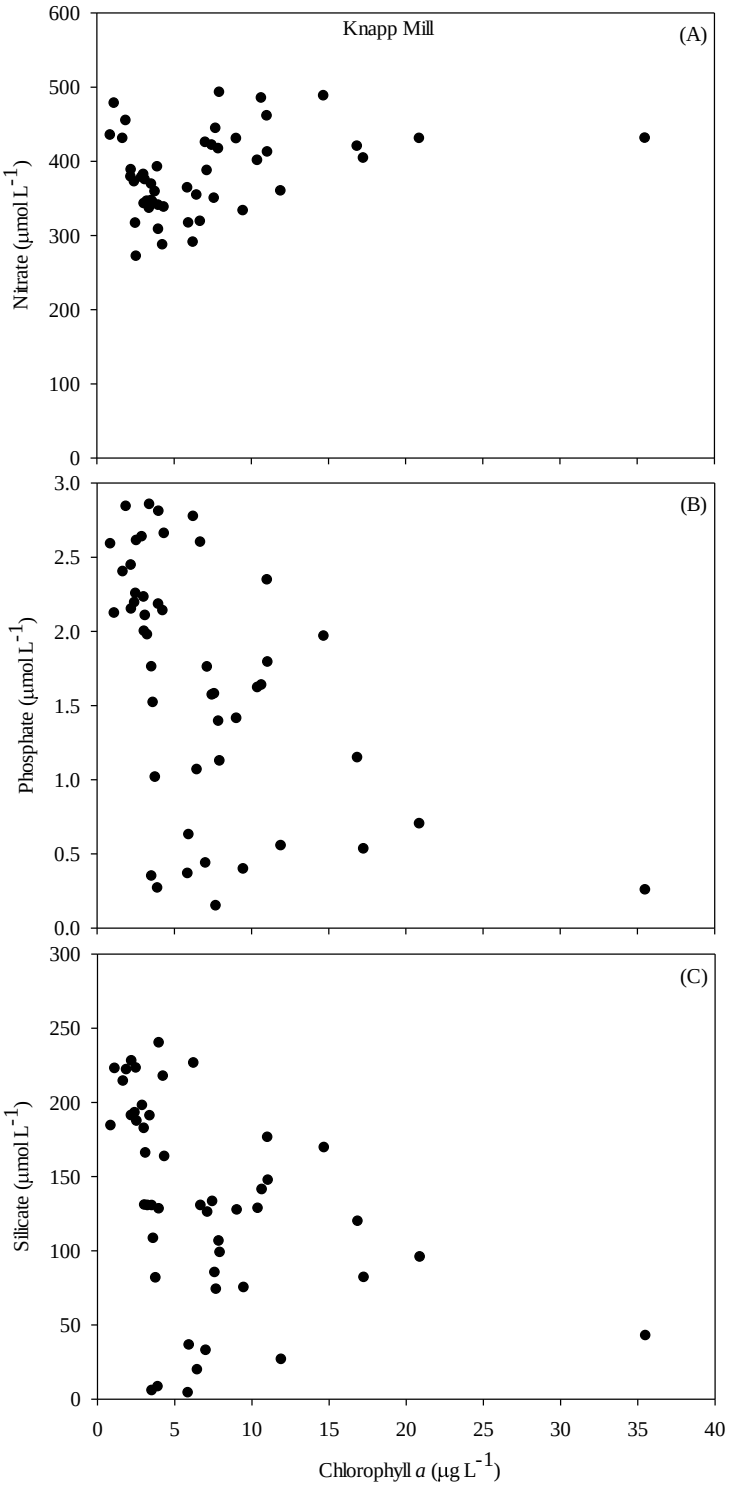


Figure 3-14: Relationship between inorganic nutrients and chlorophyll *a* concentration at Knapp Mill on the Hampshire Avon, (A) nitrate, (B) phosphate, (C) silicate.

### 3.3.2.2 Phytoplankton accessory pigment

A High Performance Liquid Chromatography (HPLC) method was used to determine the concentration of a number of phytoplankton accessory pigments including chlorophyll *a* in sample collected from Throop on the Stour and Knapp Mill on the Avon. Chlorophyll *a*

concentrations measured by HPLC were consistently lower than the concentration measured by fluorescence (Figure 3-15 A and B). It has been previously reported that lower HPLC concentrations may reflect interference by accessory pigments in the determination of chlorophyll *a* by fluorescence (Trees *et al.*, 1985; Trees *et al.*, 2000).

The discrepancy between chlorophyll *a* concentrations determined by fluorescence and HPLC analysis in riverine samples seems to be magnified at high chlorophyll *a* concentrations. This is clearly seen on the five days of peak chlorophyll *a* concentrations over 20 µg $L^{-1}$ at Throop during the diatom bloom and on the two days of high concentrations at Knapp Mill due to high abundance of the diatom, *Stephanodiscus* species. The HPLC chlorophyll *a* concentrations were lower than the fluorescence determination by around threefold.

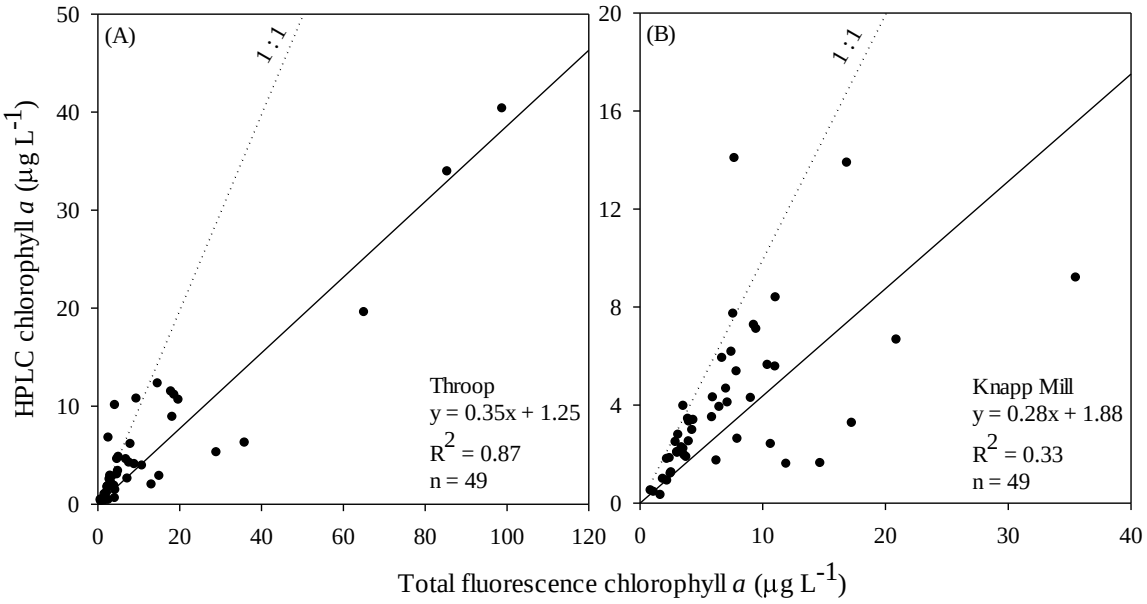


Figure 3-15: Comparison of chlorophyll *a* measurements by HPLC and fluorometer during April 2013 to April 2014 at (A) Throop and (B) Knapp Mill. The solid lines represent the linear regression for each set of data and equation for this line and correlation coefficient are shown. The dash lines represent the 1:1 agreement line.

In this study, the HPLC method detected up to 16 pigments some of which can be used as biomarkers to distinguish between phytoplankton groups as described in Table 2-2. As also shown by Trees *et al.* (2000) and Ali (2003), there were good correlations between chlorophyll *a* and both total pigment concentrations (all pigments including chlorophyll *a*) or total accessory pigment concentrations (without chlorophyll *a*), as shown in Figure 3-16

and Figure 3-17, which were irrespective of phytoplankton composition and pigment content.

The temporal successions of eight major pigments, namely chlorophyll *a* (Chl *a*), peridinin (Peri), fucoxanthin (Fuco), alloxanthin (Allo), lutein (Lut), chlorophyll *b* (Chl *b*), diadinoxanthin (Dia), and β carotene (β caro) at Throop and Knapp Mill (Figure 3-18 and Figure 3-20) as well as eight minor pigments chlorophyll *c3* (Chl *c3*), chlorophyll *c2* (Chl *c2*), 19'Butanoyloxyfucoxanthin (19' But), 19'Hexanoyloxyfucoxanthin (19' Hex), violaxanthin (Vio), prasinoxanthin (Pra), divinyl chlorophyll *a* (DV Chl *a*), and zeaxanthin (Zea) from both study sites are shown in Figure 3-19 and Figure 3-21. Variations in the ratios of accessory pigments to chlorophyll *a* (Figure 3-22 to Figure 3-25) reflected changes in the taxonomic composition of the phytoplankton population.

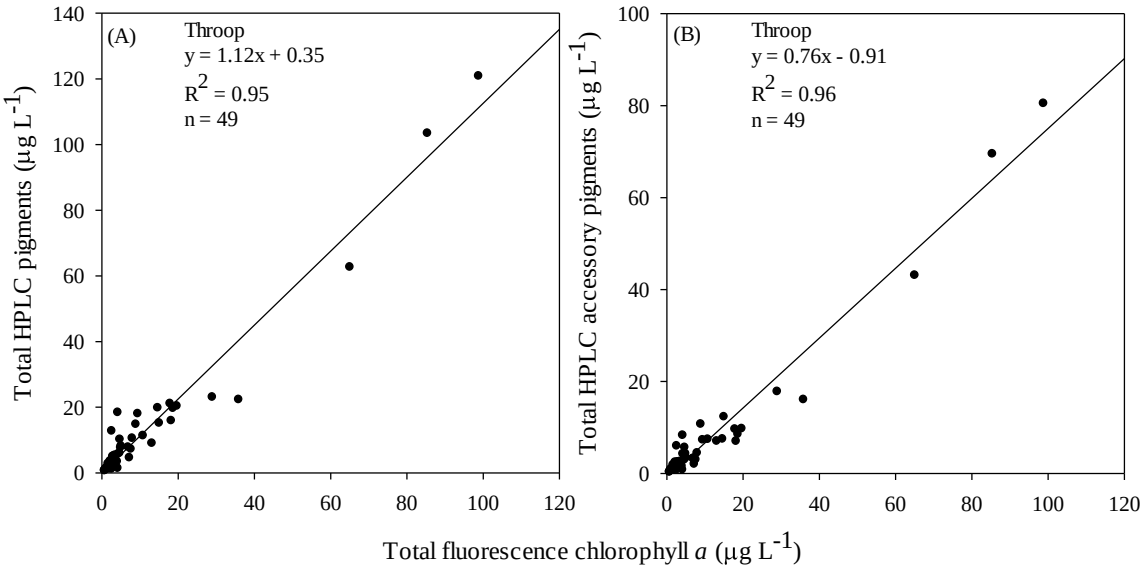


Figure 3-16: Relationship of chlorophyll *a* concentration to total HPLC pigments and total HPLC accessory pigments at Throop on the Stour River during April 2013 to April 2014.

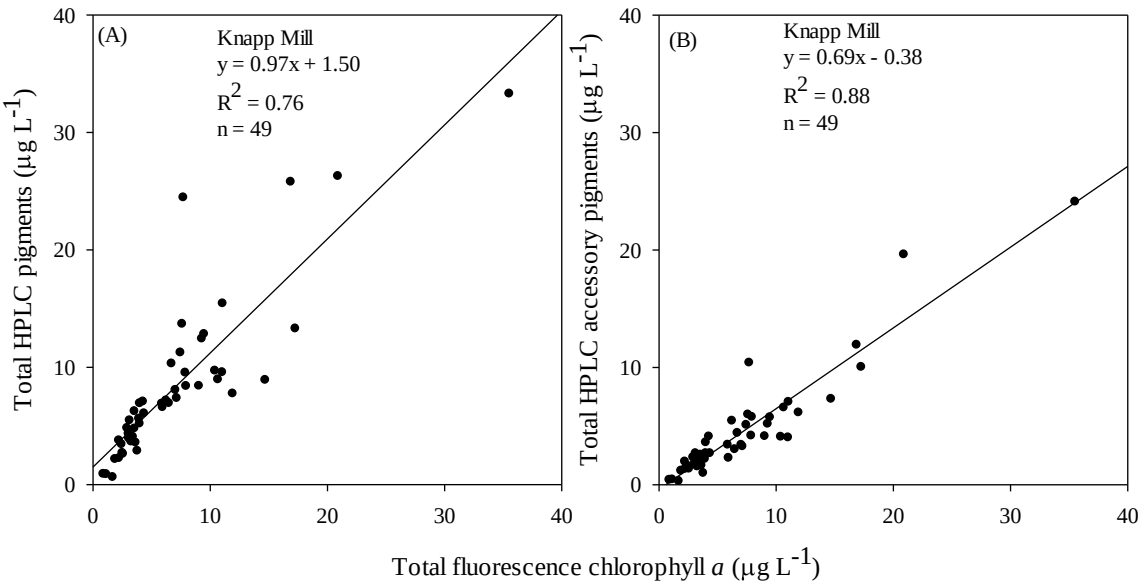


Figure 3-17: Relationship of chlorophyll *a* concentration to total HPLC pigments and total HPLC accessory pigments at Knapp Mill on the Hampshire Avon River during April 2013 to April 2014.

***Throop, River Stour***

Temporal changes of HPLC determined chlorophyll *a* concentration at Throop (Figure 3-18) generally followed distributions described previously for fluorometric determination (see Figure 3-8 A), although absolute concentration varied (Figure 3-18 A). Fucoxanthin, diadinoxanthin, and β carotene pigments displayed a similar seasonal distribution to chlorophyll *a*, with maxima of 55.0, 12.7, 4.1 µg $L^{-1}$ on 10th May 2013 (week 4) followed by 45.5, 11.5, and 3.6 µg $L^{-1}$ on 3rd May 2013 (week 3) respectively (Figure 3-18 C, G, H). The diadinoxanthin and β carotene pigments showed considerably lower concentration close to zero during autumn and winter months and concentrations of fucoxanthin were also much reduced (Figure 3-18 G, H). Alloxanthin, lutein, and chlorophyll *b* concentrations showed maxima peaks during the early chlorophyll *a* events (T1 – 6) in weeks 3, 7, and 9 (Figure 3-18 D, E, F). Concentration of lutein closely followed those of chlorophyll *b* and both pigments showed a high concentration in week 9 (T5), however, the highest concentration of lutein was presented on 30th October 2013 (week 29) with concentration of 2.9 µg $L^{-1}$ as shown in Figure 3-18 E and F. Maximum concentration of peridinin was observed in week 28 and 29 (24th and 30th October 2013) with a concentration of 0.4 µg $L^{-1}$ while concentrations were close to zero during the rest of year (Figure 3-18 B).

Some of the other eight minor accessory pigments, Chl *c2*, 19'But, violaxanthin, and divinyl Chl *a* showed a similar seasonal distribution, peaking during the early chlorophyll events (T1 – 6), with maxima of 1.9, 0.6, 1.2, and 1.3 µg $L^{-1}$ on 3rd May 2013 (week 3) except violaxanthin which peaked on 14th June 2013 (week 9) as shown in Figure 3-19 B, C, E, and G. These pigments were often undetectable during the rest of year until spring 2014. However, Chl *c3*, prasinoxanthin, and zeaxanthin were detected at maximum concentration on 30th October 2013 (week 29), but with concentrations < 1.0 µg $L^{-1}$ (Figure 3-19 A, F, H). 19'Hex concentration was low throughout the whole sampling period but did reach 0.4 µg $L^{-1}$ on 27th March 2014 (week 50, T7) as illustrated in Figure 3-19 D.

***Knapp Mill, River Hampshire Avon***

Temporal changes of HPLC analysed chlorophyll *a* concentration at Knapp Mill (Figure 3-20 A) showed some differences to the distribution measured by fluorometer analysis (see Figure 3-8 C). Fucoxanthin, diadinoxanthin, and β carotene pigments displayed a similar seasonal distribution to Chl *a* by fluorescence determination, with maxima of 16.5, 3.8, 1.2 µg $L^{-1}$ on 3rd May 2013 (week 3) followed by 13.2, 3.0, and 0.9 µg $L^{-1}$ on 10th May 2013 (week 4) respectively (Figure 3-20 C, G, H). A high fucoxanthin concentration was detected on 3rd May 2013 at this site but about threefold lower than the concentration at Throop on the same day. The diadinoxanthin and β carotene pigments showed considerably higher concentration compared with the distribution at Throop. Fucoxanthin concentration was measureable throughout the sampling period (Figure 3-20 C). Lutein and Chl *b* concentrations showed maximum peak concentrations after the chlorophyll *a* events in July 2013, with maximum of 0.6 and 0.8 µg $L^{-1}$ in week 13 and 15 respectively followed by 0.5 and 0.4 µg $L^{-1}$ in November 2013 (Figure 3-20 E, F). Peridinin showed a small concentration (< 0.4 µg $L^{-1}$) from week 19 onwards as shown in Figure 3-20 B. Throughout the rest of the sampling period alloxanthin concentration was close to zero at this site, and only observed peak maxima concentrations during the K3 and K4 events (week 42 and 50), with concentration of 0.7 and 0.6 µg $L^{-1}$ respectively (Figure 3-20 D).

In general, the concentration of minor accessory pigments (Chl *c3*, Chl *c2*, 19'But, violaxanthin, prasinoxanthin, and divinyl Chl *a*) at Knapp Mill were below 1 µg $L^{-1}$, while 19'Hex and zeaxanthin pigments were undetectable throughout the sampling period (Figure 3-21). Chl *c3* concentrations varied between zero and 0.08 µg $L^{-1}$ (Figure 3-21 A) and Chl *c2* and 19'But were generally present at level below 0.5 µg $L^{-1}$ (Figure 3-21 B, C). These peaks were observed at the same time as the maximum chlorophyll *a* by fluorescence then

decreased considerably and were close to zero throughout April 2014. Low concentrations of violaxanthin were observed at Knapp Mill with concentrations close to zero except for in July 2013 when concentrations > 0.2 µg $L^{-1}$ were detected (Figure 3-21 E). Prasinoxanthin was not detected in samples collected during April to December 2013 (week 1 – 41), but did increase during both later chlorophyll events (K3 and K4) where concentrations of 0.01 and 0.02 µg $L^{-1}$ were respectively measured (Figure 3-21 F). 19'Hex and zeaxanthin pigments were not detected in samples collected at this site (Figure 3-21 D, H).

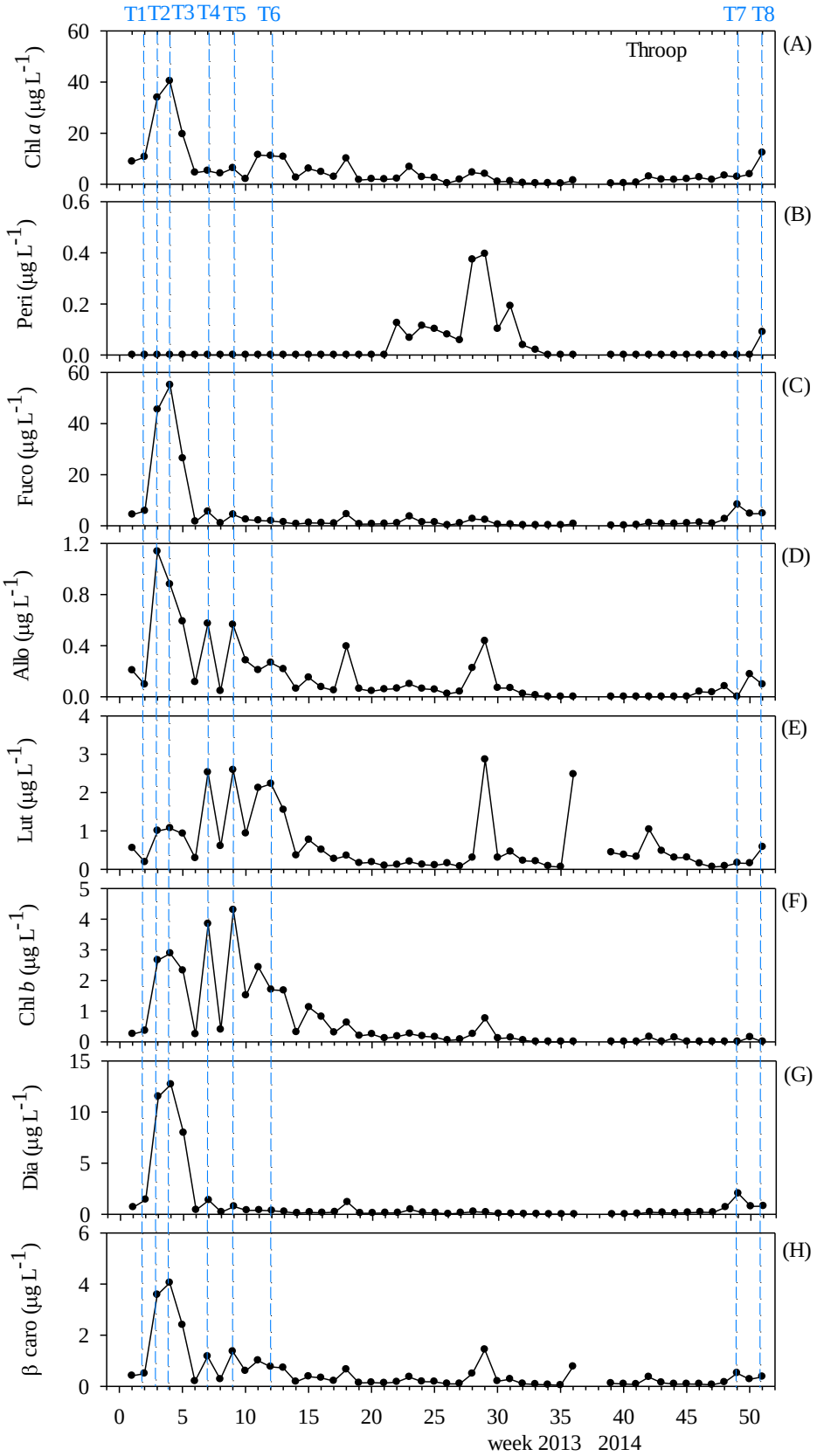


Figure 3-18: Temporal distributions of chlorophyll *a* and major accessory pigments at Throop on the Stour River. The numbers and dash lines shown above the HPLC pigment plots identify a series of chlorophyll events. Accessory pigment abbreviations are as in Table 2-2.

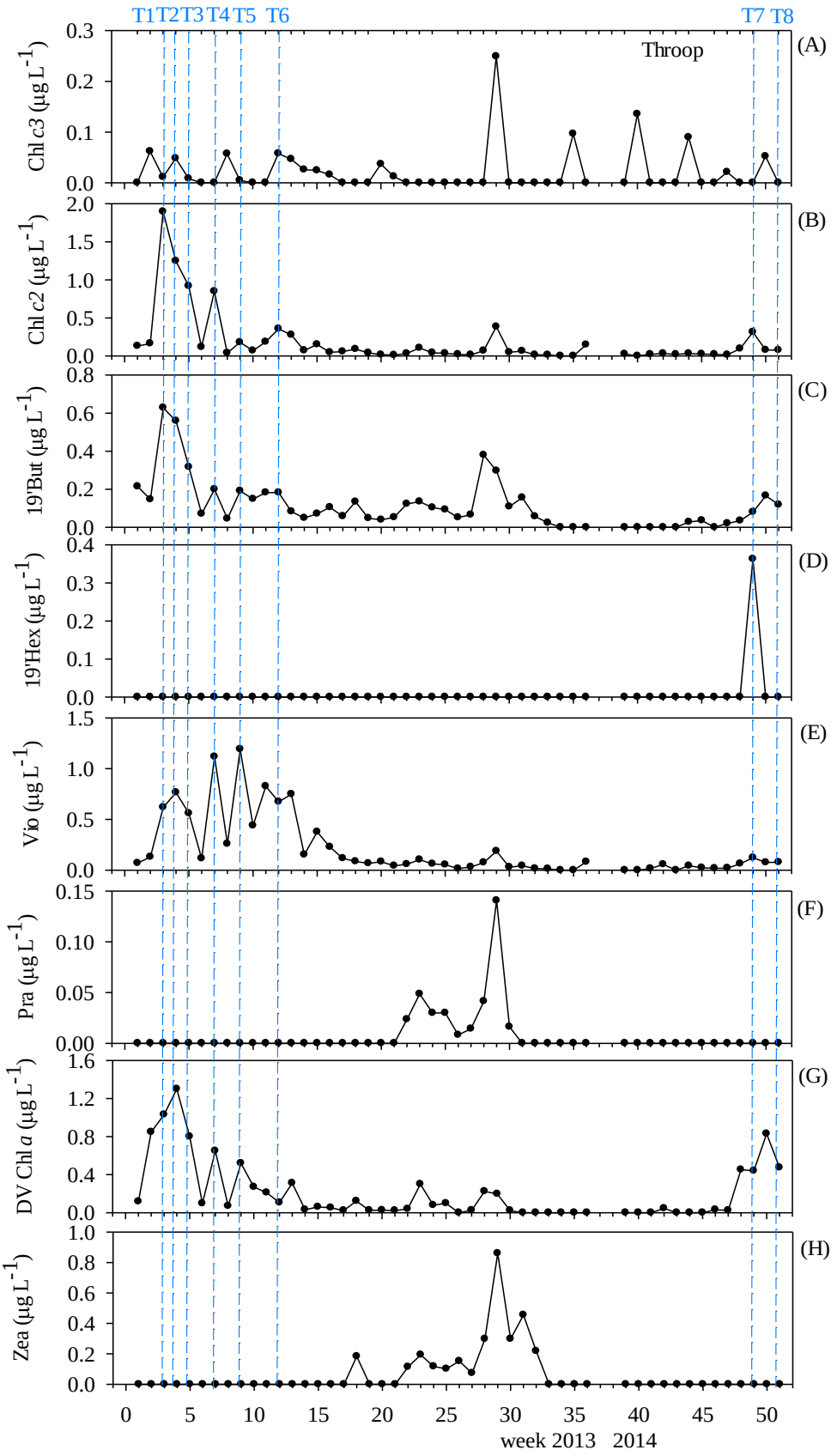


Figure 3-19: Temporal distributions of chlorophyll *a* and minor accessory pigments at Throop on the Stour River. The numbers and dash lines shown above the

HPLC pigment plots identify a series of chlorophyll events. Accessory pigment abbreviations are as in Table 2-2.

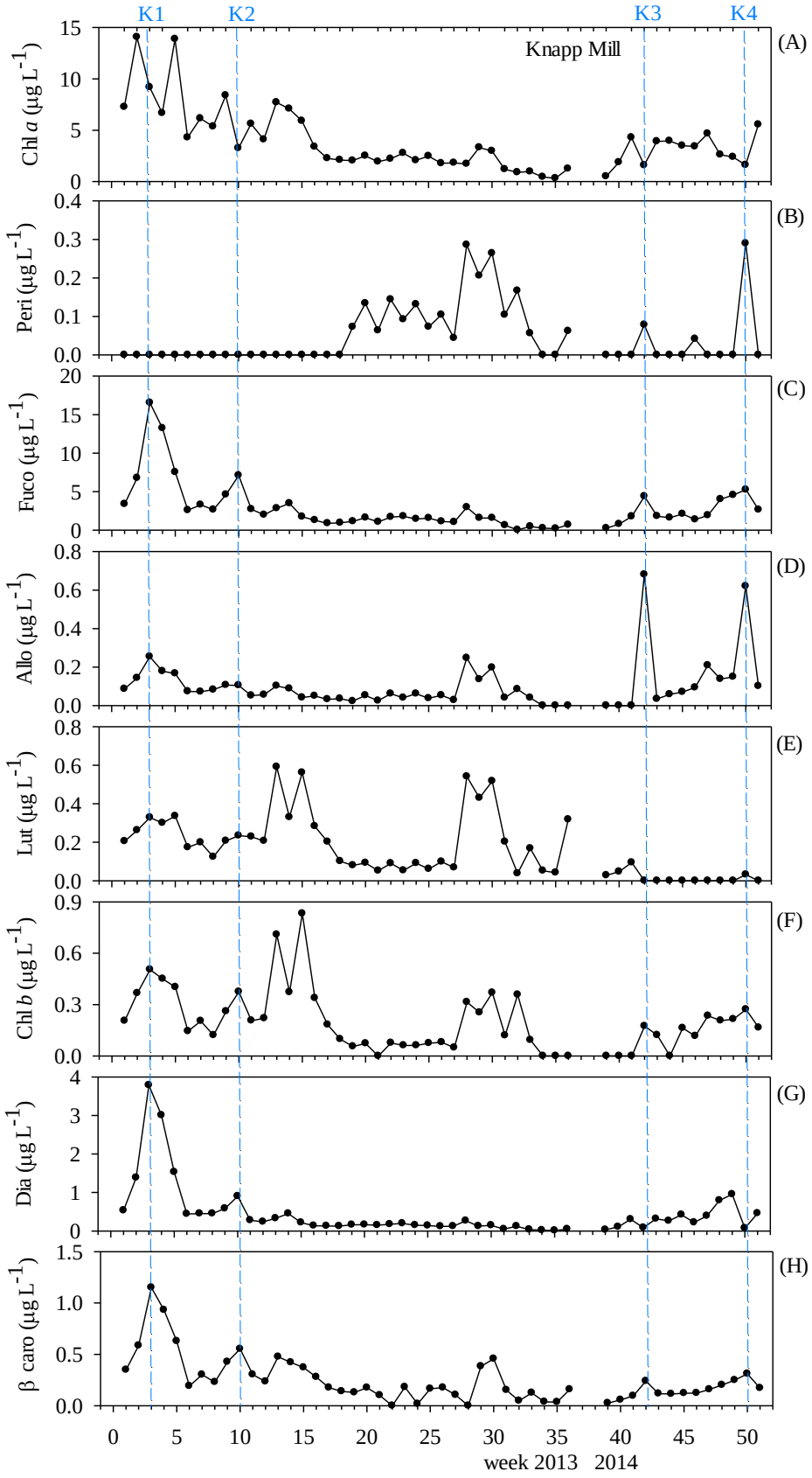

Figure 3-20: Temporal distributions of chlorophyll *a* and major accessory pigments at Knapp Mill on the Hampshire Avon River. The numbers and dash lines shown above the HPLC pigment plots identify a series of chlorophyll events. Accessory pigment abbreviations are as in Table 2-2.

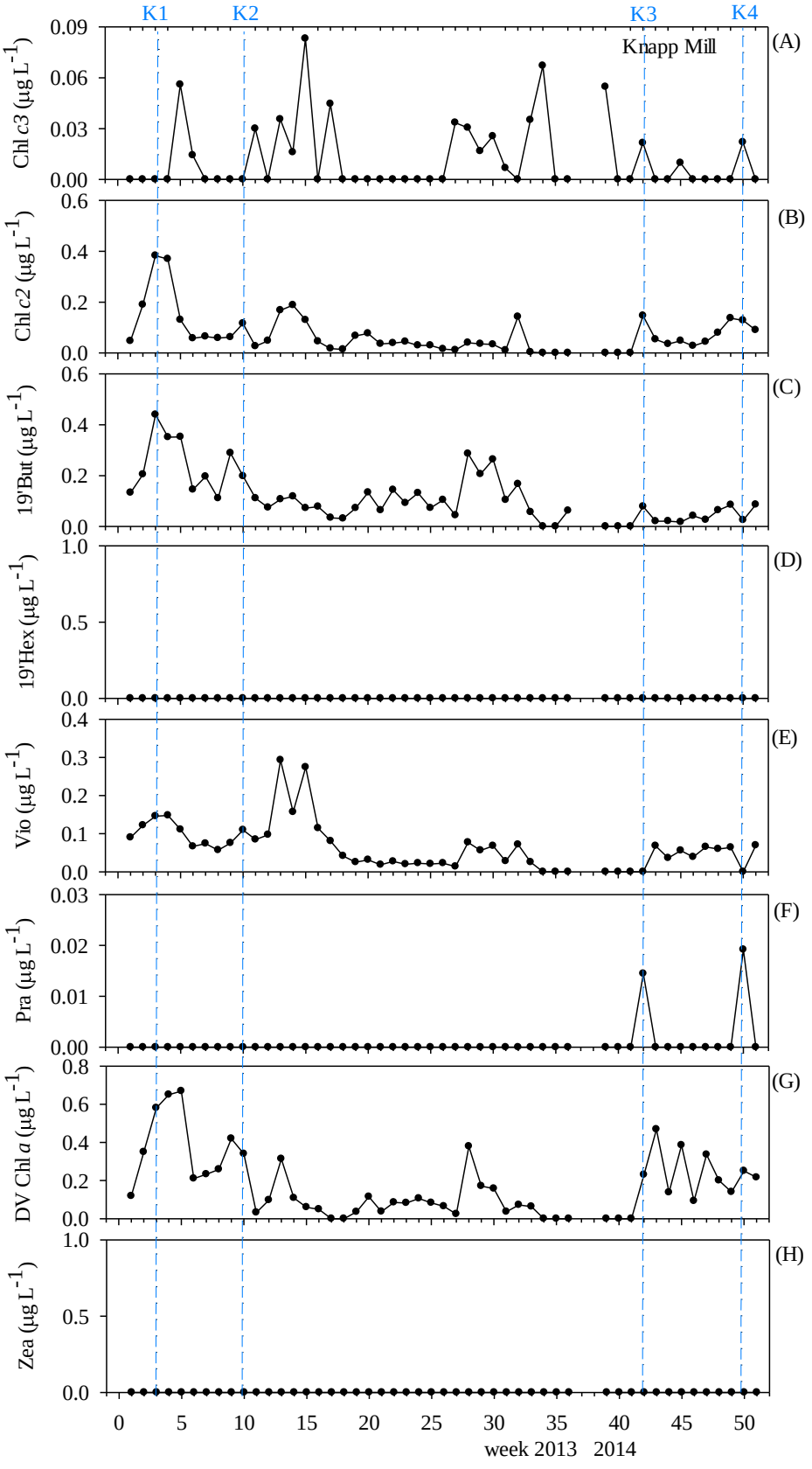

Figure 3-21: Temporal distributions of chlorophyll *a* and minor accessory pigments at Knapp Mill on the Hampshire Avon River. The numbers and dash lines shown above the HPLC pigment plots identify a series of chlorophyll events. Accessory pigment abbreviations are as in Table 2-2.

***Throop, River Stour***

Considering ratios of major accessory pigments to chlorophyll *a* (Chl *a*) for all samples from Throop, peridinin to Chl *a* ratio (Peri:Chl *a*) showed small values from September to November 2013, and was below 0.2, while ratios were zero during the rest of year (Figure 3-22 A). The fucoxanthin to Chl *a* ratio (Fuco:Chl *a*) showed consistently high values from May 2013, and were above 1, and up to 1.4 initially in this month and later up to 2.9 on 27th March 2014 (Figure 3-22 B). These high fucoxanthin to Chl *a* ratios were consistent with a high biomass of *Stephanodiscus* sp., that developed during spring 2013. Diadinoxanthin to Chl *a* ratios (Dia:Chl *a*) followed the same temporal distribution as fucoxanthin to Chl *a* ratios, indicating that diatoms were the dominant group associated with this pigment at Throop (Figure 3-22 F). Alloxanthin to Chl *a* ratios (Allo:Chl *a*) were low during most of the sampling period reaching peak values of 0.14 occasionally e.g. on 20th June 2013 (week 10, Figure 3-22 C). Lutein to Chl *a* ratios (Lut:Chl *a*) were lower than 1 throughout the sampling period, except on 17th December 2013 and 15th January 2014 (week 36 and 39, 1.7 and 1.3 respectively) and coincided with high abundances of chlorophytes (Figure 3-22 D). Chl *b* to Chl *a* ratios varied between zero and 0.8 and were in general higher in June 2013 (Figure 3-22 E) during the chlorophyll event of T4 and T5 at Throop. β carotene to Chl *a* ratios were in general lower than 0.3, except on 17th December 2013 (week 36), when this ratio was 0.5 (Figure 3-22 G).

In general, the ratio of minor accessory pigments to Chl *a* for all samples at this site were low as shown in Figure 3-23. Chl *c3* to Chl *a* ratios were low during most part of the sampling period and reached peak values of 0.3 occasionally e.g. on 9th December 2013 and 23rd January 2014 (week 35 and 40, Figure 3-23 A). Chl *c2* to Chl *a* ratios were lower than 0.2 while peak values occurring at the same time as the chlorophyll events, where this ratio was 0.2 and 0.1 and coincided with high abundance of diatoms (Figure 3-23 B). 19'But to Chl *a* ratios were quite variable at Throop (Figure 3-23 C). 19'Hex to Chl *a* ratios were generally zero, although one peak was observed of 0.1 on 27th March 2014 (week 49, Figure 3-23 D). Violaxanthin to Chl *a* (Vio:Chl *a*) and divinyl Chl *a* to Chl *a* (DV Chl *a*:Chl *a*) ratios were quite variable but were higher on similar dates (Figure 3-23 E, G).

Prasinoxanthin to Chl *a* (Pra:Chl *a*) and zeaxanthin to Chl *a* (Zea:Chl *a*) ratios were only detected from September to November 2013 (week 22 – 32, Figure 3-23 F, H).

***Knapp Mill, River Hampshire Avon***

The ratio of accessory pigments to Chl *a* for all samples at Knapp Mill showed lower values than at Throop, except fucoxanthin to Chl *a* ratios (Fuco:Chl *a*) that showed high values during each chlorophyll event (Figure 3-24). The peridinin to Chl *a* ratios showed values of zero from April 2013 to March 2014 (week 50) as shown in Figure 3-24 A. Peaks in Fucoxanthin to Chl *a* ratios followed the chlorophyll events (K2 – 4), when the ratio value was over 2, coinciding with an abundance of diatoms (Figure 3-24 B). Alloxanthin to Chl *a* ratios ranged between zero and 0.4 throughout the sampling period at this site, and higher values were detected during the K3 and K4 events (Figure 3-24 C). Lutein to Chl *a* and Chl *b* to Chl *a* ratios ranged between zero and 0.3, and were on average 0.04 and 0.6 respectively (Figure 3-24 D, E). Diadinoxanthin to Chl *a* ratios ranged between 0.04 and 0.5 throughout the sampling period. Between 28$^{th}$ June 2013 and 13$^{rd}$ March 2014 (week 11 – 47) this ratio was quite constant at below 0.2 (Figure 3-24 F). β carotene to Chl *a* ratios varied during most of the period studied, and maximum values were found at the same time as the peak chlorophyll events occurred (Figure 3-24 G).

The high values of ratios of minor accessory pigments to Chl *a* were generally detected following the four chlorophyll peak events (K1 – 4), however, the highest values of each pigment to Chl *a* ratios showed different timing with the events (Figure 3-25). In contrast to Throop, Chl *c3* to Chl *a* ratios showed similar patterns and the ratios considerably increased in December 2013 with a peak value of 0.2 detected on 2$^{nd}$ December 2013 (week 34) as shown in Figure 3-25 A. Chl *c2* to Chl *a* and 19'But to Chl *a* ratios had maximum values of 0.16 and 0.18 respectively on 18$^{th}$ November 2013 (week 32, Figure 3-25 B, C). Violaxanthin to Chl *a* and divinyl Chl *a* to Chl *a* ratios ranged between zero and 0.08, and zero and 0.2 respectively (Figure 3-25 E, G). Prasinoxanthin to Chl *a* ratios had small values during the K3 and K4 events (Figure 3-25 F). 19'Hex and zeaxanthin to Chl *a* ratios were zero as these pigments were undetected throughout the study period at Knapp Mill (Figure 3-25 D, H).

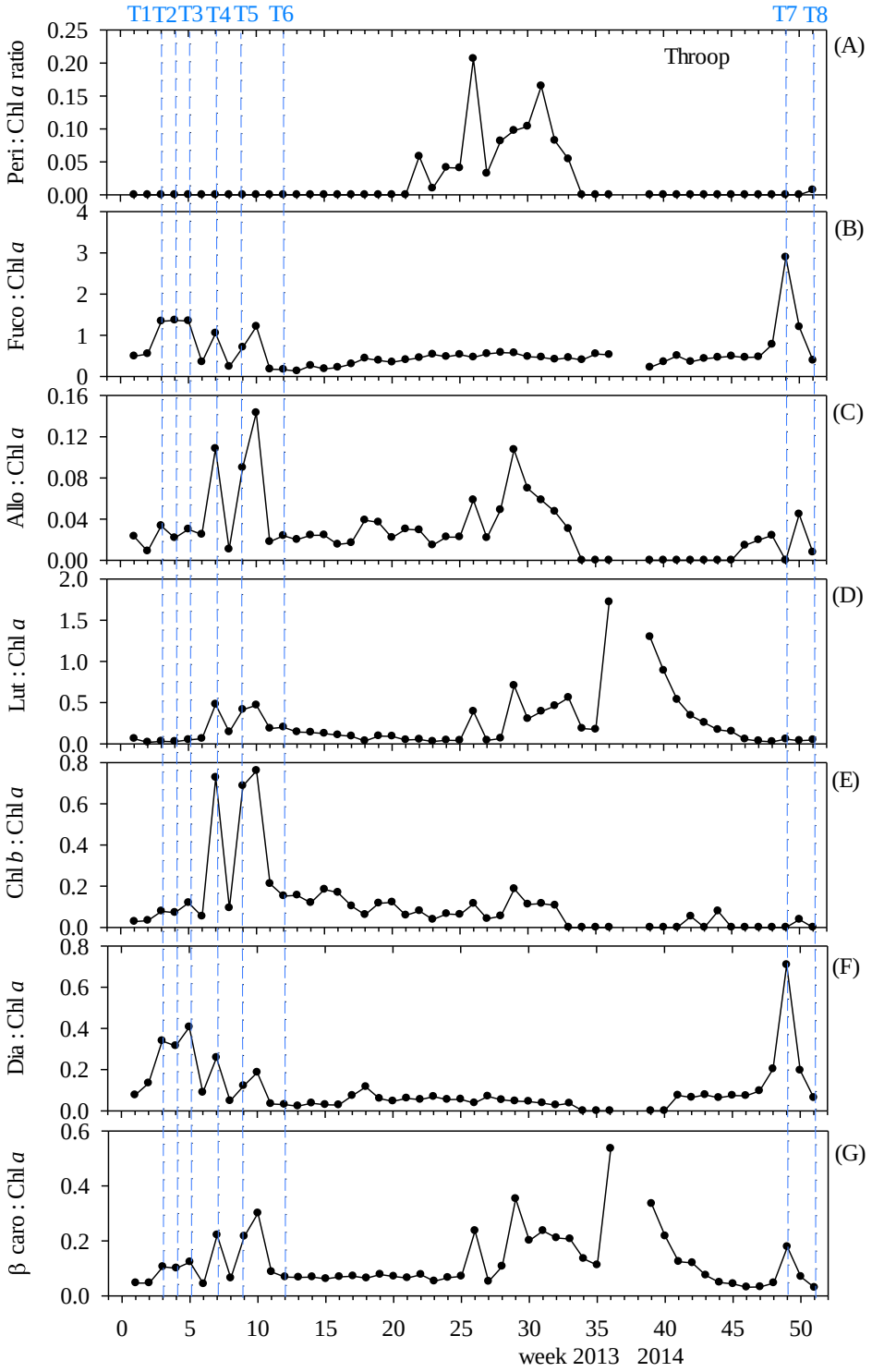


Figure 3-22: Temporal and spatial distributions of major accessory pigment to chlorophyll *a* ratios at Throop. The numbers and dash lines shown above the HPLC pigment plots identify a series of chlorophyll events. Accessory pigment abbreviations are as in Table 2-2.

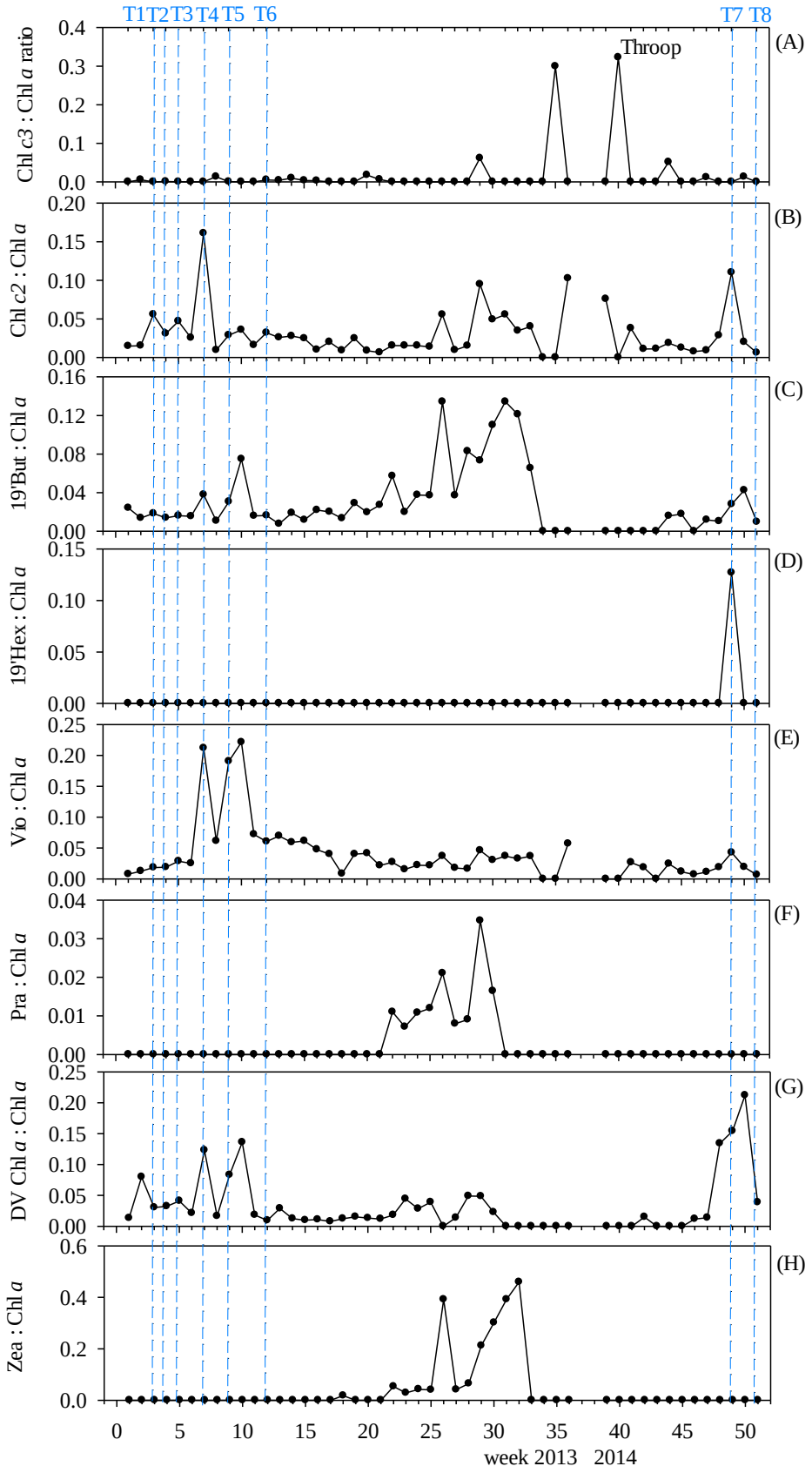


Figure 3-23: Temporal and spatial distributions of minor accessory pigment to chlorophyll *a* ratios at Throop. The numbers and dash lines shown above the HPLC

pigment plots identify a series of chlorophyll events. Accessory pigment abbreviations are as in Table 2-2.

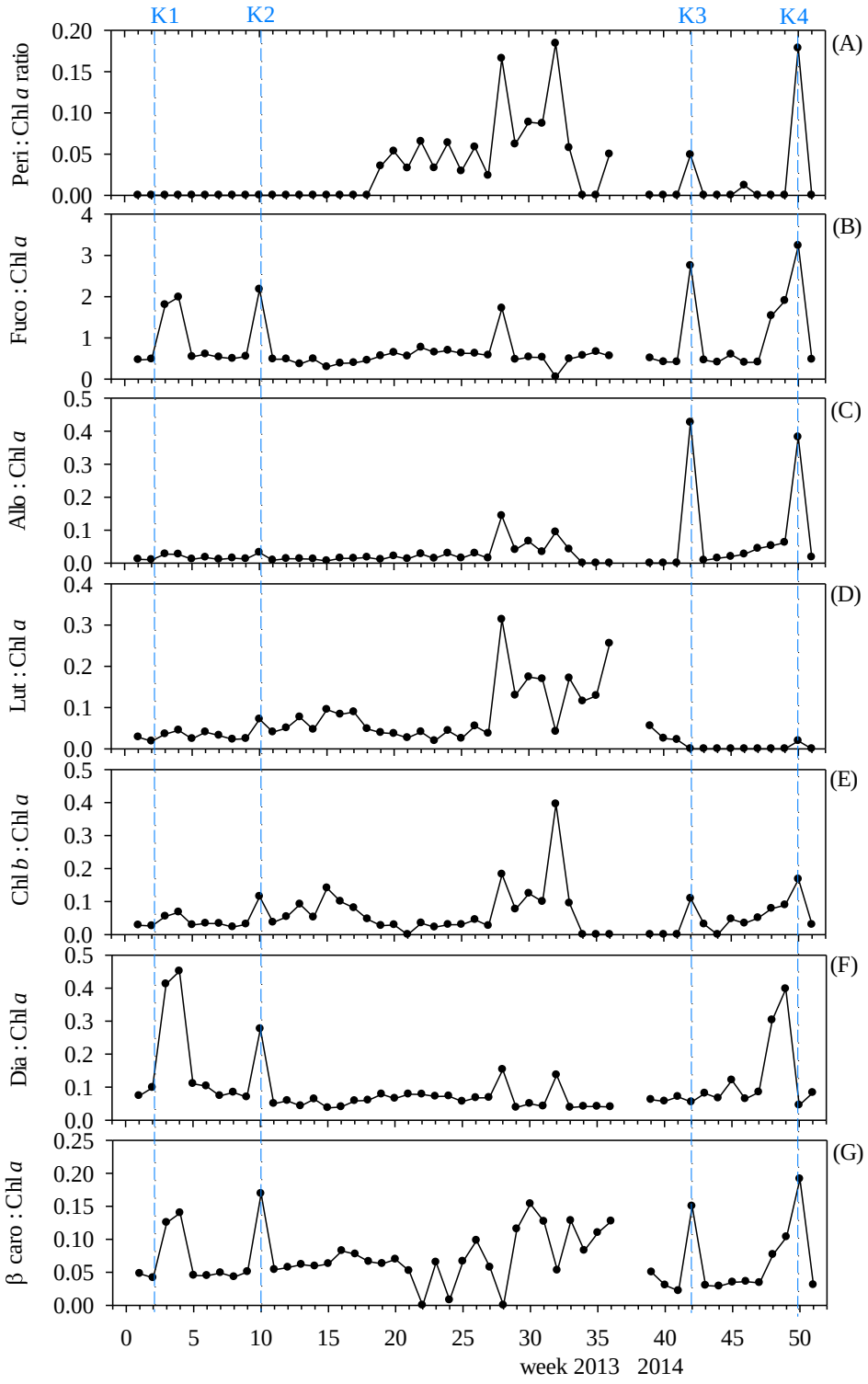


Figure 3-24: Temporal and spatial distributions of major accessory pigment to chlorophyll *a* ratios at Knapp Mill. The numbers and dash lines shown above the HPLC pigment plots identify a series of chlorophyll events. Accessory pigment abbreviations are as in Table 2-2.

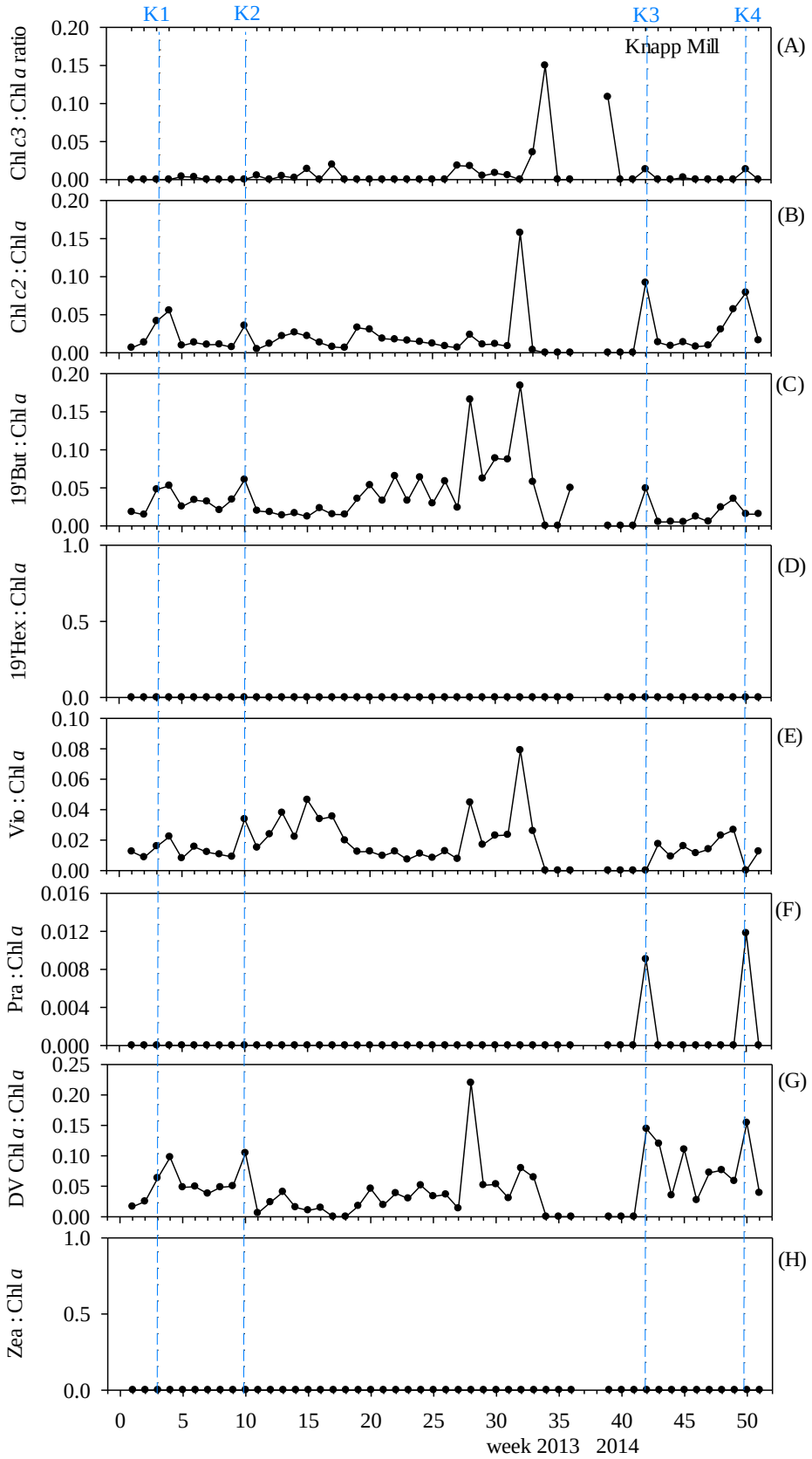


Figure 3-25: Temporal and spatial distributions of minor accessory pigment to chlorophyll *a* ratios at Knapp Mill. The numbers and dash lines shown above the HPLC pigment plots identify a series of chlorophyll events. Accessory pigment abbreviations are as in Table 2-2.

### 3.3.3 Phytoplankton taxonomic data

Cell counts of separate phytoplankton can provide useful data on the community of individual organism genera or species, and can be used to monitor the seasonal change in a particular species distribution. Species counts give information on phytoplankton abundance which can be converted to bio-volume ($\mu m^3$) and the cell carbon (µg C) as an approximate for phytoplankton biomass in the water column. In the present study the microscopic cell count (cells $mL^{-1}$), bio-volume ($\mu m^3$ $mL^{-1}$), and phytoplankton carbon biomass (µg C $L^{-1}$) were used to investigate the changes in the annual pattern of riverine phytoplankton community in the lower reaches of on the Stour and Hampshire Avon Rivers.

#### 3.3.3.1 Phytoplankton cell abundance

Riverine phytoplankton abundance on both rivers during the sampling period from April 2013 to April 2014 consisted of at least 37 diatom species, 13 chlorophytes, 2 cryptophytes, 2 cyanophytes, 2 chrysophytes, ~1 photosynthetic dinoflagellate species, and 3 ciliates. A gradient of increasing total abundance was observed from spring to summer. The phytoplankton abundances are respectively shown in Figure 3-26, Figure 3-28, and Figure 3-29 as percentage values of total cell count throughout the sampling period at Throop and Iford Bridge on the Stour River and Knapp Mill on the Hampshire Avon River.

***Throop, River Stour***

The dominant phytoplankton group was generally the diatoms, except during summer months (week 8 to 18) when chlorophytes represented the dominant group and accounted for over 50% of the total phytoplankton as shown in Figure 3-26 B. During the spring bloom events in May 2013, when the chlorophyll *a* concentration was > 60 µg $L^{-1}$ (week 3 to 5), the centric diatom *Stephanodiscus* sp. was the dominant species with a cell density of over $4.4 \times 10^4$ cells $mL^{-1}$ (Figure 3-27). A high abundance of cyanophyte species occurred after the spring diatom bloom and these were the dominant group in week 6 and 7. The small chlorophyte species, *Chlamydomonas* spp., occurred in high abundance ($1.9 – 7.9 \times 10^4$ cells $mL^{-1}$) after this diatom and cyanophyte bloom during the summer months and then the diatom group again became the main phytoplankton at Throop. In general, particularly cryptophytes, ciliates, and chrysophytes occurred together; these groups dominated from the late summer months in small proportions. Dinoflagellate populations

were found on some sampling dates after the chlorophyte bloom in summer (Figure 3-34 B).

In spring samples (week 1 – 7 and 46 – 51), the range of total phytoplankton abundance were 1.6 – 46.4 × $10^3$ and 0.5 – 5.3 × $10^3$ cells $mL^{-1}$ (spring 2013 and 2014) respectively. The monospecific bloom of the diatom *Stephanodiscus* sp. showed peaks in week 3 to 5 or chlorophyll events T1 – 3, reaching 44.0 × $10^3$ cells $mL^{-1}$ as shown in Figure 3-26 A and then a marked increase of cyanophyte species in week 6 to 7 was observed reaching 28.4 × $10^3$ cells $mL^{-1}$. From mid-April to end of March 2013, the range of total abundance was 1.6 – 46.4 × $10^3$ cells $mL^{-1}$ while from early March to mid-April 2014, lower total cell abundances were observed between 0.5 – 5.3 × $10^3$ cells $mL^{-1}$. During spring 2014, a bloom of the diatom *Stephanodiscus* sp. reached a cell abundance up to 3.3 × $10^3$ cells $mL^{-1}$ (week 49, T7). This bloom was of a much lower abundance than the spring bloom in 2013, but this diatom was still the dominant species.

In summer samples (week 8 – 20), the total abundance varied between 0.9 × $10^3$ and 85.1 × $10^3$ cells $mL^{-1}$. The highest abundance was higher than the spring peak by around twofold. The contribution of chlorophyte species became more important as a dominant group throughout most of the summer but at the end of the summer months, the diatom population again dominated together with the chlorophytes. As phytoplankton replicate in time scales ranging from hours to days then over the space of a week many changes in the composition may have occurred and subsequently might be missed in a weekly survey. From early June to mid-July 2013 (week 8 – 14), a chlorophyte bloom of *Chlamydomonas* sp. ranged in density from 19.3 – 79.9 × $10^3$ cells $mL^{-1}$. Two chlorophyll events (T5 and T6) were also observed in this season in week 9 and 12 with total abundances of 36.8 × $10^3$ and 85.1 × $10^3$ cells $mL^{-1}$, respectively. *Rhodomonas* sp. was observed along with other dominant species at the same time as this *Chlamydomonas* sp. bloom with densities between 0.3 × $10^3$ and 4.9 × $10^3$ cells $mL^{-1}$. Following the last week of July 2013 (week 8 – 15), a much lower total cell abundance was observed although chlorophyte and cryptophyte groups were still the dominant populations at that time. Following this these groups were replaced by the diatom population between week 16 and 20.

In the autumn samples (week 21 – 33), total abundance was monitored with a range of 0.2 – 2.5 × $10^3$ cells $mL^{-1}$. The diatom population was still the dominant group but with a lower density during this season. No bloom abundance of species was observed in any of

the autumn samples. Some phytoplankton species were absent several times during the autumn period, particularly dinoflagellate species.

In the winter samples (week 34 – 45), total density reached a lowest overall abundance of 28 cells $mL^{-1}$ on 30th December (week 37) and a peak cell abundance of only 569 cells $mL^{-1}$. Diatoms were still the most abundant species followed by cryptophytes, chlorophytes, and cyanophytes, respectively. The spring diatom bloom *Stephanodiscus* sp. showed gradually increasing cell numbers from 7 cells $mL^{-1}$ in week 34 to 72 cells $mL^{-1}$ in week 45. This monitoring period occurred during the high river discharge that started in week 36 at 51 $m^3$ $s^{-1}$ and up to 112 $m^3$ $s^{-1}$ on 17th December 2013 (week 38).

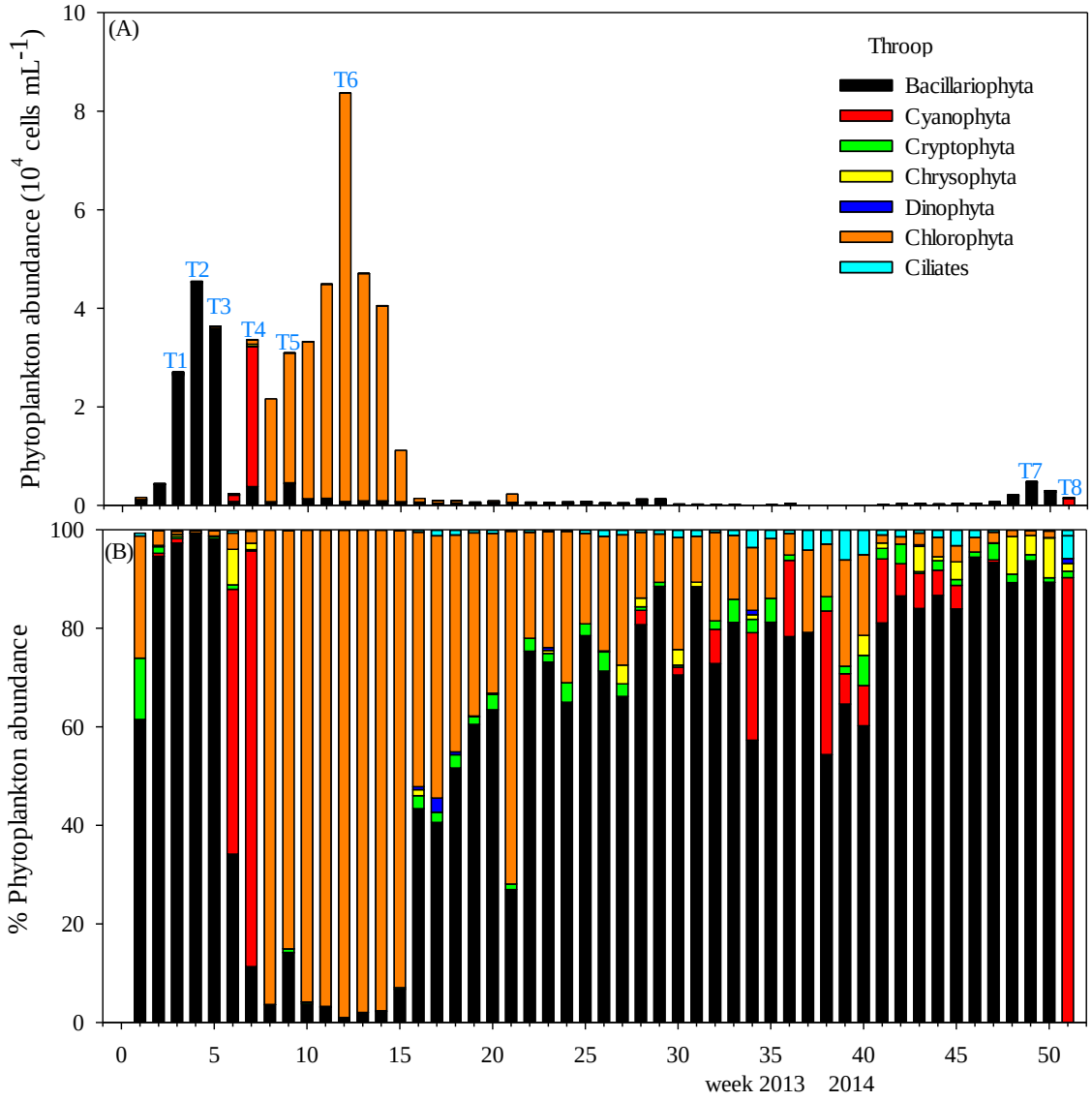


Figure 3-26: Distributions of abundance and cell count percentage for main phytoplankton groups at Throop during April 2013 – April 2014. The letters and numbers shown above the abundance bars identify a series of chlorophyll *a* events.

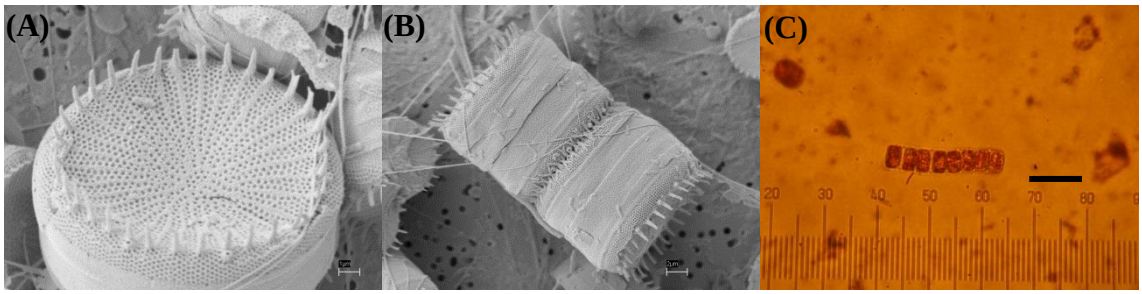


Figure 3-27: Images of the centric diatom *Stephanodiscus* sp. as observed by (A and B) scanning electron microscopy and (C) light microscopy. Scale bars are 1, 2, and 50 µm respectively.

***Iford Bridge, River Stour***

Iford Bridge on the Stour River is between Throop and the estuary and was chosen as it is directly downstream of the main sewage input into the river. This site was sampled at weekly intervals from 6th June 2013. The pattern of phytoplankton community at this site was generally similar to Throop but the percentage of cryptomonad and cyanophyte groups were found to be higher than at Throop (Figure 3-28).

In the spring samples (week 46 – 51), the range of total phytoplankton abundance were 0.4 – 4.5 × $10^3$ cells $mL^{-1}$ and the abundance variability was similar to Throop during this period. The centric diatom, *Stephanodiscus* sp. was the dominant species during spring 2014, apart from 27th March 2014 (week 49, I3), when its density was 2.5 × $10^3$ cells $mL^{-1}$. The pennate diatom, *Navicula gracilis* was the second most abundance organism at 749 cells $mL^{-1}$. On this day, high abundances of *Rhodomonas* sp. (249 cells $mL^{-1}$) were recorded as well as *Cryptomonas* sp. (130 cells $mL^{-1}$). *Dinobryon* sp. was also observed at around 200 cells $mL^{-1}$ in week 49 and 50.

In the summer samples (week 8 – 20, Figure 3-28 A), the total cell abundance varied between 0.9 × $10^3$ and 79.5 × $10^3$ cells $mL^{-1}$. The chlorophyte, *Chlamydomonas* sp. was the dominant species during this season, reaching 73.4 × $10^3$ cells $mL^{-1}$ on 4th July 2013 (week 12, I3) as shown in Figure 3-28 A. A small chlorophyte cell, *Chlorella* sp. was also abundant (3.7 × $10^3$ cells $mL^{-1}$) in week 11. A large chlorophyte, *Scenedesmus* spp. was abundant (2.6 × $10^3$ cells $mL^{-1}$) on 23rd July 2013 (week 15). The first chlorophyll event on 14th June 2013 (week 9, I1) was dominated by *Chlamydomonas* sp., *Rhodomonas* sp., and *Stephanodiscus* sp. (24.7, 8.1, and 4.1× $10^3$ cells $mL^{-1}$), respectively. *Rhodomonas* sp. was found in high numbers on 14th and 20th June 2013 (week 9 and 10), reaching 8.1 and 9.1 × $10^3$ cells $mL^{-1}$ respectively, while *Cryptomonas* sp. peaked in week 10 with an abundance

of 1.9 × $10^3$ cells $mL^{-1}$. The total abundance of summer samples sharply decreased from 24.6 × $10^3$ to 5.0 × $10^3$ cells $mL^{-1}$ after week 15.

In the autumn samples (week 21 – 33), the range of phytoplankton abundance was between 0.2 × $10^3$ and 3.0 × $10^3$ cells $mL^{-1}$. Diatom and chlorophyte species continued to be the dominant populations during week 21 to 27. Several pennate diatoms were dominant particularly *Navicula* genera and cryptomonads were still observed with low abundance. A high abundance of the cyanophyte, *Pseudo-anabaena* sp. occurred at about 1.4 × $10^3$ cells $mL^{-1}$ on 9th December 2013 (week 28). By 24th October 2013 (week 28), total cell number was higher at 1.0 × $10^3$ cells $mL^{-1}$, but on 30th October 2013 a much lower phytoplankton abundance was observed (488 cells $mL^{-1}$).

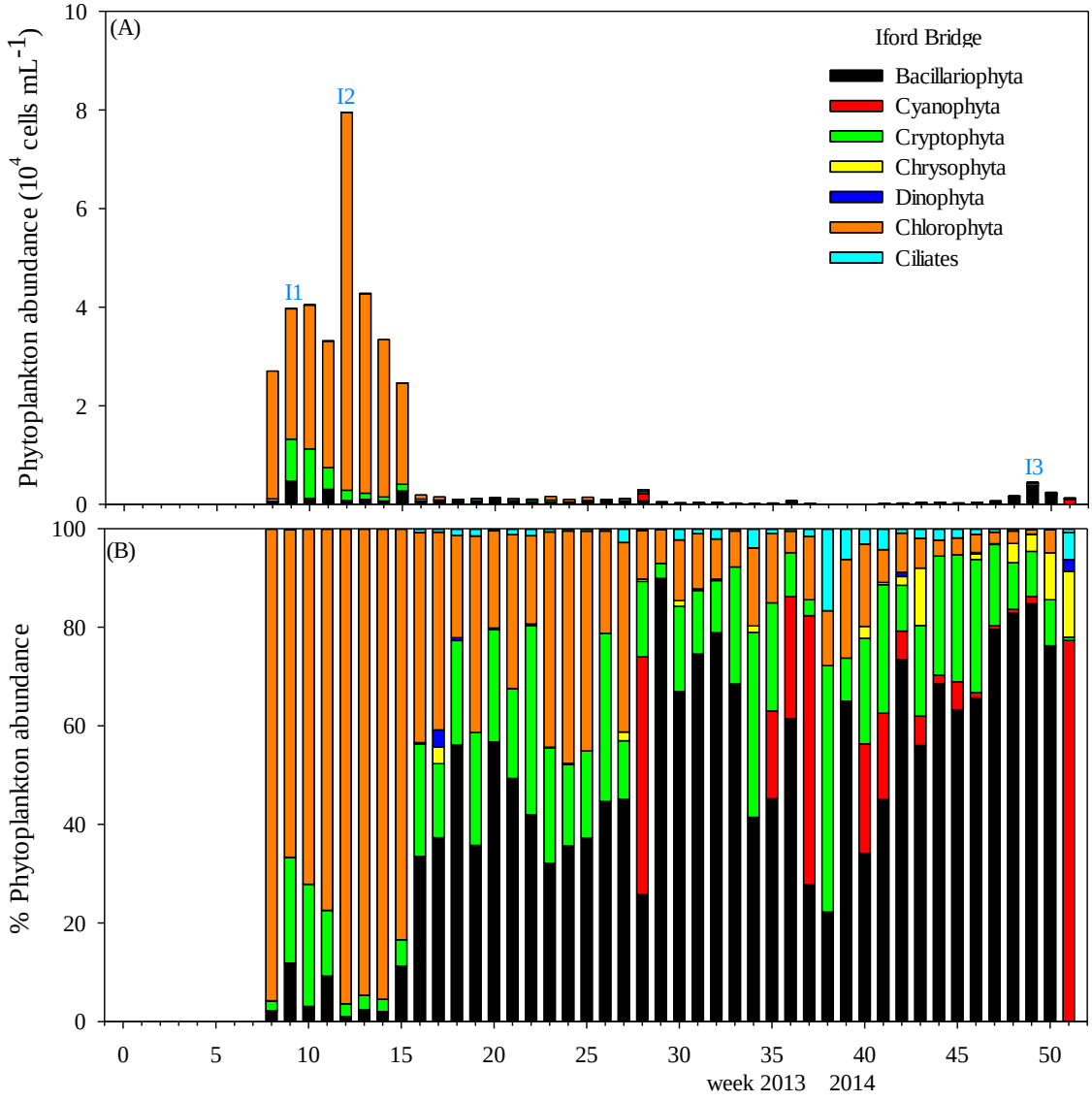


Figure 3-28: Distributions of abundance and cell count percentage for main phytoplankton groups at Iford Bridge during June 2013 – April 2014. The letters and numbers shown above the abundance bars identify a series of chlorophyll *a* events.

In the winter samples (week 34 – 45) total abundance varied between 21 and 723 cells $mL^{-1}$. A high percentage of cyanophyte community was found in this period compared with others season (Figure 3-28 B). Cryptophyte populations were a higher percentage of the total population in the winter. The spring diatom bloom of *Stephanodiscus* sp. showed low cell numbers when compared to Throop during this time.

***Knapp Mill, River Hampshire Avon***

In general, at Knapp Mill the dominant group was the diatoms, representing over 60% of the total phytoplankton counted, followed by the chlorophyte and cryptophyte populations. The chlorophyte group became the main phytoplankton group during the summer months as was also found at Throop and Iford Bridge on the River Stour. The cryptomonad community was more abundant in the summer period than during the other seasons as shown in Figure 3-29 A and B. *Stephanodiscus* sp. was also the bloom species as it was at Throop during spring 2013, but was lower in cell numbers in comparison.

In the spring samples (week 1 – 7 and 46 – 51), the range of total phytoplankton abundance was 1.9 – 6.2 × $10^3$ cells $mL^{-1}$ and 1.0 – 3.3 × $10^3$ cells $mL^{-1}$ (spring 2013 and 2014) respectively. Total abundance showed lower cell numbers than at Throop during both spring periods. The centric diatom, *Stephanodiscus* sp. was also the dominant species in spring 2013 as at Throop with a range of 1.3 – 3.8 × $10^3$ cells $mL^{-1}$ during week 1 to 5. The first chlorophyll event was on 3rd May 2013 (week 3, K1) with the highest dominance of *Stephanodiscus* sp. at 3.8 × $10^3$ cells $mL^{-1}$. The *Stephanodiscus* sp. density at this sampling site was however around sixfold lower compared to its density at Throop. The next chlorophyll event during the spring season was found on 4th April 2014 (week 50, K4) with a total abundance of 3.0 × $10^3$ cells $mL^{-1}$. During the spring months in 2013, *Rhodomonas* sp. and *Scenedesmus* spp. were observed at around 217 and 245 cells $mL^{-1}$, while *Scenedesmus* spp. became a rare species during spring 2014 and *Rhodomonas* sp. was still found in abundances close to those of spring 2013.

In the summer samples (week 8 – 20), the total abundance varied between 1.1 × $10^3$ and 22.8 × $10^3$ cells $mL^{-1}$. The abundance of the chlorophyte *Scenedesmus* spp. was over 1.0 × $10^3$ cells $mL^{-1}$ in July 2013 (week 12 – 15) and *Coelastrum* sp. was also over 1.0 × $10^3$ cells $mL^{-1}$ in week 14 to 15. On 20th June 2013 (week 10, K2) was the second chlorophyll event with a total phytoplankton abundance of 3.0 × $10^3$ cells $mL^{-1}$. *Navicula gracilis*, *Navicula* spp., and *Stephanodiscus* sp. became the dominant diatom species in week 10.

On 17th July 2013 (week 14), the centric diatom *Stephanodiscus* sp. was counted at 17.8 × $10^3$ cells $mL^{-1}$ but total chlorophyll *a* was relatively low in concentration about 9.5 µg $L^{-1}$.

In the autumn samples (week 21 – 33), the range of phytoplankton abundance was 0.8 – 2.1 × $10^3$ cells $mL^{-1}$. The diatom species were the dominant population followed by the chlorophyte and cryptophyte populations, respectively. The abundance of *Cocconeis* spp., *Navicula gracilis*, and *Navicula* spp. showed these were the main diatom species with a density less than 500 cells $mL^{-1}$.

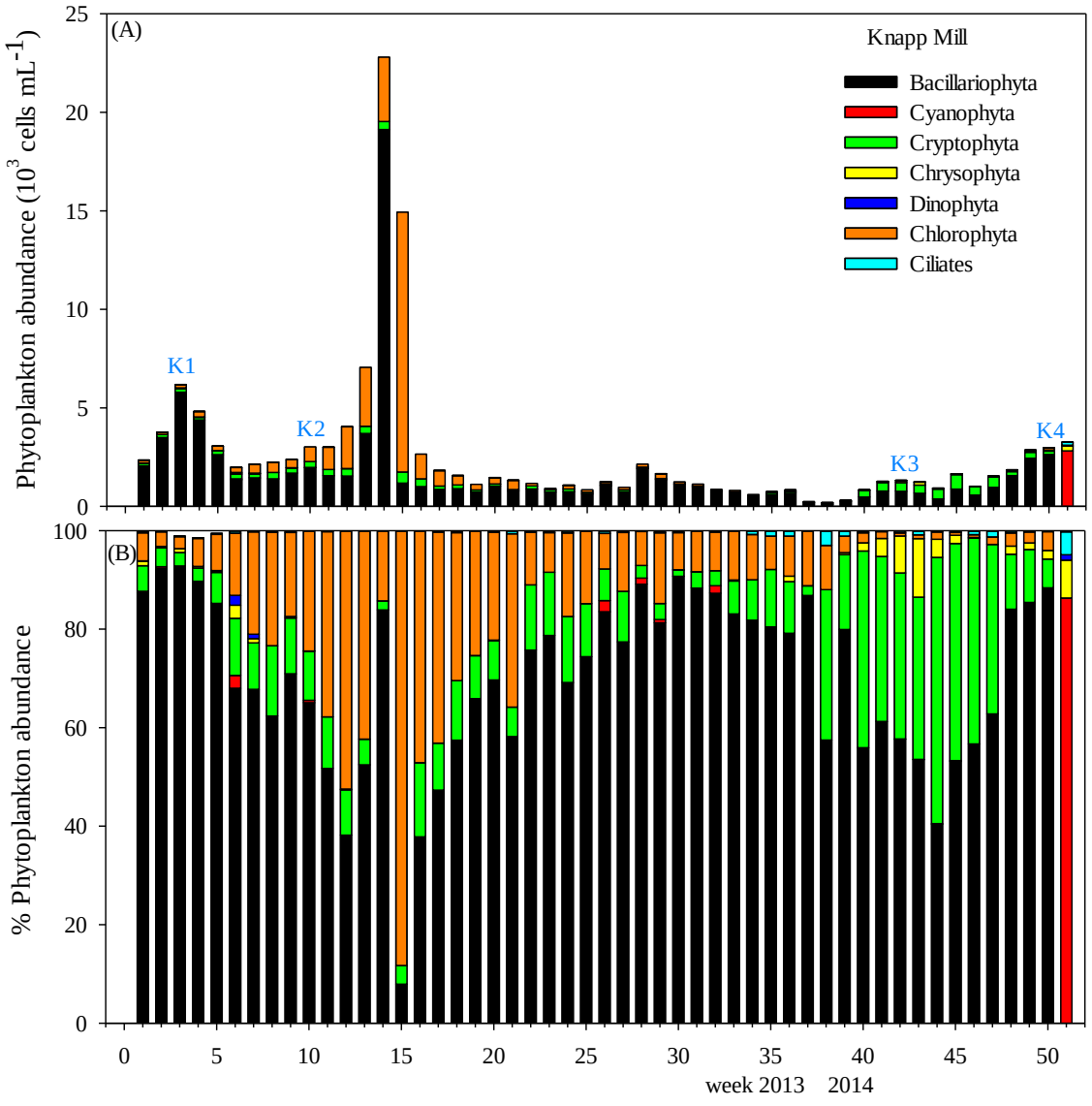


Figure 3-29: Distributions of abundance and cell count percentage for main phytoplankton groups at Knapp Mill during April 2013 – April 2014. The letters and numbers shown above the abundance bars identify a series of chlorophyll *a* events.

In the winter samples (week 34 – 45) total abundance ranged from 196 – 1654 cells $mL^{-1}$. The diatoms were still the most abundant species followed by cryptophytes, chlorophytes,

and cyanophytes respectively as was observed at Throop. This survey period coincided with the high river discharge that started in week 37 at 54 $m^3 s^{-1}$ and reached up to 94 $m^3 s^{-1}$ on 7th January 2014 (week 38).

#### 3.3.3.2 Phytoplankton bio-volume and carbon biomass

Phytoplankton carbon biomass (µg C $L^{-1}$) was calculated from cell volumes for the main species present in the rivers (see Section 2.7). Table 3-2 lists the length and width measurements, cell bio-volume and carbon content of species from the Stour and Hampshire Avon Rivers. The distribution of carbon biomass during the whole monitoring period at all riverine stations is shown in Figure 3-30, Figure 3-31, and Figure 3-32. These analyses show that the larger cells are more important when considered in terms of carbon biomass than indicated by the microscopic cell counts alone. The increase in diatom carbon biomass was accompanied by increases in the other large cells (cryptophytes) and also by higher total biomass, as measured by chlorophyll.

Measured chlorophyll *a* concentration and estimated phytoplankton carbon were positively correlated (Figure 3-33). Total carbon biomass was observed at all stations, and the best fit was found to be between total chlorophyll and total carbon biomass as shown in Figure 3-33. The slopes of the relationship give total carbon to chlorophyll *a* ratios of 38.7 as shown in Figure 3-33 and are similar to a range of 10 – 70 reported for the Southampton Water (Ali, 2003; Altisan, 2006), but the ratio of this study is lower than from what would be expected from the literature (e.g. The ratio is 51 at San Francisco Bay, Wienke and Cloern (1987)).

*Stephanodiscus* sp. was among the most abundant species at Throop during the spring bloom (week 3 – 5) as shown in Figure 3-30. Although this species was an important component of the phytoplankton population, it does not contribute highly to the phytoplankton carbon in other periods because of its small size (Table 3-2). Phytoplankton with cell sizes of over 20 µm in length were not important in terms of abundance, however, contribute greatly to the total bio-volume and carbon biomass. As an example *Diatoma vulgare* was less abundant than *Stephanodiscus* sp. but because of its larger size, contributes greatly to the total carbon (Table 3-2).

Table 3-2: Examples of linear dimensions, cell bio-volume (µm$^3$) and carbon content of main phytoplankton species from the rivers.

| Species | Length (µm) | Width (µm) | Bio-volume (µm$^3$) | µg C cell$^{-1}$ |
|---|---|---|---|---|
| **Bacillariophyta** | | | | |
| *Amphora* sp. | 19.4 | 10.0 | 916 | 73 |
| Centric diatoms | 5.8 | 15.8 | 883 | 71 |
| *Cocconeis* sp. | 20.3 | 12.9 | 773 | 63 |
| *Diatoma vulgare* | 42.5 | 18.8 | 10009 | 505 |
| *Melosira* sp. | 20.6 | 20.0 | 6280 | 346 |
| *Nitzschia acicularis* | 20.1 | 4.6 | 109 | 13 |
| Pennate diatoms | 22.5 | 10.0 | 19625 | 873 |
| *Stephanodiscus* sp. | 11.9 | 10.2 | 1227 | 92 |
| **Cyanophyta** | | | | |
| *Merismopedia* sp. | 7.5 | 7.5 | 281 | 43 |
| *Pseudo-anabaena* sp. | 4.0 | 2.5 | 8 | 2 |
| **Cryptophyta** | | | | |
| *Cryptomonas* sp. | 17.6 | 11.1 | 1022 | 145 |
| *Rhodomonas* sp. | 7.5 | 5 | 184 | 29 |
| **Chrysophyta** | | | | |
| *Dinobryon* sp. | 11.6 | 5.0 | 164 | 26 |
| *Synura sphagnicola* | 11.1 | 8.6 | 294 | 45 |
| **Chlorophyta** | | | | |
| *Chlamydomonas* sp. | 4.6 | 2.5 | 100 | 16 |
| *Chlorella* sp. | 2.8 | 2.8 | 30 | 5 |
| *Scenedesmus* spp. | 10.4 | 4.4 | 212 | 33 |

***Throop, River Stour***

Total carbon biomass varied between 7 and 4542 µg C L$^{-1}$ and the mean value was 490 ± 979 µg C L$^{-1}$ (n=51). High phytoplankton biomass was observed on the Stour River, mainly because of the *Stephanodiscus* sp. bloom in May 2013. After this diatom bloom, a considerably lower phytoplankton biomass was recorded, however, the diatom community was still a dominant population throughout the monitoring programme. The increase in chlorophyte biomass was accompanied by an increase in other large cells particularly cryptophytes and also by higher total biomass as measured by chlorophyll as shown in Figure 3-30.

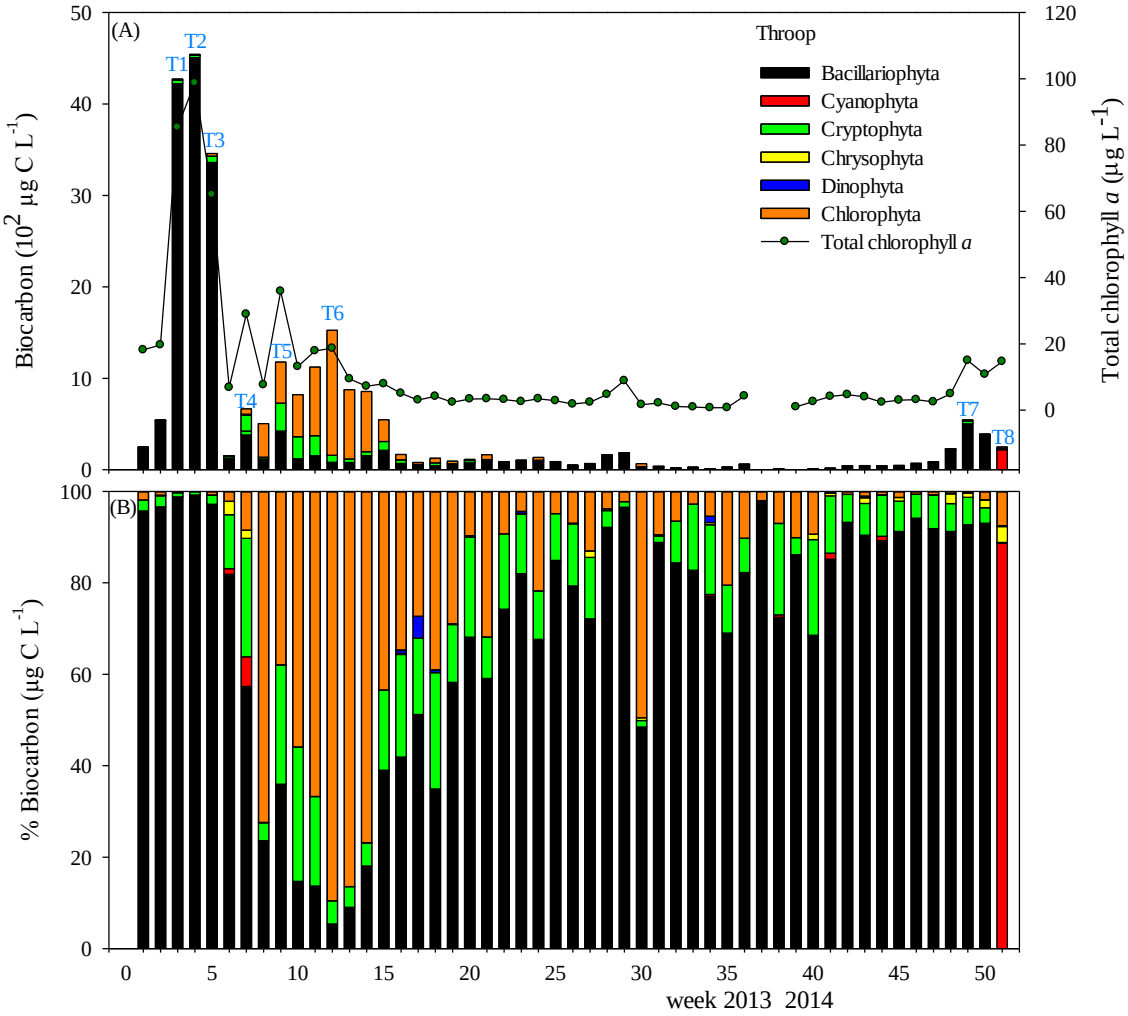


Figure 3-30: Distributions of carbon biomass and percentage for main phytoplankton groups at Throop during April 2013 – April 2014. The letters and numbers shown above the abundance bars identify a series of chlorophyll events.

***Iford Bridge, River Stour***

At this monitoring site, total carbon biomass varied from 2 to 1420 µg C $L^{-1}$ with a mean value of 249 ± 363 µg C $L^{-1}$ (n=44). The first peak of carbon biomass on 14$^{th}$ June 2013 was composed of diatoms, cryptomonads, and chlorophytes, while the second peak on 4$^{th}$ July 2013 (week 12, I2) was dominated by high biomass of chlorophyte species, *Chlamydomonas* sp. The last peak of biomass was measured on 27$^{th}$ March 2014 (week 49, I3) and consisted of two main diatom species, *Stephanodiscus* sp. and *Navicula gracilis*.

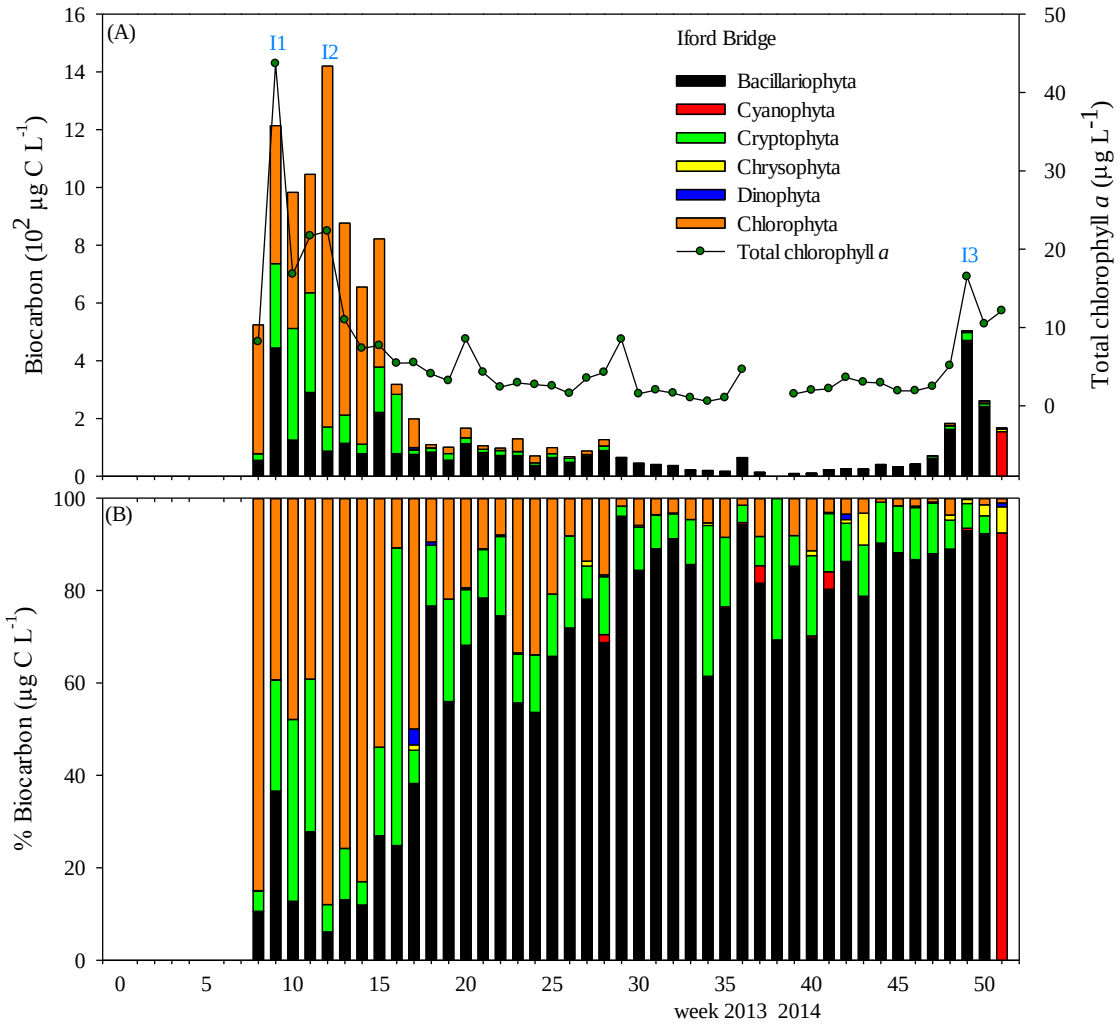


Figure 3-31: Distributions of carbon biomass and percentage for main phytoplankton groups at Iford Bridge during June 2013 – April 2014. The letters and numbers shown above the abundance bars identify a series of chlorophyll events.

***Knapp Mill, River Avon***

In general, total carbon biomass ranged from 24 to 1915 µg C $L^{-1}$ and the mean value was 263 ± 331 µg C $L^{-1}$ (n=51). The first peak of carbon biomass was observed on 3rd May 2013 (week 3, K1) and was mainly composed of the diatoms, *Diatoma vulgare* and *Stephanodiscus* sp., while the next peak in carbon biomass on 20th June 2013 (week 10, K2) is due to the pennate diatom, *Navicula gracilis*. On 17th July 2013 (week 14) a high peak of biomass was observed comprised of the centric diatom *Stephanodiscus* sp. but did not coincide with a high concentration of chlorophyll. It may be that the chlorophyll *a* concentration was underestimated at that time. The third and last peaks of carbon biomass were observed in the late winter and in spring 2014 (week 42 and 50) and were dominated by the diatom population.

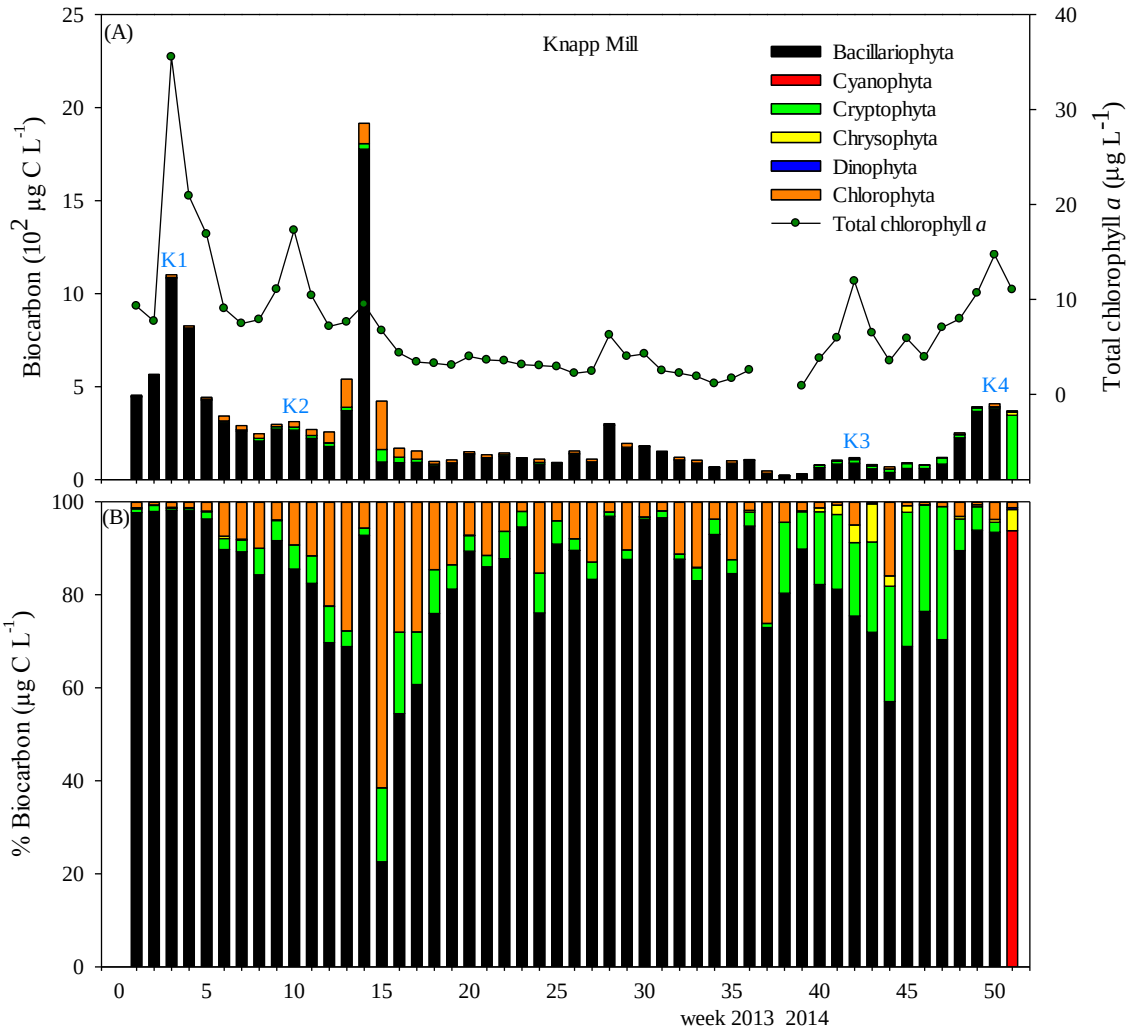


Figure 3-32: Distributions of carbon biomass and percentage for main phytoplankton groups at Knapp Mill during April 2013 – April 2014. The letters and numbers shown above the abundance bars identify a series of chlorophyll events.

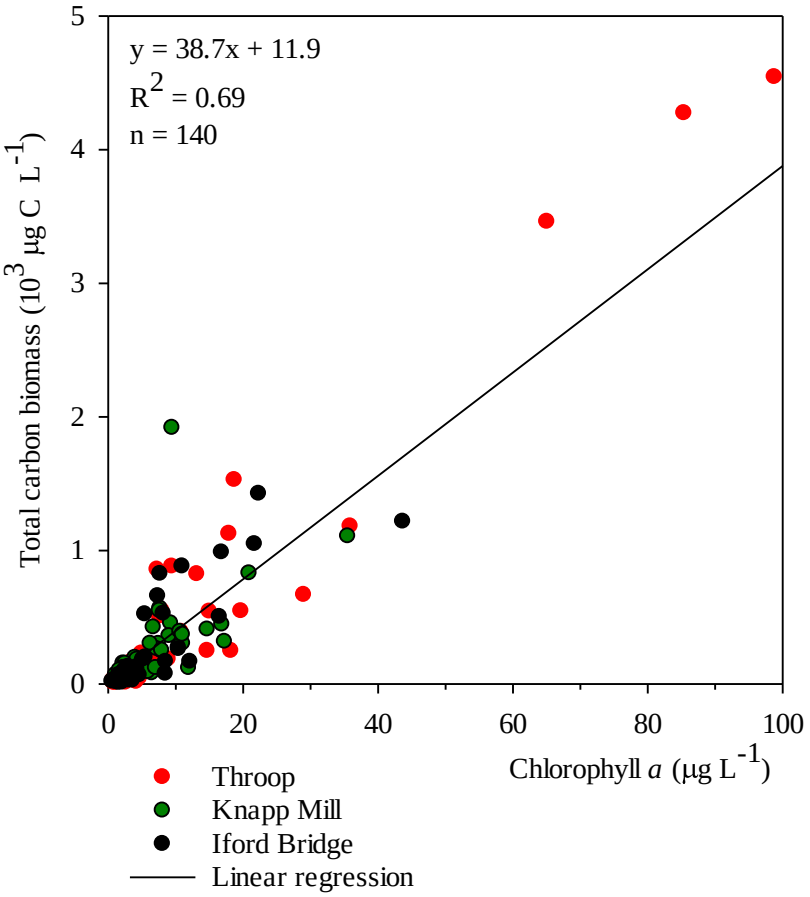


Figure 3-33: Correlation between total carbon biomass and total chlorophyll *a* concentration at three riverine sites.

### 3.3.3.3 Phytoplankton species composition

At Throop, five out of the eight chlorophyll events identified in Figure 3-8 A included samples with a chlorophyll concentration greater than 20 µg $L^{-1}$. The phytoplankton cell counts and biomass values for these samples are summarised in Table 3-3. Phytoplankton cell counts at Iford Bridge during the chlorophyll events are also shown in Table 3-3. The most numerous cell types were diatoms in most chlorophyll events (spring months), except in week 9 and 12 (summer) each with a single dominant species, *Stephanodiscus*. The other chlorophyll events (week 9 and 12) included a mixed assemblage of phytoplankton species. Cryptophytes and chlorophytes had a greater number of species contributions together than in other weeks, although some species appeared at only one time, while others appeared in many weeks.

The phytoplankton cell types identified at Knapp Mill are summarised in Table 3-4 for the four chlorophyll events. The most numerous cell types were the diatoms as on the Stour River. The diatom populations were dominated by several species but on one occasion

(week 3), *Stephanodiscus* sp. was present in appreciable numbers. The diatom cell numbers tended to decrease from spring samples to late winter. The other dominant diatom species, *Diatoma vulgare*, was present during the spring bloom at this station. Furthermore, chlorophyte numbers were very variable with a similar seasonal trend as observed on the Stour River.

When phytoplankton cell numbers are converted to bio-volume ($\mu m^3$) or carbon (µg C) biomass (Table 3-5 and Table 3-6) a different picture emerges of the community composition. The phytoplankton biomass contributions to the different chlorophyll events are shown in terms of the highest species contributors within the group, and the dominant group within similar samples. The diatoms were highly dynamic in terms of shifting from one species to another over the sampling period. The diatom carbon biomass was high, but varied from time to time. The diatoms were composed of *Stephanodiscus* sp., *Coscinodiscus* spp., *Diatoma vulgare*, *Navicula gracilis*, and *Melosira* sp. The highest biomass was obtained during the spring bloom and was dominated by *Stephanodiscus* sp. (T1 – T3, K1 chlorophyll events). The cryptomonads contributed to almost all peaks at different biomass values and times and were dominated by *Cryptomonas* sp. and *Rhodomonas* sp. during the chlorophyll events during summer months (week 9 and 12) on the Stour River. Other groups, such as the chlorophyte group were present with comparable biomass values at the same time as the cryptophyte group was peaking.

Table 3-3: Phytoplankton species counts (cells $mL^{-1}$) for the high chlorophyll samples at Throop (T1 – 8) and Iford Bridge (I1 – 3) on the Stour River. All species counted from settled 10 mL samples are listed.

| **Chlorophyll *a* events** | **T1** | **T2** | **T3** | **T4** | **T5** | **I1** | **T6** | **I2** | **T7** | **I3** | **T8** |
|---|---|---|---|---|---|---|---|---|---|---|---|
| **weeks** | **3** | **4** | **5** | **7** | **9** | | **12** | | **49** | | **51** |
| **Chlorophyll *a* (µg $L^{-1}$)** | **85.4** | **98.8** | **65.0** | **28.9** | **35.9** | **43.7** | **18.7** | **22.3** | **15.0** | **16.5** | **14.7** |
| **Bacillariophyta** | | | | | | | | | | | |
| *Amphora* spp. | 16 | 14 | 14 | 35 | 81 | 60 | 40 | 39 | 64 | 48 | 45 |
| *Bacillaria paxillifer* | - | - | - | 12 | 23 | 29 | 35 | 23 | 12 | 11 | 54 |
| *Cocconeis* spp. | - | 6 | 13 | 46 | 82 | 77 | 171 | 206 | 8 | 8 | 25 |
| *Coscinodiscus* spp. | 1,722 | 225 | - | - | 16 | 5 | 11 | 22 | 1 | - | 1 |
| *Diatoma vulgare* | 557 | 318 | 77 | 95 | 38 | 35 | 9 | 11 | 7 | 5 | 7 |
| *Licmorphora* sp. | 22 | 7 | 13 | 15 | 26 | 29 | 19 | 38 | 35 | 22 | 19 |
| *Melosira* sp. | 158 | 23 | 21 | 11 | 15 | 15 | 8 | 11 | 11 | 11 | 32 |
| *Navicula gracilis* | 695 | 152 | 101 | 63 | 68 | 54 | 30 | 26 | 53 | 74 | 60 |
| *Navicula* spp. | - | 54 | 102 | 168 | 256 | 172 | 134 | 154 | 54 | 57 | 15 |
| *Nitzschia acicularis* | 552 | 271 | 185 | 67 | 93 | 19 | 21 | 26 | 10 | 97 | 19 |
| *Nitzschia* sp. | 29 | 29 | 36 | 40 | 63 | 45 | 43 | 63 | 32 | 22 | 43 |
| Pennate diatoms | 175 | 38 | 39 | 8 | 19 | 14 | 20 | 13 | 27 | 21 | 19 |
| *Pleurotaenium* sp. | 49 | 36 | 40 | 15 | 6 | 5 | 2 | 4 | 25 | 26 | 16 |
| *Stephanodiscus* sp. | 22,252 | 44,020 | 35,113 | 3,094 | 3,559 | 4,050 | 204 | 168 | 3,397 | 2,536 | 19 |
| **Cryptophyta** | | | | | | | | | | | |
| *Cryptomonas* sp. | 110 | 27 | 304 | 998 | 1,137 | 394 | 294 | 215 | 14 | 13 | 33 |
| *Rhodomonas* sp. | 789 | 841 | 865 | 963 | 4,932 | 8,116 | 1,188 | 1,821 | 38 | 27 | 13 |
| **Chrysophyta** | | | | | | | | | | | |
| *Dinobryon* sp. | 109 | - | 18 | 433 | - | - | - | - | 18 | 13 | 11 |
| *Synura sphagnicola* | 18 | 28 | 5 | 9 | 7 | 2 | - | - | 4 | 20 | 6 |
| **Chlorophyta** | | | | | | | | | | | |
| *Actinastrum* sp. | - | 25 | 102 | 108 | 924 | 768 | - | - | - | - | 5 |
| *Ankistrodesmus* sp. | 66 | 30 | 72 | 467 | 374 | 319 | 215 | 223 | 16 | 6 | 9 |
| *Chlamydomonas* ssp. | - | 19 | - | - | 19,664 | 24,658 | 79,902 | 73,410 | - | - | 1 |
| *Chlorella* sp. | - | - | - | - | 4,722 | - | 301 | 727 | - | 1 | 7 |
| *Coelastrum* sp. | - | - | - | - | 40 | 137 | 645 | 692 | - | 4 | - |
| *Kirchneriella* sp. | - | 12 | 32 | - | 131 | 96 | 344 | 626 | 1 | - | 1 |
| *Pediastrum* sp. | - | - | 20 | - | - | - | - | - | - | - | 19 |
| *Scenedesmus* sp. | 82 | 38 | 94 | 258 | 403 | 416 | 1,409 | 912 | 16 | 21 | 16 |

Table 3-4: Phytoplankton species counts (cells $mL^{-1}$) for the high chlorophyll samples at Knapp Mill on the Hampshire Avon River. All species counted from settled 10 mL samples are listed.

| **Chlorophyll *a* events** | **K1** | **K2** | **K3** | **K4** |
|---|---|---|---|---|
| **weeks** | **3** | **10** | **42** | **50** |
| **Chlorophyll *a* (µg $L^{-1}$)** | **35.5** | **17.3** | **11.9** | **14.7** |
| **Bacillariophyta** | | | | |
| *Amphora* spp. | 57 | 46 | 18 | 168 |
| *Bacillaria paxillifer* | 18 | 41 | - | 40 |
| *Cocconeis* spp. | - | 132 | 5 | 95 |
| *Coscinodiscus* spp. | 38 | 7 | - | 11 |
| *Diatoma vulgare* | 732 | 155 | 25 | 90 |
| *Licmorphora* sp. | 94 | 176 | 21 | 80 |
| *Melosira* sp. | 104 | 25 | 59 | 208 |
| *Navicula gracilis* | 181 | 439 | 11 | 346 |
| *Navicula* spp. | 8 | 485 | 23 | 157 |
| *Nitzschia acicularis* | 291 | 12 | 169 | 68 |
| *Nitzschia* sp. | 8 | 29 | 35 | 68 |
| Pennate diatoms | 205 | 4 | 15 | 32 |
| *Pleurotaenium* sp. | 154 | 7 | 77 | 39 |
| *Stephanodiscus* sp. | 3,821 | 399 | 30 | 985 |
| **Cryptophyta** | | | | |
| *Cryptomonas* sp. | - | 64 | 50 | 33 |
| *Rhodomonas* sp. | 170 | 236 | 395 | 141 |
| **Chrysophyta** | | | | |
| *Dinobryon* sp. | - | - | - | 1 |
| *Synura sphagnicola* | 49 | 1 | 100 | 52 |
| **Chlorophyta** | | | | |
| *Actinastrum* sp. | - | - | - | 23 |
| *Ankistrodesmus* sp. | 22 | 22 | 7 | 18 |
| *Chlamydomonas* sp. | 20 | 69 | - | - |
| *Chlorella* sp. | - | 50 | - | - |
| *Coelastrum* sp. | - | 63 | - | - |
| *Kirchneriella* sp. | - | 38 | - | 2 |
| *Pediastrum* sp. | 13 | - | - | 9 |
| *Scenedesmus* sp. | 98 | 464 | - | 53 |

Table 3-5: Phytoplankton species biomass (µg C $L^{-1}$) for the high chlorophyll samples at Throop (T1 – 8) and Iford Bridge (I1 – 3) on the Stour River.

| **Chlorophyll *a*** | **T1** | **T2** | **T3** | **T4** | **T5** | **I1** | **T6** | **I2** | **T7** | **I3** | **T8** |
|---|---|---|---|---|---|---|---|---|---|---|---|
| **weeks** | **3** | **4** | **5** | **7** | **9** | | **12** | | **49** | | **51** |
| **Chlorophyll *a* (µg $L^{-1}$)** | **85.4** | **98.8** | **65.0** | **28.9** | **35.9** | **43.7** | **18.7** | **22.3** | **15.0** | **16.5** | **14.7** |
| **Total carbon (µg C $L^{-1}$)** | **4,274** | **4,544** | **3,461** | **666** | **1,180** | **1,216** | **1,528** | **1,424** | **543** | **504** | **249** |
| **Bacillariophyta** | | | | | | | | | | | |
| *Amphora* spp. | 1 | 1 | 1 | 3 | 6 | 4 | 3 | 3 | 5 | 3 | 3 |
| *Bacillaria paxillifer* | - | - | 0 | - | 1 | 1 | 1 | 1 | 4 | 3 | 4 |
| *Cocconeis* spp. | - | 0 | 1 | 3 | 5 | 5 | 11 | 13 | 1 | 1 | 2 |
| *Coscinodiscus* spp. | 1,479 | 193 | - | - | 14 | 4 | 9 | 19 | - | - | - |
| *Diatoma vulgare* | 282 | 161 | 39 | 48 | 19 | 18 | 5 | 5 | 4 | 3 | 4 |
| *Licmorphora* sp. | 1 | 0 | 0 | 0 | 1 | 1 | 0 | 1 | 1 | 1 | 0 |
| *Melosira* sp. | 55 | 8 | 7 | 4 | 5 | 5 | 3 | 4 | 4 | 4 | 11 |
| *Navicula gracilis* | 173 | 38 | 25 | 16 | 17 | 13 | 8 | 6 | 134 | 186 | 149 |
| *Navicula* spp. | - | 1 | 2 | 3 | 4 | 3 | 2 | 3 | 1 | 1 | 2 |
| *Nitzschia acicularis* | 7 | 4 | 2 | 1 | 1 | 1 | 0 | 0 | 1 | 1 | 0 |
| *Nitzschia* sp. | 3 | 3 | 3 | 3 | 4 | 4 | 4 | 6 | 1 | 1 | 1 |
| Pennate diatoms | 152 | 33 | 34 | 7 | 16 | 12 | 17 | 11 | 24 | 18 | 16 |
| *Pleurotaenium* sp. | 16 | 12 | 13 | 5 | 2 | 2 | 1 | 1 | 8 | 9 | 5 |
| *Stephanodiscus* sp. | 2,050 | 4,055 | 3,234 | 285 | 328 | 373 | 19 | 15 | 313 | 234 | 18 |
| **Cryptophyta** | | | | | | | | | | | |
| *Cryptomonas* sp. | 16 | 4 | 44 | 144 | 165 | 57 | 43 | 31 | 22 | 19 | 5 |
| *Rhodomonas* sp. | 23 | 24 | 25 | 28 | 143 | 235 | 34 | 53 | 11 | 8 | 4 |
| **Chrysophyta** | | | | | | | | | | | |
| *Dinobryon* sp. | 3 | - | 0 | 11 | - | - | - | - | 5 | 4 | 0 |
| *Synura sphagnicola* | 1 | 1 | 0 | 0 | 0 | 0 | - | - | 0 | 1 | 0 |
| **Chlorophyta** | | | | | | | | | | | |
| *Actinastrum* sp. | - | 1 | 5 | 5 | 46 | 38 | - | - | - | - | 0 |
| *Ankistrodesmus* sp. | 6 | 3 | 7 | 43 | 34 | 29 | 20 | 20 | 2 | 1 | 1 |
| *Chlamydomonas* sp. | - | 0 | - | - | 315 | 395 | 1,278 | 1,175 | - | - | 0 |
| *Chlorella* sp. | - | - | - | - | 25 | - | 2 | 4 | - | 0 | 0 |
| *Coelastrum* sp. | - | - | - | - | 0 | 1 | 7 | 8 | - | 0 | - |
| *Kirchneriella* sp. | - | 0 | - | - | 1 | 0 | 1 | 3 | 0 | - | 0 |
| *Pediastrum* sp. | - | - | 12 | - | - | - | - | - | - | - | 12 |
| *Scenedesmus* sp. | 3 | 1 | 3 | 9 | 13 | 14 | 47 | 30 | 1 | 1 | 1 |

Table 3-6: Phytoplankton species biomass (µg C $L^{-1}$) for the high chlorophyll samples at Knapp Mill (K1 – 4) on the Hampshire Avon River.

| **Chlorophyll *a* events** | **K1** | **K2** | **K3** | **K4** |
|---|---|---|---|---|
| **weeks** | **3** | **10** | **42** | **50** |
| **Chlorophyll *a* (µg $L^{-1}$)** | **35.5** | **17.3** | **11.9** | **14.7** |
| **Total carbon (µg C $L^{-1}$)** | **1,105** | **316** | **119** | **408** |
| **Bacillariophyta** | | | | |
| *Amphora* spp. | 4 | 3 | 1 | 12 |
| *Bacillaria paxillifer* | 1 | 1 | - | 1 |
| *Cocconeis* spp. | - | 8 | 0 | 6 |
| *Coscinodiscus* spp. | 32 | 6 | - | 9 |
| *Diatoma vulgare* | 370 | 78 | 12 | 46 |
| *Licmorphora* sp. | 2 | 5 | 1 | 2 |
| *Melosira* sp. | 36 | 9 | 20 | 72 |
| *Navicula gracilis* | 45 | 109 | 3 | 86 |
| *Navicula* spp. | - | 8 | 0 | 3 |
| *Nitzschia acicularis* | 4 | 0 | 2 | 1 |
| *Nitzschia* sp. | 6 | 6 | 1 | 2 |
| Pennate diatoms | 179 | 3 | 13 | 28 |
| *Pleurotaenium* sp. | 51 | 2 | 26 | 13 |
| *Stephanodiscus* sp. | 352 | 31 | 3 | 91 |
| **Cryptophyta** | | | | |
| *Cryptomonas* sp. | - | 9 | 7 | 5 |
| *Rhodomonas* sp. | 5 | 7 | 11 | 4 |
| **Chrysophyta** | | | | |
| *Dinobryon* sp. | - | - | - | 0 |
| *Synura sphagnicola* | 2 | 0 | 4 | 2 |
| **Chlorophyta** | | | | |
| *Actinastrum* sp. | - | - | - | 1 |
| *Ankistrodesmus* sp. | 2 | 2 | 1 | 2 |
| *Chlamydomonas* sp. | 0 | 1 | - | - |
| *Chlorella* sp. | - | 0 | - | - |
| *Coelastrum* sp. | - | 1 | - | - |
| *Kirchneriella* sp. | - | 0 | - | 0 |
| *Pediastrum* sp. | 8 | - | - | 6 |
| *Scenedesmus* sp. | 3 | 15 | - | 2 |

#### 3.3.3.4 Seasonal succession of phytoplankton taxa and pigments

Phytoplankton seasonal successions in terms of carbon biomass on the Stour and Hampshire Avon Rivers are shown in Figure 3-34 and Figure 3-35. They show the absolute contribution of different phytoplankton groups, over the whole sampling period, with the eight chlorophyll events indicated by dashed lines at Throop. The diatom, cryptomonad and chlorophyte populations are represented by the species data in Table 3-5 and Table 3-6. The main biomass peaks on the River Stour for diatoms (chlorophyll events T1 – T3, *Stephanodiscus* sp.) were earlier than the peaks for chrysophytes (T4, *Dinobryon* sp.), while cryptomonads (T4, T5, I1, *Cryptomonas* sp. and *Rhodomonas* sp.) and chlorophytes (T6 and I2) occurred in the summer period. Meanwhile, the phytoplankton seasonal succession at Knapp Mill shows a different pattern to Throop or Iford Bridge. Subsequently, group succession is present as phytoplankton species carbon biomass as shown in Table 3-5 and Table 3-6. The phytoplankton succession was initiated by the small diatom *Stephanodiscus* sp., in late spring, with three peaks and also the highest diatom biomass peaks at that time. The cryptomonad group peaked in early summer, followed by chlorophyte peaks. At all study sites, the summer peaks were comprised of cryptomonads and chlorophytes together with *Cryptomonas* sp. and *Chlamydomonas* sp.

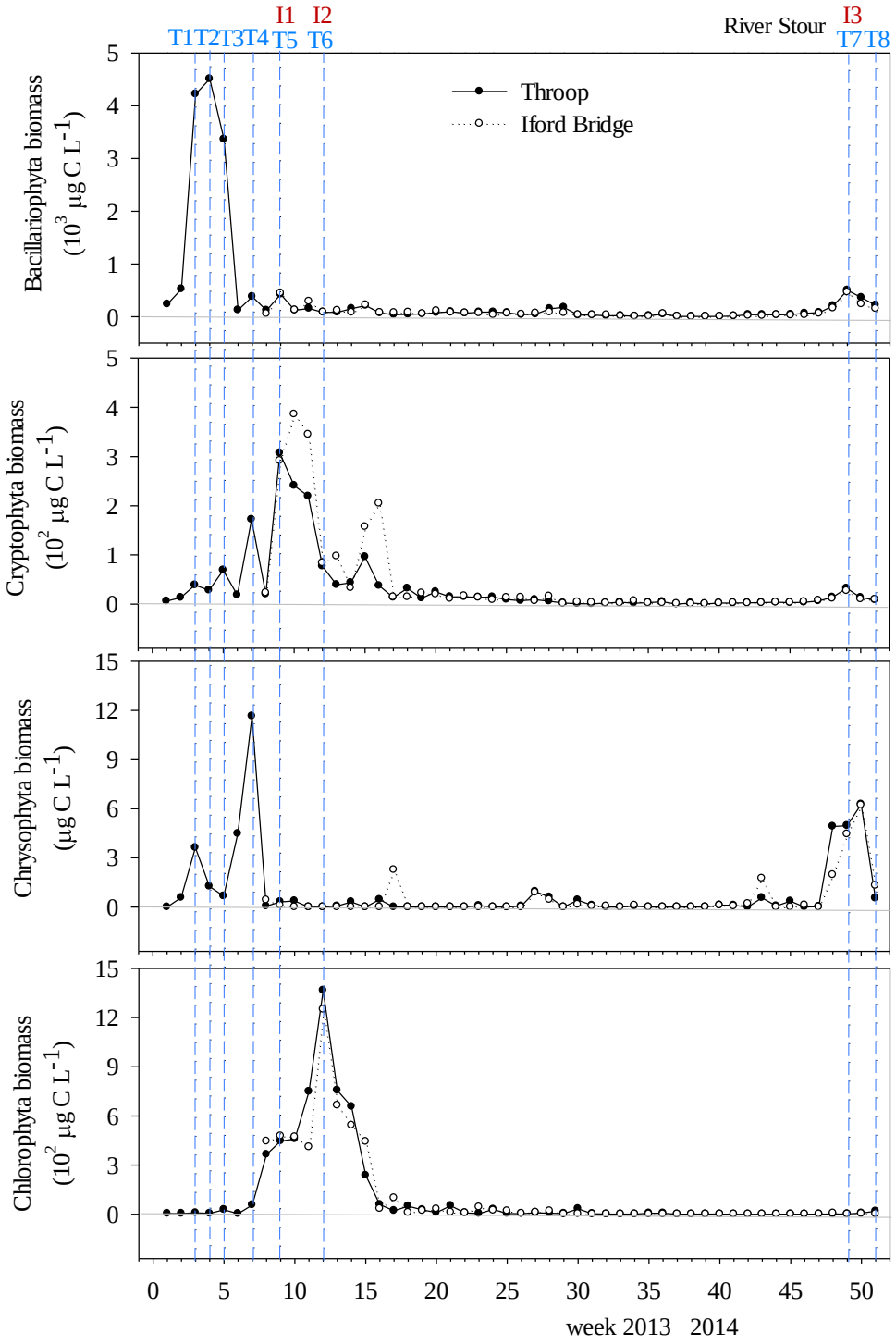


Figure 3-34: The succession of phytoplankton groups at Throop and Iford Bridge on the Stour River. Symbols in upper panel apply to all panels.

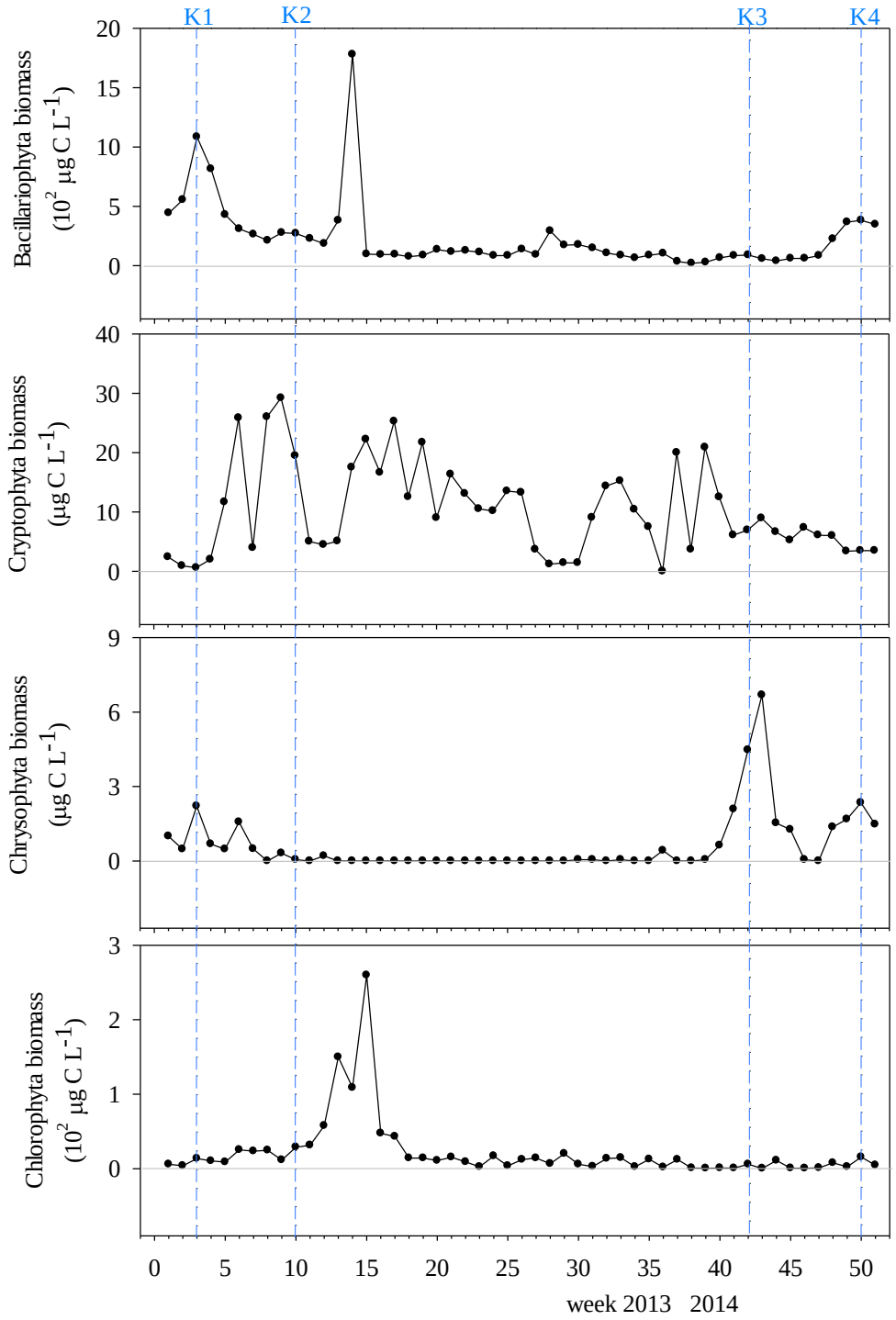


Figure 3-35: The succession of phytoplankton groups at Knapp Mill on the Hampshire Avon River.

### 3.3.4 Measurements of $F_v/F_m$

A bench-top Fluorescence Induction and Relaxation (FIRe) was used to measure the photosynthetic physiological parameters ($F_v/F_m$) both in total and size fractionated populations in riverine samples. The FIRe instrument was used to study the size fractions of phytoplankton only during spring and summer 2013, but total populations were

investigated throughout the sampling period as described in the method chapter (see Section 2.8).

The change of $F_v/F_m$ ratios of water samples from the three sites (Throop, Iford Bridge, and Knapp Mill) are shown in Figure 3-36 D – F compared with the annual concentration of chlorophyll *a* (Figure 3-36 A – C). The range of total $F_v/F_m$ efficiency was 0.02 – 0.71, 0.2 – 0.72, and 0.11 – 0.65 at Throop, Iford Bridge, and Knapp Mill respectively. Figure 3-36 D and F shows the $F_v/F_m$ values in the 2.0 – 20.0 µm range were greater and contributed most to the total $F_v/F_m$ ratio as this size fraction also contributed greater to the total concentration of chlorophyll at Throop and Knapp Mill as shown in Figure 3-36 A and C. The mean $F_v/F_m$ efficiency of nano-phytoplankton was 0.46 ± 0.17 (n = 13) at Throop and 0.45 ± 0.12 (n = 13) at Knapp Mill, while the pico-phytoplankton community (0.2 – 2 µm) had the mean of $F_v/F_m$ values of 0.11 ± 0.06 (n = 13) and 0.15 ± 0.08 (n = 12) at Throop and Knapp Mill, respectively.

The high values of $F_v/F_m$ efficiency occurred at the same time as the maximum surface chlorophyll concentration in both spring periods. Broadly, $F_v/F_m$ decreases sharply from summer to winter and then increase again in spring at all study sites. The nano-phytoplankton (2 – 20 µm) was the main community on the Stour and Hampshire Avon Rivers, which supports the size-fractionated chlorophyll results. Although the pico-phytoplankton population does not vary obviously in $F_v/F_m$ during the highly productive bloom period, this cell size shows a slight increase in photosynthetic energy conversion efficiency during periods of high chlorophyll concentration at Throop (Figure 3-36 D).

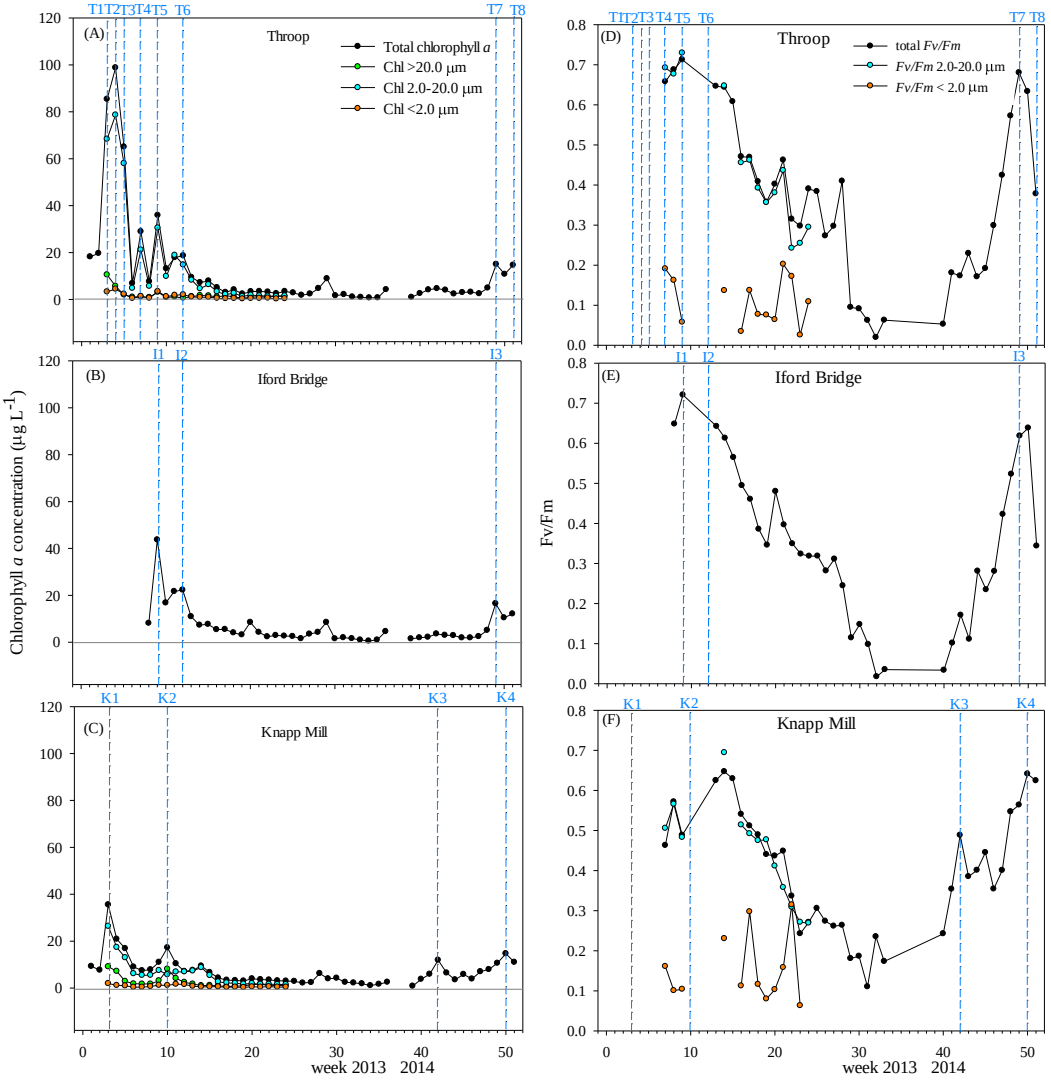


Figure 3-36: Chlorophyll *a* concentration in µg $L^{-1}$ (A – C) and photosynthetic energy conversion efficiency ($F_v/F_m$, unit-less) (D – F). The numbers and dash lines shown above the chlorophyll *a* and the photosynthetic efficiency curve identify each chlorophyll event from the three study sites. Symbols in upper panel apply to all panels.

### 3.3.5 Phytoplankton abundance and total red fluorescence by flow cytometry

Preserved samples from both rivers were analysed with a CytoSense flow cytometer. The measurements for the three stations were exported using the CytoClus software to Excel and all plots were composed using this programme. The CytoSense results from each of total fluorescence (FLR and FLO) are illustrated in Figure 3-37.

Phytoplankton pattern was investigated throughout the sampling period from all study sites (Throop, Iford Bridge, and Knapp Mill) on the Stour and Hampshire Avon Rivers. The results from the CytoSense revealed a sharp change in abundance at low spatial scale from

week 5 to 6 on both rivers (Figure 3-37 A and C). The highest values in total red fluorescence, used as a proxy for phytoplankton chlorophyll *a* content, were observed at all riverine sites (Figure 3-37) during spring with a maximum of $24 \times 10^8$, $2.4 \times 10^8$, and $2.6 \times 10^8$ a.u. $mL^{-1}$ at Throop, Iford Bridge, and Knapp Mill respectively. The highest values at Throop and Knapp Mill were mainly observed during the *Stephanodiscus* spring bloom (week 3 and 4), but at Iford Bridge were observed in spring 2014 (week 49), although no samples were taken from this site during weeks 1 – 7. In terms of total orange fluorescence a maximum of $6.7 \times 10^7$, $1.6 \times 10^7$, and $1.5 \times 10^7$ a.u. $mL^{-1}$ was observed at Throop, Iford Bridge, and Knapp Mill respectively. Spring samples corresponded to the highest values the mean total red fluorescence at all sites (Table 3-7) confirming the importance of the spring bloom of *Stephanodiscus* sp. to the total chlorophyll concentration and HPLC pigments in particular at Throop followed by Iford Bridge and Knapp Mill, which was characterized by the lowest total red fluorescence in almost every season except in winter.

Phytoplankton abundance estimates by microscopy and CytoSense flow cytometry were compared as shown in Figure 3-37. As expected, recorded flow cytometry abundance and microscopic counting were positively a weak correlated as the CytoSense flow cytometer can discriminate between wide quantities of cells in a broad size range (1 – 800 µm) based on their optical properties (Dubelaar and Jonker, 2000). The microscopic technique is limited with cell sizes < 10 µm and fixation may change phytoplankton shape, particularly in fragile organism and flagellar species. This present study used acid Lugol's iodine solution to preserve all microscopic samples therefore the fixation may have instantly caused phytoplankton cells to shrink (Montagnes *et al.*, 1994). The correlation of abundance estimate between the CytoSense and the traditional microscopy is shown in Figure 3-38.

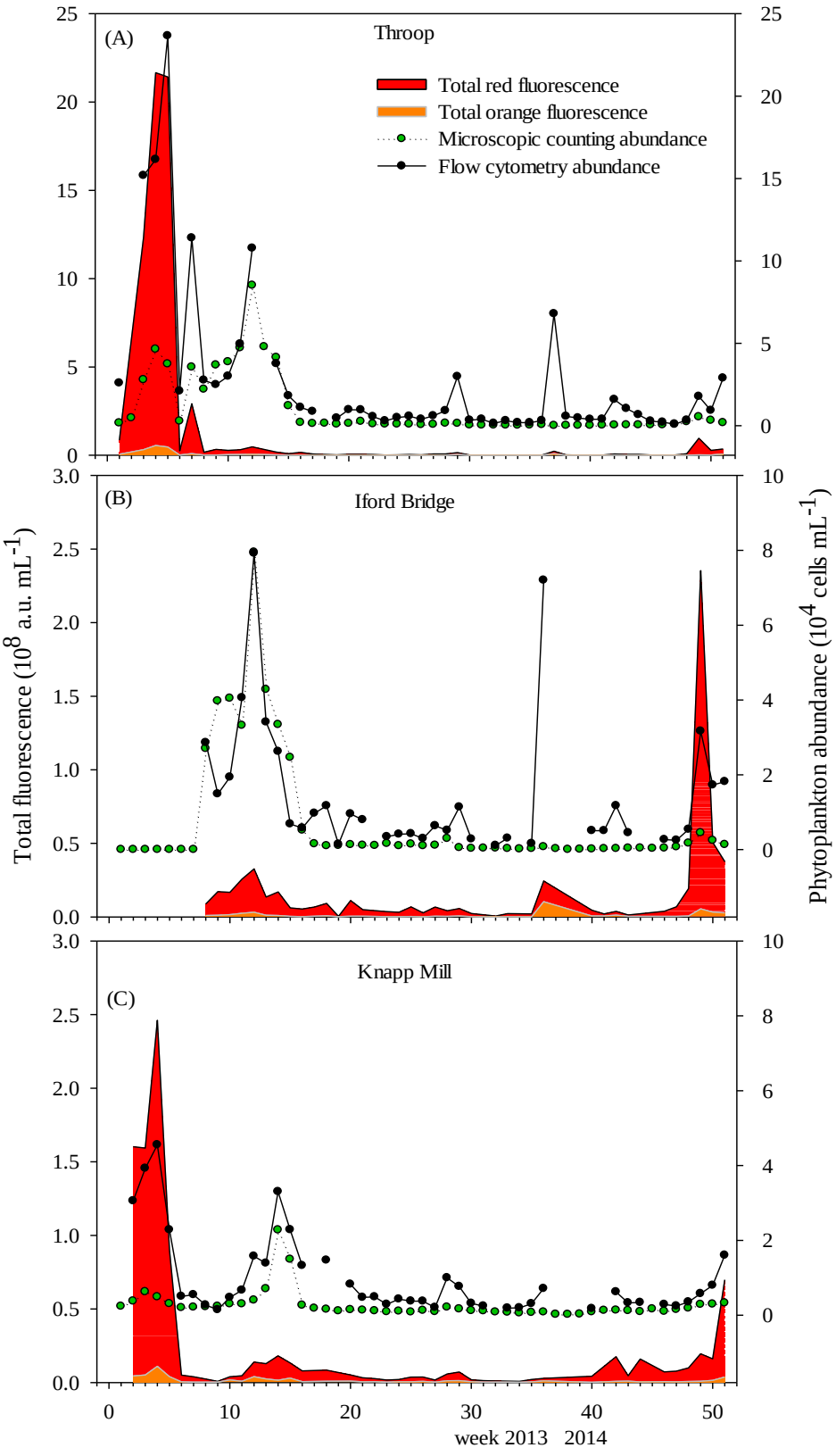


Figure 3-37: Seasonal distribution of red and orange fluorescence and phytoplankton abundance at Throop (A), Iford Bridge (B), and Knapp Mill (C). The solid line and black circles symbol are flow cytometric analysis. The dash line and green circles symbol are microscopic analysis. Note different scale in A on both y axes. Symbols in upper panel apply to all panels.

Table 3-7: Mean red and orange fluorescence (a.u. $mL^{-1}$), with standard deviation, for each season.

| | Mean values ($10^6$) ± standard deviation ($10^6$) | | | |
|---|---|---|---|---|
| | spring | summer | autumn | winter |
| **Throop**: | | | | |
| total red fluorescence | 155.03 ± 36.08 | 21.04 ± 14.69 | 4.75 ± 4.37 | 6.34 ± 8.28 |
| total orange fluorescence | 5.9 ± 4.7 | 4.08 ± 4.98 | 0.92 ± 1.42 | 2.08 ± 3.68 |
| **Iford Bridge**: | | | | |
| total red fluorescence | 60.36 ± 88.05* | 14.11 ± 9.79 | 4.36 ± 2.12 | 8.28 ± 12.79 |
| total orange fluorescence | 2.63 ± 2.37* | 1.43 ± 1.29 | 0.40 ± 0.23 | 3.29 ± 6.32 |
| **Knapp Mill**: | | | | |
| total red fluorescence | 24.88 ± 53.12 | 9.12 ± 6.03 | 3.62 ± 2.07 | 8.26 ± 8.12 |
| total orange fluorescence | 2.01 ± 2.85 | 1.89 ± 1.51 | 0.96 ± 0.70 | 0.89 ± 0.60 |

* = only spring 2014 values

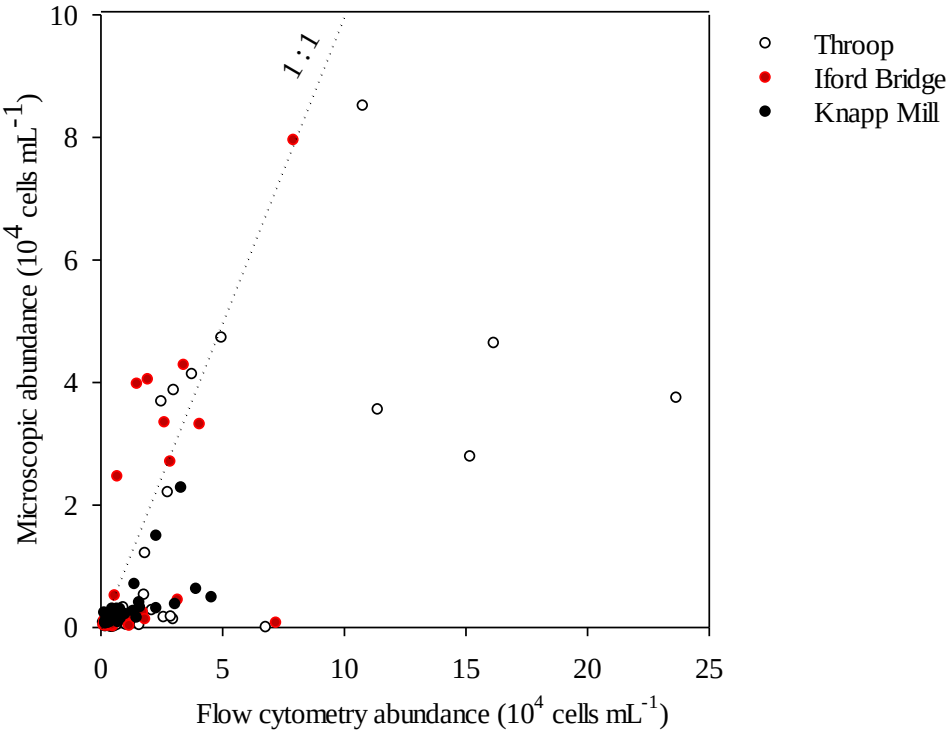


Figure 3-38: Correlation between flow cytometry abundance and microscopic cell count at Throop, Iford Bridge, and Knapp Mill.

Cytograms were determined by CytoSense according to the optical properties of cells or particles and attributed to different species from the three study sites as shown in Figure 3-39, Figure 3-40, and Figure 3-41. Cytograms were defined for every chlorophyll *a* event.

Red circles indicate red fluorescence (a.u.) area per cell versus FWS length per cell (a.u.) in a cytogram the *Stephanodiscus* sp. bloom during springtime (week 3, 4, 5, and 49), while green circles show a cytogram with a dominance of chlorophytes particularly *Chlamydomonas* spp. during early summer (week 7, 9, and 12 on the Stour River).

Diatoms showed the higher FLR and FWS signals because this group contains large cells with high chlorophyll *a* per cell (Figure 3-39 and Figure 3-40) as previous flow cytometry studies in marine water have also found (Rutten *et al.*, 2005; Bonato *et al.*, 2015).

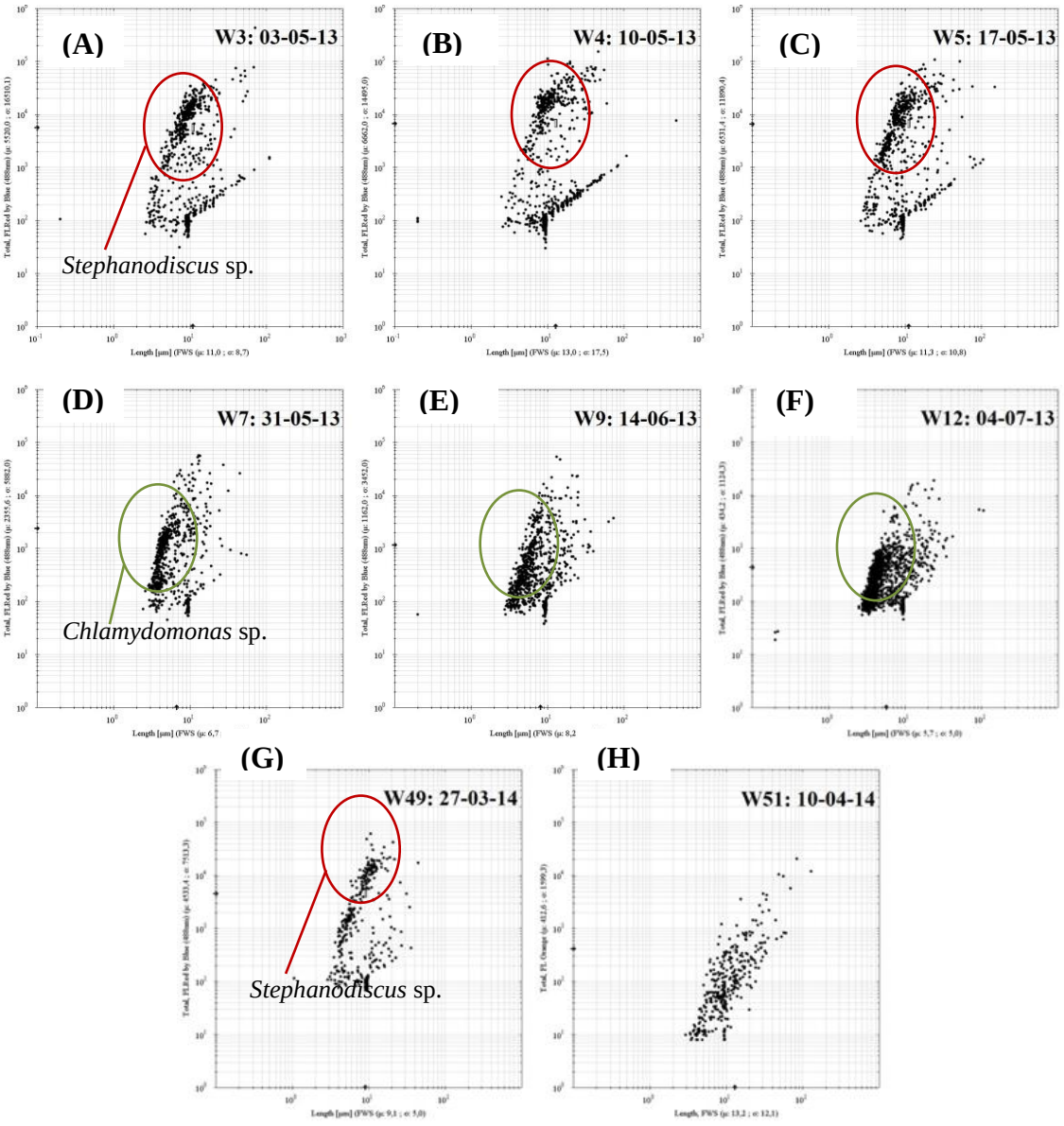


Figure 3-39: CytoSense cytograms defined for each chlorophyll event at Throop, in which red fluorescence area per cell (a.u.) versus FWS length per cell (a.u) cytograms. (x axis is length (µm) and y axis shows total red fluorescence at 488 nm).

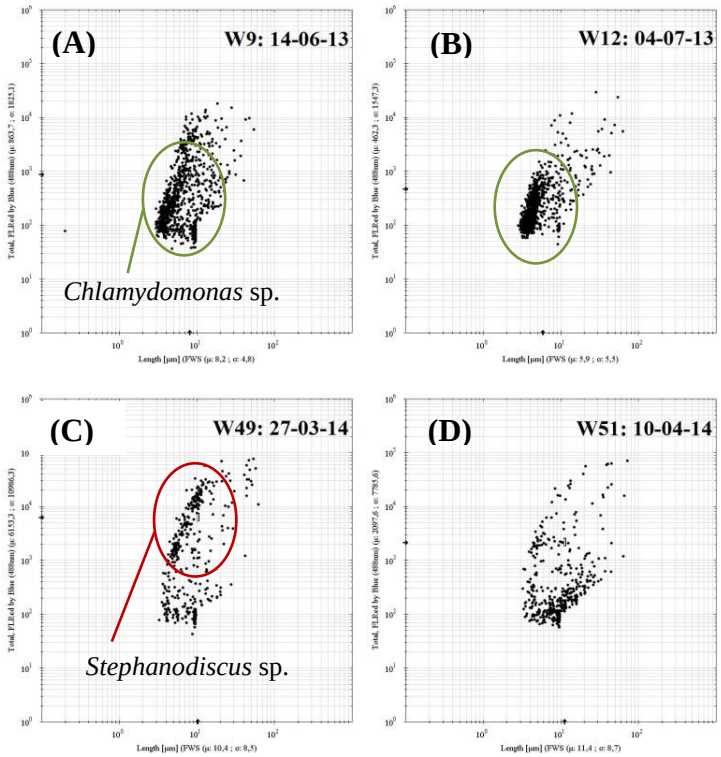


Figure 3-40: CytoSense cytograms defined for each chlorophyll event (week 9, 12, 49, and 51) at Iford Bridge, in which red fluorescence area per cell (a.u.) versus FWS length per cell (a.u) cytograms. (x axis is length (µm) and y axis shows total red fluorescence at 488 nm).

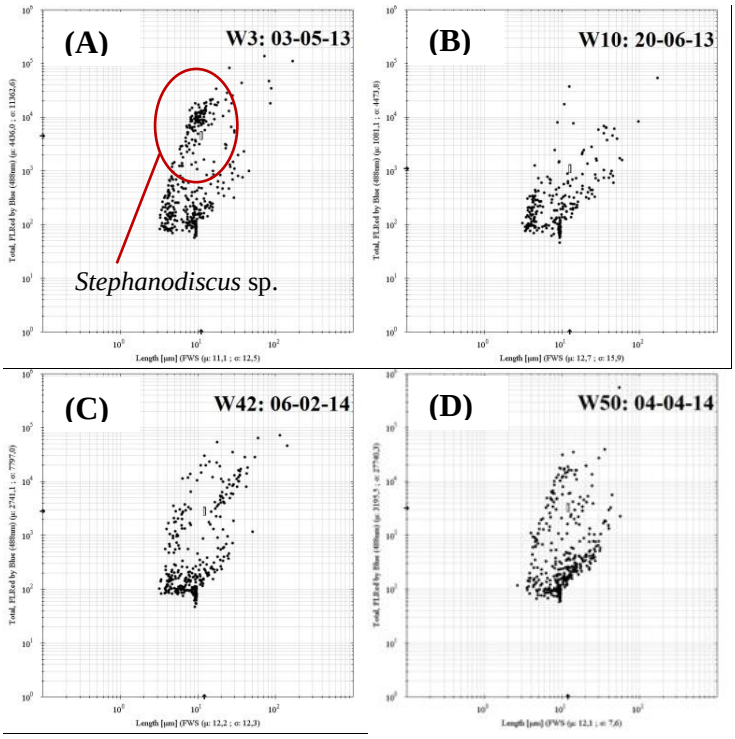


Figure 3-41: CytoSense cytograms defined for each chlorophyll event (week 3, 10, 42, and 50) at Knapp Mill, in which red fluorescence area per cell (a.u.) versus FWS

length per cell (a.u) cytograms. (x axis is length (µm) and y axis shows total red fluorescence at 488 nm).

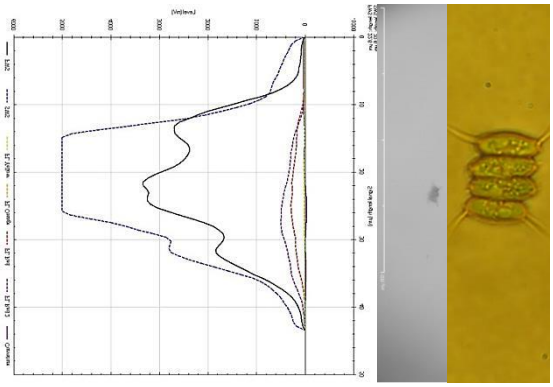

Figure 3-42: Right: "*Scenedesmus*" type colony of 4 asymmetrical cells (photo under inverted microscope). Middle: The colony image by CytoSense camera. Left: signal course of the measured scatter and fluorescence emission of particle by CytoSense measurements.

### 3.3.6 Multivariate data analysis and interpretation

The environmental (physical and chemical) data and biological (carbon biomass and accessory pigments) data collected during April 2013 to April 2014 were analysed by multivariate analysis. The analyses were carried out in several steps; first, grouping of environmental parameters by similarity or dissimilarity using Euclidean distance; second, grouping of phytoplankton species using the Bray-Curtis Similarity Index using the PRIMER-E software; and third, correlation of environmental variables to phytoplankton groups was performed using the CANOCO software.

Two types of analysis have been carried out, dendrogram for hierarchical clustering of samples and a non-matric multidimensional scaling (nMDS) to indicate group similarity and distance between sample groups in two-dimensional space. The stress level for each nMDS ordinal plot is used as an indicator of how the plot organises the distribution. Stress levels of < 0.1 indicated good ordination, 0.1 – 0.2 a useful two-dimensional display of clusters, and > 0.2 a random placement in two dimensions (see Clarke *et al.* (2014) for further details). SIMPER analysis was used to calculate the percentage similarity of each sample group and the dissimilarity between each pair of groups using the PRIMER-E version 7.0 software (Clarke *et al.*, 2014).

### 3.3.6.1 Environmental data analyses

Cluster and nMDS analysis of environmental parameters were performed on a normalised Euclidean distance with previous log (x+1) transformation. The environmental variables including; river flow, water temperature, oxygen saturation, suspended particulate matter, nitrate, phosphate, and silicate concentrations were clustered to give groups with the lowest distance between pairs of samples.

***Throop, River Stour***

Groups A - F were defined from the dendrogram for hierarchical clustering as shown in Figure 3-43. The Euclidean distance between most of the groups A – F ranged from 2.6 – 3.3. A majority of samples are in group E followed by C, F, D, A, and B. The data were then analysed by nMDS to provide a two-dimensional distance plot in Figure 3-44 which shows more clearly how samples are grouped. The plot stress (0.11) indicated a good two-dimensional representation of the data (Clarke *et al.*, 2014). A seasonal pattern to group distribution can be distinguished from the plot: group E represents mainly the summer and early autumn samples, group C a mixture of the late autumn and winter, group F a mixture of the late autumn and early winter. Group D was mainly the late spring, while group A includes two spring samples.

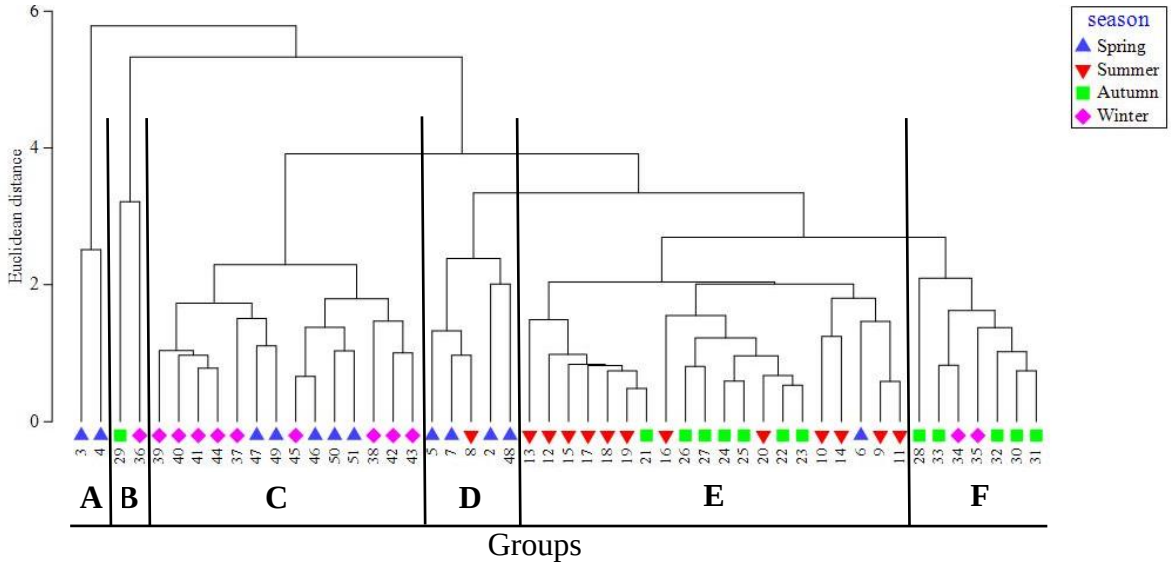


Figure 3-43: Dendrogram for hierarchical clustering of Throop samples defined by environmental parameters. Numbers indicate the sample weeks.

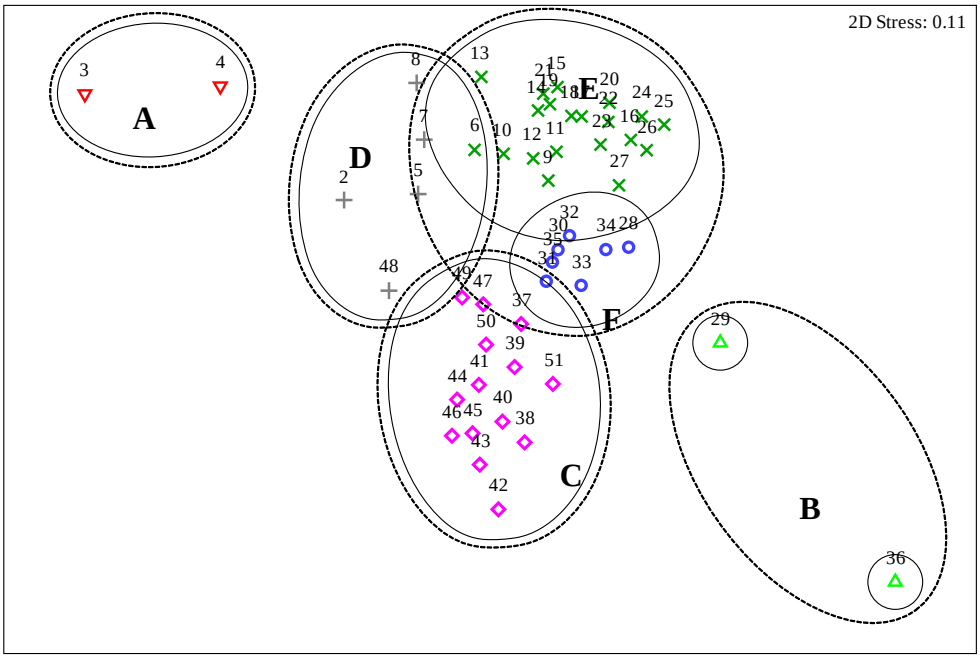


Figure 3-44: nMDS plot of environmental parameter groups at Throop on the Stour River. Numbers indicate the sample weeks. Dash line is 3.3 of the Euclidean distance and solid line indicates 2.6 of the distance.

Silicate and phosphate concentrations were the most important environmental parameters for defining the sample group during the spring bloom (week 3, 4, and 5) including the peak chlorophyll event in the early summer (week 7) as shown in Table 3-8. Several environmental factors were subsequently the majority factors to group definition at Throop. Seasonal changes in nitrate concentration and river flow rate were the dominant parameters in defining the environmental group during the winter 2013 to the early spring 2014 months. Group B was characterised by increasingly high SPM values and river flow rate. During the flooding event from week 36, nitrate was generally high concentration, silicate was relatively low and river flow continued to decrease. All the high chlorophyll samples were in group A, C, D, and F when the levels of river flow were less than 30 $m^3$ $s^{-1}$. In the summer (group E) the river flow was < 20 $m^3$ $s^{-1}$, and phosphate concentrations were beginning to increase, probably phosphate diluted by high river flows as it tends to come from point sources such as sewage treatment works and slurry.

Table 3-8: Main characteristics of sample groups defined by environmental parameters at Throop on the Stour River. The peak chlorophyll samples in Table 3-3 are indicated by sample weeks in bold.

| Group | Sample week no. | Parameter % contribution | Average square distance |
|---|---|---|---|
| A | **3**, **4** | silicate (73), phosphate (14), oxygen saturation (13) | 3.16 |
| B | 29, 36 | SPM (85), river flow (8) | 5.17 |
| C | 37, 38, 39, 40, 41, 42, 43, 44, 45, 46, 47, **49**, 50, **51** | nitrate (50), river flow (13) | 2.07 |
| D | 2, **5**, **7**, 8, 48 | phosphate (44), nitrate (19), silicate (16), temperature (12) | 2.25 |
| E | 6, **9**, 10, 11, **12**, 13, 14, 15, 16, 17, 18, 19, 20, 21, 22, 23, 24, 25, 26, 27 | oxygen saturation (35), nitrate (17), phosphate (16), temperature (15), silicate (15) | 1.76 |
| F | 28, 30, 31, 32, 33, 34, 35 | nitrate (37), temperature (33), river flow (11) | 1.43 |

***Iford Bridge, River Stour***

The environmental variables showing a pattern as present at Throop, except SPM data which was not included at Iford Bridge, were clustered to give groups with the lowest distance between pairs of samples. The cluster dendrogram shows separation at a normalised distance of 2.6 into six groups (A – F) as shown in Figure 3-45. Group C had 17 samples followed by group D, E, F, B, and A respectively. All winter samples were in group E, almost all summer and early autumn samples in group C, almost all spring 2014 samples in group F, and late autumn and early winter in group D. Group A has only one sample from week 8, while group B includes two samples from weeks 25 and 27. The results indicate a high distance of environmental factors in week 8 from all other weeks.

The nMDS plot of the Iford Bridge data provides a two-dimensional distance plot (Figure 3-46) which shows more clearly how the samples were grouped. A stress of 0.1 indicated a good representation of the environmental parameters as at Throop. A seasonal pattern to group distribution can be distinguished from the plot: group E represents the winter

samples, group F the spring 2014 samples, group C the early summer samples, and group D the late autumn and early winter samples. Group C was the summer and a mixture from the early autumn samples.

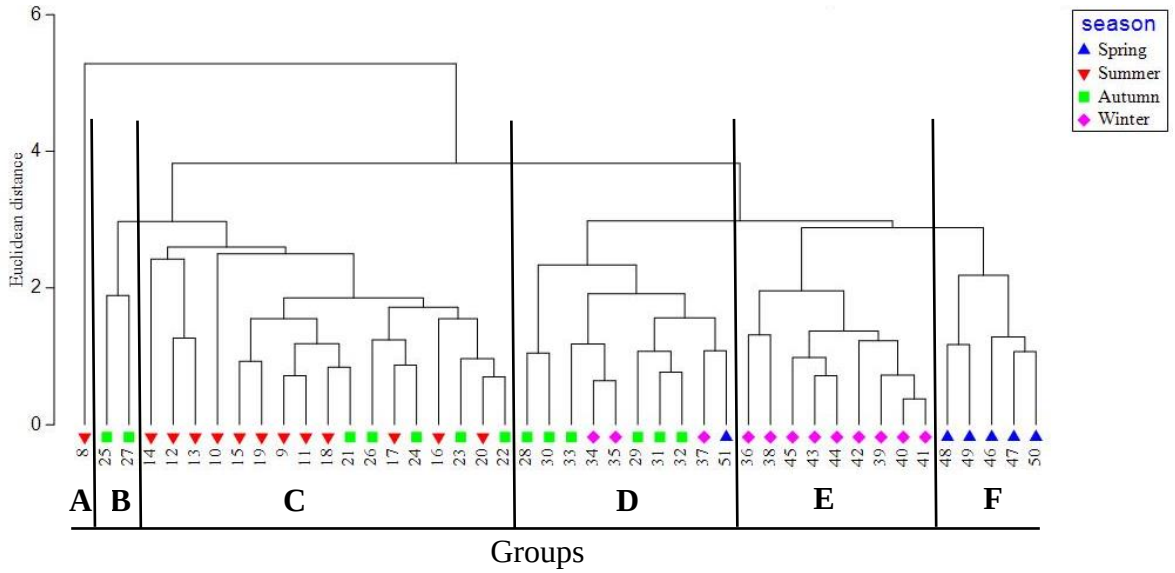


Figure 3-45: Dendrogram for hierarchical clustering of Iford Bridge samples defined by environmental parameters. Numbers indicate the sample weeks.

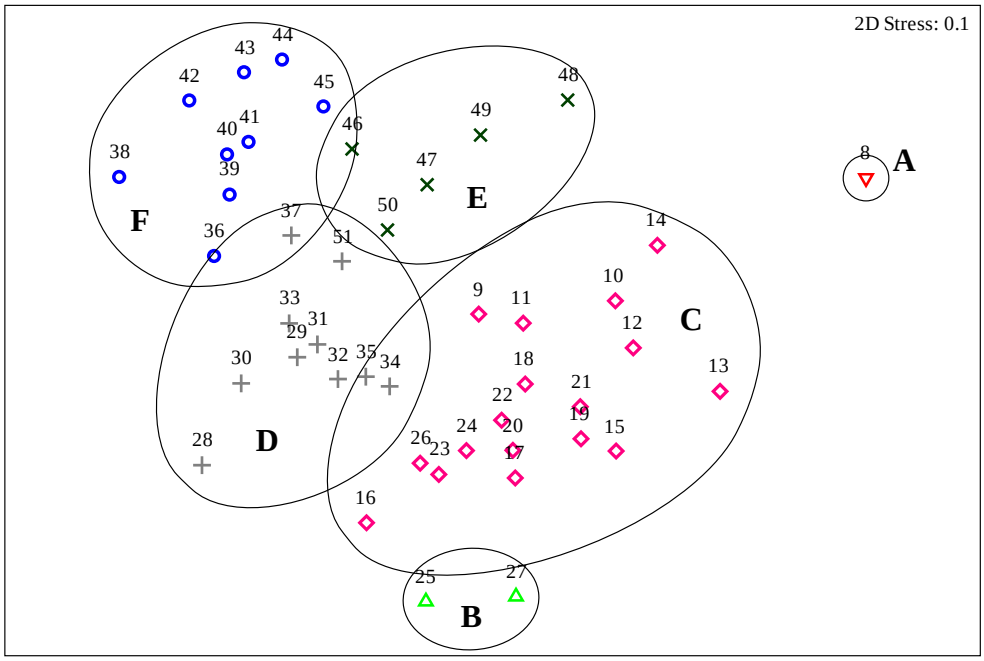


Figure 3-46: nMDS plot of environmental parameter groups at Iford Bridge on the Stour River. Numbers indicate the sample weeks and solid line is 2.6 of the Euclidean distance.

Group specifications are summarised in Table 3-9. Oxygen saturation and silicate concentration were the most important environmental parameters for defining the sample

group during the summer 2013 bloom (week 9 and 12), while the peak chlorophyll events in the spring (week 49 and 51) also occurred with these environment contributions. The oxygen saturation value was subsequently the majority factor to group definition at Iford Bridge site during the autumn – winter (group D and E). Otherwise, seasonal change in the silicate and nitrate concentrations were the dominant parameters in defining the environmental groups in almost every other sample week excluding during spring 2014 (group F). Group B was characterised by increasing nitrate concentration. All the high chlorophyll samples were in group C, D, and F when the levels of river flow were less than 30 $m^3 s^{-1}$.

Table 3-9: Main characteristics of sample groups defined by environmental parameters at Iford Bridge on the Stour River. The peak chlorophyll samples in Table 3-3 are indicated by sample weeks in bold.

| Group | Sample week no. | Parameter % contribution | Average square distance |
|---|---|---|---|
| A | 8 | single sample | - |
| B | 25, 27 | nitrate (45), oxygen saturation (41) | 1.79 |
| C | **9**, 10, 11, **12**, 13, 14, 15, 16, 17, 18, 19, 20, 21, 22, 23, 24, 26 | oxygen saturation (36), silicate (27), nitrate (18), phosphate (10) | 2.34 |
| D | 28, 29, 30, 31, 32, 33, 34, 35, 37, **51** | oxygen saturation (20), water temperature (16), river flow (15), silicate (12) | 1.95 |
| E | 36, 38, 39, 40, 41, 42, 43, 44, 45 | oxygen saturation (68), nitrate (17) | 1.80 |
| F | 46, 47, 48, **49**, 50 | silicate (45), nitrate (23), oxygen saturation (13), water temperature (10) | 1.25 |

***Knapp Mill, River Avon***

Seven groups (A – G) were defined by the dendrogram for hierarchical clustering as shown in Figure 3-47. The Euclidean distance between groups at Knapp Mill was 2.8. Group E was a mixed sample and the largest, with 17 samples followed by group C with 9 samples. Group A had 7 samples and the others between 5 and 6 samples. Group E included mixed

samples from spring 2013, summer, and the early autumn. Group A samples were almost all from winter, while group B samples represented the spring 2013 and 2014. Group C included all seasons except summer samples. Group G corresponded to samples in autumn, while group F had only one sample from week 38.

The nMDS analysis of the environmental data provide a two-dimensional distance plot (Figure 3-48) which shows more clearly how the samples are grouped at Knapp Mill. The plot stress was 0.13 which indicated a very good two-dimensional representation of the data. The plot distinguishes the samples of group D, E, and G before the flooding event, while group A samples indicate weeks after the flooding event.

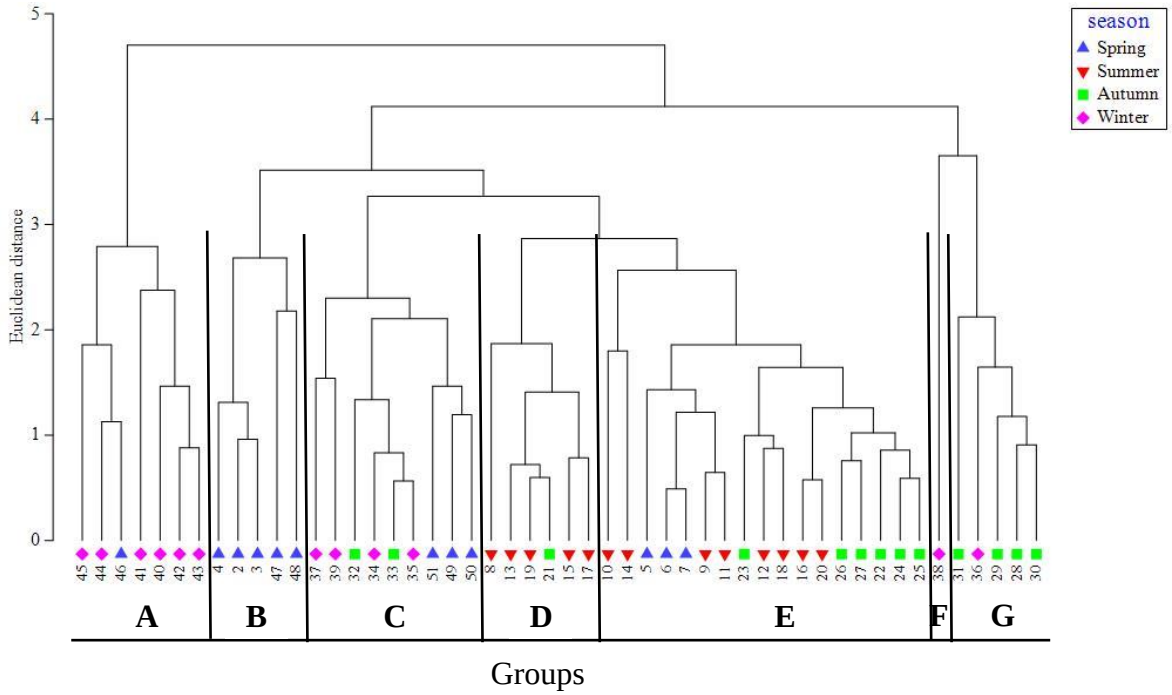


Figure 3-47: Dendrogram for hierarchical clustering of Knapp Mill samples defined by environmental parameters. Numbers indicate the sample weeks.

The group specifications are shown in Table 3-10. Four samples from the chlorophyll events are indicated in bold. Nonspecific environmental factors were the most important factor in defining the groups at this station. Chlorophyll concentration was high in spring and summer (group B, C, and E), but not in autumn. River flow rate became the main environmental parameter that influenced a grouping during high flow rates (group C). The SPM concentration showed as the major factor that influenced grouping either the decreasing river flow (group B) or a small peak river flow in group G.

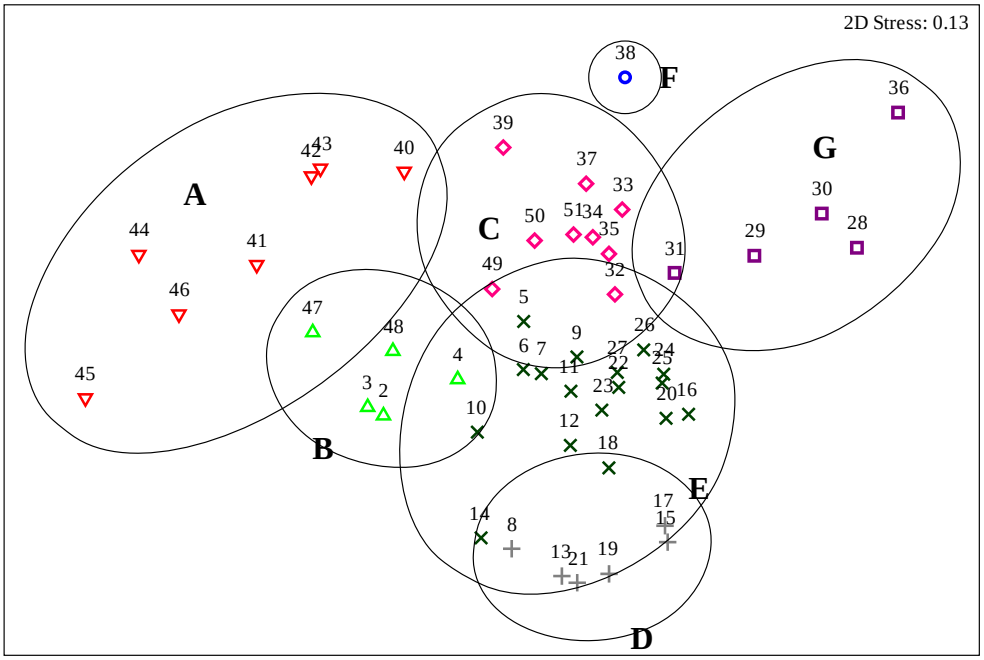


Figure 3-48: nMDS plot of environmental parameter at Knapp Mill on the Hampshire Avon River. Numbers indicate the sample weeks and solid line indicates 2.8 of the Euclidean distance.

Table 3-10: Main characteristics of sample groups defined by environmental parameters at Knapp Mill on the Hampshire Avon River. The peak chlorophyll samples in Table 3-4 are indicated by sample weeks in bold.

| Group | Sample week no. | Parameter % contribution | Average square distance |
|---|---|---|---|
| A | 40, 41, **42**, 43, 44, 45, 46 | oxygen saturation (40), silicate (40) | 3.09 |
| B | 2, **3**, 4, 47, 48 | SPM (35), phosphate (16), river flow (14), silicate (11), oxygen saturation (11) | 2.64 |
| C | 32, 33, 34, 35, 37, 39, 49, **50**, 51 | river flow (40), water temperature (16), nitrate (15), SPM (15) | 2.01 |
| D | 8, 13, 15, 17, 19, 21 | nitrate (34), phosphate (27), oxygen saturation (17) | 1.08 |
| E | 5, 6, 7, 9, **10**, 11, 12, 14, 16, 18, 20, | oxygen saturation (21), nitrate (16), water temperature (13) | 1.82 |

| | | | |
|---|---|---|---|
| | 22, 23, 24, 25, 26, 27 | | |
| F | 38 | single sample | - |
| G | 28, 29, 30, 31, 36 | SPM (65), nitrate (10) | 1.59 |

### 3.3.6.2 Phytoplankton taxa and biomass data analyses

The phytoplankton carbon biomass data (µg C $L^{-1}$) were transformed to the fourth root before illustrating by simple shade plot. Bray-Curtis similarity was performed between each pair of samples and clustering of this matrix to represent the similarity association in the cluster and nMDS plots. A one-way ANOSIM analysis comparing each group suggested that they were significantly different in composition.

***Throop, Stour River***

Figure 3-49 gives the shade plot for the most important species contributing to carbon biomass for Throop samples. The diatom species show a clear pattern of large biomass group followed by the cryptophyte and chlorophyte biomass groups. The highly dominant diatom species, *Stephanodiscus* sp., gave the most weight in the late spring 2013 (week 3, 4, and 5), while the chlorophyte species; *Chlamydomonas* sp. contributed most to biomass after the diatom bloom (week 8 – 14). The crytophyte species, *Cryptomonas* sp. and *Rhodomonas* sp. distinguished highly during summer time. Low phytoplankton biomass was observed during the winter months.

Cluster analysis of phytoplankton carbon biomass from Throop samples during April 2013 to April 2014 demonstrated six major clusters of samples (A – F) with a similarity level range of about 60 – 62% (Figure 3-50). The nMDS analysis showed a two-dimensional spatial representation of the similarities within sampled weeks based on the composition and biomass values (Figure 3-51). The plot with a stress of 0.11 indicates a good ordination and no real prospect of misinterpretation, which is not surprising, as many species are closely distributed over time as defined in Clarke *et al.* (2014). The one-way ANOSIM analysis comparing each group suggested that they were significantly different in composition with permutation numbers of 999 ($P$ = 0.001, R statistic from pairwise tests varied 0.63 to 1), and that the clustered groups are well separated, given that the R sample statistic values are close to 1 (Clarke *et al.*, 2014). Taxonomic cumulative contribution approximated 90% of the average similarity within each group is shown in Table 3-11.

The groups follow a seasonal pattern: group A and F consist of winter samples during the high river flow, group B and E contain almost entirely samples in spring of 2013 and 2014, group C is a set of early summer samples, and group D and F overlap all seasons. The lowest dissimilarity was between groups C and D at 32%, and the highest dissimilarity was between groups A and C at 81%. The average dissimilarity between the seasonal groups was 42%, for spring-summer (B and C), and 41% for the mixed groups (D and F).

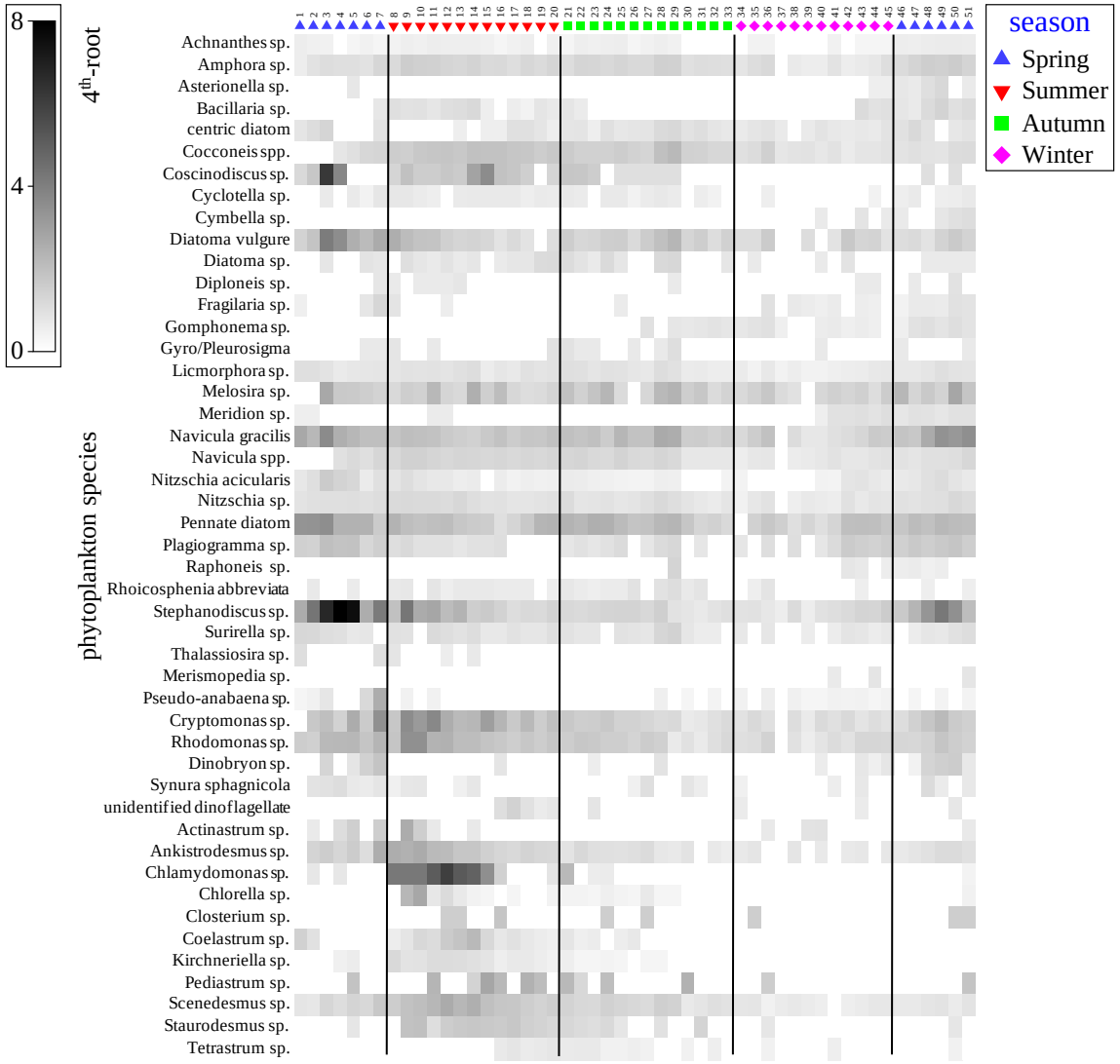


Figure 3-49: Shade plot indicating carbon biomass of each phytoplankton species ($4^{th}$-root transformed data on a log scale) for Throop samples. Numbers indicate the sample weeks.

The results of the SIMPER analysis at Throop are summarised in Table 3-11 and show how the groups are distinguished in terms of the carbon biomass of particular species. The diatom, *Stephanodiscus* sp., dominated spring groups (B and E) when the river flow was still low. In the late autumn and winter (group F), the pennate diatom, *Navicular gracilis*,

and the centric diatom, *Cocconeis*, were the main species. Group C is characterised by summer samples with a high component of chlorophyte and cryptophyte species and a low component of diatoms. Phytoplankton species during the late summer to the early autumn (group D) included various combinations of the diatom group. Another notable feature is the significant contribution of *Stephanodiscus* in group B

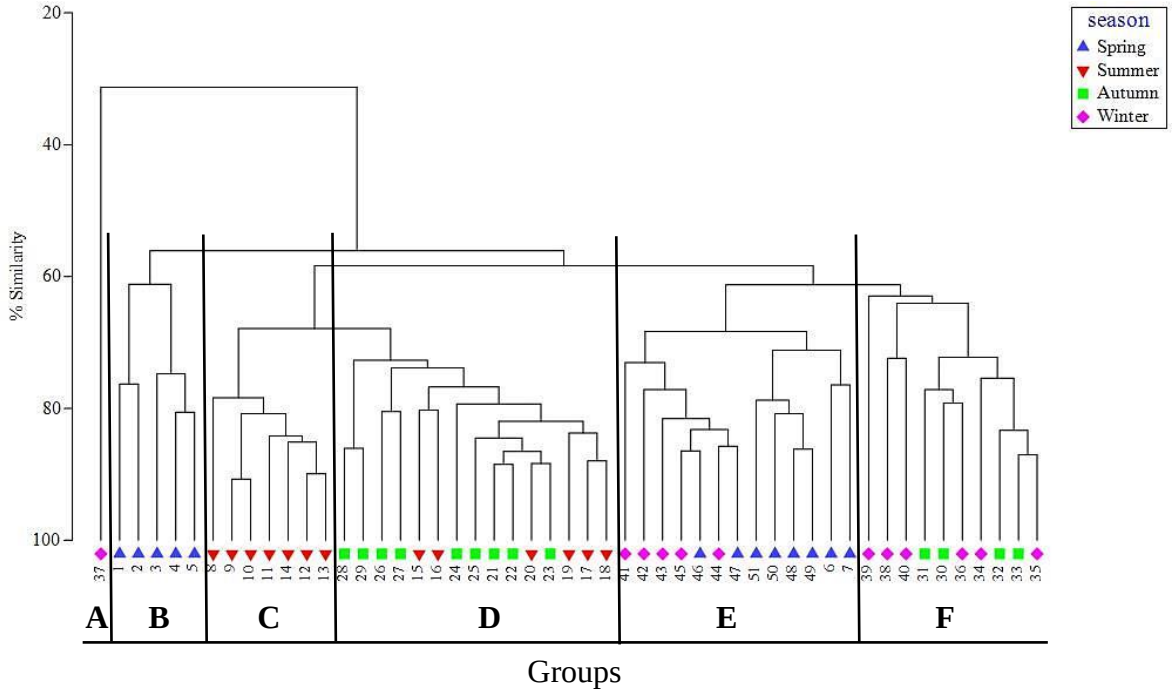


Figure 3-50: Dendrogram for hierarchical clustering of samples defined by phytoplankton carbon biomass at Throop on the Stour River. Numbers indicate the sample weeks.

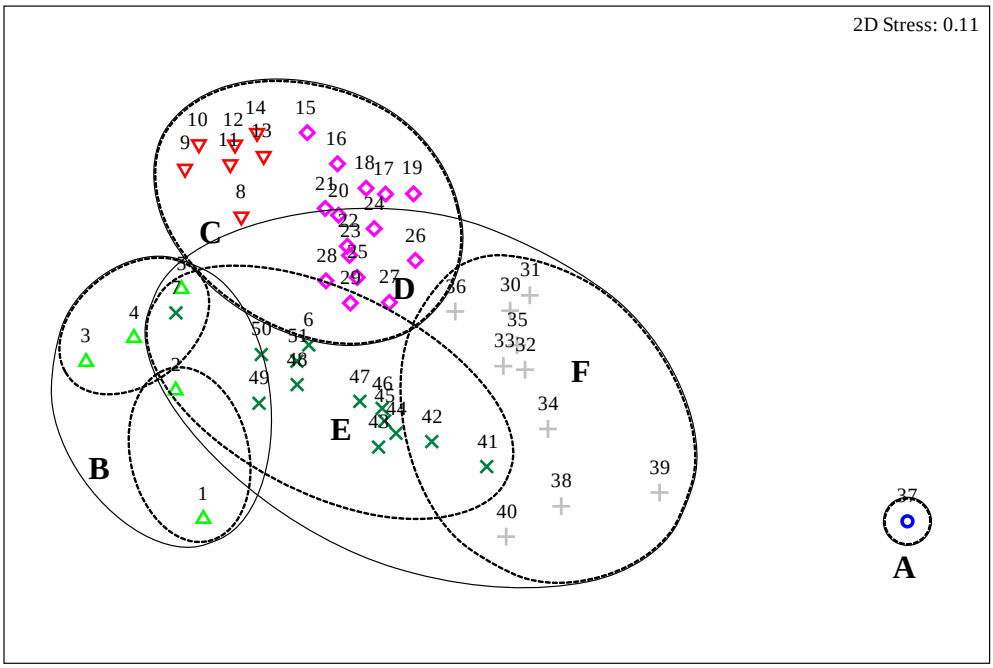

Figure 3-51: nMDS plot of samples defined by phytoplankton species/taxon carbon biomass at Throop on the Stour River. Numbers indicate the sample week. Dash line is 62% of the similarity and solid line indicates 60%.

Table 3-11: All characteristics of sample groups by phytoplankton species at Throop on the Stour River. The peak chlorophyll events in table are identified by sample weeks in bold.

| Group | Sample week no. | Species average carbon biomass as % contribution | % of similarity |
|---|---|---|---|
| A | 37 | single sample | - |
| B | 1, 2, **3**, **4**, **5** | *Stephanodiscus* (17), Pennate diatom (11), *Navicula gracilis* (9) | 67.3 |
| C | 8, **9**, 10, 11, **12**, 13,14 | *Chlamydomonas* (12), *Cryptomonas* (6), *Rhodomonas* (6) | 81.9 |
| D | 15, 16, 17, 18, 19, 20, 21, 22, 23, 24, 25, 26, 27, 28, 29 | *Navicula gracilis* (7), Pennate diatom (7), *Cocconeis* (6) | 77.4 |
| E | 6, **7**, 41, 42, 43, 44, 45, 46, 47, 48, **49**, 50, **51** | Pennate diatom (8), *Stephanodiscus* (7), *Navicular gracilis* (7) | 72.5 |
| F | 30, 31, 32, 33, 34, 35, 36, 38, 39, 40 | *Navicula gracilis* (9), *Cocconeis* (8), Pennate diatom (8) | 69.3 |
| | spring | *Stephanodiscus* (10), Pennate diatom (9), | 67.4 |
| | summer | *Cryptomonas* (7), *Rhodomonas* (6) | 75.1 |
| | autumn | *Navicula gracilis* (8), Pennate diatom (8) | 73.0 |
| | winter | Pennate diatom (10), *Cocconeis* (9) | 60.7 |

Phytoplankton were present at Throop throughout the sampling period, but some of them increased rapidly to become dominant species in particular weeks. The phytoplankton species successions are not clear between the phytoplankton species groups. However, *Stephanodiscus* which contributed most to peak chlorophyll concentrations was grouped in both B and E, and could be considered as a spring species that was associated with the environmental spring groups A and D (Table 3-8). *Chlamydomonas* and *Cryptomonas*

contributed highly to group C and are classified as summer species, and associated with the environmental group E in Table 3-8, which is characterised by high nutrients and low river flow in spring-summer period. Other groups overlap in terms of time and numbers of important species. Group A contained no samples with high chlorophyll levels and had different important species to the other groups, but the diatoms were the dominant phytoplankton type. The conclusion is that the diatom group was the main phytoplankton population throughout the monitoring programme at this station.

***Iford Bridge, Stour River***

The chlorophyte group show a clear pattern as the largest group at Iford Bridge followed by the cryptomonad and diatom species because the sampling programme at this site started after the spring diatom bloom during week 3 to 5 at Throop. The highly dominant diatom species, *Stephanodiscus* sp., gave the most weight in the early summer 2013 (week 9 and 11) and the spring 2014 (week 47 – 51), while *Chlamydomonas* sp. contributed most to biomass after the diatom bloom (week 8 – 15). *Cryptomonas* sp. and *Rhodomonas* sp. were distinguished highly during the summer period at the same time as the population of chlorophytes was increasing (Figure 3-52). During winter months (week 34 – 41) the phytoplankton carbon biomass was lower than during other seasons.

The results of phytoplankton carbon biomass at this station from the hierarchical clustering analysis are illustrated in the dendrogram (Figure 3-53). The one-way ANOSIM analysis comparing each group suggested that they were significantly different in composition with permutation numbers of 999 ($P$ = 0.001, R statistic from pairwise tests varied 0.64 to 1). There are five groups (A – E). There was also 1 single sample (group A). Group B is represented by summer samples from week 8 – 15, while almost all spring samples are in group D (week 43 – 51). Group C and E present combined samples.

The two-dimensional nMDS plot in Figure 3-54 has a low stress of 0.08, which indicates good ordination and no real prospect of misinterpretation. Group B represents all the phytoplankton biomass in the summer period, while group C was mixed within the late summer and the early autumn samples. Almost all the spring 2014 samples are represented in group D. Group E samples are from mixed seasons. Group A has only one sample from week 38 that was collected during the highest winter river flow rate on the Stour River as recorded at Throop.

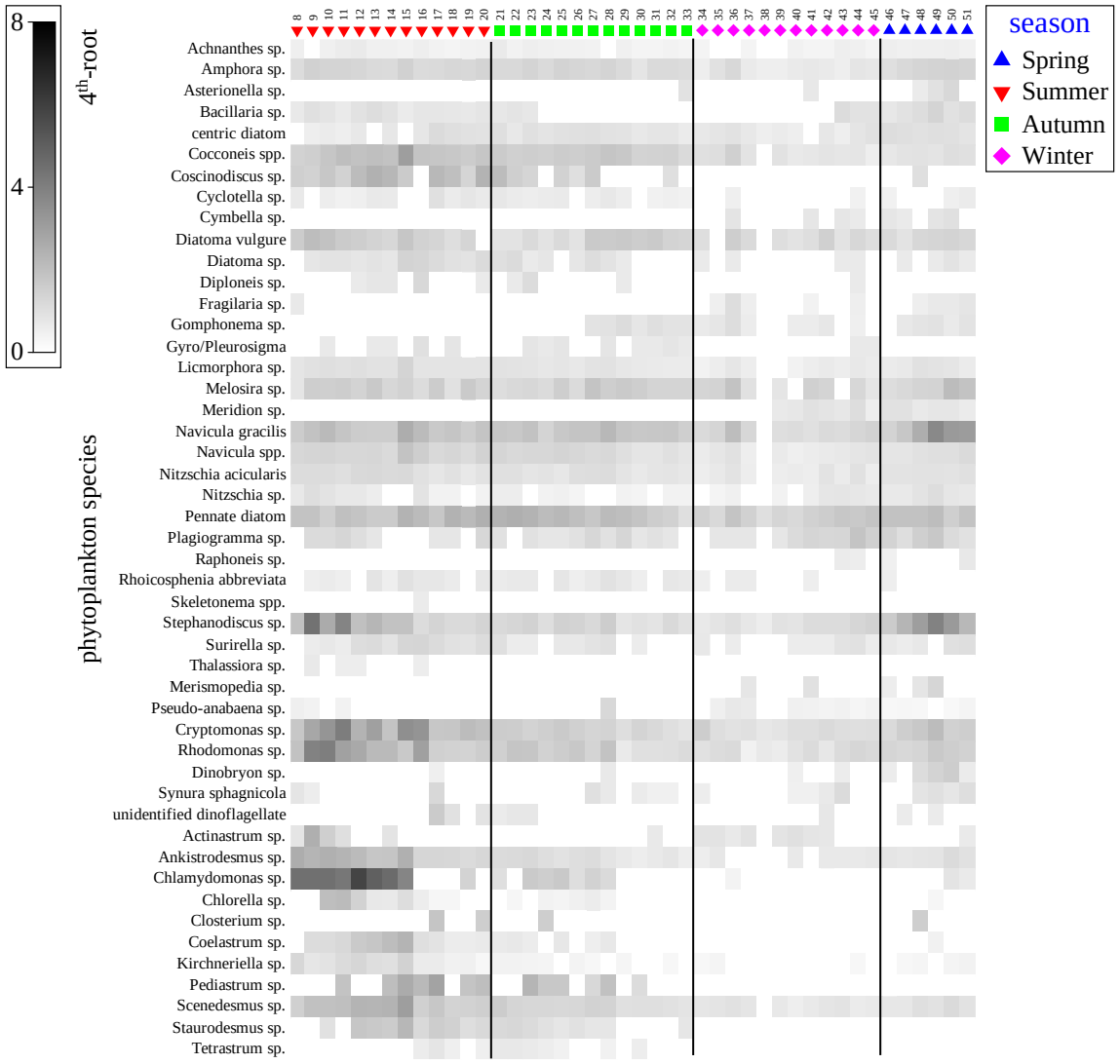


Figure 3-52: Shade plot indicating carbon biomass of each phytoplankton species ($4^{th}$-root transformed data on a log scale) for Iford Bridge samples. Numbers indicate the sample weeks.

Further analysis of the groups was based on species carbon biomass using SIMPER test, which determines the dominant species of each group, using percentage contribution and mean biomass in a similar way as at Throop. The results are summarised in Table 3-12. The contribution and biomass at Iford Bridge showed a similar pattern to Throop. Diatoms were the major contributors to most of the groups for almost every season except in summer. The chlorophyte and cryptophyte groups (*Chlamydomonas*, *Cryptomonas*, and *Rhodomonas*) made a high contribution and were present mainly in the summer period and peak chlorophyll events in week 9 and 12. Meanwhile, the other events in week 49 and 51 (I3 and I4) occurred in group D with a dominance of diatoms species.

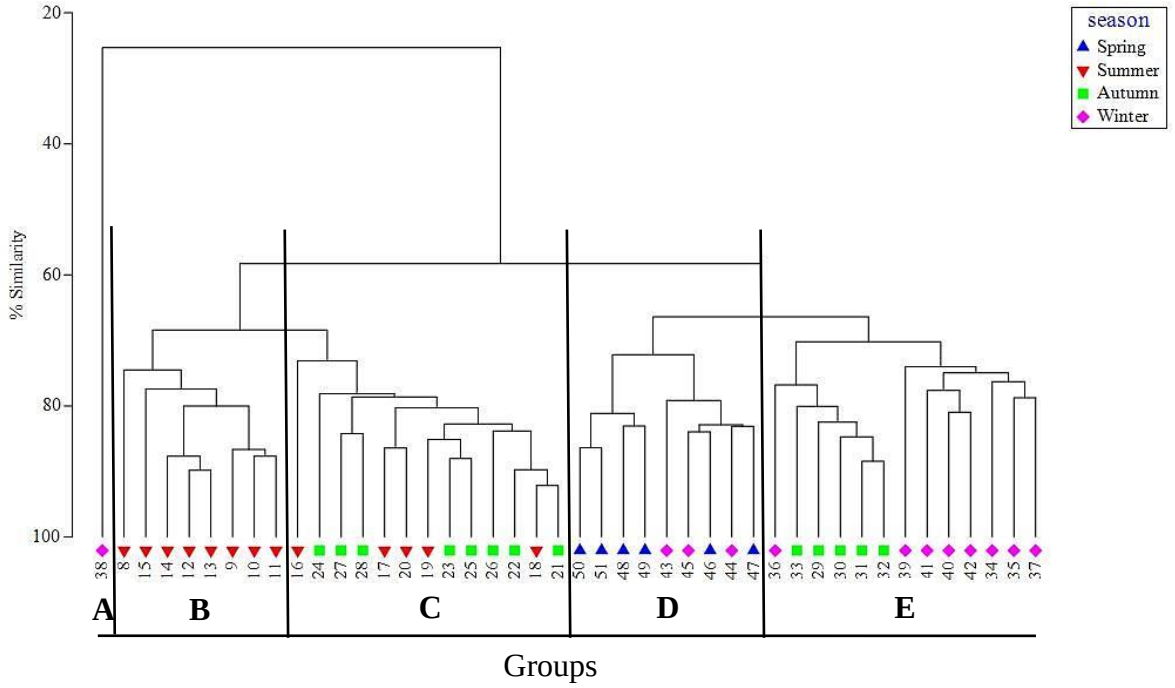


Figure 3-53: Dendrogram for hierarchical clustering of samples defined by phytoplankton carbon biomass at Iford Bridge. Numbers indicate the sample weeks.

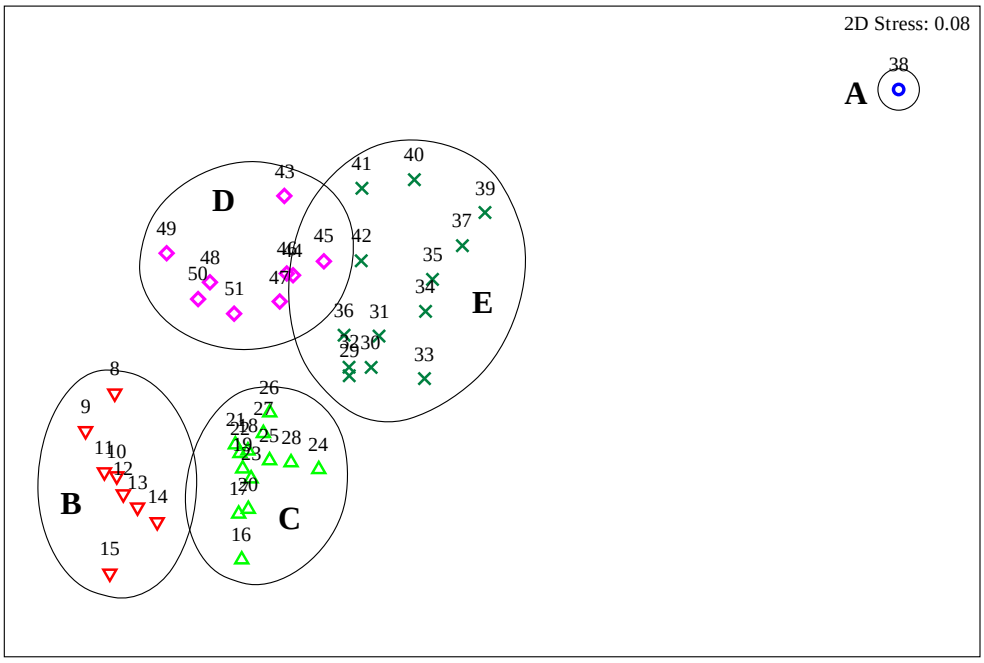


Figure 3-54: nMDS plot of samples defined by phytoplankton species/taxon carbon biomass at Iford Bridge on the Stour River. Numbers indicate the sample week at 70% similarity

Table 3-12: Main characteristics of sample groups by phytoplankton species at Iford Bridge. The peak chlorophyll events in table are identified by sample weeks in bold.

| Group | Sample week no. | Species average carbon biomass as % contribution | % of similarity |
|---|---|---|---|
| A | 38 | single sample | - |
| B | 8, **9**, 10, 11, **12**, 13, 14, 15 | *Chlamydomonas* (12), *Cryptomonas* (6), *Rhodomonas* (6) | 79.7 |
| C | 16, 17, 18, 19, 20, 21, 22, 23, 24, 25, 26, 27, 28 | Pennate diatom (8), *Navicula gracilis* (6), *Cocconeis* (6), *Cryptomonas* (6), *Rhodomonas* (6) | 79.9 |
| D | 43, 44, 45, 46, 47, 48, **49**, 50, **51** | Pennate diatom (8), *Stephanodiscus* (7), *Navicula gracilis* (7) | 76.5 |
| E | 29, 30, 31, 32, 33, 34, 35, 36, 37, 39, 40, 41, 42 | Pennate diatom (9), *Navicula gracilis* (6), *Melosira* (7), *Cryptomonas* (7) | 73.6 |
| | spring | Pennate diatom (8), *Stephanodiscus* (7) | 75.9 |
| | summer | *Cryptomonas* (7), Pennate diatom (6), *Rhodomonas* (6) | 74.1 |
| | autumn | Pennate diatom (8), *Navicula gracilis* (8), *Cocconeis* (7) | 75.8 |
| | winter | Pennate diatom (12), *Cryptomonas* (9) | 63.8 |

***Knapp Mill, Avon River***

The shade plot of Knapp Mill phytoplankton samples shows some differences to the Stour River stations. The chlorophytes and cryptophytes were not the dominant group in summer time as they were at both sampling sites on the Stour River, however, the diatom species were the major group throughout the sampling period. The diatoms *Stephanodiscus* sp., *Navicula gracilis*, and *Navicula gracilis* were the dominant species on the Avon River as shown in Figure 3-55.

The hierarchical clustered analysis is plotted as a dendrogram in Figure 3-56 to indicate the species similarity distribution. Most groups were defined with a similarity level of 72% (B – E) with each group containing ≥ 8 samples. Group A contained three samples with a similarity level of 65%. The low similarity of this group can be attributed to the presence of rare species.

A two-dimensional nMDS plot (Figure 3-57) with a stress of 0.13 gives an acceptable representation of the data. Group distribution follows seasonal patterns: group A are winter samples during the flooding period, group B samples are mixed late summer-early winter communities, group C is almost entirely summer samples, and D and E are spring season groups.

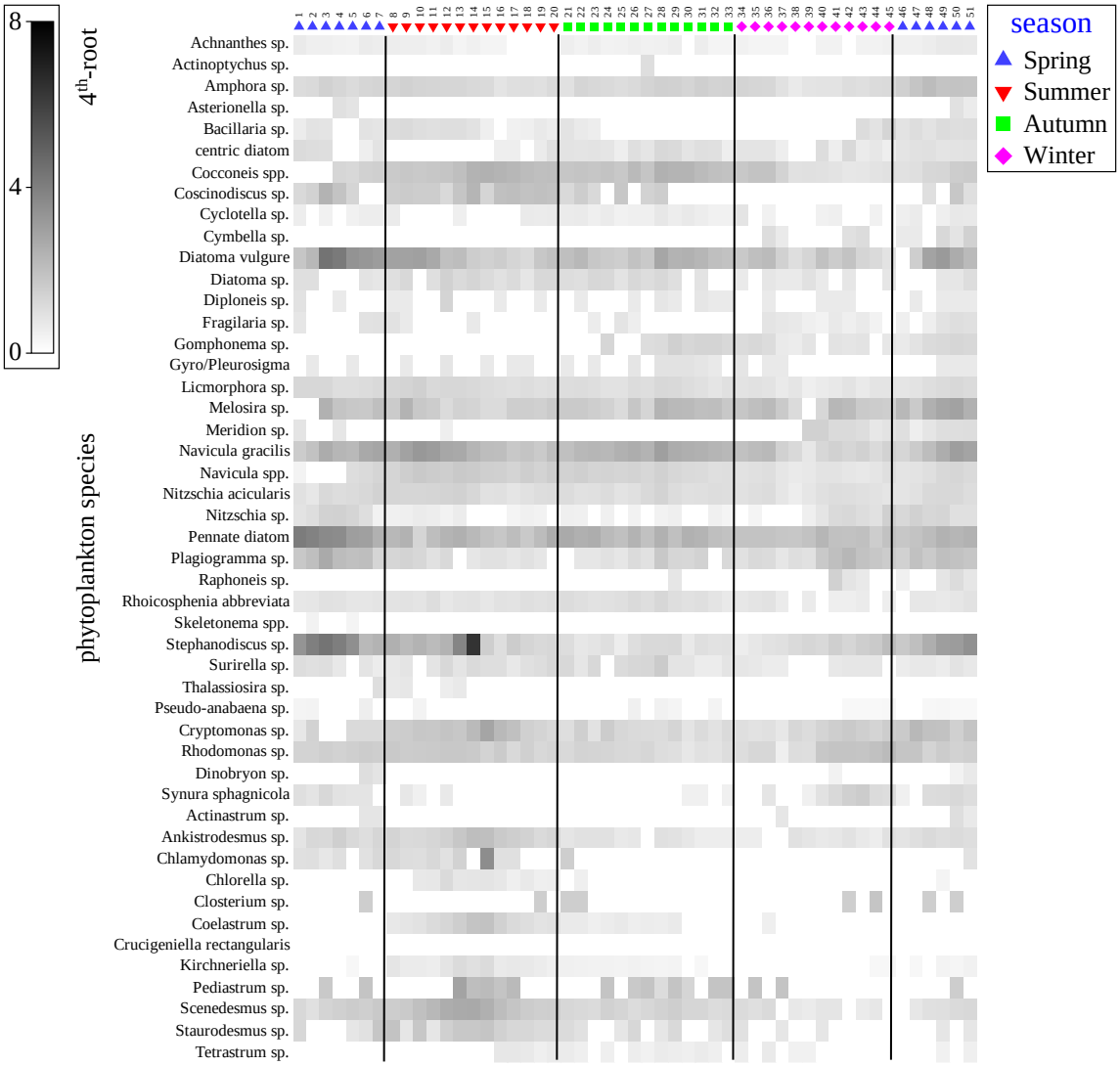


Figure 3-55: Shade plot indicating carbon biomass of each phytoplankton species ($4^{th}$-root transformed data on a log scale) for Knapp Mill samples. Numbers indicate the sample weeks.

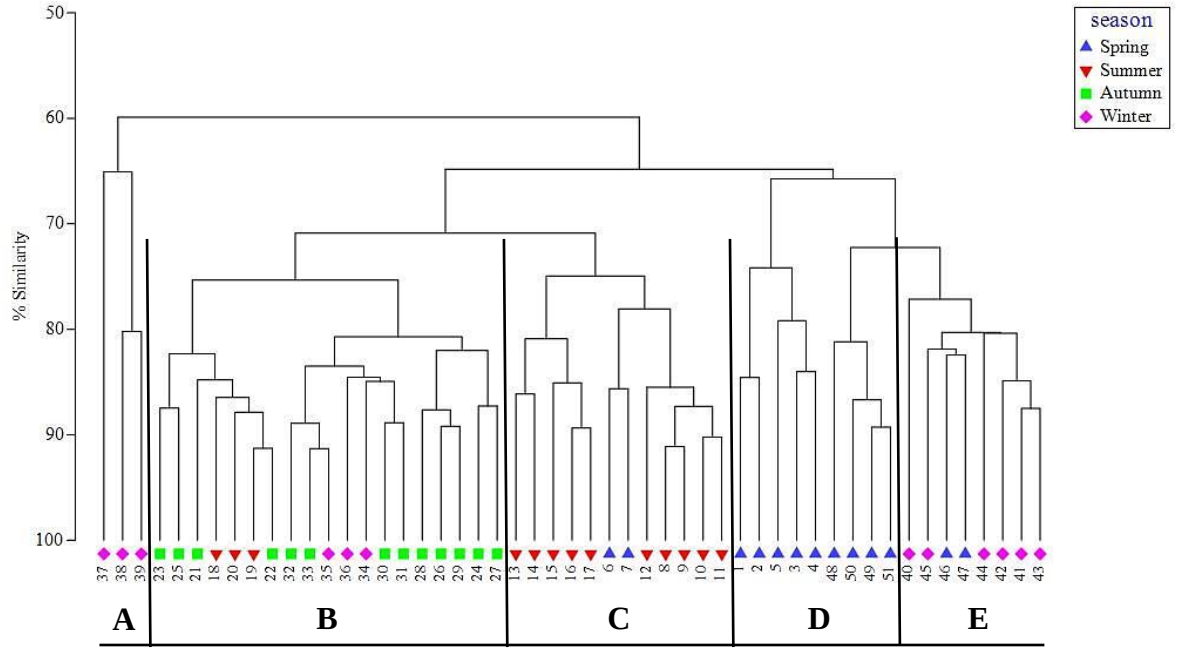


Figure 3-56: Dendrogram for hierarchical clustering of samples defined by phytoplankton carbon biomass at Knapp Mill station. Numbers indicate the sample weeks.

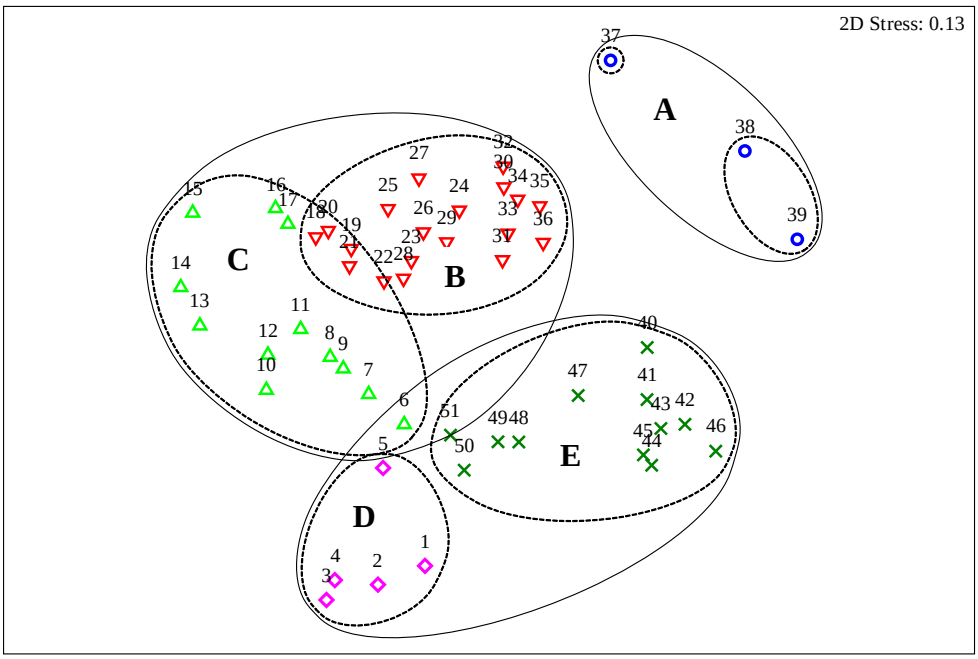


Figure 3-57: nMDS plot of samples defined by phytoplankton species/taxon carbon biomass at Knapp Mill. Numbers indicate the sample week. Dash line is 65% of the similarity and solid line indicates 72%.

The SIMPER analysis of the groups was obtained from species data and the results are summarised in Table 3-13. The phytoplankton succession can be described as starting with a mixed sample in group B, shifting to summer diatom bloom in group C, with *Navicula gracilis* and *Diatoma vulgare* sp. as the dominant species. The spring 2013 samples (group

D) mainly contained *Stephanodiscus* sp. as did the diatom bloom at Throop. In the mixed group E, diatoms were present and it included the cryptomonads species, *Rhodomonas* sp. The chlorophyte species, *Scenedesmus* spp. contributed especially highly to the summer group C.

Table 3-13: Main characteristics of sample groups by phytoplankton species at Knapp Mill on the Hampshire Avon River. The peak chlorophyll events in table are identified by sample weeks in bold.

| Group | Sample week no. | Species average carbon biomass as % contribution | % of similarity |
|---|---|---|---|
| A | 37, 38, 39 | Pennate diatom (13), *Diatoma vulgare* (8), *Stephanodiscus* (7), *Cocconeis* (7) | 70.1 |
| B | 18, 19, 20, 21, 22, 23, 24, 25, 26, 27, 28, 29, 30, 31, 32, 33, 34, 35, 36 | *Navicula gracilis* (8), Pennate diatom (8), *Cocconeis* (7), *Diatoma vulgare* (7) | 79.4 |
| C | 6, 7, 8, 9, **10**, 11, 12, 13, 14, 15, 16, 17 | *Navicula gracilis* (7), Pennate diatom (6), *Diatoma vulgare* (6), *Stephanodiscus* (6), *Scenedesmus* (6) | 78.7 |
| D | 1, 2, **3**, 4, 5 | *Stephanodiscus* (13), Pennate diatom (12), *Diatoma vulgare* (9) | 77.2 |
| E | 40, 41, **42**, 43, 44, 45, 46, 47, 48, 49, **50**, 51 | Pennate diatom (7), *Melosira* (7), *Plagiogramma* (7), *Rhodomonas* (6) | 76.9 |
| | spring | *Stephanodiscus* (8), Pennate diatom (8), *Pleurotaenium* (7), *Navicula gracilis* (6) | 71.6 |
| | summer | *Navicula gracilis* (7), Pennate diatom (6), *Cocconeis* (6), *Scenedesmus* (6) | 80.1 |
| | autumn | *Navicula gracilis* (9), Pennate diatom (8), *Cocconeis* (7), *Navicula gracilis* (7) | 80.5 |
| | winter | Pennate diatom (10), *Diatoma vulgare* (9), *Navicula gracilis* (7), *Melosira* (6) | 71.2 |

### 3.3.6.3 Accessory pigment analyse

Data for the accessory pigments were normalised by fourth root transformation before illustrating by simple shade plot as for the carbon biomass data, calculated using the Bray-Curtis Similarity Index, and hierarchical clustering used to define groups with similarities. The similarity percentage analysis (SIMPER) routine was also used to explore the similarities within groups of samples. No HPLC pigment data from Iford Bridge station are present in this study.

***Throop, Stour River***

The shade plot of Throop samples shows representations of the pigment data matrices. The matrix indicates with full black the weighted pigment and white representing absence of the pigment as for the phytoplankton carbon biomass in Section 3.3.6.2. Chlorophyll *a* and fucoxanthin were the main accessory pigments at this station. The highest fucoxanthin concentration occurred during the spring *Stephanodiscus* sp. bloom (week 3, 4, and 5) as shown in Figure 3-58. Diadinoxanthin and chlorophyll *c2* are biomarkers of several phytoplankton groups, and were simultaneously high during the spring bloom. It seems that many phytoplankton groups were growing together to form the bloom based on the high concentrations of these pigments.

The hierarchical clustering used to define groups with similarities ranged from 77 – 79%. The results of hierarchical cluster analysis demonstrated as a dendrogram (Figure 3-59), showed seven phytoplankton groups (A – G). All groups had ≥ 3 samples. Group G had all winter samples during the high winter flood period, while the samples from high chlorophyll events (week 3 – 5) were present in group B. Group D is large with a number of mixed samples (13 samples). Group E is also a combination of spring and summer seasons.

The two-dimensional nMDS plot in Figure 3-60 with a stress of 0.09 indicates a good ordination and no real prospect of misinterpretation, which is not surprising, as many pigments are closely distributed over time. The groups follow a seasonal pattern: group A and G consist of winter samples during the flooding event, group C and F are all samples in spring, group B is all samples during the spring bloom of 2013, group D overlap all seasons.

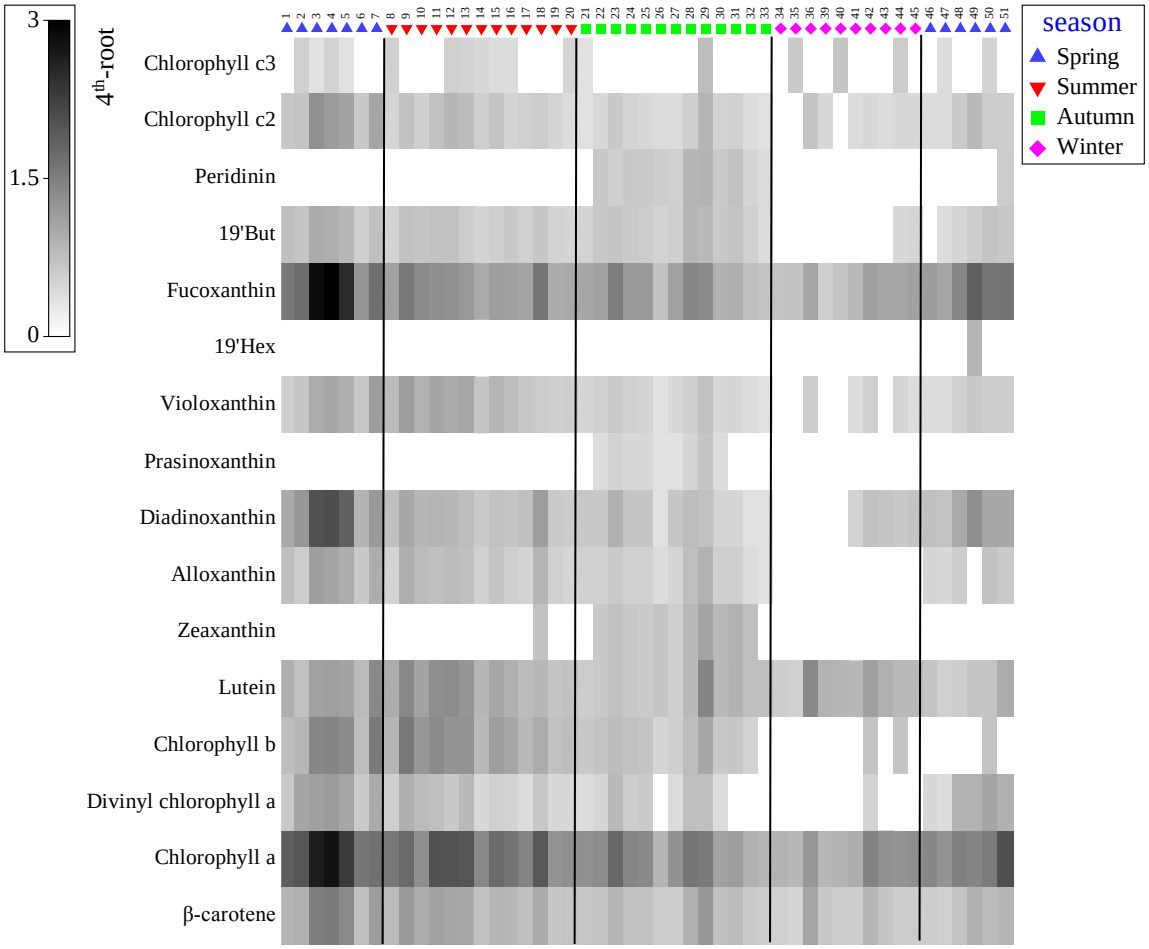


Figure 3-58: Shade plot indicating accessory pigments ($4^{th}$-root transformed data on a log scale) for Throop samples. Numbers indicate the sample weeks.

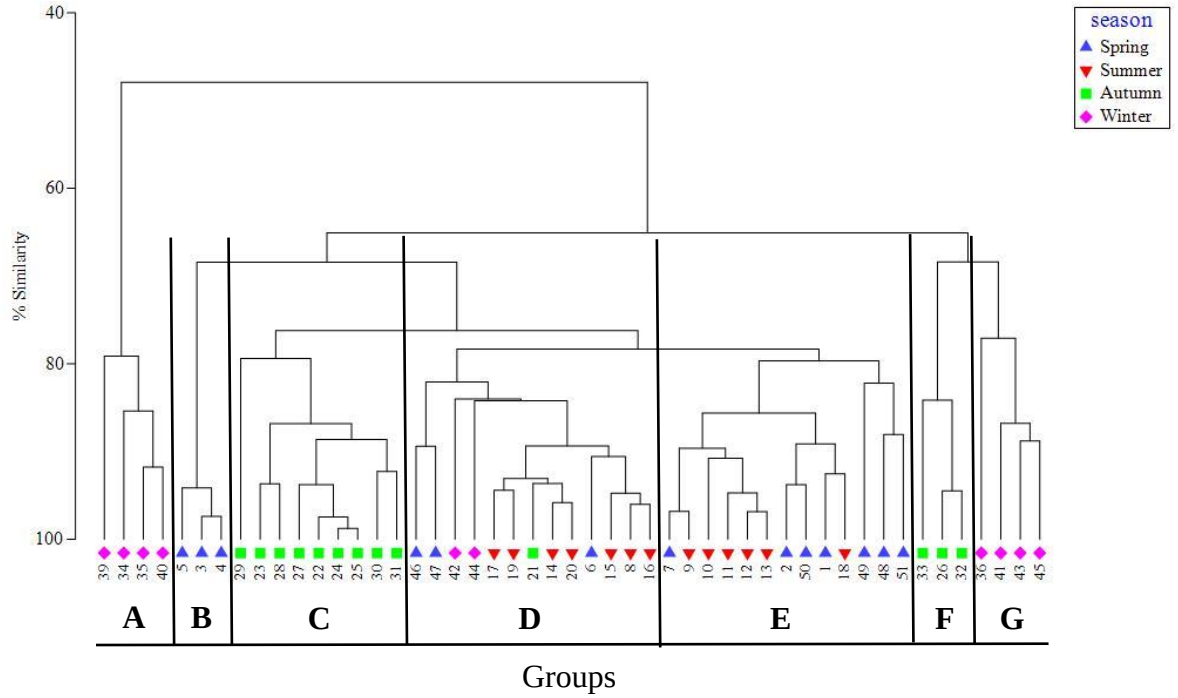


Figure 3-59: Dendrogram for hierarchical clustering of Throop samples defined by HPLC pigments at 77 and 79% of similarity level. Numbers indicate the sample weeks.

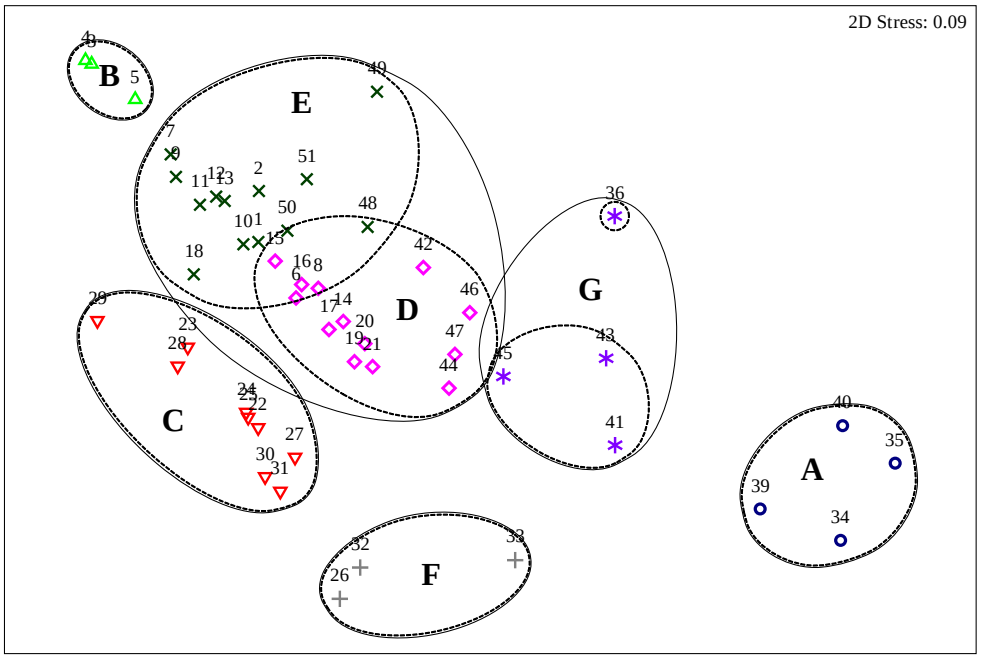


Figure 3-60: nMDS plot of samples defined by HPLC pigments at Throop on the Stour River. Numbers indicate the sample week. Dash line is 79% of the similarity and solid line indicates 77%.

The group specifications are summarised in Table 3-14. Group B samples were characterised by fucoxanthin concentration in week 3, 4, and 5 during the *Stephanodiscus* bloom. The source of the fucoxanthin in samples at that time is not readily distinguished

from the cell count data (Figure 3-34), and this anomaly may be indicative of under sampling of large diatoms in the relatively small volume (10 mL) water samples used for cell counts compared to the large volumes (500 – 1000 mL) used for HPLC analysis. Group D contained a large number of sampling weeks, while the other group E are similar with fucoxanthin as the main accessory pigment followed by lutein as a biomarker of chlorophytes.

Table 3-14: Main characteristics of sample groups in terms of photosynthetic pigment composition at Throop on the Stour River. The peak chlorophyll events in table are identified by sample weeks in bold.

| Group | Sample week no. | Pigments (% contribution) | % of similarity |
|---|---|---|---|
| A | 34, 35, 39, 40 | chlorophyll *a* (31), fucoxanthin (23), lutein (22) | 83.3 |
| B | **3**, **4**, **5** | fucoxanthin (16), chlorophyll *a* (15), diadinoxanthin (12), β carotene (9), chlorophyll *b* (9), chlorophyll *c2* (7), lutein (7) | 95.2 |
| C | 22, 23, 24, 25, 27, 28, 29, 30, 31 | chlorophyll *a* (14), fucoxanthin (12), β carotene (8), zeaxanthin (7), chlorophyll *b* (7), 19'But (7), peridinin (7), diadinoxanthin (7) | 87.4 |
| D | 6, 8, 14, 15, 16, 17, 19, 20, 21, 42, 44, 46, 47 | chlorophyll *a* (19), fucoxanthin (15), lutein (10), diadinoxanthin (8), β carotene (9), violaxanthin (7), chlorophyll *b* (7) | 86.8 |
| E | 1, 2, **7**, **9**, **10**, 11, **12**, 13, 18, 48, **49**, **50** | chlorophyll *a* (17), fucoxanthin (15), diadinoxanthin (10), β carotene (9), lutein (9), divinyl chlorophyll *a* (8), violaxanthin (7) | 84.8 |
| F | 26, 35, 39 | chlorophyll *a* (16), fucoxanthin (13), lutein (13), β carotene (11), 19'But (8), chlorophyll *c2* (7) | 87.6 |
| G | 36, 41, 43, 45 | chlorophyll *a* (25), fucoxanthin (21), lutein (19), β carotene (14) | 82.3 |

***Knapp Mill, Avon River***

The shade plot of accessory pigment samples shows representations of the pigment data matrices. Chlorophyll *a* and fucoxanthin concentrations were again the main accessory pigments at this station. The highest fucoxanthin concentration occurred during spring 2013 as shown in Figure 3-61. Diadinoxanthin, a biomarker of several phytoplankton groups, was simultaneously high during the spring bloom as it was at Throop. It seems that many phytoplankton groups were growing together and blooming from the high concentration of this pigment. 19'Hex, prasinoxanthin, and zeaxanthin showed low concentrations throughout the sampling period.

The hierarchical clustering used to define groups with similarities produced results in the range of 76%. The results of hierarchical clustered analysis demonstrated as a dendrogram (Figure 3-62), showed seven phytoplankton groups (A – G). Each group had ≥ 3 samples, except group B with just one sample from week 32. Group A had all winter samples during the high winter flood period. The samples in the peak chlorophyll events (week 3 and 10, K1 and K2) were presented in group C that includes a mixture of seasons, while the other chlorophyll events in week 42 and 50 (K3 and K4) occurred in group E. Group F is large with a number of mixed samples (21 samples).

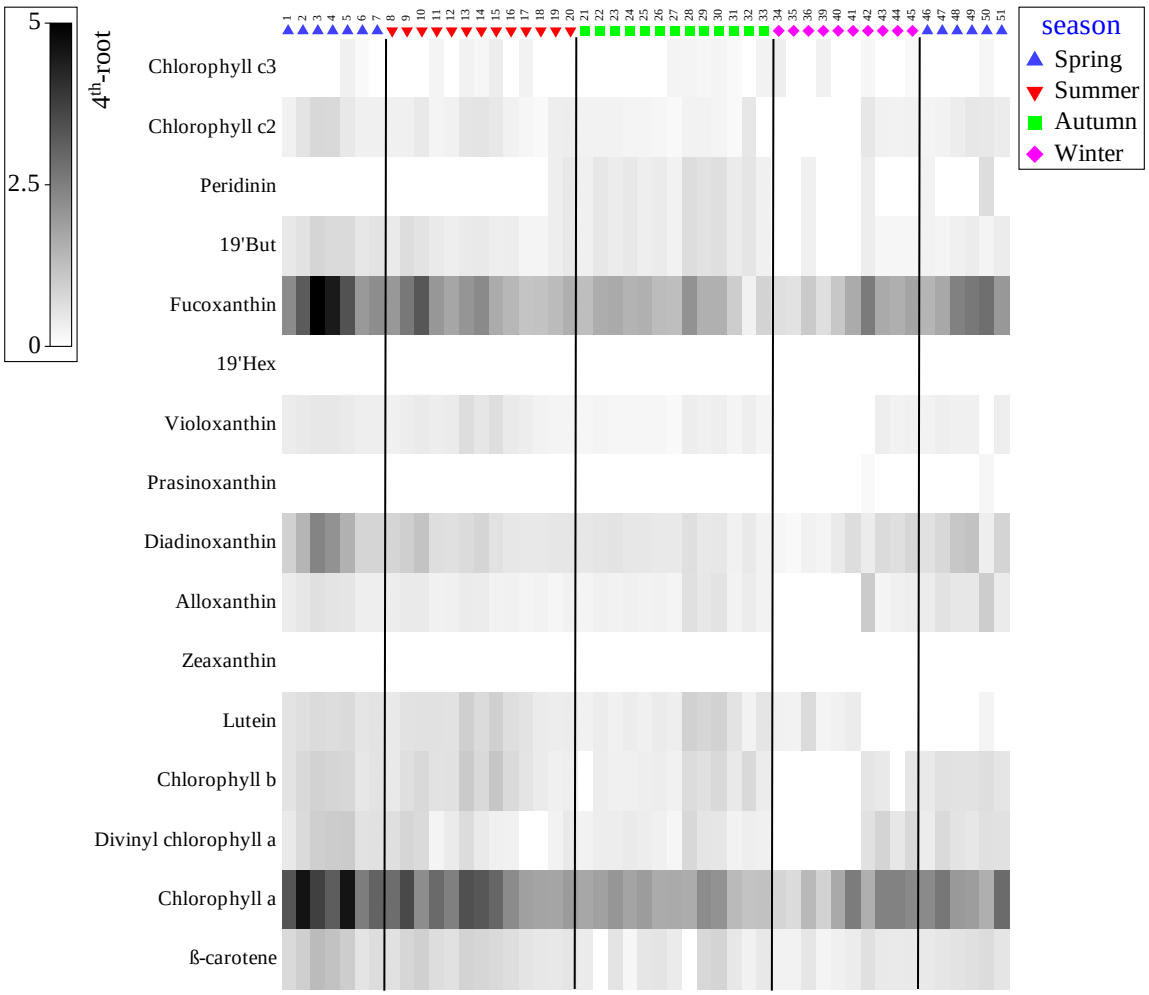


Figure 3-61: Shade plot indicating accessory pigments ($4^{th}$-root transformed data on a log scale) for Knapp Mill samples. Numbers indicate the sample weeks.

The two-dimensional nMDS plot in Figure 3-63 with a stress of 0.08 indicates a good ordination and no real prospect of misinterpretation, which is not surprising, as many pigments are closely distributed over time. The groups follow a seasonal pattern: group E and F consist of winter samples during the massive flooding event, group A is all samples in spring 2014 (week 42 and 50), group B, C, and D overlap all seasons.

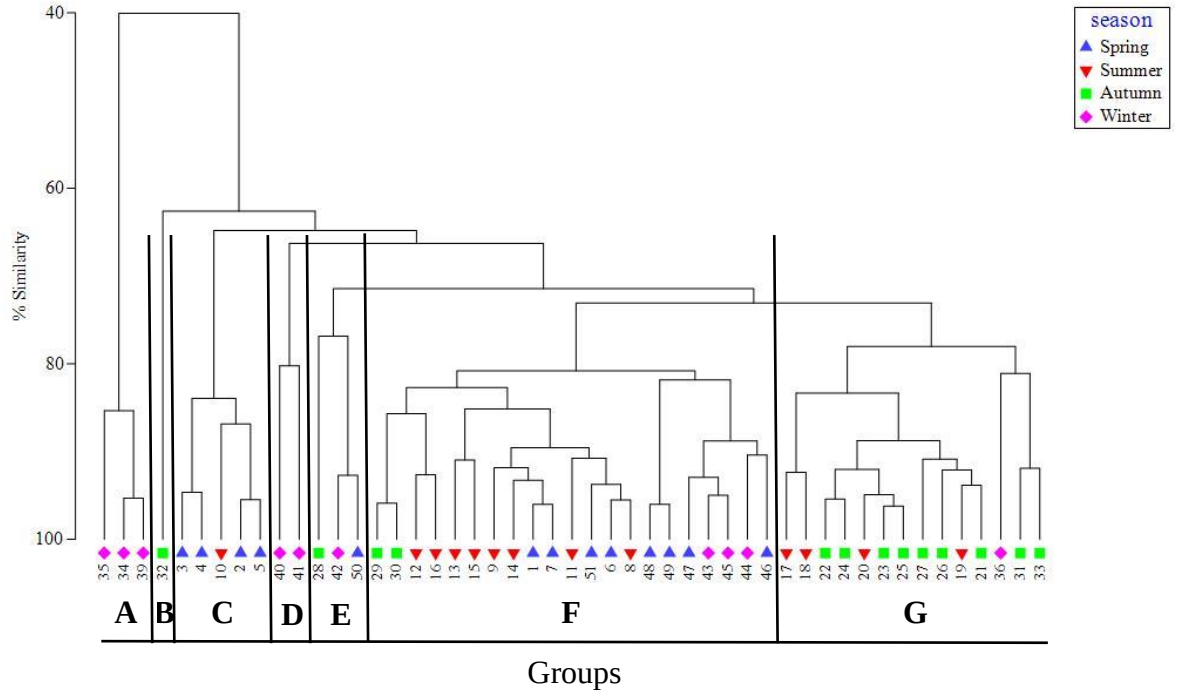


Figure 3-62: Dendrogram for hierarchical clustering of Knapp Mill samples defined by HPLC pigments at 76% of similarity level. Numbers indicate the sample weeks.

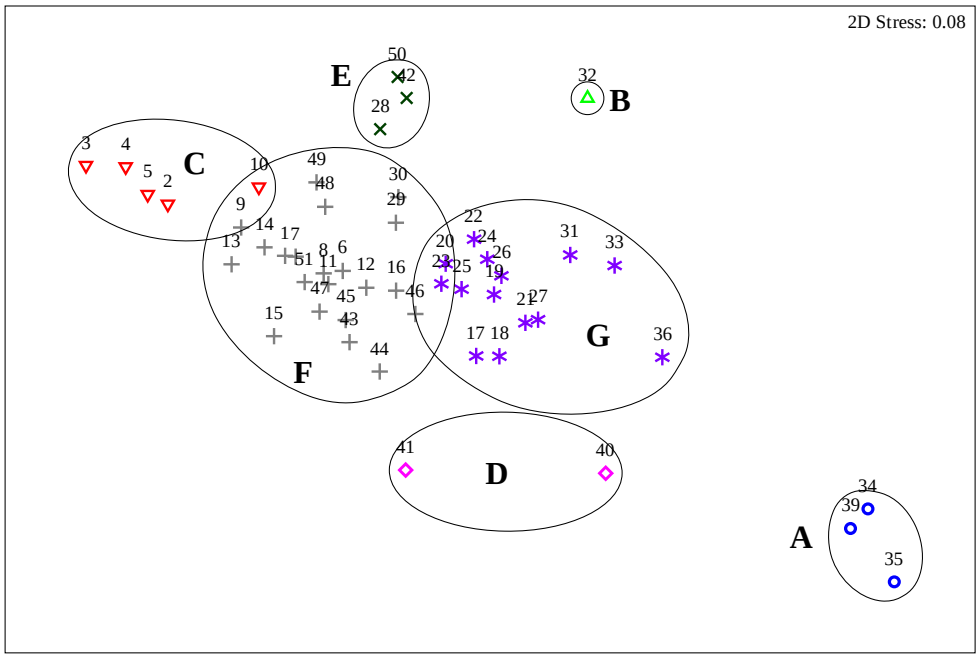


Figure 3-63: nMDS plot of samples defined by HPLC pigments at Knapp Mill on the Hampshire Avon River. Numbers indicate the sample week at 76% of similarity level.

The group specifications of accessory pigments at this station are summarised in Table 3-15. Group A and E samples were characterised by fucoxanthin concentration in the peak chlorophyll events (week 3, 4, 42, and 50). The source of the fucoxanthin in samples at that

time is not readily distinguished from the cell count data (Figure 3-35), and this anomaly may be indicative of under sampling of large diatoms in the relatively small volume (10 mL) water samples used for cell counts compared to the large volumes (500 – 1000 mL) used for HPLC analysis. Group F has a large number of sampling weeks, while group A, D, and G are similar with chlorophyll *a* as the main pigment followed by fucoxanthin as a biomarker of diatoms.

Table 3-15: Main characteristics of sample group in terms of photosynthetic pigment composition at Knapp Mill on the Hampshire Avon River. The peak chlorophyll events in table are identified by sample weeks in bold.

| Group | Sample week no. | Pigments (% contribution) | % of similarity |
|---|---|---|---|
| A | 34, 35, 39 | chlorophyll *a* (37), fucoxanthin (29), lutein (11) | 88.7 |
| B | 32 | single sample | - |
| C | 2, **3**, 4, 5, **10** | fucoxanthin (26), chlorophyll *a* (23), diadinoxanthin (11), β carotene (7) | 86.7 |
| D | 40, 41 | chlorophyll *a* (45), fucoxanthin (29) | 80.2 |
| E | 28, **42**, **50** | fucoxanthin (30), chlorophyll *a* (21), alloxanthin (10), divinyl chlorophyll *a* (8), chlorophyll *b* (7) | 82.1 |
| F | 1, 6, 7, 8, 9, 11, 12, 13, 14, 15, 16, 29, 30, 43, 44, 45, 46, 47, 48, 49, 51 | chlorophyll *a* (32), fucoxanthin (23), diadinoxanthin (8), β carotene (7), chlorophyll *b* (6) | 83.7 |
| G | 17, 18, 19, 20, 21, 22, 23, 24, 25, 26, 27, 31, 33, 36 | chlorophyll *a* (30), fucoxanthin (22), diadinoxanthin (7), β carotene (7), lutein (7) | 84.4 |

#### 3.3.6.4 Relation of environmental and biological parameters

Multivariate analysis based on environmental parameters and on phytoplankton characteristics have shown how samples are grouped in terms of similarity. Examination of the two phytoplankton characteristics including species carbon biomass and accessory pigments gave a different grouping. Seasonal changes could be clearly distinguished on the basis of environmental factors, but were less well defined by the phytoplankton data. To

address more directly the question of how environmental conditions affected the phytoplankton community, a further analysis was performed using the CANOCO software as described under statistical analysis in Chapter 2.

***Throop, River Stour***

Environmental variables that explained the variance (explanatory variables) in the carbon biomass of phytoplankton taxa at Throop were investigated using RDA. The ordination diagram in Figure 3-64 revealed associations between each taxon and the explanatory variables. Proximity of taxa to the environmental variables (arrows) in the same or opposite direction suggests negative or positive correlations, whereas no proximity suggest a weak or no correlation and the longer the arrow the stronger the correlation.

The associations in the ordination diagram (Figure 3-64) show that the carbon biomass of riverine diatoms (Bacillariophyta) was correlated positively with water temperature and phosphate concentration and high biomass occurred during summer months. Chrysophyta and cyanophyta groups dominate in water where nitrate concentrations were high. Meanwhile, cryptophyta and chlorophyta were found in relatively warmer waters with high oxygen saturation. Dinoflagellate biomass was positively correlated with phosphate concentrations. All phytoplankton biomass was negatively correlated with river flow, SPM, and silicate concentrations at Throop. River discharge was inversely correlated with water temperature that led to a phosphate maximum in summer, probably the phosphate maximum was more related to low river flow as this would have reduced its dilution.

The x axis of the analysis explained most of the variance (eigenvalue = 48.9%, cumulative percentage variance between biomass and environmental parameters = 89.6%), whereas all canonical axes explained 99.9% of the variance as shown in Figure 3-64 and Table 3-16. This means a) the arrows displayed closer to the x axis explained most of the variability in the data and b) the environmental variables explained almost 100% of the variation of the taxa, when all four axes were analysed together.

Forward selection indicated that from all seven environmental parameters (Table 3-16) included in the analysis, only four environmental factors explained the variance in the phytoplankton carbon biomass when analysed together. When all the forward selected variables were analysed together (conditional effects, referred as $\lambda_a$, Table 3-16), the water temperature value was the most significant explanatory variable ($\lambda_a = 0.44$, $P = 0.001$), followed by silicate concentration ($\lambda_a = 0.04$, $P = 0.006$), Although there was no significant

difference ($\lambda_a$ = 0.03, $P$ = 0.086 and $\lambda_a$ = 0.02, $P$ = 0.057), river flow and phosphate concentrations also had a slight influence as explanatory variables (Table 3-16). Other environmental factors (nitrate, oxygen saturation, and SPM) were not significantly explanatory variables and possibly did not influence the phytoplankton carbon biomass pattern at Throop on the Stour River.

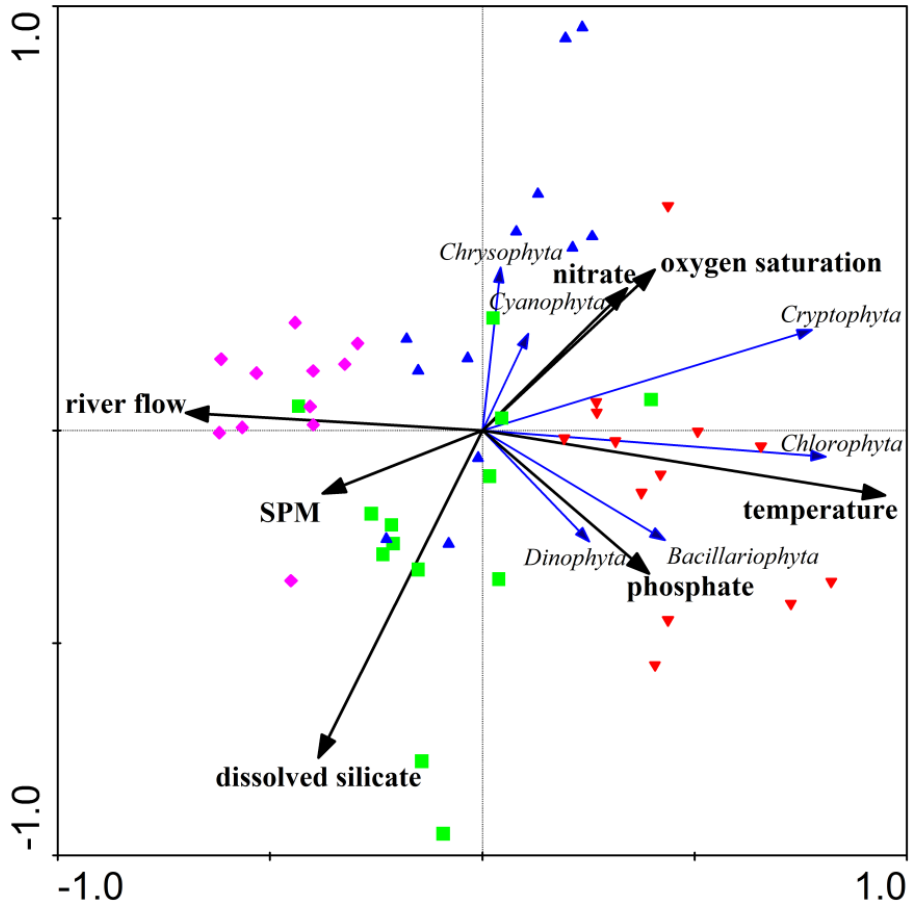


Figure 3-64: Ordination diagram generated from redundancy analysis (RDA) at Throop. Triplot represents taxa carbon biomass (blue thin lines), the significant explanatory variables (black thick lines) and weekly sampling (closed colour symbols; blue = spring, red = summer, green = autumn, pink = winter).

The nMDS plot of phytoplankton group biomass was not clearly correlated with the environmental factors to show how different parameters influence biomass pattern (Figure 3-65). The patterns of seasonality with river flow rate (early winter) and water temperature (summer and autumn) are clearly shown. Highest phytoplankton carbon biomass was found in spring because of the centric diatom *Stephanodiscus* bloom, followed by the samples in summer time. Both periods of high biomass were presented during low river discharge as shown in Figure 3-65 A and D.

Table 3-16: Eigen factor (λ) of each explanatory variable in order of the variance explained when analysed as single factor ($\lambda_1$, marginal effects) or when included in the model where other forward selected variables are analysed together ($\lambda_a$, conditional effects). Significant *P*-values (*$P < 0.1$) and (** $P < 0.05$) represent the variables that together explain the variation in the analysis at Throop.

| **Marginal Effects** | | **Conditional Effects** | | | | |
|---|---|---|---|---|---|---|
| Variable | $\lambda_1$ | Variable | $\lambda_a$ | *P* | *F* | |
| temperature | 0.44 | temperature | 0.44 | 0.001** | 37.26 | |
| river flow | 0.24 | silicate | 0.04 | 0.006** | 3.72 | |
| silicate | 0.10 | river flow | 0.03 | 0.086* | 2.12 | |
| %oxygen | 0.09 | phosphate | 0.02 | 0.057* | 2.56 | |
| phosphate | 0.08 | nitrate | 0.01 | 0.695 | 0.53 | |
| SPM | 0.07 | %oxygen | 0.00 | 0.765 | 0.42 | |
| nitrate | 0.06 | SPM | 0.01 | 0.972 | 0.12 | |
| | | | | | | |
| Axes | | 1 | 2 | 3 | 4 | Total variance |
| Eigenvalues : | | 0.489 | 0.038 | 0.015 | 0.003 | 1 |
| biocarbon-environment correlations : | | 0.851 | 0.656 | 0.322 | 0.254 | |
| Cumulative percentage variance | | | | | | |
| of biocarbon data : | | 48.9% | 52.7% | 54.2% | 54.5% | |
| of biocarbon-environment relation: | | 89.6% | 96.6% | 99.3% | 99.9% | |
| Sum of all eigenvalues | | | | | | 1 |
| Sum of all canonical eigenvalues | | | | | | 0.546 |

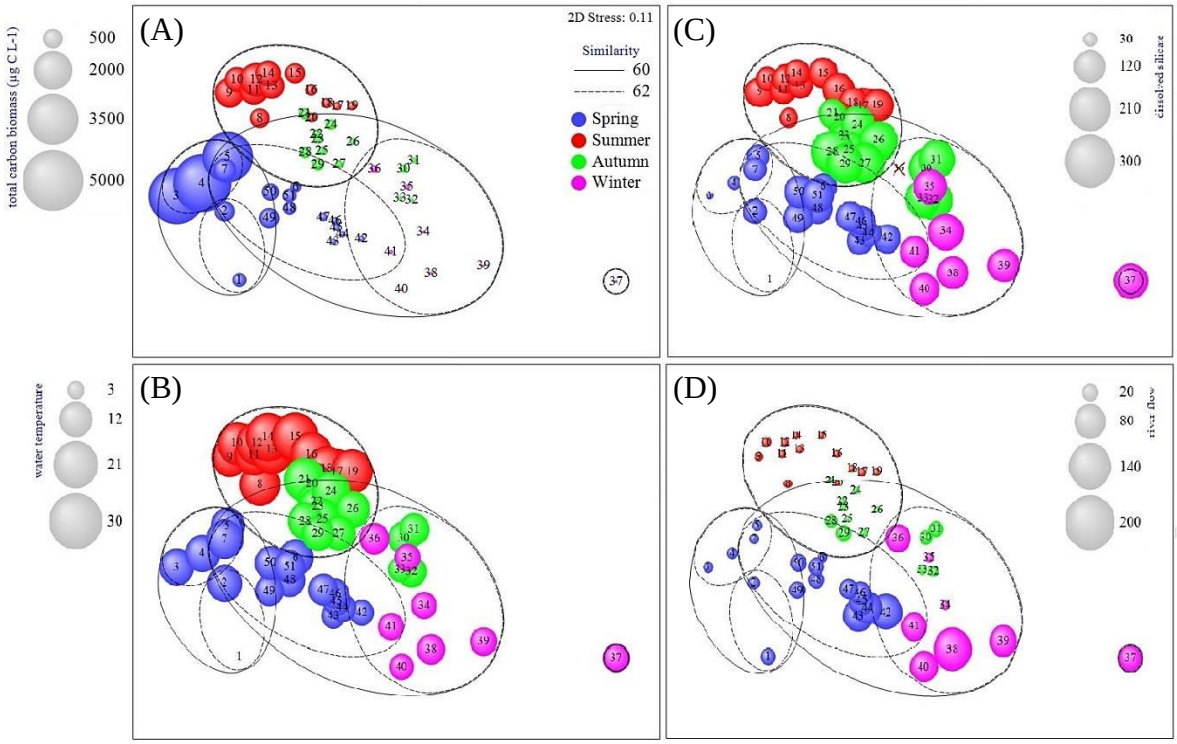


Figure 3-65: nMDS plot representing the mean biomass values in terms of carbon biomass (A), water temperature (B), silicate concentration (C) and river flow (D) at Throop. The bubble sizes represent the value of the environmental parameter.

***Iford Bridge, River Stour***

At this sampling point, the associations in the ordination diagram (Figure 3-66) show that the carbon biomass of riverine diatoms was strongly and positively correlated with nitrate concentrations and found highest biomass during summer months as at Throop. In addition, the diatom biomass was negatively related to the river discharge and silicate concentrations. Chrysophyta and cyanophyta groups showed no relationship with environmental factors. Meanwhile, cryptophyta and chlorophyta were found in relatively warmer waters with high oxygen saturation and in particular chlorophyte biomass was strongly and positively correlated with temperature. Dinoflagellate biomass was correlated with phosphate concentration as was seen at Throop.

The x axis of the analysis explained most of the variance (eigenvalue = 65.8%, cumulative percentage variance between biomass and environmental parameters = 89.5%), whereas all canonical axes explained 100% of the variance as shown in Figure 3-66 and Table 3-17. Forward selection indicated that of all six environmental parameters (as no SPM values (Table 3-17) were included in the analysis), three environmental parameters explained the variance in the phytoplankton carbon biomass when analysed together as described at

Throop. When all the forward selected variables were analysed together (conditional effects, referred as $\lambda_a$, Table 3-17), the water temperature value was the most significant explanatory variable ($\lambda_a$ = 0.60, $P$ = 0.001) as at Throop, followed by river flow ($\lambda_a$ = 0.05, $P$ = 0.005), and silicate concentrations ($\lambda_a$ = 0.02, $P$ = 0.072). River flow and phosphate concentration also had a slight influence as explanatory variables (Table 3-16). Other environmental factors (nitrate, phosphate, and oxygen saturation) were not significant explanatory variables and possibly did not influence the phytoplankton carbon biomass pattern at the Iford Bridge site on the Stour River. River flow was inversely correlated with concentration of nitrate that led to high nitrate values in late summer and autumn at this site.

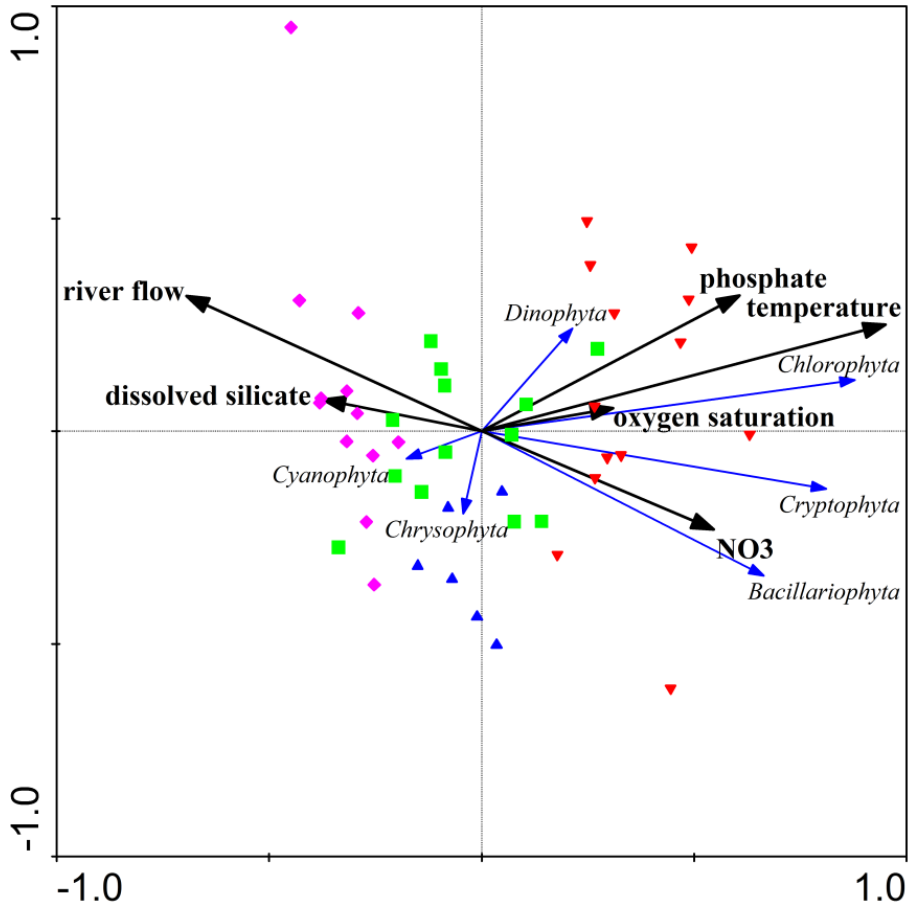


Figure 3-66: Ordination diagram generated from redundancy analysis (RDA) at Iford Bridge site. Triplot represents taxa carbon biomass (blue thin lines), the significant explanatory variables (black thick lines) and weekly sampling (closed colour symbols; blue = spring, red = summer, green = autumn, pink = winter).

Table 3-17: Eigen factor (λ) of each explanatory variable in order of the variance explained when analysed as single factor ($\lambda_1$, marginal effects) or when included in the model where other forward selected variables are analysed together ($\lambda_a$, conditional effects). Significant *P*-values (*$P < 0.1$) and (** $P < 0.05$) represent the variables that together explain the variation in the analysis at Iford Bridge.

| **Marginal Effects** | | **Conditional Effects** | | | | |
|---|---|---|---|---|---|---|
| Variable | $\lambda_1$ | Variable | $\lambda_a$ | *P* | *F* | |
| temperature | 0.60 | temperature | 0.60 | 0.001** | 62.35 | |
| river flow | 0.32 | river flow | 0.05 | 0.005** | 6.15 | |
| phosphate | 0.25 | silicate | 0.02 | 0.072* | 2.48 | |
| nitrate | 0.20 | phosphate | 0.01 | 0.330 | 1.10 | |
| silicate | 0.09 | nitrate | 0.01 | 0.381 | 0.97 | |
| %oxygen | 0.07 | %oxygen | 0.01 | 0.368 | 1.03 | |
| | | | | | | |
| Axes | | 1 | 2 | 3 | 4 | Total variance |
| Eigenvalues : | | 0.658 | 0.031 | 0.004 | 0.003 | 1 |
| biocarbon-environment correlations : | | 0.895 | 0.556 | 0.319 | 0.491 | |
| Cumulative percentage variance | | | | | | |
| of biocarbon data : | | 65.8% | 68.9% | 69.3% | 69.6% | |
| of biocarbon-environment relation: | | 94.5% | 99.0% | 99.5% | 100% | |
| Sum of all eigenvalues | | | | | | 1 |
| Sum of all canonical eigenvalues | | | | | | 0.697 |

The nMDS plot of phytoplankton group biomass at Iford Bridge was not clearly correlated with the environmental factors to show how different parameters influence biomass pattern (Figure 3-67). The patterns of seasonality with river flow rate (early winter) are clearly shown. However highest phytoplankton carbon biomass was found in summer months, followed by the samples in spring 2014. Both periods of the high biomass were present during low river discharge as shown in Figure 3-67 A and C as seen above at Throop.

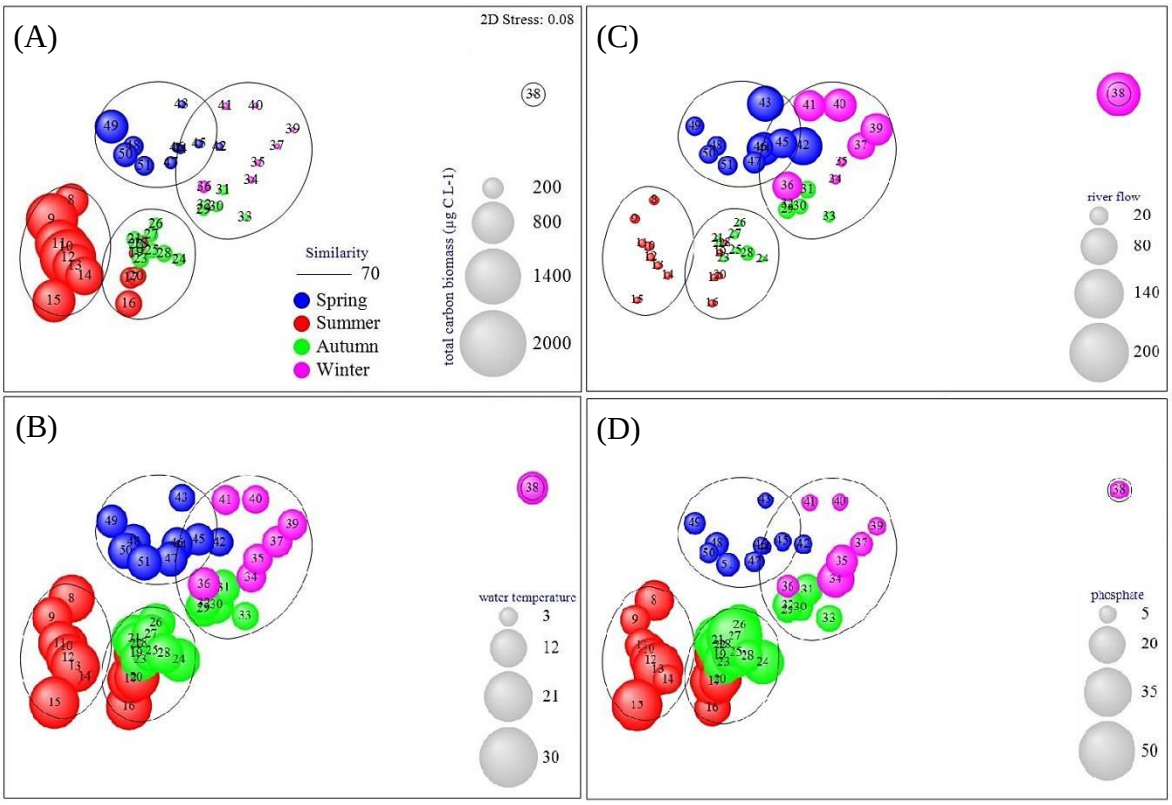


Figure 3-67: nMDS plot representing the mean biomass values in terms of carbon biomass (A), water temperature (B), river flow (C), and phosphate concentration (D) at Iford Bridge. The bubble sizes represent the value of the environmental parameter.

***Knapp Mill, River Hampshire Avon***

The associations in the ordination diagram (Figure 3-68) show that the carbon biomass of riverine diatoms was slightly positively correlated with oxygen saturation, phosphate, and silicate concentration. In addition, the diatom biomass showed a negative relationship with river discharge as was seen on the Stour River. Chrysophyte biomass showed a strong relationship with river discharge. Meanwhile, cryptomonad biomass was found to correlate negatively with high SPM concentrations. Chlorophyte biomass was correlated with water temperature. Nitrate concentrations from this spot sampling do not show any relationship with phytoplankton groups.

The x axis of the analysis explained most of the variance (eigenvalue = 27.4%, cumulative percentage variance between biomass and environmental parameters = 82.3%), whereas all canonical axes explained 100% of the variance as shown in Figure 3-68 and Table 3-18. Forward selection indicated that of all seven environmental parameters (Table 3-18) included in the analysis, three environmental factors explained the variance in the

phytoplankton carbon biomass when analysed together. When all the forward selected variables were analysed together (conditional effects, referred as $\lambda_a$, Table 3-18), the water temperature was the most significant explanatory variable ($\lambda_a$ = 0.25, $P$ = 0.001), followed by silicate concentration ($\lambda_a$ = 0.12, $P$ = 0.001), and river flow had a slight influence as an explanatory variable ($\lambda_a$ = 0.04, $P$ = 0.045). Other environmental factors (nitrate, phosphate, SPM, and oxygen saturation) were not significant explanatory variables and possibly did not influence the phytoplankton carbon biomass pattern at Knapp Mill gauging station on the Hampshire Avon River.

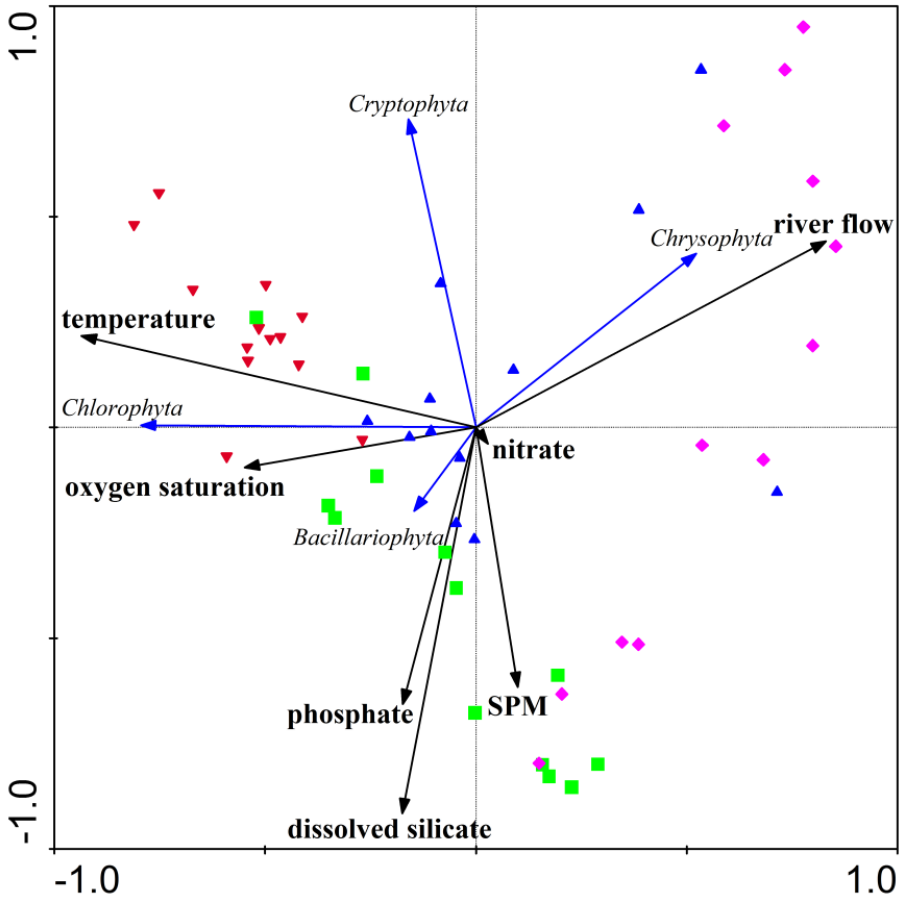


Figure 3-68: Ordination diagram generated from redundancy analysis (RDA) at Knapp Mill site. Triplot represents taxa carbon biomass (blue thin lines), the significant explanatory variables (black thick lines) and weekly sampling (closed colour symbols; blue = spring, red = summer, green = autumn, pink = winter).

Table 3-18: Eigen factor (λ) of each explanatory variable in order of the variance explained when analysed as single factor ($\lambda_1$, marginal effects) or when included in the model where other forward selected variables are analysed together ($\lambda_a$, conditional effects). Significant *P*-values (*$P < 0.1$) and (** $P < 0.05$) represent the variables that together explain the variation in the analysis at Knapp Mill.

| **Marginal Effects** | | **Conditional Effects** | | | | |
|---|---|---|---|---|---|---|
| Variable | $\lambda_1$ | Variable | $\lambda_a$ | *P* | *F* | |
| temperature | 0.25 | temperature | 0.25 | 0.001** | 15.82 | |
| river flow | 0.22 | silicate | 0.12 | 0.001** | 9.14 | |
| silicate | 0.12 | river flow | 0.04 | 0.045** | 3.16 | |
| %oxygen | 0.08 | nitrate | 0.02 | 0.315 | 1.15 | |
| phosphate | 0.07 | phosphate | 0.01 | 0.364 | 1.00 | |
| SPM | 0.06 | SPM | 0.01 | 0.490 | 0.78 | |
| nitrate | 0.02 | %oxygen | 0.00 | 0.822 | 0.29 | |
| | | | | | | |
| Axes | | 1 | 2 | 3 | 4 | Total variance |
| Eigenvalues : | | 0.274 | 0.134 | 0.0444 | 0.001 | 1 |
| biocarbon-environment correlations : | | 0.823 | 0.774 | 0.382 | 0.120 | |
| Cumulative percentage variance | | | | | | |
| of biocarbon data : | | 27.4% | 40.7% | 45.1% | 45.2% | |
| of biocarbon-environment relation: | | 60.5% | 90.1% | 99.8% | 100% | |
| Sum of all eigenvalues | | | | | | 1 |
| Sum of all canonical eigenvalues | | | | | | 0.452 |

The nMDS plot of phytoplankton group biomass at Knapp Mill site was not clearly correlated with the environmental factors to show how different parameters influence biomass pattern (Figure 3-69). The patterns of seasonality with river flow rate are clearly shown as on the Stour River. Highest phytoplankton carbon biomass was found in spring and summer months as was as at Throop and were also present during low river discharge as shown in Figure 3-69 A and C.

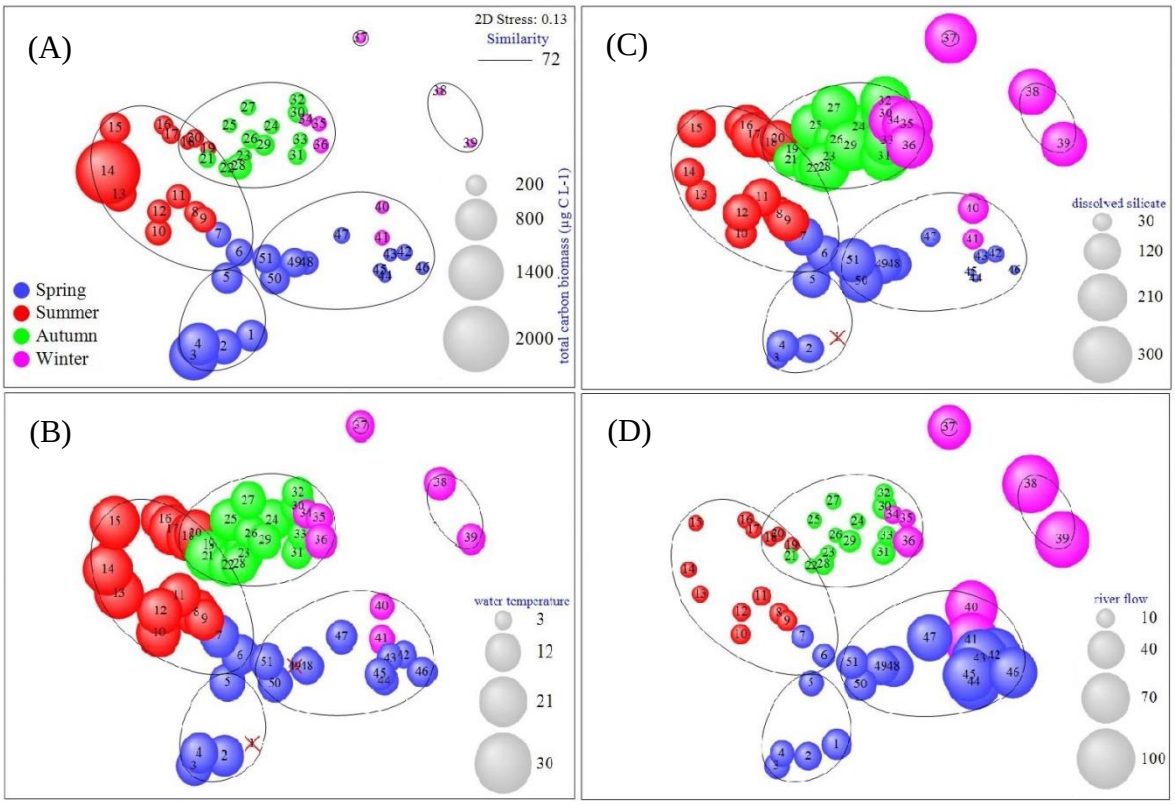


Figure 3-69: nMDS plot representing the mean biomass values in terms of carbon biomass (A), water temperature (B), silicate concentration (C), and river flow (D) at Knapp Mill. The bubble sizes represent the value of the environmental parameter.

## 3.4 Discussion

In this chapter, the seasonal pattern of biological parameters (phytoplankton species abundance, pigments, and estimated species biomass), environmental parameters (water temperature, suspended particulate matter, oxygen saturation, and river flow), and chemical parameters (nitrate, phosphate, and silicate concentrations) at Throop and Iford Bridge on the Stour River and the Hampshire Avon Rivers at Knapp Mill during April 2013 to April 2014 were described. The water samples were collected at weekly intervals from the three sites on the two main rivers discharging freshwater into the Christchurch Harbour estuary. Multivariate analysis was used to establish relationships between biological and environmental factors. The objective of this study was to monitor the seasonal changes in both riverine phytoplankton on both rivers in terms of species composition and cell size. This study takes into account the whole phytoplankton community, in terms of its carbon biomass, accessory pigments and also in relation to the chlorophyll, size fractionated chlorophyll, and photosynthetic efficiency of phytoplankton.

The seasonal distribution of riverine phytoplankton on the Hampshire Avon and Stour Rivers is similar to that in other temperate rivers, for example in the St. Lawrence River (Basu *et al.*, 2000), the Humber and the Thames (Neal *et al.*, 2006), and the Rhine and Elbe Rivers (Hardenbicker *et al.*, 2014). The biomass of chlorophyll *a* and carbon are relatively high in spring and summer up to 98.8 µg $L^{-1}$ and low in autumn and winter < 1.0 µg $L^{-1}$ while temperature is low and river discharge is high (Montesanto *et al.*, 2000; Neal *et al.*, 2006; Phlips *et al.*, 2010; Hardenbicker *et al.*, 2014).

*Phytoplankton biomass response to nutrients*

In addition to river discharge, riverine phytoplankton biomass may be strongly related to nutrient concentrations (Basu *et al.*, 2000; Sabater *et al.*, 2008). In the present study it was shown that phosphate and nitrate concentrations were important chemical factors controlling the phytoplankton dynamics in the Stour River both at Throop and Iford Bridge, while in the Hampshire Avon River at Knapp Mill only the phosphate concentration was significant. According to Reynolds (1984) nitrate concentrations in rivers are high due to receiving considerable inputs of drainage from agriculture soils, groundwater or treated sewage effluent. However, phosphate concentrations were depleted in both rivers when chlorophyll registered the peak concentrations. The observed depletion of phosphorus is commonly observed in large eutrophic rivers during mass phytoplankton growth e.g. the Middle Loire (Picard and Lair, 2005). An obvious consequence is that the arrival of higher phosphate concentrations to the Stour River could further enhance phytoplankton biomass of the river. In some rivers, for example in the Thames, phosphate is not a limiting factor due to the high concentration (Whitehead *et al.*, 2015). Silicate availability showed a strong negative correlation with phytoplankton carbon biomass in particular in the Stour as indicated by the CANACO and was low in concentration in both rivers during the spring diatom bloom. Several studies have reported that decreased silicate availability is often a factor in the termination of diatom blooms and as diatoms are dominating phytoplankton communities in both the Stour and Hampshire Avon Rivers, silicate concentrations could have temporarily limited phytoplankton growth as was reported by van Steveninck *et al.* (1992) for the Rhine River and by Whitehead *et al.* (2015) for the Thames. In contrast to lakes where nutrient concentrations are of high importance for the regulation of phytoplankton, they are of low importance in rivers as they are typically present in non limiting concentrations. Therefore, the observed increase in mean chlorophyll *a* concentrations in the Stour River was mainly a consequence of higher nutrient concentrations in particular phosphate concentration. In the Hampshire

Avon River, however, where nutrient concentrations were lower, chlorophyll *a* concentrations were also considerably lower.

*Phytoplankton biomass response to hydrodynamics*

The reduction in river discharge was the most important regulating factor for phytoplankton spring bloom dynamics in both rivers. The data show that the decrease in discharge was partially related to the spring increase in both phytoplankton in the Stour and Hampshire Avon Rivers, whereas increasing water temperature (and an associated increase in light availability) was a stronger predictor for the maximum concentration of chlorophyll *a* during the spring-summer. In the Stour, the occurrence of the maximum of the diatom spring bloom was significantly correlated to the end of the high winter flow rate period. Therefore, the reduction in discharge explained the maximum spring biomass in the Stour River. The mean annual dischange in 2013 (April – December) and 2014 at Knapp Mill were 13.7 and 30.5 $m^3 s^{-1}$, respectively, whereas the mean annual discharge during 1969 to 2000 was 15.2 $m^3 s^{-1}$ at Fordingbridge on the Hampshire Avon River (Heywood and Walling, 2003). For the Knapp Mill gauging station, the discharge in 2014 exceeded a high range of flow due to the storm which occurred in January 2014 with the highest daily flow rate reaching up to 101.6 $m^3 s^{-1}$. Increasing retention times mainly improve the conditions for the planktonic development in riverine ecosytems (Reynolds, 2000; Lucas *et al.*, 2009). The discharge increases the dilution effect as well as the decline in light climate, and the shorter residence time of rivers also reduces the phytoplankton abundance in the river ecosystem (Everbecq *et al.*, 2001). Negative correlations between river flow rate and chlorophyll *a* have also been reported concerning seasonal short term development of phytoplankton in rivers of eastern England (Neal *et al.*, 2006), the Mississippi River in the USA (Bukaveckas *et al.*, 2011), and long term in German rivers (Hardenbicker *et al.*, 2014). A contrasting river discharge was found in the Stour, the lower flow during the high productive period had mostly higher phytoplankton biomass than the Hampshire Avon.

In the present study, water temperature was an important factor controlling the phytoplankton community both in the Stour and the Hampshire Avon. This suggests that the direct effect on phytoplankton is of high importance and should be a main focus concerning plankton regulation in lotic habitats together with discharge conditions and nutrient availability. A dynamic phytoplankton model reported by Whitehead *et al.* (2015) showed temperature is a limitation to phytoplankton growth in the Thames whereas, temperature has a minor effect on phytoplankton development in larger rivers such as in

the Rhine and the Elbe (Hardenbicker *et al.*, 2014). Typically, maximum rates of phytoplankton biomass in terms of chlorophyll concentration and abundance occur when water temperature and nutrient inputs are both high leading to spring bloom conditions as observed at Throop and Knapp Mill. High chlorophyll concentrations also occurred at Iford Bridge, where the higher nitrate concentrations than seen at Throop upstream on the Stour River were related to the main sewage input from Holdenhurst Sewage Works thus further favouring phytoplankton development before flowing into the Christchurch Harbour estuary.

Comparing the suspended particulate matter (SPM) load and its influence on phytoplankton biomass dynamics in both rivers there was no significant effect on phytoplankton biomass, neither in the Stour at Throop, nor in the Hampshire Avon at Knapp Mill. This suggests that the direct effect of SPM on phytoplankton is of less importance and the main focus concerning phytoplankton regulation in rivers has to be on discharge conditions (Hardenbicker *et al.*, 2014). SPM concentration in the Avon River within the upper and middle catchments at Fordingbridge gauging station were reported at a maximum of 0.232 g $L^{-1}$ during a large magnitude storm in December 1999 (Heywood and Walling, 2003), while from this study SPM maxima was measured of 0.038 g $L^{-1}$ at Knapp Mill (week 36) and 0.135 g $L^{-1}$ at Throop on the Stour River. The maximum SPM concentrations from all study sites were recorded when the river flow rate was over 100 $m^3$ $s^{-1}$ in winter 2013.

*Changes in phytoplankton taxa and biomass*

In the present study the size distribution of chlorophyll *a* in both rivers were examined during the productive period (May – September 2013). Nano-phytoplankton (2 – 20 µm in diameter) were the dominant group in terms of biomass followed by pico-phytoplankton (< 0.2 µm) and micro-phytoplankton size (> 20 µm), respectively. The pico-sized phytoplankton were found to be greatest importance in the Thames by Read *et al.* (2014) using a flow cytometry measurements throughout the summer period. This indicates that the smaller phytoplankton are important organism in these riverine ecosystems although the population size differs in other studies.

High chlorophyll concentrations detected in the Stour at Throop compare to occasional measurements made by the Environment Agency at this site but phytoplankton counts are not routinely made. The present study has shown that the phytoplankton community in lower reaches of the Stour and Hampshire Avon is a typical riverine diatom community

dominated by species of *Stephanodiscus*, *Coscinodiscus*, *Diatoma*, *Navicula*, and *Melosira*. Similar species have been reported in a German lowland river, the Kielstau catchment (Wu *et al.*, 2011) but with different dominant species. The highest abundance of phytoplankton in both rivers occurred between April and May for diatoms and between June and July for the other phytoplankton groups as reported by Read *et al.* (2014) and Whitehead *et al.* (2015) in the Thames. The chlorophytes dominated the community throughout the summer period at all study sites as well as in the Thames at Wallingford (Read *et al.*, 2014).

The centric diatom *Stephanodiscus* sp. is considered a common diatom in eutrophic freshwaters of Europe and this diatom is capable of intense spring blooms (Stoermer *et al*., 1972; Krammer and Lange-Bertalot, 1991), both references cited by Hawryshyn *et al.* (2012). It seems that the Stour River may be considered to be eutrophic during low spring discharge when *Stephanodiscus* sp. abundance was observed at over $4.4 \times 10^4$ cells $mL^{-1}$ with 98.8 µg $L^{-1}$ of chlorophyll *a* at Throop. Major diatom blooms in spring and summer, correlated with depletion of soluble reactive phosphate and silicate concentrations. The small chlorophyte species, *Chlamydomonas* spp., was observed in high density ($1.9 – 7.9 \times 10^4$ cells $mL^{-1}$) and was the dominant species during early summer months on the Stour River. In both rivers, the diatoms were the main phytoplankton groups during the autumn-winter time with a low abundance during high river discharge.

*The uses of HPLC and flow cytometry to monitoring riverine phytoplankton community*

Inverted optical microscopy is the reference tool to assess the community composition of major phytoplankton groups such as diatoms, cryptomonads, chlorophytes, and dinoflagellates. This technique has limitations for cells that are less than 10 µm or fragile cells, however, that could be lost during the preservation process. Within this study acid Lugol's iodine solution was used to preserve all microscopic samples. Because the identification of phytoplankton species often relies on features that cannot be seen in preserved samples due to loss of pigmentation, it is recommended that a qualitative fresh water sample from the same river is viewed (if possible) before the actual count to determine which groups of phytoplankton are dominant. Pigment analysis using HPLC provides useful data about whole community diversity and the contribution of each phytoplankton pigment group. In particular, accessory pigments quantified by HPLC analysis is a useful tool with which to investigate phytoplankton community structure from their marker pigments. However some pigments are common to more than one group of phytoplankton limiting the diagnostic value of those pigments in mixed communities. For

example peridinin is often stated as a indicator pigment for dinoflagellates however some dinoflagellate species are known to contain fucoxanthin rather than peridinin. In the present study, the spring bloom on the Stour River was comprised of a combination of pigments including fucoxanthin, diadinoxanthin, and chlorophyll *b* that indicate several phytoplankton groups were present and not only the diatoms. The centric diatom *Stephanodiscus* sp. was the dominant species from the microscopic observation whilst other species were observed in low abundance. Microscopy and the preservation have limitations for small phytoplankton cells or fragile cells that could be lost during the cell counting.

The CytoSense flow cytometer is a useful instrument to estimate phytoplankton abundance and is less time consuming than microscopy. The CytoSense also measures phytoplankton cell size from 1 µm up to 800 µm and was demonstrated to be a viable alternative approach for monitoring the changing seasonal patterns of abundance and composition of phytoplankton in both rivers. In the present study, flow cytometry showed distinct variation in cell density throughout the sampling period, with a general pattern of high abundance during the spring to summer period and lower abundance during autumn to winter at all study sites as was reported by Read *et al.* (2014) for the Thames. Sharp shifts in phytoplankton abundance were observed during the spring 2013 and 2014. These results were marked by an increase in phytoplankton abundance and red fluoresence as shown in Section 3.3.5. The total abundance from CytoSense data correlated with a low significance ($R^2 = 0.39$) with the microscopic counts (Figure 3-38), suggesting that the traditional counting method underestimates the phytoplankton abundance. Nevertheless, in contrast to marine and estuarine systems where phytoplankton communities are well established (Moreira-Turcq *et al.*, 2001; Lin *et al.*, 2012; Bonato *et al.*, 2016), its application to freshwater ecosystems is less and has almost thoroughly been focused on lakes and reservoirs (Dubelaar *et al.*, 2004; Read *et al.*, 2014). Read *et al.* (2014) pointed out that flow cytometry has the potential to become a routine monitoring technique to replace some of the current water quality monitoring parameters required in the future.

*The production of riverine phytoplankton*

In the present study, photosynthetic energy conversion efficiency ($F_v/F_m$) using a bench-top Fluorescence Induction and Relaxation (FIRe) was investigated at all study sites throughout the sampling period and size-fractions were also analysed during a productive period in 2013. The rates of photosynthesis for the three riverine stations showed similar

seasonal patterns. The highest values occurred during the spring and decreased through summer with the nano-phytoplankton community showing to be the most efficient cells in the population. Several previous studies have reported maximum phytoplankton photosynthetic efficiency ($F_v/F_m$) occurred during thermal stratification, for example in the Salzkammergut lake-distrct in Austria (Kaiblinger and Dokulil, 2006). Measurement of $F_v/F_m$ using the FIRe is a convenient and relatively inexpensive method with a wide range of past and future ecophysiological applications (Parkhill *et al.*, 2001). In contrast to published results, continuous measurements of riverine samples showed that values of $F_v/F_m$ were close to measurements of culture experiments and remained constant (~0.6 – 0.7) during the spring period as reported by Parkhill *et al.* (2001). The Hampshire Avon River at Knapp Mill had a lower efficiency than at Throop and Iford Bridge on the Stour River during the spring bloom, however, in general all efficiencies from the three sites showed the same pattern following the chlorophyll concentrations throughout the sampling period.

Hierarchical cluster and CANOCA analysis revealed the presence of any distinct spatial patterns, although, distinct phytoplankton communities were recorded during the different sampling periods. The species abundance in terms of carbon biomass and pigment content were highest in the spring-summer, decreasing from autumn to winter particularly during the winter flood period at all sites. The results of the study provide important insights into the various parameters that influence riverine phytoplankton population composition in both the lower Stour and Avon Rivers. Canonical correspondence analysis can be used to determine whether variables such as hydrology or nutrients are important in controlling phytoplankton populations. For example, total phosphate and dissolved inorganic nitrogen were of equal importance in controlling the variation in structure of riverine phytoplankton assemblages in a German lowland river, the Kielstau catchment (Wu *et al.*, 2011). However, in large rivers e.g. the Rhine and Elbe Rivers the same methods have indicated that climate related factors such as discharge or light conditions have a high potential to regulate phytoplankton spring bloom dynamics (Hardenbicker *et al.*, 2014).

As a result, seasonality plays an important role in the control of phytoplankton growth and community composition and the relationship between phytoplankton biomass and environmental parameters shows that river discharge and water temperature represent the main factors controlling the carbon biomass in the Stour and Avon rivers. Lower summer river discharges leading to a longer water residence times resulted in higher phytoplankton biomass. Nutrient concentration, particularly silicate and phosphate, were also implicated

in controlling phytoplankton growth particularly on the Stour River. In particular, phosphate concentration was a main chemical factor influencing phytoplankton during the spring when the low river discharge and high temperature occurred at Throop, compared at Knapp Mill. The diatoms were the main community of riverine phytoplankton in both the Stour and Hampshire Avon Rivers in particular during the spring-summer, however, the chlorophytes and cryptophytes became dominant groups during the summer from both rivers.

## 3.5 Conclusion

In summary, this study has demonstrated the occurrence of spring diatom blooms in the Stour River at Throop with high chlorophyll *a* concentration suggesting that the Stour River should be considered to be a eutrophic river. It can be concluded that despite the interaction of complex regulation mechanisms in the Stour and Hampshire Avon, the main factors influencing the riverine phytoplankton community was related to both nutrient availabilily and the optimal climate conditions. Furthermore, the changes in river flow and nutrient concentration on the Stour and Hampshire Avon Rivers which directly flow into the Christchurch Harbour estuary potentially affect the phytoplankton community in the estuary during low tide. The annual dynamic of river discharge could imply potential changes to the estuarine phytoplankton community through its impact on the nutrient delivery to the estuary supporting high levels of phytoplankton productivity. The potential impact of a change in estuarine phytoplankton population is to be discussed in later chapters.

# Chapter 4: The response of the estuarine phytoplankton community to change in macronutrients input to in a shallow temperate estuary, Christchurch Harbour, UK

## 4.1 Abstract

The influence of changes in the nutrient inputs from the Stour and Hampshire Avon Rivers discharges on the annual response of phytoplankton community at Mudeford Quay at the estuary entrance to Christchurch Harbour were investigated at weekly intervals from April 2013 to April 2014. It is important to understand the response of different phytoplankton groups to nutrient concentrations and other hydrological parameters during different seasons. There are significantly several potential environmental factors controlling the phytoplankton biomass including salinity, oxygen saturation, river discharge, temperature, and silicate concentrations. Inorganic nutrient concentrations were generally much higher during low river discharge, but decreased during the winter flood. The chlorophyll *a* maximum was observed during the late spring and decreased during the autumn and winter similar to that detected at Throop on the Stour. Phytoplankton carbon biomass and accessory pigments displayed a similar pattern at those in the rivers. This suggests that nutrient availability and river discharge could have been important in determining the variation in phytoplankton biomass and composition in the estuary. Diatoms were a dominant component of the phytoplankton biomass and community throughout the sampling period and positively related to silicate concentrations. Dinoflagellates e.g. *Kryptoperidinium foliaceum* were observed in high abundance at higher salinity values during summer months and spring blooms of nano-sized phytoplankton occurred in low salinity water dominated by *Stephanodiscus* sp. This suggests that the river discharge is important factor influencing the phytoplankton community and primary production in the microtidal shallow Christchurch Harbour estuary.

## 4.2 Introduction

The Christchurch Harbour estuary receives freshwater from principally two rivers, the Stour and the Hampshire Avon. Results from the previous chapter showed that the riverine phytoplankton populations in the lowest reaches of both rivers were present a high abundance and biomass during spring-summer and it was shown that phosphate and nitrate concentrations were important chemical factors controlling the phytoplankton dynamics in both rivers. In this study environmental factors controlling phytoplankton abundance and biomass at the estuary entrance was investigated on the same sampling dates as samples were collected from the three riverine sites in order to better understand the condition influence estuarine phytoplankton populations at the estuary entrance during low tide.

## 4.3 Results

### 4.3.1 Environmental data

Weekly sampling was carried out at, Mudeford Quay, at low tide on the same days as the three riverine stations (Figure 2-1), between April 2013 and April 2014 (see the sampling date in Appendix A). Observations of physical factors, inorganic nutrients, total chlorophyll *a*, chlorophyll *a* size fractions, phytoplankton abundance, phytoplankton production, and phytoplankton pigments are presented in this chapter.

#### 4.3.1.1 Salinity

The annual change in surface water salinity at Mudeford Quay, at the entrance of Christchurch Harbour is shown in Figure 4-1. The estuarine surface salinity determined using a YSI 6600 multiprobe ranged 0.2 – 22.5 and showed generally high salinity values over of 15 between 4$^{th}$ July and 16$^{th}$ October 2013 (week 12 – 27), when daily river flow rates at both lowest gauging stations on the River Stour and Avon was under 10 $m^3$ $s^{-1}$. The salinity decreased from values of 22.5 (23$^{rd}$ July 2013, week 15) in the summer month, down to 0.2 during the high river flows in the winter period when daily river flow rate was over 20 $m^3$ $s^{-1}$. The seasonal changes in salinity indicated that the estuarine water was directly impacted on by the river discharge from both rivers. Salinity values suggest that stratification at the mouth of the estuary is mainly driven by the input of the riverine water, as indicated by the lower surface salinity values during the winter flood period.

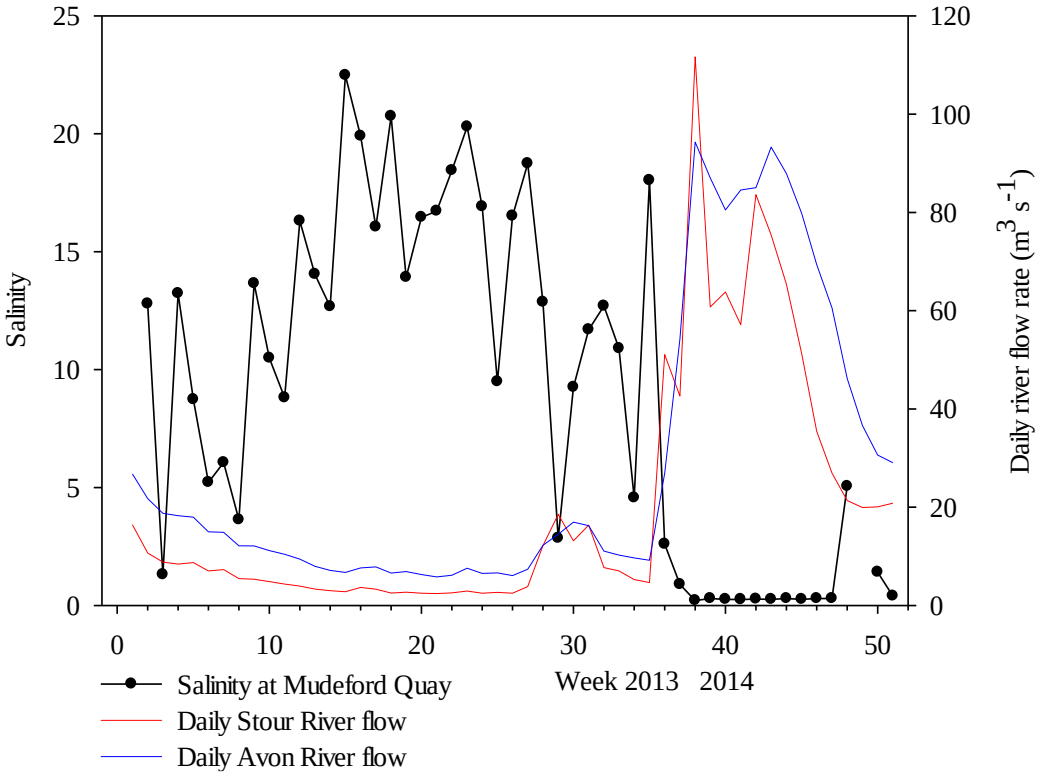


Figure 4-1: Change of surface salinity values at Mudeford Quay and daily Stour and Hampshire Avon River flow form April 2013 to April 2014. Red solid line indicates a daily Stour River flow and blue solid line shows a daily Avon River flow.

#### 4.3.1.2 Suspended particulate matter

The range of suspended particulate matter (SPM) at Mudeford Quay at low tide was 0.005 – 0.141 g $L^{-1}$. The maximum SPM value was in November 2013 (week 30) and the minimum SPM was in February 2014 (week 45) as shown in Figure 4-2. Although the SPM varied throughout the sampling at this sampling site, the SPM values increased predictably towards the autumn months and decreased towards the winter. The SPM average value at Mudeford Quay was higher (0.025 g $L^{-1}$) than at Throop and Knapp Mill (0.012 and 0.009 g $L^{-1}$). During week 29 to 33, the range of both river flow rates was 12 – 18 $m^3$ $s^{-1}$, SPM values were sharply increase up to 0.141 g $L^{-1}$ (week 30) and down to 0.010 g $L^{-1}$ (week 33) when the flow rate decreased to ~10 $m^3$ $s^{-1}$. The next peak of SPM occurred in the early winter flood up to 0.123 g $L^{-1}$ then decreased during the following high flow period. It should be note that the high SPM concentrations at Mudeford Quay followed the rate of river flow into the estuary during the study period.

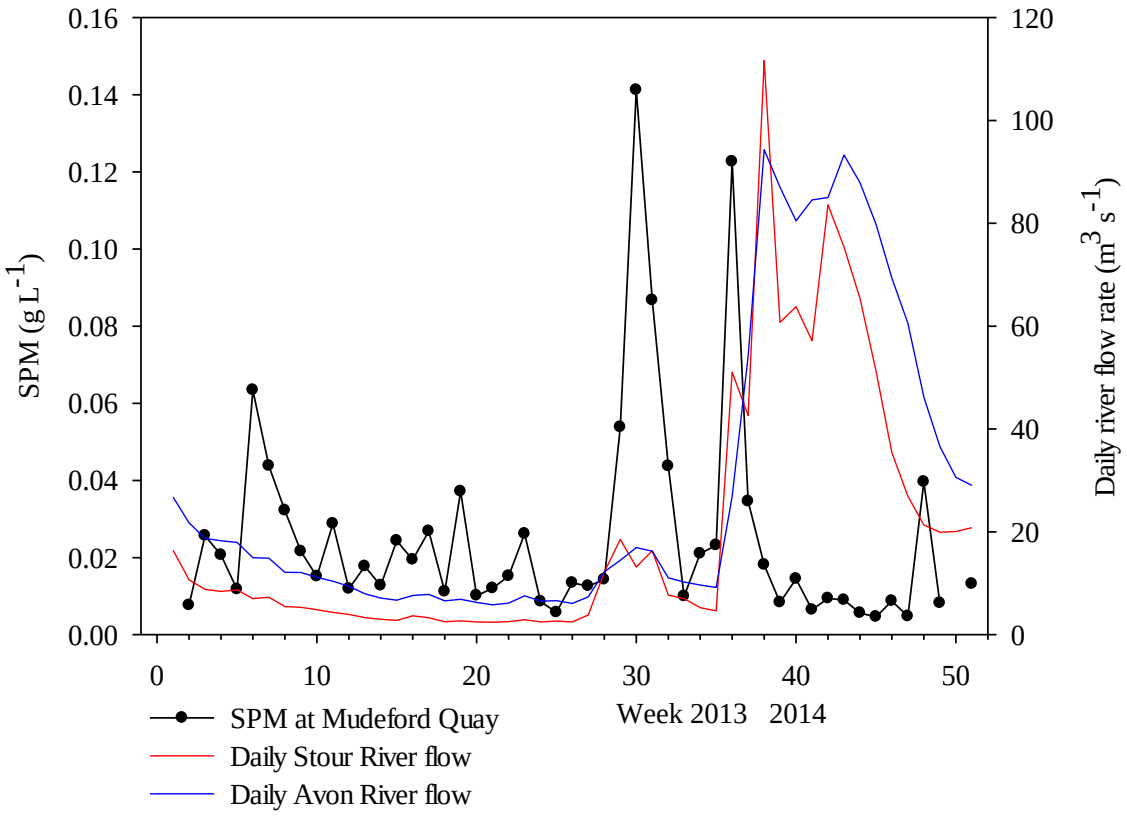


Figure 4-2: The change of suspended particulate matter (SPM) concentrations at Mudeford Quay compare to daily Stour and Avon River flows. Red solid line indicates a daily Stour River flow and blue solid line shows a daily Avon River flow

#### 4.3.1.3 Chemical parameters: Inorganic nutrients

The changes in the major inorganic nutrients, nitrate, phosphate, and silicate concentrations at the Christchurch Harbour estuary entrance, at Mudeford Quay, were determined at low tide on weekly collected samples from the same days as the three river stations. The seasonal mean concentrations of each nutrient are presented in Table 4-1.

In general, the surface nitrate concentration showed a consistent seasonal pattern (Figure 4-3 A), concentrations with reduced in summer from high concentrations in the spring, and increased again in the autumn. Phosphate concentrations showed a different pattern to nitrate with, concentrations increased from low values in the spring to high concentrations in the summer and autumn and decreased again during the winter flood (Figure 4-3 B). In terms of silicate change, concentration gradually increased from spring to winter and the highest concentration was measured with river flow was high then dropped follow the river flow decrease (Figure 4-3 C).

The mean concentration of nitrate, phosphate, and silicate at this site during the sampling period were 338 ± 98 (n=50), 6 ± 3 (n=49), and 87 ± 46 (n=49) µmol $L^{-1}$, respectively. Nitrate concentration ranged from 148 µmol $L^{-1}$ (July 2013, week 15) to 541 µmol $L^{-1}$ (December 2013, week 34), phosphate concentration ranged from 1 µmol $L^{-1}$ at the end of February 2014 (week 44) to 11 µmol $L^{-1}$ in October 2013 (week 25), and silicate concentration ranged from 24 µmol $L^{-1}$ (February 2014, week 44) to 189 µmol $L^{-1}$ (December 2013, week 37) as shown in Figure 4-3.

Inorganic nutrient concentrations at Mudeford Quay showed a similar pattern to the river stations particularly in comparison to both study sites (Throop and Iford Bridge) on the Stour River. This difference may relate to nutrients in the Stour having a higher concentration than in the Hampshire Avon as described in previous chapter (see Section 3.3.1.3).

Nitrate and silicate concentrations generally showed a decrease as salinity increased, but phosphate concentrations had a positive scatter with salinity (Figure 4-4). The maximum concentrations of nitrate were twofold higher in the low salinity (0 – 5) compared to the high salinity (> 20) water as shown in Figure 4-4 A.

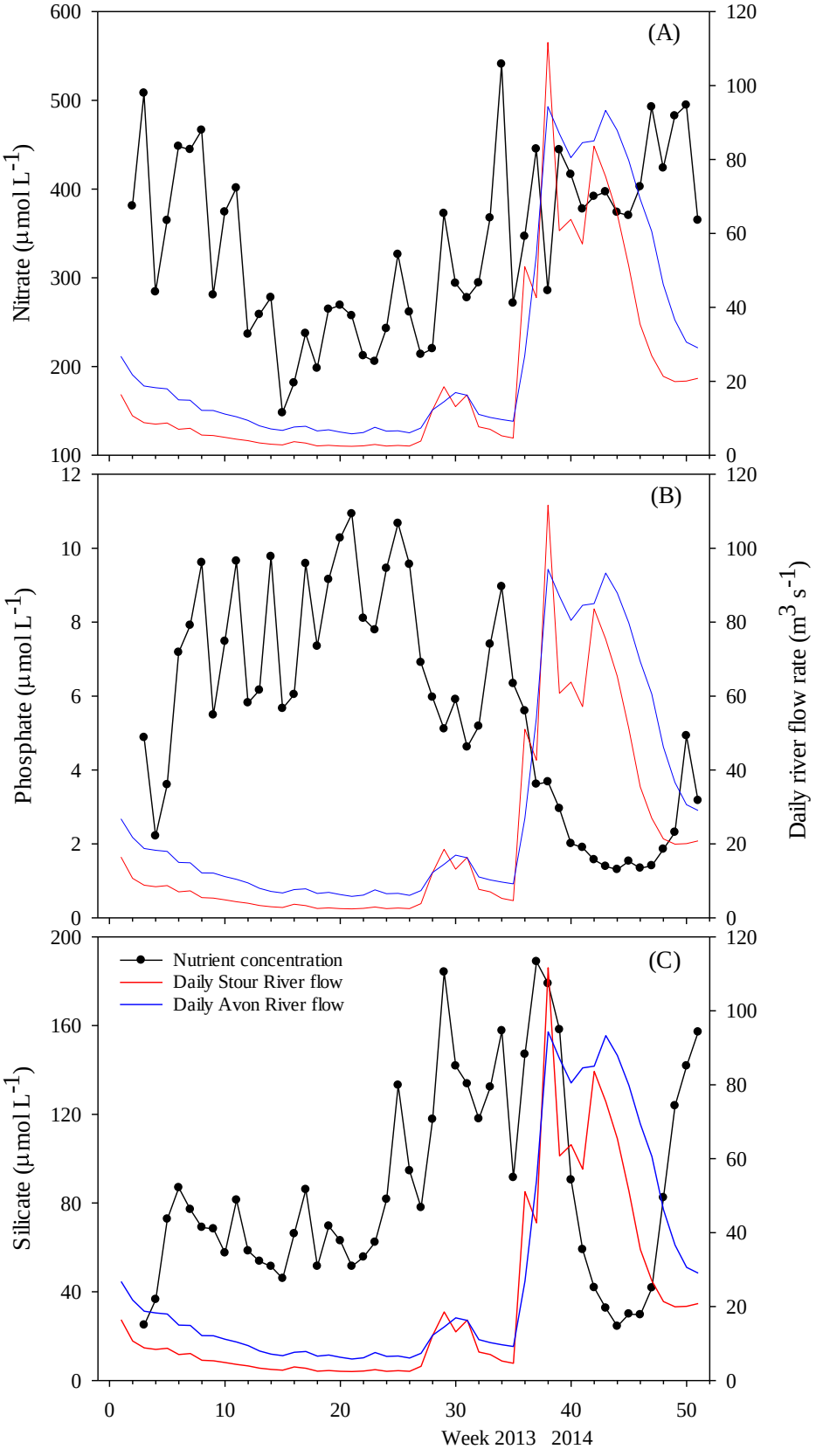


Figure 4-3: Surface inorganic nutrient changes at Mudeford Quay, Christchurch Harbour (A) nitrate, (B) phosphate, and (C) silicate. Red solid line indicates the daily Stour River flow and blue solid line shows the daily Avon River flow. Symbols in lower panel apply to all panels.

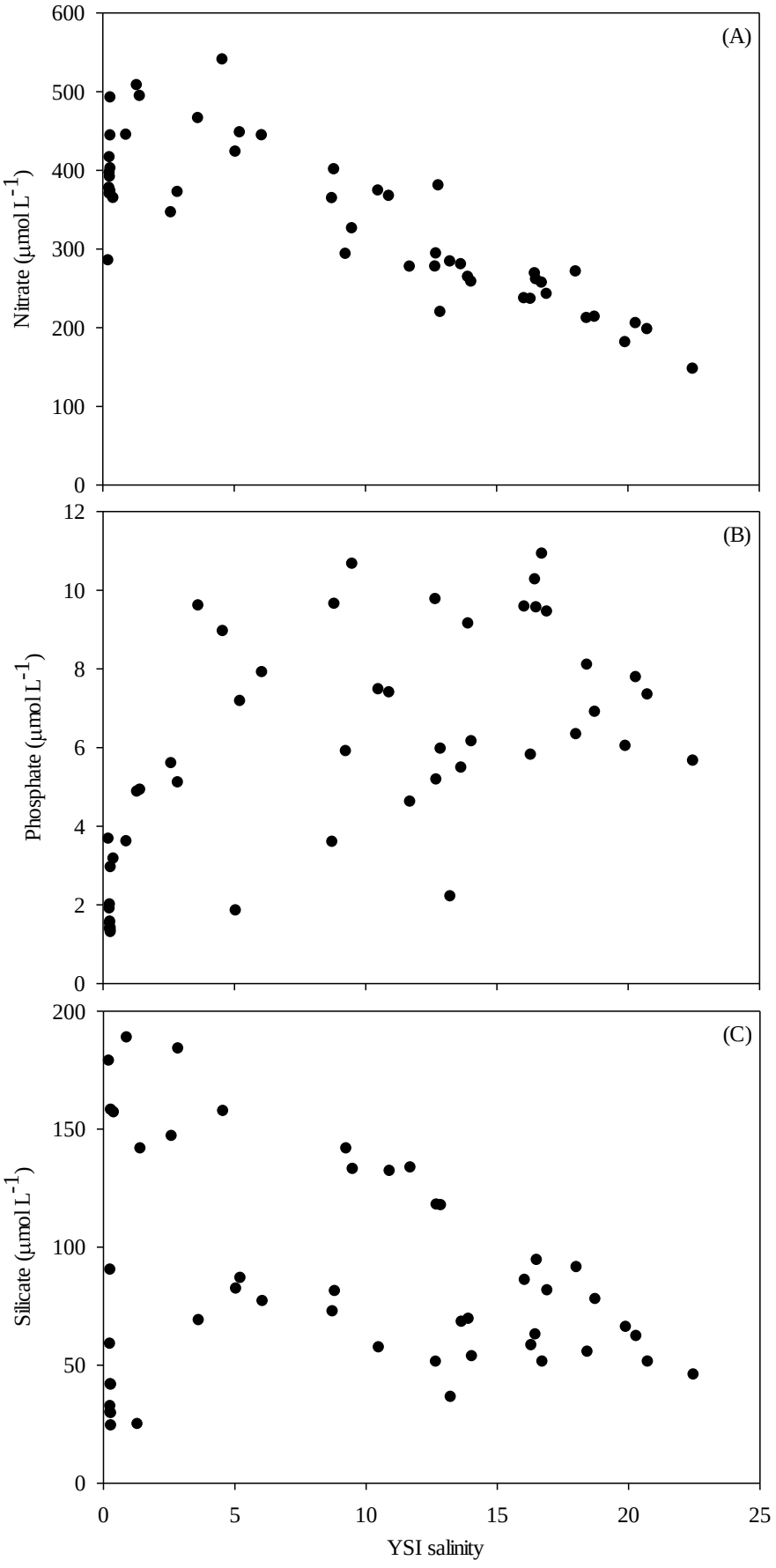


Figure 4-4: Relationship between inorganic nutrient concentrations and YSI salinity measurements at Mudeford Quay, (A) nitrate, (B) phosphate, (C) silicate.

Table 4-1: The seasonal means of nitrate, phosphate, and silicate concentrations (µmol $L^{-1}$) at Mudeford Quay.

| | mean values ± standard deviation (µmol $L^{-1}$) | | | |
|---|---|---|---|---|
| Inorganic nutrients | spring | summer | autumn | winter |
| Nitrate | 338 ± 98 | 276 ± 90 | 273 ± 57 | 388 ± 72 |
| Phosphate | 6 ± 3 | 8 ± 2 | 8 ± 2 | 3 ± 2 |
| Silicate | 87 ± 46 | 63 ± 12 | 107 ± 40 | 100 ± 63 |

The silicate to phosphate (Si:P), nitrate to phosphate (N:P), and nitrate to silicate (N:Si) ratio at Mudeford Quay are shown in Figure 4-5 and the seasonal means of these surface ratios are illustrated in Table 4-2. The N:P and N:Si ratios for this study site tended to decrease gradually from spring to winter, and increase sharply during the winter flood between week 38 and 47. The Si:P ratio fluctuated most widely between the late autumn to spring 2014 (week 28 – 51), and also the high ratios occurred during that period. The highest value of the N:P ratio occurred on 13rd March 2014 (week 46), while the peak nitrate to silicate ratio was determined on 3rd May 2013 (week 3).

The N:P generally ranged between 23 and 350. These ratios are significant greater than the Redfield ratio of 16 for typical marine waters similar to that observed for the riverine N:P ratio. The N:Si and Si:P varied generally 1 – 20 and 4 – 53, respectively.

Nutrient ratio can indicate which particular nutrient might affect phytoplankton growth and succession, but the river flow rate or the water residence time perhaps mainly controlled the variation of nutrient ratios in this estuary. Christchurch Harbour is a small shallow estuary and the Stour and Hampshire Avon Rivers flow directly into the estuary and at low tide until flush out towards the English Channel. The water samples were collected from the surface at low tide to estimate nutrient flow through the estuary. The nutrient ratio in the water can be compared with the Redfield ratio for N:P of 16:1 also for Si:P of 16:1. The high N:P and Si:P ratios were observed in early spring 2014 (week 47 and 49, respectively) indicate that relatively low phosphate concentrations may be the reason for high ratio at the estuary entrance. The N:Si ratio was 20 on 3rd May 2013 (week 3) due to high concentration of nitrate (508 µmol $L^{-1}$) was measured on that day. Residence time of the Christchurch Harbour estuary is estimated to be 65.9 hours or 2.7 days during the spring following the formulas of Dyer (1997) (Charlie Thompson, personal communication).

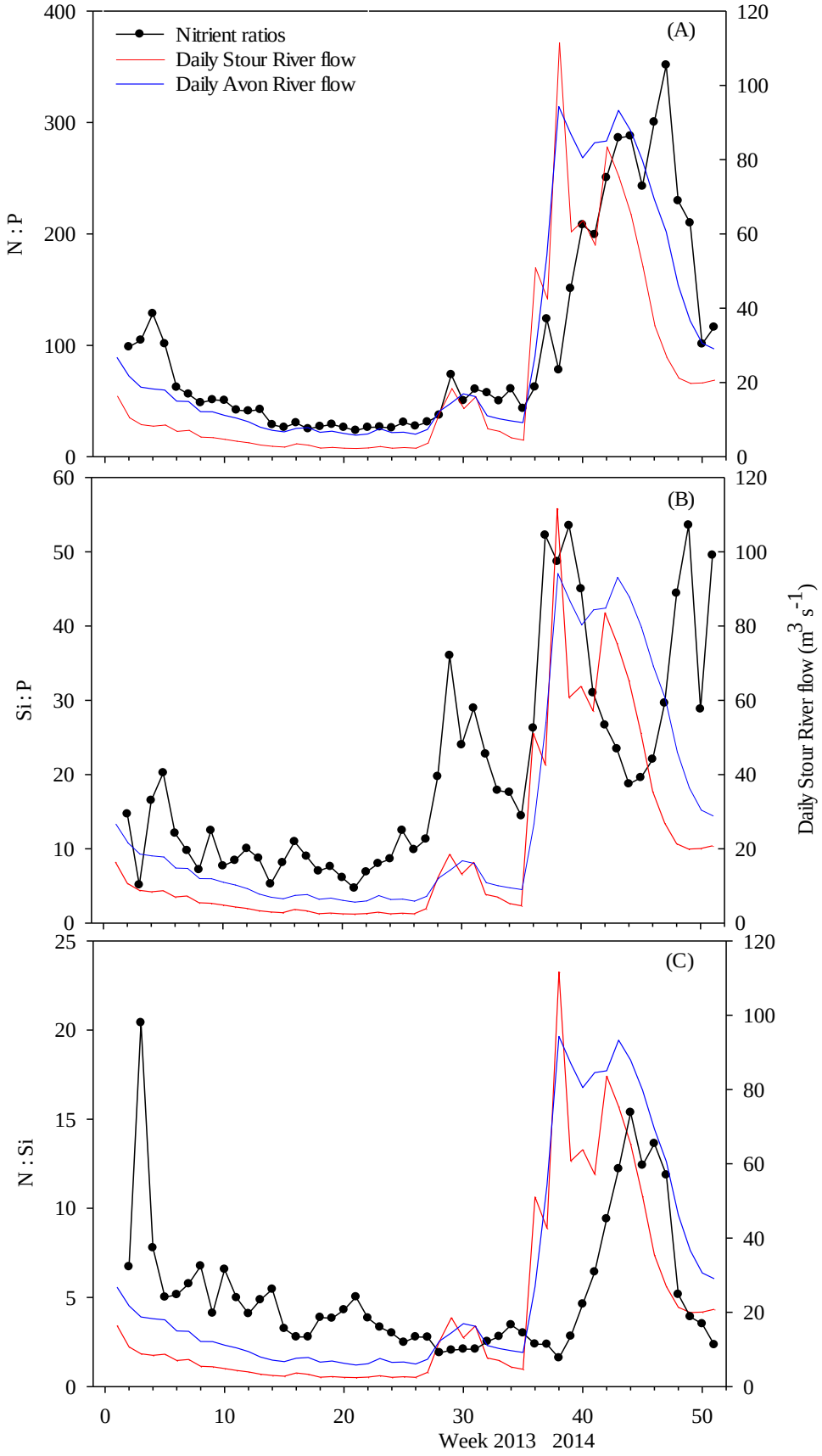


Figure 4-5: Si:P, N:P, and N:Si ratio at Mudeford Quay. Red solid line indicates a daily Stour River flow and blue solid line shows a daily Avon River flow. Symbols in upper panel apply to all panels.

Table 4-2: The seasonal means of surface nitrate to phosphate ratio (N:P), nitrate to silicate ratio (N:Si), and silicate to phosphate ratio (Si:P) at Mudeford Quay.

| | mean values ± standard deviation | | | |
|---|---|---|---|---|
| Ratio | spring | summer | autumn | winter |
| N:P | 96 ± 89 | 36 ± 10 | 40 ± 16 | 165 ± 91 |
| N:Si | 5 ± 4 | 4 ± 1 | 3 ± 1 | 6 ± 5 |
| Si:P | 20 ± 15 | 8 ± 2 | 16 ± 10 | 31 ± 15 |

### 4.3.2 Phytoplankton pigments

#### 4.3.2.1 Total chlorophyll *a* and chlorophyll *a* size fractions

Annual changes in total surface chlorophyll *a* concentrations and size fractions for the estuarine station are illustrated in Figure 4-6. The numbers (M1 – 9) and dash lines are shown above the chlorophyll *a* curve to identify chlorophyll events when chlorophyll *a* concentration was over of 15 µg $L^{-1}$. Total chlorophyll *a* concentrations ranged from 0.9 µg $L^{-1}$ (15$^{th}$ January 2014, week 39) to 44.0 µg $L^{-1}$ (3$^{rd}$ May 2013, week 3) coinciding with the spring diatom bloom event at Throop on the Stour River, followed by three small peaks of ~15 to ~22 µg $L^{-1}$ (week 6, 11, 19), and one small peak at the early April 2014 (week 50). The distribution showed a similar pattern with the total chlorophyll *a* concentrations at all riverine stations as the highest concentration occurred during the spring months.

The distributions of chlorophyll *a* size fractions at this study site during the productive period are illustrated on Figure 4-6 with total chlorophyll *a* concentration. A good agreement between total sum chlorophyll *a* and chlorophyll size fractions is shown in Figure 4-7, with slope 0.81, and an $R^2$ value of 0.96, pronouncing confidence that the size fraction procedure from this site was not associated with significant loss of phytoplankton cells.

The pattern of the chlorophyll *a* size fractions distribution during the productive period at the estuary entrance is illustrated in absolute units and as percentages in Figure 4-8. The mean percentages for each size fraction were: > 20 µm, 24% (maximum 47% in week 23); 2 – 20 µm 62% (maximum 86% in week 5); < 2 µm 15% (maximum 35% in week 21). The maximum percentage of each size fraction occurred the same sampling days as the riverine size fractions particularly at Throop on the Stour River.

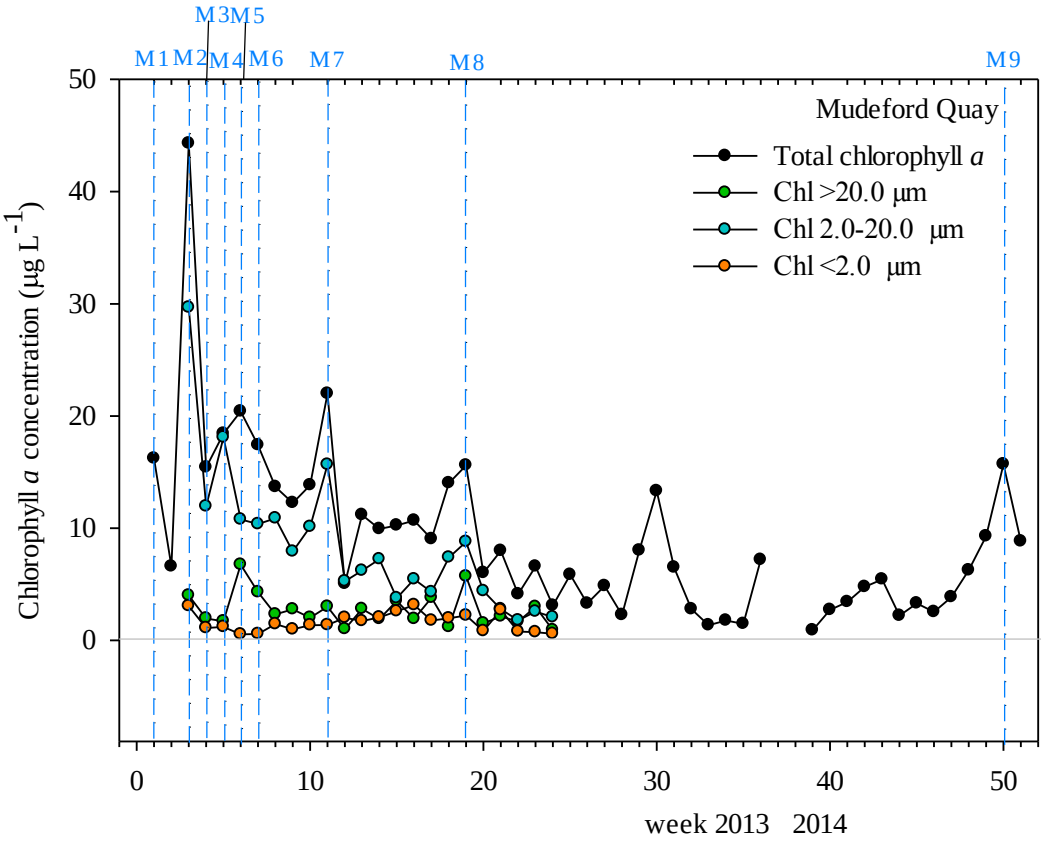


Figure 4-6: Seasonal distribution of total chlorophyll *a* and three sizes fractionated chlorophyll *a* concentrations at Mudeford Quay. The numbers and dash lines shown above the chlorophyll *a* curve identify a series of chlorophyll events.

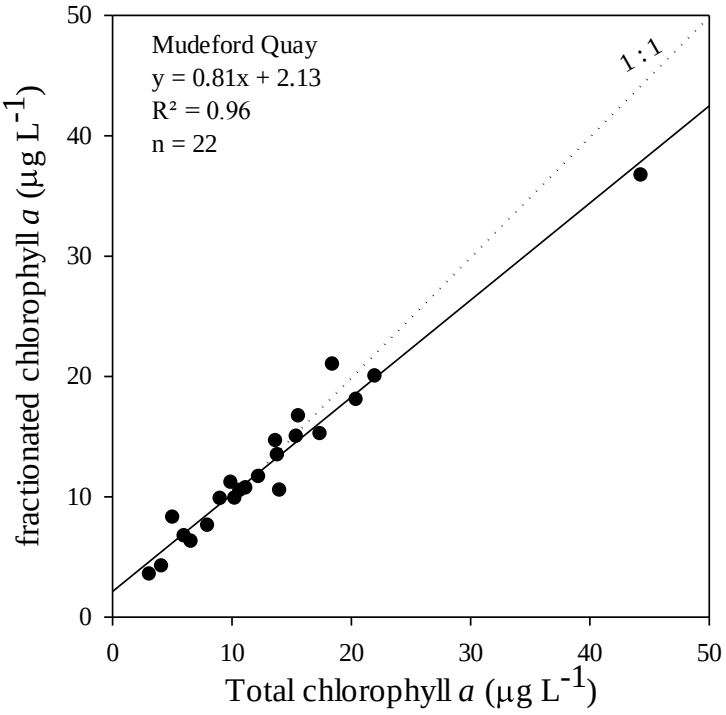


Figure 4-7: Correlation between total chlorophyll *a* and sum size fractions at Mudeford Quay. The dash line represents the 1:1 agreement line.

The three size fraction classes shown in Figure 4-8 indicate the 2 – 20 µm size (nano-phytoplankton) fractions was the highest group than the others, corresponding to this cell range identifiable under the light inverted microscope. The mean percentage of the 2 – 20 µm fraction was observed to be 62% (range 37 – 86%), with the correlation between total chlorophyll *a* and the 2 – 20 µm gave $R^2 = 0.96$ (n = 22) at this site.

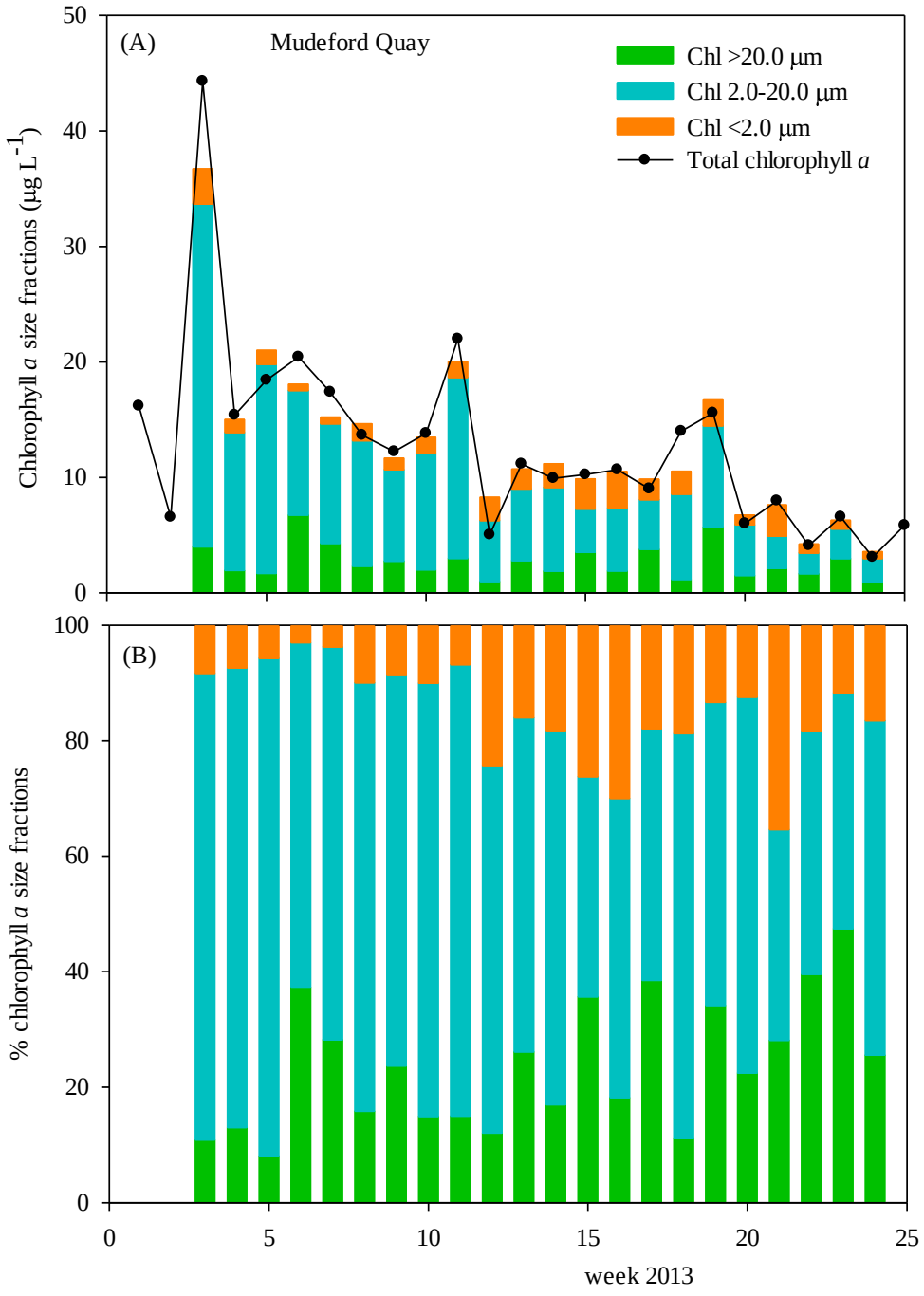


Figure 4-8: Distributions of chlorophyll *a* size fractions during the high productive period (A) and distributions of chlorophyll *a* size fractions expressed as percentages (B) at Mudeford Quay.

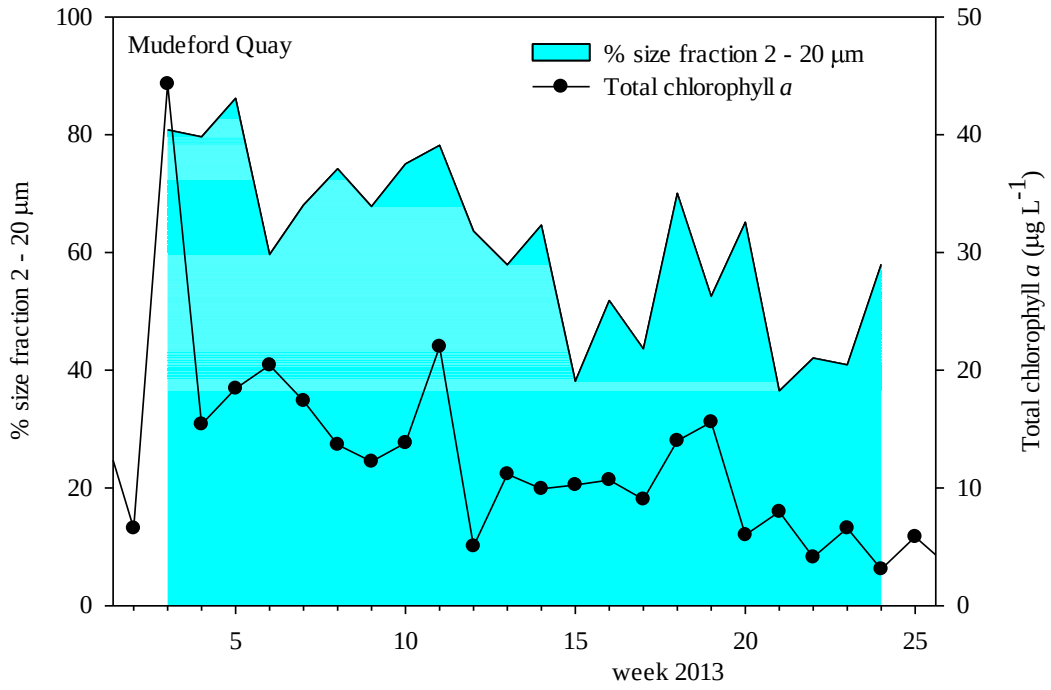


Figure 4-9: Total chlorophyll *a* and percentages of 2 – 20 µm chlorophyll *a* fraction at Mudeford Quay.

The relationship between chlorophyll concentrations and nutrients at Mudeford Quay are shown in Figure 4-10. No obvious relationships have in evident from the data.

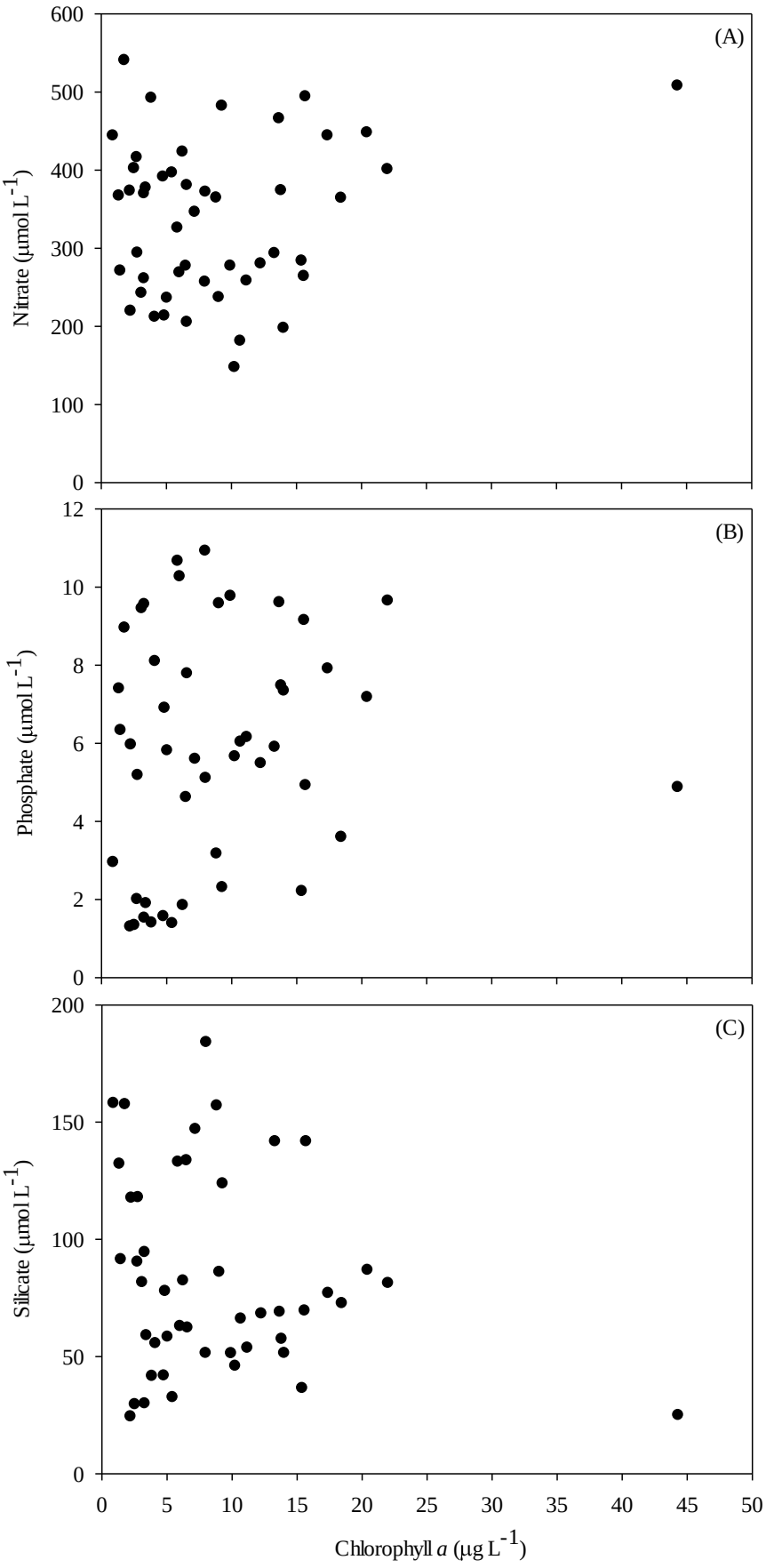


Figure 4-10: Relationship between inorganic nutrients and chlorophyll *a* concentration at Mudeford Quay, (A) nitrate, (B) phosphate, (C) silicate.

#### 4.3.2.2 Phytoplankton accessory pigment

High performance liquid chromatography (HPLC) method was used to measure the concentration of a number of estuarine phytoplankton accessory pigments as sampled from both riverine stations at Throop and Knapp Mill on the Stour and Hampshire Avon Rivers. Chlorophyll *a* concentrations measured by HPLC at Mudeford Quay were consistently lower than concentration measured by fluorescence (Figure 4-11 C). The discrepancy between chlorophyll *a* concentrations determined by fluorescence and HPLC analysis in estuarine samples seems to be magnified at high chlorophyll *a* concentrations as seen for riverine samples in the previous chapter. This is clearly seen on the three days of peak chlorophyll *a* concentrations over 20 µg $L^{-1}$ during the diatom bloom.

In the present study, the HPLC method detected up to 16 pigments some of which can be used as biomarkers to distinguish between phytoplankton groups as described in Table 2-2. There were good correlations between chlorophyll *a* and both total pigment concentrations (all pigments including chlorophyll *a*) or total accessory pigment concentrations (without chlorophyll *a*), as shown in Figure 4-11, which were irrespective of phytoplankton composition and pigment content.

The temporal successions of eight major pigments, namely chlorophyll *a* (Chl *a*), peridinin (Peri), fucoxanthin (Fuco), alloxanthin (Allo), lutein (Lut), chlorophyll *b* (Chl *b*), diadinoxanthin (Dia), and β carotene (β caro) at Mudeford Quay (Figure 4-12) as well as eight minor pigments chlorophyll *c3* (Chl *c3*), chlorophyll *c2* (Chl *c2*), 19'Butanoyloxyfucoxanthin (19'But), 19'Hexanoyloxyfucoxanthin (19'Hex), violaxanthin (Vio), prasinoxanthin (Pra), divinyl chlorophyll *a* (DV Chl *a*), and zeaxanthin (Zea) from Mudeford Quay is shown in Figure 4-13. Variations in the ratio of accessory pigments to chlorophyll *a* (Figure 4-14 to Figure 4-15) reflected changes in the taxonomic composition of the phytoplankton population similar to the riverine samples.

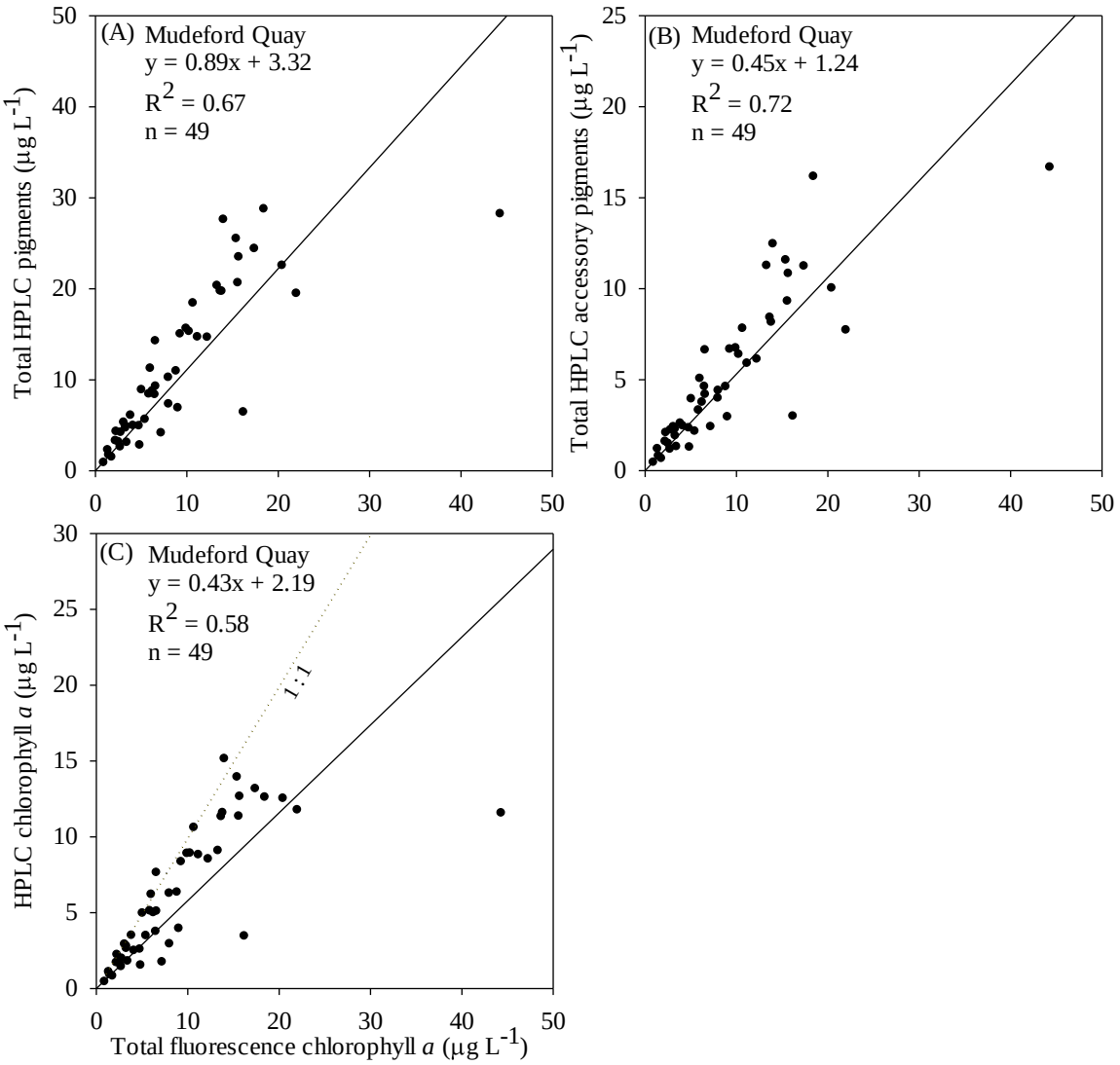


Figure 4-11: Relationship of total fluorescence chlorophyll *a* to total HPLC pigments and total HPLC accessory pigments (A and B), and HPLC chlorophyll *a* (C) at Mudeford Quay. The solid lines represent the linear regression for each set of data and equation for this line and correlation coefficient shown. The dash lines represent the 1:1 agreement line on figure C.

Similar to the riverine samples, HPLC determined chlorophyll *a* concentration at Mudeford Quay (Figure 4-12) generally followed distributions described previously for fluorometric determination (see Figure 4-6), although absolute concentration varied (Figure 4-12 A). Fucoxanthin and diadinoxanthin showed a similar seasonal distribution to Chl *a*, with maxima of 9.9 and 2.9 µg $L^{-1}$ on 3rd May 2013 (week 3) followed by 7.7 and 2.5 µg $L^{-1}$ on 17th May 2013 (week 5) respectively (Figure 4-12 C and G). Low concentrations of peridinin were observed between week 17 and week 32 (6th August to 18th November 2013) with concentrations below 0.05 µg $L^{-1}$ while concentrations were close to zero during the rest of year (Figure 4-12 B). Alloxanthin, lutein, and chlorophyll *b*

concentrations showed maxima peaks during the early chlorophyll *a* events (M1 – M6) in weeks 4, 7, and 5 (Figure 4-12 D, E, F). Concentration of chlorophyll *b* closely followed those of lutein but both pigments showed a high concentration during the early chlorophyll events, however, the highest concentration of chlorophyll *b* was present on 17$^{th}$ May 2013 (week 5) with concentration of 2.6 µg L$^{-1}$ as shown in Figure 4-6 E and F. Maximum concentration of β carotene was detected in week 30 (4$^{th}$ November 2013) with concentration of 1.3 µg L$^{-1}$ while concentrations were below 1.0 µg L$^{-1}$ during the rest of year (Figure 4-6 H).

Low concentrations of chlorophyll *c3* were observed at the Mudeford Quay during 2013 – 2014 (Figure 4-13 A). This pigment was present a highest concentration on 31$^{st}$ May 2013 (week 7, M6) at ~0.2 µg L$^{-1}$, and several small peaks were measured at this study site until the end the sampling period. Chlorophyll *c2* was found in high concentrations in samples in May 2013, both maxima of 0.6 µg L$^{-1}$ (Figure 4-13 B).

On 4$^{th}$ November 2013 (week 30) high concentration of 19'But was detected of 1.2 µg L$^{-1}$, that did not relate to chlorophyll events (Figure 4-13 C). However, this pigment presented high concentrations during the spring months in 2013; concentrations were below 0.4 µg L$^{-1}$ during the rest of year. 19'Hex was generally present in high concentrations from 10$^{th}$ May to 31$^{st}$ June 2013 (week 4 – 16), and after that zero and close to zero concentrations were measured (Figure 4-13 D).

Violaxanthin maximum concentrations were detected during the summer period of 0.4 µg L$^{-1}$ (Figure 4-13 E), and after that the concentrations were measured below 0.2 µg L$^{-1}$ during the rest of year. Prasinoxanthin was generally undetectable, except from 11$^{st}$ September to 18$^{th}$ November 2013 (week 22 – 32) low concentrations were observed (Figure 4-13 F).

Divinyl chlorophyll *a* was always present throughout the sampling period, and varied between zero and 0.6 µg L$^{-1}$ (Figure 4-13 G). Some peaks in divinyl chlorophyll *a* were observed in samples relative to chlorophyll events. Peak concentration of this pigment was detected at the same day with 19'But and prasinoxanthin peaks on 4$^{th}$ November 2013, with concentration of 0.6 µg L$^{-1}$. Low concentration of zeaxanthin was observed during 6$^{th}$ August to 24$^{th}$ October 2013 (week 17 – 28), and varied between 0.1 and 0.3 µg L$^{-1}$ after that the concentrations increased to 1.3 µg L$^{-1}$ on 4$^{th}$ November 2013 (Figure 4-13 H). This pigment was detected below 0.2 µg L$^{-1}$ during the rest of year.

Considering the accessory pigment to chlorophyll *a* (Chl *a*) ratios, peridinin to Chl *a* ratio showed much lower values than in both riverine samples. This ratio peaked on 11st November 2013 (week 31), when it was around 0.01 (Figure 4-14 A). Peridinin to Chl *a* ratios were zero during most part of the sampling period.

Fucoxanthin to Chl *a* ratios were higher during the spring period in 2014, and relative to the chlorophyll events (Figure 4-14 B). This ratio varied between 0.2 and 0.9 and maximum value was detected on 3rd May 2013 (week 3, M3). Low values of alloxanthin to Chl *a* ratios showed during 16th April to 31st July 2013 (week 1 – 16), and after that several small peaks occurred until the end of sampling (Figure 4-14 C).

Lutein to Chl *a* ratios were generally lower 0.1 until 18th November 2013 (week 32), then increased up to 0.4 on 17th December 2013 (week 36) as shown in Figure 4-14 D. This ratio was close to zero in February 2014. Chlorophyll *b* to Chl *a* ratios were quite constant from 3rd May to 18th November 2013, around 0.1, and after that zero and close to zero during the rest of year (Figure 4-14 E).

Diadinoxanthin to Chl *a* ratios ranged between 0.04 and 0.25 (Figure 4-14 F). Maximum values of ~0.3 and 0.2 were found on 3rd and 17th May 2013 (week 3 and 5, M2 and 4). β carotene to Chl *a* ratios showed an increase towards April and December 2013 at Mudeford Quay, reaching a peak of 0.2 on 17th December 2013, and after that this ratio decreased until the end of sampling (Figure 4-14 G).

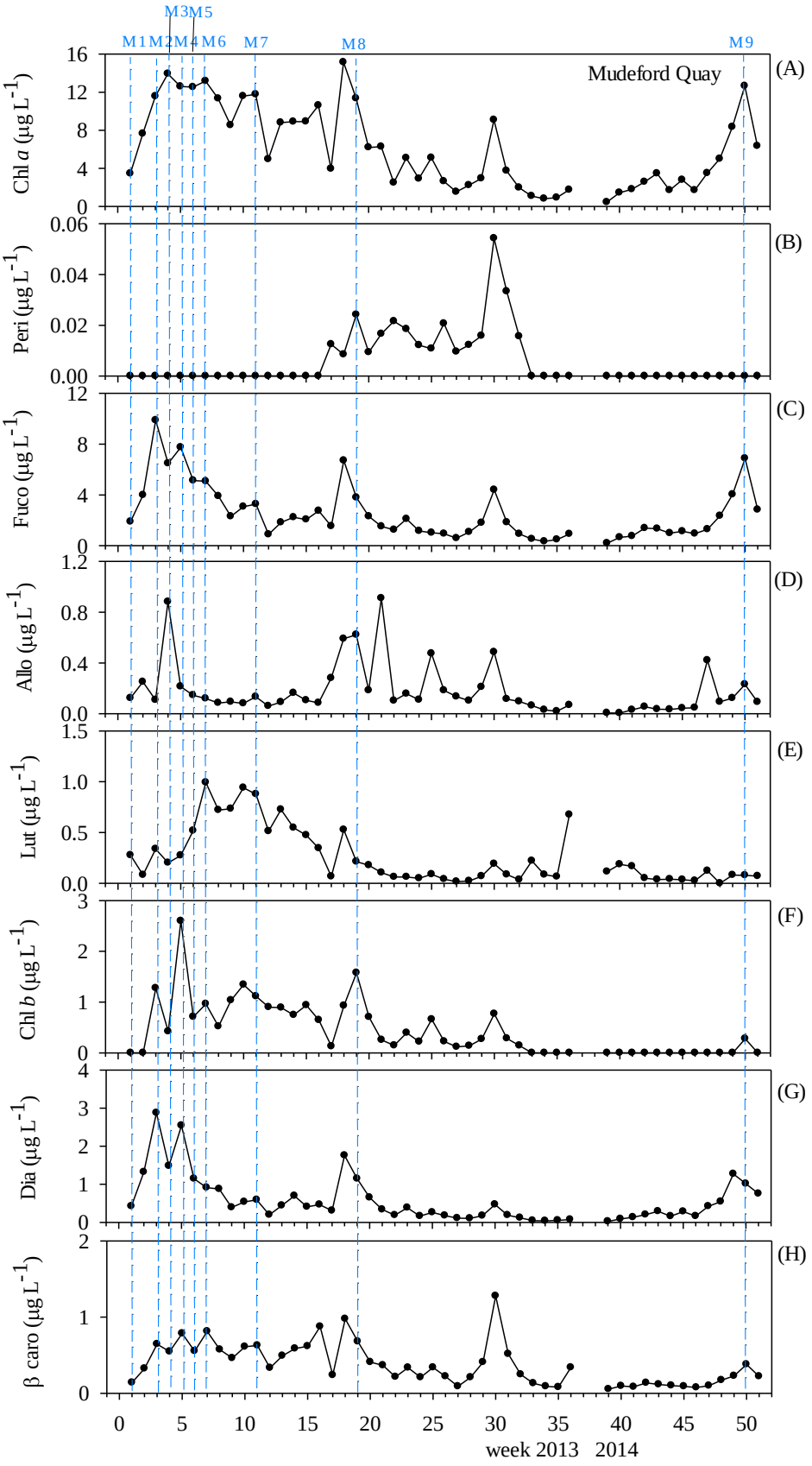


Figure 4-12: Temporal distributions of phytoplankton chlorophyll *a* and major accessory pigments at Mudeford Quay, Christchurch Harbour. The numbers and dash lines shown above the HPLC pigment plots identify a series of chlorophyll events.

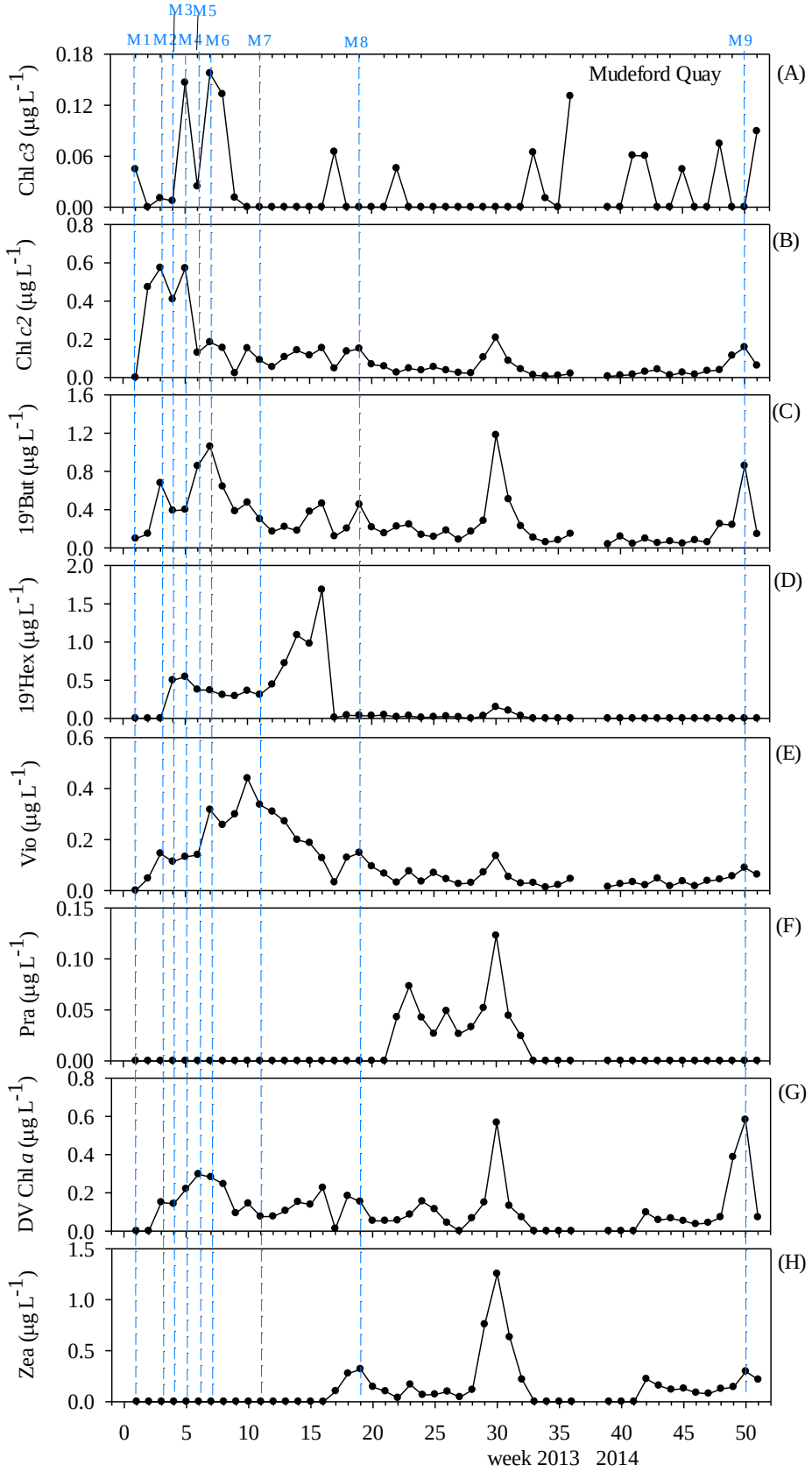


Figure 4-13: Temporal distributions of phytoplankton chlorophyll *a* and minor accessory pigments at Mudeford Quay, Christchurch Harbour. The numbers and dash lines shown above the HPLC pigment plots identify a series of chlorophyll events.

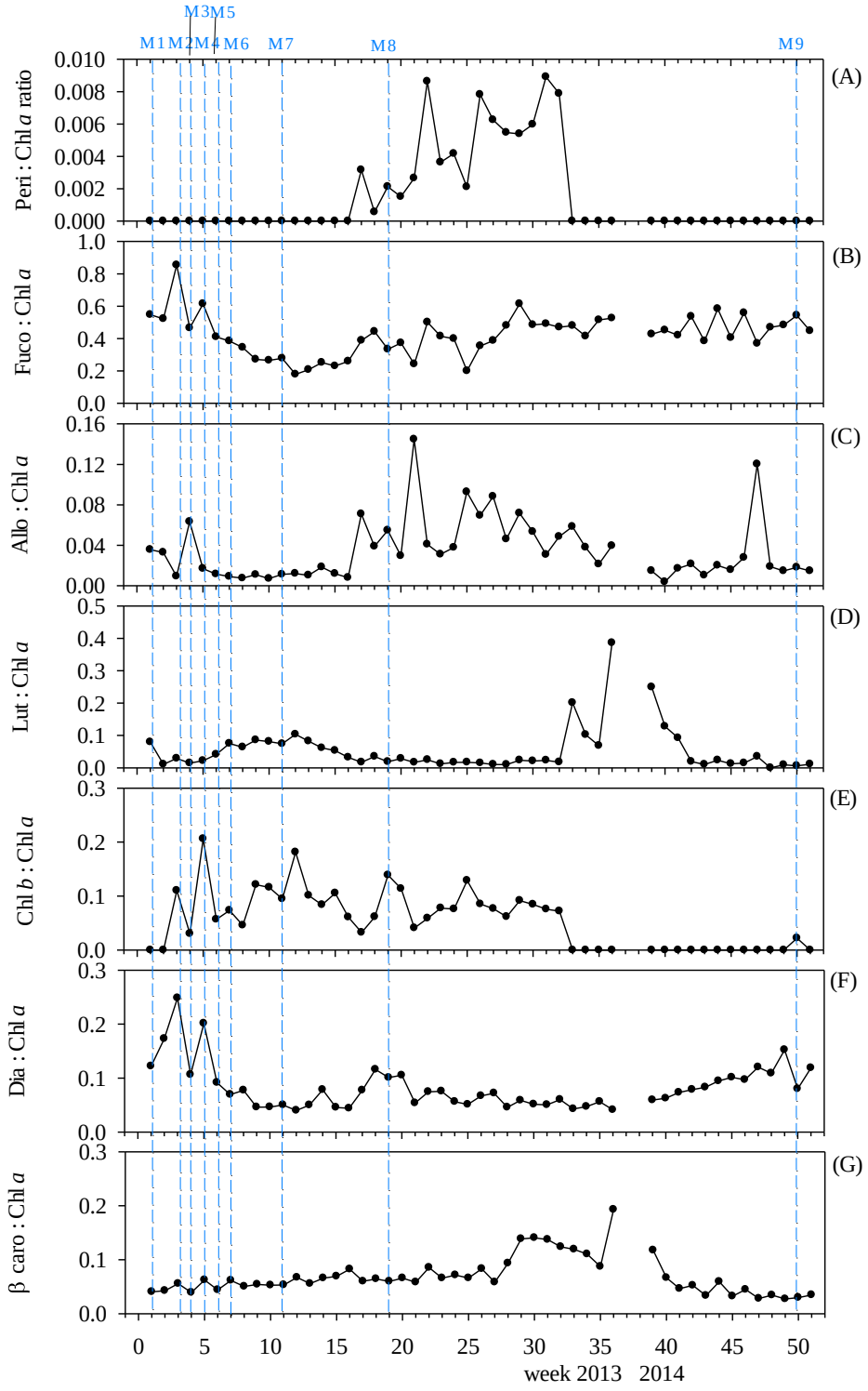


Figure 4-14: Temporal and spatial distributions of major accessory pigment to chlorophyll *a* ratios at Mudeford Quay. The numbers and dash lines shown above the HPLC pigment plots identify a series of chlorophyll events.

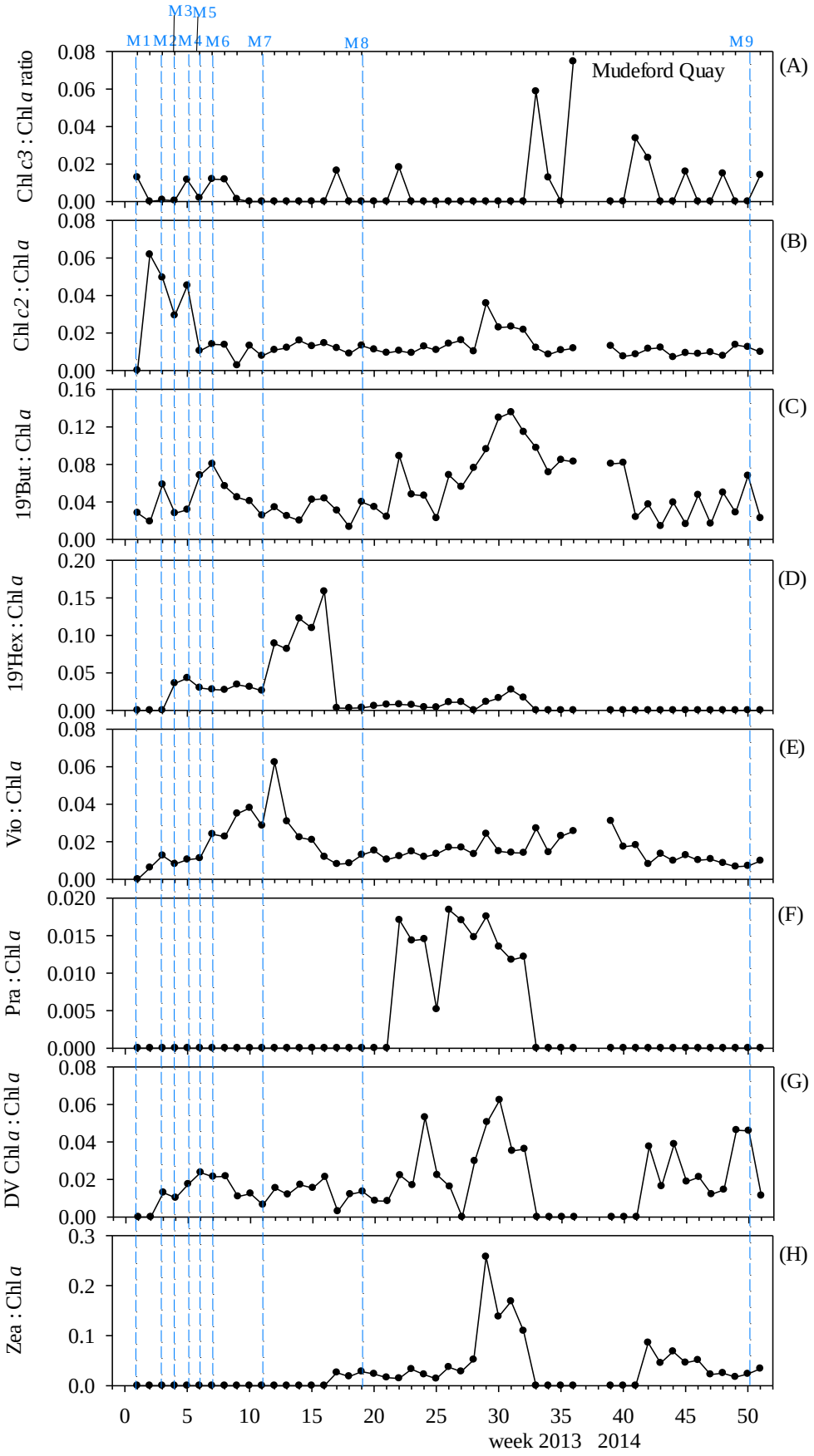


Figure 4-15: Temporal and spatial distributions of minor accessory pigment to chlorophyll *a* ratios at Mudeford Quay. The numbers and dash lines shown above the HPLC pigment plots identify a series of chlorophyll events.

### 4.3.3 Phytoplankton taxonomic data

#### 4.3.3.1 Phytoplankton cell abundance

The estuarine phytoplankton groups are shown in Figure 4-16 A as absolute values and in Figure 4-16 B as percentage values for cell counts throughout the sampling period at low tide from April 2013 to April 2014 at Mudeford Quay. The most abundant group was the diatom group contributing between 5% and 98% of the total phytoplankton population, followed by chlorophyte and cryptomonad groups contributing 0 – 89% and 0 – 69%, respectively, while the other groups together represented the remaining proportions at this study site. The spring period had the highest diatom contribution similar to the riverine stations.

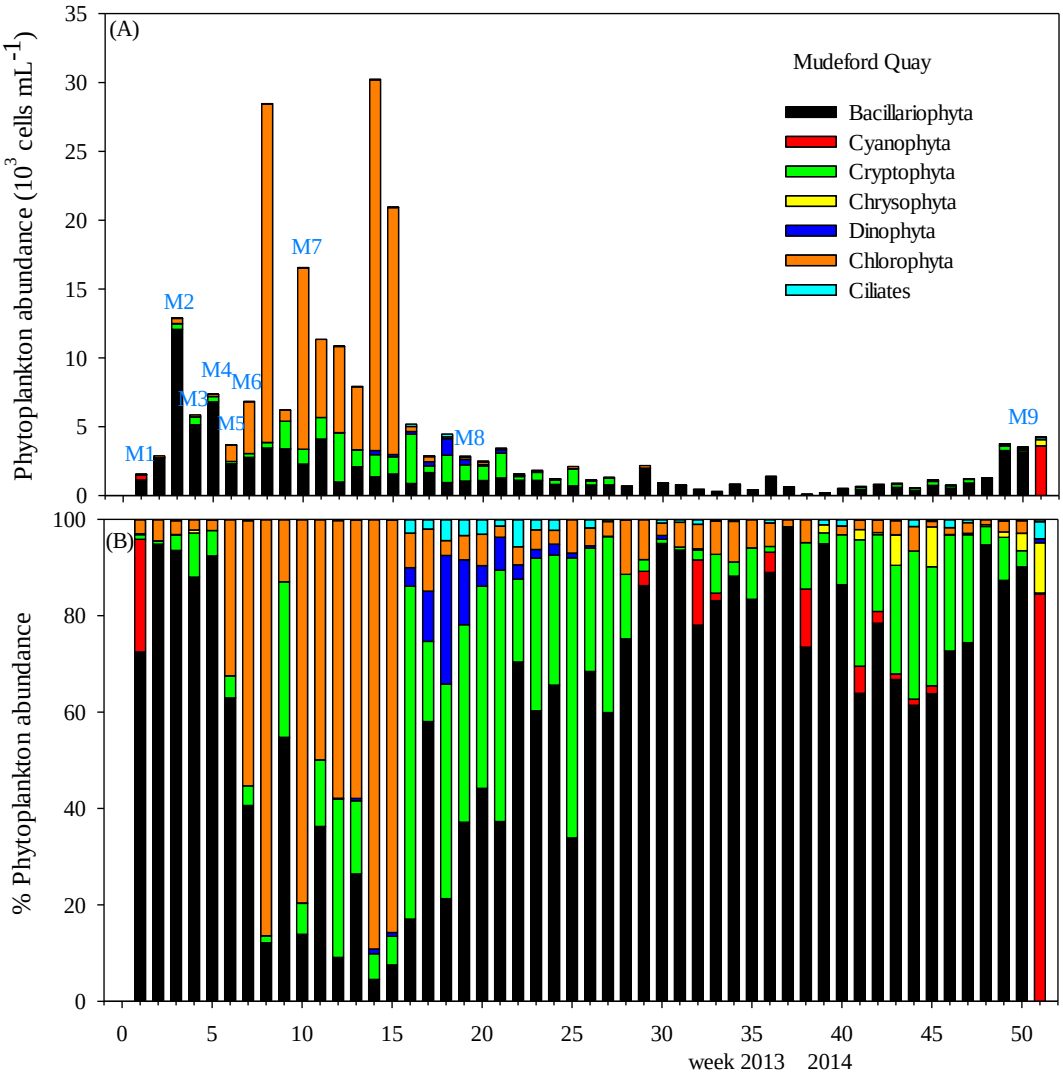


Figure 4-16: Distributions of abundance and cell count percentage for main phytoplankton groups at Mudeford Quay, Christchurch Harbour during April 2013 – April 2014. The letters and numbers shown above the abundance bars identify a series of chlorophyll *a* events.

### 4.3.3.2 Phytoplankton bio-volume and carbon biomass

Phytoplankton cell abundance was converted to carbon biomass and percentage distribution calculated for the major phytoplankton groups as shown in Figure 4-17. The diatoms gave the highest biomass values, with percentages up to 100% on 30th December 2013 (week 37), followed by dinoflagellate, chlorophyte and cryptomonad groups with percentage ranging up to 80, 58, and 56%, respectively (Figure 4-17 B). Diatoms were important throughout the sampling period, with the percentages between 9% (14th August 2013, week 18) and 100% (week 37). The chlorophyte group occurred as the main carbon biomass during the early summer (week 8 – 15), followed by the dinoflagellate group until the early autumn. The cryptomonad group increased in proportion during the chlorophyte and dinoflagellate maxima. Other phytoplankton groups (cyanophyte and chrysophyte) were relatively unimportant at this study site.

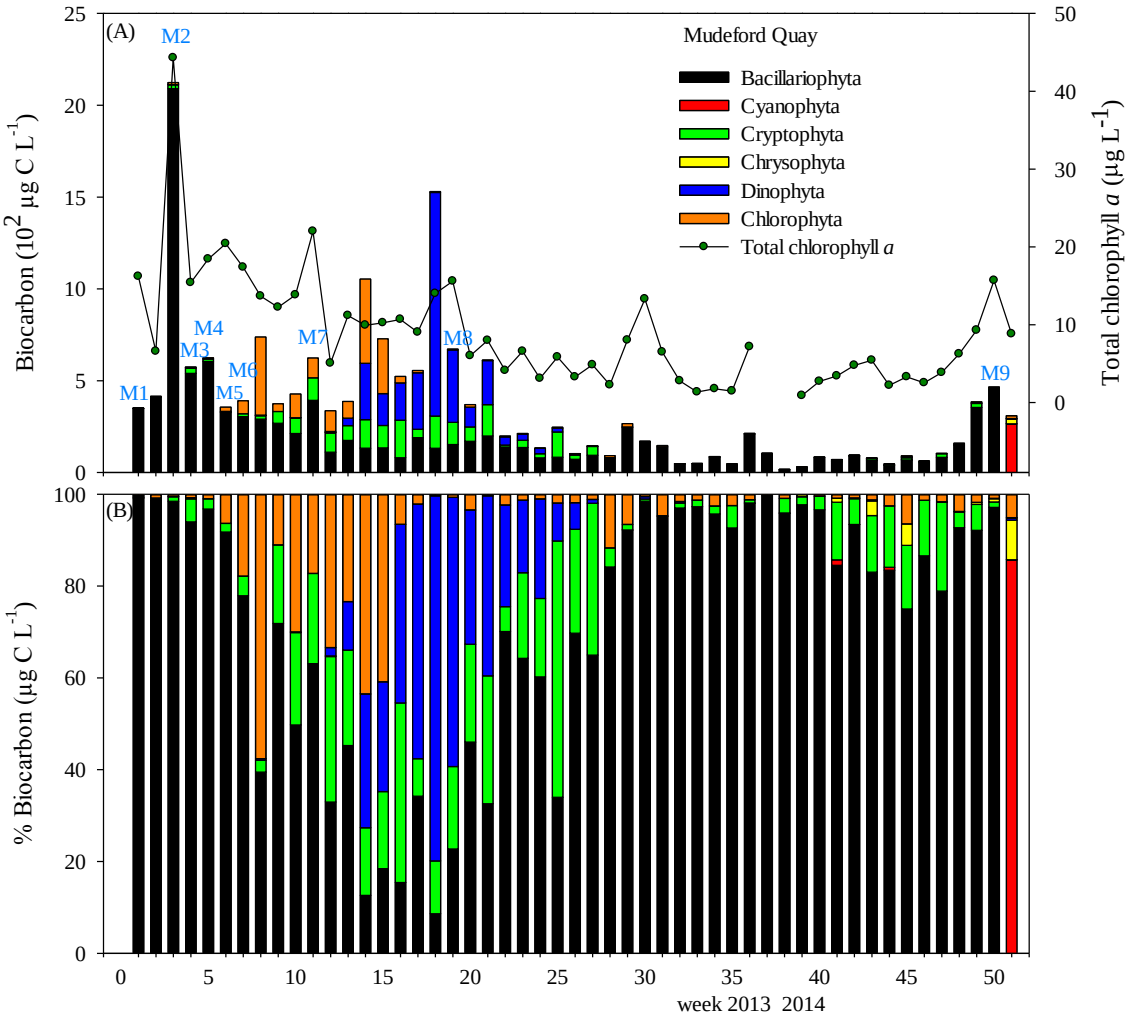


Figure 4-17: Distributions of carbon biomass and percentage for main phytoplankton groups at Mudeford Quay during April 2013 – April 2014. The letters and numbers shown above the abundance bars identify a series of chlorophyll *a* events.

The correlation between total chlorophyll *a* concentration and carbon biomass at the estuary entrance is shown in Figure 4-18. (Equation was y = 41.3x – 6.4 and $R^2$ value was 0.64). Total carbon biomass to chlorophyll ratio was 41.

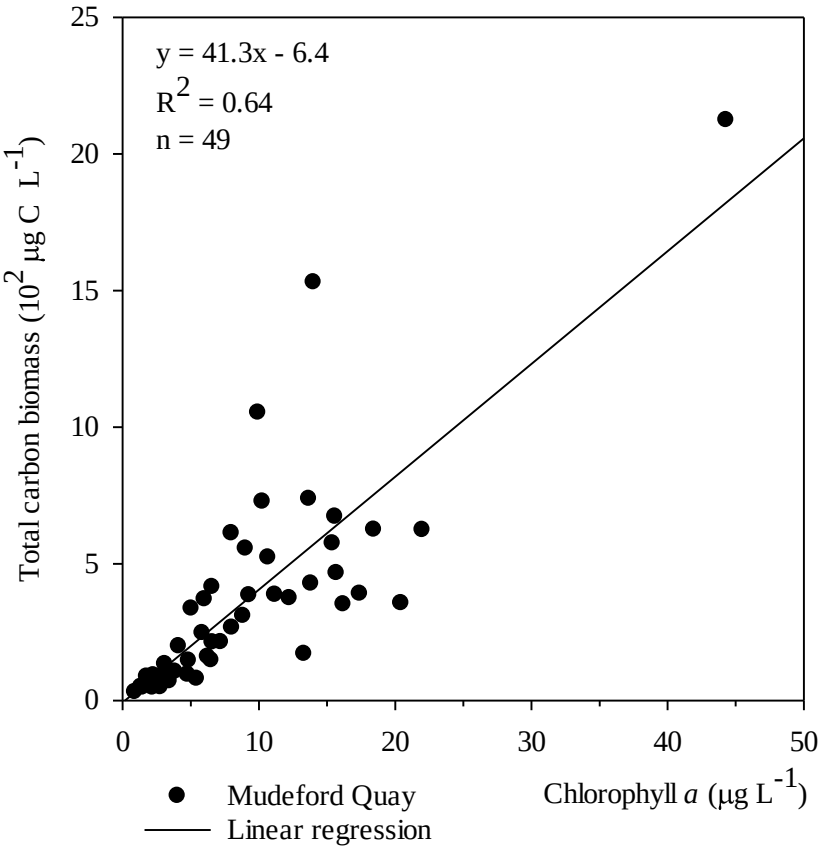


Figure 4-18: Correlation between total carbon biomass and total chlorophyll *a* concentration at Mudeford Quay.

#### 4.3.3.3 Phytoplankton species composition

The phytoplankton species cell counts and carbon concentration from maximum the chlorophyll *a* events (M 1 – 9) expressed as absolute values are shown in Table 4-3 and Table 4-4. In terms of species abundance, the chlorophyll events are quite similar. The diatom population contributed higher abundances than other groups and were the most abundant during the spring and the early summer, due to the high contribution of *Stephanodiscus* sp. and *Navicula* spp. The dinoflagellate group was less numerous at Mudeford Quay during the peak chlorophyll events, but most abundant during the summer months. *Cryptomonas* sp. and *Rhodomonas* sp. were common genera present during the high chlorophyll peak and the chlorophyte group particularly *Chlamydomonas* sp. was dominant during the late spring and summer (week 6, 7, and 11).

The phytoplankton biomass gave a different aspect of species contribution, particularly for the chlorophyte group, which represent an annual mean of 7% of total biomass. A noteworthy species was *Stephanodiscus* sp., present as a dominant species and carbon biomass at the same time as Throop during the spring diatom bloom. The highest biomass for *Stephanodiscus* sp. at Mudeford Quay was on 3rd May 2013 (week 3) with the abundance of $9.9 \times 10^3$ cells $mL^{-1}$ and the biomass of 909 µg C $L^{-1}$. The chlorophyte species, *Chlamydomonas* sp., occurred with high abundance during the early summer particularly on 28th June 2013 (week 11) up to $4.1 \times 10^3$ cells $mL^{-1}$ but had a low biomass due to its small size. *Skeletonema* sp. and *Navicula* spp. contributed high values during the summer months at this study site.

*Kryptoperidinium foliaceum* was the most abundant dinoflagellate species during the summer to autumn with up to $1.2 \times 10^3$ cells $mL^{-1}$ but they do not show in Table 4-3. This dinoflagellate species was not presented in the winter and spring months.

Table 4-3: Phytoplankton species counts (cells $mL^{-1}$) for the peak chlorophyll samples at Mudeford Quay (M1 – 9). All species counted from settled 10 mL samples are listed.

| **Chlorophyll *a* weeks** | **M1 1** | **M2 3** | **M3 4** | **M4 5** | **M5 6** | **M6 7** | **M7 11** | **M8 19** | **M9 50** |
|---|---|---|---|---|---|---|---|---|---|
| **Chlorophyll *a* (µg $L^{-1}$)** | **16.2** | **44.3** | **15.4** | **18.4** | **20.4** | **17.4** | **22.0** | **15.6** | **15.7** |
| **Bacillariophyta** | | | | | | | | | |
| *Amphora* spp. | 5 | 18 | 19 | 21 | 36 | 23 | 48 | 26 | 152 |
| *Cocconeis* spp. | - | - | 8 | 15 | 36 | 61 | 120 | 161 | 79 |
| *Diatoma vulgare* | 5 | 401 | 150 | 52 | 225 | 164 | 39 | 15 | 122 |
| *Licmorphora* sp. | 21 | 40 | 11 | 15 | 32 | 48 | 35 | 95 | 53 |
| *Melosira* sp. | - | 73 | 8 | 11 | 36 | 38 | 21 | 4 | 192 |
| *Navicula gracilis* | 21 | 159 | 64 | 46 | 150 | 166 | 161 | 110 | 476 |
| *Navicula* spp. | - | - | 777 | 1,010 | 1,094 | 1,022 | 589 | 328 | 318 |
| *Nitzschia acicularis* | 15 | 244 | 137 | 104 | 23 | 68 | 21 | 5 | 42 |
| *Nitzschia* sp. | 5 | - | - | 6 | 13 | 48 | 7 | 8 | 127 |
| Pennate diatoms | 313 | 521 | 73 | 47 | 77 | 43 | 23 | 88 | 33 |
| *Pleurotaenium* spp. | 8 | 88 | 5 | 12 | 49 | 16 | 7 | 5 | 20 |
| *Pseudo-nitzschia* spp. | - | 46 | 14 | 22 | 33 | 27 | 39 | 18 | 6 |
| *Skeletonema* spp. | 45 | 29 | - | 69 | 19 | 56 | 21 | 81 | 16 |
| *Stephanodiscus* sp. | 653 | 9,871 | 3,816 | 5,311 | 348 | 843 | 2,833 | 32 | 1,153 |
| **Dinophyta** | | | | | | | | | |
| *Kryptoperidinium* sp. | - | - | - | - | - | - | - | 386 | - |
| **Cryptophyta** | | | | | | | | | |
| *Cryptomonas* spp. | - | 89 | 115 | 22 | 15 | 74 | 667 | 749 | 19 |
| *Rhodomonas* spp. | 15 | 322 | 422 | 367 | 152 | 205 | 896 | 424 | 100 |
| **Chrysophyta** | | | | | | | | | |
| *Dinobryon* spp. | - | 7 | 5 | 1 | - | - | - | - | 127 |
| *Synura sphagnicola* | - | 11 | 32 | - | - | - | - | - | - |
| **Chlorophyta** | | | | | | | | | |
| *Actinastrum* spp. | - | - | 19 | 5 | - | 48 | 5 | - | - |
| *Ankistrodesmus* spp. | - | 45 | 15 | 32 | 34 | 100 | 161 | 13 | 13 |
| *Chlamydomonas* spp. | 20 | 182 | 66 | - | 958 | 3,330 | 4,154 | - | - |
| *Chlorella* sp. | - | - | - | - | - | - | 319 | 5 | - |
| *Coelastrum* spp. | - | 50 | - | - | - | - | 122 | - | - |
| *Kirchneriella* spp. | - | 22 | - | 13 | 95 | 158 | 220 | 11 | 2 |
| *Scenedesmus* spp. | 26 | 70 | 26 | 94 | 98 | 129 | 678 | 98 | 66 |

Table 4-4: Phytoplankton species biomass (µg C $L^{-1}$) for the peak chlorophyll samples at Mudeford Quay (M1 – 9).

| **Chlorophyll *a* events** | **M1** | **M2** | **M3** | **M4** | **M5** | **M6** | **M7** | **M8** | **M9** |
|---|---|---|---|---|---|---|---|---|---|
| **weeks** | **1** | **3** | **4** | **5** | **6** | **7** | **11** | **19** | **50** |
| **Chlorophyll *a* (µg $L^{-1}$)** | **16.2** | **44.3** | **15.4** | **18.4** | **20.4** | **17.4** | **22.0** | **15.6** | **15.7** |
| **Bacillariophyta** | | | | | | | | | |
| *Amphora* spp. | 0 | 1 | 1 | 2 | 3 | 2 | 3 | 2 | 11 |
| *Cocconeis* spp. | - | - | 1 | 1 | 2 | 4 | 8 | 10 | 5 |
| *Diatoma vulgare* | 2 | 203 | 76 | 26 | 114 | 83 | 20 | 8 | 62 |
| *Licmorphora* sp. | 1 | 1 | 0 | 0 | 1 | 1 | 1 | 2 | 1 |
| *Melosira* sp. | - | 25 | 3 | 4 | 13 | 13 | 7 | 1 | 67 |
| *Navicula gracilis* | 5 | 40 | 16 | 11 | 37 | 41 | 40 | 27 | 118 |
| *Navicula* spp. | - | - | 13 | 17 | 18 | 17 | 10 | 5 | 5 |
| *Nitzschia acicularis* | 0 | 3 | 2 | 1 | 0 | 1 | 0 | 0 | 1 |
| *Nitzschia* sp. | 0 | - | - | 0 | 0 | 2 | 0 | 0 | 4 |
| Pennate diatoms | 273 | 454 | 63 | 41 | 68 | 38 | 20 | 77 | 29 |
| *Pleurotaenium* spp. | 3 | 29 | 2 | 4 | 16 | 5 | 2 | 2 | 7 |
| *Pseudo-nitzschia* spp. | - | 5 | 1 | 2 | 3 | 3 | 4 | 2 | 1 |
| *Skeletonema* spp. | 1 | 0 | - | 1 | 0 | 1 | 0 | 1 | 0 |
| *Stephanodiscus* spp. | 60 | 909 | 352 | 489 | 32 | 77 | 261 | 3 | 106 |
| **Dinophyta** | | | | | | | | | |
| *Kryptoperidinium* sp. | - | - | - | - | - | - | - | 394 | - |
| **Cryptophyta** | | | | | | | | | |
| *Cryptomonas* spp. | - | 13 | 17 | 3 | 2 | 11 | 97 | 108 | 3 |
| *Rhodomonas* spp. | 0 | 9 | 12 | 11 | 4 | 6 | 26 | 12 | 3 |
| **Chrysophyta** | | | | | | | | | |
| *Dinobryon* spp. | - | 0 | 0 | 0 | - | - | - | - | 3 |
| *Synura sphagnicola* | - | 0 | 1 | - | - | - | - | - | - |
| **Chlorophyta** | | | | | | | | | |
| *Actinastrum* spp. | - | - | 1 | 0 | 0 | 2 | 0 | - | - |
| *Ankistrodesmus* spp. | - | 4 | 1 | 3 | 3 | 9 | 15 | 1 | 1 |
| *Chlamydomonas* spp. | 0 | 3 | 1 | - | 15 | 53 | 66 | - | - |
| *Chlorella* sp. | - | - | - | - | - | - | 2 | 0 | - |
| *Coelastrum* spp. | - | 1 | - | - | - | - | 1 | - | - |
| *Kirchneriella* spp. | - | 0 | - | 0 | 0 | 1 | 1 | 0 | 0 |
| *Scenedesmus* spp. | 1 | 2 | 1 | 3 | 3 | 4 | 22 | 3 | 2 |

#### 4.3.3.4 Seasonal succession of phytoplankton taxa and pigments

Phytoplankton seasonal succession is shown in Figure 4-19. as absolute biomass contributions from different phytoplankton groups, over the whole sampling period, with

the nine chlorophyll *a* events indicated by letters over vertical dashed lines and numbers indicating relative pigment signature.

The phytoplankton species counts are represented in Table 4-3. Higher diatom numbers were present during the second chlorophyll event (M2) and the highest diatom carbon (*Stephanodiscus* sp.) was also detected at that time. Cryptomonad and chlorophyte biomass followed the diatom peaks, associated with the seventh chlorophyll event. The peak of dinoflagellate biomass occurred during the high biomass peak of cryptomonads, but the peak was presented later the chlorophyte peak. As see in Figure 4-19, the highest biomass peak of cryptomonad and chlorophyte groups were not associated with the chlorophyll events that it seems to be the main group of the peak of chlorophyll events was the diatom group.

These peaks of diatom and dinoflagellate were associated with a peak of fucoxanthin, the fucoxanthin to chlorophyll *a* ratios are indicated with the peak numbers. The peak of dinoflagellate at Mudeford Quay was not associated with the peridinin concentration due to the dominant species, *Kryptoperidinium foliaceum*, contains fucoxanthin rather than peridinin as general biomarker of this group.

The biomass of cryptomonad group was high from the summer to autumn months (week 9 – 27) and in good agreement with the alloxanthin concentrations supporting the microscopic cell counts. The chlorophyte biomass was high during the early summer (week 8 – 15) but the biomass did not show a good agreement with the chlorophyll *b* concentration. It was indicated that there are other chlorophyll *b* continuing organisms, as the microscopic analysis showed that there were many small chlorophyte and the other flagellate organisms.

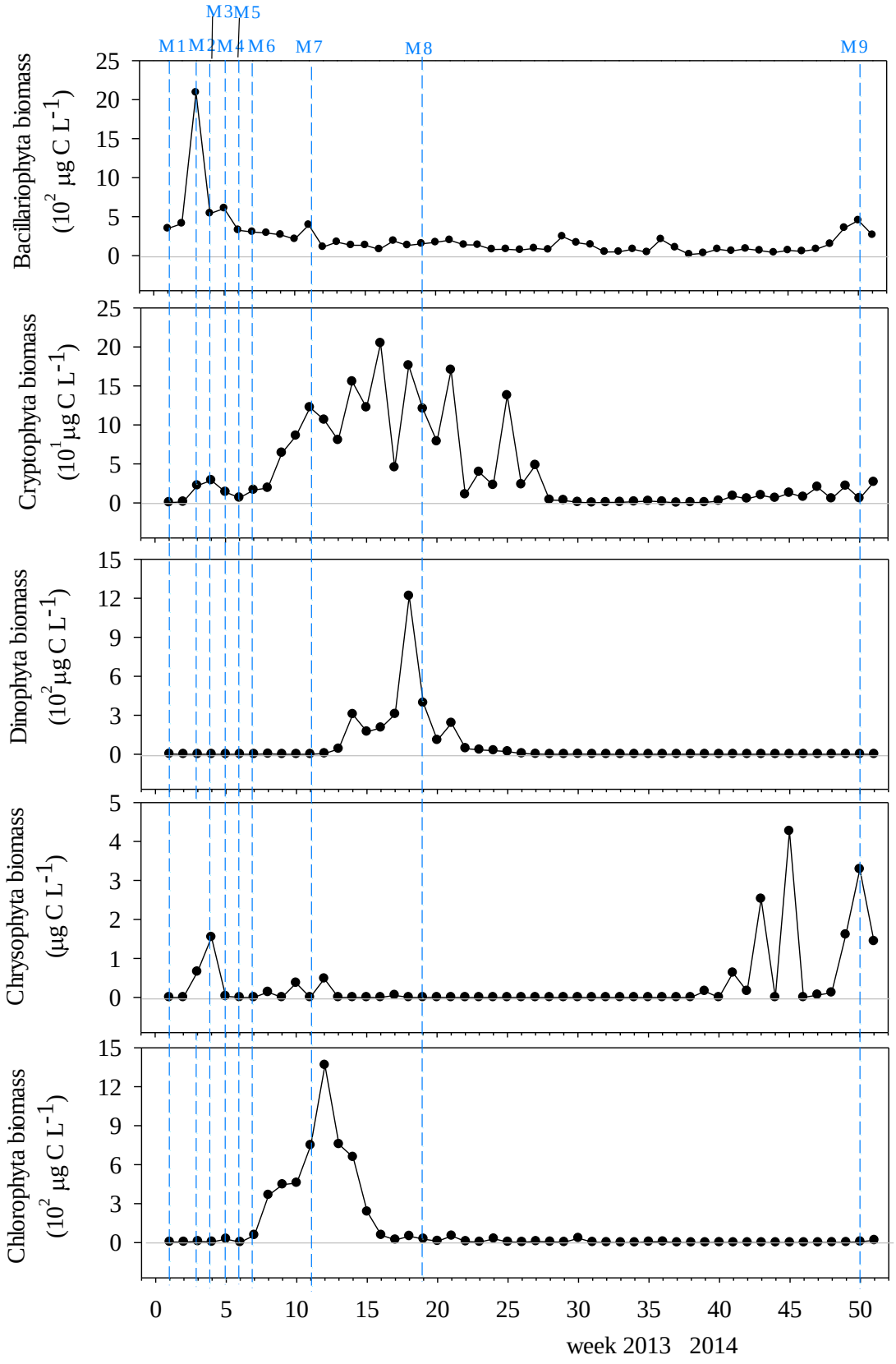


Figure 4-19: The succession of the phytoplankton group biomass, related to the chlorophyll events at Mudeford Quay. The numbers and dash lines shown above the chlorophyll *a* curve identify a series of chlorophyll events.

### 4.3.4 Measurements of $F_v/F_m$

The changes in $F_v/F_m$ ratio of water samples collected from the estuary entrance at Mudeford Quay are shown in Figure 4-20 B comparing with the annual concentration of chlorophyll *a* (Figure 4-20 A). The range of total $F_v/F_m$ efficiency was 0.14 – 0.68 which were higher values than all riverine samples (see Section **Error! Reference source not ound.**), but the maximal efficiency was less than the riverine sites. As the plot in Figure 4-20 A shows, the $F_v/F_m$ efficiency of cells in the 2.0 – 20.0 µm (nano-phytoplankton) range was greatest and contributed most to the total $F_v/F_m$ ratio, as this size fraction also contributed greater to the total concentration of chlorophyll similar to that measured at the river sites. The mean $F_v/F_m$ efficiency of nano-phytoplankton size was 0.56 ± 0.09 (n = 12), while pico-phytoplankton community had the mean of $F_v/F_m$ values of 0.19 ± 0.08 (n = 13).

The higher values of $F_v/F_m$ efficiency occurred at the same time as the maximum surface chlorophyll concentration during both spring periods. Broadly, $F_v/F_m$ decreases sharply from the summer to winter and then increases again in the spring at this study site. The nano-phytoplankton was the main community at the estuarine entrance, which supports the size fractionated chlorophyll results. Although, the pico-phytoplankton population does not obviously increase in $F_v/F_m$ during the bloom, this cell size shows a slight increase in photosynthetic energy conversion efficiency during periods of high chlorophyll concentration at Mudeford Quay as were measured at the riverine stations.

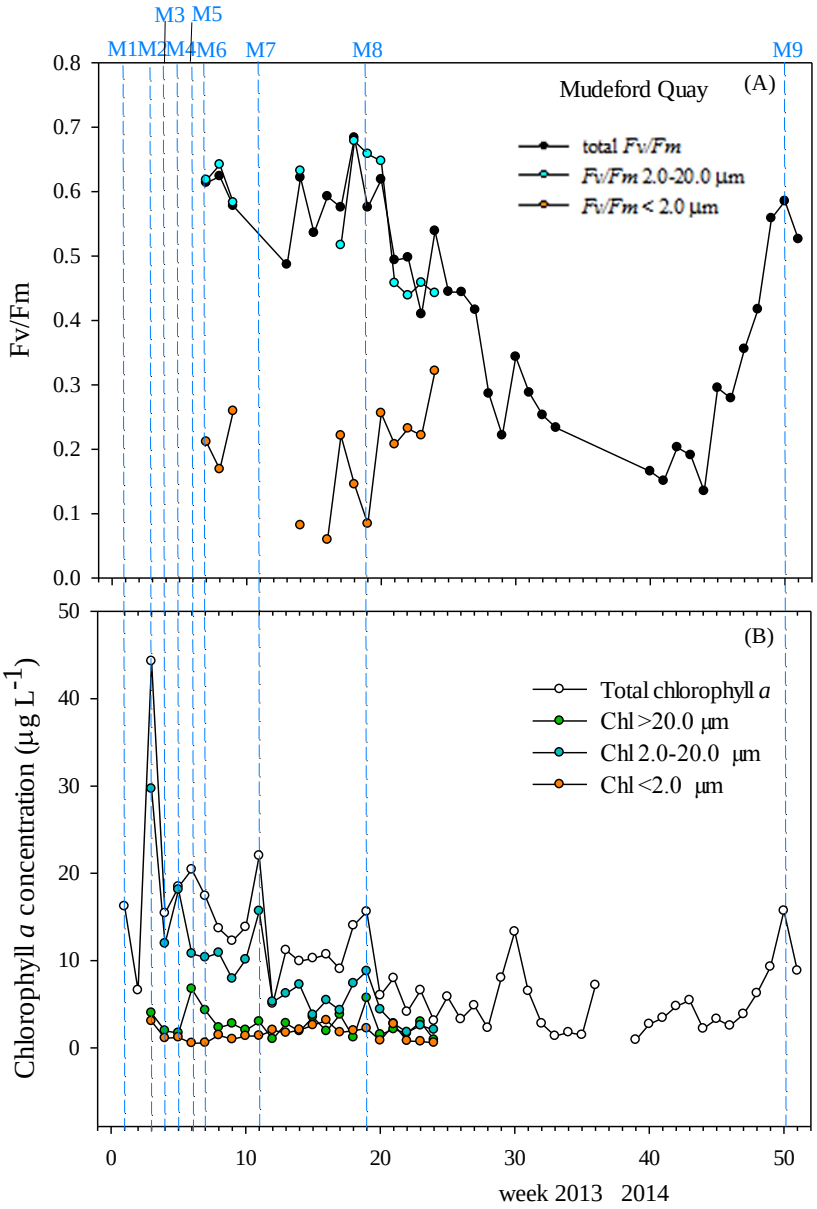


Figure 4-20: Photosynthetic energy conversion efficiency ($F_v/F_m$, unit-less) (A) chlorophyll *a* concentration in µg $L^{-1}$ (B). The numbers and dash lines shown above the photosynthetic efficiency curve and the chlorophyll *a* identify a series of chlorophyll events.

### 4.3.5 Phytoplankton abundance and total red fluorescence by flow cytometry

All estuarine samples were measured with the CytoSense flow cytometer throughout the sampling period. The analysis of total fluorescence by the flow cytometry was shown in Table 4-5 and Figure 4-21. The total red fluorescence of estuarine samples generally follows the seasonal phytoplankton abundance, associating the highest value of total red fluorescence was analysed in the spring months up to $7 \times 10^8$ a.u. $mL^{-1}$ followed by the summer, autumn, and winter months respectively. Total orange fluorescence showed

similar pattern to total red fluorescence and also the highest fluorescence was observed during the spring period (Table 4-5). In order to compare a microscopic cell count with the CytoSense counting, all analysis was plotted and the flow cytometry abundances were higher the microscopic abundance throughout the sampling period as seen from the results of riverine samples (see in Section 3.3.5). The correlation between microscopic and CytoSense flow cytometry abundance at Mudeford Quay is shown in Figure 4-22.

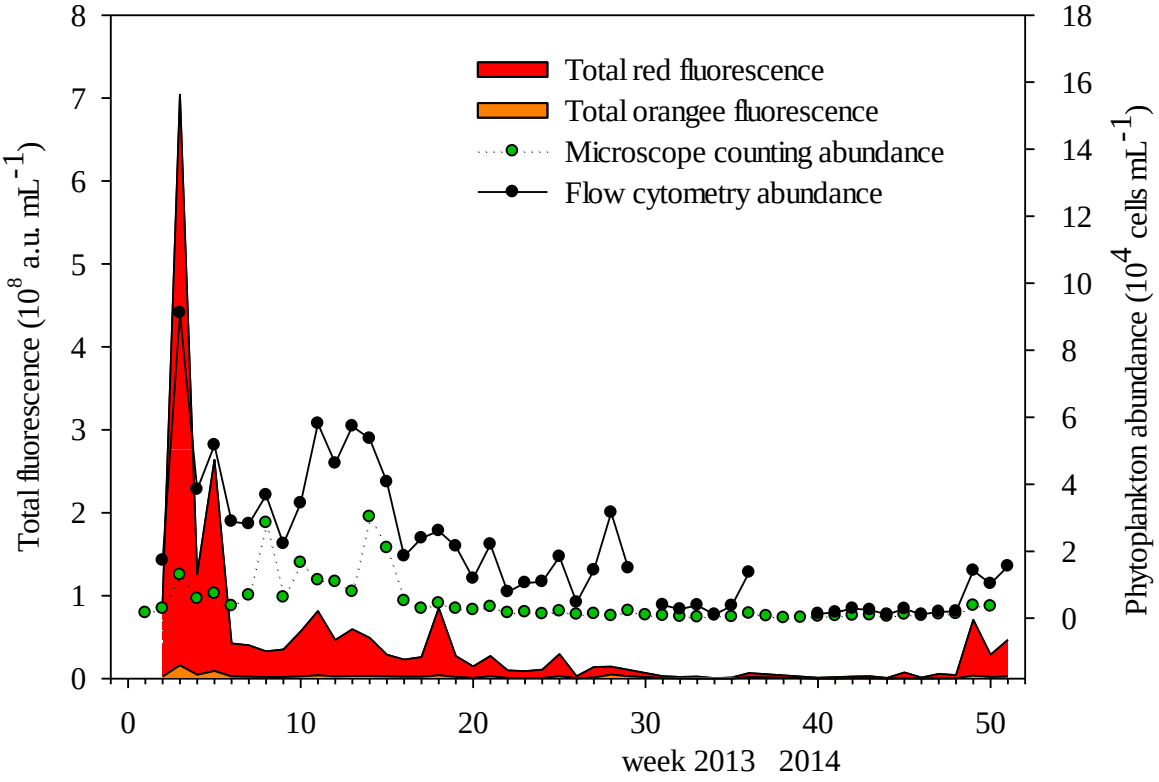


Figure 4-21: Seasonal distribution of red and orange fluorescence (a.u. $mL^{-1}$) and phytoplankton abundance (cells $mL^{-1}$) at Mudeford Quay. The solid line and black circles symbol are flow cytometry abundance. The dotted line and green circles are microscopic abundance.

Table 4-5: Mean red and orange fluorescence (a.u. $mL^{-1}$), with standard deviation, for each season; mean (bold) and range of variation (parentheses).

| | mean values ($10^6$) ± standard deviation ($10^6$) | | | |
|---|---|---|---|---|
| | spring | summer | autumn | winter |
| total red fluorescence | **46.73 ± 108.90** | **43.49 ± 22.09** | **11.23 ± 9.14** | **2.77 ± 2.54** |
| | (1.17 – 704.19) | (14.68 – 84.94) | (1.93 – 29.37) | (0.59 – 7.34) |
| total orange | **2.16 ± 2.69** | **2.53 ± 0.88** | **1.52 ± 1.46** | **0.37 ± 0.52** |
| fluorescence | (0.16 – 15.81) | (0.75 – 3.98) | (0.22 – 4.93) | (0.07 – 1.73) |

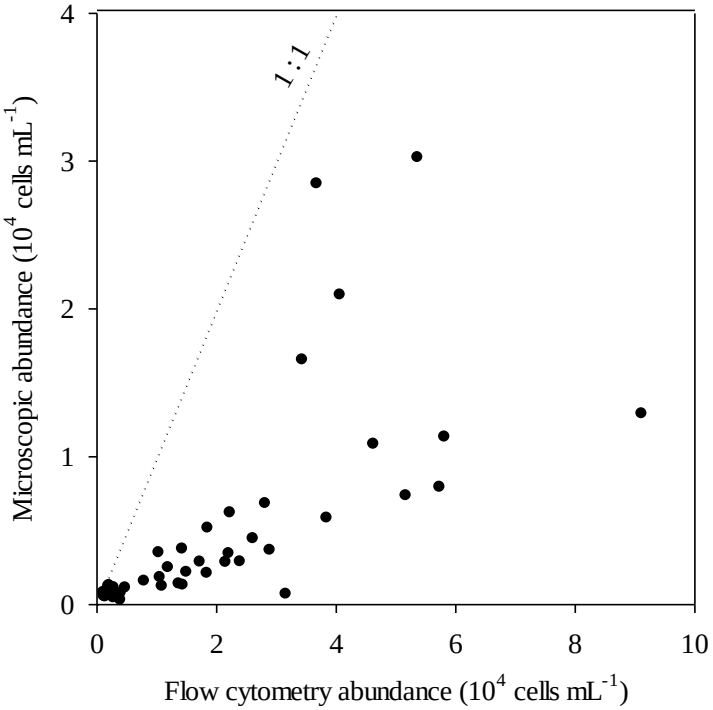


Figure 4-22: Correlation between flow cytometry abundance and microscopic cell count at Mudeford Quay.

### 4.3.6 Multivariate data analysis and interpretation

The environmental (physical and chemical) data and biological (carbon biomass and accessory pigments) data collected at Mudeford Quay during April 2013 to April 2014 were analysed by multivariate analysis as was examined the three riverine stations. The analyses were carried out in several steps; first, grouping of environmental parameters by similarity or dissimilarity using Euclidean distance; second, grouping of phytoplankton species using the Bray-Curtis Similarity Index using the PRIMER-E software; and third, correlation of environmental variables to phytoplankton groups was performed using the CANOCO software.

Two types of analysis have been carried out first a dendrogram analysis for hierarchical clustering of samples and non-matric multidimensional scaling (nMDS) to indicate group similarity and distance between sample groups in two-dimensional space. The stress level for each nMDS ordinal plot is used as an indicator of how the plot organises the distribution. Stress levels of < 0.1 indicated good ordination, 0.1 – 0.2 are useful 2-dimensional display of clusters, and > 0.2 a random placement in two dimensions (see Clarke *et al.* (2014) for further details). SIMPER analysis was used to calculate the

percentage similarity of each sample group and the dissimilarity between each pair of groups using the PRIMER-E version 7.0 software (Clarke *et al.*, 2014).

#### 4.3.6.1 Environmental data analyses

Cluster and nMDS analysis of environmental data are based on a normalised Euclidean distance with previous log transformation of the data. The cluster and nMDS included the variables nitrate, phosphate, silicate, SPM, river flow rate, water temperature, oxygen saturation, salinity, and turbidity (Figure 4-23 and Figure 4-24). The stress of nMDS was 0.15. corresponding to a good ordination with no real propect of a misleading interpretation (Clarke *et al.*, 2014). The cluster dentrogram shows separation at a normalised Euclidean distance of 3.1 into six major groups (Group A – F, Figure 4-23).

These results indicate high percentage contribution of environmental parameters in week 30, 31, and 36 from other sampling weeks (group C, Figure 4-23 and Figure 4-24) indicating SPM, river flow rate, and salinity data by the SIMPER analysis as shown in Table 4-6. Group A included late winter 2013 and early spring 2014 (week 41 – 47) considering a high percentage contribution of silicate concentration and water temperature. Group B corresponded to early winter 2013 and spring 2014 samples and also included two high peak chlorophyll samples in week 1 and 51 (Table 4-6). Group D refers to "autumn" samples at Mudeford Quay (week 20 – 35), considering by high contribution of nitrate concentration and water temperature. Whereas group E is composed of samples from summer months and also included a high peak chlorophyll sample in week 19. Group F of both cluster and nMDS included late spring and early summer 2013 samples and also included a large number of peak chlorophyll events in this group (week 3, 4, 5, 6, and 11). All inorganic nutrients (nitrate, phosphate, and silicate concentrations) showed an important parameter of high percentage contributions in group F as shown in Table 4-6.

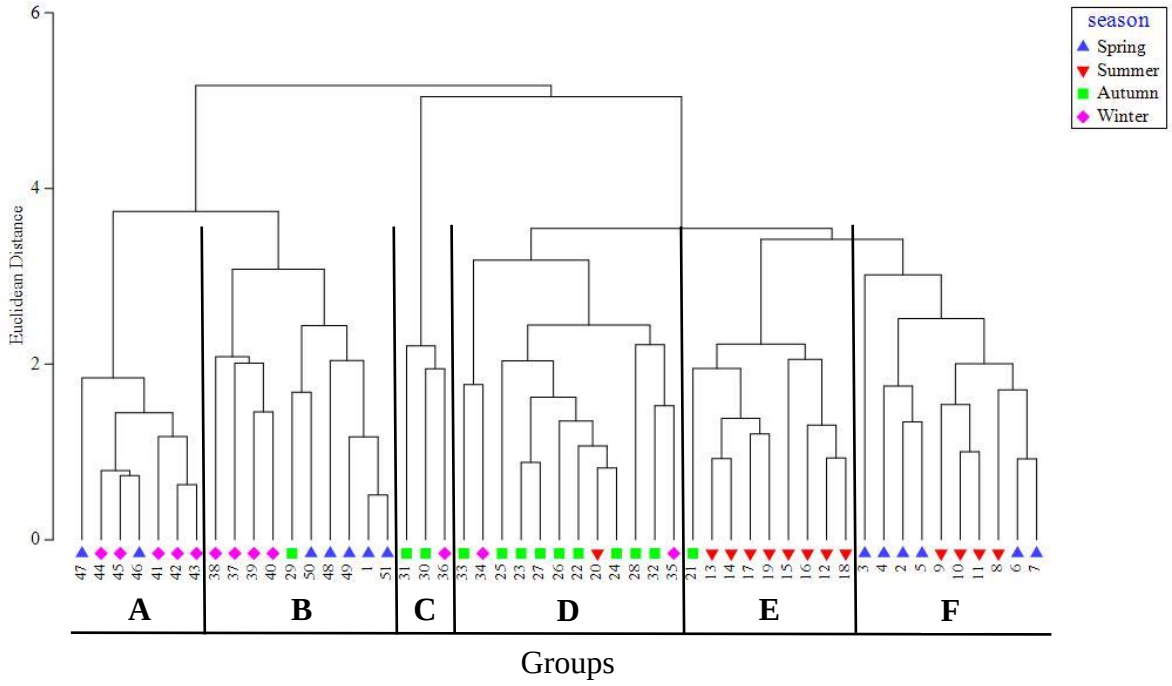


Figure 4-23: Dendrogram for hierarchical clustering of Mudeford Quay samples defined by environmental parameters. Numbers indicate the sample weeks.

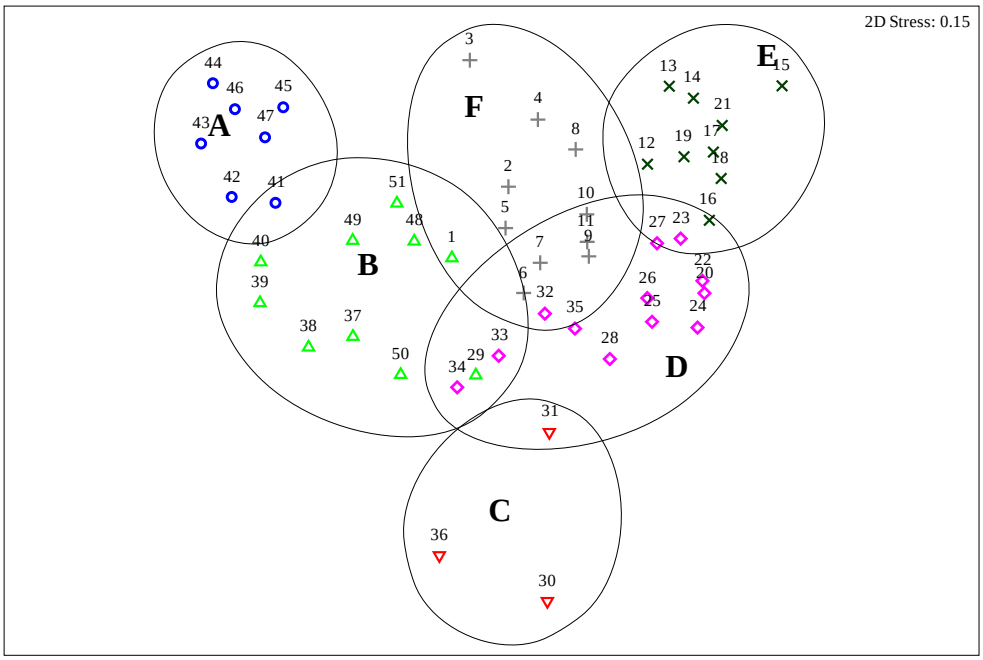


Figure 4-24: nMDS plot of environmental parameter groups at Mudeford Quay. Numbers indicate the sample weeks and solid line is 3.1 of the Euclidean distance.

Table 4-6: Main characteristics of sample groups defined by environmental parameters at Mudeford Quay. The peak chlorophyll samples in Table 4-3 are indicated by sample weeks in bold.

| Group | Sample week no. | Parameter % contribution | Average square distance |
|---|---|---|---|
| A | 41, 42, 43, 44, 45, 46, 47 | silicate (26), water temperature (21), turbidity (18), oxygen saturation (13), nitrate (10) | 1.0 |
| B | **1**, 29, 37, 38, 39, 40, 48, 49, **50**, 51 | oxygen saturation (20), SPM (11), water temperature (11), river flow (11), turbidity (10) | 3.4 |
| C | 30, 31, 36 | SPM (44), salinity (19), river flow (13) | 2.1 |
| D | 20, 22, 23, 24, 25, 26, 27, 28, 32, 33, 34, 35 | nitrate (27), water temperature (26), silicate (12), oxygen saturation (8) | 3.0 |
| E | 12, 13, 14, 15, 16, 17, 18, **19**, 21 | oxygen saturation (30), nitrate (23), turbidity (21), phosphate (10) | 2.1 |
| F | 2, **3**, **4**, **5**, **6**, **7**, 8, 9, 10, **11** | silicate (22), phosphate (18), oxygen saturation (16), nitrate (13), SPM (12), salinity (10) | 3.1 |

#### 4.3.6.2 Phytoplankton taxa and biomass data analyses

A shade plot indictes the most important species contributing to carbon biomass at Mudeford Quay in the Christchurch Harbour estuary is shown in Figure 4-25. In general, the diatom species show a clear pattern of larger groups followed by the cryptophyte and chlorophyte groups throughout the sampling period. The high abundance of diatom species, *Stephanodiscus* sp., gave the most weight in the late spring 2013 (week 3, 4, and 5), and the pennate diatoms showed the weight in week 1 – 3 with the chlorophyte species; *Chlamydomonas* sp. contributed most to biomass after the diatom bloom (week 8 – 15). During week 12 to 27, the dinoflagellate, *Kryptoperidinium foliaceum*, had the most weight comparing with other weeks during the sampling period. The crytophyte species, *Cryptomonas* sp. and *Rhodomonas* sp. distinguished highly between late spring and mid-autumn, whereas *Scenedesmus* spp. presented a high abundance during the summer months

more than the other seasons. Low phytoplankton biomass was observed during the winter months particularly the chlorophytes group (Figure 4-25).

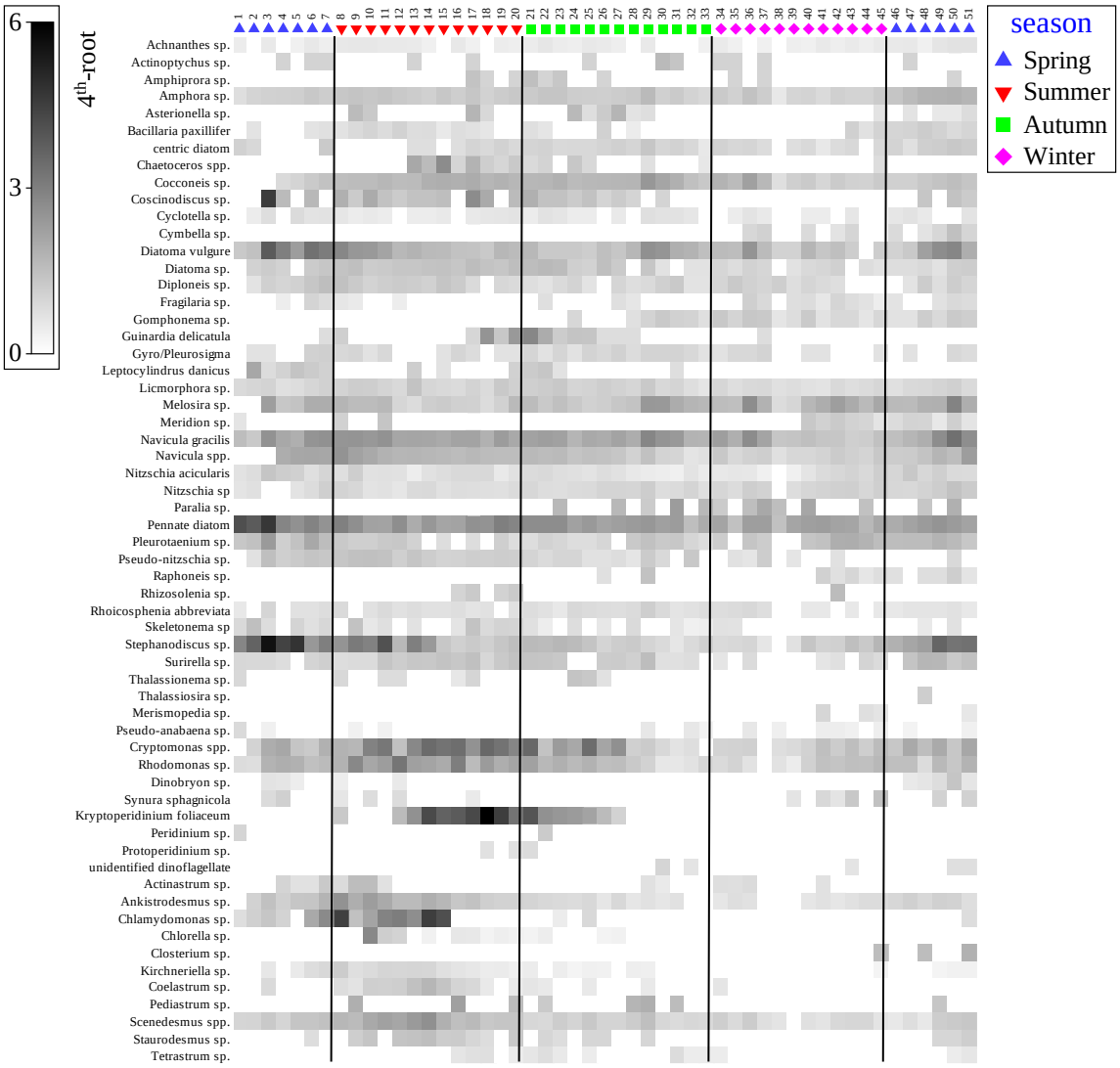


Figure 4-25: Shade plot indicating carbon biomass of each phytoplankton species ($4^{th}$-root transformed data on a log scale) for Mudeford Quay samples. Numbers indicate the sample weeks.

Cluster and nMDS analysis of phytoplankton biomass taxa are based on Bray-Curtis similarities as shown in Figure 4-26 and Figure 4-27. The stress of nMDS was 0.13, which indicated a potential useful 2-dimensional picture, though too much reliance should not be placed on the detail of the plot, and cross-check of any conclusions should be made against those from an alternative method, like the superimposition of cluster groups (Clarke *et al.*, 2014). Seven groups can be identified at 60 – 62% Bray-Curtis similarity level on cluster as shown in Figure 4-26. Two groups are composed of two samples, group A (week 38 and 39) and group B (week 1 and 2) and correspond to samples when pennate diatoms was

dominant, a percentage contribution of species average carbon biomass was 14 and 21% by SIMPER analysis (Table 4-7). Group C represents samples from weeks during the late autumn to early winter 2013. Similar to the species contribution of group A and B, pennate diatoms were a main contribution of carbon biomass. Group D refers to the late winter 2013 and spring 2014 samples. Group E is composed of three peaks of chlorophyll events (week 3, 4, and 5) in spring 2013. *Stephanodiscus* sp. is the dominant species in group E followed by pennate diatom and *Diatoma vulgare*.

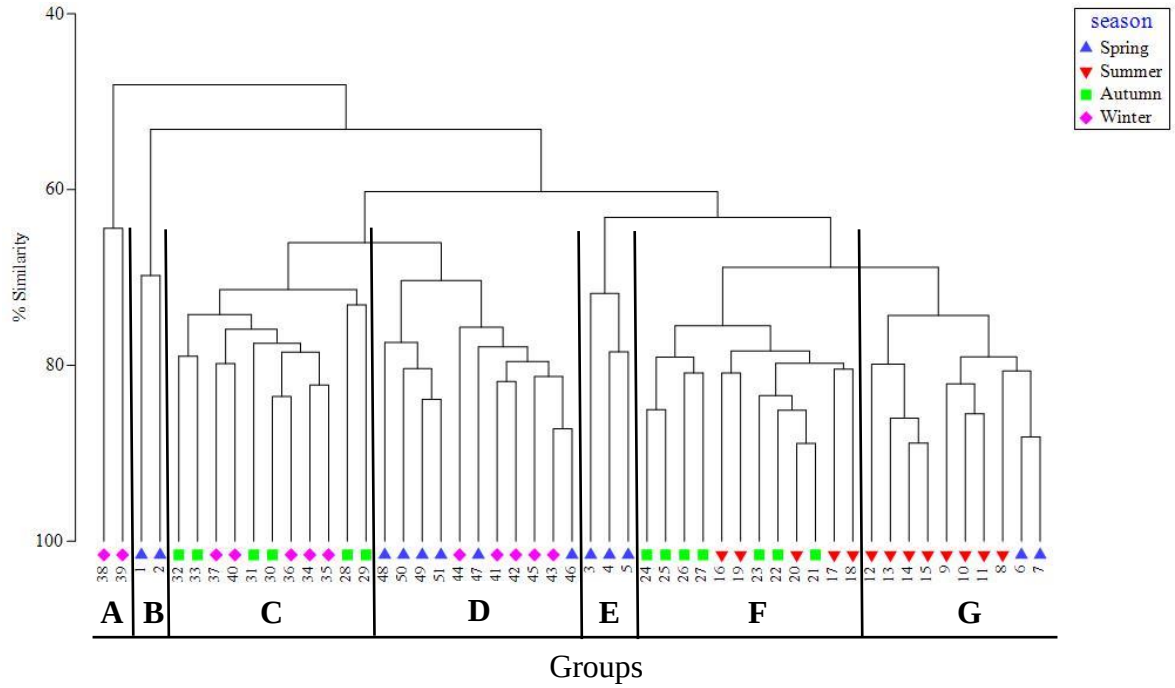


Figure 4-26: Dendrogram for hierarchical clustering of samples defined by phytoplankton carbon biomass at Mudeford Quay. Numbers indicate the sample weeks.

Group F includes samples from the late summer and early autumn 2013 and *Cryptomonas* spp., pennate diatom, and *Kryptoperidinium foliaceum* are the important biomass taxa to contribute this group. Group G is formed by summer samples and two samples of spring 2013, considering *Chlamydomonas* sp. and several diatom species were the most biomass taxa of the grouping.

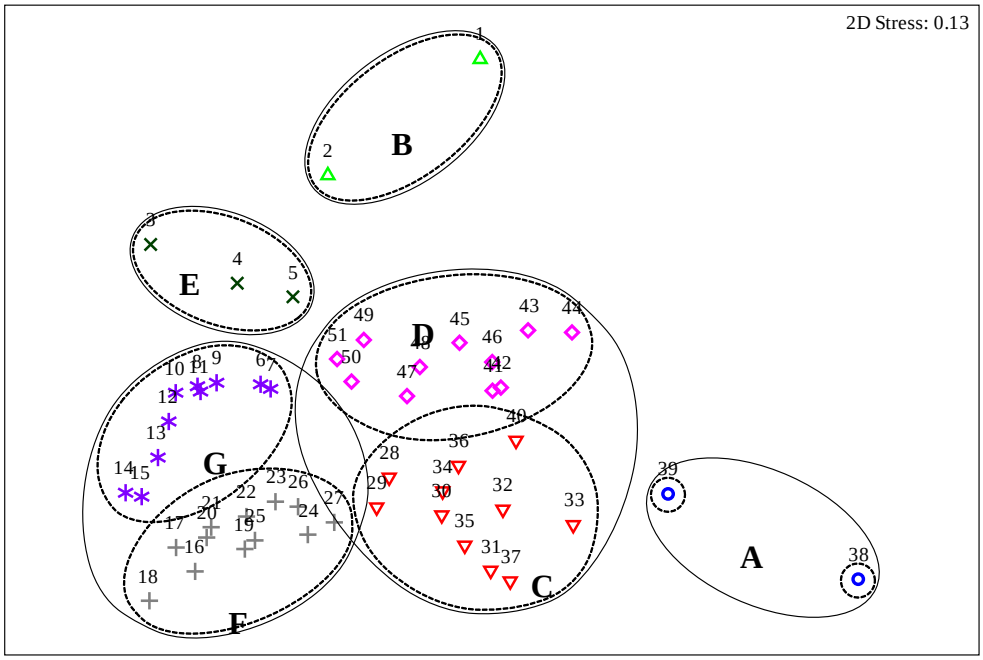


Figure 4-27: nMDS plot of samples defined by phytoplankton species/taxon carbon biomass at Mudeford Quay. Numbers indicate the sample week. Dash line is 62% of the similarity and solid line indicates 60%.

Table 4-7: All characteristics of sample groups by phytoplankton species. The peak chlorophyll events in table are identified by sample weeks in bold.

| Group | Sample week no. | Species average carbon biomass as % contribution | % of similarity |
|---|---|---|---|
| A | 38, 39 | Pennate diatom (14), *Navicula gracilis* (13), *Diatoma vulgare* (11), *Melosira* sp. (8), *Diploneis* sp. (8), *Cryptomonas* spp. (8), *Cocconeis* sp. (7), *Licmorphora* sp. (7), *Navicula* spp. (7) | 64.4 |
| B | **1**, 2 | Pennate diatom (21), *Stephanodiscus* sp. (15), *Pleurotaenium* sp.(7), *Diatoma vulgare* (7), *Navicula gracilis* (7) | 69.8 |
| C | 28, 29, 30, 31, 32, 33, 34, 35, 36, 37, 40 | Pennate diatom (8), *Navicula gracilis* (8), *Diatoma vulgare* (7), *Melosira* sp. (7), *Cocconeis* sp. (6), *Amphora* sp. (5) | 74.6 |
| D | 41, 42, 43, 44, 45, 46, 47, 48, 49, **50**, 51 | Pennate diatom (7), *Melosira* sp. (7), *Pleurotaenium* sp. (6), *Stephanodiscus* sp. (6), *Navicula gracilis* (5), *Cryptomonas* spp. (5), *Rhodomonas* sp.(5) | 74.5 |
| E | **3**, **4** , **5** | *Stephanodiscus* sp. (15), Pennate diatom (9), *Diatoma vulgare* (8), *Navicula gracilis* (6) | 74.0 |
| F | 16, 17, 18, **19**, 20, 21, 22, 23, 24, 25, 26, 27 | *Cryptomonas* spp.(7), Pennate diatom (7), *Kryptoperidinium foliaceum* (7), *Navicula gracilis* (6), *Cocconeis* sp.(5), *Rhodomonas* sp. (5) | 80.0 |
| G | **6**, **7**, 8, 9, 10, **11**, 12, 13, 14, 15 | *Chlamydomonas* sp. (6), Pennate diatom (6), *Navicula gracilis* (6), *Stephanodiscus* sp. (6), *Diatoma vulgare* (5), *Cryptomonas* spp.(5), *Rhodomonas* sp. (5) | 77.7 |

### 4.3.6.3 Relation of environmental and biological parameters

A RDA analysis (Figure 4-28) shows the occurrence of main phytoplankton carbon biomass in relation to the selected environmental variables (nitrate, phosphate, silicate, SPM, river flow rate, water temperature, oxygen saturation, salinity, and turbidity). The first axis (x-axis) of the analysis explained most of the variance (eigenvalue = 12.9%, cumulative percentage variance between taxa and environmental parameters = 37.8%), whereas all canonical axes explained 92.4% of the variance (axis 1, $P < 0.001$; all axes, $P < 0.001$). This means that the arrows displayed closer to x-axis explained most of the variability in the data and environmental variables explained almost 100% of the variation of the selected taxa biomass when all four axes were analysed together.

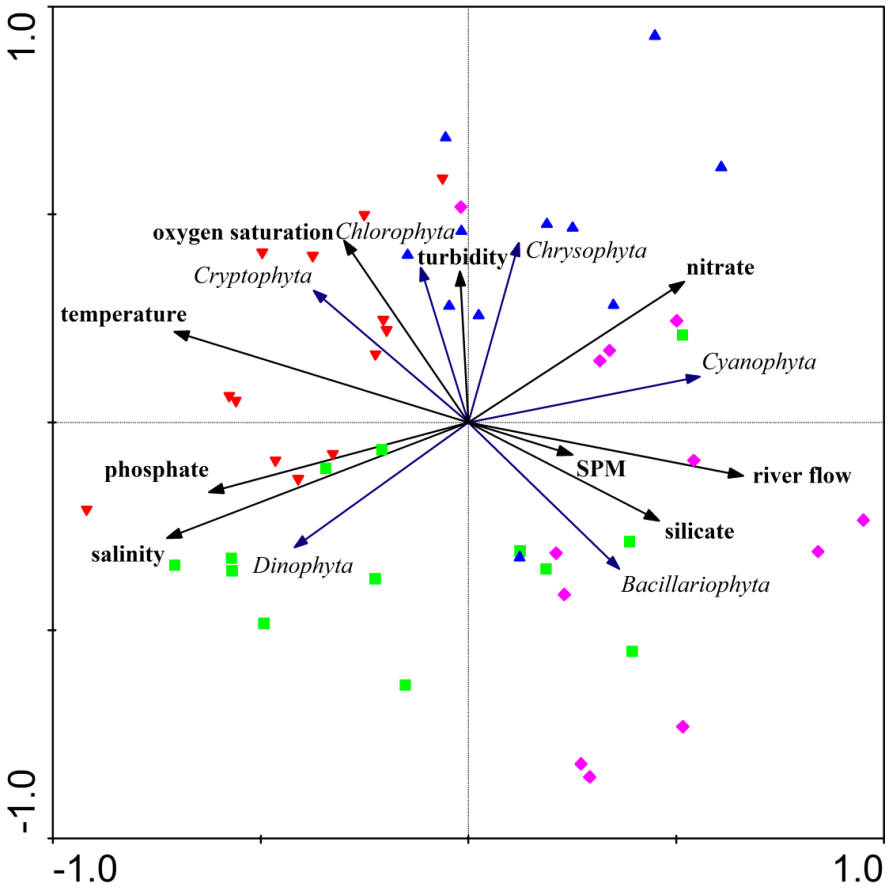


Figure 4-28: Result of RDA analysis, relationships between carbon biomass of main phytoplankton group and selected environmental variables at Mudeford Quay in the Christchurch Harbour estuary during spring 2013 to spring 2014. Triplot represents taxa carbon biomass (blue thin lines), the significant explanatory variables (black thick lines) and weekly sampling (closed colour symbols; blue = spring, red = summer, green = autumn, pink = winter).

Forward seletion showed that of all nine environmental parameters (Table 4-8) included in the RDA analysis, only three environmental factors (salinity, oxygen saturation, and river flow rate) explained the variance in the phytoplankton taxa biomass when analysed together. All the forward-selected variables were analysed together (conditional effects, referred to $\lambda_a$ in Table 4-8), salinity was the most significant explanatory variable ($\lambda_a$ = 0.09, $P$ = 0.001), followed by oxygen saturation ($\lambda_a$ = 0.05, $P$ = 0.024) and river flow ($\lambda_a$ = 0.05, $P$ = 0.015) as shown in Table 5-8. Although not significantly ($P < 0.05$) different ($\lambda_a$ = 0.04, $P$ = 0.065), silicate concentrations also had a minor influence as an explanatory variable (Table 4-8). Nutrient concentrations (nitrate and phosphate), turbidity, SPM, and water temperature were not significant explanatory variables in this analysis.

Table 4-8: Eigen factor ($\lambda$) of each explanatory variable in order of the variance explained when analysed as single factor ($\lambda_1$, marginal effects) or when included in the model where other forward selected variables are analysed together ($\lambda_a$, conditional effects). Significant $P$-values (*$P < 0.1$) and (** $P < 0.05$) represent the variables that together explain the variation in the analysis at Mudeford Quay.

| **Marginal Effects** | | **Conditional Effects** | | | | |
|---|---|---|---|---|---|---|
| Variable | $\lambda_1$ | Variable | $\lambda_a$ | $P$ | $F$ | |
| salinity | 0.09 | salinity | 0.09 | 0.001** | 4.53 | |
| temperature | 0.08 | %oxygen | 0.05 | 0.024** | 2.65 | |
| phosphate | 0.07 | silicate | 0.04 | 0.065* | 2.13 | |
| nitrate | 0.06 | river flow | 0.05 | 0.015** | 2.78 | |
| river flow | 0.06 | phosphate | 0.03 | 0.180 | 1.45 | |
| silicate | 0.05 | turbidity | 0.02 | 0.358 | 1.12 | |
| %oxygen | 0.04 | SPM | 0.02 | 0.244 | 1.30 | |
| turbidity | 0.03 | temperature | 0.01 | 0.598 | 0.79 | |
| SPM | 0.02 | nitrate | 0.01 | 0.763 | 0.52 | |
| | | | | | | |
| Axes | | 1 | 2 | 3 | 4 | Total variance |
| Eigenvalues : | | 0.129 | 0.088 | 0.068 | 0.029 | 1 |
| biocarbon-environment correlations : | | 0.745 | 0.625 | 0.588 | 0.449 | |
| Cumulative percentage variance | | | | | | |
| of biocarbon data : | | 12.9% | 21.7% | 28.6% | 31.5% | |
| of biocarbon-environment relation: | | 37.8% | 63.7% | 83.8% | 92.4% | |
| Sum of all eigenvalues | | | | | | 1 |
| Sum of all canonical eigenvalues | | | | | | 0.341 |

The nMDS plot of phytoplankton group biomass was not clearly correlated with the environmental factors to show how different parameters influence biomass pattern (Figure 4-27). The patterns of seasonality with the river flow rate and salinity are clearly shown as bubble plots (Figure 4-29). High phytoplankton carbon biomass was found in the spring

because of the diatom community, followed by the samples in the summer months (Figure 4-29 A).

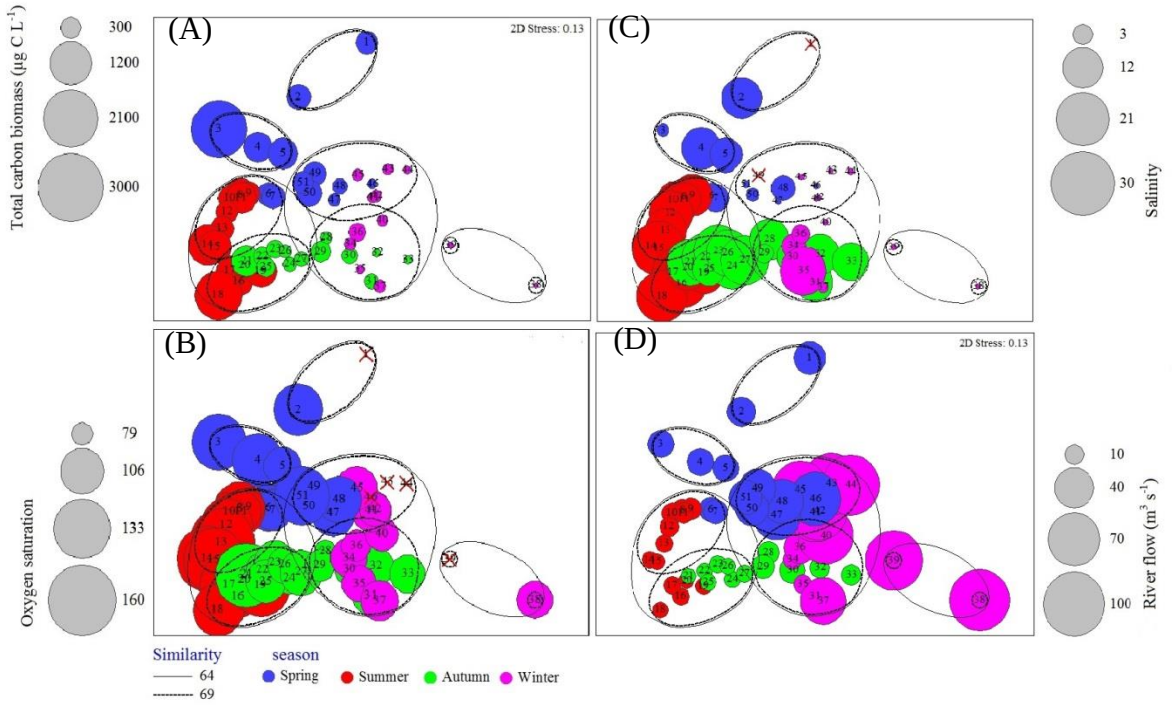


Figure 4-29: nMDS plot representing the mean biomass values in terms of carbon biomass (A), oxygen saturation (B), salinity (C) and river flow (D) at Mudeford Quay. The bubble sizes represent the value of the environmental parameter

## 4.4 Discussion

In this chapter, the seasonal pattern of biological parameters (phytoplankton species abundance, pigments, and estimated species biomass), environmental parameters (salinity, water temperature, suspended particulate matter, oxygen saturation, and river flow), and chemical parameters (nitrate, phosphate, and silicate concentrations) at the estuary entrance Mudeford Quay during mid-April 2013 to mid-April 2014 are described. Multivariate analysis was used to establish relationships between biological and environmental factors. The objective of this study was to investigate the factors influencing the phytoplankton populations at the entrance to Christchurch Harbour at the low tide over an annual period.

*Phytoplankton biomass response to nutrients*

Nutrients in estuaries are generally supplied by river discharge which supports phytoplankton growth (Saeck *et al.*, 2013; Sin *et al.*, 2013). In the present study, the nitrate and silicate concentrations were much higher in the low salinity water than at higher

salinities (Figure 4-4). This suggests that riverine nutrients are important sources of nutrients for phytoplankton in the estuary, and at some periods of the year dominated in Christchurch Harbour particularly during low tide.

In the present study, there were no consistent patterns of phytoplankton biomass (chlorophyll *a*) associated with the nutrient concentrations at Mudeford Quay. However, silicate concentrations had a minor influence on phytoplankton carbon biomass and particularly the diatom biomass when all selected environmental factors were analysed together by the RDA analysis (Figure 4-28). When chlorophyll *a* and fucoxanthin concentrations peaked (44.0 and 9.9 µg $L^{-1}$ respectively) on 3rd May 2013, *Stephanodiscus* sp. cell counts were at a maximum of $9.9 \times 10^3$ cells $mL^{-1}$ and the silicate concentration was low. Paerl and Justić (2011) stated that diatoms being strongly depend on silicon for growth can be limited by its availability in estuaries.

In general, riverine nutrients are important sources for new production of phytoplankton in estuaries (Lancelot and Muylaert, 2011). In estuarine systems, nitrogen and phosphorus can stimulate phytoplankton growth because growth of freshwater phytoplankton is general limitied by phosphorus, while nitrogen often limits the growth of marine phytoplankton (Hecky and Kilham, 1988; Howarth and Marino, 2006). The relative abundance of nitrogen to phosphorus (N:P ratio) has been shown to affect phytoplankton biomass. In the present study N:P ratios reached over 200 in the low salinity water during late winter and varied from 23 to 36 in summer slightly above the Redfield ratio of 16:1. Paerl and Justić (2011) indicated that the Redfield ratio of N:P can be greatly exceeded when freshwater runoff tend to be N enriched and lead to strong P limitation. During spring and summer blooms, the ratio of N:P reached 128:1 (chlorophyll concentration of 44.0 µg $L^{-1}$, 10th June 2013) and down to 56:1 when the concentration decreased < 20.0 µg $L^{-1}$ (31st June 2013). In Tolo Harbour in Hong Kong Anderson *et al.* (2002) reported that the dinoflagellate cell numbers increased as the annually averaged N:P ratio fell from 20:1 to 11:1 between 1982 and 1989.

*Phytoplankton biomass response to hydrodynamics*

In the present study the salinity was strongly correlated with phytoplankton carbon biomass and in particularly with the dinoflagellate biomass and showed negatively a strong relationship with nitrate concentration (Figure 4-28). The dinoflagellates were present during the summer months under low river discharge conditions and at high salinity values. Paerl and Justić (2011) demonstrated that some non-toxic dinoflagellate blooms in

temperate estuaries are linked to seasonal pattern of freshwater, salinity, and light availability. While the diatom biomass showed positive a correlation with silicate, SPM, and both river flow rates and had a negative strong relation with water temperature, indicating the diatoms at the harbour entrance at low tide were mainly freshwater diatom species e.g. the centric diatom *Stephanodiscus* sp. was dominant during the late spring and the early summer 2013. This species was also in high abundance in the Stour River and it could be considered that the river discharges this diatom into the estuary during low tide. Moreover, this centric diatom species is a freshwater planktonic diatom (Bellinger and Sigee, 2010), and it is a common diatom species in eutrophic freshwater of Europe region (Belcher and Swale, 1979). In the present study the nano-phytoplankton were observed as a main component size during the summer months, in agreement with Sin *et al.* (2015) in the Youngsan River estuary where it was reported that the nano-phytoplankton blooms developed in freshwater dominated by *Stephanodiscus* sp.

Freshwater discharged from the Stour and Hampshire Avon Rivers was suggested to be the main source of nutrients in the estuary based on the high nutrient concentrations and salinity collected throughout the sampling period. The river discharge was a hydrodynamic factor controlling the phytoplankton carbon bimass from the RDA analysis. The river discharge was positively correlated with diatom and cyanophyte biomass and also showed a negative correlation with water temperature, suggesting carbon biomass was high during high flow rates.

*Changes phytoplankton taxa and biomass*

Phytoplankton blooms generally developed during the late spring to summer which were composed of the nano-phytoplankton in particularly the centric diatom *Stephanodiscus* sp. (Figure 4-6). A small autumn bloom was observed only in week 30 (3$^{rd}$ November 2013) with a chlorophyll concentration of < 15 µg $L^{-1}$. Depletion of silicate concentration may have contributed to the termination of the diatom blooms in May 2013. Ha *et al.* (2003) and Sin *et al.* (2015) also reported that diatoms favour freshwater at low temperates and a high silicate concentration. Chlorophytes, chrysophytes, and cryptophytes were positively correlated with turbidity, confirming the dependence on light available to these phytoplankton groups.

At Mudeford Quay, late spring blooms developed in April and May and were composed of the diatom *Stephanodiscus* sp., and other diatoms which favour coldwater. The percentage contributions of diatom to total phytoplankton abundances changed from high (95%) in

April to low (12%) in June. This caused an increase in the phytoplankton community structure from diatoms in the spring to chlorophytes in the summer. The spring bloom of *Stephanodiscus* sp. was also reported for the Youngsan River estuary (Sin *et al.*, 2015), and opimal growth of *Stephanodiscus* sp. was in < 7 ºC in freshwater with low river discharge of < 100 $m^3 s^{-1}$ for the Nakdong River (Ha *et al.*, 2003). The dominance of diatoms continued until May (41%), although the total abundance of phytoplankton and chlorophyll *a* concentration decreased to as low as $6.3 \times 10^3$ cells $mL^{-1}$ and 5.0 µg $L^{-1}$, respectively on 4th June 2013. Nutrients, especially nitrate, were almost depleted in June (week 12, Figure 4-3), suggesting that phytoplankton growth was limited by nutrients. Dinoflgellates, primarily *Kryptoperidinium foliaceum* (10 – 27%), increased in August when salinity was high and low river discharge continued, their abundance peaked in mid-August. Increased salinity, temperature, and longer water residence times during the summer months may be important in initialling *K. foliaceum* developement. Salinity increased to as high as 20 due to a reduction of freshwater discharge down to 2 and 6 $m^3 s^{-1}$ during *K. foliaceum* growth period, suggesting that the species favours higher salinity water and additionally it is species known to favour high water temperatures (Figueroa *et al.*, 2009).

Although diatoms (carbon biomass) displayed a relationship with SPM and river flow similar to that of cyanophyte (Figure 4-28), the changes of diatoms to total abundances increased during the summer 2013 to the spring 2014 (Figure 4-16 B), whereas the contributions of cyanophytes were observed only occasionally during the autumn and winter. The increase in taxonomic composition in the summer months may have affected the optimal conditions of phytoplankton development. As a result of almost all accessory pigment concentration increases during the summer (Figure 4-12 and Figure 4-13), indicating that most phytoplankton groups competed and had a rapid growth during that time. The abundance of flagellate groups (chlorophyte, chrysophyte, and cryptophyte) were closely related to turbidity and oxygen saturation in the estuary, and inversely correlated with diatoms. Increased flushing in the estuary may also have affected the gradients of phytoplankton production by changing light availability through tidally driven resuspension of sediments in the microtidal estuary. Byun *et al.* (2007) reported the effect of tidally driven resuspension of sediments on light availability in the macrotidal estuary of Youngsan River Bay.

The volume of river discharged during the sampling was less than 20 $m^3 s^{-1}$ during April to November 2013 from both river gauging stations but with high volume in December 2013 to February 2014. Salinity also decreased close to zero with high discharge over 60 $m^3 s^{-1}$

at Mudefor Quay in January and February 2014 (Figure 4-1). Concentrations of chlorophyll *a*, accessory pigment, carbon biomass, and changes in the contributions of taxonomic groups, also differed between normal flow and flood conditions, suggesting that the response of phytoplankton and water characteristics to river discharges depend on the volumn of discharge into the Christchurch Harbour estuary. However, the total chlorophyll *a*, accessory pigment, carbon biomass, and the dominant diatom and dinoflagellate peaks during the spring-summer low flow period were similar to several other temperate estuaries. This suggests that the river discharge is an important factor influencing the phytoplankton community and primary production in microtidal and shallow estuaries like Christchurch Harbour.

## 4.5 Conclusion

In conclusion hydrological conditions strongly affected annual phytoplankton abundance and composition at the entrance in the shallow estuarine system. However, from this data set, a significant correlation between the chlorophyll *a* concentration and freshwater discharge from the combined Stour and Hampshire Avon Rivers was observed. This increase in chlorophyll *a* concentration during low flow periods was found to be associated with an increase in the abundance of the dinoflagellate population in the summer months. These temporal changes in the phytoplankton community were not explained by environmental factors at one station. An estuary transect sampling programme was then considered to determine the distribution of summer estuarine phytoplankton during low river discharge period. The increase in salinity moving into Chirstchurch Harbour was also considered an influence on phytoplankton distribution, confirming a shift to summer dinoflagellates in the Christchurch Harbour estuary.

# Chapter 5: Distribution and succession of estuarine phytoplankton during high productivity periods in Christchurch Harbour

## 5.1 Abstract

The factors controlling the spatial and temporal patterns of summer phytoplankton populations occurring in Christchurch Harbour, a shallow temperate UK south coast estuary, have been investigated. Water samples were collected from six sites corresponding to the upper, middle, and lower reaches of the estuary at fortnightly intervals at high tide between May and September 2014. Water samples were analysed for nitrate, phosphate, and silicate concentrations plus chlorophyll concentration and phytoplankton abundance. High chlorophyll 'bloom' events were detected in the middle of the estuary during these high tide surveys, increasing from early to late summer. Reduced river discharge in summer months led to an increase in higher salinity water in the mid estuary with associated peaks in phytoplankton abundance. Different populations of estuarine phytoplankton were observed over the course of the summer with dinoflagellate blooms dominated by *Kryptoperidinium foliaceum*, occurring in the mid estuary. Multivariate analysis revealed that irradiance attenuation coefficient (*k*), salinity, oxygen saturation, temperature, nitrate, and silicate were major factors controlling phytoplankton carbon biomass from the transect sampling. The results of the present study provide improved understanding into the distribution of estuarine phytoplankton communities in the shallow temperate, Christchurch Harbour estuary during the summer.

## 5.2 Introduction

In the two previous chapters an intensive programme of monitoring both water quality and phytoplankton communities at weekly intervals from April 2013 to April 2014 at three stations in the Stour and Hampshire Avon Rivers and during low tide at the estuary entrance at Mudeford Quay is presented. The influence of reduced river discharge rates, and increased water residence times in the estuary during summer 2014 was then investigated. In order to further investigate the factors controlling the pattern of summer phytoplankton populations occurring in Christchurch Harbour fortnightly surveys were conducted at high tide between May and September 2014. The aim of this study was to quantify the estuarine phytoplankton collected from six sites along the salinity gradient and investigate how they would respond to changes in river inputs. Changes in natural estuarine phytoplankton uptake rates of nitrogen (nitrate and ammonium) and bicarbonate using stable isotope incubation experiments were conducted throughout the sampling period. The same physical and chemical parameters were measured as previously at the three stations in the rivers and the estuary entrance. In this chapter, results from eight surveys of the six sampling sites in Christchurch Harbour are presented and discussed in terms of the factors influencing summer phytoplankton populations within the estuary.

## 5.3 Results

### 5.3.1 Environmental data

Eight fortnightly samplings transect were conducted at high tide during summer months of 2014 (May to September) throughout the Christchurch Harbour estuary. The six estuarine stations were similar to those sampled previously by the local Environmental Agency i.e. The Run at Mudeford (RM, 0 km), Ferry Pontoon (FP, 0.4 km), Blackberry Point (BP, 1.6 km), Grimbury Marsh (GM, 2.5 km), Christchurch Quay (CQ, 3.5 km), and Tuckton Bridge (TB, 4.0 km) see Figure 2-3. The objective of conducting these surveys was to investigate the effect of phytoplankton growth on the water quality and nutrient cycling throughout the estuary during spring and summer months.

The Christchurch Harbour estuary is characterized by shallow waters (depth = 1.3 – 3.0 m along the whole transect at the time of sampling). The estuarine study sites are defined as: lower – RM and FP; middle – BP and GM; upper – CQ and TB in this chapter. A map of

the estuary showing the location of the sampling stations is presented in Chapter 2 (see Section 2.1.2, Figure 2-3).

#### 5.3.1.1 River flow

Daily mean of river flow rates in 2014 from both lowest gauging stations on the Stour and Hampshire Avon Rivers which discharge freshwater into the estuary are presented in Figure 5-1. In general, both discharge rates followed a seasonal pattern, with the high flow period from winter months decreasing later in the year. The Avon River had mostly higher flow rates than the Stour River at Throop, except during mid-October to mid-December 2014 where the Stour had a high discharge (Figure 5-1 A). The lowest discharge (< 20 $m^3$ $s^{-1}$) was recorded during summer months and when the transect sampling was conducted in Christchurch Harbour (Figure 5-1 B).

#### 5.3.1.2 Salinity

During the summer months of 2014, salinity profiles were determined at each station at high tide and data is illustrated in Figure 5-2. Salinity increased with depth, displaying maximum values near the bottom and increased towards the lower-estuarine sites. The salinity ranged from 0.2 to 34.5, with the expected trend ranging from high coastal water salinity at the Run at Mudeford (RM) to brackish water at Tuckton Bridge (TB). The values increased at all stations in August 2014 particularly near the bottom and then decreased towards the estuarine entrance in September 2014. Ferry Pontoon (FP) showed a wide range in salinity, from 2.5 to 34.4 (Figure 5-3), while Tuckton Bridge (TB) had the narrowest range, from 0.2 to 21.3. Values at TB were generally similar to those at Christchurch Quay (CQ), whilst Ferry Pontoon (FP) values corresponded with the Run at Mudeford (RM). During this time Grimbury Marsh (GM) and Blackberry Point (BP) values were intermediate. The high salinity values during the summer months in 2014 observed at TB are related to lower freshwater input and the water being measured at high tide.

Salinity at the depth of Niskin water samples is shown as a pink circle in each plot (Figure 5-2). These salinity values were measured later using a refractometer in the NOCS laboratory. Sub-surface salinity reached a maximum in August 2014 at the lower-estuarine stations (RM and FP). However, relatively low salinity water (~0) was detected at the upper-estuarine station due to inputs from the river.

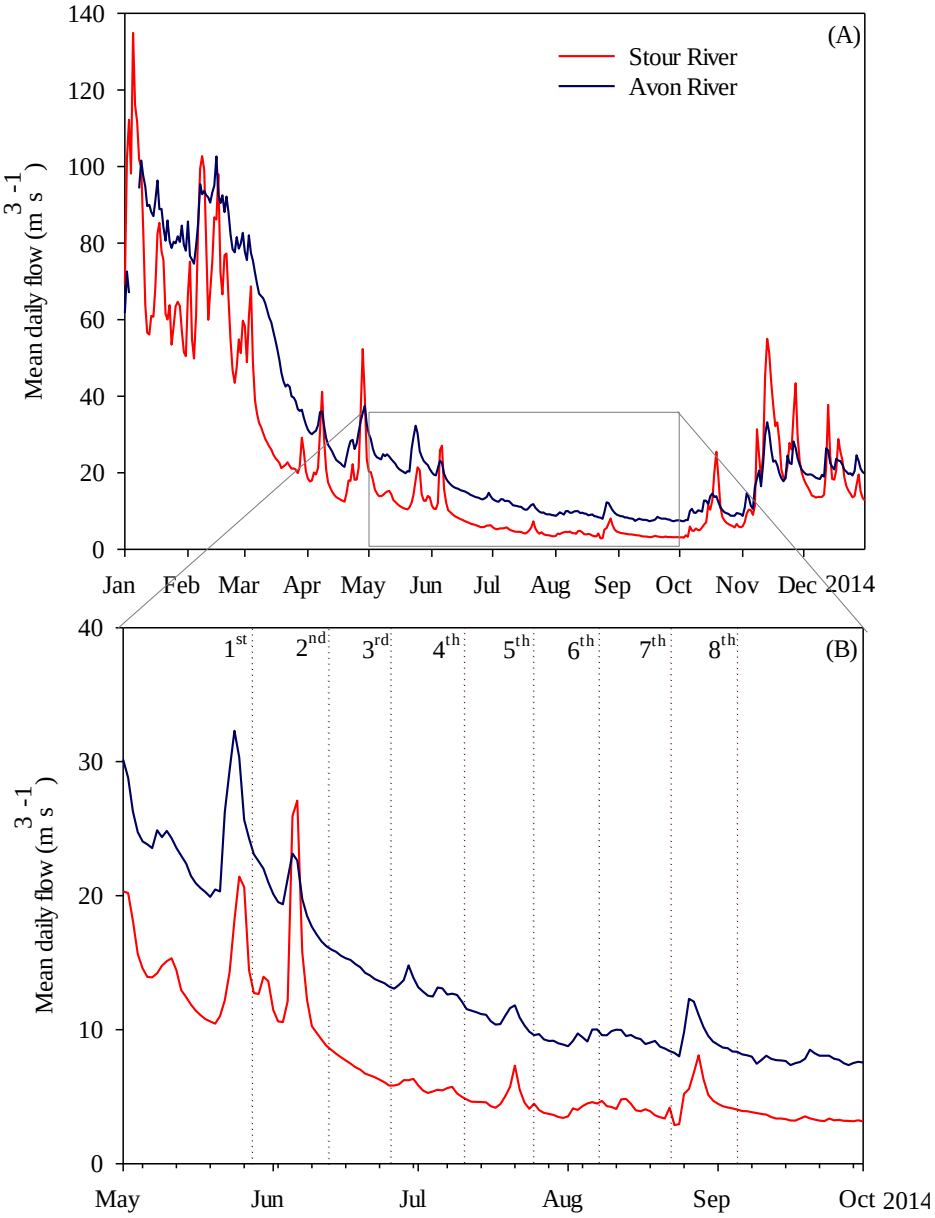


Figure 5-1: Mean daily flow ($m^3$ $s^{-1}$) of the Stour River (red solid line) and the Hampshire Avon River (blue solid line) in 2014 (Environmental Agency). B shows river flow during the sampling described here and dash lines represent each of the sampling date.

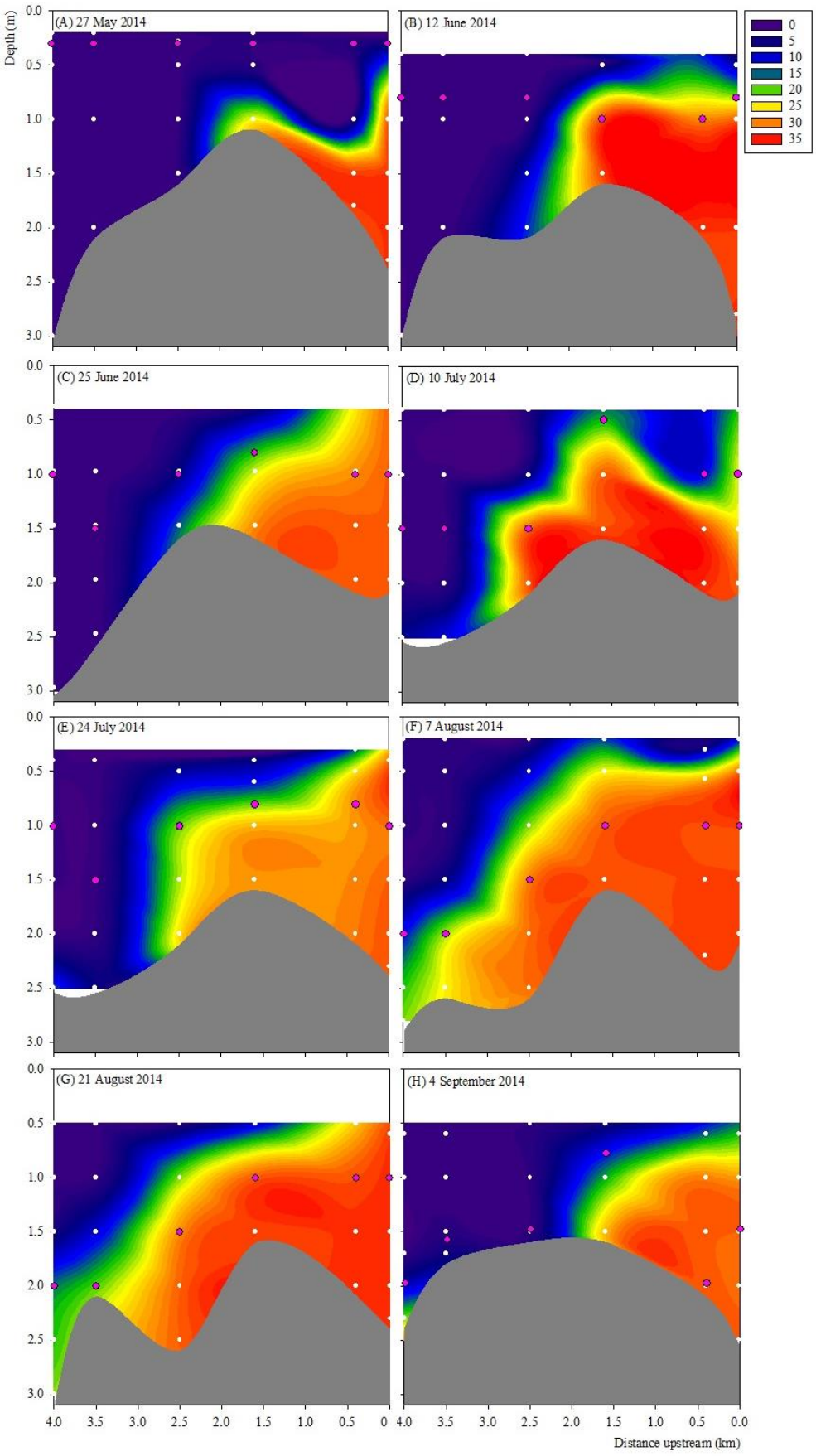


Figure 5-2: Vertical distribution of salinity at the six estuarine stations during the summer months of 2014 around high water. Pink circles show the water sampling depths and white circles where measurements using the YSI 6600 multiprobe.

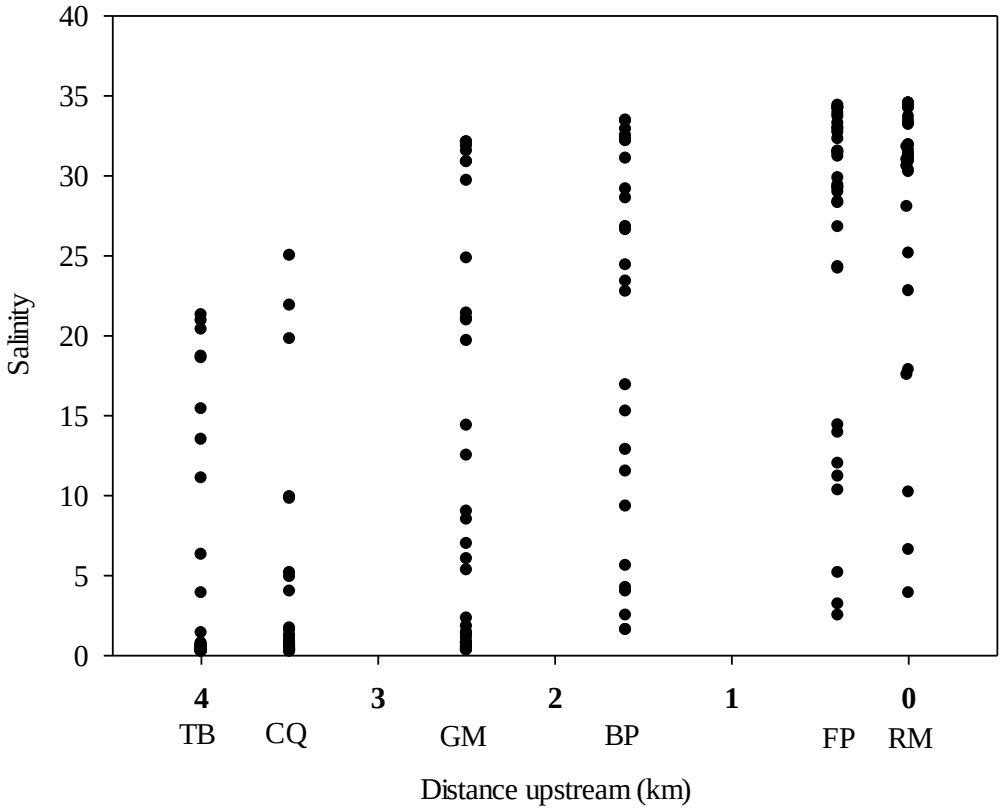


Figure 5-3: Salinity observations along the Christchurch Harbour estuary from May to September 2014 using the YSI 6600 multiprobe.

#### 5.3.1.3 Water temperature

Vertical water temperatures at the different locations in the Christchurch Harbour estuary are shown in Figure 5-4 and, follow the normal seasonal pattern. The maximum temperature recorded was 21.7 ºC in July 2014 (Figure 5-4 E) at the surface and the minimum temperature was 8.4 ºC in May 2014 (Figure 5-4 A) at the upper-estuarine stations (TB and CQ). In terms of the surface temperatures all stations were similar, apart from 24$^{th}$ July 2014, when the RM station temperatures (~20 ºC) at the entrance of the estuary were about 2 ºC higher than in the other parts of the estuary. Thermal homogeneity of the water column was observed throughout the sampling period due to the shallowness of the estuary (maximum depth 3.0 m at TB) and tidal mixing.

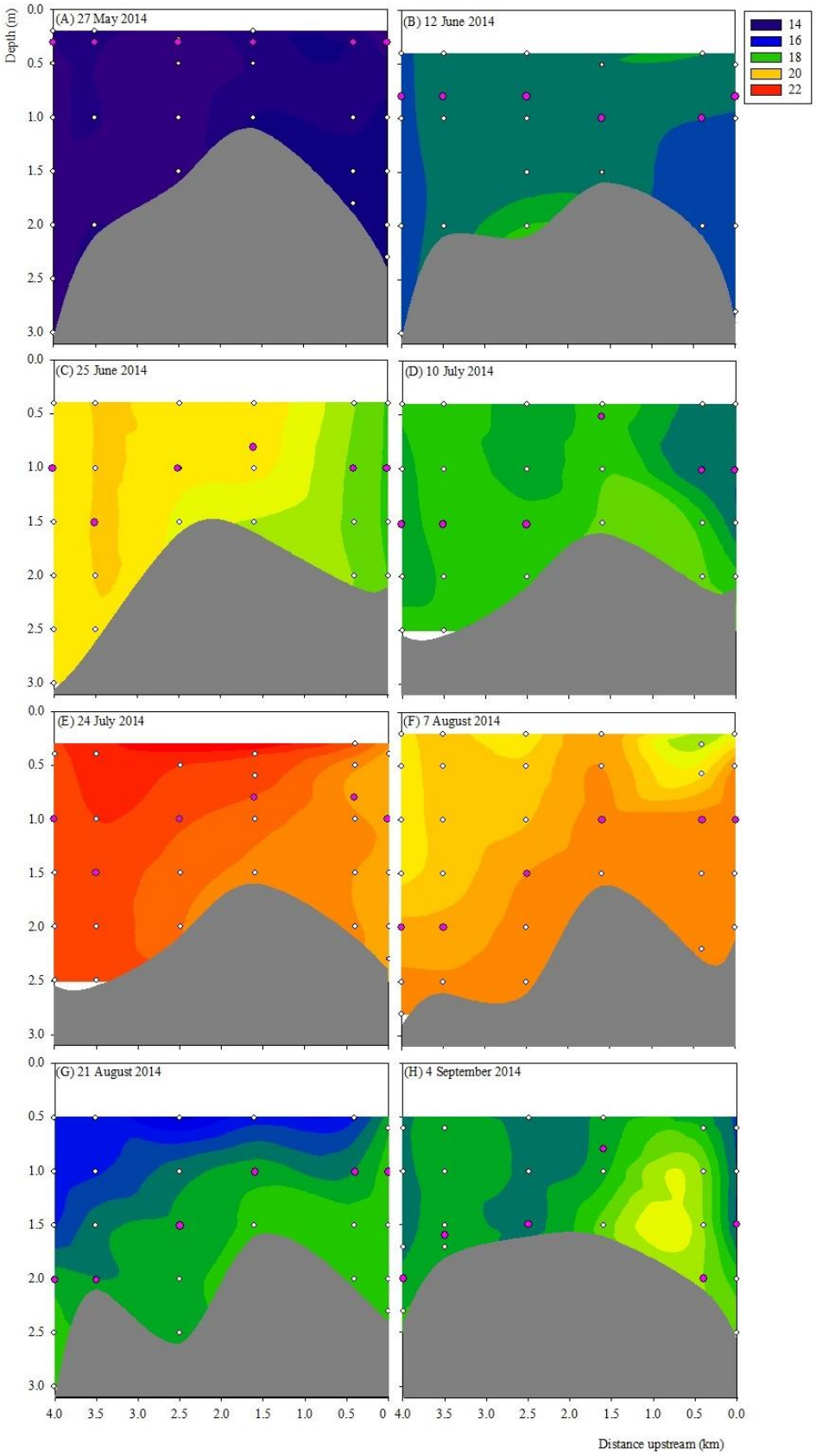


Figure 5-4: Vertical distribution of temperature (ºC) at the six estuarine stations during the summer months of 2014 around high water. Pink circles show the water sampling depths and white circles where the vertical measurements were made using the YSI 6600 multiprobe.

#### 5.3.1.4 Oxygen saturation

In general, oxygen saturations were high at the mid- to lower-estuarine stations as shown in Figure 5-5. Oxygen saturation values varied between 47.8 and 146.5%. The distribution of oxygen saturation values from the YSI 6600 multiprobe measurements showed a consistent seasonal pattern; saturation increased from the lower-estuarine reaches towards to the mid-estuary in July 2014, and decreased from the mid-estuary towards to the upper estuary in August 2014. The BP station had the highest saturation value at 1.5 m on 10$^{th}$ July 2014 and the TB station showed the lowest value at 2.3 m on 4$^{th}$ September 2014.

The higher oxygen saturation values were found (> 100%) in the sub-surface, corresponding with the higher temperatures measured particular in the middle and lower reaches. The GM and BP sites showed the highest oxygen saturation concentration during the sampling period (Figure 5-5 C – D), later microscopic analysis revealed this was related to a dinoflagellate (*Kryptoperidinium foliaceum*) bloom (Figure 5-5 D).

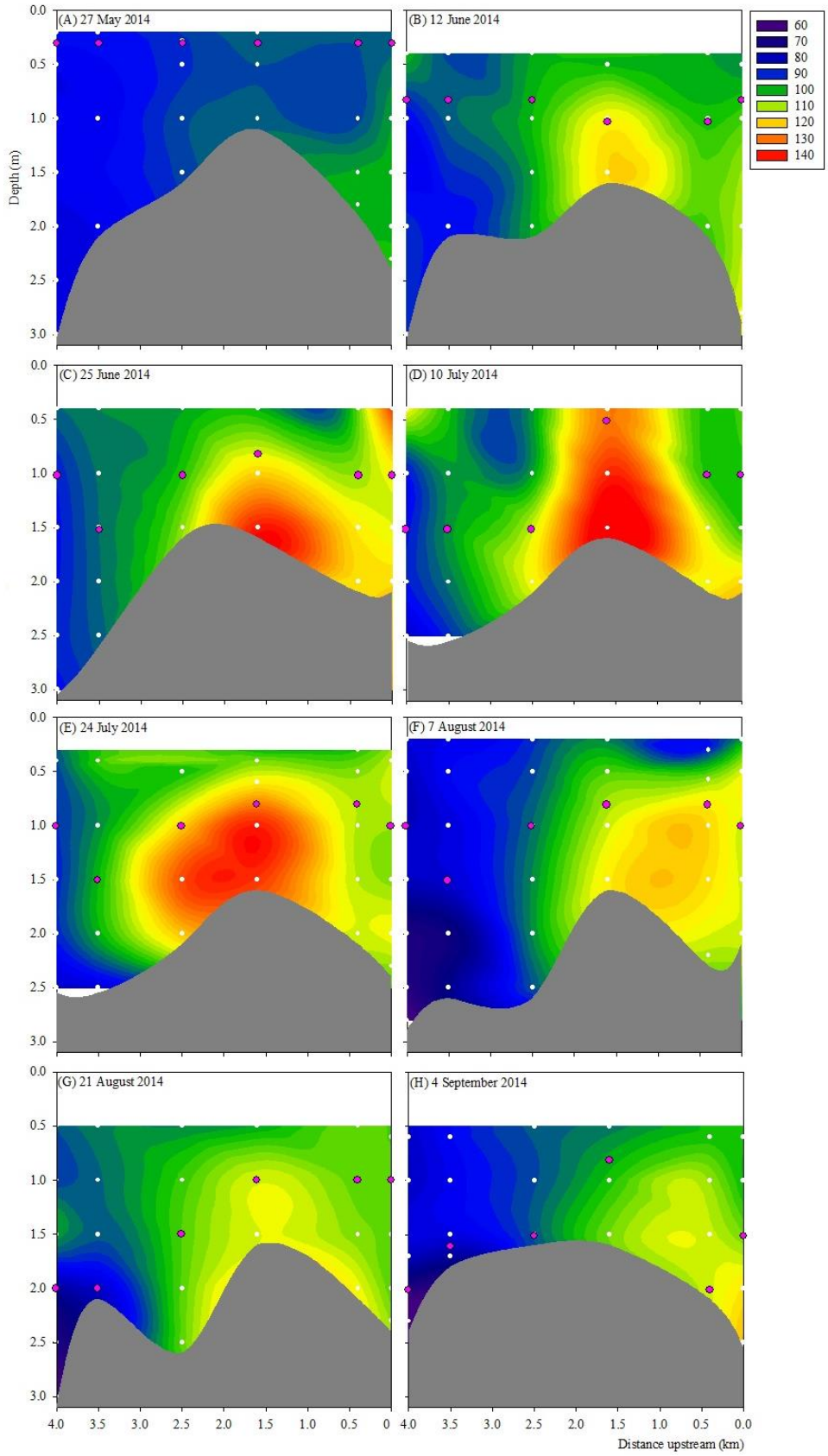


Figure 5-5: Vertical distribution of oxygen saturations at the six estuarine stations during the summer months of 2014 around high water. Pink circles show the water sampling depths and white circles present the depth of measurements from the YSI 6600 multiprobe.

#### 5.3.1.5 Turbidity

During the transect surveys in 2014, turbidity varied between zero and 80 NTU. Turbidity values were generally observed to be < 30 NTU (Figure 5-6), except close to the bottom where up to 80 NTU were observed at upper and mid-estuarine stations on 7th August and 4th September 2014 (Figure 5-6 F and H). The likely reason for this the upper estuary high turbidity is due to influence of the turbid water discharge from the Stour River. On 4th September 2014, the higher turbidity values in the mid estuary may be due to the shallow water depth with suspended sediment stirred up from the estuarine benthos.

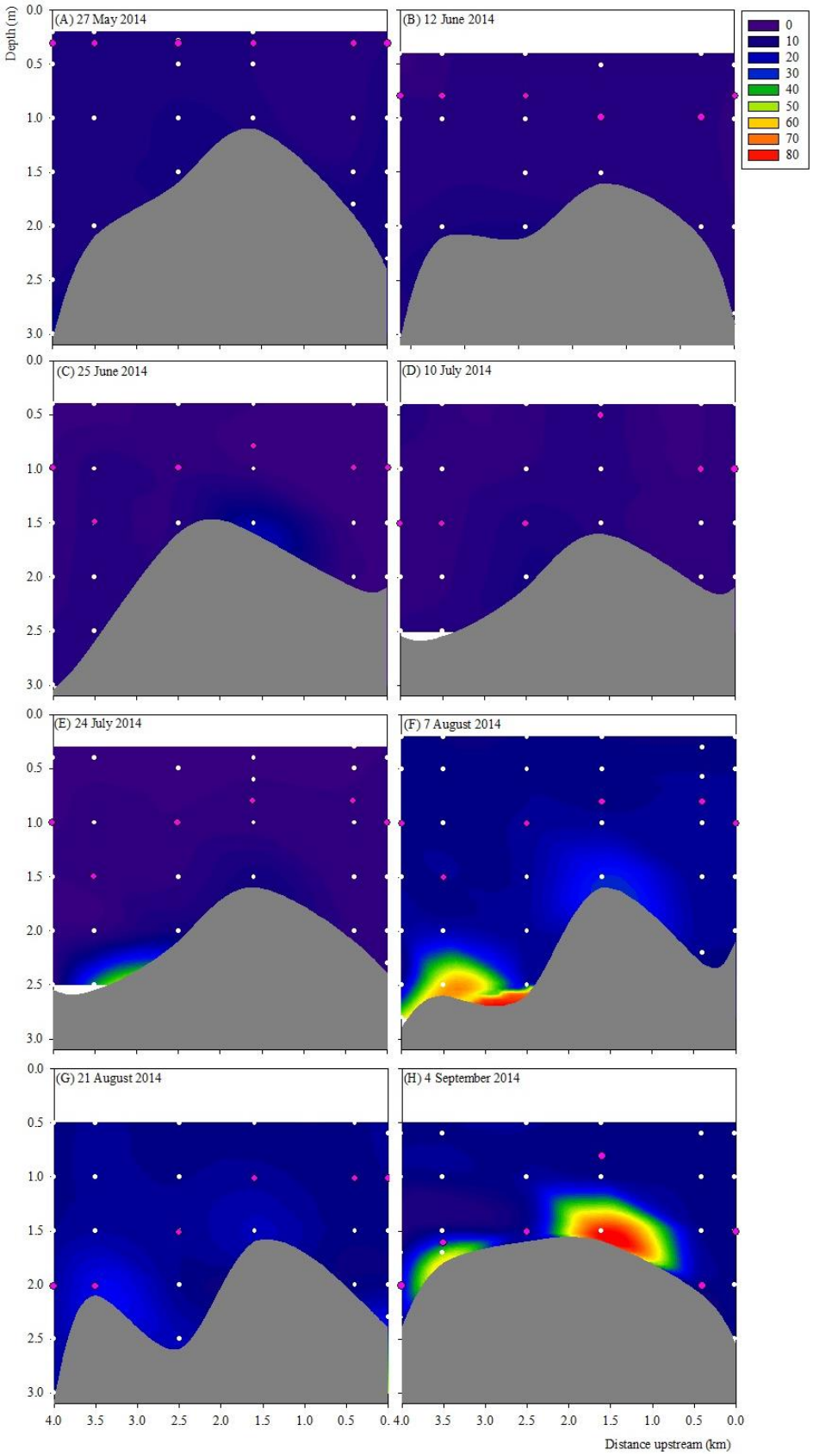


Figure 5-6: Vertical distribution of turbidity (NTU) at the six estuarine stations during the summer months of 2014 around high water. Pink circles show the water sampling depths and white circles present the depth of measurements from the YSI 6600 multiprobe.

#### 5.3.1.6 Chemical parameters: Inorganic nutrients

In general, the distributions of the major inorganic nutrients, nitrate, phosphate, and silicate showed consistently high concentrations in the upper-estuarine reaches (CQ and TB) as shown in Figure 5-7. The highest concentration of inorganic nutrients concentration varied with time and location in the estuary. The CQ and TB stations had generally the highest concentration of inorganic nutrients and the concentrations at RM were the lowest.

*Nitrate*

Higher nitrate concentrations were generally observed at the TB, CQ, and GM stations throughout the sampling period, particularly in July 2014. Mean nitrate concentrations at the TB, CQ, and GM stations were 480 ± 126 (n=8), 489 ± 129 (n=8), and 303 ± 133 (n=8) µmol $L^{-1}$ respectively. Comparing mean concentrations for the BP, FP, and RM stations were much lower 191 ± 136 (n=8), 142 ± 101 (n=8), 119 ± 101 (n=8) µmol $L^{-1}$ respectively as shown in Figure 5-7 A. During the transect sampling, nitrate concentrations at TB and CQ stations peaked initially on 10$^{th}$ July 2014 (~703 µmol $L^{-1}$), then decreased to around 300 µmol $L^{-1}$ on 7$^{th}$ August 2014, and rose again in September 2014. During survey on 10$^{th}$ July 2014, a concentration of 297 µmol $L^{-1}$ of nitrate was recorded at the GM station where the dinoflagellate bloom of *Kryptoperidinium foliaceum* occurred. In contrast, the BP, FP, and RM stations had nitrate concentrations between 135 and 216 µmol $L^{-1}$.

Nitrate concentration versus salinity plots for each sampling day showed that in general higher nitrate concentrations were observed in the low salinity measured end of the estuary (the TB and CQ stations) as shown in Figure 5-9 and Appendix B. On most dates nitrate removal led to non-conservative behaviour. On the first sampling day (27$^{th}$ May 2014), samples were only collected at the surface and showed little change in concentration over a limited range of salinity (0.5 – 4). The bloom of *Kryptoperidinium foliaceum* on 10$^{th}$ July 2014 and of *Cryptomonas* sp on 24$^{th}$ July 2014 had a small impact on the nitrate concentrations at the mid estuary sites (see Appendix B). It is clear that high nitrate concentrations were associated with the river water particularly from the Stour River, as shown by high nitrate concentrations measured at the TB and CQ stations.

*Phosphate*

There was a clear gradient in phosphate concentration along the estuary, with higher concentrations found at the TB and CQ stations and reduced concentrations at the GM, BP,

FP, and RM stations as shown in Figure 5-7 B. Average concentrations of phosphate for the sampling period were 16 ± 5 (TB), 16 ± 6 (CQ), 5 ± 4 (GM), 3 ± 4 (BP), 3 ± 2 (FP), and 2 ± 2 (RM) µmol $L^{-1}$. A pattern of variation was observed, particularly at TB, CQ, GM, and BP, with a peak in phosphate concentrations in September 2014. At the FP and RM stations, phosphate concentrations were lower.

Phosphate concentration versus salinity plots for each day of sampling showed that higher phosphate concentrations were associated with the lowest salinities as with nitrate, at the TB and CQ stations (Figure 5-9 and Appendix C). In general, phosphate concentrations markedly decreased with salinities above 15 (particular the RM and FP stations), suggesting a marked removal between the GM and BP stations. On 4th September 2014 a marked removal of phosphate occurred between the BP and FP stations (see Appendix C).

*Silicate*

Silicate concentrations varied between 8 and 183 µmol $L^{-1}$ as shown in Figure 5-7 C. High silicate concentrations were observed at the TB, CQ, and GM stations throughout the sampling period, with the highest concentration of 183 µmol $L^{-1}$ at the GM on 27th May 2014. A marked increase in silicate concentration was observed at all stations during the first survey that then decreased sharply in following surveys. It is possible that as only the surface water sample was collected at each station and not at the maximum fluorescence depth as on the other sample dates removal processes may have been missed. The silicate concentrations peaked again on 4th September 2014 along the estuary but not at the FP and RM stations, probably reflecting the increased river discharge (Figure 5-1 B) before the last transect and the input of silicate into the estuary.

Silicate concentration versus salinity plots showed that high silicate concentrations were associated with the less saline water, indicating the pronounced freshwater input at upper estuary stations (Figure 5-9 and Appendix D). Silicate concentration generally decreased following the salinity gradient, due primarily to dilution with saline water. On same dates (10th July, 24th July, and 7th August 2014) silicate concentrations at GM were above the dilution line (see Appendix D) suggesting summer silicate concentrations in the Avon River water which flows into the harbour between CQ and GM was higher than in the Stour.

*Nutrient ratios*

The nitrate to phosphate, silicate to phosphate, and nitrate to silicate ratios are shown in Figure 5-8. In general, the N:P and Si:P ratios for all stations tended to decrease gradually from May to September 2014, and peaked suddenly on 10$^{th}$ July 2014 particularly at the GM and BP stations, although the N:Si ratio showed a reverse pattern. The highest values of the N:P and Si:P ratios were found at the mid-estuarine stations (GM and BP) as shown in Figure 5-8 A and B, while the highest value of the N:Si ratio was observed at the upper-estuarine stations (TB and CQ) on the same day that the highest value of N:P ratio occurred at GM. The N:Si ratios were high at the upper-estuarine stations (TB and CQ) on 10$^{th}$ July 2014, and tended to decrease towards September 2014, perhaps because of lower silicate on that day.

Nutrient ratios can indicate which particular nutrient might influence phytoplankton growth and succession. The nutrient ratios in the water column can be compared with the Redfield ratio for N:P of 16:1 and also for Si:P of 16:1. The high N:P and Si:P ratios measured on 27$^{th}$ May and 10$^{th}$ July 2014 indicate that relatively low phosphate concentrations may be the reason for high ratios at the upper-estuary stations (TB and QC) in May 2014, while relatively high nitrate and silicate concentrations could be the reason for high ratios at the mid-estuarine stations (GM and BP). The N:Si ratios were generally < 4 at the mid- and lower-estuarine stations and > 4 at the upper stations on the same day, perhaps due to higher concentrations of nitrate at the upper stations than the lower stations due to freshwater inputs.

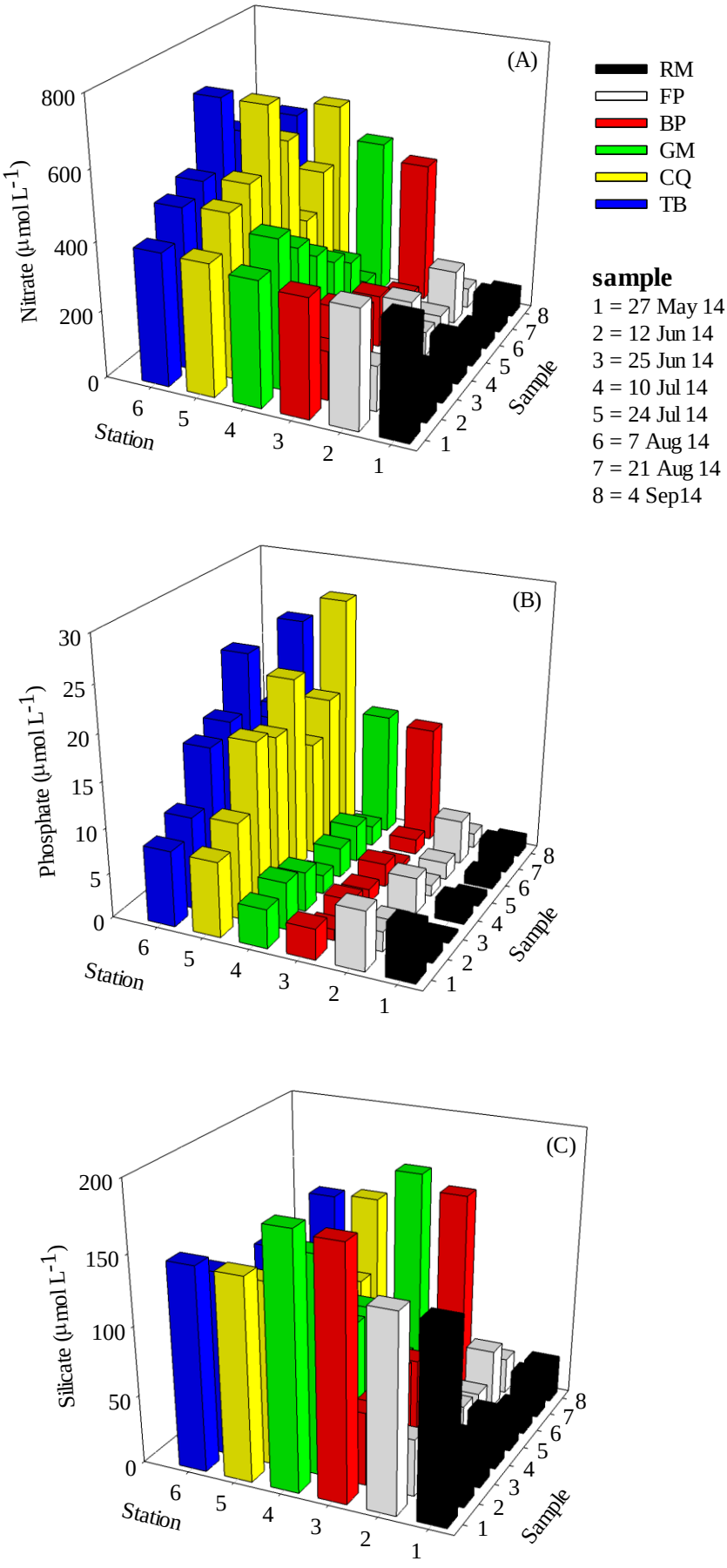


Figure 5-7: Inorganic nutrient distributions (µmol $L^{-1}$) at the six estuarine stations during the summer months in 2014, (A) nitrate, (B) phosphate, and (C) silicate.

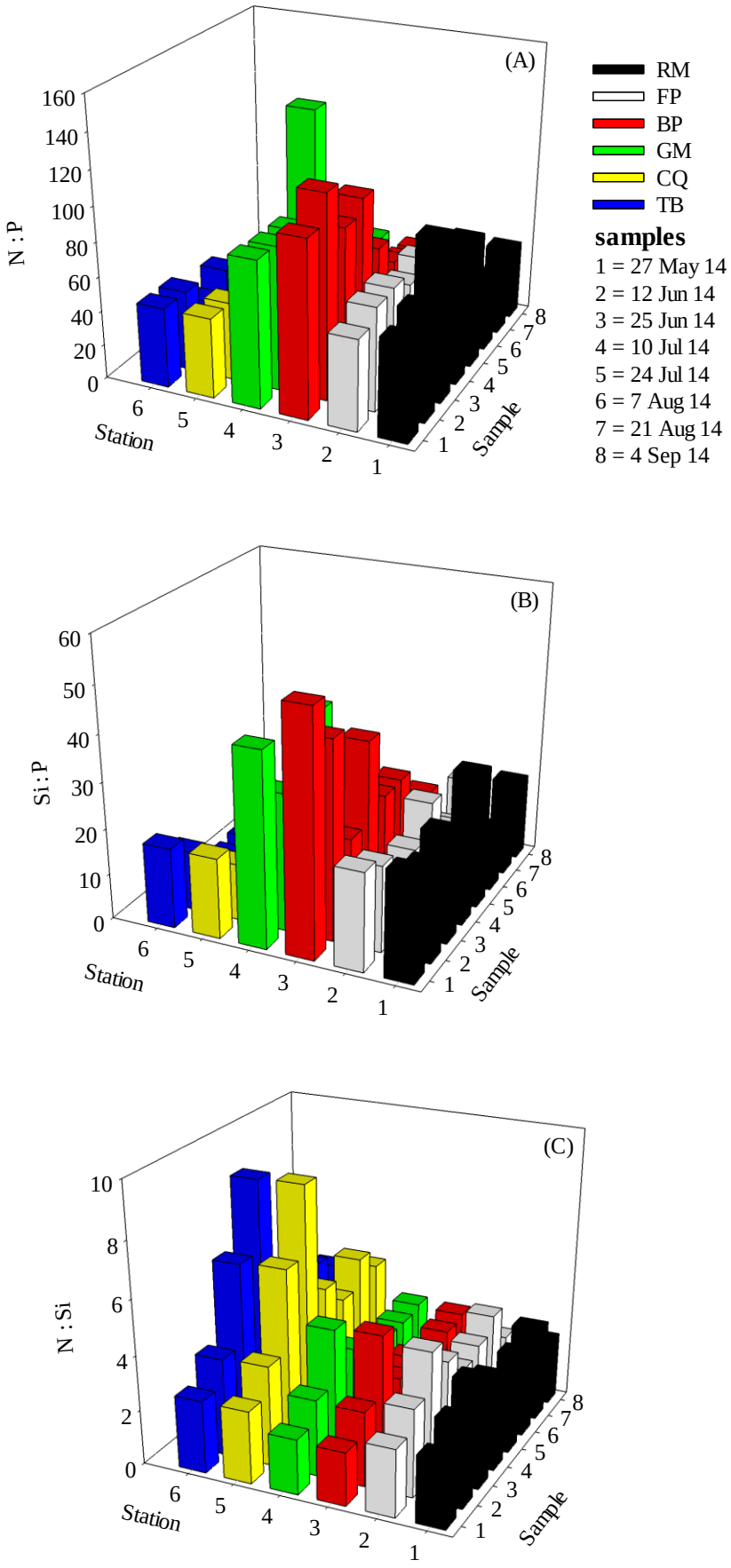


Figure 5-8: Changes in N:P, Si:P, and N:Si ratio distributions at the six estuarine stations during the summer months in 2014.

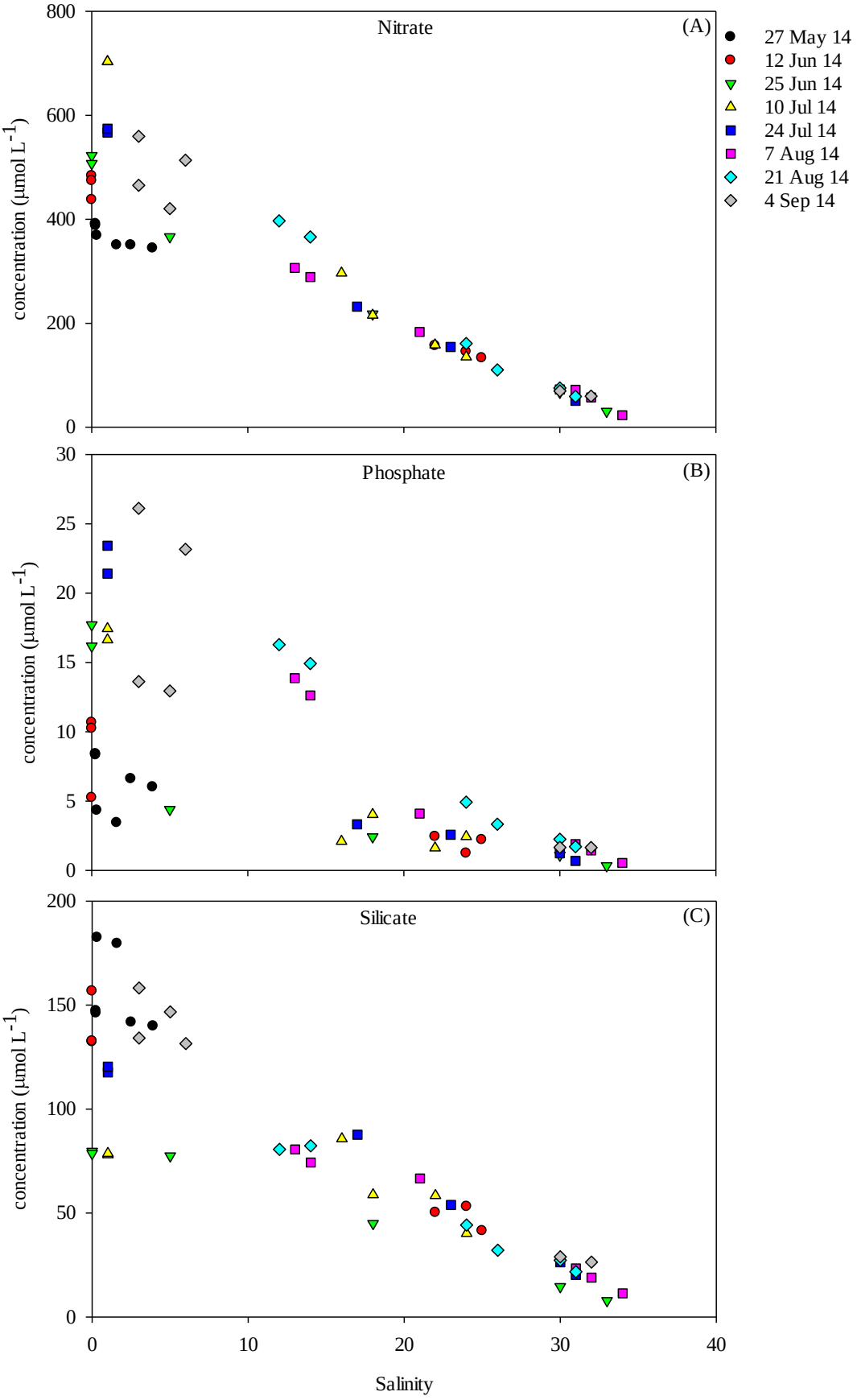


Figure 5-9: Inorganic nutrient distribution (µmol $L^{-1}$) versus salinity for each day of sampling at the six estuarine stations during the summer months in 2014, (A) nitrate, (B) phosphate, and (C) silicate.

### 5.3.1.7 Irradiance

The irradiance attenuation coefficient (*k*) was calculated for all stations throughout the sampling period from *in situ* measurements as shown in Figure 5-10 and Table 5-1. The mean *k* values from the transect stations were generally over 1 $m^{-1}$, except the RM station and showed no clear temporal variation trend. The highest *k* value was 3.9 $m^{-1}$ on 10$^{th}$ July at the GM station and was associated with the high chlorophyll *a* concentration.

Table 5-1: Irradiance attenuation coefficient (*k*) values at the six estuarine stations in Christchurch Harbour during the summer months in 2014; mean (bold) and range of values (parentheses).

| Station | *k* ($m^{-1}$) |
|---|---|
| Run at mudeford | **0.7** (0.4 – 0.9) |
| Ferry Pontoon | **1.0** (0.7 – 1.4) |
| Blackberry Point | **0.9** (0.5 – 1.7) |
| Grimbury Marsh | **1.6** (0.9 – 3.9) |
| Christchurch Quay | **1.3** (1.1 – 1.8) |
| Tuckton Bridge | **1.2** (0.9 – 1.7) |

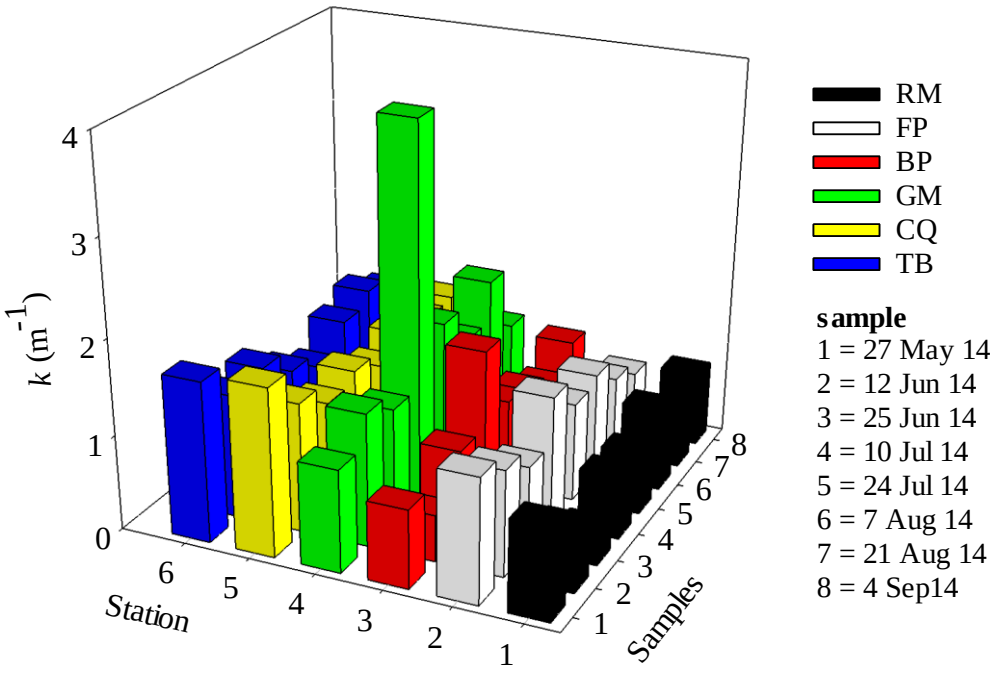


Figure 5-10: Pattern of attenuation coefficient (*k*) for the six estuarine stations during the summer months in 2014.

### 5.3.2 Phytoplankton pigments

#### 5.3.2.1 Total chlorophyll *a*

Contour plots of vertical profiles of chlorophyll *a* concentration determined from the YSI 6600 multiprobe are shown in Figure 5-11. High concentrations were generally detected near the bottom, with the highest value at 2 m (96 µg $L^{-1}$) at the GM station on 10th July 2014 as shown in Figure 5-11 D. High values of > 20 µg $L^{-1}$ were firstly observed at 1.5 m at the mid-estuarine station (GM) on 25th June 2014 and continued to be detected at this station until 21st August 2014 (Figure 5-11 C – G). High chlorophyll values were detected at the lower estuarine stations on the final sampling day in September 2014 (Figure 5-11 H).

A good agreement between measurements of acetone extracted chlorophyll *a* concentration from the water samples collected at each site during the eight transects and the chlorophyll fluorescence detected at the same depth using the YSI 6600 multiprobe is shown in Figure 5-12 A with an $R^2$ value of 0.86 and a slope of 0.9.

Chlorophyll *a* concentrations measured in the collected water samples from each estuarine station are illustrated in Figure 5-13. The chlorophyll *a* concentration varied between 1.8 and 93.0 µg $L^{-1}$ with mean concentrations of 3.8 ± 2.3 (RM), 4.3 ± 2.9 (FP), 9.3 ± 4.1 (BP), 26.4 ± 29.3 (GM), 10.5 ± 5.1 (CQ), and 13.6 ± 9.7 (TB) µg $L^{-1}$.

The high chlorophyll *a* concentration (93.0 µg $L^{-1}$) in the sample collected at 1.5 m at the GM station on 10th July 2014 was dominated by the dinoflagellate, *Kryptoperidinium foliaceum* and the next chlorophyll peak that occurred on 21st August 2014 at the mid- and upper estuary was dominated by *Cryptomonas* species. The high chlorophyll *a* concentrations of 36.9 and 21.0 µg $L^{-1}$ detected at the TB and CQ stations on 21st August 2014 also contained high abundance of cryptophytes. Lower chlorophyll *a* concentrations were generally measured between the RM and BP stations throughout the sampling period. Lower chlorophyll *a* concentrations were also measured at the TB, CQ, and GM stations between 27th May and 25th June 2014 (Figure 5-13).

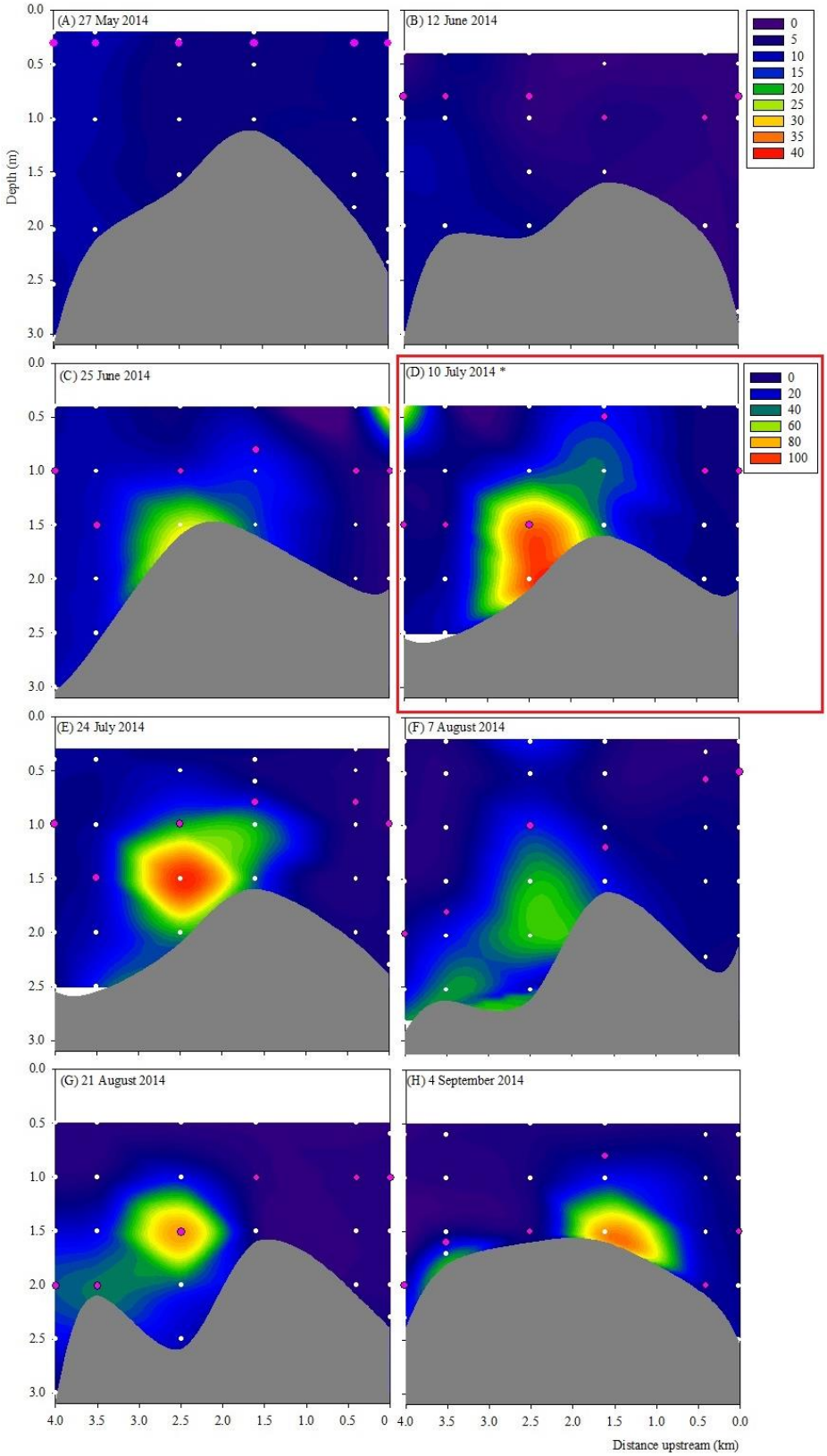


Figure 5-11: Vertical distribution of chlorophyll *a* concentration (µg $L^{-1}$) derived from the YSI 6600 multiprobe at the six estuarine stations during the summer months in 2014 around high water. Pink circles show the water sampling depths and white circles present the vertical measurements from the multiprobe. Note change of contour scale on D.

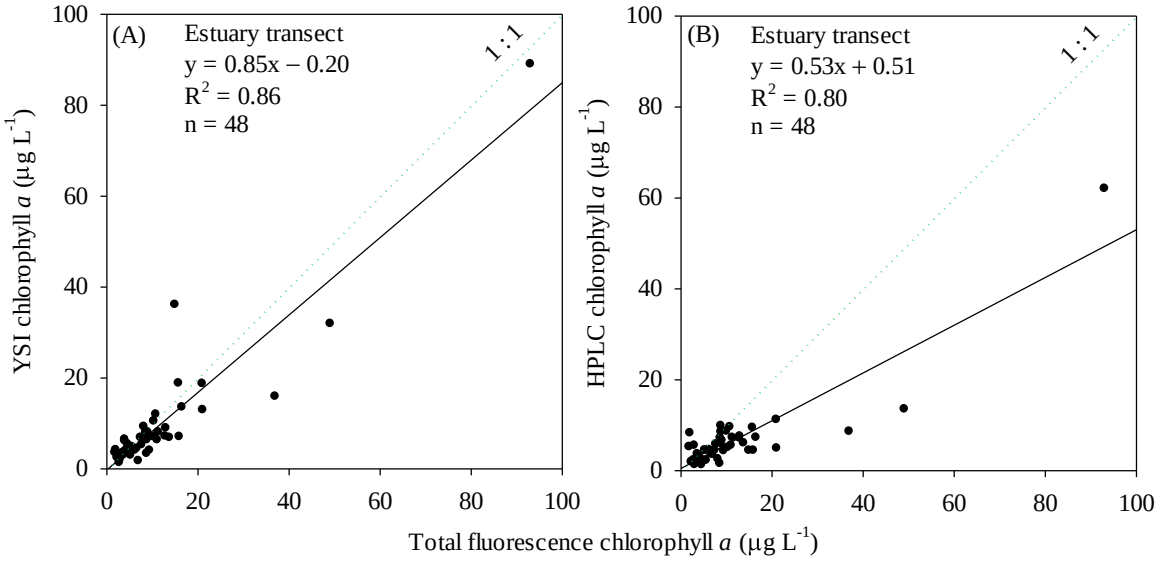


Figure 5-12: Comparison of chlorophyll *a* concentration determined from the YSI 6600 multiprobe and from acetone extracts of water samples collected at each site (A) and comparison between HPLC chlorophyll *a* and total fluorescence chlorophyll *a* at the six estuarine stations is shown in B.

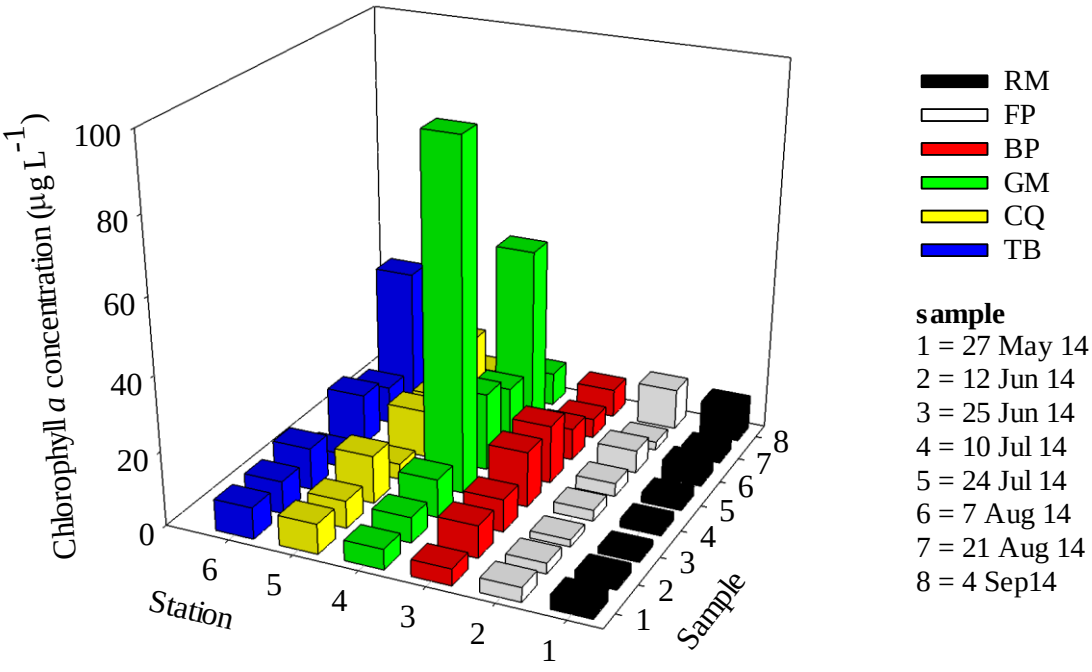


Figure 5-13: Distribution of total chlorophyll *a* at the six estuarine stations during summer in 2014.

### 5.3.2.2 Phytoplankton accessory pigment

As previously observed from the samples collected each week from Mudeford Quay in 2013 – 2014 (close the transect station of the Run at Mudeford (RM) as described in Section 4.3.2.2). Fucoxanthin was the main accessory pigment but peridinin also detected during the summer and autumn months. However, the spot samples collected in 2013 – 2014 were from the surface at low tide and, probably reflected the pigment contained the river phytoplankton populations.

Values of chlorophyll *a* measured by fluorescence were higher than values of chlorophyll *a* measured by HPLC, although there was a correlation between the two measurements (Figure 5-12 B), with an $R^2$ value of 0.8 and a slope of 0.5. Based on the HPLC data, the fluorescence chlorophyll *a* was highly correlated to both total HPLC pigment and total accessory pigment, giving $R^2$ values of 0.94 and 0.98 and slopes of 1.2 and 0.7 respectively (Figure 5-14).

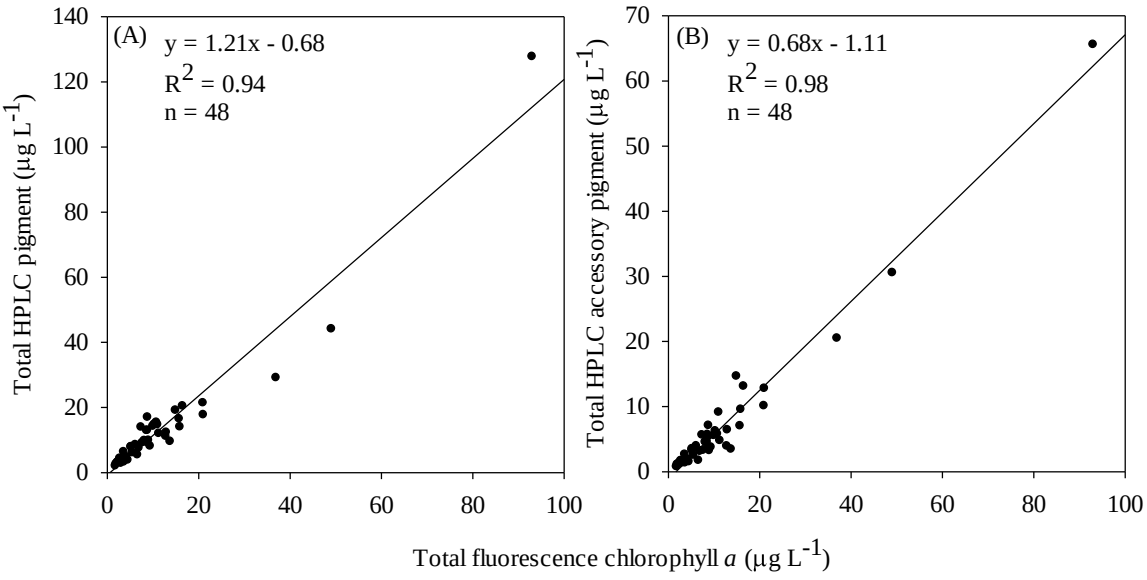


Figure 5-14: Relationships of fluorescence chlorophyll *a* to (A) total HPLC pigment and (B) total HPLC accessory pigments at the six estuarine stations during the transect sampling in 2014.

All HPLC phytoplankton pigments from the estuarine transect stations are compared in Figure 5-15 and Figure 5-16, and variations in the pigment to chlorophyll *a* ratios are shown in Figure 5-17 and Figure 5-18.

The temporal changes in HPLC determined chlorophyll *a* followed those described previously for fluorescence derived chlorophyll *a* (see Figure 5-13), although absolute

values varied (Figure 5-15 A). Peridinin, fucoxanthin, diadinoxanthin, β carotene, chlorophyll *c2*, and zeaxanthin displayed a similar trend to chlorophyll *a*, with maxima at the GM station of 0.8, 41.5, 9.9, 3.4, 4.7, and 2.0 µg $L^{-1}$ on 10$^{th}$ July 2014 respectively (Figure 5-15). These pigments showed considerably lower values at the other stations.

Concentrations of fucoxanthin closely followed those of diadinoxanthin and zeaxanthin, and these pigments peaked at the GM station on 10$^{th}$ July 2014 (Figure 5-15 C, G, and Figure 5-16 H). At the BP station the same temporal trend of high values was observed on the same day with lower concentrations. High fucoxanthin, diadinoxanthin, and zeaxanthin concentrations were observed at the GM station. At the other stations these pigments peaked on different days while concentrations were close at the GM station except during the dinoflagellate bloom on 10$^{th}$ July 2014. Fucoxanthin, peridinin, diadinoxanthin, β carotene, chlorophyll *c2*, and zeaxanthin concentrations peaked sharply at the GM station on 10$^{th}$ July 2014, indicating several phytoplankton populations developed at the same time.

Chlorophyll *b* showed a different pattern, peaking mostly at the TB and CQ stations on 21$^{st}$ August 2014, with maxima at the TB of 2.6 µg $L^{-1}$ and the CQ of 1.1 µg $L^{-1}$ (Figure 5-15 F). This pigment was often found to be 0.5 µg $L^{-1}$ lower than the other stations in the estuary.

Peridinin concentration was low throughout the whole estuary, except the GM station during the phytoplankton bloom on 10$^{th}$ July 2014, with a peak concentration of 0.8 µg $L^{-1}$ (Figure 5-15 B). While at the other stations, values were generally observed > 0.4 µg $L^{-1}$ throughout the sampling period.

Increased amounts of alloxanthin were measured after the phytoplankton bloom on 21$^{st}$ August 2014 at the GM, TB, and CQ stations with peak concentration of 11.1, 6.2, and 3.1 µg $L^{-1}$ respectively (Figure 5-15 D). Low concentrations of alloxanthin (< 0.1 µg $L^{-1}$) were detected occasionally at the RM and FP stations.

Lutein showed a different trend to chlorophyll *a* with peaks on 26$^{th}$ July 2014 at the TB and CQ stations of 0.7 µg $L^{-1}$ (Figure 5-15 E).

Violaxanthin was generally present at concentration below 0.4 µg $L^{-1}$ (Figure 5-16 E) with peaks at the upper stations (TB and CQ) on 26$^{th}$ July 2014, when 0.3 µg $L^{-1}$ was detected. Several other smaller peaks were detected at the BP and CQ stations. Divinyl chlorophyll *a* showed a different temporal pattern to the other pigments along the estuary, with

maximum concentration measured on 4th September 2014 at the FP station of 2.5 µg $L^{-1}$ (Figure 5-16 G).

Low concentrations of 19'But and prasinoxanthin were detected throughout the estuary with 19'But undetectable from 10th July 2014 (Figure 5-16 C), while prasinoxanthin was detected at some stations and sampling days (Figure 5-16 F). Prasinoxanthin was often detected at the FP station with low concentration (< 0.1 µg $L^{-1}$). 19'Hex pigment was undetectable in all samples collected during the transect surveys in 2014 (Figure 5-16 D).

Considering ratios of accessory pigment to chlorophyll *a* (Chl *a*) for all transect samples, fucoxanthin to Chl *a* ratios showed consistently high values throughout the sampling period for all transect samples, and was up to 1.2 initially at the BP station on 10th July 2014 (Figure 5-17 B). This high fucoxanthin to Chl *a* ratio was consistent with the high biomass of *Kryptoperidiniun foliaceum*, which developed in the mid-estuary, then moved down estuary in July 2014 thus indicating that dinoflagellates were the main group associated with this pigment in the estuary. This ratio varied from 0.1 to 1.2 during the summer months.

Peridinin to Chl *a* ratios varied between zero to 0.05 and in general were higher in the mid estuary towards the lower estuary (Figure 5-17 A). In July 2014 during *K. foliaceum* bloom in the GM station, this ratio presented consistently low values and were quite variable in the estuary.

Alloxanthin to Chl *a* ratios were quite variable and were high on some occasions and followed the temporal pattern of alloxanthin concentration, with the TB, CQ, and GM stations having consistently high values on 21st August 2014 and sharply decreasing on the next sampling day (Figure 5-17 C). Before the peak day the ratio was low and it is possible that there was low numbers of cryptophytes present during the dinoflagellate bloom.

Lutein to Chl *a* ratios were lower than 0.1 during the summer months (Figure 5-17 D). Peak values occurred in July 2014 particularly at the TB and CQ stations and coinciding with a high abundance of the chlorophyte group.

Chlorophyll *b* to Chl *a* ratios varied between zero and 0.5 (Figure 5-17 E) and followed the temporal pattern of chlorophyll *b* concentration. Peak values were observed to sharply increase on 21st August 2014 at the CQ station.

Diadinoxanthin to Chl *a* ratios were < 0.2 during the sampling period except on 21st August 2014 at the BP station, where this ratio was 0.4 (Figure 5-17 F). β carotene to Chl *a* ratios were generally lower than 0.1 (Figure 5-17 G), except on 10th July 2014 and 21st August 2014 at the mid- and upper estuarine stations when the ratio increased to > 0.2.

Considering the ratios of minor accessory pigment to Chl *a* for samples collected along the Christchurch Harbour estuary, chlorophyll *c3* to Chl *a* ratios showed much lower values than the other pigments to Chl *a* ratios (Figure 5-18 A). This ratio peaked at the RM and GM stations on 7th August 2014, with values of 0.018 and 0.015 respectively. Chlorophyll *c2* to Chl *a* ratios varied between zero and 0.24 and two peaks occurred at the TB station on 10th July and 21st August 2014, with values of 0.15 and 0.24 respectively (Figure 5-18 B).

19'But to Chl *a* ratios were observed in May and July 2014, with low values at some stations particular at the upper and mid estuary (Figure 5-18 C). 19'Hex was undetectable at all stations during the transect sampling and so ratios of this pigment to Chl *a* were zero (Figure 5-18 D).

Violaxanthin to Chl *a* ratios varied between zero and 0.06 and were detected at all stations (Figure 5-18 E). The high values occurred often in the upper and mid estuary, however, a value of zero was detected on 10th July 2014 at the GM station during the dinoflagellate bloom. It is possible that no phytoplankton group associated with this pigment were present at this station. Prasinoxanthin to Chl *a* ratios were quite low along the estuary (Figure 5-18 F) with maximum values of 0.04 on 25th June 2014 at the FB station.

Divinyl chlorophyll *a* to Chl *a* ratios ranged between zero and 0.45 (Figure 5-18 G). At the BP station this ratio peaked on 10th July 2014, with value of 0.45 and at the FP station on 4th September 2014, with a similar value. Zeaxanthin to Chl *a* ratios were quite constant along the estuary, with values below 0.04 except on 10th July 2014 at the BP station, when this ratio was 0.15 (Figure 5-18 H).

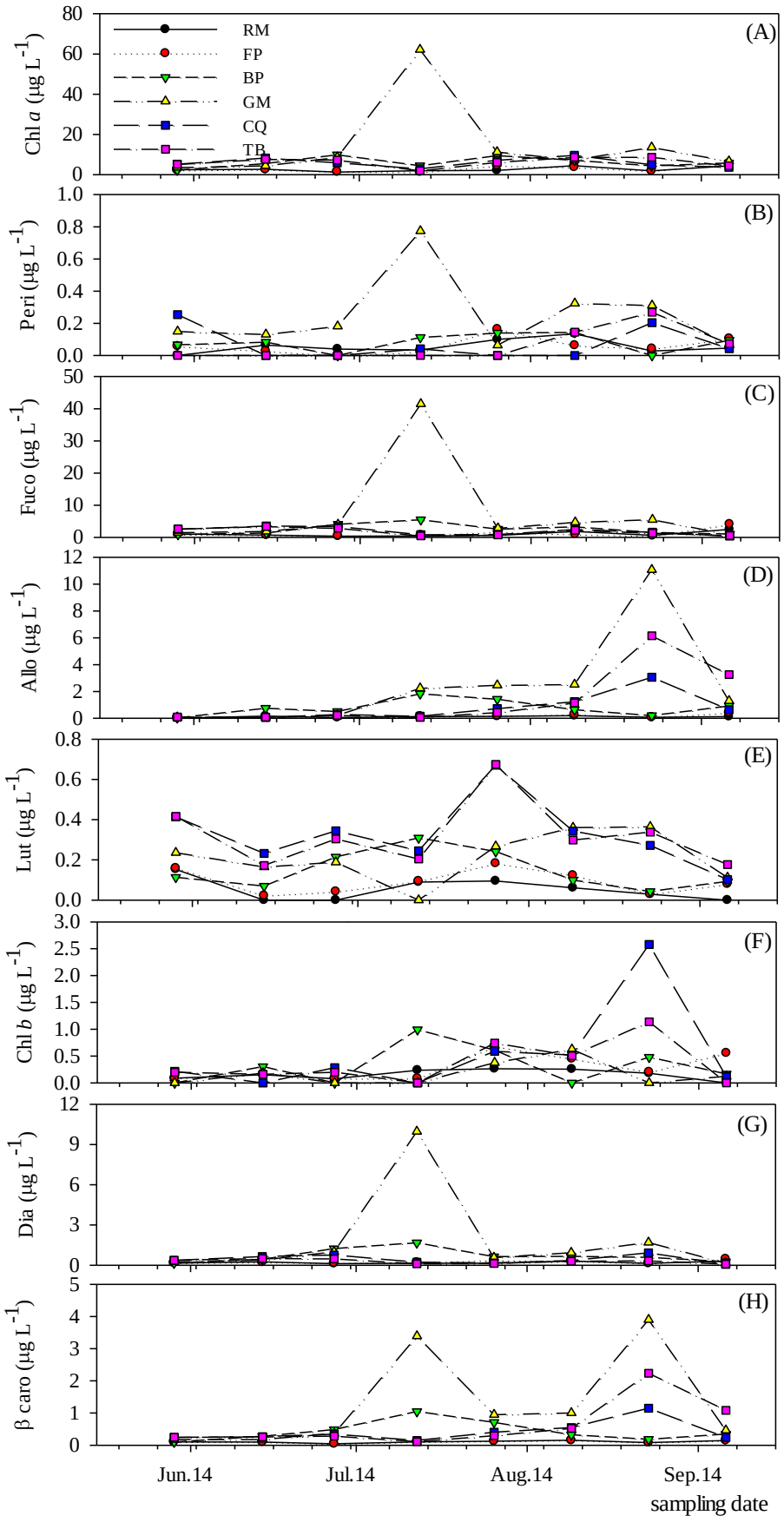


Figure 5-15: Temporal and spatial distributions of major accessory pigments at the six estuarine stations along the Christchurch Harbour estuary during the summer months in 2014. Symbols in upper panel apply to all panels.

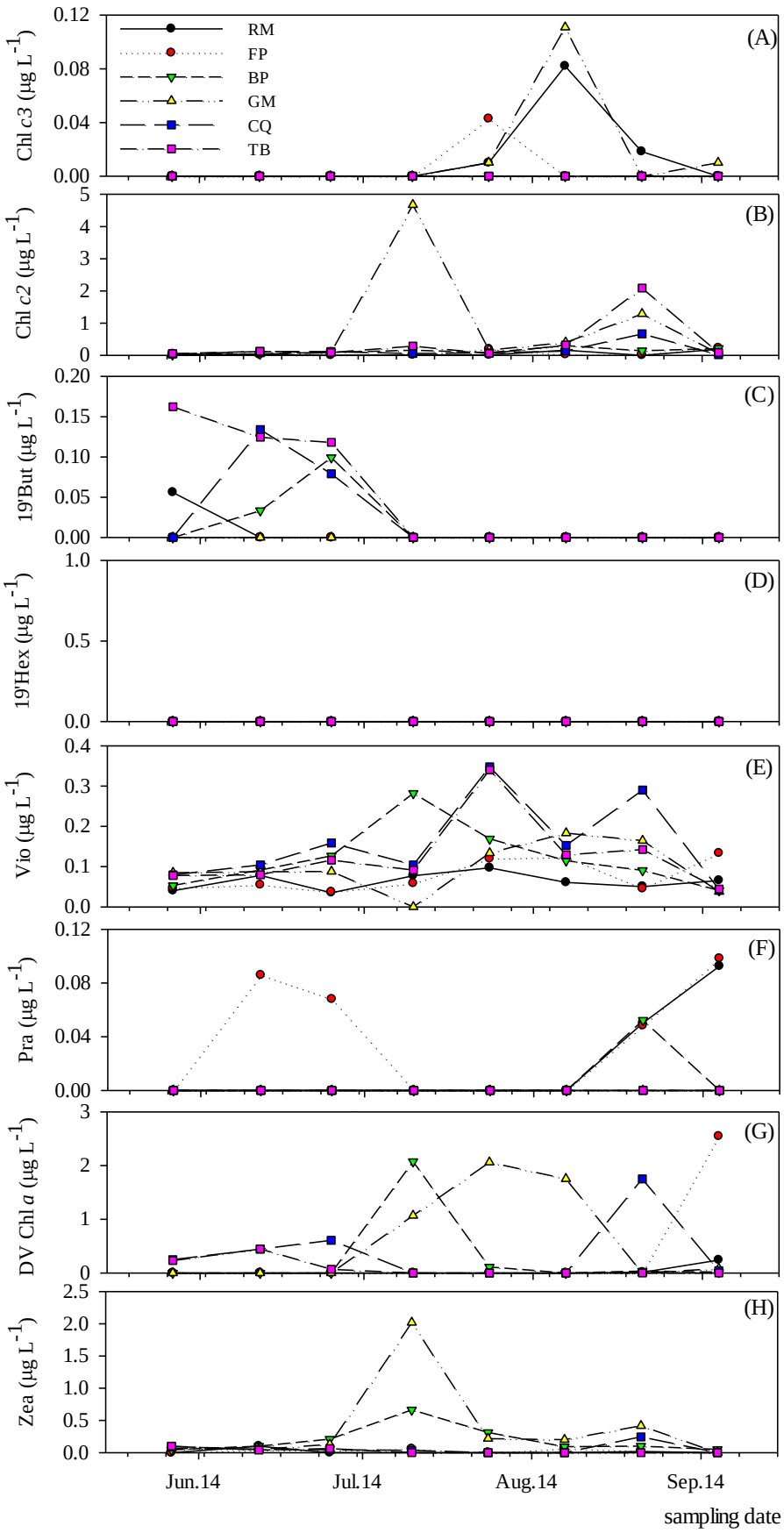


Figure 5-16: Temporal and spatial distributions of minor accessory pigments at the six estuarine stations in the Christchurch Harbour estuary during the summer months in 2014. Symbols in upper panel apply to all panels.

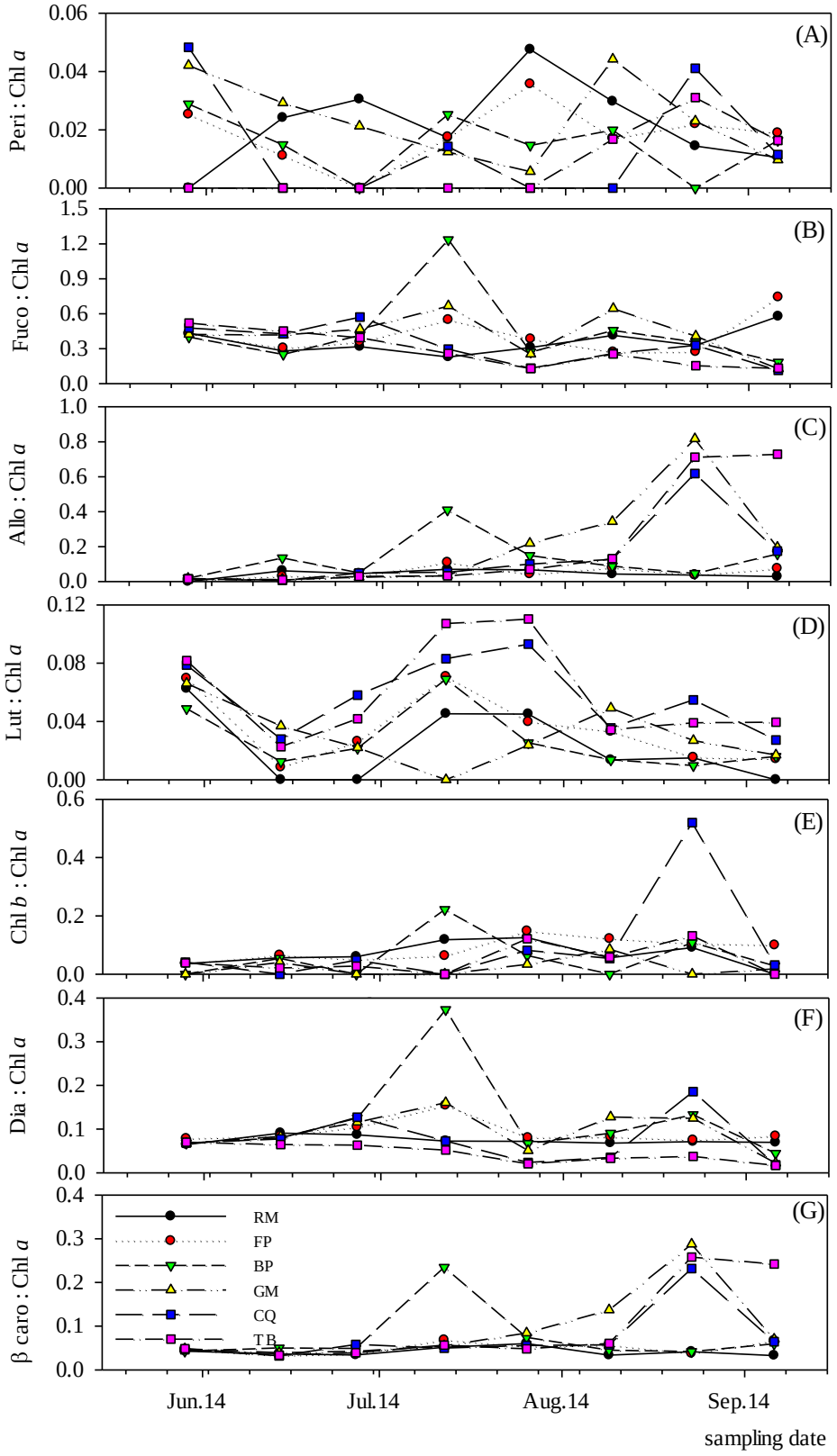


Figure 5-17: Temporal and spatial distributions of major accessory pigments to chlorophyll *a* ratios at the six estuarine stations in the Christchurch Harbour estuary during the summer months in 2014. Symbols in lower panel apply to all panels.

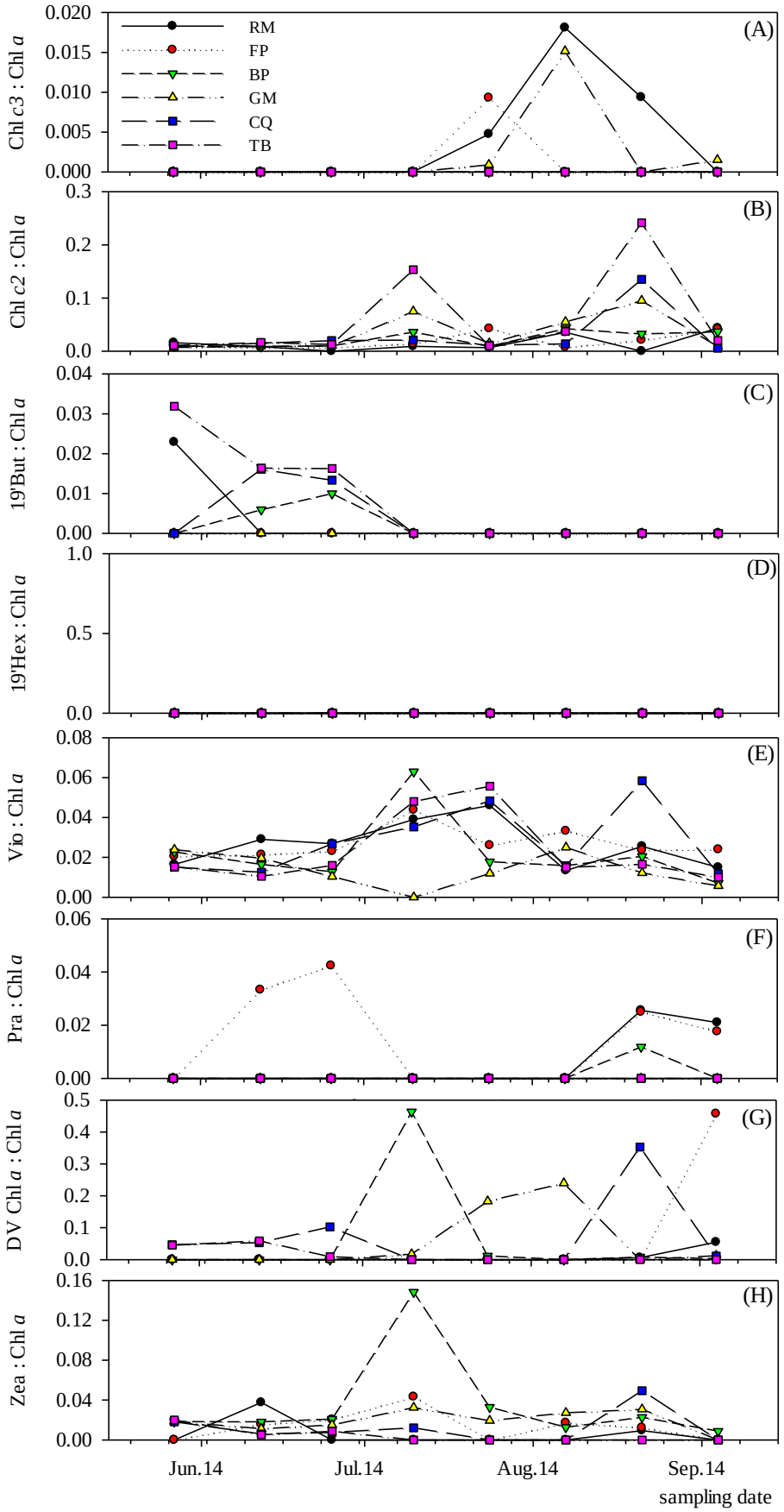


Figure 5-18: Temporal and spatial distributions of minor accessory pigments to chlorophyll *a* ratios at the six estuarine stations in the Christchurch Harbour estuary during the summer months in 2014. Symbols in upper panel apply to all panels.

### 5.3.3 Phytoplankton taxonomic data

#### 5.3.3.1 Phytoplankton cell abundance

In general, estuarine phytoplankton abundance showed a similar pattern to chlorophyll *a* concentrations. A gradient of increasing total abundance and biomass was observed at all stations from the RM to TB station. The sampling stations along the estuary showed differences in the temporal pattern of species dominance and composition during the productive period in 2014. Chlorophyte dominance generally occurred in the upper estuary (TB and CQ), while dinoflagellates with cryptomonads, and diatoms dominanted in the mid (GM and BP) and lower estuary (FP and RM) respectively during the summer months in 2014 (Figure 5-19).

At the RM station, the abundant species (*Chaetoceros* spp., *Guinardia delicatula*, *Navicula* spp., and *Nitzschia* spp.) were mainly diatoms, peaking on 7$^{th}$ August 2014 (*Chaetoceros* spp. up to 5.9 × 10$^{3}$ cells mL$^{-1}$ (Figure 5-19 A). *Guinardia delicatula* was the dominant species on 4$^{th}$ September 2014 (1.2 × 10$^{3}$ cells mL$^{-1}$), and the chlorophyll *a* peak showed a higher concentration than the peak on 7$^{th}$ August 2014 due to the dominant diatom, *G. delicatula* having a larger cell size compared with *Chaetoceros* spp. Moreover, the total abundance was up to 7.9 × 10$^{3}$ cells mL$^{-1}$ on 7$^{th}$ August 2014, while on 4$^{th}$ September 2014 at this station it was only 2.0 × 10$^{3}$ cells mL$^{-1}$. All the cryptophytes (*Cryptomonas*, *Rhodomonas*, and *Teleaulax* spp.) were observed at high abundance (> 300 cells mL$^{-1}$) throughout the sampling period, while a lower cell abundance of dinoflagellates were found (< 100 cells mL$^{-1}$) at this station. On 10$^{th}$ July 2014, an exceptional bloom of the dinoflagellate *Kryptoperidinium foliaceum* (Figure 5-20) reached cell abundance up to 18.3 × 10$^{3}$ cells mL$^{-1}$ at the GM station. This bloom seems not to have been concentrated towards the RM station by tidal advection on this date, possibly because the sample was collected at high tide. Chlorophyte abundance was above 500 cells mL$^{-1}$ from May to July 2014 and then dropped below 50 cells mL$^{-1}$ on 21$^{st}$ August 2014 at this station. The chlorophyte species *Chlorella* spp. was the dominant species in May and July 2014 and was followed by *Pyramimonas* sp. and *Scenedesmus* spp. later in July 2014. The diatoms were the dominant population at this station and ranged between 26 and 85% of the total number of cells followed by cryptophyte and chlorophyte populations with a range of 6 – 49% and 2 – 29% respectively (Figure 5-19 G).

At the FP station, lower cell numbers were observed relative to the RM station, although the phytoplankton abundance had a similar temporal pattern to the RM station (Figure 5-19

B). Total phytoplankton abundance varied between $1 \times 10^3$ and $6.9 \times 10^3$ cells $mL^{-1}$ throughout the summer months. The diatom population was also the main percentage of population at this station followed by cryptophytes and chlorophytes respectively (Figure 5-19 H). From 27th May to 24th July 2014, the diatoms population ranged $0.8 – 1.8 \times 10^3$ cells $mL^{-1}$ followed by the cryptophyte and chlorophyte populations that varied 166 – 802 and 249 – 661 cells $mL^{-1}$ respectively. The pennate diatoms showed high cell abundances in May to July 2014 particularly *Navicula* spp. The centric diatom *Chaetoceros* spp. was dominant on 7th August 2014 ($4.4 \times 10^3$ cells $mL^{-1}$) as well as at the RM station then during the next two sampling dates, 21st August 2014 and 4th September 2014, this species decreased down to 79 and 5 cells $mL^{-1}$ respectively. On 4th September 2014, *Guinardia delicatula* was present at $1.1 \times 10^3$ cells $mL^{-1}$ with chlorophyll concentration of 11.0 µg $L^{-1}$. Among the dinoflagellates cell abundances range 0 – 278 cells $mL^{-1}$ and high abundance occurred on 7th August 2014, while the chlorophyte group ranged from 39 to 769 cells $mL^{-1}$. The highest chlorophyte population was observed on 25th June 2014, with *Chlorella* spp. abundance of 624 cells $mL^{-1}$. The cryptophyte group occurred throughout the sampling period with high abundance up to $1.2 \times 10^3$ cells $mL^{-1}$ on 7th August 2014 following the dinoflagellate bloom at the GM station on 10th July 2014.

Higher cell numbers occurred at the BP station, relative to the previous two stations in the lower estuary (RM and FP) as shown in Figure 5-19 C. Low phytoplankton abundance was observed from 27th May to 25th June 2014 and 21st August to 4th September 2014, and total cell numbers varied between $1.6 \times 10^3$ and $5.1 \times 10^3$ cells $mL^{-1}$. Cryptophytes were the dominant group during this period, and pennate diatoms followed in abundance. On 10th July 2014, total phytoplankton abundance increased to $9.7 \times 10^3$ cells $mL^{-1}$ and was characterised by a mixed assemblage of chlorophyte, cryptophyte, and dinoflagellate species, including *Pyramimonas* sp. ($4.2 \times 10^3$ cells $mL^{-1}$), *Cryptomonas* spp. ($1.7 \times 10^3$ cells $mL^{-1}$), and *Kryptoperidinium foliaceum* ($1.5 \times 10^3$ cells $mL^{-1}$). *Rhodomonas* spp. (573 cells $mL^{-1}$) was also abundant on this day and *Teleaulax* spp. was found at this station during all sampling dates except for 27th May 2014, showing abundance that varied between 16 (4th September 2014) and $2.2 \times 10^3$ cells $mL^{-1}$ (12nd June 2014). On 10th July 2014 an increase in *K. foliaceum* abundance was observed, and this may have been caused by the concentration of this dinoflagellate moving downwards from the GM station. *K. foliaceum* abundance at this station was highest on 24th July 2014 ($1.6 \times 10^3$ cells $mL^{-1}$) and sharply decreased on 7th August 2014 (106 cells $mL^{-1}$). On 24th July 2014, *Rhodomonas* spp. was present in high abundance ($6.6 \times 10^3$ cells $mL^{-1}$). The centric diatom

*Chaetoceros* spp. became the dominant species on 7th August 2014 ($5.9 \times 10^3$ cells $mL^{-1}$) with *Stephanodiscus* sp. also present at $2.1 \times 10^3$ cells $mL^{-1}$.

At the GM station, phytoplankton abundance varied between $1.2 \times 10^3$ and $26.3 \times 10^3$ cells $mL^{-1}$ (Figure 5-19 D). The dinoflagellate species *Kryptoperidinium foliaceum* was the main species present on 10th July 2014 ($18.3 \times 10^3$ cells $mL^{-1}$) followed by *Rhodomonas* spp. on 24th July 2014 ($13.7 \times 10^3$ cells $mL^{-1}$) and *Cryptomonas* spp. on 21st August 2014 ($10.9 \times 10^3$ cells $mL^{-1}$) respectively. On 24th July 2014 the chlorophytes *Pyramimonas* sp., *Scenedesmus* spp. and other chlorophytes were the most abundant species ($5 \times 10^3$ cells $mL^{-1}$). However, on the next sampling date, on 7th August 2014, high densities of cryptomonads were observed ($11.9 \times 10^3$ cells $mL^{-1}$), together with a mixed assemblage of diatoms including *Chaetoceros* spp. and *Stephanodiscus* sp. ($1.5 \times 10^3$ and $1.8 \times 10^3$ cells $mL^{-1}$). *K. foliaceum* was extremely abundant ($18.3 \times 10^3$ cells $mL^{-1}$) with total chlorophyll concentration of 93 µg $L^{-1}$ on 10th July 2014. On the next sampling date (24th July 2014) the small cryptophyte *Rhodomonas* spp. was most abundant ($15.4 \times 10^3$ cells $mL^{-1}$, 20.9 µg Chl *a* $L^{-1}$). In June 2014 the chlorophyte species presented high abundance up to $3.3 \times 10^3$ and $2.4 \times 10^3$ cells $mL^{-1}$ and then sharply decreased during the dinoflagellate bloom on 10th July 2014 and increased again on the next sampling date (24th July 2014) $5 \times 10^3$ cells $mL^{-1}$. On 27th May 2014 the diatoms dominated at this station (79%) followed by the cholorophyte group in June 2014 with 70 and 45% respectively (Figure 5-19 J). On 10th July 2014 the dinoflagellate community showed the highest proportion of phytoplankton representing 71% of the total abundance and then later sampling dates the cryptophyte group was the dominant phytoplankton (62 – 84%).

At the CQ station, lower cell numbers were observed on 25th May 2014, relative to the previous stations (Figure 5-19 E). High chlorophyte abundances occurred in June 2014 and total cell numbers varied between $25.1 \times 10^3$ and $39.6 \times 10^3$ cells $mL^{-1}$. *Chlorella* spp. was the dominant chlorophyte species during this period. On 10th July 2014, total phytoplankton abundance decreased to $2.1 \times 10^3$ cells $mL^{-1}$ and rose again on 24th July 2014 with a high abundance of cryptophyte cells ($2.2 \times 10^3$ cells $mL^{-1}$). Following this day cryptophytes were dominant followed by diatoms throughout the sampling period. *Chaetoceros* spp. and *Stephanodiscus* sp. were observed at $1.5 \times 10^3$ and $3.2 \times 10^3$ cells $mL^{-1}$ on 7th August 2014 at this station (Figure 5-2 F).

At the TB station, total phytoplankton abundance was comparable to the CQ station and ranged between $1.6 \times 10^3$ and $39.6 \times 10^3$ cells $mL^{-1}$ (Figure 5-19 F). Freshwater

chlorophytes were more numerous in June and July 2014 and included *Chlorella* spp. on 12$^{nd}$ and 25$^{th}$ June 2014, *Coelastrum* spp. and *Scenedesmus* spp. ($1.1 \times 10^3$ and $1.2 \times 10^3$ cells mL$^{-1}$) on 24$^{th}$ July 2014. On 7$^{th}$ August 2014 high diatom cell abundance was observed, with *Chaetoceros* spp. and *Stephanodiscus* sp. dominant species, suggesting mixing of freshwater from the Stour River and coastal water at this station. On this sampling date the cryptophytes *Cryptomonas* spp. and *Rhodomonas* spp. were also the dominant species, representing $1.4 \times 10^3$ and $1.1 \times 10^3$ cells mL$^{-1}$ respectively. On the next sampling date (21$^{st}$ August 2014) *Cryptomonas* spp. increased in cell numbers to $2.9 \times 10^3$ cells mL$^{-1}$, while *Rhodomonas* spp. was 368 cells mL$^{-1}$. The proportion of each phytoplankton group showed a similar pattern to the CQ station as shown in Figure 5-19 L. The chlorophyte group showed a high percentage of phytoplankton abundance in June and July 2014 (60 – 94%) and then on 7$^{th}$ August 2014 the diatoms increased in proportion (55%). On 21$^{st}$ August and 4$^{th}$ September 2014 the cryptophyte population became the major percentage of phytoplankton cell numbers, representing 81 and 80% respectively.

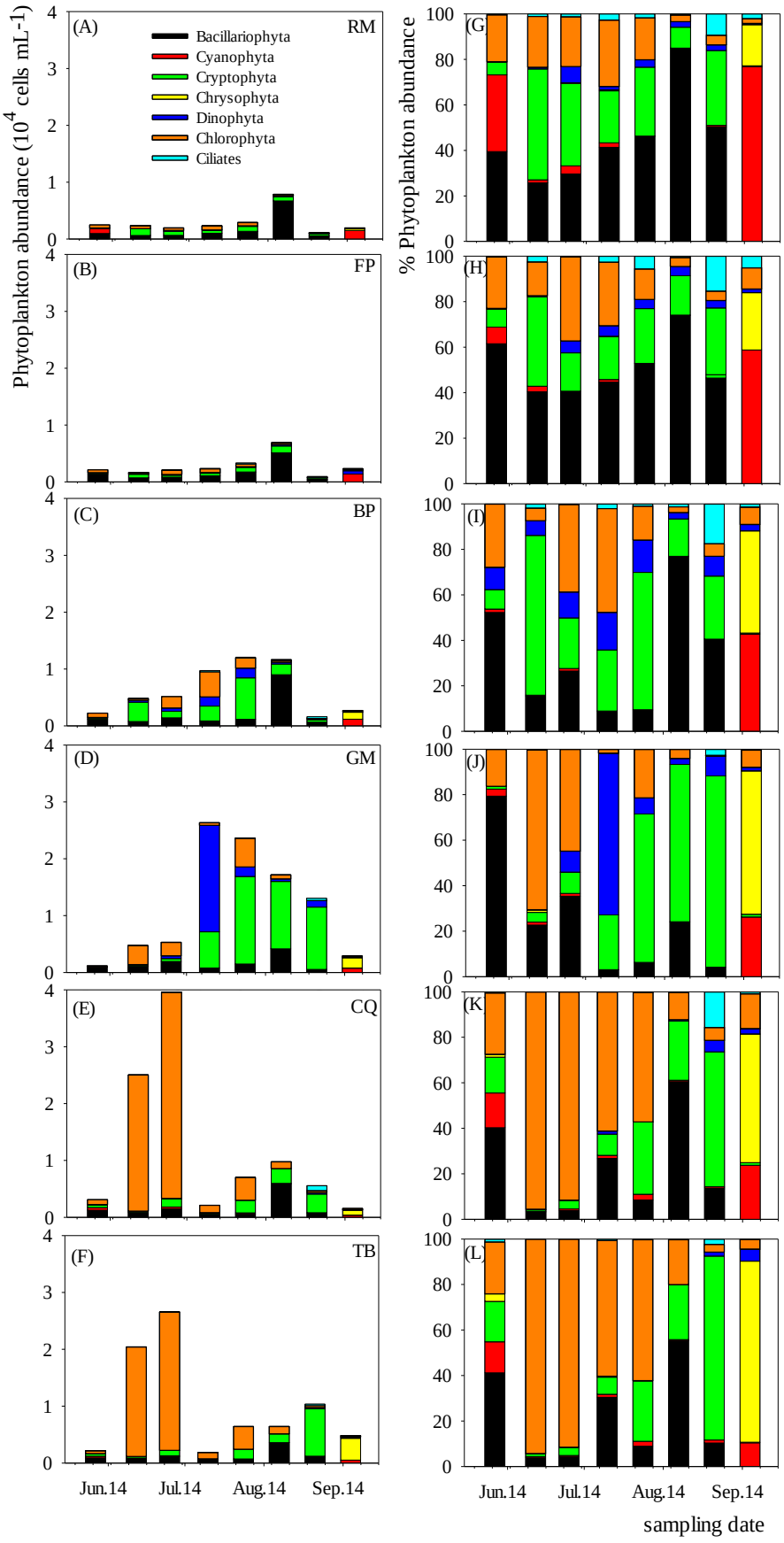


Figure 5-19: Phytoplankton abundance in cells $mL^{-1}$ (A – F) and percentages (G – L) for the main phytoplankton groups at the six estuarine stations during the transect sampling in 2014. Bar colours in upper panel apply to all panels.

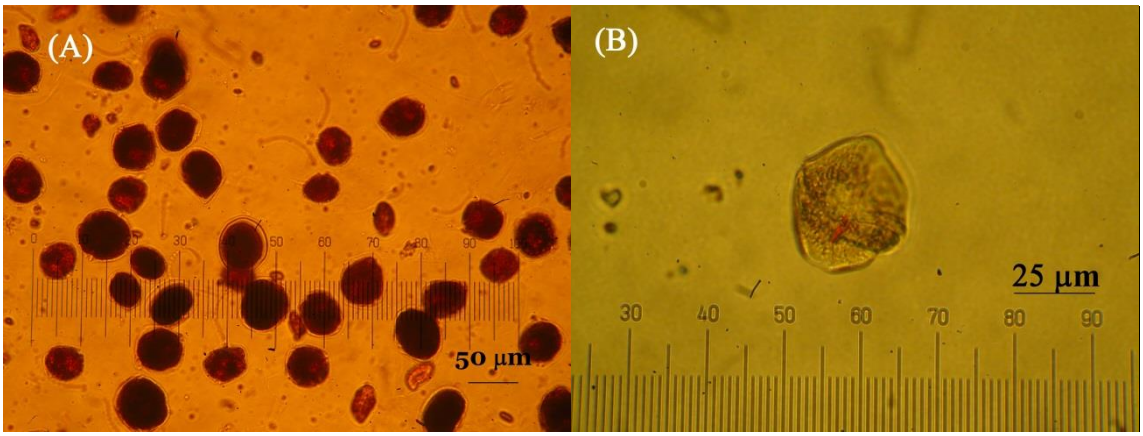


Figure 5-20: The dinoflagellate species, *Kryptoperidinium foliaceum*, at Grimbury Marsh on 10th July 2014, Lugol's fixation (A) and live cell (B).

#### 5.3.3.2 Phytoplankton bio-volume and carbon biomass

Phytoplankton cell numbers were converted to carbon biomass and percentage distribution (Figure 5-21) following published equations (see Section 2.7).

*Kryptoperidinium foliaceum* and *Cryptomonas* spp. were among the most abundant species in the estuary, particularly in the mid and upper estuary zones during the summer months in 2014. These species are an important component of the phytoplankton community and they also contribute significantly to phytoplankton carbon biomass due to their large size. Smaller species (< 20 µm long), that are important in terms of cell abundance; do not contribute greatly to the carbon component, e.g. *Chaetoceros* spp. and *Rhodomona*s spp. Some species, such as *Guinardia delicatula* was less abundant than *Chaetoceros* spp., but they contributed significantly to the total carbon biomass due to their larger size.

High phytoplankton biomass was observed during July to August 2014 in the estuary, mainly due to the *K. foliaceum* and *Cryptomonas* spp. bloom at the GM and BP stations. In May and June 2014, considerably lower phytoplankton biomass occurred, except in the upper estuary. While in the lower estuary (RM and FP) higher carbon biomass was present on the last sampling date.

The correlation between chlorophyll *a* and carbon biomass for the estuarine stations is shown in Figure 5-22. The carbon biomass to chlorophyll ratio was 171, which is comparable to that observed with the spot sampling at Mudeford Quay in 2013 – 14 in the previous chapter.

Phytoplankton carbon biomass varied between 106 µg C $L^{-1}$ on 12nd June 2014, and 606 µg C $L^{-1}$ on 7th August 2014 at the RM station (Figure 5-21 A) and between 107 µg C $L^{-1}$ on

27th May 2014, and 524 µg C $L^{-1}$ on 7th August 2014 at the FP station (Figure 5-21 B). The first peak of carbon biomass from both sites was observed on 7th August 2014 due to *Chaetoceros* spp., while the later peak on 4th September 2014 reflected the high biomass of *Guinardia delicatula*.

At BP, the carbon biomass ranged between 268 µg C $L^{-1}$ on 27th May 2014 and $2.1 \times 10^3$ µg C $L^{-1}$ on 24th July 2014 (Figure 5-21 C). Two peaks of phytoplankton carbon biomass in July 2014 were $1.9 \times 10^3$ and $2.1 \times 10^3$ µg C $L^{-1}$ when *K. foliaceum* was the main contributor followed by the cryptophyte carbon biomass. At the GM station, the dinoflagellate *K. foliaceum* represented nearly 96% of the carbon biomass on 10th July 2014 ($18.7 \times 10^3$ µg C $L^{-1}$). The carbon content at this station varied between 125 µg C $L^{-1}$ on 27th May 2014 and $19.6 \times 10^3$ µg C $L^{-1}$ on 10th July 2014.

At CQ, the phytoplankton carbon biomass varied between 196 µg C $L^{-1}$ on 4th September 2014 and 913 µg C $L^{-1}$ on 7th August 2014 (Figure 5-21 E). Diatoms composed the main carbon biomass in May 2014 (*Navicula* sp. and *Diatoma vulgare*) and then the chlorophyte carbon biomass was dominated by *Chlorella* spp. and *Pediastrum* spp.in June and July 2014.

At the Stour River end of the estuary (TB station), the total carbon biomass varied between 163 µg C $L^{-1}$ on 10th July 2014 and $1.4 \times 10^3$ µg C $L^{-1}$ on 21st August 2014 (Figure 5-21 F). The freshwater chlorophytes such as *Pediastrum* spp., *Scenedesmus* spp., and small *Chlorella* spp. were important contributors to the total biomass from May to July 2014. On 7th August 2014 the diatoms and cryptophytes were dominant, representing 352 and 184 µg C $L^{-1}$.

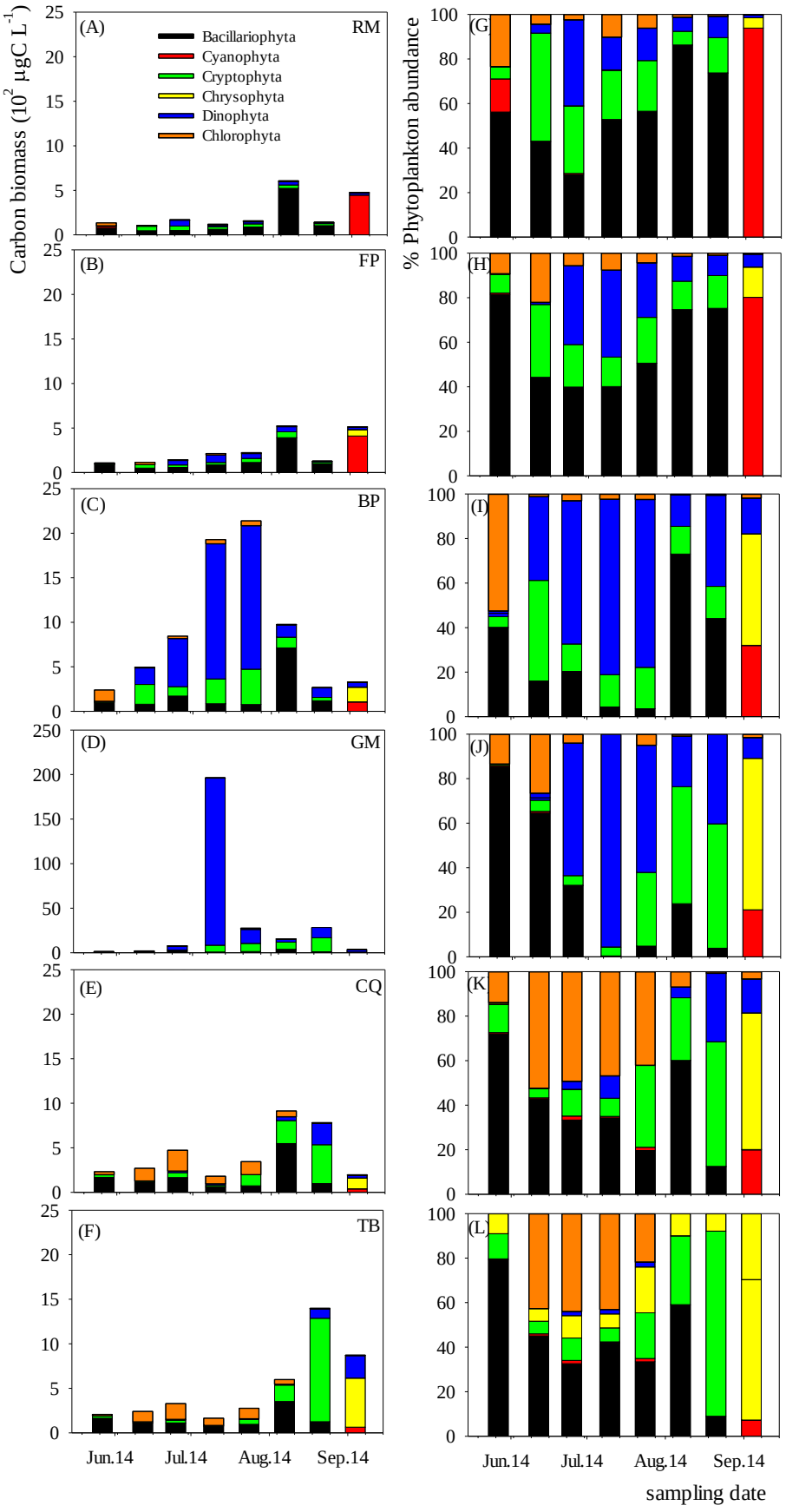


Figure 5-21: Phytoplankton carbon biomass in µg C $L^{-1}$ (A – F) and percentages (G – L) for the main phytoplankton groups at the six estuarine stations during the summer period in 2014. Note change of y scale on D.

The ratio of carbon biomass to chlorophyll *a* varied between 20 and 211 along the estuary during the summer months in 2014 (Figure 5-23). The highest value was associated with the *K. foliaceum* bloom at the GM station on 10th July 2014. The bloom of cryptophytes presented a lower carbon:Chl *a* ratio compared to *K. foliaceum*. The highest carbon to chl *a* ratio at the lower and upper estuary (RM, FP, TB, and CQ) was observed in August 2014, while the mid estuarine stations (GM and BP) presented the highest values in July 2014.

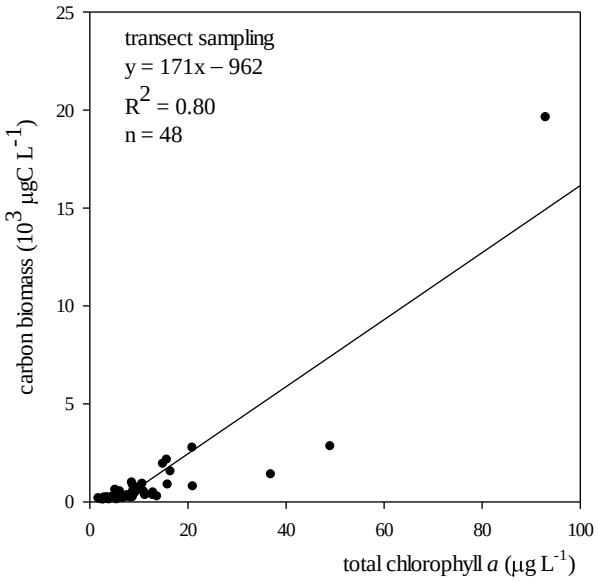


Figure 5-22: Correlation between total phytoplankton carbon biomass (µg C $L^{-1}$) and total chlorophyll *a* (µg $L^{-1}$) for the six estuarine stations during the summer months in 2014.

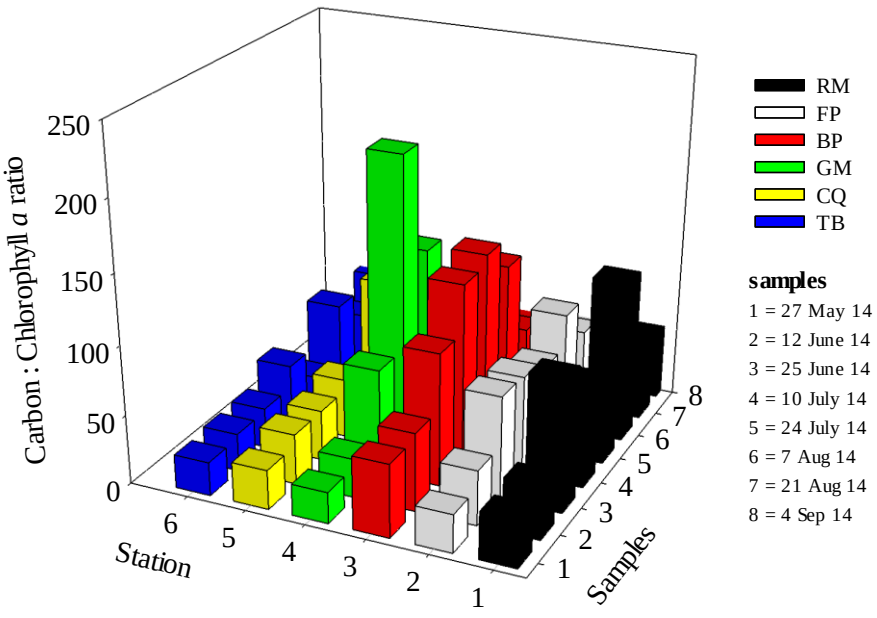


Figure 5-23: Carbon biomass to chlorophyll *a* ratio during the transect sampling in the Christchurch Harbour estuary.

#### 5.3.3.3 Phytoplankton species composition

The phytoplankton species cell counts and carbon biomass for three of the transect sampling stations are given in Table 5-2 and Table 5-3. In terms of species abundance, the stations are quite different as described in Sections 5.3.3.1 and 5.3.3.2. The species contribution was shown to differ depending on the sampling location and salinity value. The freshwater phytoplankton populations generally occurred in the surface water and the upper-estuarine stations (TB and CQ), while at the other stations (RM and FP) there was a combination of freshwater and marine species. In addition dinoflagellates were most abundant at the GM station, due to the high contribution of *Kryptoperidinium foliaceum*. The cryptomonad, (*Crpytomonas* and *Rhodomonas*) were also present during the *K. foliaceum* blooms at the GM station and these increased after the dinoflagellate bloom decreased. The coastal diatom species, *Chaetoceros* spp. and *Skeletonema* spp, were mainly observed in August 2014 as high salinity values moved towards the upper estuary (see Section 5.3.1.1).

The phytoplankton biomass values give a different perspective on the species contributions, particularly for diatoms, which had a total biomass less than that of dinoflagellates. A noteworthy species was *Chaetoceros* spp., that was present at almost all stations but with high contributions at the FP and GM stations particularly in August 2014. *Skeletonema* sp. was only found at the FP and RM stations. *Cryptomonas* and *Rhodomonas* sp. contributed the highest biomass at the GM, CQ, and TB stations.

The diatom species, *Chaetoceros* spp., was observed in high abundance up to $4.4 \times 10^3$ cells $mL^{-1}$ at the FB station but represented only a small amount of carbon biomass 338 µg C $L^{-1}$ due to this species having a small cell size.

Table 5-2: Example of phytoplankton abundance (cells $mL^{-1}$) at three estuarine stations during the transect sampling in 2014. Stations are selected to represent the lower (FP), mid (GM), and upper (TB) parts of the estuary.

| **date** | **12nd June 2014** | | | **10th July 2014** | | | **7th August 2014** | | | **21st August 2014** | | |
|---|---|---|---|---|---|---|---|---|---|---|---|---|
| **station** | **FP** | **GM** | **TB** | **FP** | **GM** | **TB** | **FP** | **GM** | **TB** | **FP** | **GM** | **TB** |
| **Chlorophyll *a* (µg $L^{-1}$)** | **2.9** | **6.9** | **8.8** | **3.0** | **93.0** | **3.6** | **6.1** | **16.5** | **10.0** | **2.2** | **49.0** | **36.9** |
| **Bacillariophyta** | | | | | | | | | | | | |
| *Amphora* spp. | 19 | 61 | 60 | 38 | 40 | 46 | 5 | 15 | 13 | 4 | 2 | 12 |
| *Bacillaria paxillifer* | - | 40 | 4 | 11 | 15 | 41 | - | - | 82 | - | - | - |
| *Chaetoceros* spp. | 12 | - | - | 77 | 12 | - | 4,400 | 1,509 | 1,199 | 79 | 53 | 12 |
| *Cocconeis* spp. | 18 | 162 | 79 | 77 | 89 | 137 | 40 | 225 | 212 | 19 | 59 | 156 |
| *Diatoma vulgare* | 5 | 57 | 6 | 9 | 22 | 5 | - | 11 | 7 | - | 2 | 5 |
| *Gomphonema* spp. | 9 | 106 | 61 | 42 | 53 | 45 | 7 | 39 | 46 | 6 | 15 | 18 |
| *Guinardia delicatula* | 7 | - | - | 14 | - | - | 5 | 2 | - | 170 | 174 | 43 |
| *Licmorphora* sp. | 4 | 83 | 22 | 20 | 46 | 30 | 5 | 2 | 9 | - | - | 20 |
| *Melosira* sp. | 9 | 18 | 18 | 7 | 16 | 5 | - | 12 | 9 | 9 | 7 | 9 |
| *Navicula* sp1. | 30 | 104 | 77 | 100 | 91 | 74 | 19 | 84 | 183 | 19 | 62 | 102 |
| *Navicula* spp. | 235 | 91 | 129 | 397 | 225 | 82 | 60 | 152 | 137 | 27 | 63 | 281 |
| *Nitzschia acicularis* | 76 | 6 | 2 | 64 | 16 | 5 | 193 | 62 | 25 | 15 | 5 | 5 |
| *Nitzschia* sp. | 7 | 53 | 28 | 34 | 29 | 18 | - | 18 | 137 | - | 7 | 281 |
| Pennate diatoms | 20 | 34 | 19 | 26 | 45 | 15 | 13 | 27 | 32 | 7 | 9 | 16 |
| *Pseudo-nitzschia* | 79 | 21 | 12 | - | 14 | - | 49 | 15 | 13 | 7 | 16 | 14 |
| *Skeletonema* spp. | - | - | - | - | - | - | 5 | - | - | - | - | - |
| *Stephanodiscus* sp. | 14 | 88 | 122 | 9 | 6 | 7 | 2 | - | 23 | - | 5 | 38 |
| **Dinophyta** | | | | | | | | | | | | |
| *K. foliaceum* | - | 4 | - | 79 | 18,306 | 2 | 26 | 326 | 8 | 8 | 1,113 | 91 |
| **Cryptophyta** | | | | | | | | | | | | |
| *Cryptomonas* spp. | 102 | 28 | 50 | 101 | 4,822 | 47 | 174 | 2,344 | 1,131 | 84 | 10,877 | 7,842 |
| *Rhodomonas* spp. | 310 | 29 | 23 | 163 | 1,435 | 32 | 579 | 9,364 | 410 | 55 | 54 | 533 |
| **Chrysophyta** | | | | | | | | | | | | |
| *Dinobryon* spp. | - | - | 2 | - | - | 2 | - | - | - | - | - | - |
| *Synura sphagnicola* | - | 49 | 2 | 5 | - | - | - | - | - | - | - | - |
| **Chlorophyta** | | | | | | | | | | | | |
| *Ankistrodesmus* spp. | 6 | 63 | 19 | 63 | 22 | 64 | 63 | 33 | 63 | 27 | 5 | 8 |
| *Chlamydomonas* spp. | 5 | 39 | 109 | 39 | 2 | 179 | 39 | 188 | 511 | 8 | 18 | 172 |
| *Chlorella* sp. | 155 | 23 | 18,586 | 23 | 26 | 177 | 23 | - | 2 | - | - | - |
| *Coelastrum* spp. | 23 | 106 | 246 | 106 | 70 | 141 | 106 | 106 | 23 | 70 | - | 13 |
| *Kirchneriella* spp. | 5 | 28 | 11 | 28 | 20 | 46 | 28 | 29 | 45 | 14 | 2 | 15 |
| *Pyramimonas* sp. | - | - | - | 158 | 123 | - | 158 | 86 | 54 | 32 | 5 | 29 |
| *Scenedesmus* spp. | 9 | 206 | 218 | 206 | 158 | 366 | 206 | 220 | 501 | 117 | 19 | 103 |

Table 5-3: Example of phytoplankton carbon biomass (µg C $L^{-1}$) at three estuarine stations during the transect sampling in 2014. Stations are selected to represent the lower (FP), mid (GM), and upper (TB) parts of the estuary.

| **date** | **12nd June 2014** | | | **10th July 2014** | | | **7th August 2014** | | | **21st August 2014** | | |
|---|---|---|---|---|---|---|---|---|---|---|---|---|
| **station** | **FP** | **GM** | **TB** | **FP** | **GM** | **TB** | **FP** | **GM** | **TB** | **FP** | **GM** | **TB** |
| **Chlorophyll *a* (µg $L^{-1}$)** | **2.9** | **6.9** | **8.8** | **3.0** | **93.0** | **3.6** | **6.1** | **16.5** | **10.0** | **2.2** | **49.0** | **36.9** |
| **Bacillariophyta** | | | | | | | | | | | | |
| *Amphora* spp. | 1 | 4 | 4 | 3 | 3 | 3 | 0 | 1 | 1 | 0 | 0 | 1 |
| *Bacillaria paxillifer* | - | 1 | 0 | 0 | 0 | - | - | - | 2 | - | - | - |
| *Chaetoceros* spp. | 1 | - | - | 6 | 1 | - | 338 | 116 | 92 | 6 | 4 | 1 |
| *Cocconeis* spp. | 1 | 10 | 5 | 5 | 6 | 9 | 3 | 14 | 13 | 1 | 4 | 10 |
| *Diatoma vulgare* | 2 | 29 | 3 | 5 | 11 | 2 | - | 21 | 4 | 1 | 15 | 2 |
| *Gomphonema* spp. | 1 | 6 | 3 | 2 | 3 | 2 | 0 | 2 | 2 | 0 | 1 | 1 |
| *Guinardia delicatula* | 2 | - | - | 5 | - | - | 2 | 1 | - | 57 | 58 | 14 |
| *Licmorphora* sp. | 0 | 2 | 1 | 1 | 1 | 1 | 0 | 0 | 0 | - | - | 1 |
| *Melosira* sp. | 3 | 6 | 6 | 3 | 6 | 2 | - | 4 | 3 | 3 | 2 | 3 |
| *Navicula* sp1. | 8 | 26 | 19 | 25 | 23 | 18 | 5 | 21 | 45 | 5 | 15 | 25 |
| *Navicula* spp. | 4 | 2 | 2 | 7 | 4 | 1 | 1 | 3 | 2 | 0 | 1 | 5 |
| *Nitzschia acicularis* | 1 | 0 | 0 | 1 | 0 | 0 | 3 | 1 | 0 | 0 | 0 | 0 |
| *Nitzschia* sp. | 0 | 2 | 1 | 1 | 1 | 1 | - | 1 | 0 | - | 0 | 0 |
| Pennate diatoms | 1 | 2 | 1 | 2 | 3 | 1 | 1 | 2 | 2 | 0 | 1 | 1 |
| *Pseudo-nitzschia* | 8 | 2 | 1 | - | 1 | - | 5 | 2 | 1 | 1 | 2 | 1 |
| *Skeletonema* spp. | - | - | - | - | - | - | 0 | - | - | 1 | - | - |
| *Stephanodiscus* sp. | 1 | 8 | 11 | 1 | 1 | 1 | 1 | - | 2 | 1 | 0 | 3 |
| **Dinophyta** | | | | | | | | | | | | |
| *K. foliaceum* | - | 4 | - | 80 | 18,715 | 2 | 26 | 333 | 8 | 8 | 1,138 | 94 |
| **Cryptophyta** | | | | | | | | | | | | |
| *Cryptomonas* spp. | 15 | 4 | 7 | 15 | 698 | 7 | 25 | 339 | 164 | 12 | 1,573 | 1,134 |
| *Rhodomonas* spp. | 15 | 1 | 1 | 8 | 72 | 2 | 29 | 469 | 21 | 3 | 3 | 27 |
| **Chrysophyta** | | | | | | | | | | | | |
| *Dinobryon* spp. | - | - | 0 | - | - | 0 | - | - | - | - | - | - |
| *Synura sphagnicola* | - | 2 | 0 | 0 | - | - | - | - | - | - | - | - |
| **Chlorophyta** | | | | | | | | | | | | |
| *Ankistrodesmus* spp. | 1 | 2 | 6 | 6 | 2 | 6 | 2 | 3 | 6 | 1 | 0 | 1 |
| *Chlamydomonas* spp. | 0 | 1 | 1 | 0 | 0 | 2 | 0 | 2 | 5 | 0 | 0 | 2 |
| *Chlorella* sp. | 1 | 15 | 98 | 0 | 0 | 1 | - | 2 | 0 | - | 0 | - |
| *Coelastrum* spp. | 0 | 1 | 3 | 1 | 1 | 2 | 1 | 1 | 0 | 0 | - | 0 |
| *Kirchneriella* spp. | 0 | 0 | 0 | 0 | 0 | 0 | 0 | 0 | 0 | 0 | 0 | 0 |
| *Pyramimonas* sp. | 0 | 0 | - | 1 | 1 | - | 0 | 1 | 0 | 0 | 0 | 0 |
| *Scenedesmus* spp. | 0 | 8 | 7 | 7 | 5 | 12 | 4 | 7 | 17 | 1 | 1 | 3 |

#### 5.3.3.4 Succession of phytoplankton taxa and pigments

Phytoplankton succession over the summer period in 2014 is shown in Figure 5-24 as absolute contributions of carbon for different phytoplankton groups. High dinoflagellate numbers were observed on 10th July 2014 at the GM station and the highest dinoflagellate carbon biomass of *Kryptoperidinium foliaceum* was on the same day (Figure 5-24 B). The diatom carbon biomass followed the dinoflagellate peak at all stations due to *Chaetoceros* spp. and *Guinardia* spp. being the dominant populations (Figure 5-24 A). The next most dominant was the cryptophyte biomass peaking at the GM and TB stations (Figure 5-24 C). The chlorophyte biomass was highest in the upper-estuarine stations as shown in Figure 5-24 D.

These peaks in dinoflagellate and diatom biomass were associated with a peak of the peridinin and fucoxanthin (Figure 5-15 B and C). However, the peak in dinoflagellate biomass on 10th July at the GM station was not associated with a high peridinin concentration as *K. foliaceum* contains fucoxanthin rather than peridinin as a biomarker pigment.

The cryptomonad biomass was higher at GM and the upper estuary stations after the dinoflagellate bloom. The peaks in biomass at these stations showed good agreement with the alloxanthin concentration, as this is a marker pigment for Cryptomonads. The chlorophyll *b* concentrations from the transect sampling did not show good agreement with the chlorophyte biomass, suggesting that small flagellates may not have been effectively enumerated in Lugols samples.

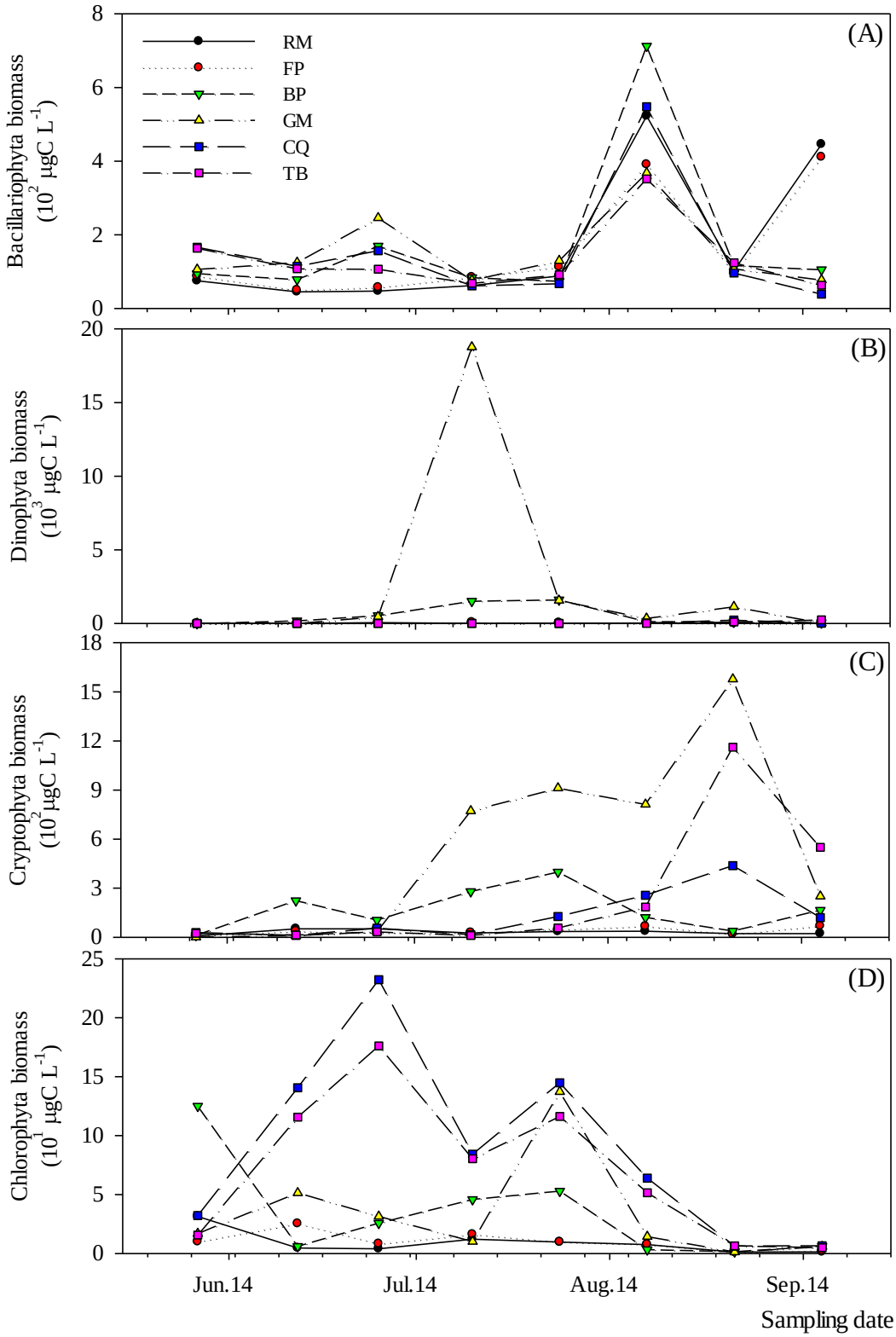


Figure 5-24: The succession of the phytoplankton group biomass at the six estuarine stations. Symbols in upper panel apply to all panels.

### 5.3.4 Phytoplankton abundance and total red fluorescence by flow cytometry

Total red and orange fluorescence of phytoplankton samples were measured using the CytoSense flow cytometer (Figure 5-25), and average red and orange fluorescence values for all estuarine samples are given in Table 5-4. The highest values of total red fluorescence was detected at the GM station, with a maximum of $245 \times 10^7$ a.u. $mL^{-1}$ on 10th July 2014 during the dinoflagellate bloom (Figure 5-25 D). The highest value in total orange fluorescence was also observed at the same site and sampling day, with a maximum of $8.8 \times 10^7$ a.u. $mL^{-1}$. The RM station had the lowest averages of both total red and orange fluorescence, while the highest fluorescences were observed at GM during the transect sampling.

Cell counts derived from CytoSense analysis where significantly higher than cell counts estimated from Lugol's preserved samples. This is due to the many small cells (< 5 µm) that are counted by the CytoSense not generally visible by microscopic counts

Table 5-4: Mean red and orange fluorescence ($10^7$ a.u. $mL^{-1}$) by the CytoSense flow cytometer, with standard deviation for six estuarine stations.

| | Mean values ($10^7$) ± standard deviation ($10^7$) | |
|---|---|---|
| Station | total red fluorescence | total orange fluorescence |
| Run at Mudeford | 16.5 ± 6.5 | 1.0 ± 0.4 |
| Ferry Pontoon | 100.8 ± 21.2 | 9.9 ± 23.4 |
| Blackberry Point | 42.9 ± 44.2 | 2.4 ± 1.9 |
| Grimbury Marsh | 411.1 ± 904.9 | 16.1 ± 31.9 |
| Christchurch Quay | 69.2 ± 68.7 | 5.9 ± 9.0 |
| Tuckton Bridge | 77.4 ± 101.3 | 11.5 ± 21.1 |

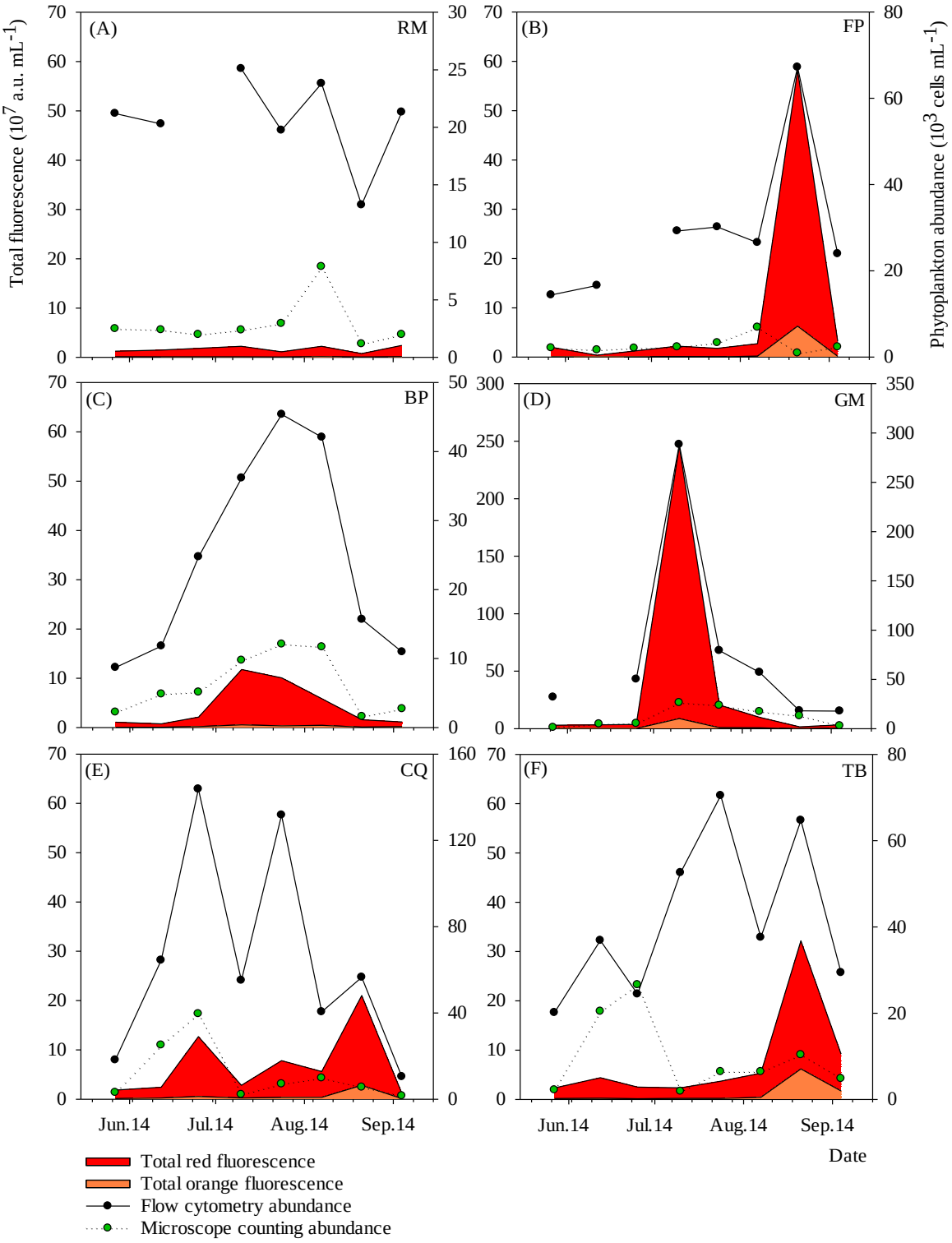


Figure 5-25: Distribution of red and orange fluorescence ($10^7$ a.u. $mL^{-1}$) and phytoplankton abundance (cells $mL^{-1}$) for the six estuarine stations. The solid line and black circles symbol are flow cytometry abundance. The dotted lines and green symbols are microscopic abundance. Note change of scale on all second y axis and y axis on figure D.

### 5.3.5 Nutrients uptake rates

Uptake rates of nitrogen (ammonium and nitrate) and carbon by the natural estuarine phytoplankton in the Christchurch Harbour estuary during the summer transects in 2014 as estimated by stable isotope uptake are shown in Table 5-5 and Figure 5-26. No nutrient uptake rates were measured on samples collected from the first estuarine transect sampling. In general, the nitrate and carbon uptake rates followed the chlorophyll concentrations observed (Figure 5-13, Figure 5-26 A and C), while the highest uptake rates were most significantly at the GM station during the dinoflagellate bloom on 10$^{th}$ July 2014. Uptake rates of ammonium were consistently higher than uptake rates of nitrate (Table 5-5) in all incubations. Both nitrogen and carbon uptake rates also tended to be higher in less saline water (CQ and TB), and mid-estuarine waters (BP and GM) than in more saline samples (RM and FP).

The uptake rates of nitrateand carbon were particularly high for the *Kryptoperidinium foliaceum*-dominated sample from the GM station on 10$^{th}$ July 2014 (8.63 µmol-N L$^{-1}$ h$^{-1}$, and 15.88 µmol-C L$^{-1}$ h$^{-1}$, respectively) The next peak of carbon uptake was also at GM coincident with a peak of chlorophyll on 21$^{st}$ August 2014 although nitrate uptake rates were lower. The upper estuarine stations (TB and CQ) had lower nitrate uptake rates than GM and uptake generally followed the pattern of chlorophyll concentration (Figure 5-26). The lower estuarine stations (RM and FP) had rates of < 0.4 µmol-N L$^{-1}$ h$^{-1}$ and < 3.0 µmol-C L$^{-1}$ h$^{-1}$ of nitrogen and carbon respectively throughout the sampling.

During the sampling period, the nitrogen uptake rates for nitrate and ammonium were generally < 2 and 0.5 µmol-N L$^{-1}$ h$^{-1}$, respectively, except on 10$^{th}$ July 2014 at the GM station (Figure 5-26 A and B). The carbon uptake rates were generally < 5 µmol-C L$^{-1}$ h$^{-1}$ at all study sites, except the GM site on two sampling days which corresponded to high nitrate uptake (Figure 5-26 C). Figure 5-27 shows scatter plots of nitrate, ammonium and carbon uptake rates compared with chlorophyll and cell carbon concentrations for all incubations. Carbon uptake rates (µmol-C L$^{-1}$ h$^{-1}$) compared with fluorescence derived chlorophyll concentrations (µg L$^{-1}$) and phytoplankton carbon biomass (µg C L$^{-1}$) for all stations on each of the sampling days (except for the first sampling date) showed a positive relationship (Figure 5-27 E and F). In contrast, however, similar plots comparing nitrate and ammonium uptake rates with chlorophyll and carbon biomass concentration showed more scatter (Figure 5-27 A– D).

Table 5-5: Nitrogen and carbon uptake rates in the Christchurch Harbour estuary; mean (bold) and range of variation (parentheses) during the productive summer period in 2014.

| Station | **Nitrate** µmol-N $L^{-1}$ $h^{-1}$ | **Ammonium** µmol-N $L^{-1}$ $h^{-1}$ | **Carbon** µmol-C $L^{-1}$ $h^{-1}$ |
|---|---|---|---|
| Run at mudeford | **0.14** (0.04 – 0.27) | **0.09** (0.04 – 0.21) | **0.72** (0.26 – 1.89) |
| Ferry Pontoon | **0.21** (0.08 – 0.34) | **0.09** (0.04 – 0.14) | **0.83** (0.39 – 2.58) |
| Blackberry Point | **0.43** (0.04 – 1.04) | **0.08** (0.03 – 0.11) | **1.23** (0.00 – 3.44) |
| Grimbury Marsh | **2.13** (0.54 – 8.63) | **0.17** (0.02 – 0.43) | **4.54** (0.48 – 15.88) |
| Christchurch Quay | **0.98** (0.44 – 1.38) | **0.23** (0.11 – 0.47) | **1.32** (0.44 – 2.85) |
| Tuckton Bridge | **1.00** (0.41 – 1.81) | **0.21** ( 0.09 – 0.29) | **1.48** (0.23 – 4.16) |

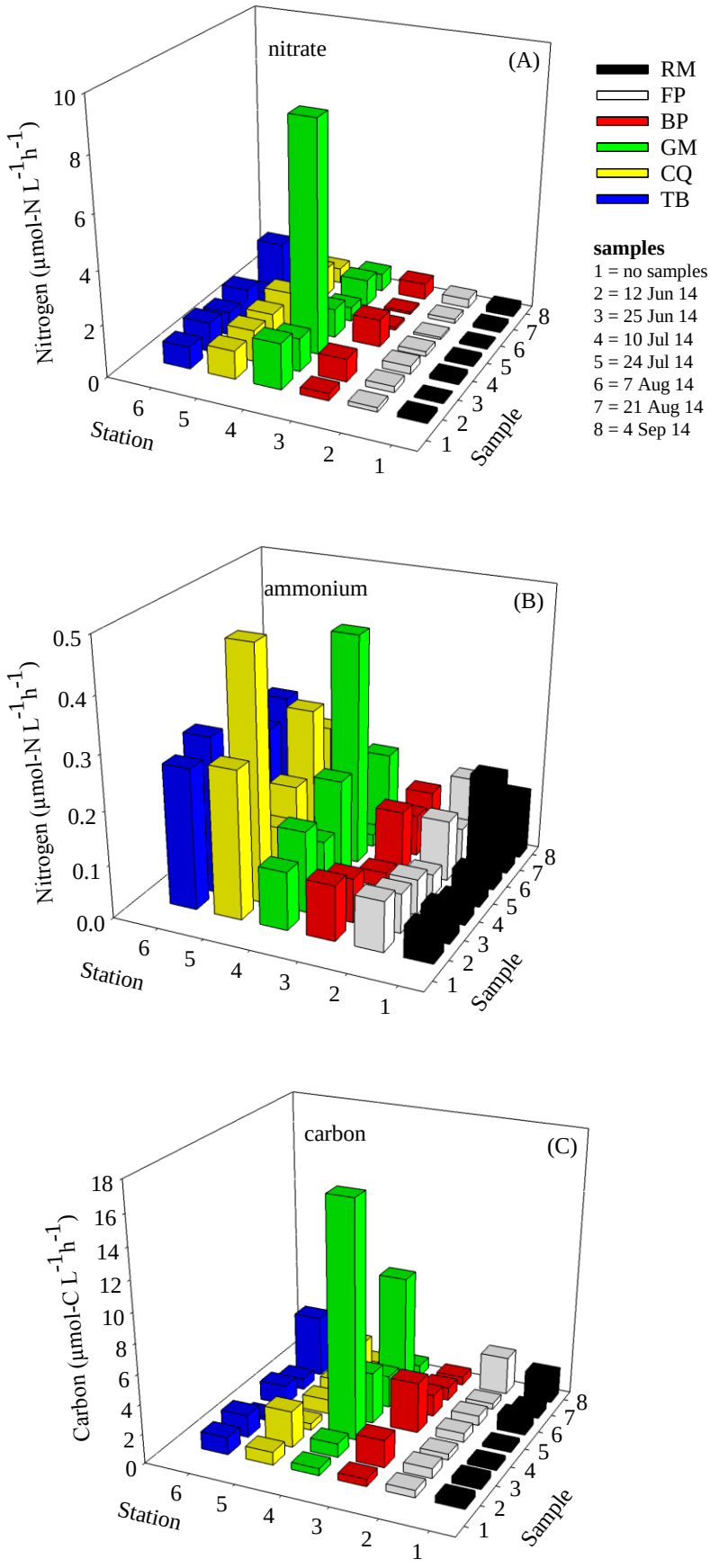


Figure 5-26: Nitrogen and carbon uptake rates (A) nitrate, (B) ammonium, and (C) carbon during transect sampling in the Christchurch Harbour estuary for the six estuarine stations.

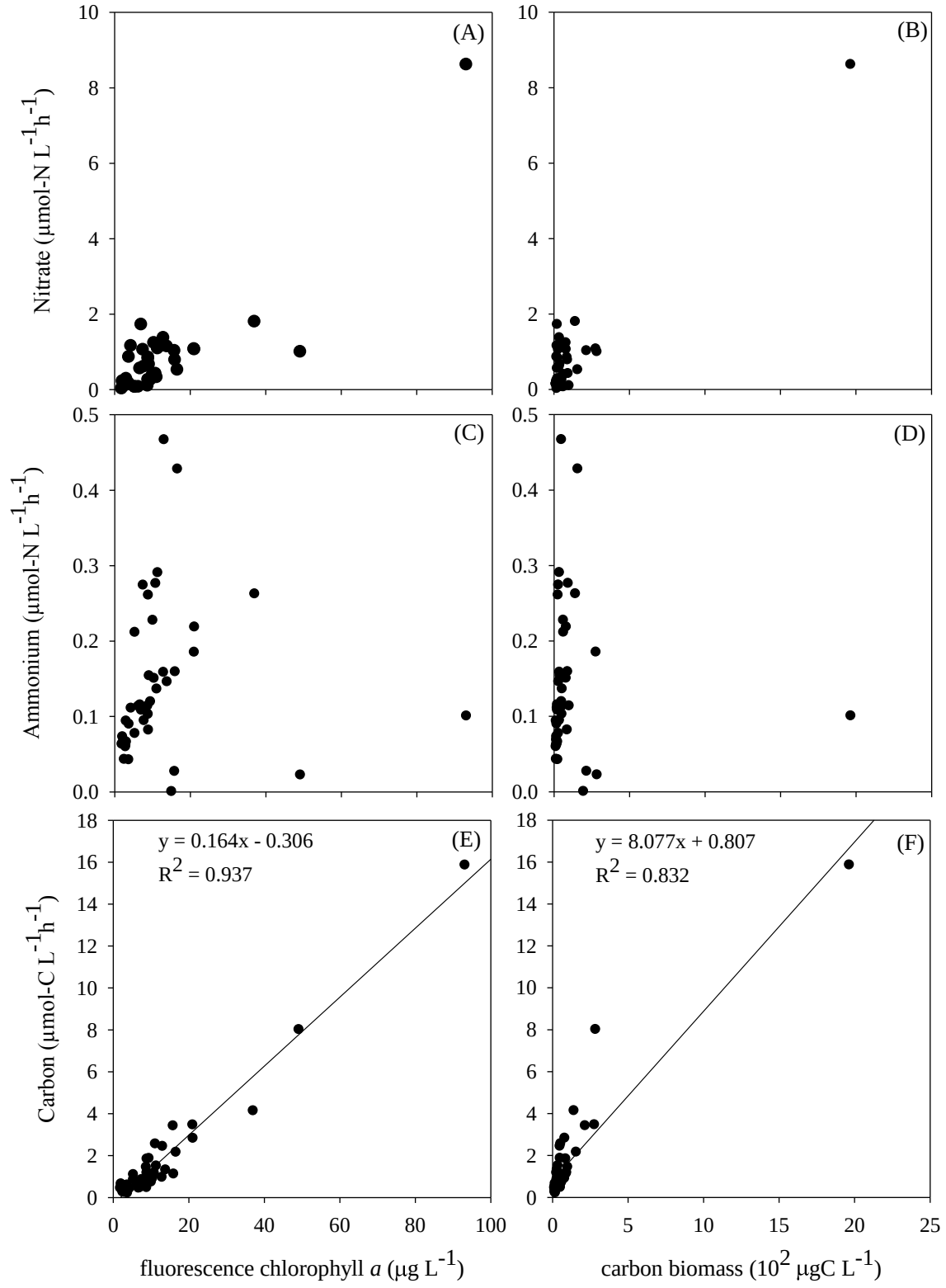


Figure 5-27: Relationship between nutrients uptake rates and fluorescence derived chlorophyll *a* concentrations (A – C), and carbon biomass (D – E) during summer 2014 along the Christchurch Harbour estuary.

### 5.3.6 Multivariate data analysis and interpretation

In order to better understand linkages between variable multivariate analysis that provides statistical methods for the study of the cooperative relationships of variables in data that contain inter-correlations was used. The patterns of relationships between samples can be described by ordination (nMDS) or by cluster analysis. CANOCO was used identify any temporal pattern of phytoplankton community change in the Christchurch Harbour estuary.

#### 5.3.6.1 Environmental data analyses

Cluster and nMDS analysis of environmental data are based on a normalised Euclidean distance after previous log transformation of the data. The cluster and nMDS analysis included the variables nitrate, phosphate, silicate, salinity, irradiance attenuation coefficient (*k*), water temperature, oxygen saturation, and turbidity (Figure 5-28 and Figure 5-29). The stress of nMDS was 0.13. corresponding to a good ordination with no real prospect of a misleading interpretation (Clarke *et al.*, 2014). The cluster dentrogram shows separation at a normalised Euclidean distance of 2.9 into seven major groups (Figure 5-28).

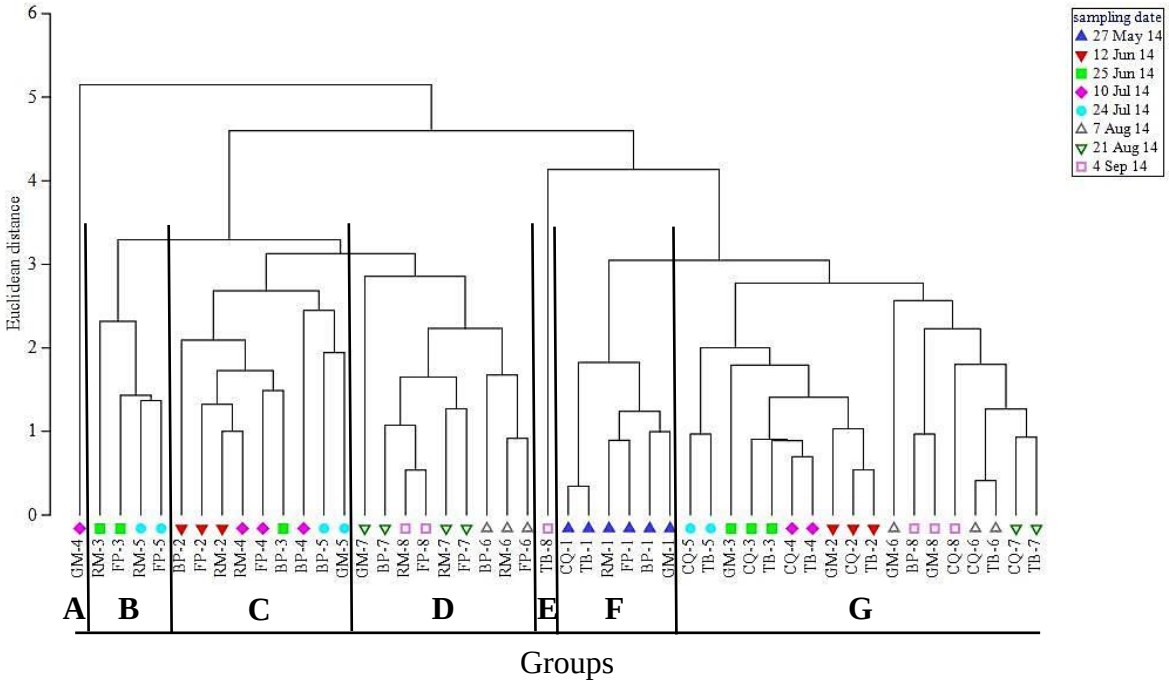


Figure 5-28: Dendrogram for hierarchical clustering of fortnightly transect samples defined by selected environmental parameters. The abbreviation of each marker refers to the station names, followed by the fortnightly sample.

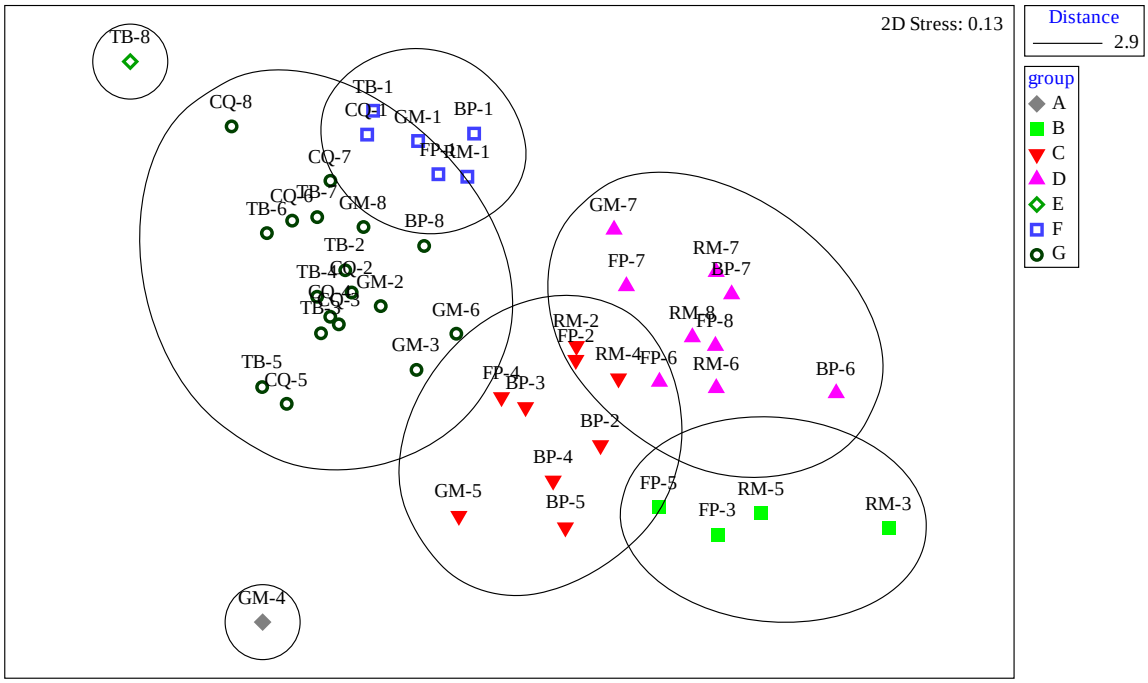


Figure 5-29: nMDS plot of environmental parameter groups for fortnightly transect sampling. The abbreviation of each marker refers to the station name, followed by the fortnightly sample.

These results indicate no average square distance of environmental parameters at Tuckton Bridge (TB) and Grimbury Marsh (GM) stations from other stations on 10th July and 4th September 2014 (group A and E) and low square distance of samples collect on 27th May 2014 at all stations using SIMPER analysis, considering *k*, salinity, and phosphate data, as those samples were grouped together in group F as shown in Table 5-6. Indeed, all samples in group F were collected only from the surface and not at the depth of the highest fluorescence as done on other sampling days. Group G corresponds to samples from the upper and middle estuarine stations throughout the sampling period except on 27th May 2014, with grouping by turbidity, oxygen saturation, temperature, and phosphate variables (see Table 5-6). Group B includes the lower stations (RM and FP) on 25th June and 24th July 2014, while group C contains samples of these stations plus BP and GM from June to July 2014. Group D is mostly composed of samples from August to September 2014 at the middle and lower estuarine stations with grouping by *k*, temperature, salinity, and nitrate variables (see Table 5-6). The *k* variable was an important parameter assembling the samples in group B, C, D, and F.

Table 5-6: Main characteristics of sample groups defined by selected environmental parameters for fornightly transect sampling. The abbreviation of each marker refers to the station name, followed by the fortnightly sample.

| Group | Station & Sample | Parameter % contribution | Average square distance |
|---|---|---|---|
| A | GM-4 | single sample | - |
| B | RM-3, RM-5, FP-3, FP-5 | *k* (39), silicate (21), temperature (12), nitrate (10) | 1.90 |
| C | RM-2, RM-4, FP-2, FP-4, BP-2, BP-3, BP-4, BP-5, GM-5 | *k* (38), temperature (23), oxygen saturation (17) | 2.75 |
| D | RM-6, RM-7, RM-8, FP-6, FP-7, FP-8, BP-6, BP-7,GM-7 | *k* (28), temperature (21), salinity (19), nitrate (14) | 2.44 |
| E | TB-8 | single sample | - |
| F | RM-1, FP-1, BP-1, GM-1, CQ-1, TB-1 | *k* (56), salinity (23), phosphate (10) | 1.20 |
| G | BP-8, GM-2, GM-3, GM-6, GM-8, CQ-2, CQ-3, CQ-4, CQ-5, CQ-6, CQ-7, CQ-8, TB-2, TB-3, TB-4, TB-5, TB-6, TB-7 | turbidity (42), oxygen saturation (18), temperature (12), phosphate (11) | 2.89 |

#### 5.3.6.2 Phytoplankton taxa and biomass data analyses

A shade plot (Figure 5-30) indictes the most important species for carbon biomass from transect samples. The cryptomonad and dinoflagellate groups show a clear pattern followed by the diatom and chlorophyte groups from May to September in 2014. The abundant dinoflagellate species, *Kryptoperidinium foliaceum*, gave the most weight in July particularly in the mid-estuary, while the cryptomonads species, *Cryptomonas* sp. and *Rhodomonas* sp. was the major biomass after the dinoflagellate bloom in August 2014. The cryptophyte species, *Cryptomonas* sp. and *Rhodomonas* sp. were most dominant during the summer time. The riverine diatom species *Diatoma vulgare* had the most biomass in the samples from May to June 2014, whereas, the coastal diatom species such as *Chaetoceros*

spp. and *Guinardia delicatula* had a significant biomass as salinity increased mid-estuary in August and September 2014. The carbon biomass of the pennate diatom *Navicula* sp.1 had a high weighting throughout the sampling period.

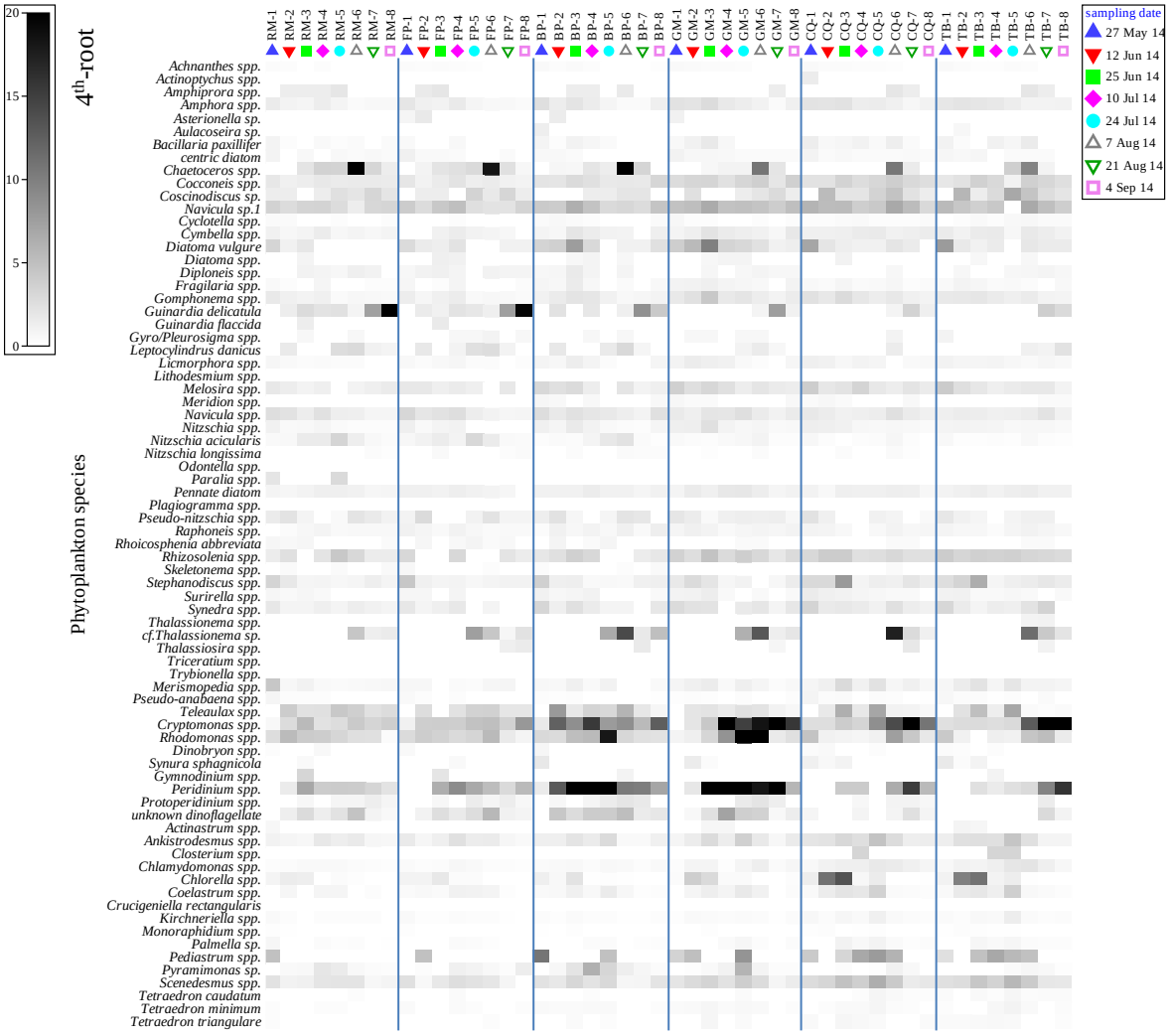


Figure 5-30: Shade plot indicating carbon biomass of each phytoplankton species ($4^{th}$-root transformed data on a log scale) for transect samples. The abbreviation of each marker refers to the station name, followed by the fortnightly sample.

Cluster and nMDS analysis of phytoplankton species carbon biomass are based on Bray-Curtis similarities. The stress of nMDS was 0.16, which indicates a potential useful 2-dimensional picture, though too much reliance should not be placed on the detail of the plot, and cross-checks of any conclusions should be made against those from an alternative method, like the superimposition of cluster groups (Clarke *et al.*, 2014). Four biomass groups can be identified at 69% Bray-Curtis similarity level in the clusters (Figure 5-31) and on the nMDS analysis (Figure 5-32).

Group A is composed of all samples that were collected on 27th May 2014 plus the samples at the TB and CQ stations between June and July 2014, considering several phytoplankton species were group together using the SIMPER analysis (Table 5-7). Group B represents samples from the middle and lower estuarine stations on 21st August and 4th September 2014, while group D is mainly composed of the high biomass samples from the RM and FP stations between June and mid-August 2014. Furthermore, these two groups were close on the 2D nMDS plot as shown in Figure 5-32 and the samples in group B had the highest percentage of similarity (Table 5-7). Group C mostly represents samples from the mid- and upper estuary throughout the sampling period except the samples collected on 27th May 2014 and the dinoflagellate bloom sample (GM-4) is included with this group.

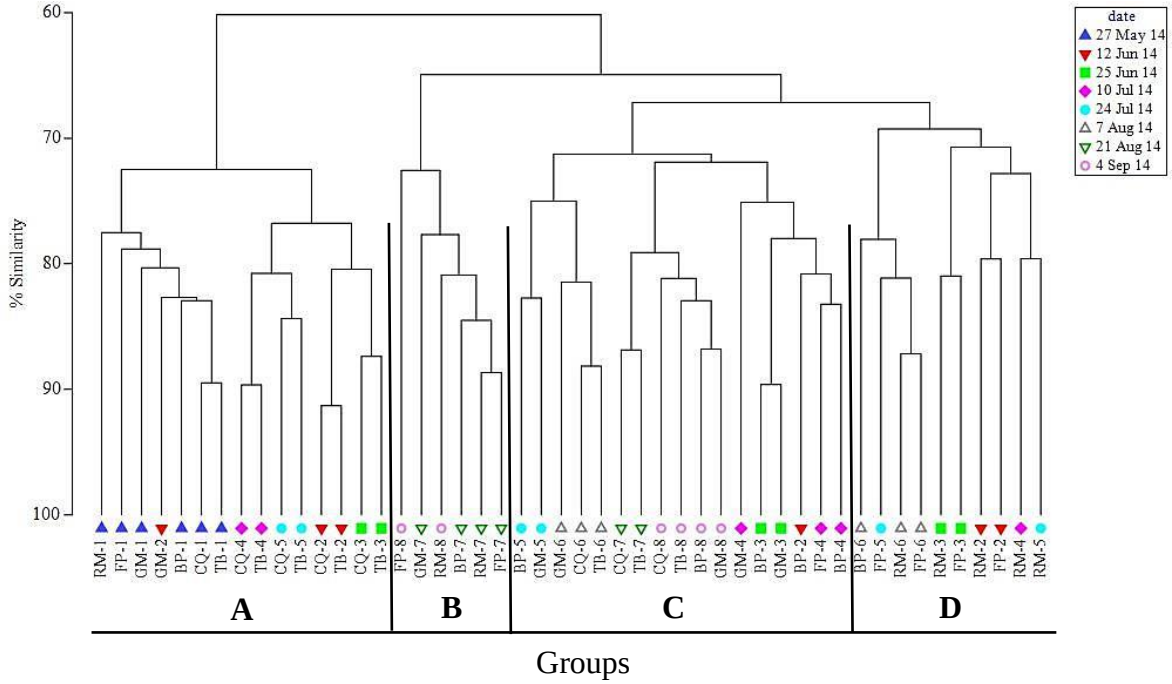


Figure 5-31: Dendrogram for hierarchical clustering of samples defined by phytoplankton carbon biomass for transect samples. The abbreviation of each marker refers to the station name, followed by the fortnightly sample.

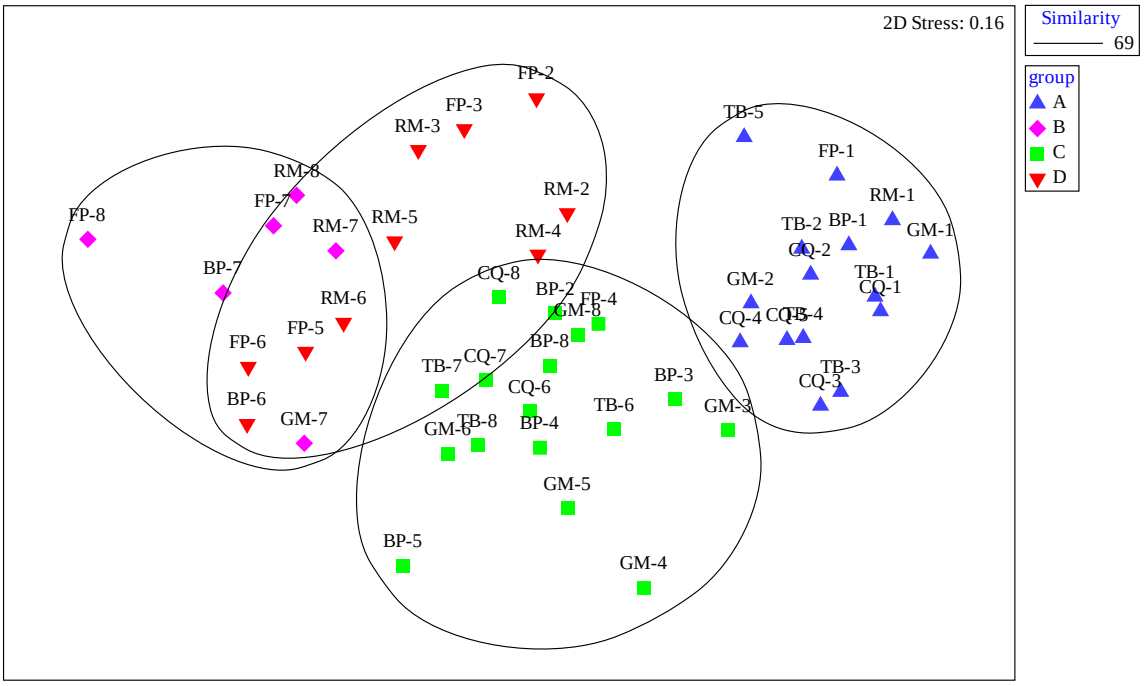


Figure 5-32: nMDS plot of samples defined by phytoplankton species/taxon carbon biomass for transect samples. The abbreviation of each marker refers to the station name, followed by the fortnightly sample.

Some temporal changes are entering to note. Species in the mid- and upper estuary from group A, initially present in the first sampling day on 27th May 2014 were not replaced by the other species at these stations. Whereas, the lower estuary changed from cryptomonads and dinoflagellate species from group C and D during June to the mid-August 2014. These biomass species assemblages were later observed to be abundant in the middle estuary and were probably flushed out from the estuary during this period. A major species from group B in the mid- and lower estuary on 21st August and 4th September 2014 was the marine species *Guinardia delicatula* and this gave up to a 9.3% contribution as shown in Table 5-7.

*Rhodomonas* spp., *Cryptomonas* spp., and *Kryptoperidinium foliaceum* were important contributors to several groups. Some groups are differentiated by the species associated with these biomass species and others by the percentage of contribution of these species, that peak at group C. Their cell sizes are large compared with other species and occurred in high abundance during the sampling period. *Cryptomonas* spp. and *K. foliaceum* are the important biomass contributors in the groups.

Table 5-7: All characteristics of sample groups by phytoplankton species for transect samples during the high productive period of 2014 in the Christchurch Harbour estuary.

| Group | Station and sample | Species average carbon biomass as % contribution | % of similarity |
|---|---|---|---|
| A | RM-1, FP-1, BP-1, GM-1, CQ-1, TB-1, GM-2, CQ-2, TB-2, CQ-3, TB-3, CQ-4, TB-4, CQ-5, TB-5 | *Navicula* sp.1 (4.9), *Scenedesmus* spp. (4.4), *Rhizosolenia* spp. (4.4), *Cocconeis* spp.(3.9), *Melosira* spp. (3.8), *Stephanodiscus* spp. (3.8), *Amphora* spp. (3.6) | 75.9 |
| B | RM-7, FP-7, BP-7, GM-7, RM-8, FP-8 | *Guinardia delicatula* (9.3), *Cryptomonas* spp. (6.4), *Kryptoperidinium foliaceum* (5.9), *Navicula* sp.1 (5.3), *Coscinodiscus* sp. (4.5), *Teleaulax* spp. (4.1), *Rhizosolenia* spp. (4) | 78.3 |
| C | BP-2, BP-3, GM-3, FP-4, BP-4, GM-4, BP-5, GM-5, GM-6, CQ-6, TB-6, CQ-7, TB-7, BP-8, GM-8, CQ-8, TB-8 | *Cryptomonas* spp. (7.8), *Kryptoperidinium foliaceum* (7.5), *Navicula* sp.1 (5), *Rhodomonas* spp. (4.4), *Cocconeis* spp. (3.9), *Scenedesmus* spp.(3.5), *Rhizosolenia* spp. (3.5) | 73.8 |
| D | RM-2, FP-2, RM-3, FP-3, RM-4, RM-5, FP-5, RM-6, FP-6, BP-6 | *Rhodomonas* spp. (5.5), *Cryptomonas* spp.(5.5), *Kryptoperidinium foliaceum* (4.7), *Navicula* sp.1 (4.7), unidentified dinoflagellate (4.2), *Teleaulax* spp. (4.2), *Chaetoceros* spp. (4.1), *Navicula* spp. (3.5), *Cocconeis* spp. (3.5) | 72.1 |

### 5.3.6.3 Relation of environmental and biological parameters

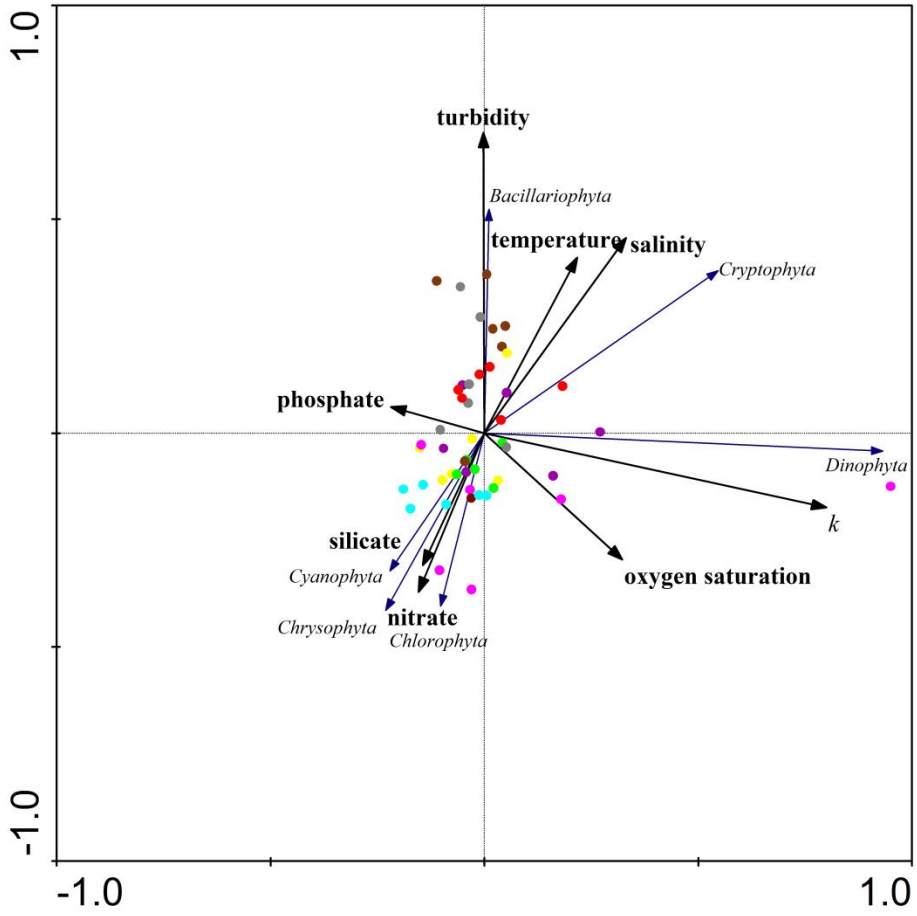


Figure 5-33: Result of RDA analysis, relationships between carbon biomass of main phytoplankton groups and selected environmental variables in the Christchurch Harbour estuary during the summer months in 2014. The plot represents taxa carbon biomass (blue thin lines), the significant explanatory variables (black thick lines) and fortnightly sampling (closed colour symbol; blue = 1st, green = 2nd, yellow = 3rd, pink = 4th, purple = 5th, brown = 6th, red = 7th, grey = 8th).

Constrained CANOCO RDA analysis (see Section 2.12, Figure 5-33) shows the occurrence of the main phytoplankton carbon biomass in relation to the selected environmental variables (nitrate, phosphate, silicate, water temperature, oxygen saturation, salinity, turbidity, and irradiance attenuation coefficient (*k*)) throughout the Christchurch Harbour estuary. The first axis (x-axis) of the analysis explained most of the variance (eigenvalue = 72.8%, cumulative percentage variance between taxa and environmental parameters = 93.0%, whereas all canonical axes explained 100% of the variance (axis 1, $P < 0.001$; all axes, $P < 0.001$). This means that the arrows displayed closer to the x-axis explained most of the variability in the data and environmental variables explained 100% of the variation of the selected taxa biomass when all four axes were analysed together.

Table 5-8: Eigen factor (λ) of each explanatory variable in order of the variance explained when analysed as single factor ($\lambda_1$, marginal effects) or when included in the model where other forward selected variables are analysed together ($\lambda_a$, conditional effects). Significant *P*-values (*$P < 0.1$) and (** $P < 0.05$) represent the variables that together explain the variation in the analysis for the transect sampling in 2014.

| **Marginal Effects** | | **Conditional Effects** | | | | |
|---|---|---|---|---|---|---|
| Variable | $\lambda_1$ | Variable | $\lambda_a$ | *P* | *F* | |
| *k* | 0.47 | *k* | 0.47 | 0.001** | 40.41 | |
| salinity | 0.09 | salinity | 0.20 | 0.001** | 27.49 | |
| %oxygen | 0.08 | %oxygen | 0.04 | 0.008** | 5.38 | |
| phosphate | 0.05 | nitrate | 0.03 | 0.004** | 6.13 | |
| temperature | 0.05 | temperature | 0.02 | 0.034** | 3.56 | |
| nitrate | 0.03 | silicate | 0.02 | 0.026** | 3.52 | |
| silicate | 0.02 | phosphate | 0.01 | 0.235 | 1.39 | |
| turbidity | 0.02 | turbidity | 0.01 | 0.230 | 1.43 | |
| | | | | | | |
| Axes | | 1 | 2 | 3 | 4 | Total variance |
| Eigenvalues : | | 0.728 | 0.037 | 0.016 | 0.015 | 1 |
| biocarbon-environment correlations : | | 0.930 | 0.695 | 0.612 | 0.637 | |
| Cumulative percentage variance | | | | | | |
| of biocarbon data : | | 72.8% | 76.5% | 78.1% | 79.6% | |
| of biocarbon-environment relation: | | 91.4% | 96.1% | 98.1% | 100.0% | |
| Sum of all eigenvalues | | | | | | 1 |
| Sum of all canonical eigenvalues | | | | | | 0.796 |

Forward selection showed that of all eight environmental parameters (Table 5-8) included in the RDA analysis, six environmental factors (*k*, salinity, oxygen saturation, nitrate, temperature, and silicate) explained the variance in the phytoplankton taxa biomass when analysed together. All the forward-selected variables were analysed together (conditional effects, referred to $\lambda_a$ in Table 5-8), and *k* was the most significant explanatory variable ($\lambda_a = 0.47$, $P = 0.001$), followed by salinity ($\lambda_a = 0.20$, $P = 0.001$), oxygen saturation ($\lambda_a = 0.04$, $P = 0.008$), nitrate concentrations ($\lambda_a = 0.03$, $P = 0.004$), water temperature ($\lambda_a = 0.02$, $P = 0.034$), and silicate concentrations ($\lambda_a = 0.02$, $P = 0.026$) as shown in Table 5-8. Phosphate concentrations and turbidity were not significant explanatory variables in this analysis.

## 5.4 Discussion

In this chapter the distributions of biological parameters (total chlorophyll *a*, accessory pigments, phytoplankton species abundance by microscope and flow cytometry, carbon

biomass, and nutrient uptake rates), physical parameters (salinity, water temperature, oxygen saturation, turbidity, and irradiance attenuation coefficient (*k*)), and chemical parameters (inorganic nutrients nitrate, phosphate, and silicate) were compared at eight fortnightly intervals for six sampling stations (Run at Mudeford, Ferry Pontoon, Blackburry Point, Grimbury Marsh, Christchurch Quay, and Tuckton Bridge) in the Christchurch Harbour estuary during summer months in 2014. Statistical multivariate programmes (PRIMER and CANOCO) were used to investigate relationships between the biological and environmental parameters.

The objective was to investigate how estuarine phytoplankton populations collected from the six sites along the nutrient and salinity gradients would respond to changes in the Stour and Hampshire Avon River inputs. The two rivers had a large influence on the abiotic conditions in the Christchurch Harbour estuary and also influenced phytoplankton distributions by altering both nutrient concentration and salinity.

*Nutrient distribution in the estuary*

Nutrients mainly enter the Christchurch Harbour estuary from the Stour and Hampshire Avon Rivers. The upper estuary at Tuckton Bridge and Christchurch Quay had the highest nutrient concentrations and lowest salinity values reflecting the influence of the Stour river inputs. The lower estuary stations at the Run and Ferry Pontoon in contrast showed the lowest concentrations of all nutrients and at high salinity values.

The input of nitrate, phosphate, and silicate showed similar a pattern during the productive period in 2014. From July to August 2014, saline water reached the middle estuary during high tide surveys and nitrate concentrations were reduced due to dilution with low nutrient seawater and natural estuarine phytoplankton uptake. However, higher concentrations at Tuckton Bridge and Christchurch Quay stations were observed and the low concentration of nitrate detected at the Grimbury Marsh station was reduced in July 2014 following growth of the dinoflagellate *Kryptoperidinium foliaceum*, and then in August 2014 by the cryptomonad bloom. This decrease in nutrient availability could lead to a collapse of the phytoplankton bloom, as discussed by Cebrián and Valiela (1999) for temperate ecosystems. In the present study, the average nitrate concentration in the river water was ~500 µmol $L^{-1}$, which is high when compared with other major river systems, such as the Rhine (< 310 µmol $L^{-1}$), the Colne Estuary (~400 µmol $L^{-1}$), and the Pearl River (~100 µmol $L^{-1}$) (van Bennekom and Wetsteijn, 1990; Underwood *et al.*, 1998; Dai *et al.*, 2006) but similar to other UK south coast estuaries (Nedwell *et al.*, 2002).

Phosphate concentrations remained low at Grimbury Marsh during the phytoplankton growth periods and were below the dilution line (see Appendix C) on 10th and 24th July and 7th August 2014. A peak in phosphate concentration in September 2014 may have been caused by the input of freshwater moving down to the middle estuary. Although in estuaries nitrogen is often identified as the most limiting nutrient, nitrogen and phosphorus co-limitation is also regularly observed in particular in the low salinity zone of estuaries (Paerl and Justić, 2011). However, it is unlikely that phosphate concentration is a limiting factor for phytoplankton growth in the Christchurch Harbour estuary as concentrations were high throughout the sampling period.

Silicate concentrations decreased with salinity but with an indication that the Avon River was adding silicate to the estuarine system below Christchurch Quay when river flow rates were low as evidenced by the silicate values at Grimbury Marsh plotting above the dilution line on 10th and 24th July and 7th August 2014 (see Appendix D). The base river flow of the Stour is generally less than that for the Avon in summer months (see Figure 5-1 B) and the Avon silicate concentration can be higher than the Stour.

*Nutrient uptake rates*

The use of stable isotopes provides an understanding of estuarine food webs and ecosystem function (Bouillon *et al.*, 2011). In the present study, the highest phytoplankton biomass and nutrient uptake rates were consistently recorded in the middle reaches of the estuary at Grimbury Marsh. These finding are in agreement with those of Kotsedi *et al.* (2012) in the Sundays Estuary and Dalu *et al.* (2015) in the Kowie Estuary, South Africa, while the macrotidal Southampton Water estuary showed high nutrient uptake rates in both upper and middle areas of the estuary (Torres-Valdés and Purdie, 2006). High nitrate and ammonium uptake rates of up to 0.47 and 8.63 µmol-N $L^{-1}$ $h^{-1}$, respectively measured in the middle estuary are close to those measured by Torres-Valdés and Purdie (2006) in the inner Southampton Estuary of 3.97 and 5.15 µmo-N $L^{-1}$ $h^{-1}$ for nitrate and ammonium, respectively. Uptake rates from the middle of the Christchurch Harbour estuary are higher than uptake rates observed in other European estuaries by Middelburg and Nieuwenhuize (2000a), and are also higher than some other UK estuaries such as the Thames estuary (Middelburg and Nieuwenhuize, 2000b), the Tweed estuary (Shaw *et al.*, 1998a), and the Humber estuary (Shaw *et al.*, 1998b). Kotsedi *et al.* (2012) attributed the high biomass in the Sundays estuary to the geo-hydro-morphological state of the middle reaches, which were turbid, with the intertidal sediment consisting of clay and sand. Similar sediment

characteristics (SPM) were observed in the upper and middle reaches of the Christchurch Harbour estuary, suggesting a similar situation may apply.

A wide range of carbon uptake rates by the natural estuarine phytoplankton was measured along the estuary Table 5-5. In this study, the lowest carbon uptake rate was observed in the lower reaches of the Christchurch Harbour estuary, while the highest rate occurred in the mid-estuary at Grimbury Marsh where high nitrogen uptake rates were measured. These finding are in agreement with Matson and Brinson (1990) for the Pamlico Estuary and Neuse Rivers, USA. Primary production can be estimated based on nutrient uptake (Han *et al.*, 2012) and it seems that the mid-estuary of Christchurch Harbour was an important zone of phytoplankton growth during the summer during high tide.

*Phytoplankton response to salinity and nutrient*

The concentration of chlorophyll *a* using the YSI 6600 multiprobe measurement peaked (93 µg $L^{-1}$) in waters with salinity of about 32 – 33 in the mid-estuary at Grimbury Marsh at high tide on 10$^{th}$ July 2014 (Figure 5-34). Estuarine chlorophyll *a* concentration is often highest in waters of lower salinity (Boynton *et al.*, 1982; Putland *et al.*, 2014). For example, although peak concentrations vary (e.g., 5 to 60 µg $L^{-1}$), chlorophyll *a* concentrations were highest in lower salinity waters (typically below 20) of Apalachicola Bay, USA (Putland *et al.*, 2014), the estuary of Mundaka, Spain (Ruiz *et al.*, 1998), and the Schelde Estuary, the Netherlands (Kromkamp and Peene, 1995).

Phytoplankton need many chemical elements for growth but two critical ones are nitrogen and phosphorus (Paerl and Justić, 2011). However, canonical correspondence analysis indicated that some phytoplankton carbon biomass shows a positive correlation with nitrate and silicate concentrations particularly for chlorophytes, chrysophytes, and cyanophytes throughout the sampling period but had a negative with other groups (diatoms and cryptomonads). Thus nutrient concentrations are not likely to be limiting phytoplankton growth (bloom conditions) during the summer due to the nutrient availability in the estuary. Lancelot and Muylaert (2011) stated that the response of phytoplankton to nutrient loads differs from estuary to estuary, from time to time, and from segment to segment within any part of an estuary.

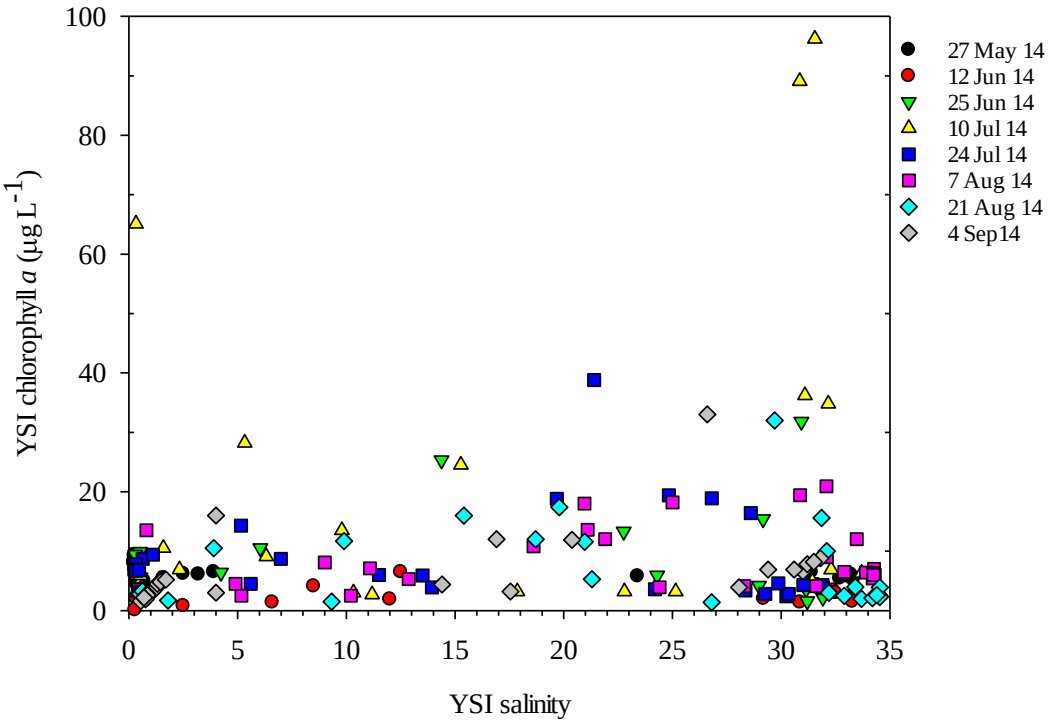


Figure 5-34: Relationship between vertical chlorophyll *a* concentrations and salinity using the YSI 6600 multiprobe measurements during summer 2014 along the Christchurch Harbour estuary.

*Phytoplankton response to hydrodynamics*

In the present study, water temperature varied from 8.4 – 21.7 ºC and positively correlated to the dinoflagellate and cryptomonad communities in the estuary during the summer blooms, suggesting they are the phytoplankton groups with a strong response to warmer temperatures. These two groups showed a reverse correlation with nutrients in the RDA analysis, suggesting that they are the phytoplankton groups with a strong response to riverine inputs of nutrients and have a high potential to use nutrient sources during photosynthesis and also have the highest nitrogen and carbon uptakes rates during their bloom periods. What controls the phytoplankton community in the estuary is not yet clear. However, such a change in the community may have impacts on other organisms in the food web as well as the water quality of the estuary. The temperature optimum for the dinoflagellate bloom of *Kryptoperidinium foliaceum* (in the range of 17 – 21 ºC) and high fucoxanthin concentration (42 µg $L^{-1}$) are in general agreement with those of Figueroa *et al.* (2009) and Manuel *et al.* (2012) that reported fucoxanthin-containing dinoflagellates had the highest division rates at the temperatures tested (19 and 23 ºC). Diatom and cryptomonad groups were also positively associated with the water temperature in the RDA analysis.

In this study, turbidity values were generally observed to be < 30 NTU and had negative correlations with freshwater phytoplankton groups (chlorophytes, chrysophytes, and cyanophytes) during the sampling period. Cloern (1987) pointed out that turbidity has been considered as the main factor controlling light availability and phytoplankton growth in estuaries. The main phytoplankton biomass groups (cryptomonads and diatoms) were positively correlated with the turbidity and also the irradiance coefficient (*k*) was high (3.9 $m^{-1}$) during the dinoflagellate bloom in the middle estuary. The spring tidal currents did not obviously cause increased estuarine turbidity and probably the narrow entrance (~40 metres long) and microtidal nature of the estuary (< 2 metres tidal range) had some impact. Furthermore, in macrotidal estuaries the dinoflagellates are usually more abundant in the summer during reduced periods of turbidity (Valdes-Weaver *et al.*, 2006).

In the previous chapter it is shown that the river flow significantly influenced the phytoplankton population at the entrance of the estuary at low tide (see Section 4.3.6.3). This factor is an important mechanism in controlling vertical stratification of the water column in the estuary because it increases the water residence time. During the summer of 2014, the river discharge was < 20 $m^3$ $s^{-1}$ from the Stour and Hampshire Avon Rivers leading to salinity intrusion into the mid-estuary and an increase in water residence times providing good conditions for growth of flagellates.

*Estuarine phytoplankton taxonomic composition*

In the present study diatoms, cryptomonads, and dinoflagellates have shown a positive correlation with salinity because these groups are adapted to dynamic estuarine environments (Lionard *et al.*, 2005). The salinity gradient had a direct influence on the composition of the phytoplankton population (Figure 5-35). Diatoms were abundant in waters with salinity between 10 and 35, and dinoflagellates and cryptomonads were also important in this salinity range (Figure 5-35 A, D, and E). However, the highest abundance of dinoflagellates was observed at a salinity of 12 (Figure 5-35 D). The chlorophytes, chrysophytes, and cyanophytes dominated at low salinity and may have been riverine species entering the upper estuary (Figure 5-35 B, C, and F). Due to the nutrient-enriched nature of estuaries, chlorophytes and cyanophytes are typically considered to be common features in low salinity waters (Carstensen *et al.*, 2015)

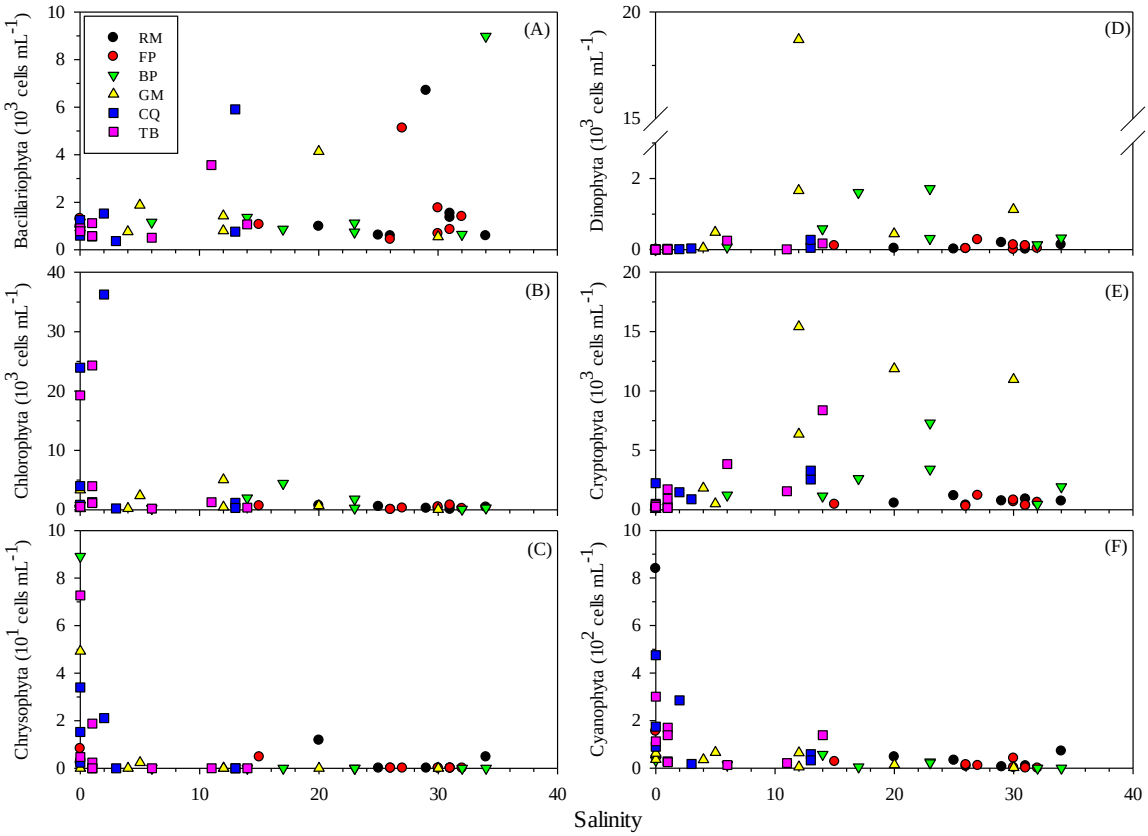


Figure 5-35: Abundance (cells $mL^{-1}$) of (A) bacillariophyta, (B) chlorophyta, (C) chrysophyta, (D) dinophyta, (E) cryptophyta, (F) cyanophyta during the Christchurch Harbour transect sampling in 2014.

This is the first comprehensive study of phytoplankton communities in the Christchurch Harbour estuary. The lower estuary was dominated by marine waters and the phytoplankton assemblages showed the same structure and temporal dynamic as those of coastal waters. During the current investigation, the dinoflagellate species, *Kryptoperidinium foliaceum*, occurred mainly in the middle reaches of the estuary, suggesting that this species can survive in relatively high salinity waters. The bloom was initiated at Grimbury Marsh on 10$^{th}$ July 2014 ($18.3 \times 10^3$ cells $mL^{-1}$), resulting in a chlorophyll *a* peak value of 93.0 µg $L^{-1}$ with a temperature of 17.3 ºC and the irradiance attenuation coefficient was 3.9 $m^{-1}$. *K. foliaceum* forms non-toxic red tide blooms in the Indian River Lagoon in the USA (Phlips *et al.*, 2011) and it has the highest growth rate between 19 and 23 ºC (Figueroa *et al.*, 2009). This bloom was not observed at other stations or sampling days in Christchurch Harbour although it is possible samples were not always collected where maximum chlorophyll levels were present. In some shallow coastal ecosystems blooms can develop only when the river discharge decreases to a level at which the water residence time is longer than the phytoplankton population doubling time

(Cloern, 1996). Phytoplankton growth rates have been estimated by combining carbon uptake rates and cell carbon concentrations for each incubation. Cell growth rates ranged from 0.4 to 1.5 $day^{-1}$ during summer months when river flow rates were reduced (Figure 5-36). Estimates of summer water residence times in the estuary under these conditions were greater than 2 days indicating that phytoplankton net growth could potentially occur in the mid estuary as was seen at Grimberry Marsh during July and August 2014. The reduced river discharge shifts the salinity gradients in river-dominated estuaries which indicate the importance of salinity changes to estuarine ecology (Attrill and Rundle, 2002). In the Taw estuary (SW England), it was shown that the major factors influencing the phytoplankton blooms in the upper and middle estuary during the summer in 2008 were two hydrodynamic processes, river flow and tidal amplitude (Maier *et al.*, 2012).

In the upper and middle estuary the cryptophyte group was the main phytoplankton species following the dinoflagellate bloom. *Rhodomonas* spp. and *Cryptomonas* spp. were respectively observed in significant numbers at Grimbury Marsh on 24th July 2014 ($13.7 \times 10^3$ cells $mL^{-1}$, 20.9 µg $L^{-1}$) and 21st August 2014 ($10.9 \times 10^3$ cells $mL^{-1}$, 49.0 µg $L^{-1}$), when temperature and salinity ranged 15.5 – 21.6 ºC and 30.2 – 33.7, respectively. In the summer period it seems that coastal water moved further into the estuary due to reduced riverine input and with increasing water temperature providing favourable conditions for the development of cryptomonads in the estuary with sustained high abundances over a period of several weeks in the middle estuary. Cryptomonads are an important components of phytoplankton ecosystems (Hill, 1991) and are common in freshwater ecosystem and often forms blooms in eutrophic lakes (Weng *et al.*, 2007). This genus also grows widely in the Chinese coastal areas and is known as a HAB species (Hu *et al.*, 2002). However, cryptomonad bloom events did not appear to affect other estuarine organisms in the Christchurch Harbour estuary.

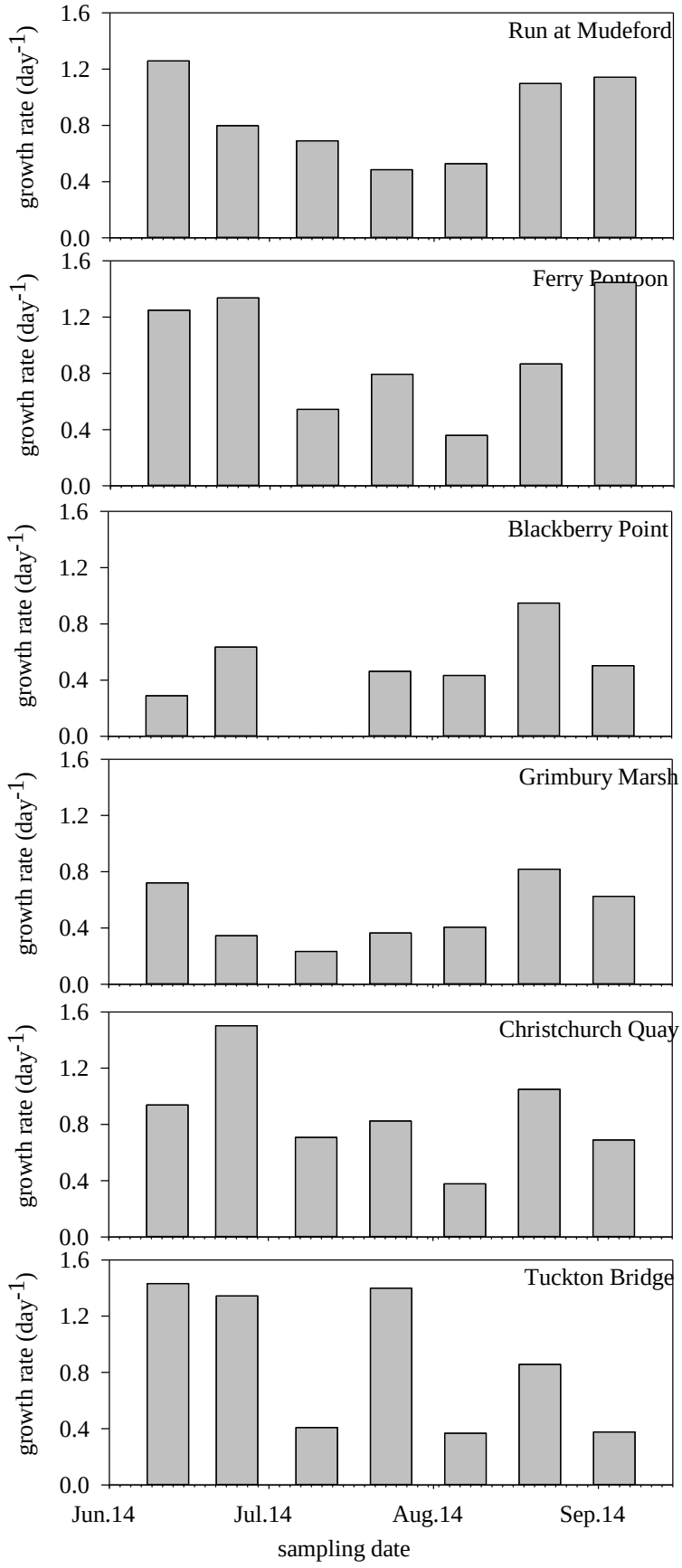


Figure 5-36: Phytoplankton growth rate (day $^{-1}$) at the six estuarine stations during the Christchurch Harbour transect sampling in 2014.

*Estuarine HPLC pigment composition*

Few studies of HPLC phytoplankton pigments have been performed in estuaries and rivers (Lionard *et al.*, 2005; Lionard *et al.*, 2008). Overall, accessory pigment composition was a good descriptor of changes observed in the phytoplankton community in Christchurch Harbour. In the present study the pigments were variable within and among sampling sites, and there were changes in pigment composition during the sampling period. In samples from the estuary transect, microscopic observations revealed that the peaks of chlorophyll *a* and of fucoxanthin at Grimbury Marsh on 10$^{th}$ July 2014 were associated with biomass of the dinoflagellate *Kryptoperidinium foliaceum* of $18.7 \times 10^3$ µg C $L^{-1}$. This species was recently observed as a fucoxanthin-containing dinoflagellate by Manuel *et al.* (2012) and does not contain peridinin which is often used as an indicator pigment for dinoflagellates. This dinoflagellate species contains a tertiary plastid from a diatom endosymbiont (Kempton *et al.*, 2002; Imanian and Keeling, 2007; Imanian *et al.*, 2010). the In contrast, fucoxanthin has been reported as the dominant accessory pigment in the Urdaibai estuary, where it was attributed to diatoms (Ansotegui *et al.*, 2001) and similarly in the Tagus estuary (Gameiro *et al.*, 2007). There are a several advantages with the HPLC method, for example, it can be used to analyse a large number of samples over an extended aquatic area and has been employed particularly in marine ecosystems (Goericke, 1998) and eutrophic estuary systems (Paerl *et al.*, 2005). However, the combined use of HPLC analysis and microscopic enumeration is still required for accurate assessment of phytoplankton communities since some pigments are found in more than one group of microalge e.g. fucoxanthin is present in diatoms, chrysophytes, and a few dinoflagellates. As stated by Millie *et al.* (1993) and Ansotegui *et al.* (2001) pigment analysis coupled with microscopic technique provides the most accurate characterisation of phytoplankton assemblages.

## 5.5 Conclusion

In this study it was found that most of the bloom species experienced strong, tidally-driven, longitudinal displacements during high tide, and that daily variations in the rate of vertical mixing by tidal stirring (Cloern, 1991) might control phytoplankton bloom dynamics. Different populations of estuarine phytoplankton were observed over the course of the summer in 2014 with blooms occurring in the middle of Christchurch Harbour often in associated with low salinity water.

# Chapter 6: Synthesis and conclusions

## 6.1 Synthesis of data and comparison with previous years

The main freshwater inputs into the Christchurch Harbour estuary occur through the rivers Stour and Hampshire Avon. River flow rates over a fourteen year period show clear seasonal variations in both rivers, with increased flow rates occurring in winter months and reduced flow rates in summer (Figure 6-1). The summer base flow rates in both rivers was similar for most of the fourteen year record shown in Figure 6-1 with the Avon base flow sustained at a slightly higher level than the Stour due it being fed by the chalk aquafer (Murray, 1966). The river Stour differs from the Hampshire Avon in winter by showing rapid increases followed by decreses in flow (i.e. flashy behaviour) due to the rapid run off from its tertiary catchment, The period of sampling undertaken during the current project coincided with a summer period of low flows (similar to previous years) in both rivers followed by sustained high rates of flow from December 2013 to March 2014 caused by high levels of winter rain fall. These exceptionally high flow rates were unusual when compared with winter flows from most of the previous years apart from the winters of 2000/2001 and 2002/2003. Seasonal changes in river flow rates will play a dominant role in controlling the water residence time within the Christchurch Harbour estuary. Estimates of water residence times calculated for the period April 2013 to April 2014 using the method of Dyer (1997) range from 1.5 to 2.5 days during summer months and decreased to between 0.3 and 0.5 days during the high flow period (December 2013 to March 2014; week 34 to 49; Figure 6-2; Appendix E). Measurements of chlorophyll concentration at Mudeford Quay over this period show that concentrations were >5 µg $L^{-1}$ when water residence times were more than 1.5 days during late spring and summer 2013 suggesting phytoplankton populations were showing net growth in this period.

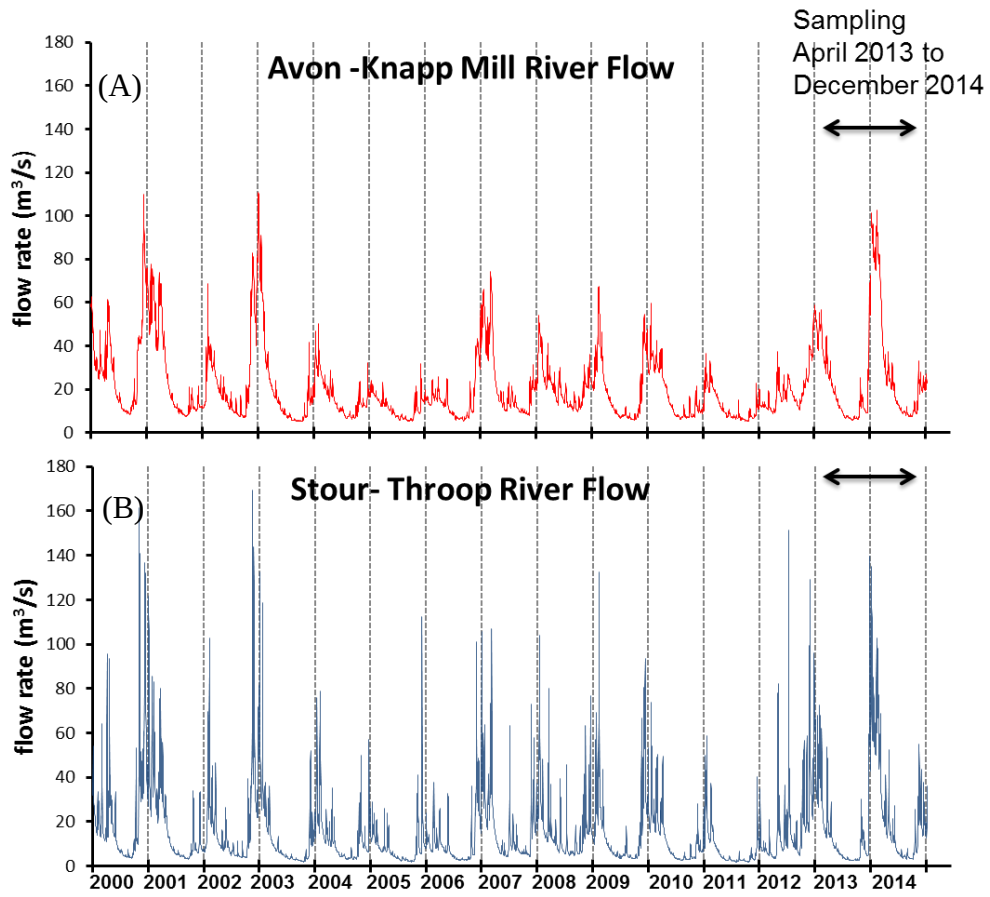


Figure 6-1: Mean daily flow ($m^3$ $s^{-1}$) of the Hampshire Avon River (A) and the Stour River (B) from 2000 to 2014 by the Environmental Agency.

Some chlorophyll *a* concentration data recorded by the Environment Agency was available in the Hampshire Avon at Knapp Mill, and within the estuary (Christchurch Quay, Grimberry Marsh, and the Run at Mudeford) for the period 1990 – 2003 (Figure 6-3). Peak concentration of chlorophyll were typically detected by the EA at Knapp Mill in some years during April (Figure 6-3 D) which was in agreement with the high concentrations detected in April 2013 during the current study (Figure 3-8 C). At Mudeford the EA data also showed similar seasonal changes in chlorophyll *a* to those detected during the weekly sampling from April 2013 to April 2014 (Figure 6-3 C and Figure 4-6). In the mid estuary at Grimmberry Marsh and Christchurch Quay the EA data indicated spring and summer chlorophyll concentrations were typically >50 µg $L^{-1}$ which compares to peak values detected during summer 2014 surveys of the estuary during this work (Figure 6-3 A, B and Figure 5-11). The European Union Water Framework Directive (C.E.C., 2000) defines a range of chlorophyll levels used in establishing the phytoplankton biological quality in all waters. In this study, some spring-summer concentrations of chlorophyll were detected over the generic thresholds (>10 µg $L^{-1}$) in both riverine and estuarine samples indicating

the Christchurch Harbour estuary and the Rivers Stour and the Hampshire Avon can be considered to be a risk boundary condition, according to classificated by Devlin *et al.* (2007).

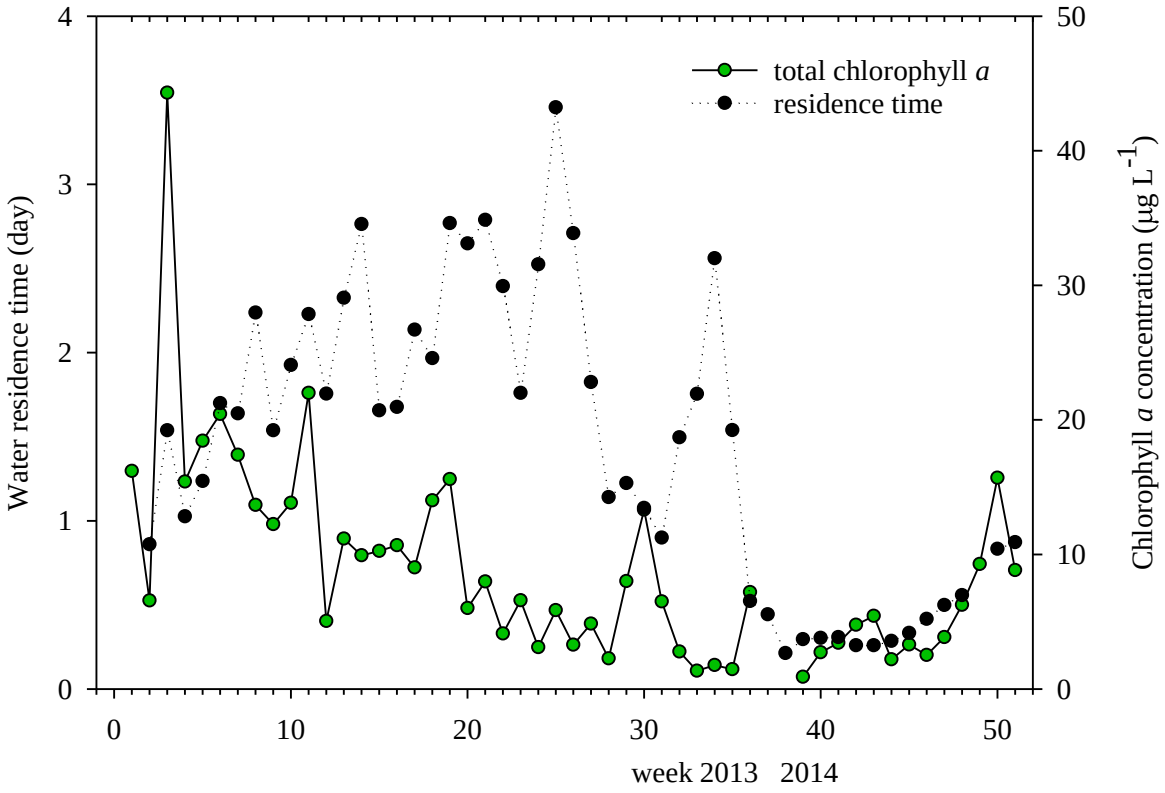


Figure 6-2: Water residence time (day) in the Christchurch Harbour estuary and concentration of chlorophyll *a* (µg $L^{-1}$) at Mudeford Quay during April 2013 to April 2014.

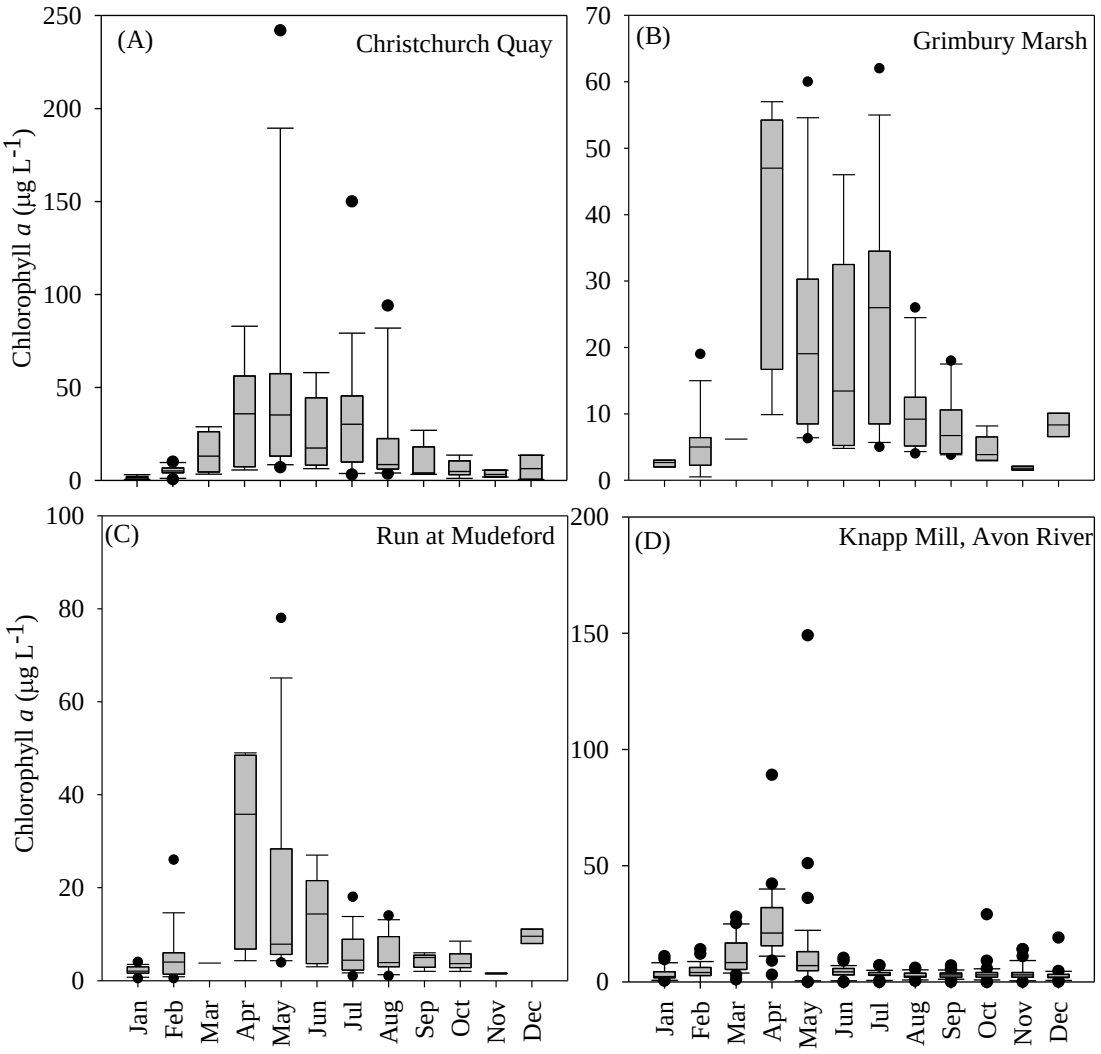


Figure 6-3: Chlorophyll *a* concentrations at Christchurch Quay (A), Grimbury Marsh (B), the Run at Mudeford (C), and Knapp Mill (D) during 1990 – 2003 by the Environment Agency.

## 6.2 Conclusions and main findings of this research

The results in this thesis have been used to determine the response of the estuarine phytoplankton community to changes in macronutrient input to the Christchurch Harbour estuary, and their role in cycling of macronutrients between aqueous and particulate forms.

In Chapter 3, it was demonstrated that the riverine phytoplankton population in the Stour River at Throop and Iford Bridge peaked during the spring period with the diatom *Stephanodiscus* sp. dominanting followed by chlorophyte species being most abundant in summer months. The nano-phytoplankton (2.0 – 20.0 µm in diameter) was the main component of phytoplankton biomass during the productive period in both rivers but with lower abundance and biomass in the Hampshire Avon River compared to the Stour. All

inorganic nutrients (nitrate, phosphate, and silicate) were found to be in high concentration in the Stour indicating this river can be considered to be eutrophic during productive periods of the year. The river discharge and water temperature were the main environmental factor controlling the changes in phytoplankton community at both rivers sites.

In Chapter 4, the changes estuarine phytoplankton community at the estuary entrance was reported for a year from April 2013 to April 2014. The pattern of changes in chlorophyll concentration and phytoplankton abundance was similar to the results for the river sites for high flow periods of the year when low salinity waters were detected at low tide at Mudeford Quay. Several environmemtal parameters were shown to be influencing the phytoplankton communities in the outer estuary during the year with the river discharge and salinity particularly important factors. The nano-sized phytoplankton were the main component of phytoplankton biomass during the productive period of the year – similar to results from the river sites.

In Chapter 5, it was demonstrated that the dinoflagellate *Kryptoperidinium foliaceum* formed blooms in the middle estuary at high tide in July 2014 followed by high abundance of cryptomonads in August 2014. The majority of freshwater phytoplankton species in terms of abundance did not penetrate saline water. The mid-estuary showed the highest nitrate and ammonium uptake rates with high rates of carbon uptake by the natural estuarine phytoplankton. Nitrate showed little evidence of non conservative behaviour in Christchurch Harbour on most sampling dates however (Appendix B) despite high uptake rates detected at mid estuary stations in July and August 2014. The irradiance attenuation coefficient ($k$) and salinity were important environmental parameters influencing the distribution of estuarine phytoplankton populations together with the high levels of nutrient availability that promoted eutrophic conditions in the middle estuary.

The following is a list of main findings from this research:

- The lower reaches of the Stour River at Throop and Iford Bridge prior to river entering the Chrischurch Harbour estuary can be considered eutrophic based on the level of macronutrients, annual mean of chlorophyll *a* concentration, and phytoplankton biomass results from the weekly surveys. This is in contrast to lower reaches of the Hampshire Avon River that has much lower concentrations of nutrients and consequently less chlorophyll is detected in these waters. Phytoplankton show seasonal changes in abundance and production in the Stour

and Hampshire Avon Rivers with increases particularly during the spring-summer period. In contrast, in the winter period, low chlorophyll *a* concentration and phytoplankton abundance was measured during periods of high river flow.

- Blooms of the diatom *Stephanodiscus* sp. observed during the late spring and early summer at Throop on the Stour River are caused by rich nutrient conditions due to winter or early spring input through rainfall and runoff and the ability of this species to grow rapidly and acclimate to light conditions that would be limiting for other phytoplankton species.
- The Christchurch Harbour estuary can be considered to be potentially eutrophic on the basis of high summer levels of chlorophyll *a*, phytoplankton biomass, and nutrients that were measured during the estuarine transects. The estuary receives a high nutrient loading from the river discharges into the system but with reduced flows in summer the increased estuarine residence time provides good conditions for growth of photosynthetic flagellates in saline waters of the mid estuary. The distribution of nutrients, chlorophyll, accessory pigments, and phytoplankton abundance at the mouth of the estuary at Mudeford Quay reflected the conditions in the rivers when sampled at low tide during high river flow periods of the year.
- Accessory pigments detected by HPLC analysis from the riverine and estuarine samples were in general a good descriptor of changes observed in the phytoplankton communities. The bloom of cryptomonads was confirmed by high levels of alloxanthin and diatoms mostly indicated from fucoxanthin concentration. In contrast, though the presence of the dinoflagellate *K. foliaceum* correlated with peaks in fucoxanthin rather than the usual dinoflagellate indicator pigment of peridinin containing. The use of microscopic observation of phytoplankton samples therefore must be used in combination with HPLC pigment analysis to confirm the presence of some species.
- The abundance of phytoplankton using microscopic techniques from both rivers and the estuary were shown to underestimate total cells detected by the CytoSense flow cytometer due to the smaller phytoplankton being omitted from the microscope counts.

## 6.3 Recommendations and future work

The results of this thesis have demonstrated that the lower reaches of the Stour River and the Christchurch Harbour estuary can be considered to be eutrophic systems. There have

been only intermittent previous data on chlorophyll and nutrient concentrations in Christchurch Harbour collected by the Environment Agency. It is suggested therefore that it is important to continue monitoring the water quality, phytoplankton species, and abundance in the estuary, particularly in the middle estuary to establish a longer temporal dataset. This dataset will help better understand the conditions promoting blooms of different phytoplankton species and it will be important to establish if any toxic species exist in the estuary. The discharge of river water to the estuary is a major source of nutrients that has little impact in non-productive months when the estuary contains little saline water. However, it has been shown that in summer months during reduced river flow conditions high water residence times in the estuary lead to development of extensive blooms of dinoflagellates that reduce the water quality of the estuary. The top-down control of phytoplankton populations in the estuary was not assessed in this research but it is likely there is minimal benthic grazing by marine filter feeders (e.g. shell fish) due to the freshwater nature of the harbour during winter. The top-down control of estuarine phytoplankton through grazing by zooplankton, benthic filter feeders, and juvenile fish would be an important future area of research as these could be important in a shallow estuary. The data sets obtained through this research could be used to validate a coupled hydrodynamic and simple phytoplankton growth model to provide a prediction of the effect of future drier summers or wetter winters on the eutrophication status of the estuary.

## Appendix A

Dates on which spot samplings were collected from the three sampling stations between 16th April 2013 and 10th April 2014.

| week | Date / Station | Throop, Stour River | Iford Bridge, Stour River | Knapp Mill, Avon River | Mudeford Quay Christchurch H. |
|---|---|---|---|---|---|
| 1 | 16-Apr-13 | √ | - | √ | √ |
| 2 | 25-Apr-13 | √ | - | √ | √ |
| 3 | 03-May-13 | √ | - | √ | √ |
| 4 | 10-May-13 | √ | - | √ | √ |
| 5 | 17-May-13 | √ | - | √ | √ |
| 6 | 23-May-13 | √ | - | √ | √ |
| 7 | 31-May-13 | √ | - | √ | √ |
| 8 | 06-Jun-13 | √ | √ * | √ | √ |
| 9 | 14-Jun-13 | √ | √ * | √ | √ |
| 10 | 20-Jun-13 | √ | √ * | √ | √ |
| 11 | 28-Jun-13 | √ | √ * | √ | √ |
| 12 | 04-Jul-13 | √ | √ * | √ | √ |
| 13 | 10-Jul-13 | √ | √ * | √ | √ |
| 14 | 17-Jul-13 | √ | √ * | √ | √ |
| 15 | 23-Jul-13 | √ | √ * | √ | √ |
| 16 | 31-Jul-13 | √ | √ * | √ | √ |
| 17 | 06-Aug-13 | √ | √ * | √ | √ |
| 18 | 14-Aug-13 | √ | √ * | √ | √ |
| 19 | 20-Aug-13 | √ | √ * | √ | √ |
| 20 | 27-Aug-13 | √ | √ * | √ | √ |
| 21 | 03-Sep-13 | √ | √ * | √ | √ |
| 22 | 11-Sep-13 | √ | √ * | √ | √ |
| 23 | 16-Sep-13 | √ | √ * | √ | √ |
| 24 | 24-Sep-13 | √ | √ * | √ | √ |
| 25 | 01-Oct-13 | √ | √ * | √ | √ |
| 26 | 11-Oct-13 | √ | √ * | √ | √ |
| 27 | 16-Oct-13 | √ | √ * | √ | √ |
| 28 | 24-Oct-13 | √ | √ * | √ | √ |
| 29 | 30-Oct-13 | √ | √ * | √ | √ |
| 30 | 04-Nov-13 | √ | √ * | √ | √ |
| 31 | 11-Nov-13 | √ | √ * | √ | √ |
| 32 | 18-Nov-13 | √ | √ * | √ | √ |
| 33 | 24-Nov-13 | √ | √ * | √ | √ |
| 34 | 02-Dec-13 | √ | √ * | √ | √ |

| week | Station<br>Date | Throop,<br>Stour River | Iford Bridge,<br>Stour River | Knapp Mill,<br>Avon River | Mudeford Quay<br>Christchurch H. |
|---|---|---|---|---|---|
| 35 | 09-Dec-13 | √ | √ * | √ | √ |
| 36 | 17-Dec-13 | √ | √ * | √ | √ |
| 37 | 30-Dec-13 | √ * | √ * | √ * | √ * |
| 38 | 07-Jan-14 | √ * | √ * | √ * | √ * |
| 39 | 15-Jan-14 | √ | √ * | √ | √ |
| 40 | 23-Jan-14 | √ | √ * | √ | √ |
| 41 | 30-Jan-14 | √ | √ * | √ | √ |
| 42 | 06-Feb-14 | √ | √ * | √ | √ |
| 43 | 13-Feb-14 | √ | √ * | √ | √ |
| 44 | 21-Feb-14 | √ | √ * | √ | √ |
| 45 | 27-Feb-14 | √ | √ * | √ | √ |
| 46 | 07-Mar-14 | √ | √ * | √ | √ |
| 47 | 13-Mar-14 | √ | √ * | √ | √ |
| 48 | 19-Mar-14 | √ | √ * | √ | √ |
| 49 | 27-Mar-14 | √ | √ * | √ | √ |
| 50 | 04-Apr-14 | √ | √ * | √ | √ |
| 51 | 10-Apr-14 | √ | √ * | √ | √ |

√ Spot samples collected.

- Samples not collected

* No HPLC experiment

## Appendix B

Nitrate (µmol $L^{-1}$) versus salinity plots for each day of sampling throughout the Christchurch Harbour estuary during the summer months in 2014. Note change of scales on the x axis.

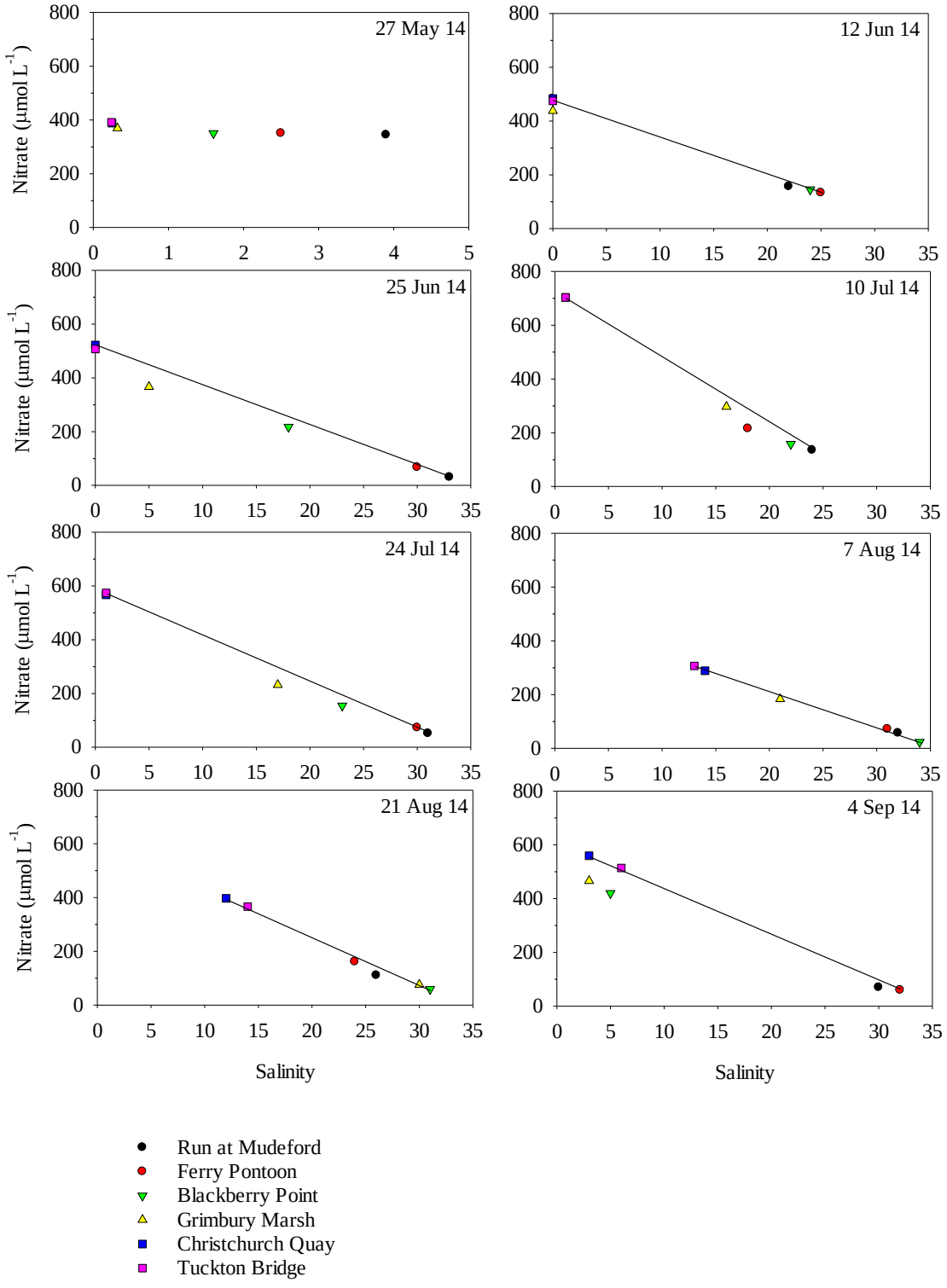

## Appendix C

Phosphate (µmol $L^{-1}$) versus salinity plots for each day of sampling throughout the Christchurch Harbour estuary during the summer months in 2014. Note change of scales on the x axis.

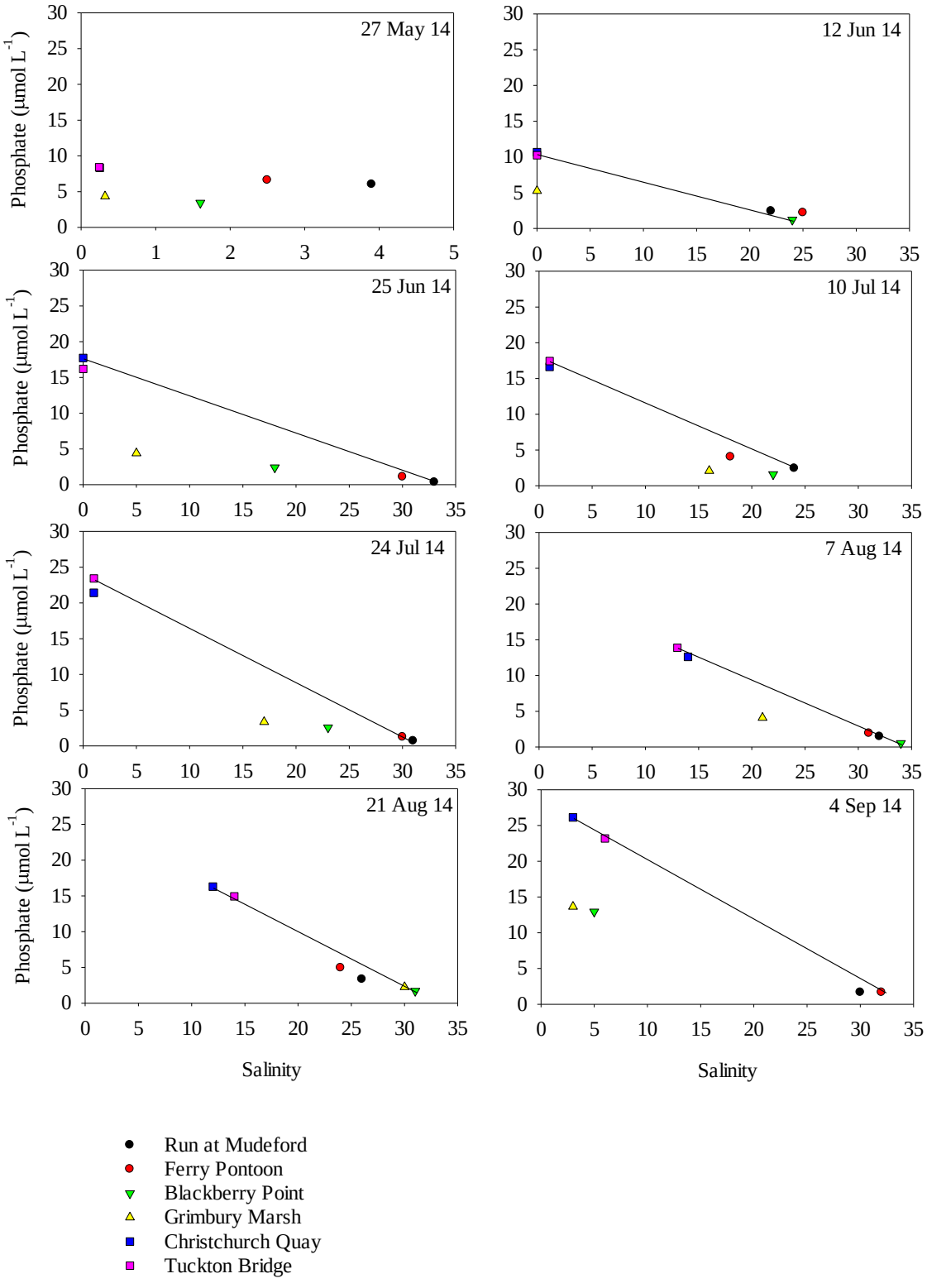

## Appendix D

Silicate (µmol $L^{-1}$) versus salinity plots for each day of sampling throughout the Christchurch Harbour estuary during the summer months in 2014. Note change of scales on the x axis.

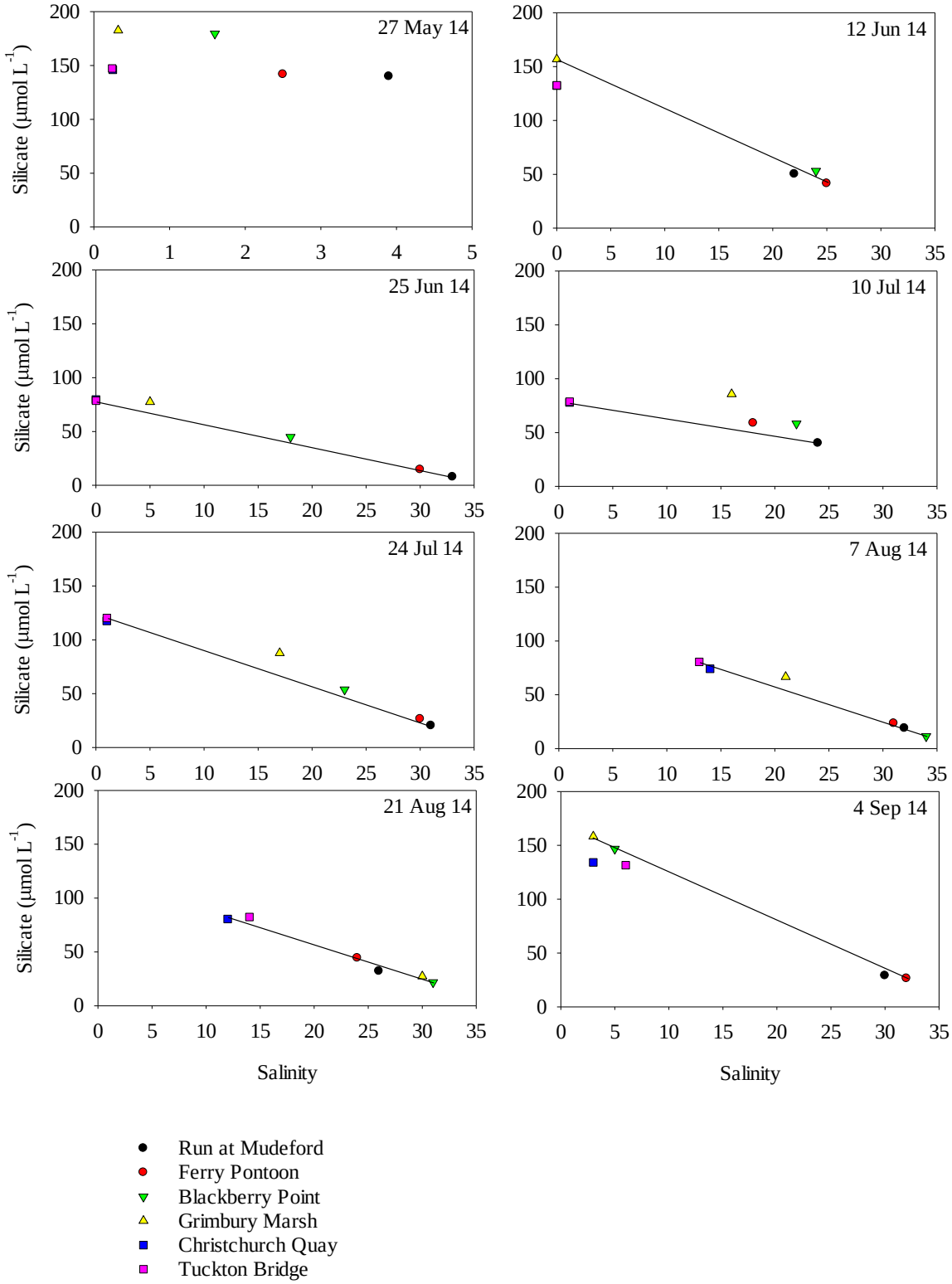

## Appendix E

Water residence time (day) in the Christchurch Harbour estuary during April 2013 to April 2014 using the formulation of Dyer (1997).

| week | Date | Throop, Stour River flow ($m^3 s^{-1}$) | Knapp Mill, Avon River flow ($m^3 s^{-1}$) | Salinity at Mudeford Quay | Residence time (day) |
|---|---|---|---|---|---|
| 1 | 16-Apr-13 | 16.4 | 26.8 | - | - |
| 2 | 25-Apr-13 | 10.7 | 21.8 | 12.8 | 0.9 |
| 3 | 03-May-13 | 8.8 | 18.7 | 1.3 | 1.5 |
| 4 | 10-May-13 | 8.4 | 18.3 | 13.2 | 1.0 |
| 5 | 17-May-13 | 8.7 | 18.0 | 8.7 | 1.2 |
| 6 | 23-May-13 | 7.0 | 15.0 | 5.2 | 1.7 |
| 7 | 31-May-13 | 7.3 | 14.9 | 6.1 | 1.6 |
| 8 | 06-Jun-13 | 5.5 | 12.1 | 3.6 | 2.2 |
| 9 | 14-Jun-13 | 5.3 | 12.1 | 13.7 | 1.5 |
| 10 | 20-Jun-13 | 4.8 | 11.2 | 10.5 | 1.9 |
| 11 | 28-Jun-13 | 4.3 | 10.4 | 8.8 | 2.2 |
| 12 | 04-Jul-13 | 4.0 | 9.4 | 16.3 | 1.8 |
| 13 | 10-Jul-13 | 3.3 | 8.0 | 14.0 | 2.3 |
| 14 | 17-Jul-13 | 3.0 | 7.1 | 12.7 | 2.8 |
| 15 | 23-Jul-13 | 2.8 | 6.7 | 22.5 | 1.7 |
| 16 | 31-Jul-13 | 3.7 | 7.6 | 19.9 | 1.7 |
| 17 | 06-Aug-13 | 3.3 | 7.8 | 16.1 | 2.1 |
| 18 | 14-Aug-13 | 2.5 | 6.6 | 20.7 | 2.0 |
| 19 | 20-Aug-13 | 2.7 | 6.9 | 13.9 | 2.8 |
| 20 | 27-Aug-13 | 2.5 | 6.3 | 16.5 | 2.6 |
| 21 | 03-Sep-13 | 2.4 | 5.8 | 16.7 | 2.8 |
| 22 | 11-Sep-13 | 2.6 | 6.1 | 18.4 | 2.4 |
| 23 | 16-Sep-13 | 2.9 | 7.6 | 20.3 | 1.8 |
| 24 | 24-Sep-13 | 2.5 | 6.5 | 16.9 | 2.5 |
| 25 | 01-Oct-13 | 2.7 | 6.6 | 9.5 | 3.5 |
| 26 | 11-Oct-13 | 2.5 | 6.1 | 16.5 | 2.7 |
| 27 | 16-Oct-13 | 3.8 | 7.4 | 18.7 | 1.8 |
| 28 | 24-Oct-13 | 12.2 | 12.2 | 12.9 | 1.1 |
| 29 | 30-Oct-13 | 18.6 | 14.5 | 2.9 | 1.2 |
| 30 | 04-Nov-13 | 13.2 | 16.9 | 9.3 | 1.1 |
| 31 | 11-Nov-13 | 16.3 | 16.2 | 11.7 | 0.9 |
| 32 | 18-Nov-13 | 7.7 | 11.1 | 12.7 | 1.5 |
| 33 | 24-Nov-13 | 7.0 | 10.2 | 10.9 | 1.8 |
| 34 | 02-Dec-13 | 5.3 | 9.7 | 4.6 | 2.6 |
| 35 | 09-Dec-13 | 4.7 | 9.2 | 18.0 | 1.5 |

| week | Date | Throop, Stour River flow ($m^3 s^{-1}$) | Knapp Mill, Avon River flow ($m^3 s^{-1}$) | Salinity at Mudeford Quay | Residence time (day) |
|---|---|---|---|---|---|
| 36 | 17-Dec-13 | 51.1 | 26.9 | 2.6 | 0.5 |
| 37 | 30-Dec-13 | 42.6 | 54.2 | 0.9 | 0.4 |
| 38 | 07-Jan-14 | 111.7 | 94.3 | 0.2 | 0.2 |
| 39 | 15-Jan-14 | 60.7 | 87.0 | 0.3 | 0.3 |
| 40 | 23-Jan-14 | 63.8 | 80.5 | 0.3 | 0.3 |
| 41 | 30-Jan-14 | 57.2 | 84.6 | 0.3 | 0.3 |
| 42 | 06-Feb-14 | 83.6 | 85.0 | 0.3 | 0.3 |
| 43 | 13-Feb-14 | 75.4 | 93.3 | 0.3 | 0.3 |
| 44 | 21-Feb-14 | 65.4 | 87.9 | 0.3 | 0.3 |
| 45 | 27-Feb-14 | 51.3 | 79.8 | 0.3 | 0.3 |
| 46 | 07-Mar-14 | 35.5 | 69.4 | 0.3 | 0.4 |
| 47 | 13-Mar-14 | 26.9 | 60.6 | 0.3 | 0.5 |
| 48 | 19-Mar-14 | 21.4 | 46.2 | 5.1 | 0.6 |
| 49 | 27-Mar-14 | 19.9 | 36.6 | - | - |
| 50 | 04-Apr-14 | 20.1 | 30.6 | 1.41 | 0.8 |
| 51 | 10-Apr-14 | 20.8 | 29.0 | 0.4 | 0.9 |

**List of Reference**

Adolf, J.E., C.L. Yeager, W.D. Miller, M.E. Mallonee and L.W. Harding Jr (2006). Environmental forcing of phytoplankton floral composition, biomass, and primary productivity in Chesapeake Bay, USA. *Estuarine, Coastal and Shelf Science,* **67**(1–2): 108-122.

Ali, E.M. 2003. *Processes and conditions influencing phytoplankton growth and bloom initiation in a macrotidal, Southampton Water.* PhD thesis, University of Southampton.

Allen, J.I., T.J. Smyth, J.R. Siddorn and M. Holt (2008). How well can we forecast high biomass algal bloom events in a eutrophic coastal sea?. *Harmful Algae,* **8**(1): 70-76.

Allen, S.E. and M.A. Wolfe (2013). Hindcast of the timing of the spring phytoplankton bloom in the Strait of Georgia, 1968–2010. *Progress in Oceanography,* **115**: 6-13.

Altisan, I.A.R. 2006. *Effects of light and nutrient gradients on the taxonomic composition, size structure and physiological status of the phytoplankton community within a temperate eutrophic estuary.* PhD thesis, University of Southampton.

Anderson, D., P. Glibert and J. Burkholder (2002). Harmful algal blooms and eutrophication: Nutrient sources, composition, and consequences. *Estuaries,* **25**(4): 704-726.

Ansotegui, A., J.M. Trigueros and E. Orive (2001). The use of pigment signatures to assess phytoplankton assemblage structure in estuarine waters. *Estuarine, Coastal and Shelf Science,* **52**(6): 689-703.

Attrill, M.J. and S.D. Rundle (2002). Ecotone or Ecocline: Ecological boundaries in estuaries. *Estuarine, Coastal and Shelf Science,* **55**(6): 929-936.

Barlow, R.G., D.G. Cummings and S.W. Gibb (1997). Improved resolution of mono- and divinyl chlorophylls a and b and zeaxanthin and lutein in phytoplankton extracts using reverse phase C-8 HPLC. *Marine Ecology Progress Series,* **161**: 303-307.

Barlow, R.G., R.F.C. Mantoura, M.A. Gough and T.W. Fileman (1993). Pigment signatures of the phytoplankton composition in the northeastern Atlantic during the

1990 spring bloom. *Deep Sea Research Part II: Topical Studies in Oceanography,* **40**(1–2): 459-477.

Basu, B.K., J. Kalff and B. Pinel-Alloul (2000). Midsummer plankton development along a large temperate river: the St. Lawrence River. *Canadian Journal of Fisheries and Aquatic Sciences,* **57**(S1): 7-15.

Belcher, H. and E. Swale (1979). *An illustrated guide to river phytoplankton*. Institue of Terrestrail Ecology, Natural Environment Reseach Council, Her Majesty's Stationery Office. 64 pp.

Bellinger, E. and D.D. Sigee (2010). *Freshwater algae : Identification and use as bioindicators*. Hoboken, GB, Wiley. 285 pp.

Bonato, S., E. Breton, M. Didry, F. Lizon, V. Cornille, E. Lécuyer, U. Christaki and L.F. Artigas (2016). Spatio-temporal patterns in phytoplankton assemblages in inshore–offshore gradients using flow cytometry: A case study in the eastern English Channel. *Journal of Marine Systems,* **156**: 76-85.

Bonato, S., U. Christaki, A. Lefebvre, F. Lizon, M. Thyssen and L.F. Artigas (2015). High spatial variability of phytoplankton assessed by flow cytometry, in a dynamic productive coastal area, in spring: The eastern English Channel. *Estuarine, Coastal and Shelf Science,* **154**: 214-223.

Bouillon, S., R.M. Connolly and D.P. Gillikin (2011). 7.07 - Use of stable isotopes to understand food webs and ecosystem functioning in estuaries. *In: Treatise on estuarine and coastal science.* E. Wolanski and D. Mclusky (eds.). Waltham, Academic Press, pp. 143-173.

Boynton, W., W. Kemp and C. Keefe (1982). A comparative analysis of nutrients and other factors influencing estuarine phytoplankton production. *In: Estuarine comparisons.* V. S. Kennedy (ed.). New York, Academic Press, pp. 69-90.

Bukaveckas, P., A. MacDonald, A. Aufdenkampe, J. Chick, J. Havel, R. Schultz, T. Angradi, D. Bolgrien, T. Jicha and D. Taylor (2011). Phytoplankton abundance and contributions to suspended particulate matter in the Ohio, Upper Mississippi and Missouri Rivers. *Aquatic Sciences,* **73**(3): 419-436.

Bury, S.J., N.J.P. Owen and T. Preston (1995). 13C and 15N uptake by phytoplankton in the marginal ice zone of the Bellingshausen Sea. *Deep Sea Research Part II: Topical Studies in Oceanography,* **42**(4–5): 1225-1252.

Byun, D.-S., X.H. Wang, M. Zavatarelli and Y.-K. Cho (2007). Effects of resuspended sediments and vertical mixing on phytoplankton spring bloom dynamics in a tidal estuarine embayment. *Journal of Marine Systems,* **67**(1): 102-118.

C.E.C. (2000). Directive 2000/60/EC of the European Parliament and of the Council of 23 October 2000 establishing a framework for Community action in the field of water policy. *Commission of the European Communities,* **77**: 1-73.

Carstensen, J. and D.J. Conley (2004). Frequency, composition, and causes of summer phytoplankton blooms in a shallow coastal ecosystem, the Kattegat. *Limnology and Oceanography,* **49**(1): 191-201.

Carstensen, J., P. Henriksen and A.-S. Heiskanen (2007). Summer algal blooms in shallow estuaries: Definition, mechanisms, and link to eutrophication. *Limnology and Oceanography,* **52**(1): 370-384.

Carstensen, J., R. Klais and J.E. Cloern (2015). Phytoplankton blooms in estuarine and coastal waters: Seasonal patterns and key species. *Estuarine, Coastal and Shelf Science,* **162**: 98-109.

Cebrián, J. and I. Valiela (1999). Seasonal patterns in phytoplankton biomass in coastal ecosystems. *Journal of Plankton Research,* **21**(3): 429-444.

Clarke, K.R., R.N. Gorley, P.J. Somerfield and R.M. Warwick (2014). *Change in marine communities: an approach to statistical analysis and interpretation.,* 3rd (ed.). Plymouth, Plymouth Marine Laboratory. 262 pp.

Clarke, K.R. and R.M. Warwick (1994). *Change in marine communities: An approach to statistical analysis and interpretation (PRIMER).* Plymouth, Plymouth Marine Laboratory. 144 pp.

Cloern, J.E. (1987). Turbidity as a control on phytoplankton biomass and productivity in estuaries. *Continental Shelf Research,* **7**(11–12): 1367-1381.

Cloern, J.E. (1991). Tidal stirring and phytoplankton bloom dynamics in an estuary. *Journal of Marine Research,* **49**(1): 203-221.

Cloern, J.E. (1996). Phytoplankton bloom dynamics in coastal ecosystems: a review with some general lessons from sustained investigation of San Francisco Bay, California. *Reviews of Geophysics,* **34**(2): 127-168.

Cloern, J.E. (2001). Our evolving conceptual model of the coastal eutrophication problem. *Marine Ecology Progress Series,* **210**: 223-253.

Conley, D.J., H. Kaas, F. Møhlenberg, B. Rasmussen and J. Windolf (2000). Characteristics of Danish estuaries. *Estuaries,* **23**(6): 820-837.

Couceiro, F., G.R. Fones, P.J. Statham, B.A. Kelly-Gerreyn, D.B. Sivyer, C.E.L. Thompson, R. Parker and C.L. Amos (2013). Impact of resuspension of cohesive sediments at the Oyster Grounds (North Sea) on nutrient exchange across the sediment–water interface. *Biogeochemistry,* **113**: 37-52.

Crawford, D.W., D.A. Purdie, A.P.M. Lockwood and P. Weissmanb (1997). Recurrent red-tides in the Southampton Water Estuary caused by the phototrophic ciliate *Mesodinium rubrum*. *Estuarine, Coastal and Shelf Science,* **45**: 799-812.

Cullen, J.J. and R.F. Davis (2003). The blank can make a big difference in oceanographic measurements. *Limnology and Oceanography Bulletin*, **12**(2): 29-35.

Dai, M., X. Guo, W. Zhai, L. Yuan, B. Wang, L. Wang, P. Cai, T. Tang and W.-J. Cai (2006). Oxygen depletion in the upper reach of the Pearl River estuary during a winter drought. *Marine Chemistry,* **102**(1): 159-169.

Dalu, T., N.B. Richoux and P.W. Froneman (2015). Distribution of benthic diatom communities in a permanently open temperate estuary in relation to physico-chemical variables. *South African Journal of Botany*.

De Jonge, V.N., M. Elliot and E. Orive (2002). Cause, historical development, effects and future challenges of a common environmental problem: eutrophication. *Hydrobiologia,* **475/476**: 1-19.

Devlin, M., M. Best, D. Coates, E. Bresnan, S. O'Boyle, R. Park, J. Silke, C. Cusack and J. Skeats (2007). Establishing boundary classes for the classification of UK marine waters using phytoplankton communities. *Marine Pollution Bulletin,* **55**(1–6): 91-103.

Domingues, R.B., T.P. Anselmo, A.B. Barbosa, U. Sommer and H.M. Galvão (2010). Tidal variability of phytoplankton and environmental drivers in the freshwater reaches of the Guadiana Estuary (SW Iberia). *International Review of Hydrobiology,* **95**(4-5): 352-369.

Dubelaar, G.B.J., P.J.F. Geerders and R.R. Jonker (2004). High frequency monitoring reveals phytoplankton dynamics. *Journal of Environmental Monitoring*, **6**(12): 946-952.

Dubelaar, G.B.J. and R.R. Jonker (2000). Flow cytometry as a tool for the study of phytoplankton. *Scientia Marina,* **64**(2): 135-156.

Dudgeon, D. (2007). *Aquatic ecology : Tropical stream ecology*. Burlington, MA, USA, Academic Press. 306 pp.

Dugdale, R. and F. Wilkerson (1986). The use of 15N to measure nitrogen uptake in eutrophic oceans; experimental considerations. *Limnology and Oceanography,* **31**(4): 673-689.

Dyer, K.R. (1997). *Estuaries: a Physical Introduction*, 2nd ed. Chichester, Wiley. 195 pp.

Eppley, R.W. (1972). Temperature and phytoplankton growth in the sea. *Fishery Bulletin,* **70**(4): 1063-1085.

Everbecq, E., V. Gosselain, L. Viroux and J.-P. Descy (2001). Potamon: a dynamic model for predicting phytoplankton composition and biomass in lowland rivers. *Water Research,* **35**(4): 901-912.

Falkowski, P.G., R.T. Barber and V. Smetacek (1998). Biogeochemical controls and feedbacks on ocean primary production. *Science*, **281**(5374): 200-206.

Ferreira, J.G., J.H. Andersen, A. Borja, S.B. Bricker, J. Camp, M. Cardoso da Silva, E. Garcés, A.-S. Heiskanen, C. Humborg, L. Ignatiades, C. Lancelot, A. Menesguen, P. Tett, N. Hoepffner and U. Claussen (2011). Overview of eutrophication indicators to assess environmental status within the European Marine Strategy Framework Directive. *Estuarine, Coastal and Shelf Science,* **93**(2): 117-131.

Figueroa, R.I., I. Bravo, S. Fraga, E. Garcés and G. Llaveria (2009). The life history and cell cycle of *Kryptoperidinium foliaceum*, a dinoflagellate with two eukaryotic nuclei. *Protist,* **160**(2): 285-300.

Gameiro, C., P. Cartaxana and V. Brotas (2007). Environmental drivers of phytoplankton distribution and composition in Tagus Estuary, Portugal. *Estuarine, Coastal and Shelf Science,* **75**(1–2): 21-34.

Gao, S. and M. Collins (1994). Tidal inlet stability in response to hydrodynamic and sediment dynamic conditions. *Coastal Engineering,* **23**: 61-80.

Gaulke, A.K., M.S. Wetz and H.W. Paerl (2010). Picophytoplankton: A major contributor to planktonic biomass and primary production in a eutrophic, river-dominated estuary. *Estuarine, Coastal and Shelf Science,* **90**(1): 45-54.

Geider, R.J., R.M. Greene, Z. Kolber, H.L. MacIntyre and P.G. Falkowski (1993). Fluorescence assessment of the maximum quantum efficiency of photosynthesis in the western North Atlantic. *Deep Sea Research Part I: Oceanographic Research Papers,* **40**(6): 1205-1224.

GEOHAB (2006). *Global ecology and oceanography of harmful algal blooms, HABs in eutrophic systems.* Paris and Baltimore, IOC and SCOR. 74 pp.

Gibb, S.W., D.G. Cummings, X. Irigoien, R.G. Barlow, R. Fauzi and C. Mantoura (2001). Phytoplankton pigment chemotaxonomy of the northeastern Atlantic. *Deep Sea Research Part II: Topical Studies in Oceanography,* **48**(4–5): 795-823.

Gillanders, B.M. and M.J. Kingsford (2002). Impact of changes in flow of freshwater on estuarine and open coastal habitats and the associated organisms. *In: Oceanography and Marine Biology, An Annual Review, Volume 40.* R. N. Gibson, M. Barnes and R. J. A. Atkinson (eds.). Taylor & Francis, pp. 233-309.

Goericke, R. (1998). Response of phytoplankton community structure and taxon-specific growth rates to seasonally varying physical forcing in the Sargasso Sea off Bermuda. *Limnology and Oceanography,* **43**(5): 921-935.

Gregg, W.W., M.E. Conkright, P. Ginoux, J.E. O'Reilly and N.W. Casey (2003). Ocean primary production and climate: Global decadal changes. *Geophysical Research Letters,* **30**(15): 1809.

Griffin, S.L. and R.J. Rippingale (2001). Zooplankton grazing dynamics: top-down control of phytoplankton and its relationship to an estuarine habitat. *Hydrological Processes,* **15**(13): 2453-2464.

Ha, K., M.-H. Jang and G.-J. Joo (2003). Winter *Stephanodiscus* bloom development in the Nakdong River regulated by an estuary dam and tributaries. *Hydrobiologia,* **506**(1-3): 221-227.

Han, A., M. Dai, S.J. Kao, J. Gan, Q. Li, L. Wang, W. Zhai and L. Wang (2012). Nutrient dynamics and biological consumption in a large continental shelf system under the influence of both a river plume and coastal upwelling. *Limnology and Oceanography,* **57**(2): 486-502.

Hardenbicker, P., S. Rolinski, M. Weitere and H. Fischer (2014). Contrasting long-term trends and shifts in phytoplankton dynamics in two large rivers. *International Review of Hydrobiology,* **99**(4): 287-299.

Harding Jr, L.W., M.E. Mallonee and E.S. Perry (2002). Toward a predictive understanding of primary productivity in a temperate, partially stratified estuary. *Estuarine, Coastal and Shelf Science,* **55**(3): 437-463.

Harris, G.P. (1986). *Phytoplankton ecology: Structure, function and fluctuation*. London, Chapman & Hall. 384 pp.

Harrison, W.G. and L.R. Harris (1986). Isotope-dilution and its effects on measurements of nitrogen and phosphorus uptake by oceanic microplankton. *Marine Ecology Progress Series*, **27**: 253-261.

Haskoning (2009). *Poole & Christchurch Bays SMP2 Sub-Cell 5f: Estuary Processes Assessment,* ABP Marine Environment Research Ltd.

Hawryshyn, J., K.M. Rühland, M. Julius and J.P. Smol (2012). Absence of evidence is not evidence of absence: Is *Stephanodiscus binderanus* (bacillariophyceae) an exotic species in the great lakes region?. *Journal of Phycology,* **48**(2): 270-274.

Hecky, R. and P. Kilham (1988). Nutrient limitation of phytoplankton in freshwater and marine environments: a review of recent evidence on the effects of enrichment. *Limnology and Oceanography,* **33**(4): 796-822.

Heywood, M. and D.E. Walling (2003). Suspended sediment fluxes in chalk streams in the Hampshire Avon catchment, UK. *Hydrobiologia,* **494**(1-3): 111-117.

Hill, D.R.A. (1991). A revised circumscription of *Cryptomonas* (Cryptophyceae) based on examination of Australian strains. *Phycologia,* **30**(2): 170-188.

Hillebrand, H., C.-D. Dörselen, D. Kirschtel, U. Pollingher and T. Zohary (1999). Biovolume calculation for pelagic and benthic microalgae. *Journal of Phycology*, **35**: 403-424.

Hilton, J., M. O'Hare, M.J. Bowes and J.I. Jones (2006). How green is my river? A new paradigm of eutrophication in rivers. *Science of the Total Environment*, **365**(1-3): 66-83.

Howarth, R.W. and R. Marino (2006). Nitrogen as the limiting nutrient for eutrophication in coastal marine ecosystems: evolving views over three decades. *Limnology and Oceanography*, **51**(1 Part 2): 364-376.

Howarth, R.W., D.P. Swaney, T.J. Butler and R. Marino (2000). Rapid Communication: Climatic Control on Eutrophication of the Hudson River Estuary. *Ecosystems*, **3**(2): 210-215.

Hu, H., Y. Li, L. Wu and Y. Qi (2002). Studies on Genus *Cryptomonas* from China seas. *Acta Oceanologica Sinica*, **21**(4): 535-540.

Imanian, B. and P.J. Keeling (2007). The dinoflagellates Durinskia baltica and Kryptoperidinium foliaceum retain functionally overlapping mitochondria from two evolutionarily distinct lineages. *BMC Evolutionary Biology*, **7**(1): 1-11.

Imanian, B., J.-F. Pombert and P.J. Keeling (2010). The complete plastid genomes of the two 'dinotoms' Durinskia baltica and Kryptoperidinium foliaceum. *PloS one*, **5**(5): e10711.

Iriarte, A. and D.A. Purdie (1994). Size distribution of chlorophyll a biomass and primary production in a temperate estuary (Southampton Water): the contribution of photosynthetic picoplankton. *Marine Ecology Progress Series*, **115**: 283-297.

James, F.C. and C.E. McCulloch (1990). Multivariate analysis in ecology and systematics: Panacea or Pandora's Box?. *Annual Review of Ecology and Systematics*, **21**: 129-166.

Jarvie, H.P., M.D. Jurgens, R.J. Williams, C. Neal, J.J.L. Davies, C. Barrett and J. White (2005a). Role of river bed sediments as sources and sinks of phosphorus across two major eutrophic UK river basins: the Hampshire Avon and Herefordshire Wye. *Journal of Hydrology*, **304**: 51–74.

Jarvie, H.P., C. Neala, P.J.A. Withersb, C. Wescottc and R.M. Acornleyc (2005b). Nutrient hydrochemistry for a groundwater-dominated catchment: The Hampshire Avon, UK. *Science of the Total Environment,* **344**: 143–158.

Jeffrey, S.W. and G.F. Humphrey (1975). New spectrophotometric equations for determining chlorophylls *a*, *b*, $c_1$ and $c_2$ in higher plants, algae and nutural phytoplankton. *Biochemie und Physiologie der Pflanzen,* **167**: 191-194.

Jeffrey, S.W. and M. Vesk (1997). Introduction to marine phytoplankton and thier pigment and signature. *In: Phytoplankton pigments in oceanography: guidelines to modern methods.* S. W. Jeffrey, R. F. Mantoura and S. W. Wright (eds.). Paris, UNESCO, pp. 37-84.

Ji, H., G. Sheng, H. Xin and Y. Sha (2009). Distribution of dissolved inorganic carbon (DIC) and its related parameters in seawater of the North Yellow Sea and off the Qingdao Coast in October, 2007. *Journal of Ocean University of China,* **8**(4): 366-376.

Kaiblinger, C. and M. Dokulil (2006). Application of fast repetition rate fluorometry to phytoplankton photosynthetic parameters in freshwaters. *Photosynthesis Research,* **88**(1): 19-30.

Kaiser, M.J., M.J. Attrill, S. Jennings, D.N. Thomas, D.K.A. Barnes, A.S. Brierley, J.G. Hiddink, H. Kaartokallio, N.V.C. Polunin and D.G. Raffaelli (2011). *Marine ecology: processes, systems and impacts.,* 2nd (ed.). USA, Oxford University Press. 501 pp.

Kempton, J.W., J. Wolny, T. Tengs, P. Rizzo, R. Morris, J. Tunnell, P. Scott, K. Steidinger, S.N. Hymel and A.J. Lewitus (2002). Kryptoperidinium foliaceum blooms in South Carolina: a multi-analytical approach to identification. *Harmful Algae*, **1**(4): 383-392.

Kimmerer, W., J. Burau and W. Bennett (1998). Tidally oriented vertical migration and position maintenance of zooplankton in a temperate estuary. *Limnology and Oceanography,* **43**(7): 1697-1709.

Kimmerer, W.J., A.E. Parker, U.E. Lidstroem and E.J. Carpenter (2012). Short-term and interannual variability in primary production in the low-salinity zone of the San Francisco Estuary. *Estuaries and Coasts,* **35**(4): 913-929.

Kirkwood, D.S. (1992). Stability of solutions of nutrient salts during storage. *Marine Chemistry,* **38**(3–4): 151-164.

Kolber, Z., J. Zehr and P. Falkowski (1988). Effects of growth irradiance and nitrogen limitation on photosynthetic energy conversion in photosystem II. *Plant Physiology,* **88**(3): 923-929.

Kolber, Z.S., O. Prášil and P.G. Falkowski (1998). Measurements of variable chlorophyll fluorescence using fast repetition rate techniques: defning methodology and experimental protocols. *Biochimica et Biophysica Acta,* **1367**: 88-106.

Kotsedi, D., J.B. Adams and G.C. Snow (2012). The response of microalgal biomass and community composition to environmental factors in the Sundays Estuary. *Water SA,* **38**: 177-190.

Kraberg, A., M. Buamann and C.-D. Dürselen (2010). *Coastal phytoplankton; photo guide for Northern European Seas.* München, Pfeil. 204 pp.

Kromkamp, J. and J. Peene (1995). Possibility of net phytoplankton primary production in the turbid Schelde Estuary (SW Netherlands). *Marine Ecology Progress Series,* **121**: 249-259.

Lancelot, C. and K. Muylaert (2011). 7.02 - Trends in estuarine phytoplankton ecology. *In: Treatise on estuarine and coastal science.* E. Wolanski and D. Mclusky (eds.). Waltham, Academic Press, pp. 5-15.

Lepš, J. and P. Šmilauer (2003). *Multivariate analysis of ecological data using CANOCO*. Cambridge University Press. 269 pp.

Levinton, J. (2011). *Marine biology: Function, biodiversity, ecology.* , 3nd ed., Oxford University Press. 588 pp.

Lin, L., J. He, Y. Zhao, F. Zhang and M. Cai (2012). Flow cytometry investigation of picoplankton across latitudes and along the circum Antarctic Ocean. *Acta Oceanologica Sinica,* **31**(1): 134-142.

Lionard, M., F. Azémar, S. Boulêtreau, K. Muylaert, M. Tackx and W. Vyverman (2005). Grazing by meso- and microzooplankton on phytoplankton in the upper reaches of the Schelde estuary (Belgium/The Netherlands). *Estuarine, Coastal and Shelf Science*, **64**(4): 764-774.

Lionard, M., K. Muylaert, A. Hanoutti, T. Maris, M. Tackx and W. Vyverman (2008). Inter-annual variability in phytoplankton summer blooms in the freshwater tidal reaches of the Schelde estuary (Belgium). *Estuarine, Coastal and Shelf Science,* **79**(4): 694-700.

Liu, Z., L. Zhang, W.-J. Cai, L. Wang, M. Xue and X. Zhang (2014). Removal of dissolved inorganic carbon in the Yellow River Estuary. *Limnology and Oceanography*, **59**(2): 413-426.

Lucas, L.V., J.E. Cloern, J.R. Koseff, S.G. Monismith and J.K. Thompson (1998). Does the Sverdrup critical depth model explain bloom dynamics in estuaries? *Journal of Marine Research,* **56**(2): 375-415.

Lucas, L.V., J.R. Koseff, J.E. Cloern, S.G. Monismith and J.K. Thompson (1999). Processes governing phytoplankton blooms in estuaries. I: The local production-loss balance. *Marine Ecology Progress Series,* **187**: 1-15.

Lucas, L.V., J.K. Thompson and L.R. Brown (2009). Why are diverse relationships observed between phytoplankton biomass and transport time. *Limnology and Oceanography*, **54**(1): 381-390.

Maier, G., G.A. Glegg, A.D. Tappin and P.J. Worsfold (2012). A high resolution temporal study of phytoplankton bloom dynamics in the eutrophic Taw Estuary (SW England). *Science of the Total Environment,* **434**: 228-39.

Maier, G., R.J. Nimmo-Smith, G.A. Glegg, A.D. Tappin and P.J. Worsfold (2009). Estuarine eutrophication in the UK: current incidence and future trends. *Aquatic Conservation: Marine and Freshwater Ecosystems*, **19**(1): 43-56.

Mann, K.H. (2000). *Ecology of coastal waters: With implications for management*. USA, Blackwell Science. 432 pp.

Manuel, Z., S. Fraga, F. Rodríguez and J.L. Garrido (2012). Pigment-based chloroplast types in dinoflagellates. *Marine Ecology Progress Series*, **465**: 33-52.

Marques, S.C., M.A. Pardal, M.J. Pereira, F. Gonçalves, J.C. Marques and U.M. Azeiteiro (2007). Zooplankton distribution and dynamics in a temperate shallow estuary. *Hydrobiologia*, **587**(1): 213-223.

Matson, E.A. and M.M. Brinson (1990). Stable carbon isotopes and the C: N ratio in the estuaries of the Pamlico and Neuse Rivers, North Carolina. *Limnology and Oceanography,* **35**(6): 1290-1300.

McLusky, D.S. and M. Elliott (2004). *The estuarine ecosystem: ecology, threats and management.* Oxford University Press. 214 pp.

McQuoid, M.R. (2005). Influence of salinity on seasonal germination of resting stages and composition of microplankton on the Swedish west coast. *Marine Ecology Progress Series,* **289**: 151-163.

Menden-Deuer, S. and E.J. Lessard (2000). Carbon to volume relationships for dinoflagellates, diatoms, and other protist plankton. *Limnology and Oceanography,* **45**(3): 569–579.

Middelburg, J.J. and J. Nieuwenhuize (2000a). Uptake of dissolved inorganic nitrogen in turbid, tidal estuaries. *Marine Ecology Progress Series,* **192**: 79-88.

Middelburg, J.J. and J. Nieuwenhuize (2000b). Nitrogen uptake by heterotrophic bacteria and phytoplankton in the nitrate rich Thames estuary. *Marine Ecology Progress Series,* **203**: 13-21.

Millie, D.F., H.W. Paerl and J.P. Hurley (1993). Microalgal pigment assessments using High-Performance Liquid Chromatography: A synopsis of organismal and ecological applications. *Canadian Journal of Fisheries and Aquatic Sciences,* **50**(11): 2513-2527.

Monsen, N.E., J.E. Cloern, L.V. Lucas and S.G. Monismith (2002). A comment on the use of flushing time, residence time, and age as transport time scales. *Limnology and Oceanography,* **47**(5): 1545-1553.

Montagnes, D.J.S., J.A. Berges, P.J. Harrison and F.J.R. Taylor (1994). Estimating carbon, nitrogen, protein, and chlorophyll a from volume in marine phytoplankton. *Limnology and Oceanography,* **39**(5): 1044-1060.

Montesanto, B., S. Ziller, D. Danielidis and A. Economou-Amilli (2000). Phytoplankton community structure in the lower reaches of a Mediterranean river (Aliakmon, Greece). *Arch Hydrobiol,* **147**: 171-191.

Moore, S.K., M.E. Baird and I.M. Suthers (2006). Relative effects of physical and biological processes on nutrient and phytoplankton dynamics in a shallow estuary after a storm event. *Estuaries and Coasts,* **29**(1): 81-95.

Moreira-Turcq, P.F., G. Cauwet and J.M. Martin (2001). Contribution of flow cytometry to estimate picoplankton biomass in estuarine systems. *Hydrobiologia,* **462**(1-3): 157-168.

Murray, J.W. (1966). A study of the seasonal changes of the water mass of Christchurch Harbour, England. *Journal of the Marine Biological Association of the United Kingdom,* **46**: 561-578.

Neal, C., J. Hilton, A.J. Wade, M. Neal and H. Wickham (2006). Chlorophyll-a in the rivers of eastern England. *Science of the Total Environment,* **365**(1): 84-104.

Nedwell, D.B., L.F. Dong, A. Sage and G.J.C. Underwood (2002). Variations of the nutrients loads to the mainland U.K. estuaries: correlation with catchment areas, urbanization and coastal eutrophication. *Estuarine, Coastal and Shelf Science,* **54**: 951-970.

Nedwell, D.B. and D.G. Raffaelli (1999). *Estuaries: Advances in ecological research*. London, Academic Press. 306 pp.

Nixon, S.W., R.W. Fulweiler, B.A. Buckley, S.L. Granger, B.L. Nowicki and K.M. Henry (2009). The impact of changing climate on phenology, productivity, and benthic-pelagic coupling in Narragansett Bay. *Estuarine, Coastal and Shelf Science,* **82**(1): 1-18.

Paerl, H.W., J. Dyble, J.L. Pinckney, L.M. Valdes, D.F. Millie, P.H. Moisander, J.T. Morris, B. Bendis and M.F. Piehler (2005). Using microalgal indicators to assess human-and climate-induced ecological change in estuaries. *In: Estuarine indicators.* S. A. Bortone (ed.). CRC press, pp. 145 - 174.

Paerl, H.W. and D. Justić (2011). 6.03 - Primary producers: Phytoplankton ecology and trophic dynamics in coastal waters. *In: Treatise on estuarine and coastal science.* E. Wolanski and D. Mclusky (eds.). Waltham, Academic Press, pp. 23-42.

Paerl, H.W., L.M. Valdes, J.L. Pinckney, M.F. Piehler, J. Dyble and P.H. Moisander (2003). Phytoplankton photopigments as indicators of estuarine and coastal eutrophication. *BioScience,* **53**(10): 953-964.

Parkhill, J.-P., G. Maillet and J.J. Cullen (2001). Fluorescence-based maximal quantum yield for psII as a diagnostic of nutrient stress. *Journal of Phycology,* **37**(4): 517-529.

Parsons, T.R., Y. Maita and C.M. Lalli (1984). *A manual of chemical and biological methods for seawater analysis.* UK, Pergamon Press. 173 pp.

Peterson, T.D., H.N.J. Toews, C.L.K. Robinson and P.J. Harrison (2007). Nutrient and phytoplankton dynamics in the Queen Charlotte Islands (Canada) during the summer upwelling seasons of 2001–2002. *Journal of Plankton Research,* **29**(3): 219-239.

Phlips, E.J., S. Badylak, M. Christman, J. Wolny, J. Brame, J. Garland, L. Hall, J. Hart, J. Landsberg, M. Lasi, J. Lockwood, R. Paperno, D. Scheidt, A. Staples and K. Steidinger (2011). Scales of temporal and spatial variability in the distribution of harmful algae species in the Indian River Lagoon, Florida, USA. *Harmful Algae,* **10**(3): 277-290.

Phlips, E.J., S. Badylak, M.C. Christman and M.A. Lasi (2010). Climatic trends and temporal patterns of phytoplankton composition, abundance, and succession in the Indian River Lagoon, Florida, USA. *Estuaries and Coasts,* **33**(2): 498-512.

Phlips, E.J., M. Cichra, F.J. Aldridge, J. Jembeck, J. Hendrickson and R. Brody (2000). Light availability and variations in phytoplankton standing crops in a nutrient-rich blackwater river. *Limnology and Oceanography,* **45**(4): 916-929.

Picard, V. and N. Lair (2005). Spatio-temporal investigations on the planktonic organisms of the Middle Loire (France), during the low water period: biodiversity and community dynamics. *Hydrobiologia,* **551**(1): 69-86.

Pinckney, J.L., H.W. Paerl and M.B. Harrington (1999). Responses of the phytoplankton community growth rate to nutrient pulses in variable estuarine environments. *Journal of Phycology,* **35**(6): 1455-1463.

Putland, J.N., B. Mortazavi, R.L. Iverson and S.W. Wise (2014). Phytoplankton biomass and composition in a river-dominated estuary during two summers of contrasting river discharge. *Estuaries and Coasts,* **37**(3): 664-679.

Read, D.S., M.J. Bowes, L.K. Newbold and A.S. Whiteley (2014). Weekly flow cytometric analysis of riverine phytoplankton to determine seasonal bloom dynamics. *Environmental Science: Processes & Impacts,* **16**(3): 594-603.

Resende, P., U. Azeiteiro and M.J. Pereira (2005). Diatom ecological preferences in a shallow temperate estuary (Ria de Aveiro, Western Portugal). *Hydrobiologia*, **544**: 77-88.

Reynolds, C.S. (1984). *The ecology of freshwater phytoplankton*. Cambridge, Cambridge University Press. 384 pp.

Reynolds, C.S. (1998). The state of freshwater ecology. *Freshwater Biology,* **39**(4): 741-753.

Reynolds, C.S. (2000). Hydroecology of river plankton: the role of variability in channel flow. *Hydrological Processes,* **14**(16-17): 3119-3132.

Reynolds, C.S. (2006). *Ecology of phytoplankton. Ecology, biodiversity, and conservation,* C. Reynolds (ed.). Cambridge University Press. 435 pp.

Round, F.E., R.M. Crawford and D.G. Mann (2007). *The diatoms; biology & morphology of the genera*. Cambridge University Press. 747 pp.

Ruiz, A., J. Franco and F. Villate (1998). Microzooplankton grazing in the Estuary of Mundaka, Spain, and its impact on phytoplankton distribution along the salinity gradient. *Aquatic Microbial Ecology,* **14**(3): 281-288.

Rutten, T.P.A., B. Sandee and A.R.T. Hofman (2005). Phytoplankton monitoring by high performance flow cytometry: A successful approach?. *Cytometry Part A,* **64A**(1): 16-26.

Sabater, S., J. Artigas, C. Duran, M. Pardos, A.M. Romani, E. Tornes and I. Ylla (2008). Longitudinal development of chlorophyll and phytoplankton assemblages in a regulated large river (the Ebro River). *Science of the Total Environment,* **404**(1): 196-206.

Saeck, E.A., W.L. Hadwen, D. Rissik, K.R. O'Brien and M.A. Burford (2013). Flow events drive patterns of phytoplankton distribution along a river–estuary–bay continuum. *Marine and Freshwater Research,* **64**(7): 655-670.

Schöl, A., V. Kirchesch, T. Bergfeld and D. Müller (1999). Model-based analysis of oxygen budget and biological processes in the regulated rivers Moselle and Saar: modelling the influence of benthic filter feeders on phytoplankton. *In: Man and River Systems.* Springer, pp. 167-176.

Shaw, P.J., C. Chapron, D.A. Purdie and A. Rees (1998a). Impacts of phytoplankton activity on dissolved nitrogen fluxes in the tidal reaches and estuary of the Tweed, UK. *Marine Pollution Bulletin,* **37**(3-7): 280-297.

Shaw, P.J., D.A. Purdie, P.S. de Frietas, A.P. Rees and I. Joint (1998b). Nutrient uptake in a highly turbid estuary (the Humber, United Kingdom) and adjacent coastal waters. *Estuaries,* **21**(4): 507-517.

Shikata, T., S. Nagasoe, T. Matsubara, S. Yoshikawa, Y. Yamasaki, Y. Shimasaki, Y. Oshima, I.R. Jenkinson and T. Honjo (2008). Factors influencing the initiation of blooms of the raphidophyte *Heterosigma akashiwo* and the diatom *Skeletonema costatum* in a port in Japan. *Limnology and Oceanography,* **53**(6): 2503-2518.

Sieburth, J.M., V. Smetacek and J. Lenz (1978). Pelagic ecosystem structure: heterotrophic compartments of the plankton and their relationship to plankton size fractions. *Limnology and oceanography,* **23**(6): 1256-1263.

Sin, Y., B. Hyun, B. Jeong and H.Y. Soh (2013). Impacts of eutrophic freshwater inputs on water quality and phytoplankton size structure in a temperate estuary altered by a sea dike. *Marine Environmental Research,* **85**: 54-63.

Sin, Y., E. Lee, Y. Lee and K.-H. Shin (2015). The river–estuarine continuum of nutrients and phytoplankton communities in an estuary physically divided by a sea dike. *Estuarine, Coastal and Shelf Science,* **163**(Part B): 279-289.

Sin, Y., R.L. Wetzel and I.C. Anderson (2000). Seasonal variations of size-fractionated phytoplankton along the salinity gradient in the York River estuary, Virginia (USA). *Journal of Plankton Research,* **22**: 1945-1960.

Statham, P.J. (2012). Nutrients in estuaries - An overview and the potential impacts of climate change. *Science of the Total Environment,* **434**: 213-27.

Stoll, M.H.C., K. Bakker, G.H. Nobbe and R.R. Haese (2001). Continuous-flow analysis of dissolved inorganic carbon content in seawater. *Analytical Chemistry,* **73**(17): 4111-4116.

Suggett, D., G. Kraay, P. Holligan, M. Davey, J. Aiken and R. Geider (2001). Assessment of photosynthesis in a spring cyanobacterial bloom by use of a fast repetition rate fluorometer. *Limnology Oceanography,* **46**(4): 802-810.

Sun, J. and D. Liu (2003). Geometric models for calculating cell biovolume and surface area for phytoplankton. *Journal of Plankton Research,* **25**(11): 1331-1346.

Tan, Y., L. Huang, Q. Chen and X. Huang (2004). Seasonal variation in zooplankton composition and grazing impact on phytoplankton standing stock in the Pearl River Estuary, China. *Continental Shelf Research,* **24**: 1949-1968.

Ter Braak, C.J.F. and P. Šmilauer (2002). *CANOCO reference manual and CanoDraw for Windows user's guide: software for canonical community ordination (version 4.5).* Ithaca, NY, USA, Microcomputer Power. 500 pp.

Tomas, C.R. (1997). *Identifying marine phytoplankton*. USA, Elsevier. 858 pp.

Torres-Valdés, S. and D.A. Purdie (2006). Nitrogen removal by phytoplankton uptake through a temperate non-turbid estuary. *Estuarine, Coastal and Shelf Science,* **70**(3): 473-486.

Trees, C.C., D.K. Clark, R.R. Bidigare, M.E. Ondrusek and J.L. Mueller (2000). Accessory pigments versus chlorophyll a concentrations within the euphotic zone: A ubiquitous relationship. *Limnology and Oceanography,* **45**(5): 1130-1143.

Trees, C.C., M.C. Kennicutt Ii and J.M. Brooks (1985). Errors associated with the standard fluorimetric determination of chlorophylls and phaeopigments. *Marine Chemistry,* **17**(1): 1-12.

Trigueros, J.M. and E. Orive (2001). Seasonal variations of diatoms and dinoflagellates in a shallow, temperate estuary, with emphasis on neritic assemblages. *Hydrobiologia,* **444**: 119-133.

Underwood, G., J. Phillips and K. Saunders (1998). Distribution of estuarine benthic diatom species along salinity and nutrient gradients. *European Journal of Phycology,* **33**(2): 173-183.

Underwood, G.J.C. and J. Kromkamp (1999). Primary production by phytoplankton and microphytobenthos in estuaries. *In: Advances in ecological research: Estuaries.* D. B. Nedwell and D. G. Raffaelli (eds.). Academic press, pp. 93-153.

UNESCO (2010). *Microscopic and molecular methods for quantitative phytoplankton analysis.* Paris, UNESCO. 101 pp.

Valdes-Weaver, L.M., M.F. Piehler, J.L. Pinckney, K.E. Howe, K. Rossignol and H.W. Paerl (2006). Long-term temporal and spatial trends in phytoplankton biomass and class-level taxonomic composition in the hydrologically variable Neuse-Pamlico estuarine continuum, North Carolina, USA. *Limnology and Oceanography,* **51**(3): 1410-1420.

van Bennekom, A.J. and F.J. Wetsteijn (1990). The winter distribution of nutrients in the Southern Bight of the North Sea (1961–1978) and in the estuaries of the Scheldt and the Rhine/Meuse. *Netherlands Journal of Sea Research,* **25**(1): 75-87.

van Steveninck, E.d.R., W. Admiraal, L. Breebaart, G. Tubbing and B. Van Zanten (1992). Plankton in the River Rhine: structural and functional changes observed during downstream transport. *Journal of Plankton Research,* **14**(10): 1351-1368.

Villegas, I. and G. de Giner (1973). Phytoplankton as a biological indicator of water quality. *Water Research,* **7**(3): 479-487.

Wehr, J.D. and J.-P. Descy (1998). Use of phytoplankton in large river management. *Journal of Phycology*, **34**(5): 741-749.

Wehr, J.D. and J.H. Thorp (1997). Effects of navigation dams, tributaries, and littoral zones on phytoplankton communities in the Ohio River. *Canadian Journal of Fisheries and Aquatic Sciences,* **54**(2): 378-395.

Weng, H.-X., Y.-C. Qin, X.-W. Sun, H. Dong and X.-H. Chen (2007). Iron and phosphorus effects on the growth of *Cryptomonas* sp. (Cryptophyceae) and their availability in sediments from the Pearl River Estuary, China. *Estuarine, Coastal and Shelf Science*, **73**(3–4): 501-509.

Wetz, M.S., H.W. Paerl, J.C. Taylor and J.A. Leonard (2011). Environmental controls upon picophytoplankton growth and biomass in a eutrophic estuary. *Aquatic Microbial Ecology,* **63**(2): 133-143.

White, J.R. and M.R. Roman (1992). Seasonal study of grazing by metazoan zooplankton in the mesohaline Chesapeake Bay. *Marine Ecology-Progress Series*, **86**: 251-251.

Whitehead, P.G., G. Bussi, M.J. Bowes, D.S. Read, M.G. Hutchins, J.A. Elliott and S.J. Dadson (2015). Dynamic modelling of multiple phytoplankton groups in rivers with an application to the Thames river system in the UK. *Environmental Modelling & Software*, **74**: 75-91.

Wienke, S.M. and J.E. Cloern (1987). The phytoplankton component of seston in San Francisco Bay. *Netherlands Journal of Sea Research*, **21**(1): 25-33.

Wu, N.C., B. Schmalz and N. Fohrer (2011). Distribution of phytoplankton in a German lowland river in relation to environmental factors. *Journal of Plankton Research*, **33**(5): 807-820.